

**THE PYROLYSIS OF FUEL NITROGEN
FROM BLACK LIQUOR**

A Thesis Submitted by

Denise M. Martin

B.S. 1989, Viterbo College

M.S. 1991, Institute of Paper Science and Technology

in partial fulfillment of the requirements
of the Institute of Paper Science and Technology
for the degree of Doctor of Philosophy,
Atlanta, Georgia

Publication Rights Reserved by the
Institute of Paper Science and Technology

September, 1995

TABLE OF CONTENTS

LIST OF FIGURES.....	vi
LIST OF TABLES.....	xi
NOMENCLATURE.....	xiii
SUMMARY.....	xvi
INTRODUCTION.....	1
BLACK LIQUOR COMBUSTION.....	2
<u>Pyrolysis</u>	3
NO _x FORMATION MECHANISMS.....	4
<u>Fuel NO</u>	5
Effect of Nitrogen Content on Conversion.....	8
Effect of Fuel Nitrogen Chemical Structure.....	9
Fuel NO _x Formation Pathways From Coal Nitrogen.....	12
Effect of Temperature/Heating Rate.....	14
NO _x DEPLETION REACTIONS.....	18
NO _x FORMATION DURING KRAFT RECOVERY BOILER OPERATION.....	20
NITROGEN IN BLACK LIQUOR.....	26
PROBLEM ANALYSIS.....	28
THESIS OBJECTIVES.....	31
EXPERIMENTAL APPROACH.....	32
RESULTS AND DISCUSSION.....	34
BLACK LIQUOR CHARACTERIZATION.....	35
<u>Source of Nitrogen in Black Liquor</u>	35
Nitrogen Content in Black Liquor.....	36
Nitrogen Species in Black Liquor.....	37
<u>Selection of Model Fuel Nitrogen Compounds</u>	38
<u>Black Liquor Elemental Analysis</u>	39
<u>Significance of Characterization</u>	40
MEASUREMENT OF TOTAL NITROGEN AS NO _x IN NITROGEN CONTAINING COMPOUNDS.....	40
<u>PCL Comparison with Other Nitrogen Methods of Analysis</u>	42
PCL vs. Kjeldahl.....	43
PCL vs. LECO.....	47
<u>Effect of Nitrogen Species on Conversion During Pyrolysis</u>	49
<u>Effect of Inorganic Composition</u>	53

PYROLYSIS OF ORGANIC FUEL NITROGEN MODEL	
COMPOUNDS	57
<u>Effect of Inorganic Compound Addition</u>	59
<u>Effect of Total Sodium</u>	60
GENERATION OF GAS PHASE NO_x PRECURSORS	62
<u>Pyrolysis of Model Fuel Nitrogen Compounds</u>	62
Effect of Oxygen During Pyrolysis	64
Comparison of Pyrolysis Results with Total Nitrogen Measurements	66
Effect of Nitrogen Species on Conversion During Pyrolysis	68
Effect of Inorganic Composition	70
Effect of Heating Rate	76
Variation in GPNP at Slow Heating Rates	76
Variation in Pyrolysis Products at High Heating Rates	78
Proline pyrolysis	79
Glutamic acid pyrolysis	84
Ammonium sulfate pyrolysis	86
Formation Pathways for Gas Phase Nitrogen Species	89
Significance of Pyrolysis Results	93
<u>Black Liquor Pyrolysis</u>	95
NO _x and NO _x Precursor Generation from Liquor Fractions	95
NO _x and NO _x Precursor Generation from Black Liquor Drops	98
Effect of Temperature	100
Effect of Addition of Known Components to Black Liquor	104
Liquor Composition Comparisons	105
Significance of Black Liquor Pyrolysis Results	110
IN SITU REACTIONS OF GAS PHASE NITROGEN SPECIES	112
<u>Effect of Residence Time</u>	112
<u>Kinetic Analysis of Gas Phase NO_x Precursor Depletion</u>	115
Determination of the Rate Equation	117
Concentration Dependency	118
Temperature Dependency	120
<u>Interpretation of Kinetic Data</u>	123
CONCLUSIONS	124
CONTRIBUTIONS	127
INSIGHT INTO FUEL NO_x FORMATION	127
RECOVERY FURNACE APPLICATION	128
<u>Alternate NO_x Control Strategies</u>	129
SUGGESTIONS FOR FUTURE WORK	131
EQUIPMENT AND METHODS	133

Pyrochemiluminescence (PCL) Nitrogen Analyzer	133
<u>Instrument Description</u>	133
<u>Operating Conditions</u>	135
Pyrolysis Using the PCL Nitrogen Analyzer	135
<u>Instrument Description</u>	135
<u>Operating Conditions</u>	135
Pyrolysis Using Gas Chromatography-Mass Spectrometry	136
<u>Instrument Description</u>	136
<u>Operating Conditions</u>	138
Black Liquor Single Drop Reactor	139
<u>Description of Apparatus and Instrumentation</u>	139
<u>Operating Conditions</u>	141
Thermogravimetric Differential Scanning Calorimeter	143
<u>Description of Apparatus and Instrumentation</u>	143
<u>Operating Conditions</u>	145
Chemical Analyses Used	148
ACKNOWLEDGMENTS	149
LITERATURE CITED	151
APPENDIX I: LIST OF MATERIALS AND EXPERIMENTAL EQUIPMENT	159
APPENDIX II: PYROCHEMILUMINESCENCE NITROGEN ANALYZER	
METHODS VERIFICATION	161
METHODS OPTIMIZATION	161
<u>Combustion Temperature</u>	161
Data Tables for Temperature Effect.....	162
<u>Sample Boat Preparation</u>	169
Analysis of Variance for Sample Boat Preparation.....	171
<u>Effect of Sample Size</u>	174
<u>Verification of Gas Loop Sample Size</u>	175
TOTAL NITROGEN MEASUREMENT	177
<u>Measurement of Multiple Fuel Nitrogen Species</u>	177
Model Fuel Nitrogen Species with NO (g).....	177
Model Fuel Nitrogen Species with NH ₃ (g).....	180
<u>Data Tables for of Multiple Nitrogen Species Measurement</u>	181
PYROLYSIS	196
<u>Temperature Profile Accuracy</u>	196
<u>Carrier Gas Flow Rate</u>	196
<u>Effect of Sample Placement</u>	197
<u>Reproducibility</u>	199
<u>Pyrolysis Data For Fixed Nitrogen Measurements</u>	200
APPENDIX III: SINGLE DROPLET REACTOR METHODS	
VERIFICATION	206

NO ANALYZER CALIBRATION.....	206
<u>Discussion</u>	208
CALCULATION OF N_{Re}	210
DETERMINATION OF STATISTICALLY SOUND SAMPLE SIZE.....	212
APPENDIX IV: SAMPLE PREPARATION.....	213
MODEL FUEL NITROGEN SPECIES.....	213
BLACK LIQUORS.....	218
SCREENING EXPERIMENTS.....	219
APPENDIX V: GPNP DATA COLLECTED UNDER COMBUSTION CONDITIONS.....	221
APPENDIX VI: THERMODYNAMIC EVALUATION OF NITROGEN SPECIES CONVERSION UNDER COMBUSTION CONDITIONS.....	261
OVERVIEW OF THERMODYNAMIC EQUILIBRIUM CALCULATIONS.....	261
<u>Example Equilibrium Compositions</u>	263
APPENDIX VII: KINETICS OF NITROGEN OXIDATION IN THE PYROTUBE.....	270
APPENDIX VIII: GPNP DATA COLLECTED UNDER PYROLYSIS CONDITIONS.....	274
APPENDIX IX: KINETICS FOR GPNP CONVERSION DURING PYROLYSIS.....	286
VERIFICATION OF HOMOGENEOUS GAS PHASE.....	286
EVALUATION OF THE EFFECT OF DISPERSION.....	289
<u>Kinetics for First-Order Reaction with Dispersion</u>	292
<u>Data for Proline Nitrogen Calibration and Kinetic Calculations</u>	297
APPENDIX X: EFFECT OF HEATING RATE ON GASEOUS NITROGEN SPECIES.....	307
PYROLYSIS GC/MS FOR PROLINE.....	309
<u>Spectral Identification of Proline Pyrolysis Products</u>	309
<u>Proline Pyrolysis Spectral Data Tables and Figures</u>	310
PYROLYSIS GC/MS FOR GLUTAMIC ACID.....	320
<u>Spectral Identification of Glutamic Acid Pyrolysis Products</u>	320
<u>Glutamic Acid Pyrolysis Spectral Data Tables and Figures</u>	321
PYROLYSIS GC/MS FOR AMMONIUM SALTS.....	329
<u>Spectral Identification of Ammonium Salt Pyrolysis Products</u>	329
<u>Ammonium Salt Pyrolysis Spectral Data Tables and Figures</u>	330
APPENDIX XI: BLACK LIQUOR NITROGEN MEASUREMENTS.....	343
PCL NITROGEN DATA.....	344
SINGLE DROP DATA.....	352

APPENDIX XII: THERMOGRAVIMETRIC DIFFERENTIAL SCANNING CALORIMETRY SCREENING EXPERIMENTS.....	377
SCREENING EXPERIMENTS OVERVIEW.....	377
RESULTS AND DISCUSSION.....	379
<u>Decomposition Onset Temperature.....</u>	380
<u>Percent Weight Loss.....</u>	382
<u>Onset Decomposition Enthalpy.....</u>	384
<u>Summary.....</u>	386
<u>Example of Weight Loss Correction Calculations.....</u>	390
DATA.....	391
<u>Analysis of Variance Tables.....</u>	393
APPENDIX XIII: DISSERTATION PUBLICATIONS.....	396
ADDITIONAL LITERATURE CITATIONS.....	397

LIST OF FIGURES

Figure 1.	Structures of fuel nitrogen species: methylamine, pyridine, and piperidine.....	11
Figure 2.	Proposed reaction pathways for coal nitrogen as a) carbazole and b) acridine to for NO _x intermediate NH ₃ . ³⁰	13
Figure 3.	Formation of HCN and NH _i from pyridinic ring rupture. ^{31, 32}	13
Figure 4.	Percent conversion of fuel nitrogen to NO for coal ²³ (◊) is about 10 times greater than for equivalent nitrogen concentrations of nitrogen in black liquor ⁵ (Δ).....	25
Figure 5.	Composition of organic fuel nitrogen species in Southern Pine I black liquor.....	37
Figure 6.	Heterocyclic nitrogen species of Southern Pine II black liquor.....	38
Figure 7.	Chemical structure of organic nitrogen: proline, glutamic acid, pyrazine, and inorganic nitrogen: ammonium nitrate (NH ₄ NO ₃).....	39
Figure 8.	Block diagram of nitrogen analyzer system.....	41
Figure 9.	Chemical structure of carbazole which was used as a nitrogen calibration standard. ⁷⁵	44
Figure 10.	Relative conversions of various model fuel nitrogen species with respect to the primary standard NO _(g)	50
Figure 11.	Inorganic component effects on organic nitrogen (as glutamic acid) conversion to GPNP for detection of total nitrogen.....	53
Figure 12.	Increased sodium hydroxide concentration decreases the organic fuel nitrogen (as tryptophan) conversion to GPNP for total nitrogen measurement compared to the NO _(g) standard.....	54
Figure 13.	Increased sodium carbonate concentration increases the inorganic nitrogen (as NH ₄ Cl) conversion to GPNP for total nitrogen measurement compared to the NO _(g) standard.....	55

Figure 14.	Effect of total sodium addition on mass loss of organic fuel nitrogen model compounds as determined with the TG-DSC (Combined data for glutamic acid and tryptophan).....	60
Figure 15.	Block diagram of nitrogen analyzer system with the controlled temperature, programmable pyrolysis furnace.....	63
Figure 16.	Reproducibility of nitrogen release profile for measurement of GPNP species during the oxidative pyrolysis (at a heating rate of 150° C/min) for aqueous glutamic acid (2.564 µg N/5 µl sample).....	64
Figure 17.	Oxygen has a negligible effect on the gas phase NO _x precursors measured for 2.564 µg/ 5 µl as proline at pyrolysis conditions.....	65
Figure 18.	Gas phase NO _x precursor measurements indicated no significant difference between inert and oxidative pyrolysis conditions.....	66
Figure 19.	Comparison of gas phase NO _x and NO _x precursor total nitrogen measurements with those for pyrolysis conditions.....	67
Figure 20.	Conversion of fuel nitrogen model compounds under pyrolysis conditions for an initial nitrogen concentration of 2.5 µg N/ 5 µl. Nitric oxide (NO _(g)) standard values are presented as a reference for comparison.....	69
Figure 21.	Linear conversion with increasing concentration of proline model fuel nitrogen species under pyrolysis conditions.....	70
Figure 22.	Effect of inorganic species on fuel nitrogen (as glutamic acid) conversion to GPNP nitrogen during pyrolysis at 150° C/min.....	71
Figure 23.	Effect of inorganic concentration on the organic fuel nitrogen (as glutamic acid) conversion to GPNP during pyrolysis at 150° C/min.....	71
Figure 24.	Effect of combined inorganics on the glutamic acid nitrogen conversion to GPNP for pyrolysis at a heating rate of 150° C/min	72
Figure 25.	Nitrogen release profiles for glutamic acid pyrolysis at 150° C/min (2.5° C/sec) to 400° C. Conditions as indicated.....	73
Figure 26.	Nitrogen release profiles for proline pyrolysis at 150° C/min (2.5° C/sec) to 400° C in an aqueous NaCl matrix.....	74
Figure 27.	No significant variation in the total GPNP measured occurs for	

	pyrolytic heating rates of 1–150° C/min.....	77
Figure 28.	Effect of heating rate programs on the nitrogen profiles of glutamic acid during pyrolysis. Program methods are a) 35° C hold for 6 sec, ramp at 50° C/min to 90° C hold for 1 min, ramp at 1° C/min to 400° C. b) 35° C hold for 6 sec, ramp at 50° C/min to 90° C hold for 1.5 min, ramp at 150° C/min to 400° C. c) 35° C hold for 6 sec, ramp at 150° C/min to 400° C, hold for 2.0 min. d) 35° C hold for 6 sec, ramp at 150° C/min to 700° C.....	78
Figure 29.	Total ion chromatogram of proline pyrolysis gas products. Heating rate of 10° C/sec Retention time a) t = 1.9 min and b) t = 2.7 min.....	80
Figure 30.	Mass spectra for proline pyrolysis. a) CO ₂ , retention time t = 1.9 min and b) C ₄ H ₇ N, retention time t = 2.7 min.....	80
Figure 31.	Relative differences in amount and fragmentation of proline pyrolytic species with increased heating rates. Data based on mass spectra obtained for a) peak 1, t = ~1.3 min and b) peak 2, t = ~2.4 min.....	82
Figure 32.	Total ion chromatogram of glutamic acid pyrolysis gas products. Heating rate of 10° C/sec.....	85
Figure 33.	Relative differences in amount and fragmentation of glutamic acid pyrolytic species with increased heating rates. Data based on mass spectra obtained for a) peak 1, t = ~1.6 min and b) peak 2, t = ~2.8 min..	86
Figure 34.	Total ion chromatogram of ammonium sulfate pyrolysis gas products. Heating rate of 10° C/sec.....	87
Figure 35.	Relative differences in amount and fragmentation of (NH ₄) ₂ SO ₄ pyrolytic species with increased heating rates. Data based on mass spectra obtained for a) peak 1, t = ~1.6 min and b) peak 2, t = ~2.2 min..	88
Figure 36.	Proposed pathway for the formation of HCN and NH ₃ from proline fuel nitrogen species.....	90
Figure 37.	Proposed pathway for the formation of NH ₃ and HCN from glutamic acid fuel nitrogen species.....	91
Figure 38.	Schematic diagram for the mass balance for nitrogen recovery determined by combustion of dry black liquor, the dried acid precipitated and the non-precipitated fractions.....	97
Figure 39.	All of the nitrogen can be accounted for in the total nitrogen	

	measurement as indicated here for So. Pine I as determined by mass balance of the liquor fractions.....	97
Figure 40.	Pyrolytic weight loss (expressed on a dry basis) for liquors at temperatures from 300–1000° C in inert N ₂	99
Figure 41.	Profiles as NO for So. Pine I liquor pyrolysis at temperatures from 400–1000° C in inert N ₂	100
Figure 42.	Nitrogen released as NO for liquor pyrolysis at temperatures from 300–1000° C in inert N ₂	101
Figure 43.	Nitrogen remaining in the char for liquor pyrolysis at temperatures from 300–1000° C in inert N ₂	102
Figure 44.	Relationship for percent nitrogen released as NO with respect to the nitrogen remaining in the char from black liquor pyrolysis at 300–1000° C in N ₂ . The (—) represents the pine liquors, (- -) represents all liquors tested.....	103
Figure 45.	Linear relationship for the nitrogen measured from the tryptophan model fuel nitrogen addition to So. Pine III black liquor.....	104
Figure 46.	Inorganic components added to So. Pine III black liquor reduce the nitrogen measured as NO _x and NO _x precursors.....	105
Figure 47.	Relationships for percent nitrogen released as NO during pyrolysis with respect to a) nitrogen, b) sodium, and c) oxygen content in the liquor. Pyrolysis at 600–1000° C in inert N ₂	106
Figure 48.	Relationships for percent nitrogen released as NO during pyrolysis with respect to a) O/N, b) C/N, c) Na/N and d) S/N ratios in the liquor. Pyrolysis at 600 and 800° C in inert N ₂	108
Figure 49.	Relationships for the GPNP measured (%N based on dry liquor solids) during pyrolysis and combustion with respect to the liquor component/liquor nitrogen ratio.....	109
Figure 50.	Gas phase NO _x precursors evolution profile with residence times of a) t = 0, b) t = 230, and c) t = 410. Model fuel nitrogen source was proline.....	112
Figure 51.	Effect of pyrolysis gas residence time on fuel nitrogen conversion to gas phase NO _x precursors during inert pyrolysis at 400° C.....	113

Figure 52.	Effect of residence time on GPNP depletion under static pyrolysis conditions where proline, glutamic acid, and pyrazine fuel nitrogen concentrations of 2.5 $\mu\text{g N/5 } \mu\text{l}$	114
Figure 53.	Effect of gas phase residence time on NO_x precursor depletion under static pyrolysis conditions where proline was the source of fuel nitrogen at the concentrations indicated.....	115
Figure 54.	Test for the first-order reaction of gas phase NO_x precursors, Eq. 22, at 673 K.....	118
Figure 55.	Conversion of gas phase NO_x precursor to N_2 during static pyrolysis is independent of initial concentration. a) 290 sec reaction time. b) 410 sec reaction time.....	120
Figure 56.	Temperature dependency of first-order rate equation.....	121
Figure 57.	Arrhenius plot for determination of activation energy for the conversion of gas phase NO_x precursors.....	122
Figure 59.	Overhead diagram of PCL nitrogen analyzer system components.....	134
Figure 60.	Block diagram for pyrolysis GC/MS.....	136
Figure 61.	Block diagram for the components of the mass selective detector.....	137
Figure 62.	Experimental block diagram for the measurement of NO_x evolved during black liquor pyrolysis.....	140
Figure 63.	Quartz tube reactor for black liquor pyrolysis, CCRG, Åbo Akademi University.....	141
Figure 64.	Block diagram for experimental equipment and data acquisition for the TG-DSC 111.....	143
Figure 65.	Schematic diagram of the TG-DSC 111 calorimeter and microbalance.....	144
Figure 66.	Thermogram regions for enthalpy and weight analysis. Region I = overall decomposition; Region II = glutamic acid decomposition; Region III = tryptophan decomposition.....	147

LIST OF TABLES

Table 1.	Types and chemical structures of coal nitrogen species which have been reported in the literature.....	10
Table 2.	Estimated yields of HCN, % of total fuel nitrogen, as a function of pyrolysis temperature for three coals. Nelson et al. ²⁹	15
Table 3.	Total nitrogen of commercial kraft black liquors by pyrochemiluminescence (PCL), Kjeldahl, and LECO methods. Reported as weight percent of dry solids.....	36
Table 4.	Elemental composition of commercial kraft black liquors reported as weight percent of dry solids.....	39
Table 5.	Experimental design (2 ³ factorial) of initial experiments.....	58
Table 6.	Effect of oxygen concentration on the response counts of 2.564 µg N as proline during pyrolysis.....	65
Table 7.	Identification of proline pyrolysis products determined by mass spectrometry.....	81
Table 8.	Identification of glutamic acid pyrolysis products determined by mass spectrometry.....	85
Table 9.	Identification of ammonium sulfate pyrolysis products determined by mass spectrometry.....	87
Table 10.	Total gas phase NO _x and NO _x precursors measured during pyrolysis at 400° C of liquor fractions. Percent N based on dry solids of each fraction.....	96
Table 11.	Total gas phase NO _x and NO _x precursors measured during total nitrogen measurement of liquor fractions. Percent N based on dry solids of each fraction.....	96
Table 12.	Percent of original liquor nitrogen accounted for by nitrogen remaining in the char or released as NO after pyrolysis at the given temperature.....	102
Table 13.	Concentrations of gas phase NO _x precursors at various reaction times where C _{Ao} = 0.0393 mol/l for T = 673 K.....	119

Table 14.	Percent conversions (Eq. 26) of gas phase NO _x precursors. Concentrations of initial reactant and the product gases are given at reaction times of 290 and 410 sec for 673 K.....	120
Table 15.	Concentration data for temperature dependency determination, C _{Ao} = 0.0366 mol/l.....	121
Table 16.	Operational parameters for the pyrolysis GC/MS experiments.....	139
Table 17.	Operating conditions for TG-DCS 111 screening experiments.....	146
Table 18.	Temperature designations for TG-DSC analysis regions.....	147
Table 19.	Summary of compositional and structural methods on which analyses of the black liquor samples was based.....	148

NOMENCLATURE

A	chemical component of interest
C	heat capacity
C_{Ao}	initial concentration of component A, mol/l
C_A	final concentration of component A, mol/l
C_p	specific heat represented by the power series: $C_p = \alpha + \beta T + \gamma T^2$
D	axial dispersion coefficient, cm^2/sec
D/uL	vessel dispersion number, dimensionless
d	diameter of the reactor, cm
E_a	activation energy for reaction, cal/mol
ΔG°_f	standard Gibbs energy of formation
ΔH°_f	standard enthalpy of formation
H	enthalpy
H_{tr}	enthalpy of phase transition
k	reaction rate constant, mol/cm^3 or sec^{-1}
k_o	pre-exponential constant, frequency factor
K	equilibrium constant
L	length, cm
m	molecular mass of a compound or atom, g/mol, as in mass-to-charge ratio (m/z)
N	normality (equivalents/L)
N_{re}	Reynolds number, dimensionless
r_A	reaction rate for A, $\text{mol}/\text{cm}^3 \cdot \text{sec}$
R	molar gas constant, 1.9872 cal/mol.K
ΔS°_f	standard entropy of formation
S	cross-sectional surface area, cm^2
S	entropy, in Appendix VI
T	temperature, ° C or ° K

T_r	transformation temperature
t	time of reaction, sec
\bar{t}	mean residence time in reactor, L/u , sec
v_o or u	volumetric feed rate, cm^3/sec
ν	kinematic viscosity
V	reactor volume, cm^3
\bar{V}	average velocity, (volumetric flow rate/cross-sectional surface area), cm/sec
X_A	conversion of A defined as $[1 - (C_A/C_{Ao})]$
z	molecular charge, as in mass to charge ratio (m/z)

Greek Symbols

ρ	density of liquid, kg/m^3
μ	fluid viscosity, cP
σ_θ^2	variance in dimensionless time
σ^2	variance of the response curve, sec^2
τ	space time, V/v_o , sec

Abbreviations

AA	atomic absorption spectroscopy
BACT	best available control technology
BLS	black liquor solids
EDTA	ethylenediaminetetraacetic acid
FT-IR	fourier transform infrared spectroscopy
GC/MS	gas chromatography/mass spectrometry
GPNP	gas phase NO _x precursors, NO plus the sum of intermediates such as HCN and NH ₃
IC	ion chromatography
ICP	inductively coupled plasma spectroscopy
ID	internal diameter
NDIR	non-dispersive infrared
NO _x	Nitrogen oxides
PCL	pyrochemiluminescence
ppm	parts per million
ppt	precipitate
RSD	relative standard deviation (standard deviation ÷ average) x 100, %
SD	standard deviation
SAOB	sulfide anti-oxidant buffer
TAPPI	Technical Association of the Pulp and Paper Industry
TG-DSC	thermogravimetric-differential scanning calorimeter

SUMMARY

NO_x emissions resulting from the combustion of black liquor arise from the fuel NO_x mechanism, that is NO_x is formed by oxidation of the chemically bound nitrogen in the fuel. The mechanism is complex and involves numerous reactions. Identification and characterization of many of these reactions has been reported and largely involve HCN and NH_3 intermediate species. However, little information exists on the details of the fuel nitrogen species decomposition to form the fuel NO_x intermediates. Thus, the present work focuses on understanding the formation of fuel NO_x intermediates during pyrolysis of black liquor.

A four-part experimental program was employed to 1) determine the chemical form of nitrogen in black liquor, 2) evaluate the analysis for nitrogen species in a total nitrogen measurement, 3) study pyrolysis with respect to the black liquor composition and operational parameters, and 4) provide an understanding of the formation processes through the formation pathway and depletion kinetics involved.

Black liquor nitrogen was found to be predominantly organic with the nitrogen bound in heterocyclic rings, both five- and six-member, and in straight-chain amines. Multiple species were present with individual compounds below the analytical detection limit for individual species making up 79% of the total organic nitrogen. The nitrogen was primarily associated with the acid-insoluble fraction of the liquor, which contains

predominantly larger molecular weight organic compounds. Little nitrogen was associated with the acid-soluble liquor fraction. Thus, emphasis was placed on nitrogen bound in organic compounds. The types of nitrogen identified in the liquors varied between and within the tree species from which the liquor was generated. Multiple forms of nitrogen suggest various pathways for NO_x formation during black liquor combustion. Model compounds were selected based on the black liquor nitrogen characterization and were used to evaluate the conversion for the total nitrogen measurement and to study nitrogen conversion to NO_x or NO_x precursors during pyrolysis.

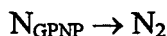
The fuel nitrogen recovery for the analytical measurement varied from 35–91% (by weight) of the original fuel nitrogen content depending on the nitrogen species chemical structure. The nitrogen chemistry proved to be more important as compared with the kinetics and thermodynamics of the experimental system. The fractional recovery of the inorganic fuel nitrogen did not change for nitrate- and ammonium-type species regardless of the compound from which the nitrogen evolved. The organic forms of nitrogen, amines and heterocyclic compounds, varied with respect to their individual bonds and structures. The variation observed indicates that intermediate reactions that lead to both N_2 and NO_x are important in understanding the overall formation of fuel NO_x .

The addition of alkali, as Na_2CO_3 and NaOH , to aqueous solutions of organic fuel nitrogen model compounds decreased the fuel nitrogen recovery by ~10%. Increased inorganic concentrations further decreased the recovery. No effect was observed for Na_2SO_4 . It is theorized that sodium carbonate decomposed and sodium hydroxide vaporized at the reaction temperature of 1100° C such that sodium species entered the gas

phase allowing reactions to occur which deplete NO_x and the NO_x precursors. Sodium sulfate does not enter the gas phase at these temperatures and had no effect. An opposite result was found for inorganic fuel nitrogen as NH_4Cl . As the Na_2CO_3 concentration, i.e. the alkali concentration, in solution increased, more NH_3 was driven into the gas phase to be detected.

Pyrolysis was assumed to initially evolve a series of gas phase NO_x precursors termed GPNP. These are the sum of all gas phase nitrogen intermediates that eventually lead to NO_x or N_2 . The oxygen concentration (0–22% O_2) did not affect the total nitrogen released. The pyrolysis heating rate employed also had little effect on the total nitrogen released at 1–150° C/min or on the gas phase composition at rates from 10–1000° C/sec. Potential pathways have been provided for fuel nitrogen conversion for pyrolysis conditions which form the HCN and NH_i intermediate species. These pathways offer further insight into the otherwise limited information for this portion of the fuel NO_x formation mechanism.

The depletion of the GPNP species to form N_2 was investigated kinetically and found to follow a first-order homogeneous irreversible gas phase reaction:



The activation energy for an assumed first-order reaction was found to be 850 cal/mol indicating a low temperature sensitivity. The low activation energy is suggestive of radical or catalytic reactions occurring in the depletion process.

The knowledge gained for the effects of fuel composition on the fuel nitrogen conversion provide a greater understanding to the overall fuel NO_x mechanism and is applicable to general stationary combustion processes and specifically to the combustion of black liquor during recovery boiler operations. Both individual nitrogen species and the related inorganic matrix have an effect of NO_x generation. Conditions that provide time for the GPNP species to react prior to oxidation may lead to lower NO_x emissions.

INTRODUCTION

The formation of NO_x from the combustion of black liquor is an important problem in the pulp and paper industry. With continued tightening of allowable air emission levels, it becomes increasingly more important to understand the source of the emission in order to minimize its generation. The emissions of nitrogen oxides (NO , NO_2 , and N_2O) are regulated by the 1990 Clean Air Act Amendments. Current allowable emissions are based on site-specific best available control technologies (BACT) and on the region within which the mill resides. Most regulated levels are approaching 100 ppm NO_x , but for some mills in heavily restricted areas, the allowable limits have dropped to as low as 50 ppm NO_x .¹ An understanding of the source of NO_x and the conditions under which it is generated is desirable for control of NO_x emissions that the pulp and paper industry faces.

Control of NO_x emissions in the recovery furnace flue gas has become an important environmental concern affecting the operation of recovery boilers. The choice of control options for effective and practical reduction is affected by the major source of NO_x . Many general NO_x control strategies employed in combustion processes are based on control of thermal NO_x and involve minimization of one or more combustion parameters such as residence time, free oxygen, and flame temperature. Techniques employed include biased firing, off-stoichiometric combustion, and low excess air firing. These methods have been employed for NO_x reduction during black liquor combustion where the principle source of NO_x is fuel nitrogen.

Studies at the IPST and elsewhere have shown that fuel NO_x is the major source of NO_x emissions during recovery furnace operations.²⁻⁵ Fuel NO_x formation is dependent upon the black liquor nitrogen content and upon the excess air. A need exists to better understand recovery furnace fuel NO_x so that appropriate control measures can be taken.

Little knowledge exists on the fundamental understanding of NO_x generation during the combustion of black liquor. Some information on NO_x formation processes can be obtained by analogies with the knowledge gained from fundamental studies of other combustion fuels, particularly coal. During coal combustion, the formation of NO_x is dominated by fuel NO_x .⁶

Knowledge of the formation mechanisms, fuel nitrogen conversion, and evolution rates during coal combustion is reviewed as a basis for investigations into the fuel nitrogen release which occurs during black liquor combustion. The current state of knowledge for NO_x formation, depletion, and control during the operation of kraft recovery boilers is also reviewed.

BLACK LIQUOR COMBUSTION

The fundamental combustion processes occurring in kraft black liquor recovery furnaces have traditionally been separated into several steps which apply to both in-flight and char bed combustion. As the liquor (drops of about 1.5 mm average diameter) is sprayed into the furnace, it undergoes drying, pyrolysis, and char burning.⁷ The nature of the combustion environment is such that overlap of stages occurs for single drops as well as on the bed.

Combustion of liquor drops begins with drying. The drop temperature raises to the boiling point where water is evaporated. As the drop or particle continues to increase in temperature, pyrolysis occurs. During pyrolysis, the volatile nitrogen species are released along with the organic compounds which are broken down to yield a volatile gas phase consisting of CO_2 , CO , H_2 , H_2O , light hydrocarbons, tars, H_2S , and some mercaptans.⁸ The volatiles mix and react with O_2 in the combustion air. The residual solid or char contains about one-half of the initial carbon, essentially all of the inorganic compounds, and very little hydrogen and oxygen.

Pyrolysis

The partially dried and slightly swollen drop begins pyrolysis at temperatures above 150°C . Further drop swelling and flame formation mark the initiation of the volatiles release and their gas phase combustion. The particle temperature very rapidly rises during the pyrolysis phase which is short lasting only 0.5–1 second. The drop temperature increases linearly with time.⁷ Pyrolysis and volatiles burning may occur up to temperatures of $> 1000^\circ\text{C}$.

During pyrolysis, the volatile yield is affected by the heating rate and the temperature level.⁸ Particle size becomes important with respect to heating rates. Smaller particles tend to heat up faster, and therefore, release volatiles more quickly than larger particles. The fixed carbon remaining at the end of pyrolysis is responsible for 6–20% of the original black liquor solids and the inorganic material may be 40% of the original solids.⁸ This makes up the material which then begins “char burning.” Burning may occur

over 1–6 seconds, depending on the initial particle size. For such conditions, 2 mm particles experience heating rates in excess of 300° C/s. Black liquor solids are typically > 62% on a wet solids basis. The organic and the volatile content at furnace conditions is expected to be in the range of 42–56% on a dry solids basis.⁸ At the end of char burning, the residue consists primarily of sodium sulfide and sodium carbonate.⁷

NO_x FORMATION MECHANISMS

The major constituent of NO_x is nitric oxide, NO, with only a small portion of the NO_x emission made up of N₂O or the further oxidized species nitrogen dioxide, NO₂. Because of this, review of NO_x formation mechanisms will primarily include the work leading to the formation of NO species. Also, because of the NO dominance, the term is used synonymously with NO_x.

The literature considers three NO_x formation mechanisms. These are thermal NO_x, fuel NO_x, and prompt NO_x. These are based on NO as the major constituent. Thermal NO_x formation, the oxidation of atmospheric nitrogen, N₂, at high temperatures, is thought to be the primary mechanism for NO_x formation in the combustion of natural gas or oil where the fuel nitrogen content is negligibly low and the combustion temperatures are very high. Fuel NO_x, oxidation of the nitrogen in the fuel, is the major contributor to the total NO_x emissions for coal combustion. The portion of NO_x created via prompt NO_x, the formation resulting from reaction of N₂ with hydrocarbons with subsequent oxidation, is considered to be negligible in most practical combustion systems. The relative amounts of each, though, depend on the fuel composition and the combustion conditions. Each of

these mechanisms was developed from studies in flame and fossil fuel combustion.⁹⁻¹² The fuel NO mechanism, which is the primary source of NO_x emissions from recovery furnace operations,²⁻⁵ is of interest here and is reviewed in more detail below. Thermal NO_x and prompt NO_x will not be considered further.

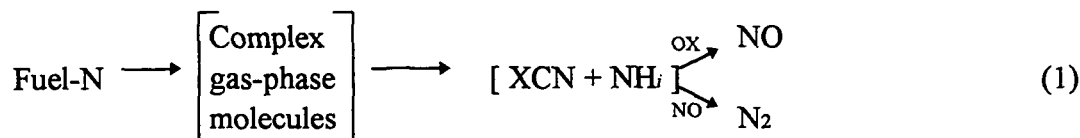
Fuel NO

The basic fuel NO_x mechanism results from coal combustion research. Fuel NO_x results from the oxidation of the fuel nitrogen during combustion. In liquid fossil fuels and pulverized coal, where the nitrogen content ranges from 0.5–2.0%¹³ and averages about 0.8% on a dry weight basis, the principal source of NO_x emissions generally is fuel nitrogen oxidation.¹²

The fuel NO_x formation mechanism has been investigated by many researchers, but the details of NO_x formation from fuel nitrogen remain unclear. Numerous reactions are believed to be involved with the conversion of fuel nitrogen to NO_x species. Several summaries of the current knowledge of the fuel NO_x mechanism for coal combustion are available.^{12, 14} On a very simplified level, the nitrogen content in the fuel can be thought to evolve through intermediates, hydrogen cyanide (HCN) and amine-type species (NH_i), which can then be oxidized to NO. A key side reaction is the practically irreversible reaction of NO with other nitrogen radicals, such as the NH_i species, that leads to N₂. Further discussion of the NO_x depletion reactions is given starting on page 18. Much detail is known of the gas phase reactions of the CN and NH_i nitrogen species to form

NO_x , yet little is known of the fuel nitrogen reactions which occur to produce the NO_x intermediates.

The fuel NO_x pathway could be accurately represented if the intermediates HCN and NH_3 were treated in parallel as the sum of $\text{XCN} + \text{NH}_i$ intermediates (Eq. 1).



Both cyanide and ammonia forms have been reported to be evolved initially from coal combustion.¹³⁻¹⁵ The identities of XCN , NH_i and OX species have not been exactly determined because of difficulty measuring intermediate and radical species during combustion processes. However, the OH radical has been suggested as a potential OX species,¹² HCN, NCO, HCNO, and CN have been suggested for XCN , and N, NH, NH_2 , and NH_3 have been indicated for the NH_i intermediates by many researchers.¹⁶⁻¹⁸ Likewise, the intermediate or transition species for the reaction pathway of the fuel nitrogen compounds to arrive at the HCN or NH_i intermediates are not fully known.

The fuel NO_x pathway in coal combustion, where the fuel nitrogen species are primarily heterocycles, upon volatilization, release HCN as the dominant species with minor formation of the NH_3 intermediate. For example, in a coal with a nitrogen content of 1.17%, about 20-30% of the fuel nitrogen was converted to HCN and about 8-10% was converted to NH_3 .¹⁹ However, both forms have been noted as the initial intermediate formed.¹³⁻¹⁵ This is discussed further in the section "Effect of Fuel Nitrogen Chemical

In pulverized coal studies, the total NO_x consisted primarily of fuel NO .¹⁵ It was noted that NH_3 appeared to be the first fuel nitrogen species evolved during early combustion. The need to know more of the intermediate nitrogen pyrolysis species was stressed in light of not being able to determine if devolatilization of nitrogen is only a function of temperature and if the evolved nitrogen species were the same for varying stoichiometric ratios for varying coals. More detail of these effects, specifically, the effect of the nitrogen content, the fuel nitrogen chemical structure, and the temperature and heating rate, on the formation of NO_x and NO_x precursors are discussed below.

Effect of Nitrogen Content on Conversion

The fractional conversion of fuel nitrogen to NO_x , with respect to the total nitrogen content of several coals during combustion, was determined in a study by Chen et al.²² The fuels ranged from 0.68 to 2.5% nitrogen and a correlation was found that reflected the trend of decreasing fuel nitrogen conversion with increasing fuel nitrogen content (i.e. conversion to NO is inversely related to $[\text{N}]$). Also, NO_x emissions were higher for those coals which exhibited a higher volatile nitrogen release as compared with the coals where more nitrogen was retained in the char or solid phase.

The general trend of increasing conversion to NO_x with decreasing fuel nitrogen concentration should not be confused with the general trend of increasing total NO_x generation with increasing fuel nitrogen concentration. At low concentrations of fuel nitrogen, relatively large conversion to NO_x is observed, but the total NO_x evolved is limited by the low initial fuel nitrogen concentration. As the fuel nitrogen concentration

increases, the actual conversion to NO_x decreases (due to the increased reactions of the intermediates with NO_x forming N_2), but the overall NO_x generation increases because of the much larger amount of fuel nitrogen available for conversion. These general relationships have been noted in many studies.^{6, 12, 16, 22}

Pershing and Wendt⁶ examined the influences on the percent conversion of fuel nitrogen in four different coals and one coal char during combustion. Fuel NO was found to contribute to greater than 75% of the total NO emissions under all conditions investigated in a laboratory combustor. The fuel nitrogen conversion to NO was 12–16% for coal char, whereas the conversion was 28% for coal with the same nitrogen content combusted under the same conditions. This suggested that fuel NO formation cannot be related solely to the fuel nitrogen content, but it must also be related to how it is bound in the coal or char. There is a possibility of the fuel nitrogen to remain in the char, but only gas phase reactions are of interest in this work. Therefore, char nitrogen pathways are not considered.

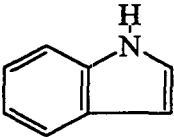
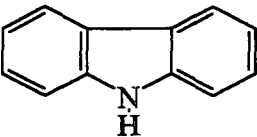
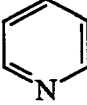
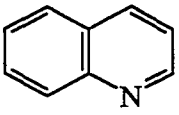
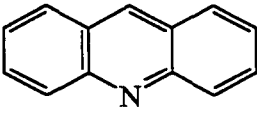
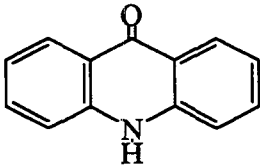
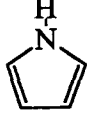
Effect of Fuel Nitrogen Chemical Structure

The chemical form of fuel nitrogen is important in the conversion to NO_x because the NO_x intermediates, HCN and NH_i , tend to convert to NO in different proportions. Coal nitrogen structures have been observed in various heterocyclic forms. The types and chemical structures are summarized in Table 1. The individual compounds can be classified into the larger groups of five-member rings, pyrrole structures, and six-member rings, pyridine structures. Typical compositions may be in the range of 50–60% of the

coal nitrogen as pyridinic type compounds and about 25–40% as pyrrolic compounds.¹³

The remaining portion can be made up of amines and anilines.²³ Specific formation of NO_x and its HCN and NH_3 precursors from these fuel nitrogen structures are discussed below and in the “Fuel NO_x Formation Pathways From Coal Nitrogen” to provide some insight into their relationship to NO_x formation.

Table 1. Types and chemical structures of coal nitrogen species which have been reported in the literature.

Type of Nitrogen Compound	Chemical Structure	Reference
Indole		23, 24
Carbazole		23-26
Pyridine		13, 23-25, 27
Quinoline		23-25, 27
Benzoquinoline or Acridine		26, 27
Acridone		23, 27
Pyrrole		13, 23, 25, 26

release is from the ring structure as a whole entity, i.e. without experiencing any structural change in the heterocyclic ring. At the higher temperatures, the rings could be broken and the nitrogen species of HCN and NH_3 were then observed.

In a determination of the fuel nitrogen release rates during rapid pyrolysis, Nelson et al.²⁹ reported the predominant NO_x precursors to be HCN and NH_3 as indicated by FT-IR. The release rates of HCN were found to be significantly different for different coals and were found to coincide with the difference in the nitrogen composition. The fuel nitrogen species were found as heterocyclic ring structures with the thermal stability of the six-member pyridine-type species being greater than that of the five-member pyrrole-type species. The thermal stability difference was exemplified in the more rapid formation of the HCN intermediate species from the coals with a higher percentage of the fuel nitrogen bound in the pyrrole-type ring structures. The proposed pathways for fuel NO_x intermediate formation from coal nitrogen as identified in the literature are discussed in the following section.

Fuel NO_x Formation Pathways From Coal Nitrogen

Hydrogen cyanide is expected as the major NO_x intermediate from heterocyclic coal nitrogen. However, both HCN and NH_3 species have been observed as the initial intermediates in the formation of NO_x from coal combustion. Reaction pathways have been presented in the literature to account for the formation of both species from the predominately heterocyclic coal nitrogen.

Nagai and Masunaga offered pathways for the carbazole and acridine type structures to yield NH_3 as an intermediate.³⁰ In both cases, they proposed that the loss of the nitrogen species as NH_3 did not occur until after ring saturation was achieved as indicated in Fig. 2.

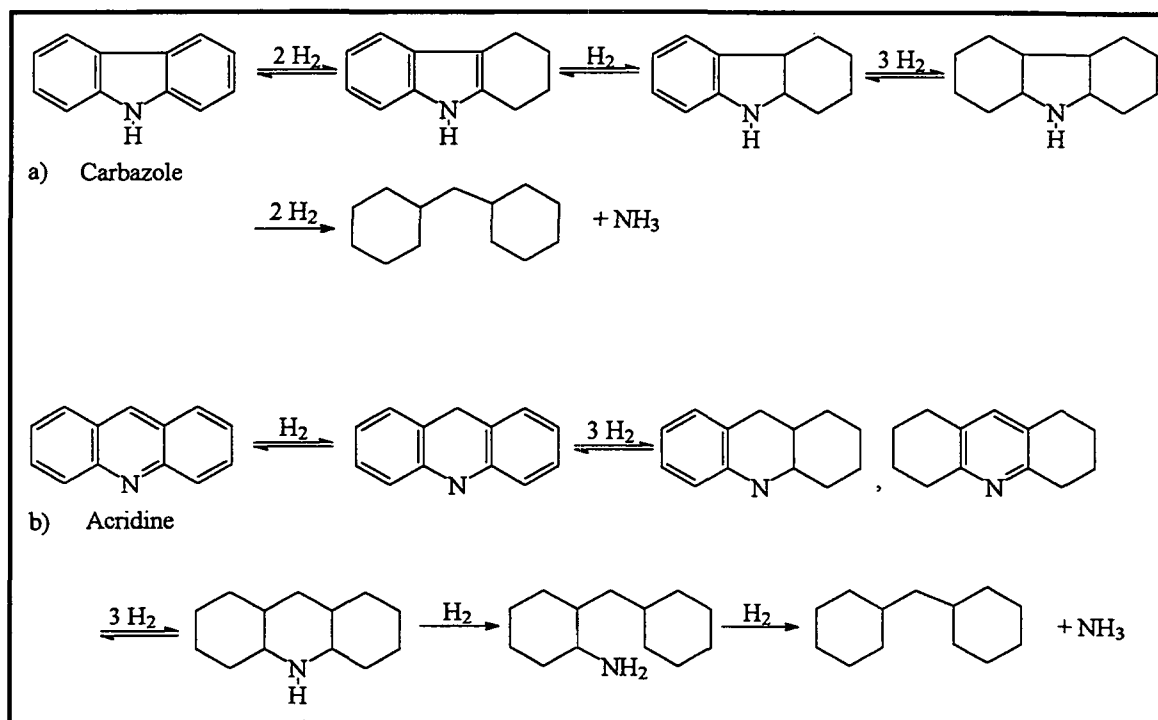


Figure 2. Proposed reaction pathways for coal nitrogen as a) carbazole and b) acridine to form NO_x intermediate NH_3 .³⁰

The formation of HCN as well as NH_i intermediates from pyridine has been proposed to occur through ring cleavage at the C-N bond.^{31, 32} As such, the formation of the CN and NH radical species results from the subsequent cleavage of the ruptured ring. This shown in Fig. 3 below.

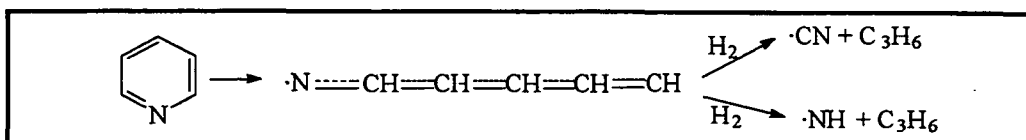


Figure 3. Formation of HCN and NH_i from pyridinic ring rupture.^{31, 32}

Fast exchange reactions involving attack of the CH and NH radicals by an O-atom lead to the formation of NO.³² It should be noted that the reaction pathways indicated above have only been hypothesized as the species involved are difficult to measure. The chemistry of NO_x intermediate formation from coal nitrogen is complex and is not completely understood. However, the pathways do suggest that both CN and NH species can be formed from the heterocyclic nitrogen compounds in the coal even though the cyanide species dominates (as much as 85% of the intermediate concentration in some cases).¹⁸ It also provides some indication as to the possible reactions which may occur during the formation of NO_x from black liquor nitrogen.

Effect of Temperature/Heating Rate

Nitrogen in coal was found to evolve late in the volatilization sequence.¹⁸ As such, the nitrogen release was initiated after the total mass release started. The nitrogen release was found to increase more as compared with the total coal mass release over a specified temperature range.¹⁸ This indicates that the fraction of nitrogen volatilized would likely increase with increases in the pyrolysis temperature. It was observed that HCN and NH₃ in the low molecular weight gases accounted for less than half of the nitrogen evolved toward the end of pyrolysis.¹⁸ This suggests the remaining amount of the evolved nitrogen to be other low molecular weight species such as N₂, NO_x, or NH_i intermediates. At higher pyrolysis temperatures, more intermediate species HCN and NH_i are present. Therefore, gas phase reactions which lead to N₂ were more likely reducing the overall conversion of the volatilized nitrogen to NO_x. The depletion reactions which occur with NH_i and NO_x are discussed in greater detail starting on page 18.

Temperature dependency of the conversion of bound nitrogen to NO_x was noted in fluidized bed coal combustion.³³ The bound nitrogen released during coal devolatilization yielded negligible amounts of NO_x until the temperature reached about 700° C. As the temperature was increased to about 900° C, the fuel-bound nitrogen accounted for two-thirds of the total NO_x observed.

Pohl and Sarofim³⁴ studied the pyrolysis of nitrogen in coal at temperatures in the range of 700–1800° C to examine the conversion of the bound nitrogen in the volatiles and char to NO_x . It was found that the nitrogen release paralleled that for the total volatiles after 10–15% of the coal had been devolatilized. The time of nitrogen and total volatiles release was found to be dependent on the coal composition.

Nelson et al.²⁹ reported the yield of HCN as a function of temperature. As observed in Table 2, HCN increased significantly for temperatures in the 700–800° C range. The source of the HCN was suggested to be from the secondary decomposition of the volatile fuel nitrogen species. These species were detected at lower temperatures and most likely come from the less thermally stable pyrrole-type species.

Table 2. Estimated yields of HCN, % of total fuel nitrogen, as a function of pyrolysis temperature for three coals. Nelson et al.²⁹

Coal #	500° C	600° C	700° C	800° C	900° C	1000° C	1025° C
1	0.1	0.9	2.2	4.3	5.5	9.2	6.0
2	--	--	1.0	3.8	7.6	9.3	10.0
3	0.3	0.7	2.3	7.0	9.8	12.0	--

While about 10% of the total fuel nitrogen was observed as HCN, a significant amount of NH_3 (< 5%) was also observed at temperatures greater than 700° C. Mackie,

et al. noted that the decomposition products of heterocyclic ring structures of aromatic compounds typically did not include significant amounts of NH_3 ,³⁵ therefore, it was suggested that other functional groups in coal, such as amines, are responsible for the NH_3 observed as a pyrolysis product. The possible formation of NH_3 from heterocyclic structures has been shown previously in Figs. 2 and 3.

A study of the evolution and reaction of the fuel nitrogen during pyrolysis and combustion of pulverized coal was conducted by Haussman and Kruger.³⁶ At heating rates typical of pulverized coal combustion, approximately 10^5 °C/sec, it was observed that the initiation of the fuel nitrogen release was slower than the initiation of the total mass release by 23%. The initial lag in the nitrogen release as compared with total mass release was also noted by Pohl and Sarofim.³⁴ However, the subsequent nitrogen release occurred faster than that for the total mass.

The rate of nitrogen release was thought to be a function of how the fuel nitrogen was bound in the coal. The lag period was thought to be characteristic of fuel nitrogen bound in the more stable heterocyclic ring, while the overall mass release was due to the decomposition of the peripheral groups or side chains.³⁶ Variations of the mass-nitrogen release ratio are observed with different coals suggesting that the nitrogen content in the volatiles and that in char varies. High heating rates were found to increase the amount of nitrogen that was found in the char residue due to shorter exposure time to the higher temperatures.

In pulverized coal combustion, the NO_x formation rate is greatest during the heterogeneous and/or homogeneous gas phase reactions where the volatile nitrogen is rapidly consumed.³⁷ The NO_x formation is largely due to oxidation of the volatile nitrogen. The conversion of fuel nitrogen to NO_x was found to increase slightly with the flame temperature, to decrease slightly with the coal nitrogen content, and to increase with the volatile content in the coal in the experimental excess oxygen conditions.³⁸

Pohl and Sarofim³⁴ found the nitrogen evolution during the early stages of coal combustion to be kinetically controlled based on knowledge of the nitrogen structure in coal and of the coal-nitrogen release mechanism. They theorized a coal nitrogen release pathway based on the coal nitrogen to be primarily heterocyclic where the primary nitrogen pyrolysis products would be HCN. They postulated that, during early stages of coal pyrolysis, volatiles are formed from the release of side chains and aliphatic links. As the aromatic rings decompose, some nitrogen is released. Likewise, Diels-Alder type secondary condensation reactions occur to form multiple ring structures where the nitrogen could be incorporated into side chains or into the multiring structure. The amount of nitrogen remaining in the char was a function of the time-temperature history of the char.

In summary, a portion of the fuel nitrogen is released into the gas phase and a portion stays in the char residue during coal combustion. The nitrogen that is released forms HCN and NH_i type intermediates based largely on the coal nitrogen structure. Heterocyclic species tend to form predominantly HCN intermediates but some NH_i has been observed in some cases. Amine type species are thought to yield predominantly NH_i

intermediates. The amount of a given intermediate is also thought to be dependent on the temperature and thermal stability of the fuel nitrogen compound. For example, pyrrole would have a higher intermediate yield than pyridine at low temperatures because pyridine is more thermally stable. Likewise, the conversion of the intermediates to NO_x appears to be dependent on the relative concentration of the intermediates, in particular the NH_i species, in the gas phase. Reactions of NH_i with NO_x can occur to deplete the NO_x that is formed. This is discussed further below.

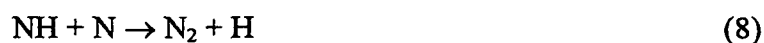
NO_x DEPLETION REACTIONS

NO_x depletion reactions are important for a complete understanding of the NO_x formation chemistry. Reactions of NO_x with other nitrogen gas phase species have been identified in Eq. 1 as a means to reduce the NO_x formed. Selective reduction of NO in the combustion gases by reaction with an injected amine type species has been demonstrated in experimental studies. Ammonia has been employed such that the reduction occurs entirely in the gas phase. The reduction can also occur on the surface of a catalyst. Chen et al.³⁹ used four selective reducing agents (ammonia, urea, cyanuric acid, and ammonium sulfate) to reduce fuel NO_x formation in fuel-lean combustion. Very high NO_x reduction levels were achieved with the addition of these agents into the fuel-rich zone of a staged combustion environment. The greatest efficiency in NO_x reduction could be obtained by combining the addition of a selective reducing agent with combustion modification. The reduction of NO to N_2 in the presence of NH_3 may potentially occur by the following series of reactions,^{12, 39}





Other reactions of the NH_i intermediates which can occur are given in the following equations.^{14, 40}



Depletion of NO_x during combustion has been indicated to also occur by other mechanisms. Reactions of the CN and NH_i intermediates with bound hydrogen atoms leading to HCN and NH_3 formation, reduction to N_2 by char carbon and carbon monoxide, and other gas phase reactions between nitrogen species reduce the NO_x emissions observed. Detailed mechanisms for the heterogeneous reduction of NO_x on bound carbon atoms were proposed by De Soete.⁴¹ Reactions with hydrocarbons which deplete NO_x formation were also found to be significant.^{39, 42, 44}

In a study by Furusawa et al.,⁴⁴ the NO reduction by char and carbon monoxide was investigated in fluidized-bed coal combustion. It was observed that the carbon dioxide produced during combustion coincided with the nitric oxide consumed. The overall reaction pathway was suggested to be the following catalytic reaction:



The char was considered to provide a catalytically active surface for the NO_x depletion reaction. In this scenario, char carbon was not consumed. However, NO was also found to be depleted by carbon-consuming reactions. At lower temperatures, NO_x depletion may be described by reactions 10 and 11. At higher temperatures, depletion is also possible by reaction 10 followed by reaction 12.



The C_f represents a free active site carbon atom, while C(O) represents carbon with a chemisorbed oxygen at the char surface. It was found that the NO_x reduction increased with temperature over the lower range in the presence of CO, H, and O. The reduction rate was enhanced by eliminating the oxide complexes at the char surface. This implies the reaction in Eq. 10 to be the important step. The depletion processes are important because they can occur simultaneous to the formation processes. As such, depletion is important to the formation processes.

NO_x FORMATION DURING KRAFT RECOVERY BOILER OPERATION

NO_x formation from recovery boiler operations is inherently lower than that from coal combustion processes because the nitrogen content in black liquor (0.1% N on average)² is much lower than that of coal (0.8% N on average).¹² The fact that the combustion air is introduced in stages in recovery boilers also provides built-in opportunities for lower NO_x emissions.

Nitrogen oxide emissions in recovery furnace flue gases were first investigated in the early seventies by Galeano and co-workers^{45, 46}. They looked at the effects of furnace operating conditions, including temperature, gaseous residence time, and air input characteristics. Low nitrogen oxide emissions were measured. Grab samples were found to average 10 ppm, with the maximum value at 50 ppm (by volume). Galeano et al.⁴⁵ concluded that the off-stoichiometric combustion methods employed in black liquor combustion typically kept NO_x emission levels very low. In the second study,⁴⁶ NO_x emissions averaged 32 ppm over a range of 0–53 ppm at combustion temperatures of 1010–1230° C.

A more detailed investigation into the emission of NO_x from kraft recovery furnaces was reported by NCASI in 1979.⁴⁷ At the time of the study, it was believed that NO_x emissions were dependent upon the combustion temperature, “instantaneous flame temperature,” the fuel-bound nitrogen, and the combustion furnace operational parameters. In the report, the NO_x emission rates from six boilers were examined along with the operating and design characteristics of each boiler. A correlation ($R^2 = 0.85$) was found to exist between the black liquor solids fired and the NO_x emission rate. Reported NO_x emissions averaged 43.8 ppm with a range of 26.3–70.9 ppm for all furnaces. At the time of the study, regulations of NO_x emissions for kraft recovery furnaces were nonexistent. However, the emission levels reported were one-third to one-half of that specified for fossil fuel-fired steam generators for that time.

NO_x emission levels did not receive industry attention until 1986, when all new permits had NO_x limits.⁴⁸ NO_x limits were established based on individual furnace capabilities and evaluation of the best available control technology (BACT). Methods to control or reduce NO_x levels have been investigated to effectively meet air quality permits. In most cases, proper combustion control is the BACT for individual recovery furnace operation.⁴⁹ Increased bed temperature and a large excess of combustion air have been shown to increase NO_x emissions,⁵⁰ but the variables which control the formation of NO_x in the combustion of black liquor are not very well understood.

Increasing liquor solids from 65% to 77–78% was reported to increase NO_x emissions from 95 ppm to an average of 133 ppm with a maximum emission level of 155 ppm.⁵¹ The emission levels were lowered from 150 to 120 ppm by reducing the combustion air temperatures, but the steam production rate was also reduced. Higher bed temperatures and a slight increase in NO_x emissions, resulting from a 23% increase in liquor solids, were reported by Barsin et al.⁵² High solids (75% +) firing technology employed by S. D. Warren Company left it difficult to meet the 77 ppm NO_x limits with bed temperatures of 1040° F.⁵³ The increase in NO_x levels with higher solids firing (80% solids) was also noted by Netherton and Osborne.⁵⁴ However, the increases in NO_x with increased black liquor solids have not been noted for all recovery boilers.⁵⁵

Note that the reported recovery boiler NO_x values cover a period of nearly twenty years and that NO_x values appear to be increasing with time. There are likely two reasons. First, the process operating conditions have changed significantly over this period of time and may account for the increase in the values. Second, the method for measurement of

NO_x has improved significantly. Lower detection limits can be achieved with greater accuracy. A combination of these two items provides some explanation for the apparent increase observed.

The primary mechanism of NO_x formation from black liquor combustion is fuel NO_x formation.²⁻⁴ Fuel NO_x formation is characterized by the fractional conversion of black liquor nitrogen to NO_x and is dependent on the fuel nitrogen content and the oxygen concentration. Until recently, little data have been reported for black liquor nitrogen conversion. Brännland et al.⁵⁶ reported 5% or less of the nitrogen in “Prenox” nitrate to be converted to NO_x emissions. However, the chemical form of nitrogen in black liquor is thought to be primarily proteinaceous with only very small amounts of nitrate present. Therefore, the nitrate conversion was likely not representative of the actual black liquor nitrogen conversion.²

A review of black liquors’ nitrogen content indicated the range to be between 0.05–0.24% nitrogen (based on dry liquor solids) with the average being 0.1%.² This is much lower than the 0.8% average for coals.¹² Nichols et al.² pointed out that if 20% of the fuel nitrogen converted to NO_x, emission levels would be in the range of 25–120 ppm (at 8% O₂) for black liquor combustion and this could account for recovery furnace NO_x emissions. Partial responsibility for the low conversion may be accounted for with NO_x depletion reactions which also can occur. NO_x depletion in the presence of molten sodium carbonate and sodium carbonate/sodium sulfide mixtures has been verified.⁵⁷ A reduction in the NO_x measured was also observed in the presence of fume species and CO.⁵⁸ Only a 5% reduction was attained with 5000 ppm of CO over a fixed bed of Na₂SO₄ at 750° C.

A reduction of 0–40% over the temperature range of 550–750° C was achieved with a fixed bed of presintered Na_2CO_3 with 5000 ppm CO present. No reduction was observed in the absence of the reducing agent, CO.

The importance of fuel NO_x in black liquor combustion was tested using both an industrial black liquor and a synthetic liquor.⁴ The contribution of thermal NO_x was eliminated by using a mixture of 21% oxygen in argon. At 65% solids, an average of 50 ppm NO_x was measured during combustion. The same NO_x levels were measured as when air was used and thus, shows no thermal NO_x to be generated. This study also indicated that fuel nitrogen release and subsequent NO_x formation occurred during both devolatilization and char burning. The percent conversion was found to increase as the fuel nitrogen decreased in the liquor. This correlation, increasing fuel nitrogen conversion to NO_x with decreasing initial fuel nitrogen content, is similar to the fuel nitrogen conversion behavior in coal combustion.¹²

In general, the highest percent conversion to NO_x occurs for fuels with the lowest nitrogen content. With 0.1% nitrogen in the fuel, a percentage similar to that of black liquors, conversion of fuel nitrogen to NO_x are reported over a range of 20–80% for various fossil fuels depending on the fuel type. Nichols et al. reported the black liquor nitrogen conversion to NO_x to be 28% in a pilot combustor and 35% in a tube furnace.⁴ These conversions are higher than other conversions reported in the literature. Aho et al. reported conversions to NO_x to be < 10%⁵ and Iisa et al reported conversions to NO_x at < 24%.⁵⁸ The black liquor conversions are also much lower than the conversion to NO_x

observed for coal combustion at equivalent fuel nitrogen concentrations. The differences are shown in Fig. 4.

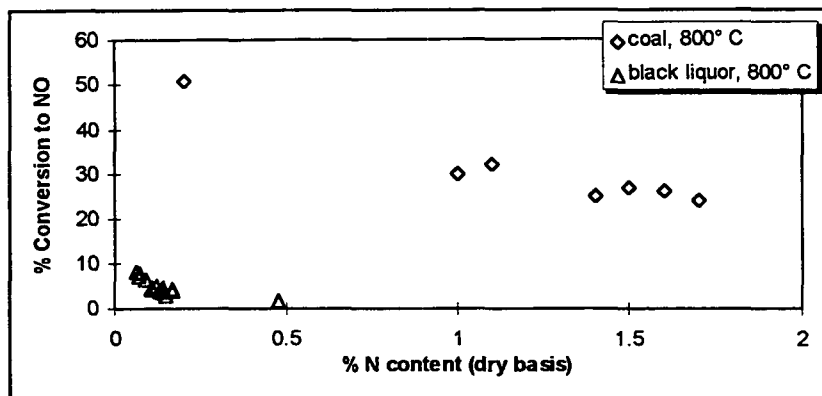


Figure 4. Percent conversion of fuel nitrogen to NO for coal²³ (◊) is about 10 times greater than for equivalent nitrogen concentrations of nitrogen in black liquor⁵ (Δ).

Percent conversion of fuel nitrogen to NO_x or NO_x intermediates from a series of black liquors has been reported for pyrolysis^{5,59} and char combustion conditions in a laboratory.⁵⁹ Black liquor pyrolysis results indicated 20–60% of the fuel nitrogen to be released with the dominant gas phase species being NH₃ (10–30% of original black liquor nitrogen).⁵ Only small amounts, 1–2%, were observed directly as NO. The remaining volatilized nitrogen was assumed to be N₂. It was also observed that the amount of nitrogen released as gas phase NO_x or precursors (GPNP), which is the sum of NO plus the oxidizable intermediate species such as HCN and NH₃, increased with increasing black liquor nitrogen content.

Similar results were reported by Forssén et al⁵⁹ during volatilization. About 35% of the liquor nitrogen was measured as GPNP, 30% of the nitrogen was found in the char, and the remaining 35% was assumed to be N₂. Combustion of the remaining char

produced NO as the major species representing about 15–20% of the original nitrogen. Char nitrogen was noted to have a greater tendency to produce NO from combustion as compared to the pyrolysis of black liquor drops.⁶⁰ Because only 30% of the original liquor nitrogen remained in the char (i.e. a lower nitrogen content), char nitrogen conversion to NO was higher.

Forssén et al. also suggested that some of the char nitrogen may be released as N₂ and some may enter the smelt stream.⁵⁹ It was further postulated that the smelt could in turn release some NO_x or N₂, and finally a portion would enter the green liquor stream. While no experimental data were collected for this postulation, NH₃ emissions have been noted at the smelt spouts,⁶¹ and nitrogen has been measured in the green liquor, green liquor dregs, and in the slaker grits.⁶²

NITROGEN IN BLACK LIQUOR

The potential nitrogen species in black liquor have been reviewed by Veverka et al.³ in an effort to better understand the source of fuel nitrogen leading to NO_x emissions in the recovery furnace flue gas. The black liquor nitrogen content is small, in the range of 0.05–0.24% (wet percent dry liquor solids) with the average being about 0.1%. The earliest available data have been reported by Niemelä in 1990 where three nitrogen compounds were identified in a structural study of the organic compounds in birch kraft black liquor.⁶³ These structures were 1-methylpyrrole, 1,3-dimethylpyrrole, and 2-methylpyridine. No concentrations were reported.

The chemical form of nitrogen in lignin is considered here since it is a major component in kraft black liquors. Two studies indicated the lignin nitrogen to be primarily amino acid in nature.^{64, 65} In general, the nitrogen in wood is 70–90% proteinaceous.^{64, 66} Other nitrogen compounds in wood consist of free amino acids, nucleic acids, alkaloids, and inorganic nitrogen (as nitrate).

An overall nitrogen material balance was used to determine if the nitrogen content in wood could account for the amount of nitrogen in black liquor.³ The black liquor nitrogen content calculated from the nitrogen in the wood was greater than the 0.1% nitrogen average reported in the literature, which suggested that all of nitrogen in black liquor comes from the wood. A Kjeldahl analysis for total nitrogen of two kraft pulps indicated that only ~ 10% of the nitrogen remained with the pulp. Therefore, the larger portion of the wood nitrogen would be washed into the black liquor stream.

Process additives can also be a source of nitrogen in black liquor. Brownstock defoamer additives and evaporator scale inhibitors which can enter the black liquor cycle may contain small amounts of nitrogen. The potential contribution of such components was evaluated by Veverka et al.³ They found, in comparison to the total nitrogen content in black liquor solids, neither additive should make a significant contribution to the total fuel nitrogen content. Other sources for nitrogen in the black liquor may arise as mills close up. However, the addition of any nitrogen from these sources is again thought to be very small by comparison to the nitrogen from the wood.

PROBLEM ANALYSIS

A fundamental understanding of the fuel nitrogen release which occurs during the pyrolysis of kraft black liquor is desirable to aid in the development of combustion techniques which minimize NO_x emissions and NO_x reduction processes. Limited knowledge of NO_x formation mechanisms exists for the combustion of black liquor and analogies are usually made with the combustion of other fuels. Background information from coal combustion and flame chemistry provides a context for investigating the formation of fuel NO_x from the oxidation of kraft black liquor pyrolysis.

The relative proportion of fuel nitrogen in black liquor is small (0.1% on average), yet, it is sufficient to produce the level of NO_x emitted for the fractional conversions cited. The nitrogen in liquor is expected to be organic in nature with only a small fraction possibly appearing as nitrate or nitrite species. The source of the organic nitrogen is from wood and therefore should be proteinaceous in nature. In coal, the nitrogen content is much higher at about 0.8% on average. The nitrogen in coal is primarily heterocyclic in nature with pyridinic and pyrrolic species dominating. The evolution of nitrogen from these heterocyclic species tends to form HCN as the predominant NO_x intermediate although NH_i species have also been measured. Nitrogen analysis of black liquor, where the nitrogen is expected to be proteinaceous, would indicate if the nitrogen is in the form of straight chain amines or as heterocyclic ring structures. The corresponding NO_x intermediates expected would then be amine (NH) or cyanide (CN) type species, respectively, based on coal nitrogen research.

The structure of the fuel nitrogen is also important in the volatiles release.

Temperature and nitrogen structure effects as noted for coal nitrogen release suggest that similar effects may occur during NO_x formation from black liquor combustion.

Temperature effects become important for fuel NO formation as temperature often is a primary variable in the release of volatile material during pyrolysis. It was noted during coal devolatilization that the release of bound nitrogen produces negligible amounts of NO_x until the temperature reached about 700°C .³³ As the temperature increased to about 900°C , the fuel nitrogen accounted for two-thirds of the total NO_x observed. An increase in the nitrogen evolved from black liquor pyrolysis with an increase in temperature was noted over the range of $300\text{--}1000^\circ\text{C}$. This suggests an increase in pyrolysis temperature, which causes an increase in the nitrogen devolatilization, may in turn cause an increase in the NO_x emissions.

The conversion of the fuel nitrogen to NO_x was affected to some extent by other operating parameters. For instance, the oxygen available,²¹ as well as the presence of other gas phase species such as the amine-type intermediates,^{12, 14, 39, 40} were important in the total conversion of coal nitrogen to NO_x . Likewise, the presence of fume species, in particular Na_2CO_3 , reduced NO_x in the presence of CO .⁵⁸ Further data to support or refute these findings is desirable.

The formation of fuel NO_x from coal combustion was described previously by the pathway given in Eq. 1, which is also shown below. This pathway does not include the nitrogen which remains in the char; however, it is thought to make a small contribution to

THESIS OBJECTIVES

The objective of this thesis is to gain an improved understanding of NO_x formation when black liquor is combusted. The major emphasis has been placed on the effect that the liquor composition and liquor nitrogen structures have on the nitrogen release.

Emphasis is placed on obtaining a better understanding of factors controlling the initial release of gaseous nitrogen compounds. In addition, the effects of pyrolysis temperature, heating rate, and the structure of the fuel nitrogen compounds on nitrogen evolution are investigated during black liquor pyrolysis. The specific objectives are as follows:

1. Evaluate the structure and amount of major nitrogen compounds, along with the inorganic components, in black liquor. This includes developing a suitable method for total nitrogen analysis.
2. Determine the effect of black liquor nitrogen structure, black liquor inorganic content, pyrolysis temperature, and heating rate on nitrogen evolved during pyrolysis.
3. Evaluate the possible pathways for formation of amine- and cyanide- type intermediates which lead to NO_x and the possible depletion which leads to N_2 .

EXPERIMENTAL APPROACH

A four-part experimental program was used. In the first phase, the quantity and chemical form of the fuel nitrogen in black liquors was determined. Compositional and structural analyses were made to determine the nature of the fuel nitrogen in the liquor. An elemental analysis of the industrial black liquors was also determined. The results of the black liquor nitrogen characterization were used to select model fuel nitrogen compounds which were used in the pyrolysis experiments. These data are presented in the section beginning on page 35.

In phase two, tests were done to measure the conversion of the nitrogen present in various model fuel nitrogen compounds to evaluate the pyrochemiluminescence (PCL) method for total nitrogen measurements. The effect of sodium carbonate and hydroxide addition to the model compounds was also evaluated. These data are presented beginning on page 40.

Phase three consisted of pyrolysis experiments for the model fuel nitrogen compounds and for the black liquors. The conversion of fuel nitrogen in model compounds to gas phase NO_x precursors was evaluated along with the effect of the inorganic sodium salts for the model compounds using the pyrochemiluminescence (PCL) nitrogen analyzer. The effect of final temperature, heating rate, and the structure of the fuel nitrogen was also determined. These data are presented and discussed beginning on page 62. In addition, compositional effects were evaluated for the pyrolysis of the liquor samples. The information gained places emphasis on understanding the effect that the

liquor composition and the nitrogen structures have on the nitrogen release and its conversion to gas phase NO_x or precursors. In addition, the effect of both compositional and operational parameters are addressed. The effects of the sodium species on volatile weight loss of model fuel nitrogen compounds were qualitatively determined as preliminary experiments. The results are presented in the section beginning on page 57. Likewise, single black liquor drop pyrolysis experiments were completed as initial experiments. These results from the black liquor pyrolysis are presented beginning on page 95.

Finally, the fourth phase included evaluation of the fuel NO_x formation mechanism. Potential pathways for the fuel nitrogen species to form the amine- and cyanide-type intermediate species, which then react to form NO_x , were proposed based on an evaluation of the initial products of pyrolysis using gas chromatography/mass spectrometry methods. Results are reported beginning on page 89. In addition, time, temperature, and concentration data were used to suggest a kinetic model for the depletion of gas phase nitrogen/ NO_x precursor species. These data are presented in the section beginning on page 112.

RESULTS AND DISCUSSION

Experimental results and discussion are presented in the following sections.

1. The first section gives the characterization of the black liquor samples. This section includes the results for the nitrogen species characterization, the use of that information in selection of model fuel nitrogen compounds, and the chemical composition of the liquors.
2. The second section discusses the total nitrogen measurements. This includes a comparison of the methods available for nitrogen measurements and the effects of the nitrogen structure and the inorganic composition on the measurements.
3. The third section covers the data for the pyrolysis of the model fuel nitrogen compounds and the black liquors. The effects of oxygen in the pyrolysis gas, heating rate, and temperature are discussed along with the effects of the fuel nitrogen structure. NO_x precursor formation pathways which were derived from the identification of pyrolysis intermediates are provided. The results of black liquor pyrolysis are also presented.
4. The fourth section discusses NO_x depletion reactions. Rates of NO_x depletion are analyzed and discussed in light of the overall NO_x formation pathway.
5. Finally, the last section summarizes the results and insight gained in the understanding of fuel NO_x formation in black liquor combustion.

BLACK LIQUOR CHARACTERIZATION

The results of chemical analysis of the kraft black liquors used in this work are given here. The data include black liquor nitrogen quantification and identification and elemental composition and identification of the sodium salt species. Selection of model fuel nitrogen compounds, for further pyrolysis studies, is also presented.

Source of Nitrogen in Black Liquor

The nitrogen in black liquor largely comes from the wood and enters the black liquor stream in the wash lines after pulping and bleaching.³ The nitrogen may be present as protein amino acids and other nonproteinaceous compounds. It is also possible for a very small fraction of the nitrogen to enter the black liquor stream through process additives such as defoamers and antiscaling agents. In most instances, however, these extraneous nitrogen sources can be neglected with respect to the much greater source from wood-lignin. As such, nitrogen from additives was not considered in this work.

A black liquor sample was acidified to precipitate the lignin and other acid insolubles and determine the nitrogen content of the precipitated fraction. In this procedure, nearly all inorganic compounds and low molecular weight carbohydrates are separated from the precipitate.⁶⁷ The acid insoluble fraction of the liquor was approximately 50% of the whole liquor on a dry solids basis. It was found that its nitrogen content on a dry solids basis was twice that of the whole liquor, indicating that the nitrogen content of the liquor is mainly associated with the acid-precipitated fraction.

Nitrogen Content in Black Liquor

The total nitrogen content in the black liquors is given in Table 3 below. All amounts were less than 0.25% N. Three methods frequently used by the pulp and paper industry and analytical laboratories to determine total nitrogen content were used for the measurements: pyrochemiluminescence (PCL), Kjeldahl, and LECO. All three methods were tested for the southern pine liquors and the results are given to two significant digits. The pyrochemiluminescence values are based on glutamic acid as a standard. A difference of ~ 11% on average is indicated between the pyrochemiluminescence values and those from the Kjeldahl method, while the difference between the Kjeldahl and the LECO total nitrogen values is much greater at ~ 41%. Further discussion on the differences in the total nitrogen measurements is given in the next section starting on page 41.

Table 3. Total nitrogen of commercial kraft black liquors by pyrochemiluminescence (PCL), Kjeldahl, and LECO methods. Reported as weight percent of dry solids.

Commercial kraft black liquor	PCL N [‡]	Kjeldahl N	LECO N
Pine	--	0.06*	--
Pine/Birch	--	0.07*	--
Eucalyptus	--	0.09*	--
Southern Pine I	0.072	0.072 [†]	0.17 [†]
Southern Pine II	0.079	0.092 [†]	0.26 [†]
Southern Pine III	0.11	0.14 [†]	0.13 [†]
Southern Pine IV	0.12	0.13 [†]	0.25 [†]

[‡]Test completed at IPST.

*Test completed at KCL.

[†]Test completed at Galbraith Labs.

Throughout this work, the pyrochemiluminescence values are used, where possible, as the total nitrogen measurement. In the case of the pine, pine/birch, and

eucalyptus liquors where no pyrochemiluminescence value is available, the Kjeldahl values are used.

Nitrogen Species in Black Liquor

A characterization of the types of organic fuel nitrogen in black liquor was made using GC/MS techniques⁶³ at IPST and protein and amino acid assays at Hazelton Laboratories.^{68, 69} Two liquors were analyzed, Southern Pines I and II. The results of the protein and amino acid assays are indicated in Fig. 5 for Southern Pine I. About 20% of the nitrogen could be accounted for from detectable amino acids. About 80% which remained was composed of compounds present at levels below the detectable limits of the analysis (< 10 ppm of a given amino acid which is equivalent to approximately $< 2\%$ of the liquor nitrogen content). That is, individual compounds with $< 2\%$ nitrogen made up $\sim 80\%$ of the total organic nitrogen. Nitrogen was found to be present both in straight chains and bound in heterocyclic ring forms. Qualitative structural information gained with the GC/MS indicated the latter were comprised of indoles, pyrazoles, and pyrimidines representing both five- and six-member ring structures.

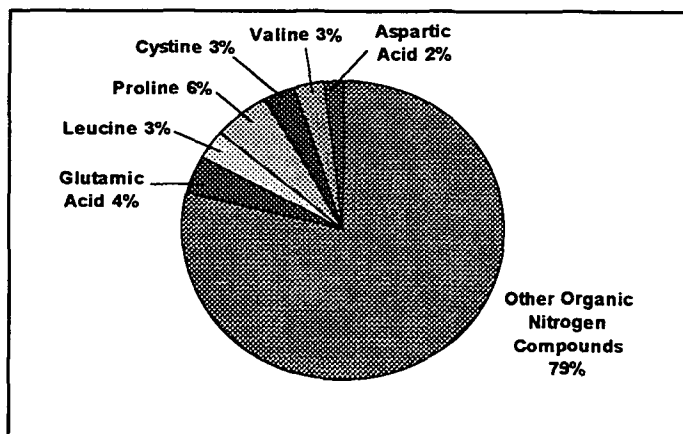


Figure 5. Composition of organic fuel nitrogen species in So. Pine I black liquor.

The results of the nitrogen structural evaluation of So. Pine II also indicated glutamic acid and heterocyclic nitrogen species to be present. The heterocyclic species included indoles, pyrimidines, and pyrazines. These species are shown in Fig. 6. Similar heterocyclic structures, pyrroles and pyridines, have been found in birch kraft black liquor.⁶³ Note that similar heterocyclic structures (pyridines, pyrroles, indoles, and carbazoles) have also been observed in coals.^{24, 25, 29}

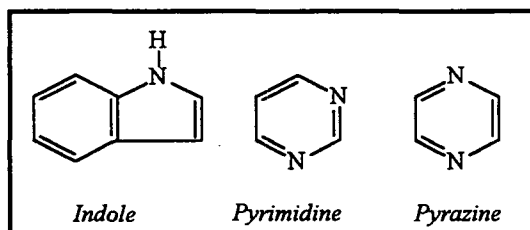


Figure 6. Heterocyclic nitrogen species of So. Pine II black liquor.

Selection of Model Fuel Nitrogen Compounds

Because of the complexity of the black liquor, model compounds of the black liquor nitrogen species were selected to be used for further study. The species selected included proline (a five-member ring), glutamic acid (a straight-chain amine), and pyrazine (a six-member ring) and were chosen based on the data presented in the previous section. Ammonium nitrate was also used because it is a common analytical nitrogen standard. The structures of these species are shown in Fig. 7. The nitrogen species were dissolved in distilled deionized water at concentrations of 0.001–0.1% N. This is the range of interest for the typical black liquor nitrogen content and its individual components. See Appendix IV for sample preparation techniques.

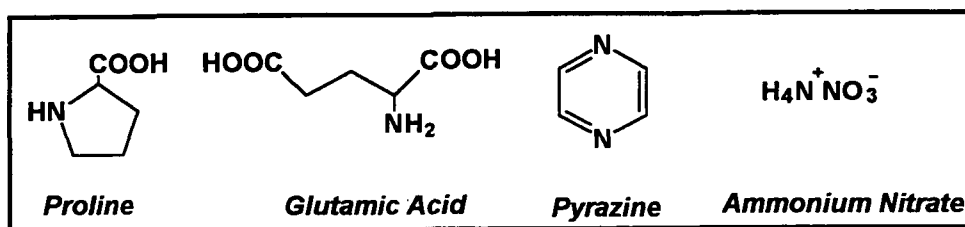


Figure 7. Chemical structure of organic nitrogen: proline, glutamic acid, pyrazine, and inorganic nitrogen: ammonium nitrate (NH_4NO_3).

Pyrolysis experiments using these model fuel nitrogen compounds were carried out to understand the individual effects of the nitrogen chemical structure and the inorganic compounds on the conversion of these species to GPNP nitrogen (the sum of fuel NO_x and its intermediates, HCN and NH_3) which occurs during pyrolysis.

Black Liquor Elemental Analysis

Further characterization of the kraft black liquors is given below. Elemental analysis is provided in Table 4. Note that the N and Na contents of these liquors varies both between species and within the same wood species (the four Southern Pine liquors).

Table 4. Elemental composition of commercial kraft black liquors reported as weight percent of dry solids.

Commercial kraft black liquor	C	H	N	S	O*	Na	K	Ca	Cl
Pine	35.8	3.6	0.06	4.6	32.6	21.0	1.8	-	0.5
Pine/Birch	33.1	3.4	0.07	5.0	30.1	25.9	1.8	-	0.6
Eucalyptus	37.3	3.6	0.09	3.4	33.2	19.0	1.8	-	1.6
Southern Pine I	34.3	3.4	0.07	5.2	33.4	19.7	2.4	0.2	0.9
Southern Pine II	31.0	4.1	0.08	2.4	33.8	21.2	1.1	0.2	0.6
Southern Pine III	37.4	3.9	0.11	4.3	36.2	16.2	2.0	1.0	0.6
Southern Pine IV	39.4	3.7	0.12	4.3	36.0	14.9	2.0	1.0	0.6

* Determined by difference.

- No observation made.

Significance of Characterization

The nitrogen content for the liquors used ranged from 0.06–0.12% N as determined by the Kjeldahl and pyrochemiluminescence methods. Black liquor fuel nitrogen was found to be primarily organic in nature. Nitrogen is present in five- and six-member heterocyclic compounds and also as straight-chain amine compounds. Variation of the nitrogen types was observed within individual species.

Since there are multiple forms of nitrogen species in the liquor, multiple pathways for the formation of the intermediate species, HCN and NH_3 , are likely. Model fuel nitrogen compounds were selected to investigate the effects of the composition on the nitrogen release during pyrolysis and to gain knowledge of the formation pathways of these fuel NO_x intermediates.

MEASUREMENT OF TOTAL NITROGEN AS NO_x IN NITROGEN CONTAINING COMPOUNDS

The measurement of total nitrogen in a given sample is the basis of much of the work presented in this thesis. Thus, the methods available were considered to determine an appropriate analysis technique for the experimental work. The methods considered were the high-temperature combustion pyrochemiluminescence (PCL) method, the Kjeldahl wet chemical method, and the low-temperature combustion LECO method. Significant differences in the nitrogen content of black liquor samples have been reported in this work (page 36) and by others.⁵⁹

The principle for the measurement of total nitrogen using the pyrochemiluminescence (PCL) nitrogen analyzer is based on an assumed 100% conversion of the fuel nitrogen to NO_x .⁷⁰ Samples are placed in a quartz boat and are inserted into a horizontal tube reactor inside of a tube furnace where they are combusted. The nitrogen analyzer system is shown in the block diagram in Fig. 8.

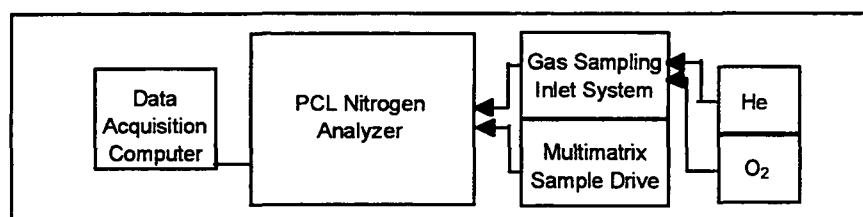


Figure 8. Block diagram of nitrogen analyzer system.

Samples were combusted at 1100°C in $> 75\%$ O_2 such that all of the fuel nitrogen was assumed to be converted to the oxidized form of nitrogen, NO . The NO and other combustion gases are sent through a membrane dryer before entering the ozone generator. Here, NO reacts with ozone, O_3 , to form excited nitrogen dioxide, NO_2^* . As the excited molecule decays, light is emitted and then detected with a photomultiplier tube within the nitrogen detector assembly.⁷⁰ The total nitrogen result is determined by the light response emitted by the unknown sample compared with that of a known standard material. The following equations chemically describe the process.



A comparison of the PCL method with the other methods available for nitrogen analysis (Kjeldahl and LECO methods) was made to determine the best method for all of the analyses to be completed in this work. The comparison of the nitrogen analysis methods is given in the next section.

PCL Comparison with Other Nitrogen Methods of Analysis

The pyrochemiluminescence (PCL) method has been compared to the Kjeldahl^{59, 71} and LECO methods for total nitrogen analysis.⁵⁹ Using the PCL method, reproducible results are achieved, but the accuracy is dependent of the choice of the standard used. Differences in the total nitrogen for organic samples was negligibly small,⁷¹ whereas the comparison of nitrogen results was poorer for black liquor samples.⁵⁹ Comparison of the test results of 17 black liquors showed that PCL total nitrogen values were lower by 20% on average than those obtained for Kjeldahl analysis.⁵⁹ On the other hand, the nitrogen content measured by the LECO method were higher by 59% on average than the Kjeldahl values.⁵⁹

The Kjeldahl analysis is a wet chemical method in which the total nitrogen of the sample is measured as ammonia. Sample preparation includes strong acid digestion, alkalization followed by distillation of the ammonia, and back titration of the excess standard base. The method assumes 100% conversion of the nitrogen in the samples to NH_3 . This assumption may not be valid for some types of nitrogen compounds depending on their chemical structure. Using this method, results within 10% of the true values can be obtained for solid samples in the range of 0.8–1.7% N.⁷² This is much greater than the

average 0.1% N in black liquor solids. Liquid samples can be measured with greater sensitivity (approximately 0.0004% N \pm 1%).⁷³

Many laboratories modify the last step of the method in order to reduce the use of hazardous chemicals and to improve the range of detection for some solid samples. For instance, detection of the ammonium ion can be done using ion chromatography.⁷⁴ Difficulty exists with this method when analyzing black liquors because of a lack of resolution between the ammonium peak and the sodium peak. Even so, nitrogen concentrations determined with the modified method were reported at \pm 4% for replicate samples.

With the LECO method, samples are combusted at a relatively low temperature (about 675° C) to oxidize the fuel-bound nitrogen along with carbon and hydrogen. Reduction of the oxidized nitrogen (NO) to N₂ occurs using a catalyst. Ultimately, N₂ is measured by thermal conductivity.

PCL vs. Kjeldahl

The lower than expected results achieved, indicated previously on page 42, from the high-temperature pyrochemiluminescence analysis can be explained by the choice of the standard used during the analysis. The PCL technique is based on a comparative response of a known nitrogen concentration with the unknown nitrogen concentration of the black liquor sample. The response is dependent on the chemical structure of the nitrogen species present and the sample matrix.⁷⁰ In the reported nitrogen analyses,⁵⁹ carbazole was used as the standard. Carbazole's chemical structure is presented in Fig. 9.

The conversion of a nitrogen species, such as carbazole where nitrogen is bound in a five-member ring, to NO is different from that of a nitrogen species in a straight-chain amine. The relative conversions of the various types of nitrogen are important in determining an accurate total nitrogen result by this method. This will be shown in the results presented in the following section, starting on page 49. In this regard, the analysis response is determined like many analytical tests. The calibration standard is used to generate a linear response throughout the concentration range of interest to which the unknown response can be compared.

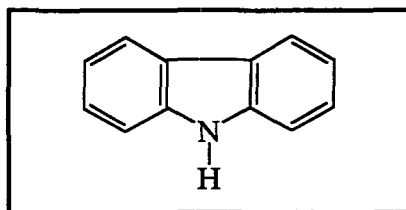
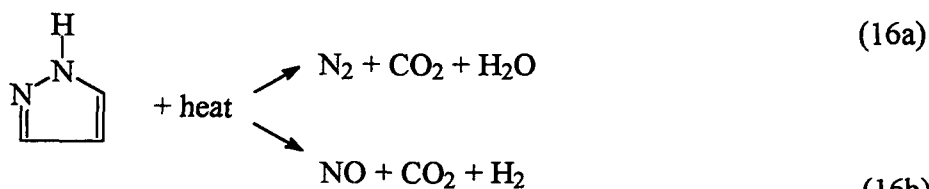


Figure 9. Chemical structure of carbazole which was used as a nitrogen calibration standard.⁷⁵

The PCL nitrogen values reported by Forssén et al.⁵⁹ for the black liquors were generated using carbazole as the calibration standard.⁷⁵ In carbazole, the nitrogen is bound in a five-member ring. This form of nitrogen is thought to represent only a small portion of the nitrogen that is present in black liquor. Nitrogen compounds with similar structures compared to that of carbazole have indicated a higher response than equivalent concentrations of amino structures. The nitrogen response from the carbazole-type structure has been as great as 44% higher than the nitrogen response from some of the amino and nitrate compounds.⁷¹ This also helps explain the lower results achieved with the combustion chemiluminescence method.

It has been established that the calibration standard and its matrix must closely represent the type of nitrogen to be analyzed and the matrix of the sample.⁷⁰ Without closely representing the type of nitrogen structure and the sample matrix, error in the analysis occurs due to changes in the conversion of the nitrogen to NO based on the differences in the chemical structure of the nitrogen compound. A similar situation may help explain the low nitrogen values for the PCL method. The calibration matrix used for the carbazole standard was toluene which is very different from the non-heterogeneous organic/inorganic nature of black liquor.

There is also an effect on the response due to the structure of the nitrogen species and its chemical bonding.⁷⁶ For example, the detection of nitrogen in pyrazole can be inhibited by the refractory nature of the compound to high-temperature oxidation or because the combustion products yield molecular nitrogen instead of nitric oxide, NO. The competing reaction is presented in Eq. 16 below. The N–N bond in the five-member ring coupled to the N=C bond is able to tautomerize forming the stronger N=N bond. Then, at high temperatures, it is released as molecular nitrogen, N₂, which cannot be measured by the combustion chemiluminescence method. The reaction identified in Eq. 16b is desirable for the combustion chemiluminescence nitrogen measurement. Similar structures with the N–N bond are measured with difficulty using this technique; however, other structures can be measured with great success.



(16b)

High conversions were observed from pyridazine, a six-member ring containing a resonant N–N bond, and from imidazole, a five-member ring with two nitrogen atoms, but without an N–N bond.⁷⁶ The conversion of species containing the N–N bond coupled to an N=C bond is high if there is sulfur, for example, substituted for the carbon at the 4-position of a pyrazole ring acting to prevent the tautomerization.

Another item which helps to explain the lower nitrogen values is a small temperature dependency that exists for some nitrogen species. (See Appendix II.) It was observed that the response was improved with increasing combustion temperature for amine-, nitrate-, and ammonium (NH₄)-type nitrogen compounds. However, the response was slightly lower with increasing temperatures for heterocyclicly bound nitrogen species. Thus, at the temperature used in the analysis, approximately 1050° C, the carbazole standard conversion was preferentially greater while the black liquor nitrogen species conversion was likely lower. The lower temperature may also explain the residue which was reported for some samples.⁷⁵

Finally, inevitable corrosion occurs when black liquor is pyrolyzed in a quartz combustion tube. As the corrosion builds up in the tube, nitrogen compounds adsorb, as well as other gas phase species, onto the corroded surface resulting in a lower nitrogen response. This can be minimized by using a ceramic lining inside the combustion tube, by

purging the combustion chamber after sample analysis to clean it, and by replacing the combustion tube when corrosion builds up. Quantification of the adsorbed nitrogen is difficult, but it has been noted to account for 5–25% of the total nitrogen measured.

PCL vs. LECO

The total nitrogen content of black liquor determined by the LECO method was higher by > 60% as compared with the PCL values.⁵⁹ The LECO analysis allows several sources of error in the nitrogen measurement. First, at lower temperatures, incomplete combustion can occur yielding volatile organics rather than the products of complete combustion. The volatile organics have a much lower thermal conductivity than a carrier gas of argon or helium.⁷⁷ A small amount of organic material results in a large decrease in the thermal conductivity and, subsequently, increases the detector temperature yielding a falsely elevated response.

Second, the amount of nitrogen present in black liquor (typically < 0.1% N based on BLS) is very small compared with carbon and hydrogen (approximately 32% and 3.5% by dry weight, respectively). Thermoconductivity detectors have a relatively low sensitivity. Thus, the LECO analysis lower limit of detection for nitrogen (~ 0.5%) becomes questionable within the concentration range of interest. Finally, the measurement of N₂ is inherently difficult because N₂ is everywhere. A small air leak during testing can result in grossly large errors for very low nitrogen concentrations which are present. These points, problems with the thermal conductivity measurement and appropriate limits

of detection, inherent within the analysis exclude the LECO method for providing reliable total nitrogen data for black liquors.

In summary, absolute values for the total nitrogen content in black liquor must be viewed critically. The above comparison of the PCL, Kjeldahl, and LECO methods identifies some of the problems currently in the area of nitrogen analysis and provides an evaluation of total nitrogen measurements between test methods. It also represents potential problems for laboratory-to-laboratory comparison of results from the same methods. Reported values between laboratories may yield significantly different results and accurate comparisons of these values would be difficult. If values were reported on a relative basis, they would likely be more valid. However, if appropriate care is taken in the analysis by matching the standard's nitrogen structure and its matrices with that of the sample, accurate measurements can be achieved. The PCL method has been used throughout the thesis work because 1) the LECO method does not provide a low enough detection limit and 2) the assumption of total conversion to NH_3 for the Kjeldahl method is not more valid than the assumption of total conversion to NO for the PCL method. The PCL method also has the advantage of shorter sampling times.

The choice of the standard used is important in obtaining an accurate result. It is difficult to determine which standard would provide the most accurate measurement for total nitrogen in black liquors because many forms of nitrogen are present (see pages 37 and 38). More work is required to determine a better standard nitrogen analysis method for black liquors and this work is being pursued by TAPPI.⁷⁸ In this thesis, NO gas was used as a primary standard for comparison of the fuel nitrogen conversion to NO for

various nitrogen sample species. For the black liquors and liquor fractions, glutamic acid was used as the standard as it was observed in black liquors (see page 37).

Effect of Nitrogen Species on Conversion

Tests were done using the PCL analyzer to evaluate the conversion of the nitrogen present in various types of model fuel nitrogen species to gas phase NO_x . The method employs combusting a small amount of sample in a high-temperature, oxygen-rich ($> 75\% \text{O}_2$) environment oxidizing all gas phase NO_x precursor (GPNP) species present to NO. Helium was used as a carrier gas. Note that the conditions employed do not generate thermal NO_x from N_2 in the atmosphere as the temperature is too low. The experimental setup was given on page 41. Further detail is given in the “Experimental Equipment and Methods” section. The effect of inorganic composition and concentration on the conversion of nitrogen to NO in several of these species was also evaluated. The results of these experiments are presented in the following sections. Complete data tables for nitrogen measurements are presented in Appendix V.

To compare the effect of the nitrogen structure on the amount of nitrogen that could be detected, several forms of organic and inorganic nitrogen were used. Nitric oxide gas ($\text{NO}_{(g)}$) was used as a primary standard. All measurements were made using the nitrogen analyzer within the concentration range of interest based on the total black liquor nitrogen content and for the content of individual nitrogen components (0.001–0.1% N). Measurement conditions were selected to maximize conversion of the fuel nitrogen.

The average relative standard deviation (RSD, %) for all analyses presented in Fig. 10 was ~5%, and the data were quite reproducible. Note that all of the nitrogen species yield less than 100% conversion by comparison to NO. Even the NH_3 (g) yield is low by approximately 17%, suggesting that the NH_3 may form NH_i intermediates which either react with themselves or with NO to yield N_2 , which is not measured in this analysis system. Possible reactions of the NH_i intermediates have been discussed on pages 18 and 19.

Thermodynamics and kinetics of the combustion environment were evaluated to explain the differences in the conversions from the various species. It was found that the results of the thermodynamic equilibrium concentration calculations did not follow what was observed experimentally, which suggests kinetic control for the reactions. The thermodynamic calculations indicated no increase in the NO or N_2 concentrations within a temperature range from 100–1100° C. (See Appendix VI.) It has been reported that the gas phase nitrogen chemistry does not follow the thermodynamic predictions.⁷⁹

If complete mixing occurs, kinetic calculations evaluating the conversion to NO from both the NH_3 and the HCN intermediate species predicted complete conversion to NO for analyzer combustion conditions and for the sizes of the samples used. (See Appendix VII.) Complete conversion was not observed, however, which suggests intermediate reactions that generate unreactive N_2 to play an important role. The possibility of depletion reactions was evaluated for pyrolysis conditions and is discussed in the section beginning on page 112.

While the differences in conversions are not fully understood, some explanation can be found in the nitrogen chemistry. For example, some species of nitrogen are capable of tautomerization allowing stronger bonds to form within the structure. This would be particularly true of heterocyclic compounds. Structures such as proline tend to have a refractory nature to high temperature oxidation and yield molecular nitrogen (N_2) instead of nitric oxide.⁷⁶ Other structures where an N-N bond exists in a five- or six-member ring coupled to an N=C are able to tautomerize, shifting the double bond around the ring thus forming the stronger N=N bond. However, the conversions of these species to NO can be improved if highly electronegative substituents such as sulfur are located on the ring withdrawing the electrons to prevent the N=N bond from forming.

The conversions of the ammonium species, NH_4Cl and $(NH_4)_2SO_4$, are similar at about 38% compared to NO. However, the NH_4NO_3 conversion is 55%. The increased conversion in the latter species is likely due to a portion of the nitrogen in the nitrate form which is noted to have a higher conversion for $AgNO_3$. See Fig. 10. Approximate averages indicate the conversion of either the nitrate or the ammonium forms of nitrogen to remain the same regardless of the compound within which they reside. However, the nitrogen in the form of nitrate tends to convert to NO_x more readily than nitrogen in ammonium compounds. In other words, the NH_4 species appear to form more N_2 . The other forms of nitrogen, such as the amine groups, vary with respect to their individual bonds and structures.

Effect of Inorganic Composition

The effect of inorganic composition and concentration on the conversion of fuel nitrogen model compounds was evaluated. Both organic and inorganic forms of nitrogen were evaluated in triplicate, at a minimum, using the PCL nitrogen analyzer at 1100° C and > 75% O₂. The results are presented and discussed here.

Equivalent concentrations of sodium carbonate and sodium hydroxide were used to prepare the alkaline solutions of glutamic acid. Each sample was measured, and the results, presented as the average percent nitrogen detected, are shown in Fig. 11. The error bars represent plus/minus one standard deviation of the mean. As indicated in the figure, the presence of sodium carbonate and sodium hydroxide reduced the amount of fuel nitrogen conversion by about 9%.

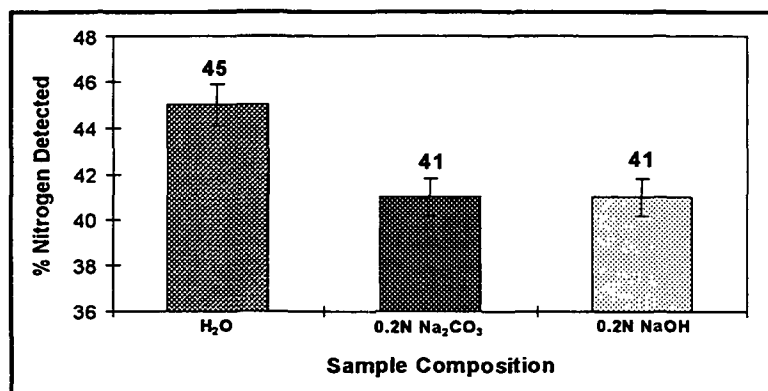


Figure 11. Inorganic component effects on organic nitrogen (as glutamic acid) conversion to GPNP for detection of total nitrogen.

The effect of different alkali concentrations was tested for organic nitrogen as tryptophan. Sodium hydroxide concentrations of 0.01, 0.1, and 1.0 normality (N) made up the solutions for 5 µl samples of tryptophan, a dinitrogen structure where the nitrogen

is bound in a 5-member heterocyclic ring and in an amine group, at concentrations of 0.2365–3.7696 $\mu\text{g N}$. The results are shown in Fig. 12 with the error bars representing plus/minus one standard deviation of the mean. In general, increasing the sodium hydroxide concentration decreases the conversion of fuel nitrogen bound in tryptophan to gas phase nitrogen species which can be detected as NO_x or NO_x precursors. The effect observed may be due to increasing the pH of the sample. It should be noted that the data presented in Figs. 11 and 12 are based on different organic nitrogen compounds, it cannot be assumed that all alkali will have the same effect over the concentration ranges tested.

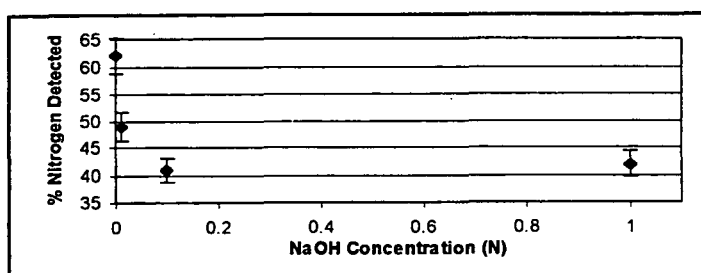


Figure 12. Increased sodium hydroxide concentration decreases the organic fuel nitrogen (as tryptophan) conversion to GPNP for total nitrogen measurement compared to the $\text{NO}_{(g)}$ standard.

The effect of alkali concentration was also tested for inorganic nitrogen. Sodium carbonate, in the range of 0–0.5 N Na_2CO_3 , was added to NH_4Cl samples in which the percent nitrogen detected was measured. An enhancement of the nitrogen response was observed as the concentration of sodium carbonate in the sample matrix increased. The average values are reported in Fig. 13 with the error bars representing the plus/minus one standard deviation of the mean.

The enhancement in the nitrogen response is likely due to the increase in the alkali concentration, which then tends to form some NH_4OH in solution which upon heating

Implications for Total Nitrogen Measurements

Conversion of fuel nitrogen compounds to NO varied from 35–91% for the nitrogen PCL measurement. The fractional conversion of the inorganic fuel nitrogen did not change for nitrate- and ammonium-type species regardless of the compound from which the nitrogen evolved. The organic forms of nitrogen, amines and heterocyclic compounds, however, were found to vary with respect to their individual bonds and structures. The variation in the fractional conversion indicated intermediate reactions that lead to N_2 are likely and may be important in understanding the overall formation of fuel- NO_x , i.e. depletion reactions which lead to the formation of N_2 must be considered in the formation of NO because the reaction pathways are thought to occur simultaneously.

A similar dependence on individual chemical structures was noted for the effect of the alkali on the conversion. The inclusion of alkali to the organic fuel nitrogen species indicated a rapid decrease in the nitrogen measured as NO.

The test indicated that the form of nitrogen is important in obtaining an accurate result. Significant differences were observed between the various forms of organic and inorganic nitrogen tested. The use of a single standard in measuring the total nitrogen in black liquor, for example, where various types of nitrogen are present can lead to an incorrect result. The results further indicated that the inorganic components also affect the gas phase organic and inorganic nitrogen species differently. This would likewise contribute to the inaccuracy of the determination of total nitrogen. Work to establish a standard method for total nitrogen analysis is being pursued by TAPPI.⁷⁸

Consideration of the results presented in this section is required when evaluating the total nitrogen content for black liquor samples or for any sample because of the differences in conversions achieved based on the nitrogen chemical structures. Further presentation and discussion of total nitrogen contents of the samples reported here are provided in terms of percent nitrogen detected based on a calibration standard, which is cited, or as a raw measurement, e.g. instrument counts. No absolute values are given unless a standard material of the same composition and nitrogen structure was employed.

PYROLYSIS OF ORGANIC FUEL NITROGEN MODEL COMPOUNDS

The effect of inorganic compounds on the pyrolysis of organic model fuel nitrogen compounds under controlled inert pyrolysis (5°C/min) from ambient to 800°C was determined using the thermogravimetric-differential scanning calorimeter (TG-DSC) in a series of initial experiments. The model compounds, glutamic acid and tryptophan, were studied in solutions of sodium salts. The total mass release was measured during pyrolysis of the dried sample. Note that the mass release is not the same as the nitrogen release. The purpose was to indicate if the addition of sodium salts to a model fuel nitrogen system would effect the decomposition of the entire compound and the temperature at which the initial decomposition occurred.

A factorial design experiment was conducted to test for significance of the effect of inorganic sodium salts on the release temperature and mass release enthalpy of two nitrogen species during slow pyrolysis. The experimental design is presented in Table 5. The inorganic components tested were Na_2SO_4 (factor a), Na_2S (factor b), and Na_2CO_3

(factor c). Each factor was tested individually and in combination with the other two factors. The base case or control for the experiment was designated “treatment combination 1” and consisted of two nitrogen compounds, glutamic acid and tryptophan, in a sodium hydroxide solution. Preparation of each treatment combination is given in Appendix IV. The nitrogen compounds were chosen based on the nitrogen structures observed in the black liquor. Glutamic acid is a straight-chain amino compound and tryptophan contains both the amino group as well as heterocyclicly bound nitrogen.

Table 5. Experimental design (2^3 factorial) of initial experiments.

Treatment Combinations	Factor A (Na ₂ SO ₄)	Factor B (Na ₂ S)	Factor C (Na ₂ CO ₃)	Experiment Number
1	-	-	-	1
a	+	-	-	2
b	-	+	-	3
ab	+	+	-	4
c	-	-	+	5
ac	+	-	+	6
bc	-	+	+	7
abc	+	+	+	8

Data was statistically analyzed using analysis of variance to determine the significance of the addition of the sodium salts to the total mass release and the temperature at which it occurs. An analysis of the effect of total sodium content on the mass release was also made. The initial results are presented briefly here as they provided the basis for further investigation. Detail of experimental set up is given in the “Experimental Equipment and Methods” section and further detail of the results is given in Appendix XII.

Effect of Inorganic Compound Addition

The temperature of the initial mass release was evaluated for the addition of inorganic components to the model compounds, glutamic acid and tryptophan. These compounds decompose at temperatures of ~ 213 and $\sim 282^{\circ}\text{C}$, respectively.⁸⁰ The addition of an inorganic sodium salt, Na_2S , Na_2SO_4 , or Na_2CO_3 , to the organic nitrogen compounds shifted the mass release onset temperature for both the glutamic acid and tryptophan to higher temperatures by $5\text{--}8^{\circ}\text{C}$ when used individually and by nearly 20°C when the salts were added in combinations. These data show that the addition of inorganic compounds to organic fuel nitrogen model compounds does affect the decomposition temperature. Since total mass release and nitrogen release are related,⁴ the nitrogen mass release should be affected in a similar manner.

The differences in mass release between the control and the addition of individual sodium salts were shown to be significant for the addition of Na_2S and Na_2CO_3 . A reduction in the mass release of $\sim 13\%$ and $\sim 4\%$ was noted for the addition of Na_2S and Na_2CO_3 , respectively, for glutamic acid. The reduction in the mass release for tryptophan was significant at $\sim 26\%$ for the addition of Na_2S and at $\sim 7\%$ for the addition of Na_2CO_3 . Additions of combinations of the inorganic compounds to the organic species also indicated a reduction in the mass release as compared with the control, although not as significant, typically being in the range of $0.5\text{--}5.0\%$. These data likewise indicate that sodium salts will have an effect on the pyrolytic mass release of the model fuel nitrogen compounds.

Effect of Total Sodium

The effect of the total sodium was evaluated by plotting the mass release versus the total sodium concentration. The weight loss decreased as total sodium increased over the range tested as seen in Fig. 14. These results are important to the overall volatiles yield and more specifically, suggest a negative effect of the total sodium may occur for the nitrogen release for black liquor pyrolysis.

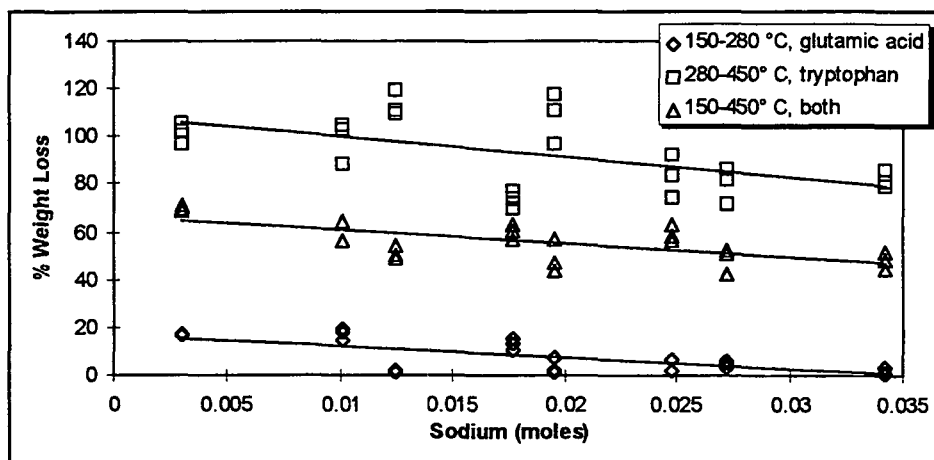


Figure 14. Effect of total sodium addition on mass release of organic fuel nitrogen model compounds as determined with the TG-DSC (Combined data for glutamic acid and tryptophan).

The temperature regions in Fig. 14 indicate the regions of mass release expected for the model compounds used in the experiments. These regions were chosen based on glutamic acid's and tryptophan's decomposition temperatures and on initial decomposition tests of each sample. Glutamic acid samples were found to decompose in the 150–280° C region, while tryptophan samples were found to decompose in the 280–450° C region. The entire 150–450° C temperature region covers the region where both compounds decompose. As such, this region provides an approximate average of both regions as expected.

In addition, increasing the sodium tends to shift the onset of the model compound decomposition to a higher temperature range. This was indicated in the previous section, “Effect of Inorganic Compound Addition.” As an example, the mass release of glutamic acid with only ~ 0.0025 moles of sodium added, was initiated at about 290°C . With ~ 0.034 moles of sodium present, the mass release was not initiated until about 310°C .

The total mass release for the individual fuel nitrogen model compounds was approximately 75% for glutamic acid and tryptophan at $150\text{--}280^{\circ}\text{C}$ and $280\text{--}450^{\circ}\text{C}$, respectively. The control, glutamic acid and tryptophan in NaOH, provided a mass release of only about 17% in the lower temperature region and 102% in the upper temperature region. The change in the mass release indicates that the initial decomposition temperature was shifted higher possibly by complexing with the sodium or through the formation of new organic sodium salts.

The total mass loss for the pure model compounds averaged 75%. However, the combined experimental mass loss of both regions of interest indicated a total mass loss of only 60%. This further suggests the potential for the nitrogen compounds to complex with the inorganic fraction and remain partially within the char residue after the completion of the pyrolysis stage. These initial experiments indicate that inorganic compounds in black liquor may have a significant effect on nitrogen release and NO_x formation.

GENERATION OF GAS PHASE NO_x PRECURSORS

The following sections present and discuss the experimental work on the pyrolysis of model fuel nitrogen compounds and on black liquor pyrolysis. Model compound pyrolysis experiments included an evaluation of the effects of inorganic compounds and concentration and pyrolysis temperatures and heating rates on the gas phase NO_x precursor nitrogen response. The effect of the inorganic components, the pyrolysis temperature, and low heating rates were determined using the pyrolysis furnace attached to the PCL analyzer. The effect of high heating rates on the pyrolysis gas composition was evaluated using the pyrolysis GC/MS techniques. Black liquor pyrolysis experiments were completed in the pyrolysis furnace attached to the PCL analyzer and in a single drop reactor. Each of the methods are described prior to presentation of the results. Information supporting the work done is presented in the appendices as indicated. Further detail of the experimental equipment is given in the “Experimental Equipment and Methods” section.

Pyrolysis of Model Fuel Nitrogen Compounds

The programmable furnace was attached to the high-temperature pyrochemiluminescence (PCL) nitrogen analyzer to be used for the pyrolysis experiments. The PCL nitrogen analyzer was previously described on pages 40 and 41. The controlled temperature pyrolysis furnace is connected to the PCL analyzer such that the pyrolysis gases directly enter the combustion chamber for the analytical measurement of the GPNP species. A schematic diagram of the pyrolysis setup is provided in Fig. 15.

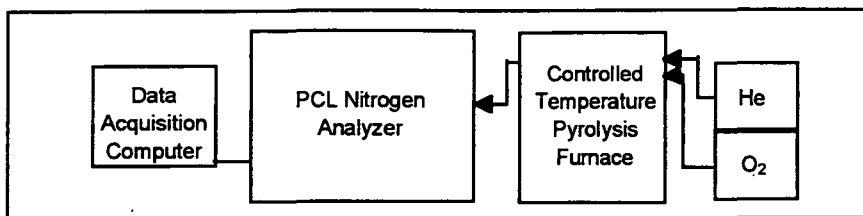


Figure 15. Block diagram of nitrogen analyzer system with the controlled temperature, programmable pyrolysis furnace.

Conversion of fuel nitrogen to GPNP species was measured under various pyrolytic conditions. Pyrolysis of several model fuel nitrogen compounds was conducted in both inert (pure helium gas) and oxidative ($\sim 15\%$ O_2 in helium) environments. The pyrolysis experiments were carried out at heating rates of $1\text{--}150^\circ\text{C}/\text{min}$ at temperatures from ambient to 700°C . The effect of gas flow rate was tested by pyrolyzing the samples both in static and dynamic ($0.170\text{ liters}/\text{min}$) environments.

Model fuel nitrogen compounds in water and alkaline solutions were tested. In this thesis, measurements of nitrogen release during pyrolysis of proline, glutamic acid, and pyrazine samples have been made for various operating conditions. The results of all pyrolysis experiments are presented and discussed in this section. Further data for pyrolysis with the programmable furnace are provided in Appendix VIII.

Measurements were made of the nitrogen release as gas phase NO_x or NO_x precursors (GPNP) during pyrolysis of the proline, glutamic acid, and pyrazine samples. A minimum of three replicates was made at each condition. Good reproducibility of the measurements was obtained; most samples indicated an RSD of $\leq 5\%$.

An example of the reproducibility for the GPNP measurements based on the nitrogen release profiles is shown in Fig. 16 for a series of three glutamic acid samples. Each sample was replicated three times. The GPNP measurement was obtained by integrating the area under the peak. Thus, a peak which is higher than a second peak yields the same integration as the second peak due to the second peak having a greater width. Therefore, while the nitrogen release profiles are not exact, the overall result provides very high reproducibility.

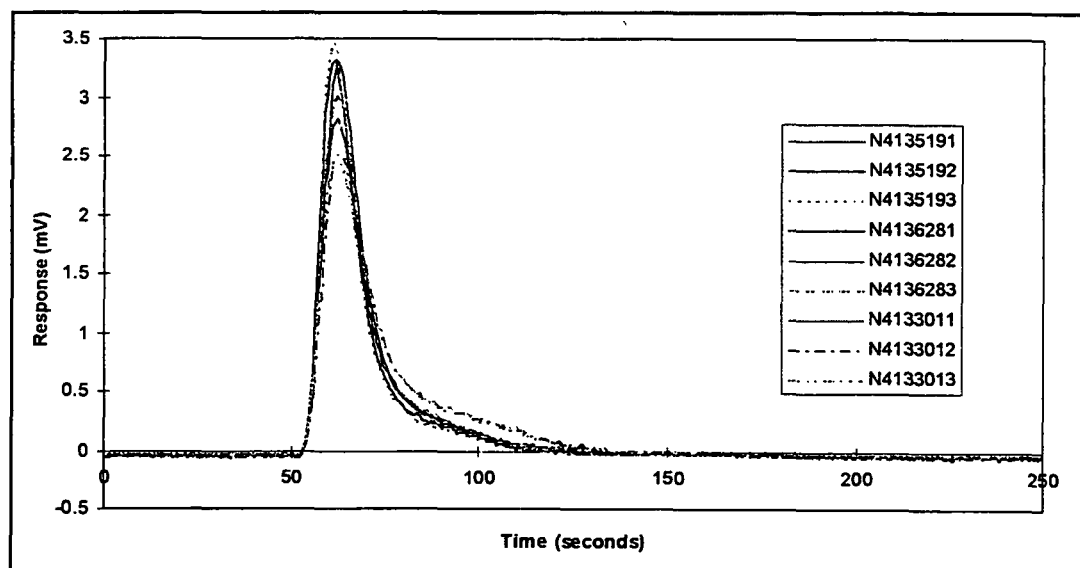


Figure 16. Reproducibility of nitrogen release profile for measurement of GPNP species during the oxidative pyrolysis (at a heating rate of 150°C/min) for aqueous glutamic acid ($2.564\text{ }\mu\text{g N/5 }\mu\text{l sample}$).

Effect of Oxygen During Pyrolysis

The effect of the oxygen concentration during pyrolysis was established by measuring the nitrogen response (counts) of $2.564\text{ }\mu\text{g N/5 }\mu\text{l}$ samples of proline in H_2O . The results are provided in Table 6 and are also shown in the Fig. 17 below. One standard deviation of the mean is indicated by the error bars. As illustrated in the figure, the

oxygen content had no statistically different effect on the nitrogen measurement during pyrolysis. This result was not anticipated as an increase in NO_x with increased oxygen has been reported for theoretical calculations² and from recovery boiler operations,⁸¹ where temperatures range of 1000–1400° C. It is possible that the effect of the concentrations at 0–22% O_2 may be overcome by the much greater oxygen concentration and the higher temperature in the combustion chamber of the nitrogen analyzer.

Table 6. Effect of oxygen concentration on the response counts of 2.564 $\mu\text{g N}$ as proline during pyrolysis.

% O_2	Counts	SD	RSD %
0	53431	1983	3.71
4	56115	416	0.74
8	51826	2775	5.35
15	54380	2291	4.21
22	54764	1007	1.84

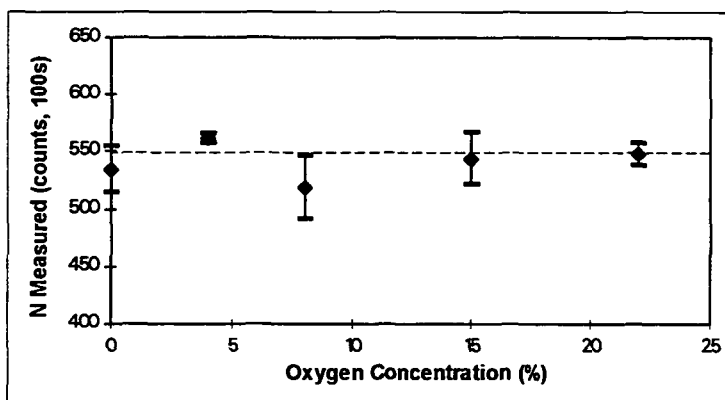


Figure 17. Oxygen has a negligible effect on the gas phase NO_x precursors measured from 2.564 $\mu\text{g N}$ / 5 μl as proline at pyrolysis conditions.

A second series of inert versus oxidative (15% O_2) pyrolysis experiments were conducted using different model fuel nitrogen compounds. The pyrolysis experiments

were conducted at a heating rate of 150° C/min. All samples were pyrolyzed (glutamic acid, proline, and pyrazine) to a final temperature of 400° C.

Figure 18 provides a comparison of the gas phase NO_x precursors measured from model fuel nitrogen samples under inert and oxidative pyrolysis conditions. As indicated in the figure, no significant differences in the pyrolytic release of GPNP species were noted for oxidative versus inert conditions. Error bars represent one standard deviation of the mean reported.

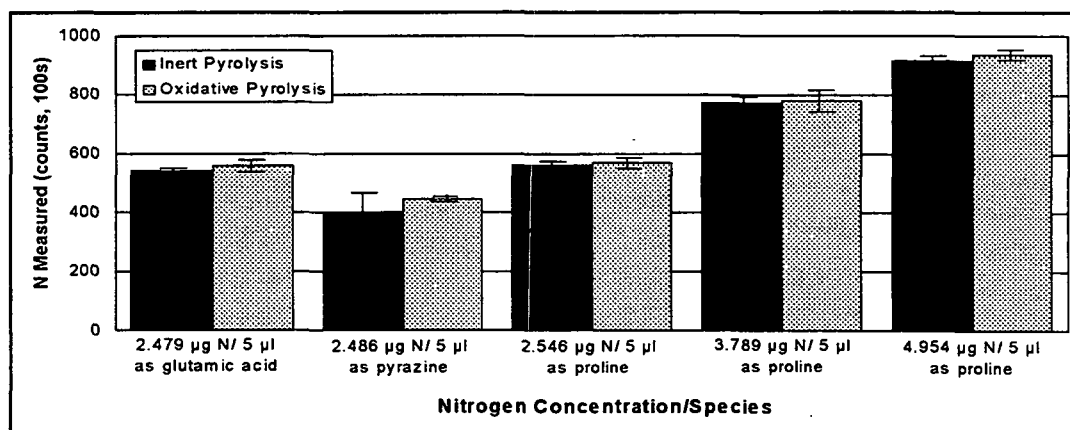


Figure 18. Gas phase NO_x precursor measurements indicated no significant difference between inert and oxidative pyrolysis conditions.

Because there is no significant effect of the oxygen present during pyrolysis on the conversion of the model fuel nitrogen species to NO_x precursors, all further results are simply presented as pyrolysis results. No distinction between inert and oxidative pyrolysis is made.

Comparison of Pyrolysis Results with Total Nitrogen Measurements

A comparison is given in Fig. 19 between the GPNP measured from model fuel nitrogen samples under pyrolysis conditions (400° C, in helium) and the total nitrogen

measurement in the PCL analyzer (1100°C , $\geq 75\%\text{O}_2$). Error bars represent one standard deviation of the reported mean. In most cases, the pyrolysis experiments gave higher levels of NO_x . The GPNP released during pyrolysis was greater for glutamic acid and proline model fuel nitrogen species than it was for the same species under the analytical measurement conditions for equivalent concentrations. However, the pyrazine nitrogen indicated poorer conversion to GPNP under pyrolytic conditions. Possible reasons for the results follow.

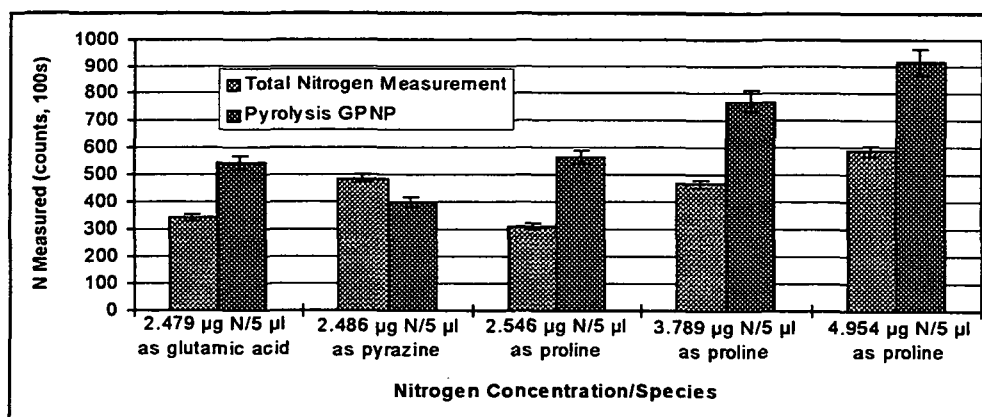


Figure 19. Comparison of gas phase NO_x and NO_x precursor total nitrogen measurements with those for pyrolysis conditions.

During the total nitrogen measurement in the PCL analyzer, the volatile nitrogen concentration remains high in the boundary layer of the sample drop as the nitrogen is given off over a shorter period of time, only ~ 20 seconds as compared with ~ 65 seconds for the nitrogen release during pyrolysis. When pyrolysis occurs prior to the total nitrogen measurement, the concentration of the volatile nitrogen species is lower at any given time and therefore, the depletion reactions which lead to N_2 are less likely to occur. Depletion reactions which occur during pyrolysis are presented in more detail starting on page 112.

The slightly lower conversion of fuel nitrogen to GPNP for pyrazine ($C_4H_4N_2$) suggests that some release of oxidizable intermediates and their conversion to N_2 rather than NO occurs within the gaseous boundary layer around the sample drop. In the case of pyrazine, no bound oxygen is present as the liquid drop volatilizes. The released nitrogen may selectively form N_2 in the immediate environment as the intermediate species react with each other in the absence of oxygen. This is also supported by the data presented later for the effect of gas phase residence time (page 112).

It is clear that the gaseous environment in which pyrolysis occurs has an effect on the amount of nitrogen from the sample that is converted to GPNP. This ultimately has an effect on the amount that is converted to NO in the combustion furnace.

The differences in conversion may result in part from the much lower heating rates at pyrolysis as compared to those obtained at higher combustion temperatures. At the lower heating rates, gas molecules would move more slowly having a lower collision frequency. As such, less opportunity would be available for the GPNP species to react with each other to form N_2 which cannot be detected with this analytical method. Only when the residence time is increased, allowing for the GPNP species to react with each other to form N_2 , does a significant decrease in the GPNP measured occur.

Effect of Nitrogen Species on Conversion During Pyrolysis

A heating rate of $150^\circ C/min$, the maximum possible for the PCL pyrolysis furnace, was chosen as a basis for further measurements. Recovery furnace heating rates are high and it is useful to use conditions as close to those encountered in an actual

recovery boiler. It should also be noted that all of the nitrogen is released by 400° C. The nitrogen in pyrazine, glutamic acid, and proline is released at temperatures of about 40, 90, and 120° C, respectively. The conversion of these model fuel nitrogen species to GPNP during pyrolysis at 400° C is given in Figs. 20 and 21 along with the error bars at ± 1 SD. From Fig. 20, it is seen that both glutamic acid and proline show similar conversions with respect to NO_(g). Glutamic acid has a conversion of about 61% while proline shows a conversion of about 62%. Pyrazine shows a lower conversion of only about 30%. The differences in chemical structures are likely responsible for the differences in conversions. Glutamic acid and proline are amino acids with amine and carboxylic acid functional groups, while pyrazine is an aromatic ring with two nitrogen atoms in the ring at 1,4 positions. Six-member heterocyclic structures are known to be more stable than either straight-chain or five-member heterocyclic nitrogen compounds.^{14, 29}

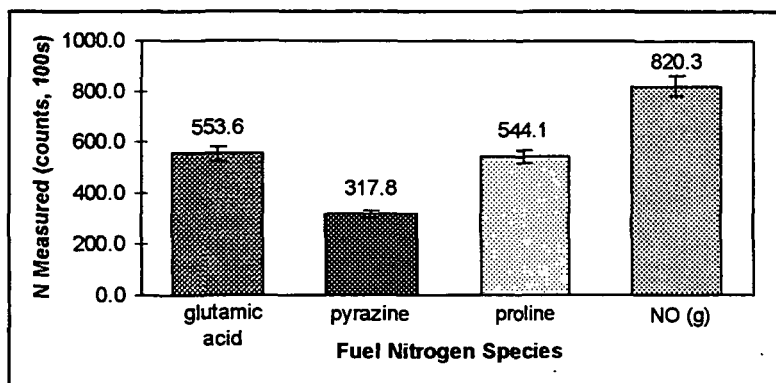


Figure 20. Conversion of fuel nitrogen model compounds under pyrolysis conditions for an initial nitrogen concentration of 2.5 $\mu\text{g N/ 5 } \mu\text{l}$. Nitric oxide (NO_(g)) standard values are presented as a reference for comparison.

compared with the control (H_2O matrix) during slow pyrolysis by 40% and 32%, respectively. This also indicates the anionic component to be important; likely as it affects the high temperature stability of the salt. The error bars represent plus/minus one standard deviation of the mean.

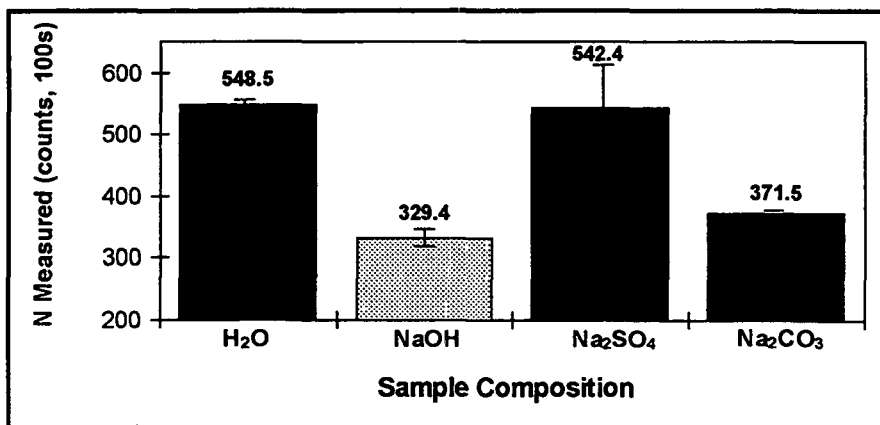


Figure 22. Effect of inorganic species on fuel nitrogen (as glutamic acid) conversion to GPNP during pyrolysis at $150^\circ\text{C}/\text{min}$.

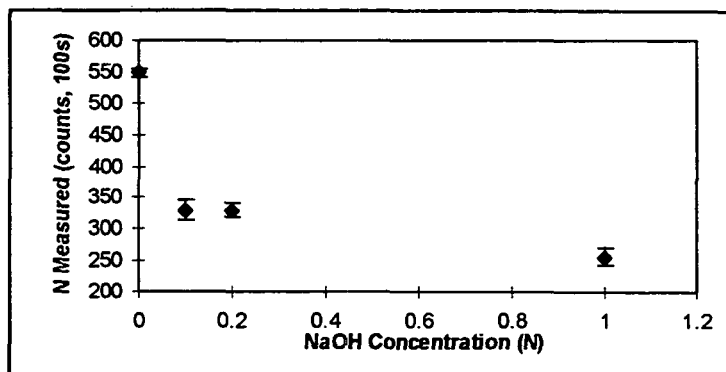


Figure 23. Effect of inorganic concentration on organic fuel nitrogen (as glutamic acid) conversion to GPNP during pyrolysis at $150^\circ\text{C}/\text{min}$.

Combinations of the sodium salt species in the matrices are indicated in Fig. 24. (Error bars represent one standard deviation of the mean reported.) The addition of the sodium mixtures was made at equivalent sodium concentrations. The salt effect follows

the order: $\text{NaOH} > \text{Na}_2\text{CO}_3 > \text{Na}_2\text{SO}_4 > \text{Na}_2\text{S}$. The Na_2S increased the measured NO_x more than predicted based on the sodium content alone. This suggests that the release of sulfur is tied to the release of the nitrogen and the evolution of one in conjunction with the other may be synergistic.

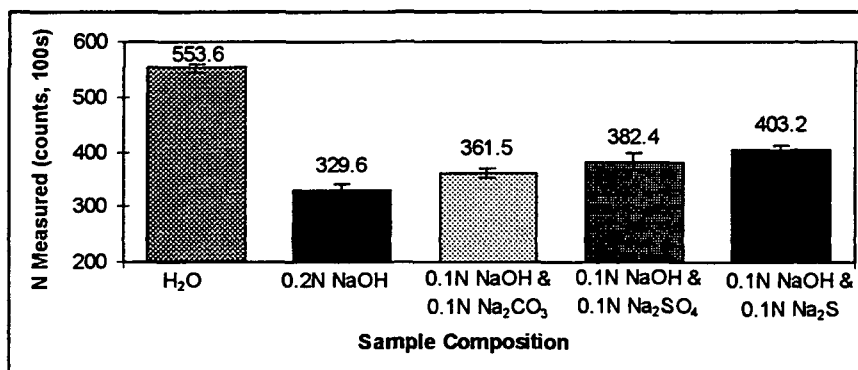


Figure 24. Effect of combined inorganics on the glutamic acid nitrogen conversion to GPNP for pyrolysis at a heating rate of 150° C/min.

Glutamic acid nitrogen release vs. time profiles are given in Fig. 25 to further compare the effects of the inorganic compounds on the GPNP measurements made during pyrolysis. These plots indicate how the addition of inorganic compounds to the sample changes the nitrogen release during pyrolysis. All nitrogen profiles shown were collected at heating rates of 150° C/min to 400° C under pyrolysis conditions. The inorganic components added to the sample are identified on each chart.

In general, the nitrogen profiles show how the inorganic compounds affect the rate of nitrogen release (slope of the initial peak), initiation temperature, and overall time of release. In plots a) and c), typical nitrogen profiles for a model fuel nitrogen compound undergoing pyrolysis is given. Both profiles exhibit a more rapid release upon initiation

(the upward slope of the peak) than is exhibited by the nitrogen decay (the downward slope of the peak).

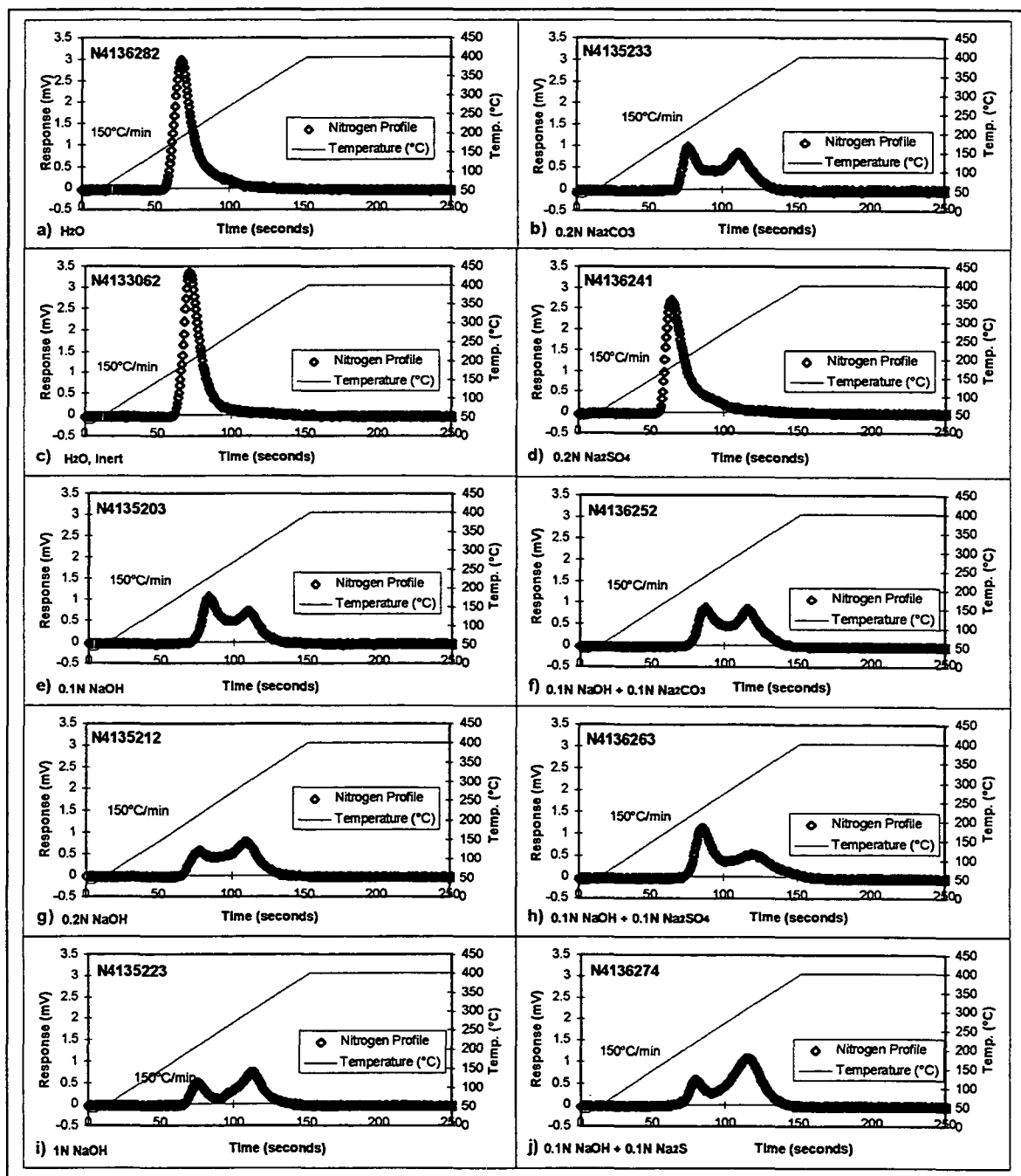


Figure 25. Nitrogen release profiles for glutamic acid pyrolysis at 150°C/min (2.5°C/sec) to 400°C. Conditions as indicated.

Significant differences, both in terms of profile shape and size, are observed when the inorganic species were added to the matrices with the exception of Na_2SO_4 (plot d in Fig. 25) and NaCl . The nitrogen release vs. time profile for proline in NaCl is given in Fig. 26. The nitrogen release profile in the presence of Na_2SO_4 or NaCl is not affected. In each of the other cases where differences in the nitrogen profile exist, the peak shape was modified from a large single peak to two smaller peaks. In previous sections, the decrease in GPNP in the presence of inorganic species was noted to be in the range of about 32–50% and will not be further discussed here.

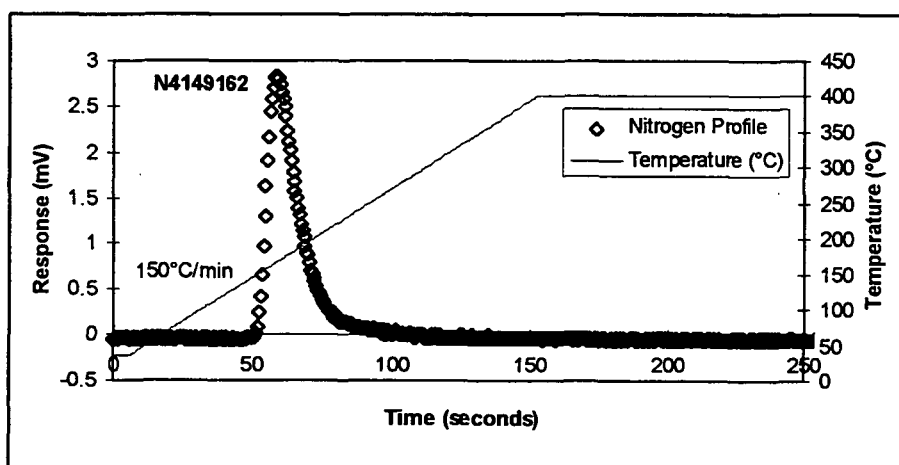


Figure 26. Nitrogen release profile for proline pyrolysis at 150° C/min (2.5° C/sec) to 400°C in an aqueous NaCl solution.

In the cases of plots e), g), and i) in Fig. 25, the inorganic concentration of NaOH is increased. From these plots, it appears that as the NaOH concentration is increased, a larger portion of the GPNP has shifted to a later time. Some variation of peak size occurs within replicates of individual samples; however, the pattern remains the same. The shift in the GPNP release may indicate that 1) some of the nitrogen is being bound either

chemically or physically with the sodium salts and is released at a later time period or 2) gas phase reactions of the sodium vapor and the GPNP are occurring. In the first case, because of the relatively low pyrolysis temperature (400°C), the sodium salts likely will not completely volatilize and the decrease in the overall GPNP in the sample may result from the nitrogen which remains bound to the sodium species in the pyrolysis residue. In the second case, sodium that does vaporize may account for the decreased concentration of GPNP due to gas phase reactions which form N_2 . The sodium species may react with the GPNP species in the gas phase to reduce the nitrogen measurement. Similar reactions have been noted for gaseous and molten sodium species.^{57, 58}

A similar shift in the peaks is observed for the addition of Na_2CO_3 (plot b) and for the combinations of the sodium species. In general, Na_2CO_3 behaves in a similar manner as NaOH indicating that the alkaline salts behave differently than the neutral salts. The plots for combined sodium species exhibit nitrogen profiles which average the two individual sodium species' profiles. The effect on the total GPNP measured was presented in an earlier section.

It should also be noted that the initiation time for the nitrogen release was increased by about 10–20 sec in all cases where sodium salts were used in the solutions. The time period in which all of the nitrogen was released also increased with the addition of the inorganic components in solution. In every case except the addition of Na_2SO_4 and NaCl , the time period nearly doubled from about 50 sec to 100 sec.

Evaluation of the response attained from Na_2SO_4 and NaCl addition indicated only a slight decrease if any in the nitrogen response. Both of these species have lower vapor pressures as compared with NaOH and Na_2CO_3 and tend to be less volatile in the temperature ranges employed. Sodium hydroxide, for example, readily vaporizes while Na_2SO_4 maintains a very low concentration in the vapor phase. Also, in aqueous solutions, SO_4^{2-} and Cl^- are neutral where CO_3^{2-} , OH^- , and S^{2-} are basic and more reactive.³¹ The model fuel nitrogen species employed in the aqueous solutions likely were chemically bound to these ions. The outcome then was that the response observed for the Na_2SO_4 and NaCl additions have little to no effect on the nitrogen released during pyrolysis at the given conditions.

Effect of Heating Rate

Variation in the total GPNP concentration was determined with respect to the applied heating rate over a range of 1–150° C/min under pyrolysis conditions with the PCL furnace. Variation in the pyrolytic gas phase composition with increased heating rates was also determined over the heating rate range of 10–1000° C/sec employing the pyrolysis GC/MS system. The results of these investigations follow.

Variation in GPNP at Slow Heating Rates. To determine the effect of heating rate on the total GPNP evolved, the GPNP was measured for the pyrolysis of glutamic acid at slow heating rates. The results are presented in Fig. 27 and indicate that no significant differences are observed. Heating rate had no effect on the GPNP formation from

glutamic acid pyrolysis over the range from 1–150° C/min. The error bars represent plus/minus one standard deviation of the mean.

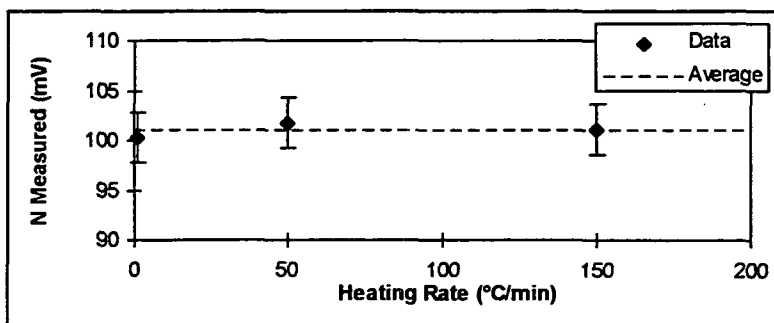


Figure 27. No significant variation in the total GPNP measured occurs for pyrolytic heating rates of 1–150° C/min.

Figure 28 shows that changing the heating rate profile changes the nitrogen release profile for glutamic acid even though the total release is unaffected. Some variation in the peak shape occurs as natural variation and can be seen within replicates of the same samples.

In plots c) and d) of Fig. 28, during the period in which the nitrogen is released, the same heating rate of 150° C/min was applied. The peaks differ slightly in these two plots. In c), the nitrogen release is slightly slower initially than it is in d). The much quicker release of nitrogen as seen in d) is paralleled with a rather large tail or shoulder at the base of the peak. This suggests that if part of the nitrogen is rapidly released the portion that remains will be released more slowly. The slower release may represent that from the core of the sample drop during pyrolysis. In general, there was no significant difference in the total nitrogen measured over the range of heating rates, from 1–150° C/min, tested under pyrolysis conditions. Note that the temperature scale on the right

vertical axis in Fig. 28 varies with the heating rate. The solid line represents the temperature changes made according to the applied rate.

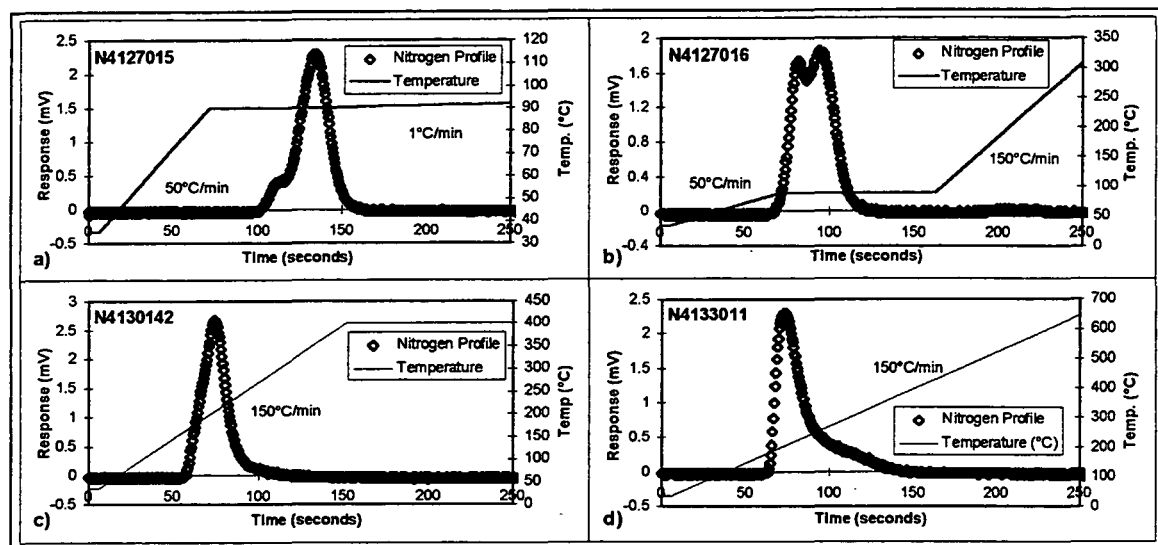


Figure 28. Effect of heating rate on the nitrogen profiles of glutamic acid during pyrolysis. Heating rate methods are a) 35° C hold for 6 sec, ramp at 50° C/min to 90° C, hold for 1 min, ramp at 1° C/min to 400° C. b) 35° C hold for 6 sec, ramp at 50° C/min to 90° C, hold for 1.5 min, ramp at 150° C/min to 400° C. c) 35° C hold for 6 sec, ramp at 150° C/min to 400° C, hold for 2.0 min. d) 35° C hold for 6 sec, ramp at 150° C/min to 700° C.

Variation in Pyrolysis Products at High Heating Rates. Much faster heating rates were possible with the pyrolysis GC/MS system. Tests on several model fuel nitrogen compounds were conducted at rates of 10–1000° C/sec, which overlap the heating rate for black liquor drops in the furnace. Information from coal pyrolysis literature indicated that the heating rate could effect the total NO_x formed.¹⁸ The effect of heating rate on the pyrolysis gases, including fuel nitrogen conversion to GPNP species or N₂, was evaluated by pyrolysis GC/MS in inert conditions for species of proline, glutamic acid, ammonium sulfate, and ammonium chloride. Solid samples of approximately 0.02–0.1 mg were

pyrolyzed inside the probe heating coil in a helium gas atmosphere at the desired heating rate. Solid proline samples were pyrolyzed in an inert environment at rates of 10, 150, 400, and 1000° C/sec. The four heating rates were used to bridge the gap between the heating rate used for the conversion data collected with the high-temperature PCL analyzer and rates found in commercial recovery boilers (300–400° C/sec).⁸

The glutamic acid, ammonium sulfate, and ammonium chloride were pyrolyzed at 10 and 400° C/sec. Pyrolysis gases were rapidly quenched, diluted, and cooled with helium so that the first products of pyrolysis could be separated and identified with the GC/MS. The results of these experiments are presented and discussed below. Details of the spectral data can be found in Appendix X.

Proline pyrolysis. A total ion chromatogram from proline pyrolysis is given in Fig. 29. Data were collected to a 15 min retention time. The majority of the gas phase products came through the column quickly as noted by the larger area under the curve at the shorter retention times. These peaks are represented by the lower molecular weight gas phase species such as CO₂. Other gas products, water, for example, may also be present within an individual peak. A few very small peaks were noted at retention times between 6 and 15 min and these species are thought mainly to be the condensation products of secondary reactions of the pyrolytic species. Such reactions under pyrolytic conditions have been noted in the literature.⁸²

The identity of the gas product is derived from the mass spectrum of the main molecule and its chemical fragments. Figure 30 presents typical mass spectra with the

corresponding pyrolytic gas species identified. Data for the major pyrolytic species, and those of particular interest, have been tabulated and are presented in Table 7.

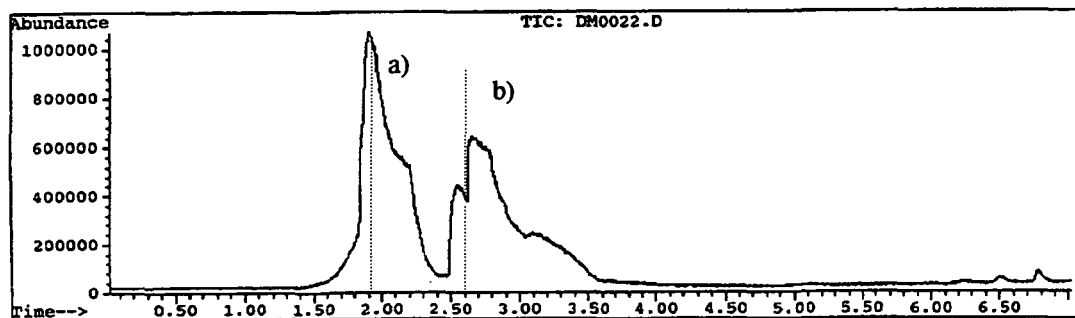


Figure 29. Total ion chromatogram of proline pyrolysis gas products. Heating rate of 10°C/sec . Retention time a) $t = 1.9$ min and b) $t = 2.6$ min.

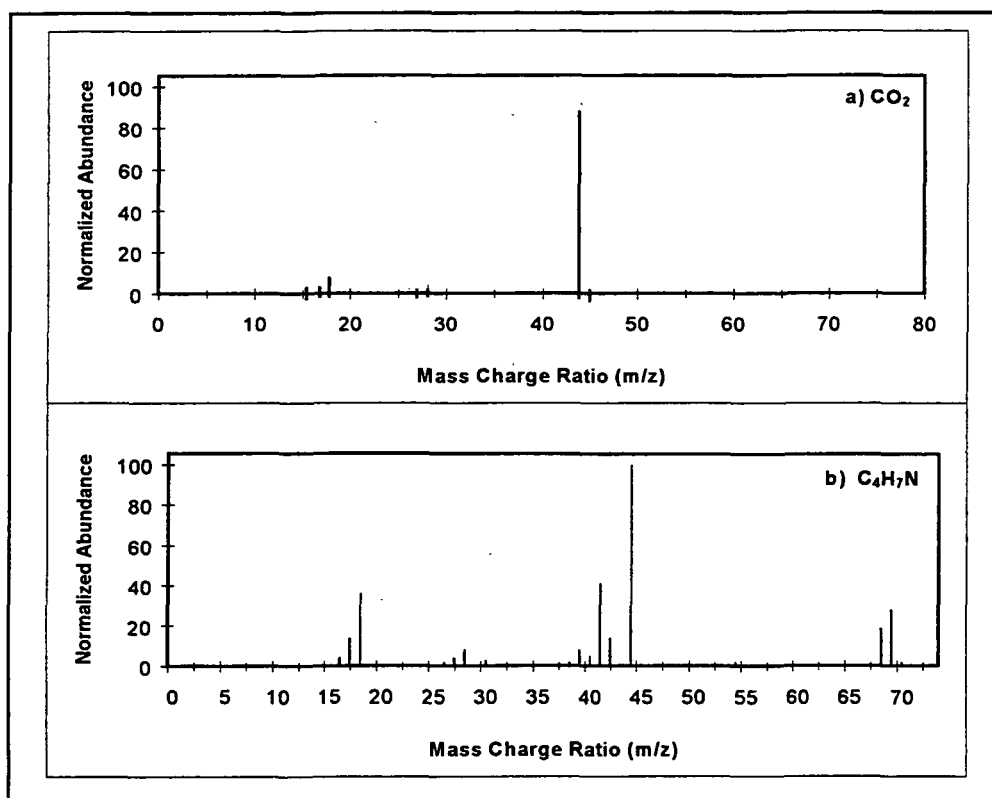


Figure 30. Mass spectra for proline pyrolysis. a) CO_2 , retention time $t = 1.9$ min and b) $\text{C}_4\text{H}_7\text{N}$, retention time $t = 2.6$ min.

The dominant pyrolysis product, CO_2 ($m/z = 44$), appears in the mass spectrum at retention time $t = 1.9$ min (Fig. 30 a), but CO_2 is also present in the peak at 2.6 min in Fig

30 b) along with the proline decomposition product 3-pyrroline, C_4H_7N ($m/z = 69$). (This indicates that a clean separation of the pyrolytic gases on the GC column was not obtained.) Signals related to water (18, 17, and 16) were also observed. Other reaction products from proline pyrolysis appear to be pyrrolidine, C_4H_9N ($m/z = 71$). These components, which elute at retention times of 2.6 and 2.7 min, are likely the primary products of the loss of CO_2 from proline during pyrolysis.

Species identification has been tabulated and is presented in Table 7 for the major components of interest. The presence of the carrier gas, helium is noted in the mass spectra at some retention times and is an indication that some of the pyrolytic species are present in very small amounts. Also, the larger pyrolytic components are present due to condensation reactions of the smaller molecular weight species. Again, the original data are available in Appendix X.

Table 7. Identification of proline pyrolysis products determined by mass spectrometry.

<u>Retention Time (min)</u>	<u>Mass Charge Ratio (m/z)^a</u>	<u>Pyrolytic Species</u>	<u>Mass Spectral Fragments^b</u>	<u>Normalized Abundance^c</u>
1.9/2.1	44	CO_2		100
2.6	69	C_4H_7N		72
	42		C_3H_6 or C_2H_4N	36
	41		C_3H_5 or C_2H_3N	100
2.7	71	C_4H_9N		63
	70		C_4H_8N	43
	43		C_3H_6 or C_2H_4N	100
	41		C_3H_5 or C_2H_3N	95
6.2	123	$C_8H_{13}N$		14
6.5	109	$C_7H_{11}N$		100 ^d
6.8	123	$C_8H_{13}N$		100

^a Only mass to 150 were recorded; higher mass may have been present.

^b Suggested molecular composition.

^c All abundances have been normalized to the highest abundance, base peak which is assigned the value of 100. Only signals with normalized abundance > 10%.

^d Helium was not allowed to be the base peak in this case.

The proline pyrolysis results indicated only small changes over the range of heating rates employed. The greatest change was noted between 10° to 150° C/sec. Each spectra was normalized to an abundance of 100 units as determined by the experimental mass spectral line of the highest abundance, or base peak. Representative changes are given in Fig. 31.

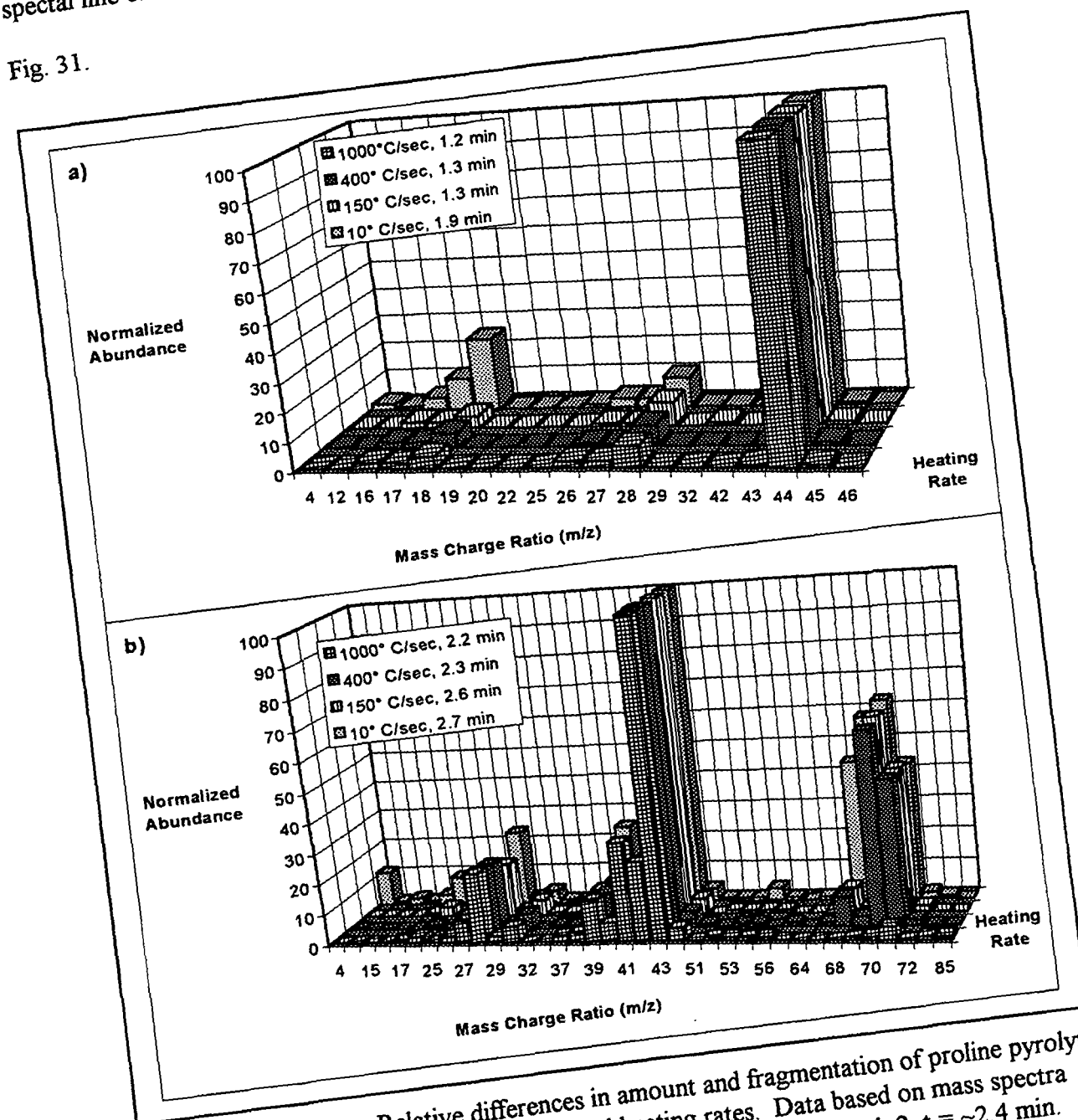


Figure 31. Relative differences in amount and fragmentation of proline pyrolytic species with increased heating rates. Data based on mass spectra obtained for a) peak 1, $t \approx 1.3$ min and b) peak 2, $t \approx 2.4$ min.

In Fig. 31 a), the change in amount and fragmentation of CO₂ (at $m/z = 44$) is presented as a bar chart through the normalized abundance and mass ratios for the normalized mass spectral series. The same is presented in Fig. 31 b) for the C₄H₇N pyrolytic species ($m/z = 69$). The parent ion, CO₂, in Fig. 31 a) is clearly shown on the chart as the dominant pyrolysis gas at the mass charge ratio of 44. No change in the relative amounts of CO₂ was observed as the heating rate increased. A combination of species may be contributing to the $m/z = 28$ signal, including ethylene (C₂H₄), protonated hydrogen cyanide (HCNH), and carbon monoxide (CO). The peak at 18 represents water while the peak at 4 represents the He carrier gas in the system.

In Fig. 31 b), the parent peak at 69 is taken to be the unsaturated nitrogen heterocycle, 3-pyrroline, C₄H₇N. The peaks at 43, 42, 41, and 28 are likely fragment ions of 3-pyrroline. As the heating rate increases less of the higher molecular weight pyrolysis products are present as more of the intermediate species are converted to CO₂. Likewise, the separation of species at retention times 2.6 and 2.7 min is not observed at the higher heating rates. At 150 and 400° C/sec, mass charge ratios of 70 and 71 are more prevalent than those of 68 and 69 as indicated at 10 °C/sec. Only a small portion of the gases are present at $m/z = 71$ at the highest heating rate. Even though at higher rates a more complete pyrolysis is observed, in terms of the overall composition, CO₂ dominates all species and no new compounds are formed. Therefore, the change in heating rate can be assumed to not greatly affect the pyrolytic species composition.

More water is present in Fig. 31 a) at the lowest heating rate than at the other heating rates. As the heating rate increases, the amount of CO₂ present in the

chromatograph increases indicating the pyrolysis reaction to be moving to completion faster. In b), the fragments due to electron impact at 68 and 41 lose intensity at the higher heating rates. At 1000° C/sec, the parent ion is barely present indicating the pyrolysis reactions to be occurring more rapidly such that the fragment species that originally result from the electron impact now likely result from pyrolysis. Again, more CO₂ is generated in the process.

Overall, however, little change in the gas phase composition occurs over this range of heating rates. This finding supports the results of the kinetic evaluation of the in situ reactions, discussed in detail starting on page 112, where the dependence on temperature was weak and the residence time for reaction was more important. Further species identification from the gas chromatographs and mass spectral data is presented along with spectral interpretation information in Appendix X.

Glutamic acid pyrolysis. Similar results were achieved for glutamic acid pyrolysis GC/MS. The dominant pyrolysis gas was CO₂. Other pyrolytic gases, present in small amounts, included pyrrole and other heterocyclic nitrogen structures. These species are present due to condensation reactions which can occur in the gas phase. The total ion chromatogram for the glutamic acid pyrolysis gases is given in Fig. 32. The identified species have been summarized and are given in Table 8 for a heating rate of 10° C/sec. Again, detailed spectral information and identification is provided in Appendix X.

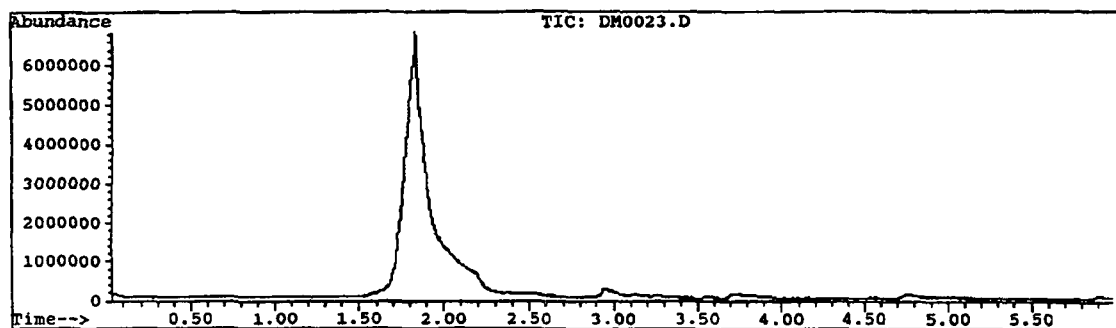


Figure 32. Total ion chromatogram of glutamic acid pyrolysis gas products. Heating rate of 10° C/sec.

Table 8. Identification of major glutamic acid pyrolysis products determined by mass spectrometry.

<u>Retention Time (min)</u>	<u>Mass Charge Ratio (m/z)^a</u>	<u>Pyrolytic Species</u>	<u>Mass Spectral Fragments^b</u>	<u>Normalized Abundance^c</u>
1.8	44	CO ₂		100
2.3	18	H ₂ O		100
	17		OH	39
2.9	67	C ₄ H ₅ N		100
	41		C ₂ H ₃ N	36
			HCNH,	
	28		CH ₂ N, C ₂ H ₄ , or CO	14
	18		NH ₄ ⁺	14
4.7	95	C ₆ H ₉ N		75
	94		C ₆ H ₈ N	55
	80		C ₅ H ₆ N	100

^a Only mass to 150 were recorded; higher mass may have been present.

^b Suggested molecular composition.

^c All abundances have been normalized to the highest abundance, base peak which is assigned the value of 100. Only signals with normalized abundance > 10%.

The increased heating rate did not greatly affect the pyrolysis gas phase

composition as seen in Fig. 33. The data presented is taken from the normalized mass

spectrum, used to identify the gas phase species. The greatest change noted is the

difference in the retention time values for the gas species. At the higher heating rates, the

retention time is lower. This is expected because the initial volatilization temperature is

attained faster with higher heating rates. The difference of 0.6 min for CO₂ release, as

seen in the legend of Fig. 33 a), cannot be solely accounted for in the differences in the time-to-temperature for the two heating rates.

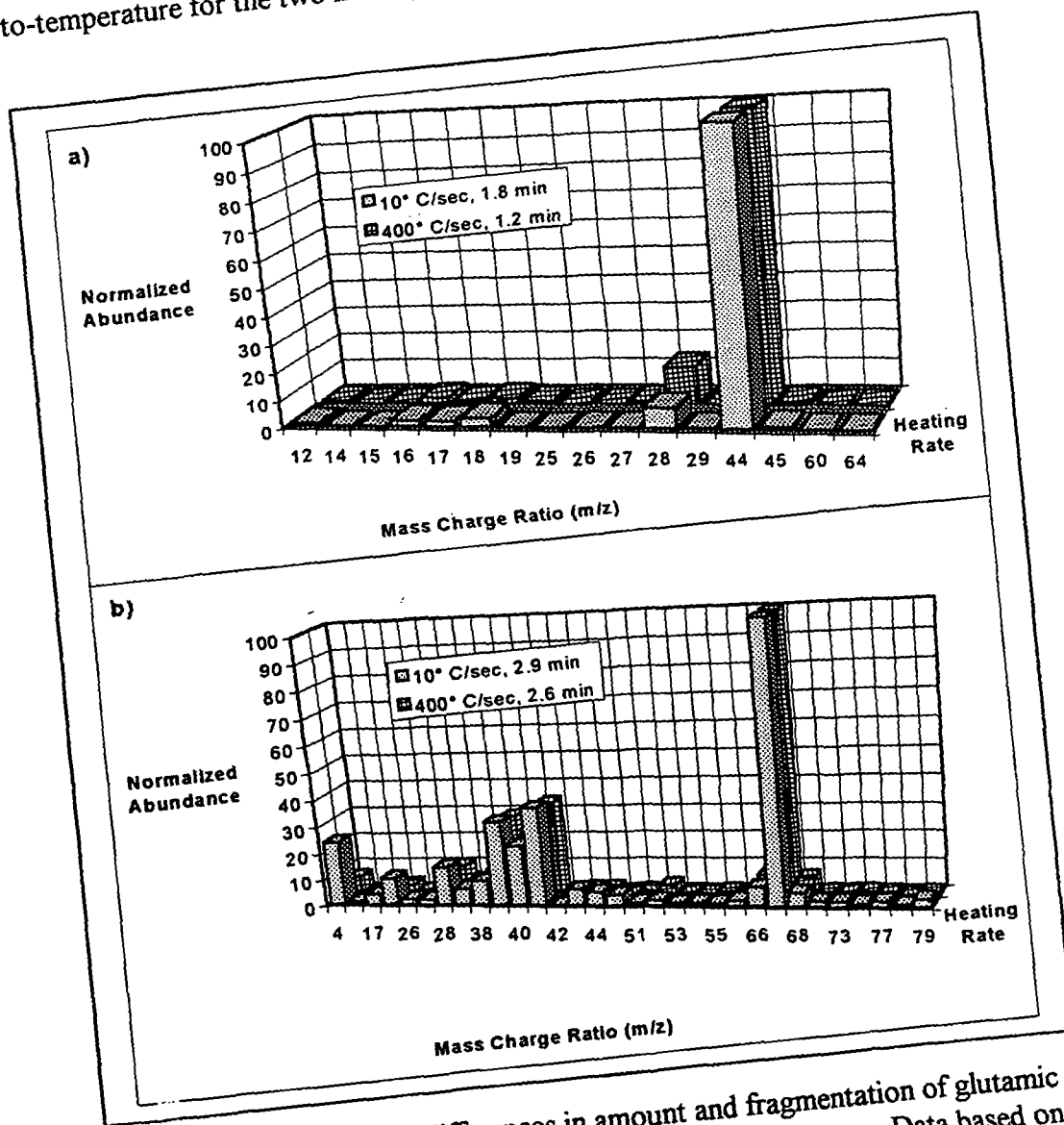


Figure 33. Relative differences in amount and fragmentation of glutamic acid pyrolytic species with increased heating rates. Data based on mass spectra obtained for a) peak 1, $t \approx 1.6$ min and b) peak 2, $t \approx 2.8$ min.

Ammonium sulfate pyrolysis. The total ion chromatogram for the ammonium sulfate pyrolysis at a heating rate of 10° C/sec is given in Fig. 34, while the species identified from the mass spectra are presented in Table 9.

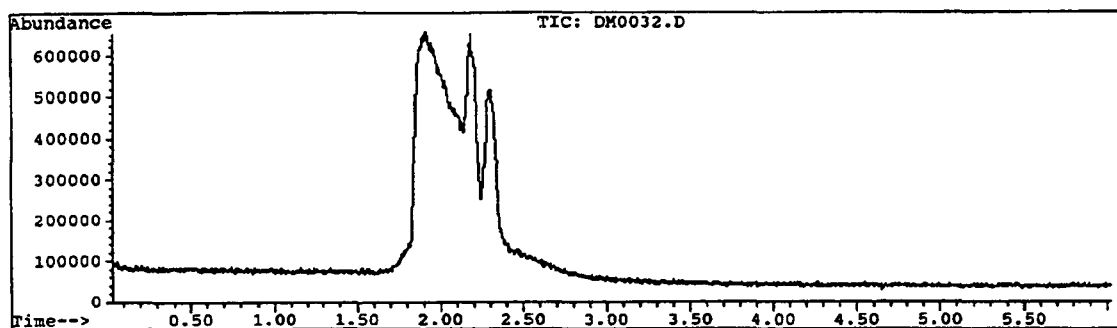


Figure 34. Total ion chromatogram of ammonium sulfate pyrolysis gas products. Heating rate of 10° C/sec.

Table 9. Identification of ammonium sulfate pyrolysis products determined by mass spectrometry.

<u>Retention Time (min)</u>	<u>Mass Charge Ratio (m/z)^a</u>	<u>Mass Spectral Assignments^b</u>	<u>Normalized Abundance^c</u>
1.9/2.2	18	NH ₄ , H ₂ O	34
	17	NH ₃ , OH	89
	16	NH ₂ , O	100
	15	NH	29
2.3	64	SO ₂	100
	48	SO	42

^a Only mass to 150 were recorded; higher mass may have been present.

^b Suggested molecular composition.

^c All abundances have been normalized to the highest abundance, base peak which is assigned the value of 100. Only signals with normalized abundance > 10%.

Comparison of the pyrolytic gas species' normalized spectra indicated little change

in the gas composition due to an increased heating rate as seen in Fig. 35. A shift to

shorter retention times of the pyrolytic gases in the column was observed at the higher

heating rate. At both rates, 10° C/sec and 400° C/sec rates, the dominant species were

ammonia and sulfur dioxide. Other species observed included NH₄, N₂, He, and CO₂ in

small amounts. In Fig. 35 b), the amount of He (m/z = 4) and NH₄ (m/z = 18) observed,

relative to SO₂ (m/z = 64) in the system, is much greater at 400° C/sec. This is probably

due to the decreased concentration of SO₂ at the given retention time and heating rate.

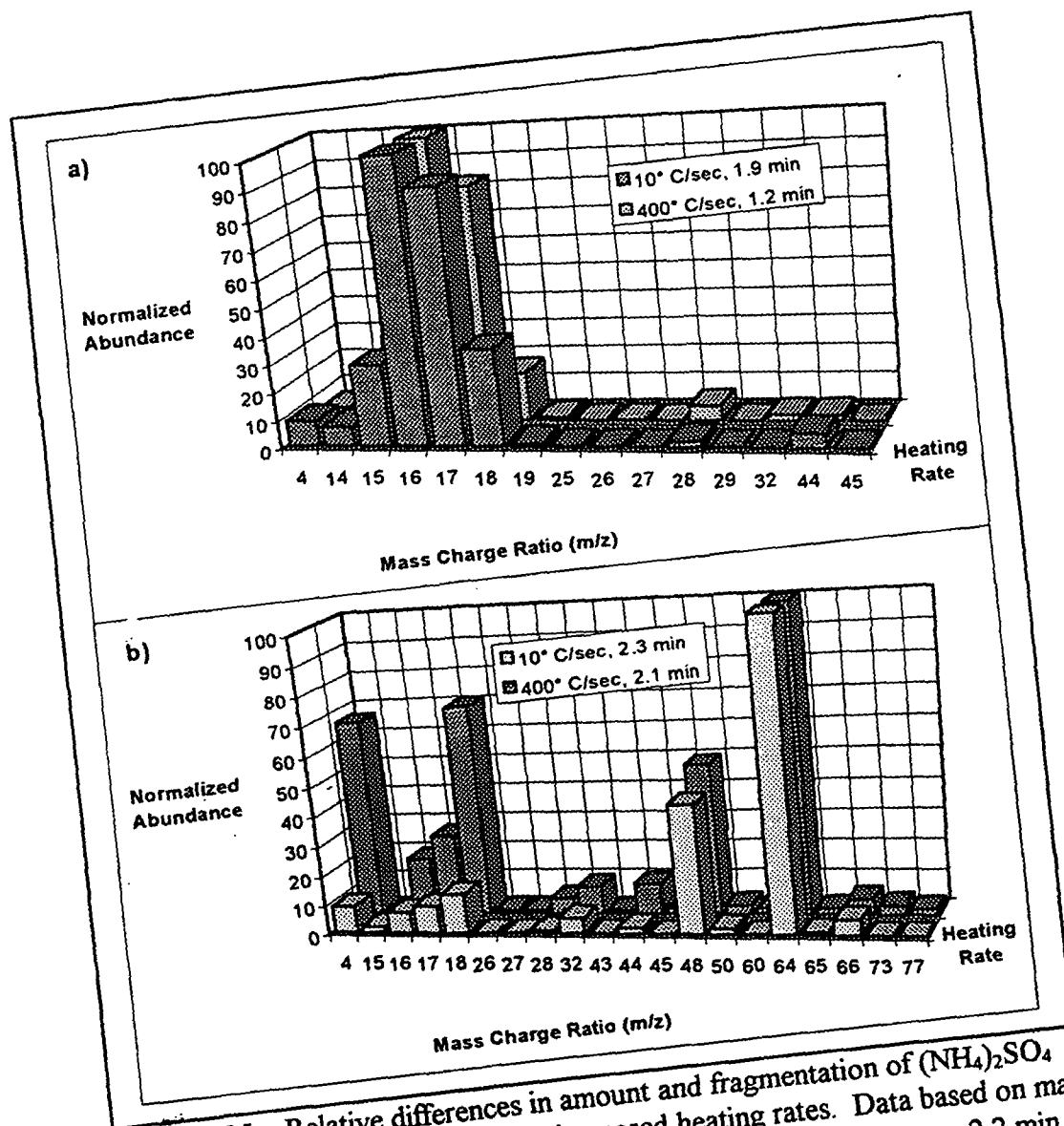


Figure 35. Relative differences in amount and fragmentation of $(\text{NH}_4)_2\text{SO}_4$ pyrolytic species with increased heating rates. Data based on mass spectra obtained for a) peak 1, $t \approx 1.6$ min and b) peak 2, $t \approx 2.2$ min.

In summary, the heating rate has little effect on the gas phase nitrogen species for several types of model fuel nitrogen compounds as observed by pyrolysis GC/MS. It should be noted that the pyrolysis GC/MS equipment precluded testing of compounds such as NH_4Cl because the decomposition gases recombined in the low temperature quench employed before injection into the GC.

Formation Pathways for Gas Phase Nitrogen Species

In general, various nitrogen species from pyrolysis, including simple and heterocyclic forms, were determined along with CO_2 , which was the dominant pyrolysis gas. Decomposition pathways were developed based on examination of the species represented in the chromatogram and the mass spectra. For instance, CO_2 can be formed from the generation of formic acid (CH_2O_2) which results from the sequential loss of water and carbon monoxide from an amino acid parent molecule.⁸⁵ Various forms of nitrogen species were also observed in the pyrolytic gases; however, little to none of the simple fuel nitrogen pyrolysis products, such as N_2 , HCN , or NH_3 , were directly observed.

Two possible explanations arise to account for the lack of simple pyrolysis gas phase NO_x intermediates, HCN and NH_3 , etc., in the mass spectrum. First, the smaller gases have very similar molecular weights and the column on the GC, originally selected to separate organic nitrogen heterocycles, could not effectively separate these lower molecular weight gases. Two gases, air and NH_3 (g), were injected directly into the GC. The chromatogram of air verified that only one peak is observed at about one minute with the mass spectrum indicating the combination of oxygen and nitrogen to be present. The chromatogram of NH_3 (g) indicated a small peak at 1.0 min and a weak ionization from the mass spectrum. This suggests that the NH_3 is being purged with the He prior to entering the mass spectrometer.

Second, reactions of the CN and NH_i intermediate species may be occurring. These reactions were noted in previous discussion on pages 18 and 19. As such, any

ammonia that is produced during pyrolysis may be reacting or is likely being masked within the peak of the more common pyrolysis gases, such as CO_2 , H_2O , N_2 , and O_2 , which come off the column at nearly the same time. Close observation of the mass spectra at low retention times indicates the possibility of multiple species per peak, with NH_3 possibly present in the dominant CO_2 peak, as indicated by the weak abundances at mass/charge ratios of 14, 15, 16, and 17.

The mass spectral evidence indicates that 3-pyrrolidine forms during proline pyrolysis, most likely by a simple decarboxylation (Fig. 36). While HCN and NH_i were not directly observed in the mass spectra for the proline pyrolysis products, several studies suggest that nitrogen heterocycles do generate HCN and NH_i species upon pyrolysis.^{13, 28, 29, 32, 35, 82-84} Detailed pathways for NO and N_2 formation from HCN and NH_i is readily available in the literature.^{12, 14-17}

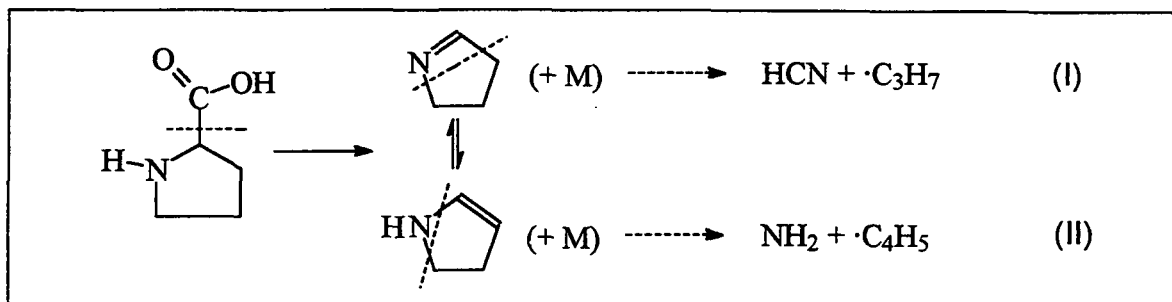


Figure 36. Proposed pathway for the formation of HCN and NH_i from proline fuel nitrogen species.

In pathways (I) and (II), the loss of the carboxylic functional group initiates the proline fuel nitrogen model compound decomposition. The rapid loss of the carboxylic acid group is thought to form the simple heterocyclic isomeric species, $\text{C}_4\text{H}_7\text{N}$ ($m/z = 69$),

which was noted in the mass spectrum at retention time 2.6 min. Ring cleavage of the simple C–N bond has been noted to initiate pyrolysis reactions.^{82, 84} Ring cleavage at the C–N bond, indicated by the dashed lines in the figure, may occur to give the HCN and NH_i (fuel NO_x intermediates) along with the hydrocarbon species.

Similarly, the mass spectral data from the glutamic acid pyrolysis indicates that CO₂ is lost and pyrrole is formed (Fig. 37). Pyrolysis of pyrrole is expected to give HCN and NH_i as intermediates in the generation of fuel NO_x.^{32, 35, 82–84} The proposed pathway is provided in Fig. 37. Again, the pathway only provides for the possible formation of gas phase NO_x precursors as the subsequent detailed pathways for NO and N₂ formation are readily available in the literature.^{12, 14–17}

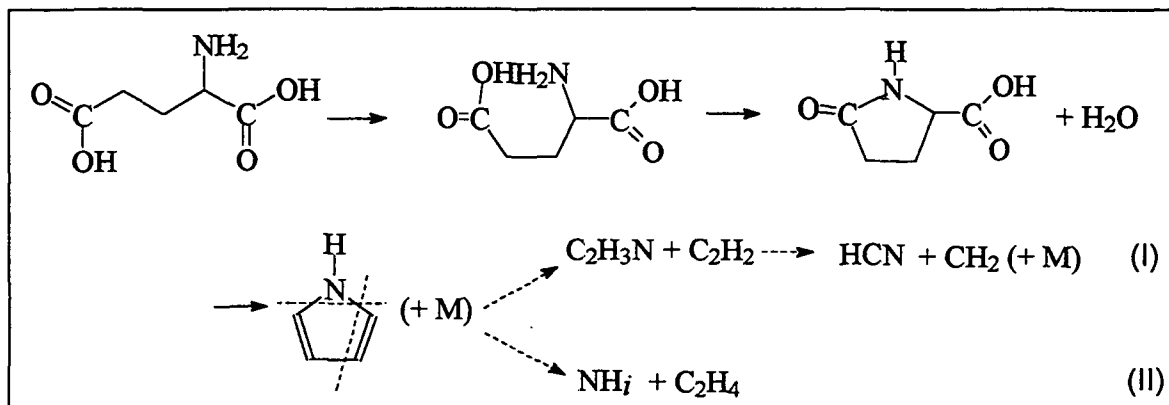


Figure 37. Proposed pathway for the formation of NH_i and HCN from glutamic acid fuel nitrogen species.

It is interesting to note that combinations of straight-chain and heterocyclic nitrogen compounds can be present in the pyrolysis gases irrespective of the nature of the compounds' initial chemical structure. However, glutamic acid is probably a special case as it contains a sufficient number of carbons between the amine and carboxyl groups to

form a cyclic structure (and H₂O) as indicated above in the first steps of Fig. 37.

Cyclization will not occur if the functional group is an aryl- or alkyl-type structure. The outcome, however, of evaluating the formation pathways indicates that both CN and NH₂ pathways are possible from amino acid pyrolysis.

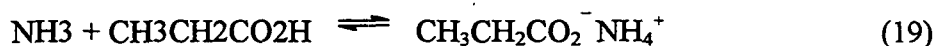
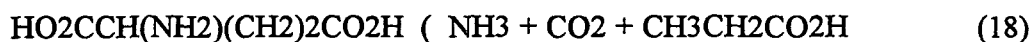
While the results of the ammonium sulfate pyrolysis were straight forward with the pyrolysis products being NH₃ and SO₂, the expected products of the NH₄Cl pyrolysis, HCl and NH₃, were not measured. With ammonium chloride, the presence of ammonia was observed in some cases; however, good reproducibility was not achieved due to low abundance of the species. The spectra contained a high degree of noise and the ammonia pyrolysis gas was difficult to distinguish from the background of the spectrum.

It is thought that the initial pyrolysis products were NH₃ and HCl and that these species were purged with the He or recombines prior to mass spectral analysis (Eq. 17). This reaction has been noted in the literature.⁸⁶ Deposits were noted within the pyroprobe interface to the GC suggesting the reaction of ammonium chloride to be a reversible reaction. The deposits were not analyzed but they provide some visible evidence for such a reaction.



This reaction, which consumes any ammonia formed from inert pyrolysis, may also be applicable to the reactions which occur with the amino acid species, such as glutamic acid. A postulated reaction, paralleled to that in Eq. 17, is indicated in Eq. 18. Here, ammonia may form after the loss of the CO₂. The ammonia could then react with the

remaining carboxylic acid species which would tie up the ammonia in the reversible reaction which subsequently could form ammonium propionate (Eq. 19). Residues were noted in the sample holder after the glutamic acid pyrolysis.



It should be emphasized that the above reactions are considered only because of the rapid cooling which occurred with the helium quench during the pyrolysis GC/MS experiments. Other experimental apparatus may give different results.

Significance of Pyrolysis Results

Under pyrolysis conditions using the furnace attached to the PCL analyzer, the amino acid fuel nitrogen compounds indicated higher rates of conversion than under conditions for the PCL total nitrogen analytical measurement. The conversion of pyrazine, a di-nitrogen heterocyclic compound indicated poorer conversion to GPNP as compared with glutamic acid and proline. This implies that the gas conditions and temperatures at which individual types of compounds are pyrolyzed or combusted plays a role in the overall conversion to GPNP.

The effects of the inorganic compounds followed the same trends under pyrolysis conditions as they did for total GPNP measurement. It was noted that an increase in the inorganic concentration enhanced the effect observed on the conversion to GPNP. Little to no difference was observed in the nitrogen conversion for inert vs. oxidative pyrolysis

suggesting the high temperature and oxygen content of the analytical chamber to overwhelm any effects observed directly from the pyrolysis environment.

Heating rate had a negligible effect on the gas phase composition. Intermediate gas phase nitrogen species, which were identified from pyrolysis GC/MS, were used to postulate several potential pathways for the formation of HCN and NH_i intermediates. This information provides new insight into the reaction pathways of black liquor fuel nitrogen species conversion to fuel NO_x .

Black Liquor Pyrolysis

Black liquors were pyrolyzed to obtain gas phase NO_x and NO_x precursor (GPNP) measurements for the whole liquors and for the liquor fractions. Nitrogen was also measured as NO released with volatiles and as that which remained in the char from black liquor drop pyrolysis. The results of these experiments are presented here along with a comparison of results based on the various liquor compositions. All supporting data for black liquor pyrolysis, both GPNP data and single drop data, are presented in Appendix XI.

NO_x and NO_x Precursors Generation from Black Liquor Fractions

Gas phase NO_x and NO_x precursor measurements were made for the four southern pine liquors and for their acid precipitated and non-precipitated fractions using the PCL analyzer. Total nitrogen measurements were made using the PCL analyzer described previously on pages 41 and 42. Samples were combusted at 1100°C in $> 75\% \text{O}_2$. Pyrolysis experiments were conducted using the controlled temperature furnace attached to the PCL analyzer in inert conditions at 400°C . The pyrolysis furnace was previously described on pages 62 and 63. More experimental detail is found in the “Experimental Equipment and Methods” section. The results of the measurements along with the nitrogen profiles are presented and discussed here. Information on sample preparation is given in Appendix IV.

Results of gas phase NO_x and NO_x precursor measurements taken during pyrolysis of the acid precipitated and non-precipitated fractions and of the whole black liquor are

given in Table 10. Data for the total nitrogen analytical measurement are given in Table 11. Based on the analytical total nitrogen measurement, the values for nitrogen released during pyrolysis were determined. It was found that 53.4, 35.5, 86.8, and 89.3% of the nitrogen was released on average as GPNP during pyrolysis for Southern Pine I, II, III, and IV liquors, respectively, at 400° C. Very good reproducibility was achieved for individual liquors as indicated by the standard deviations (Std. Dev.) given in the tables. Differences in the nitrogen release due to black liquor composition are discussed later in this section.

Table 10. Total gas phase NO_x and NO_x precursors measured during pyrolysis at 400° C for liquor fractions. Percent N based on dry solids of each fraction.

Fraction	So. Pine I		So. Pine II		So. Pine III		So. Pine IV	
	Avg.	Std. Dev.	Avg.	Std. Dev.	Avg.	Std. Dev.	Avg.	Std. Dev.
Acid ppt	0.123	0.002	0.157	0.006	0.200	0.016	0.224	0.007
Non-ppt	0.011	0.002	0.010	0.003	0.060	0.005	0.072	0.005
Whole Liquor	0.038	0.002	0.028	0.002	0.098	0.001	0.103	0.004

Table 11. Total gas phase NO_x and NO_x precursors measured during total nitrogen measurement of liquor fractions. Percent N based on dry solids of each fraction.

Fraction	So. Pine I		So. Pine II		So. Pine III		So. Pine IV	
	Avg.	Std. Dev.	Avg.	Std. Dev.	Avg.	Std. Dev.	Avg.	Std. Dev.
Acid ppt	0.177	0.001	0.211	0.002	0.296	0.011	0.292	0.002
Non-ppt	0.023	0.004	0.019	0.001	0.066	0.003	0.073	0.007
Whole Liquor	0.072	0.003	0.079	0.009	0.113	0.007	0.115	0.011

A nitrogen mass balance, as depicted in Fig. 38, was done for the combustion and pyrolysis of the acid precipitated and the non-precipitated fractions and whole liquor.

Figure 39 indicates a 106.4% nitrogen recovery (dry solids basis) for the Southern Pine I fractions and whole liquor measurements. The recovery is based on a comparison of the initial black liquor nitrogen measurement with the sum of the acid precipitated and non-precipitated fractions as indicated in Fig. 39 for the Southern Pine I liquor. The nitrogen mass balance for pyrolysis of the same liquor fractions from Southern Pine II provided a 135% recovery. This indicates that more nitrogen was released as gas phase NO_x or NO_x precursors during pyrolysis from the acid precipitated and the non-precipitated fractions than from the whole liquor pyrolysis. Compositional effects may be responsible for the nitrogen release differences and are considered in more detail below.

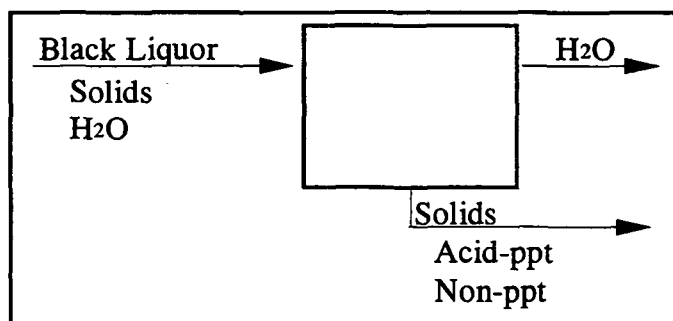


Figure 38. Schematic diagram for the mass balance for the total nitrogen analytical determination within dry black liquor, the dried acid precipitate and the non-precipitated fractions.

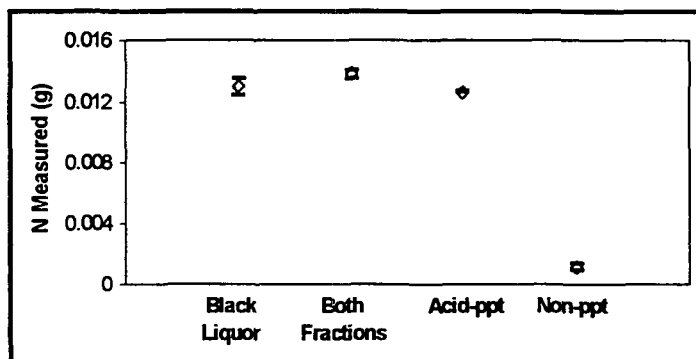


Figure 39. All of the nitrogen can be accounted for in the total nitrogen measurements as indicated here for So. Pine I liquor as determined by mass balance on the liquor fractions.

The data in Fig. 39 shows that up to 97% of the total black liquor nitrogen can be accounted for in the acid precipitated fraction. This was confirmed by independent measurements of the nitrogen content in the remaining non-precipitated fraction which was shown to contain only 3–6% of the total black liquor nitrogen. Closure of the nitrogen balance was achieved at levels of $\pm 10\%$. Therefore, black liquor fuel nitrogen is associated with the acid precipitated, lignin component of the liquor.

NO_x and NO_x Precursors Generation from Black Liquor Drops

The nitrogen measurements during the pyrolysis of black liquor drops were completed for four kraft black liquors; pine, a pine-birch blend, eucalyptus, and a southern pine (Southern Pine I). Samples were pyrolyzed from 300–1000° C at 100° C intervals in N₂ in a drop tube furnace where the drop was suspended in the gas flow. Pyrolysis gases were measured for the total NO_x content using a chemiluminescence NO_x analyzer. Nitrogen remaining in the char was measured by the PCL method (at EMPA). Further experimental detail is provided in the “Experimental Equipment and Methods” section.

In general, the pyrolytic weight loss for the liquors was similar throughout the temperatures tested with the averages indicated in Fig. 40. The standard deviations calculated for the replicates of these measurements were very low as shown by the error bars in the figure. This indicated a high degree of reproducibility for the measurements. A noticeable increase in the weight loss of approximately 30% was observed between 800 and 900° C for all liquors. It was also noted at the low temperatures, from 300–500° C,

that little to no fuming was visibly observed and the degree of swelling for the particles was small but increasing with temperature. It was estimated from char particle observations that maximum swelling occurred at 800° C. At 600–1000° C, the deposition of fume was noted on the lower portion of the quartz reactor.

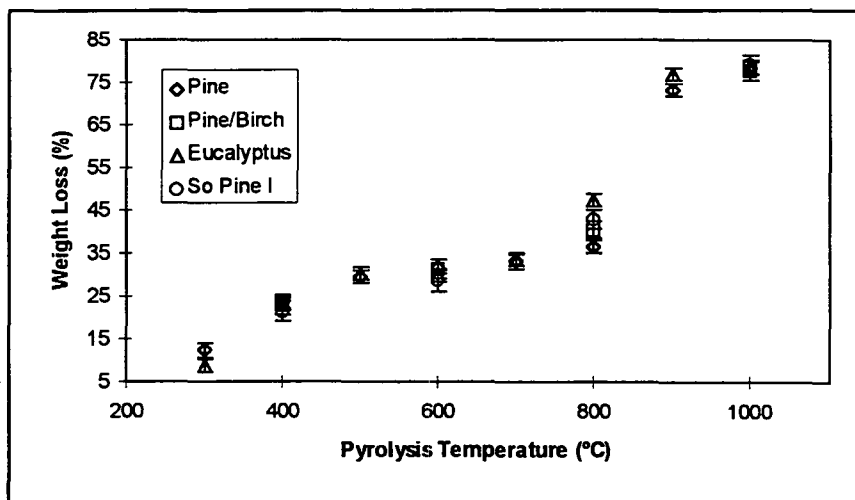


Figure 40. Pyrolytic weight loss (expressed on a dry basis) for liquors at temperatures from 300–1000° C in inert N₂.

Examples of the profile for nitrogen release as NO at various pyrolysis temperatures is given in Fig. 41 for the Southern Pine I liquor. At the lowest temperatures, in plot a), the level of nitrogen release was very small. The roughness of the profile curve indicates the nitrogen release to be occurring slowly.

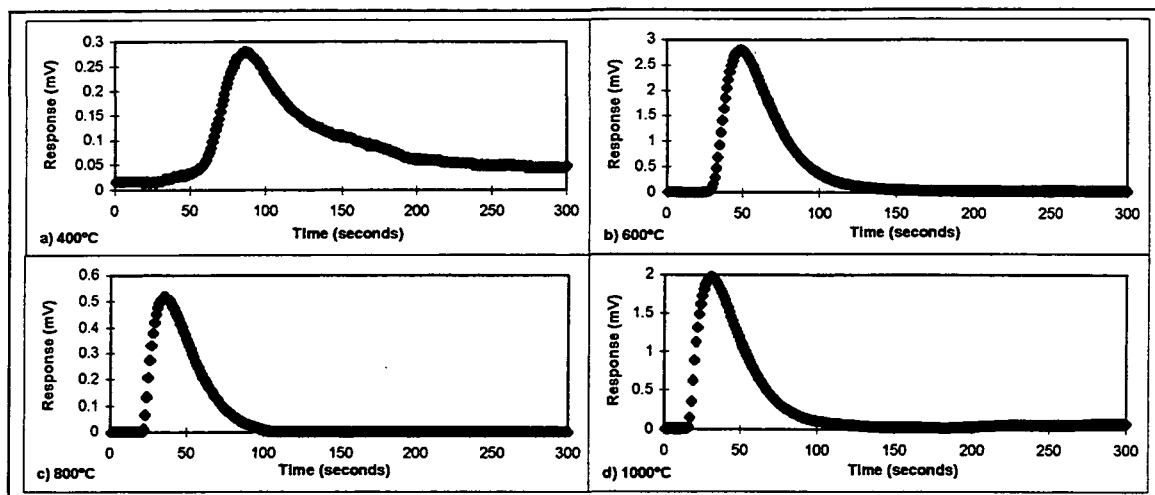


Figure 41. Profiles as NO for So. Pine I liquor pyrolysis at temperatures from 400–1000° C in inert N₂.

It was assumed that the pyrolysis stage of black liquor combustion was not yet completed at the end of the 300 sec pyrolysis period for the low temperatures, as indicated by the tar-like substance and the low relative swollen volume observed for the drops. At slightly higher temperatures, as seen in Fig 41 b) at 600° C, the nitrogen release was slow by comparison to the higher temperatures as indicated by the upward slope of the peak. Less nitrogen was released than at the higher temperatures in plots c) and d). These profiles show single peaks for the nitrogen release as NO. This was also observed by Aho et al;⁵ however, they also reported multiple peaks for NH₃ measurements.

Effect of Temperature. Quantification of the effect of temperature on the nitrogen release as NO is indicated in Fig. 42. Likewise, the nitrogen that was found to remain in the char after pyrolysis is presented in Fig. 43. The release of nitrogen as NO appears to stabilize at about 8–10 % for the four liquors at a temperature greater than or equal to 600° C. The range reported is similar to the 3–5 % N as NO reported by Aho et al.⁵ The

three pine type liquors show similar values at nearly all temperatures while the eucalyptus liquor tends to have slightly lower values.

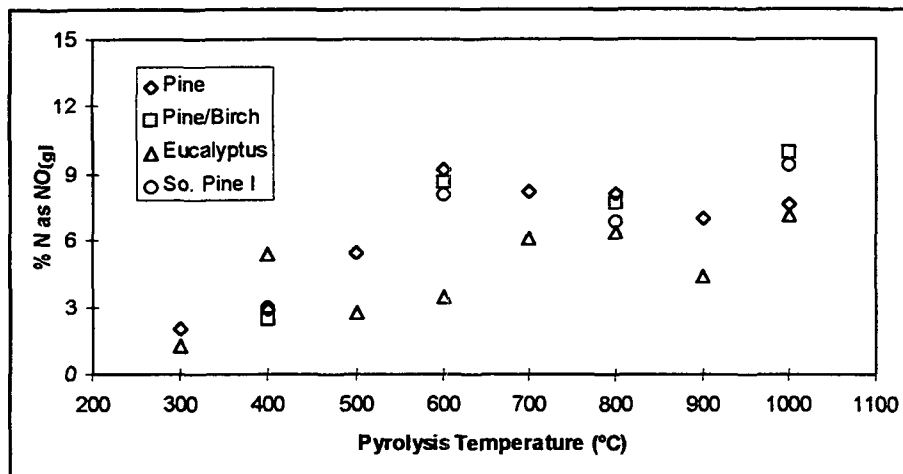


Figure 42. Nitrogen released as NO for liquor pyrolysis at temperatures from 300–1000° C in inert N₂.

Results of the nitrogen remaining in the char exhibit a very low quantity of nitrogen volatilizing at lower temperatures of 300–400° C—in the range of 10–15% of the total nitrogen in the liquors. As the temperature increases, the nitrogen retained, or conversely, the total nitrogen released, plateaus at about 50%. Thus, the nitrogen in the char comprises 50% of the original liquor nitrogen after pyrolysis while the other 50% is volatilized to form NO (8–10%), N₂, and GPNP intermediates such as HCN and NH₃. The quantity of NH₃ observed during black liquor pyrolysis has been reported to be 10–30%.⁵ The difference in the total nitrogen was defined as N₂ while no HCN was measured.

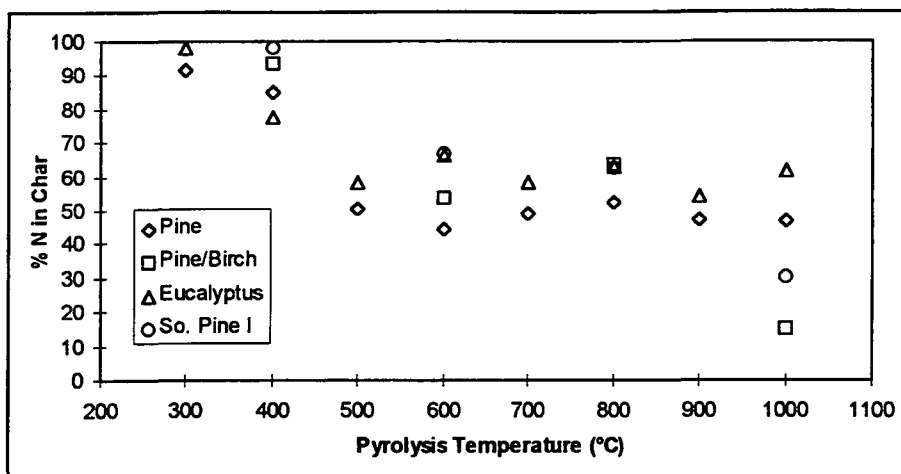


Figure 43. Nitrogen remaining in the char for liquor pyrolysis at temperatures from 300–1000° C in inert N₂.

Amounts of nitrogen remaining in the char after black liquor pyrolysis have been reported at levels of ~30%.^{5, 59} The data presented in Figs. 42 and 43 have been tabulated and are given in Table 12 as the total amount of nitrogen accounted for during the pyrolysis of black liquor drops either in the form of char-nitrogen or as nitrogen released as NO. Any amount less than 100% indicated in the table must represent the remaining liquor-nitrogen volatilized as GPNP intermediates or as N₂.

Table 12. Percent of original liquor nitrogen accounted for by nitrogen remaining in the char or released as NO after pyrolysis at the given temperature.

T (° C)	Pine	Pine/Birch	Eucalyptus	So Pine I
300	93.84	--	99.23	--
400	87.81	95.79	82.77	100.99
500	56.14	--	61.27	--
600	53.71	62.18	69.95	74.74
700	57.05	--	64.32	--
800	60.61	71.22	69.31	69.25
900	54.24	--	58.79	--
1000	54.42	25.1	68.81	39.96

At the lower temperatures, nearly 100% of the total nitrogen can be accounted for by the nitrogen released as NO or that which remains in the char. As the temperature for pyrolysis increases, the relative amounts of total nitrogen volatilized and of that as NO increase as seen previously in Figs. 42 and 43. Consideration of nitrogen released as NO, with respect to the nitrogen remaining in the char, yields the correlation depicted in Fig. 44. As the nitrogen remaining in the char increases, the amount of NO measured from pyrolysis decreases. The correlation representing only the pine liquors is given by the solid line ($R^2 = 0.80$) while that representing all four liquors is indicated by the dashed line ($R^2 = 0.68$). The slopes of each line remain about the same, however, the inclusion of the eucalyptus liquor causes a slight downward shift. The correlation, nonetheless, remains good considering the data represent four different liquors over a range of pyrolysis temperatures.

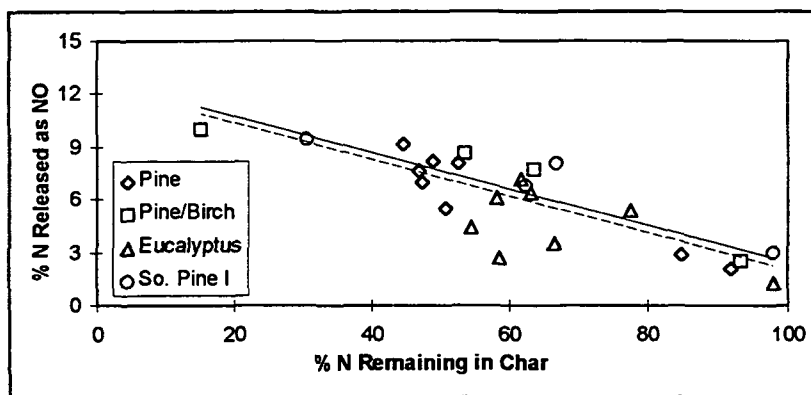


Figure 44. Relationship for percent nitrogen released as NO with respect to the nitrogen remaining in the char from black liquor pyrolysis at 300–1000° C in N_2 . (—) represents the pine liquors, (---) represents all liquors tested.

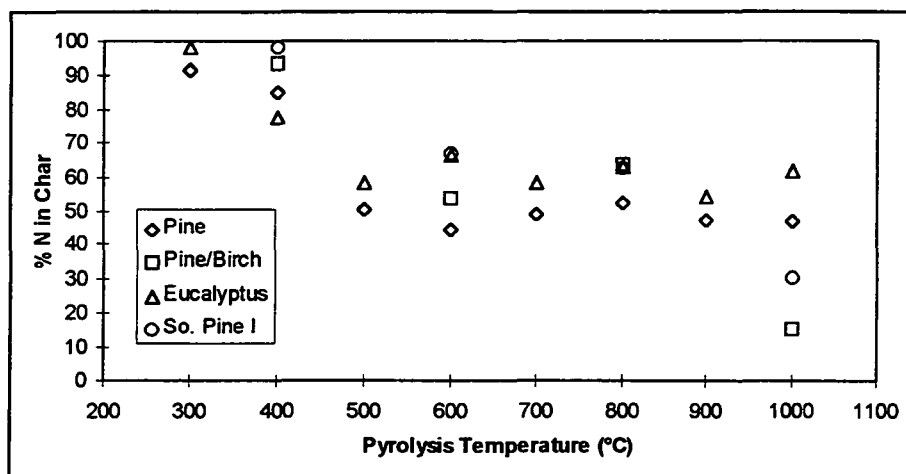


Figure 43. Nitrogen remaining in the char for liquor pyrolysis at temperatures from 300–1000° C in inert N₂.

Amounts of nitrogen remaining in the char after black liquor pyrolysis have been reported at levels of ~30%.^{5, 59} The data presented in Figs. 42 and 43 have been tabulated and are given in Table 12 as the total amount of nitrogen accounted for during the pyrolysis of black liquor drops either in the form of char-nitrogen or as nitrogen released as NO. Any amount less than 100% indicated in the table must represent the remaining liquor-nitrogen volatilized as GPNP intermediates or as N₂.

Table 12. Percent of original liquor nitrogen accounted for by nitrogen remaining in the char or released as NO after pyrolysis at the given temperature.

T (° C)	Pine	Pine/Birch	Eucalyptus	So Pine I
300	93.84	--	99.23	--
400	87.81	95.79	82.77	100.99
500	56.14	--	61.27	--
600	53.71	62.18	69.95	74.74
700	57.05	--	64.32	--
800	60.61	71.22	69.31	69.25
900	54.24	--	58.79	--
1000	54.42	25.1	68.81	39.96

At the lower temperatures, nearly 100% of the total nitrogen can be accounted for by the nitrogen released as NO or that which remains in the char. As the temperature for pyrolysis increases, the relative amounts of total nitrogen volatilized and of that as NO increase as seen previously in Figs. 42 and 43. Consideration of nitrogen released as NO, with respect to the nitrogen remaining in the char, yields the correlation depicted in Fig. 44. As the nitrogen remaining in the char increases, the amount of NO measured from pyrolysis decreases. The correlation representing only the pine liquors is given by the solid line ($R^2 = 0.80$) while that representing all four liquors is indicated by the dashed line ($R^2 = 0.68$). The slopes of each line remain about the same, however, the inclusion of the eucalyptus liquor causes a slight downward shift. The correlation, nonetheless, remains good considering the data represent four different liquors over a range of pyrolysis temperatures.

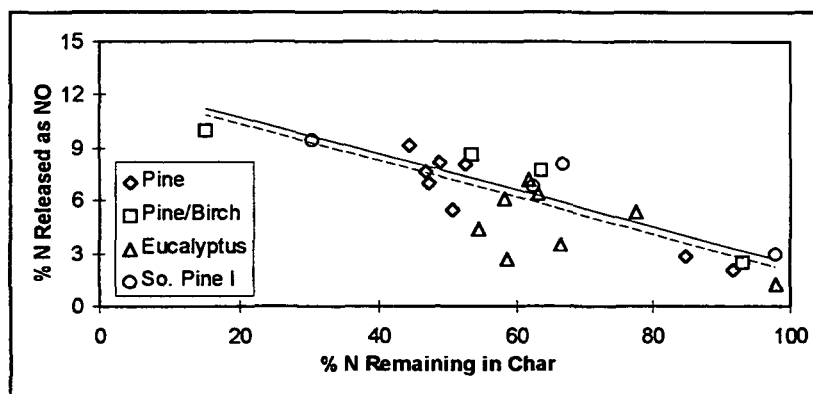


Figure 44. Relationship for percent nitrogen released as NO with respect to the nitrogen remaining in the char from black liquor pyrolysis at 300–1000° C in N₂. (—) represents the pine liquors, (— —) represents all liquors tested.

Effect of Addition of Known Components to Black Liquor. Samples of Southern Pine III black liquor were spiked with tryptophan as a model fuel nitrogen compound to investigate the effect of the whole liquor composition on the fuel nitrogen conversion to NO_x and NO_x precursors (GPNP). The resulting GPNP was measured and is reported in Fig. 45. The relationship indicates that the GPNP species measured increases linearly with increasing concentrations of the model fuel nitrogen addition in the black liquor. The percent nitrogen detected as GPNP was 29.5% when compared to the $\text{NO}_{(g)}$ standard. This result follows that presented previously in Fig. 12 (on page 54) which showed the percent nitrogen detected to range from 62% down to about 43% with increasing NaOH concentration. These results from the addition of the model fuel nitrogen species to the black liquor supports the results discussed earlier, with the inorganic composition of the black liquor reducing the nitrogen conversion to NO_x and NO_x precursors.

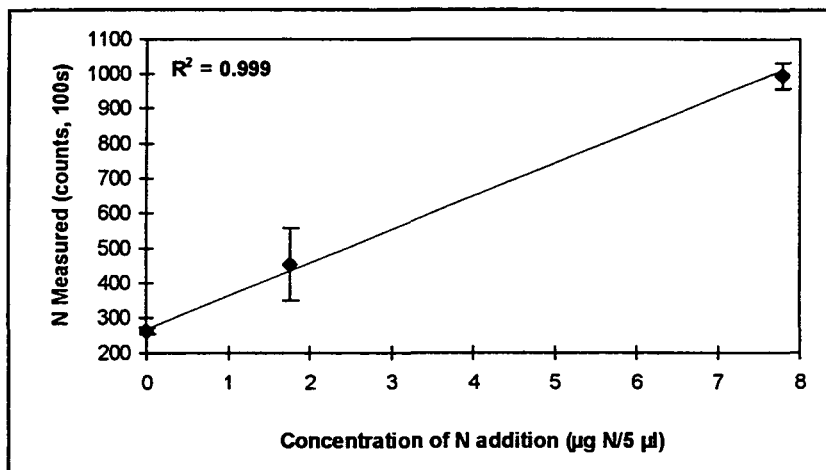


Figure 45. Linear relationship for the nitrogen measured from the tryptophan model fuel nitrogen addition to Southern Pine III black liquor.

literature.⁵ In each plot, the representative equation is given along with the correlation coefficient, R^2 , providing a measure to judge the fit of the data. The data represented in Fig. 47 indicate a reasonable fit considering the plots contain data for 14 liquors over a range of temperatures (600–1000° C). A slightly better fit may be attained, for instance, if only one temperature is considered for all of the liquors—pyrolysis at 800° C provided a correlation coefficient of $R^2 = 0.81$ for the relationship between % N released as NO vs. the % N in the liquor. The relationships presented in Fig. 47 further support the low temperature sensitivity of fuel NO_x formation which was also observed in the kinetic and heating rate evaluations.

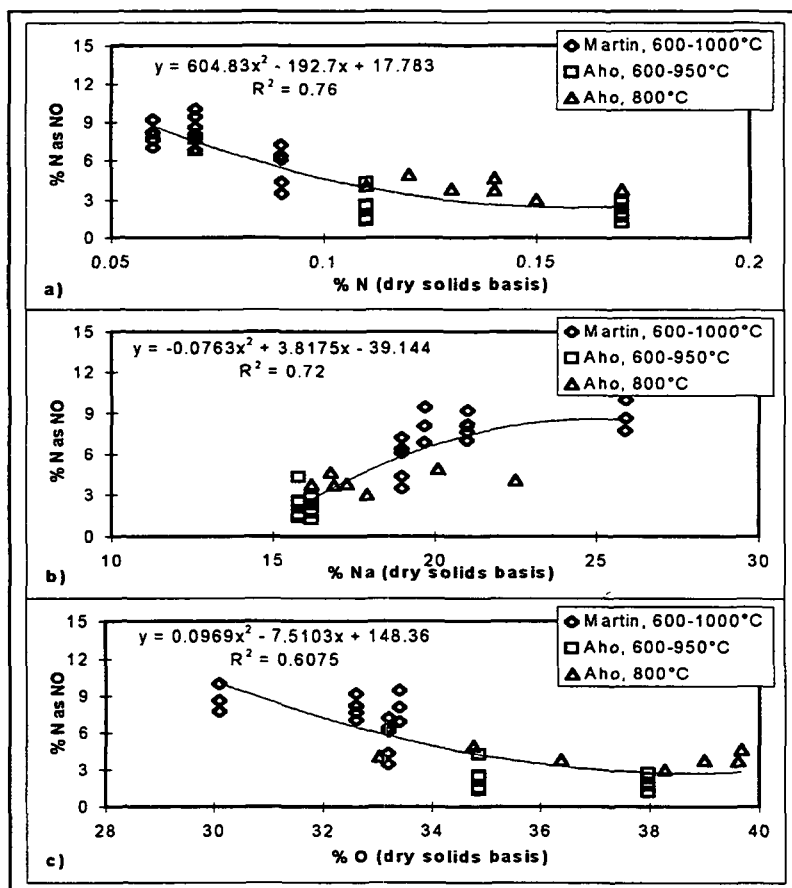


Figure 47. Relationships for percent nitrogen released as NO during pyrolysis with respect to a) nitrogen, b) sodium, and c) oxygen content in the liquor. Pyrolysis at 600–1000° C in inert N_2 .

Basic relationships for recovery furnace data have been reported by Clement and Barna.⁸⁷ They reported linear correlations for the relationship between the nitrogen in the liquor and the NO_x emissions ($R^2 = 0.37$) and for the conversion to NO_x based on the liquor nitrogen content ($R^2 = 0.56$). The data employed for the various liquors in this work, pyrolyzed on a laboratory scale, provided a better fit. Relationships were examined for other elemental components as well; however, the correlation coefficients were low indicating high error, and therefore, would not be of significance in future work.

Relationships for the major liquor component content, oxygen, carbon, sodium, and sulfur, divided by the nitrogen content are presented in Fig. 48. The relationships for these components with respect to the amount of nitrogen measured as NO show good fit for the range of liquors for pyrolysis at 600 and 800° C.

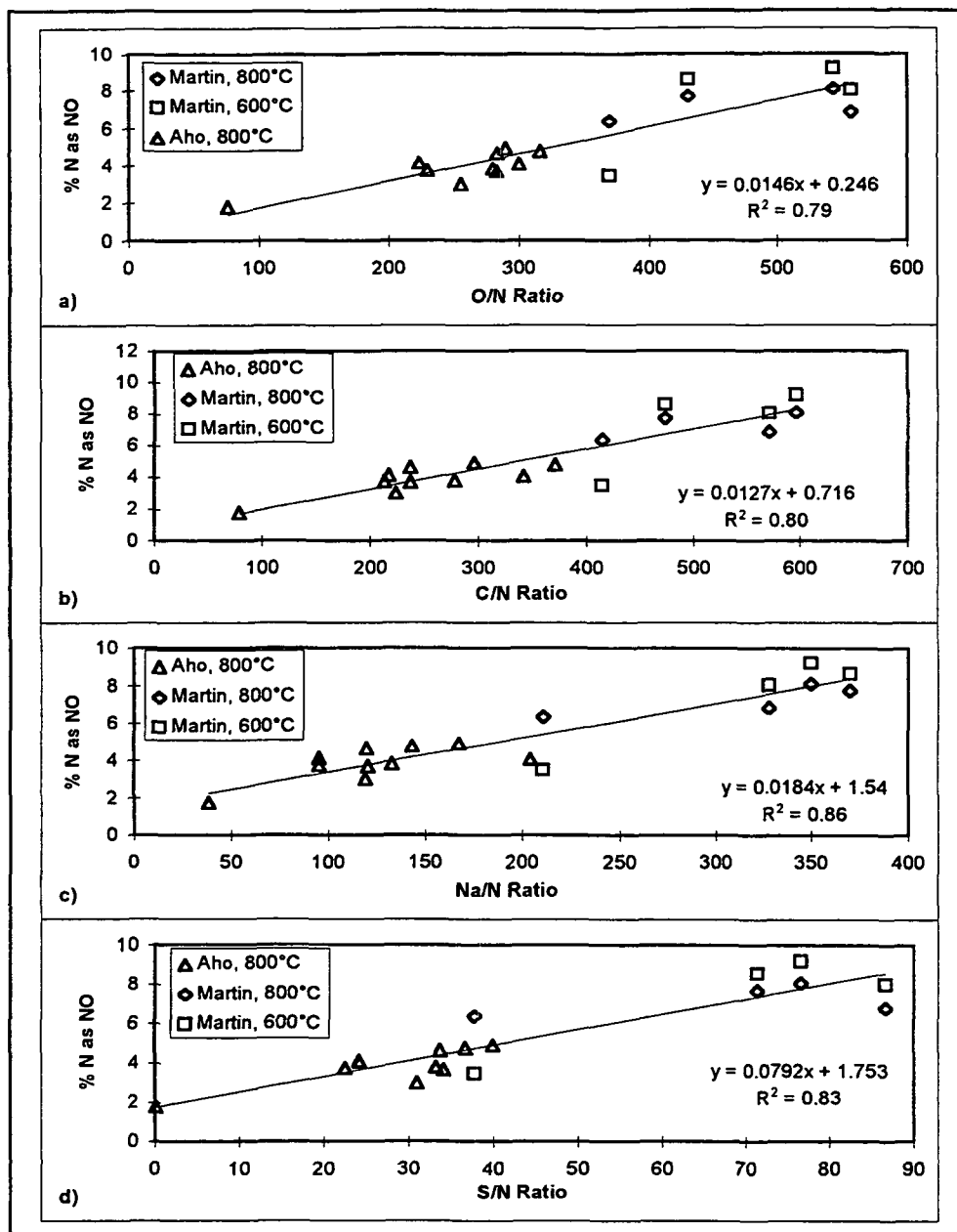


Figure 48. Relationships for percent nitrogen released as NO during pyrolysis with respect to a) O/N, b) C/N, c) Na/N and d) S/N ratios in the liquor. Pyrolysis at 600 and 800° C in inert N₂.

Relationships for the GPNP nitrogen measurements (%N based on black liquor dry solids) under pyrolysis and combustion conditions were also plotted for the southern pine liquor compositions. The data is presented in Fig. 49 for the ratios of the liquor

The general relationships observed for the conversion to NO_x and NO_x precursors with respect to the liquor component/liquor nitrogen ratios are opposite those previously noted for the relationships indicated for the conversion to NO. (See Fig. 48.) While it is recognized that the liquor components are by definition related to each other, the possibility of the more dominant species to control the gas phase chemistry exists. For example, a trade off in the amount of SO_x and NO_x has been noted for combustion of black liquor⁸⁸ as well as for high sulfur coals.⁸⁹ It is thought that SO_2 (g) influences the nitrogen chemistry which results in a catalytic reduction of NO to N_2 . The relationship for the S/N ratios, plotted as Fig. 49 d), suggest this possibility. At low S/N ratios, the amount of sulfur relative to the nitrogen content is low and therefore, the GPNP nitrogen concentration, which includes NO, is high. As the ratio increases, the sulfur content relative to the nitrogen also increases. At the higher ratios, less GPNP nitrogen is measured.

Significance of Black Liquor Pyrolysis Results

Gas phase NO_x and NO_x precursor measurements of fractionated liquor samples during both analytical combustion and liquor pyrolysis further verified that black liquor nitrogen is primarily organic in nature. Gas phase NO_x and NO_x precursor release during pyrolysis indicated a range of values from 35% to nearly 90% as compared with the measurements made during analytical combustion.

Single drop pyrolysis indicated volatiles release to plateau for temperatures from 500–700° C before increasing further with the release of sodium species at temperatures

up to 1000° C. It was found that little nitrogen was converted to NO at temperatures of 300–400° C. Yet, at temperatures $\geq 600^{\circ}\text{C}$, the NO formation was fairly steady indicating about an 8% average of the original liquor nitrogen to convert to NO. Similarly, the nitrogen remaining in the char was found to stabilize at about 50% on average based on the original liquor nitrogen for $T \geq 500^{\circ}\text{C}$. The nitrogen unaccounted for was thought to be released as fuel NO_x intermediates, such as NH₃ and HCN, and also as N₂.

The addition of known compounds supports the results achieved with model compounds in terms of the inorganic addition effects. These results help bridge the gap between the results obtained for the model fuel nitrogen compounds and for the application of these results to industrial processes.

Simple relationships were noted for the nitrogen released as NO or as intermediate gas phase species, with respect to composition, for the liquors. Good correlations were achieved, with respect to the nitrogen, sodium, and oxygen species in all cases. These relationships can be used for initial evaluation of a mill's potential to emit NO_x based on liquor composition.

IN SITU REACTIONS OF GAS PHASE NITROGEN SPECIES

Effect of Residence Time

The effect of residence time in the gas phase on the conversion of the fuel nitrogen species to gas phase NO_x precursors was evaluated using the PCL pyrolysis furnace. Several experiments were conducted where the gases were held in a static inert environment for a given time before the GPNP concentration was measured. A typical nitrogen profile of the release with time and temperature is shown in Fig. 50 for a) $t = 0$ sec delay, b) $t = 230$ sec delay, and c) $t = 410$ sec delay. Static conditions were maintained during the heat up period to 400°C .

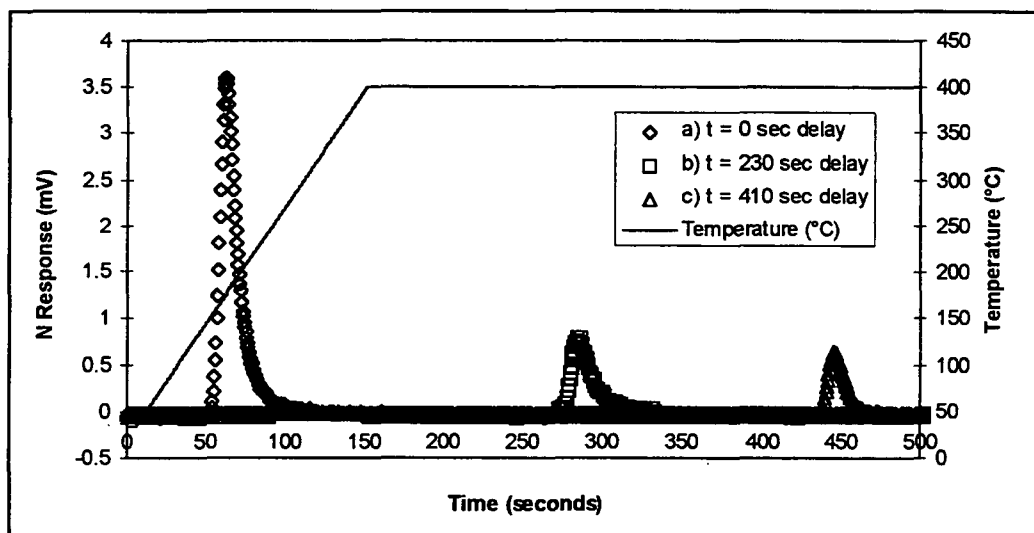


Figure 50. Gas phase NO_x precursors evolution profile with residence times of a) $t = 0$, b) $t = 230$, and c) $t = 410$. Model fuel nitrogen source was proline.

An example of the depletion data is presented in Fig. 51 for model fuel nitrogen compounds, glutamic acid and proline, at concentrations of $2.5\ \mu\text{g N}$. The first column

represents the nitrogen released as gas phase NO_x precursors under pyrolytic conditions with continuous gas flow during heating to and at 400°C . This represents the control or base test result for each sample where $t = 0$. The second column represents the total nitrogen released as GPNP as determined after the given time delay. The difference between the two values represents the effect of the gas phase residence time on the GPNP detected.

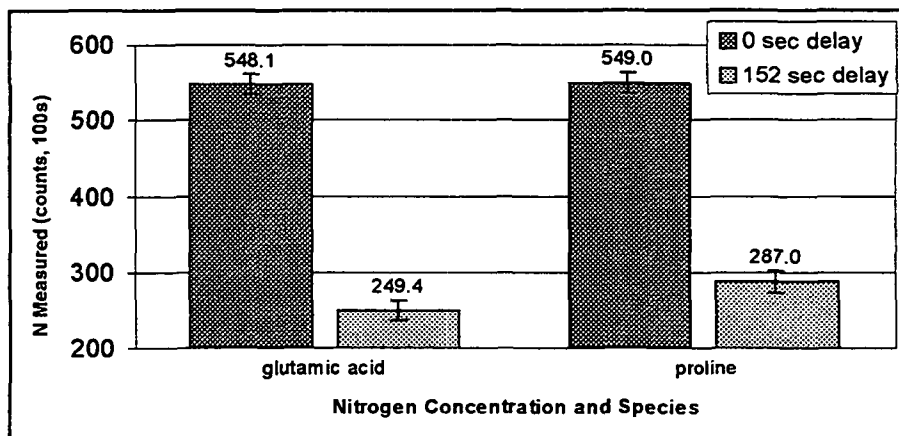


Figure 51. Effect of pyrolysis gas residence time on fuel nitrogen conversion to gas phase NO_x precursors during pyrolysis at 400°C .

Reduction of the measured gas phase NO_x precursors is 54.5% for glutamic acid and 47.7% for the proline with an increased residence time of 152 sec. Further, the GPNP species from glutamic acid appear to react with each other more readily to deplete the total GPNP concentration measured as compared to the those from heterocyclic bound nitrogen in proline. Heterocyclic nitrogen species are known to be more stable than straight-chain amines.^{16, 76}

The increased residence time allowed the gas phase NO_x intermediates, such as HCN and NH_3 , to remain at a high concentration allowing for reactions to occur

generating N_2 . When no residence time is allowed for the gases to react, the gas phase NO_x precursors remained as intermediates until undergoing the high-temperature, excess-oxygen combustion in the next chamber of the furnace where the species were easily oxidized then immediately measured.

Similar behaviors were exhibited by pyrazine and glutamic acid. The effect of residence time on the depletion of the NO_x intermediate pyrolytic gases is shown in Figures 52 and 53. Significant depletion is noted after the initial increase in residence time. Gas phase NO_x intermediate measurements from proline and glutamic acid exhibited a decrease of 80 and 85% after 290 seconds and of 86 and 88% after 410 seconds, respectively, while pyrazine had a decrease of 48 and 64% for the same residence times. Again, the increased stability of the heterocyclic nitrogen species is exhibited by the pyrazine gas phase species. Pyrazine is a six-member aromatic, heterocyclic di-nitrogen compound and would tend to exhibit greater stability than a five-member nitrogen heterocycle, such as proline. This is shown explicitly in Fig. 52.

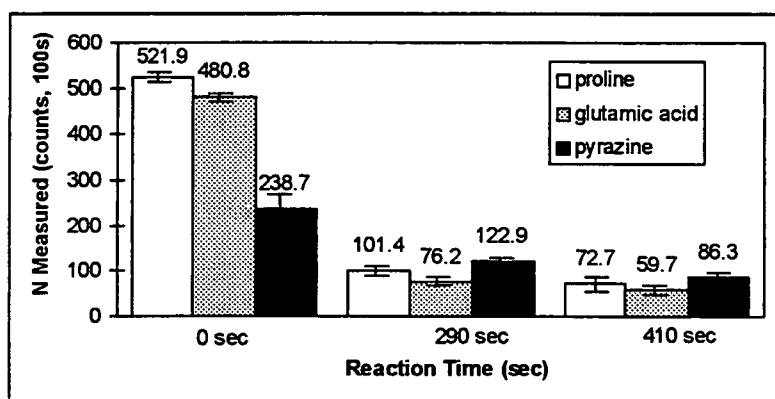


Figure 52. Effect of residence time on the GPNP depletion under static pyrolysis conditions for proline, glutamic acid, and pyrazine fuel nitrogen species at concentrations of $2.5 \mu\text{g N}/5 \mu\text{l}$.

The measurements from proline pyrolysis at various concentrations indicated the depletion to be consistent. For the range of concentrations indicated in Fig. 53, the depletion was $78.3\% \pm 3.8\%$ at 290 seconds and $84.7\% \pm 1.2\%$ at 410 seconds. Again, constant conversion over a range of concentrations suggests a first-order reaction to be occurring. This hypothesis of a first-order reaction was further investigated and the results are presented in the following section.

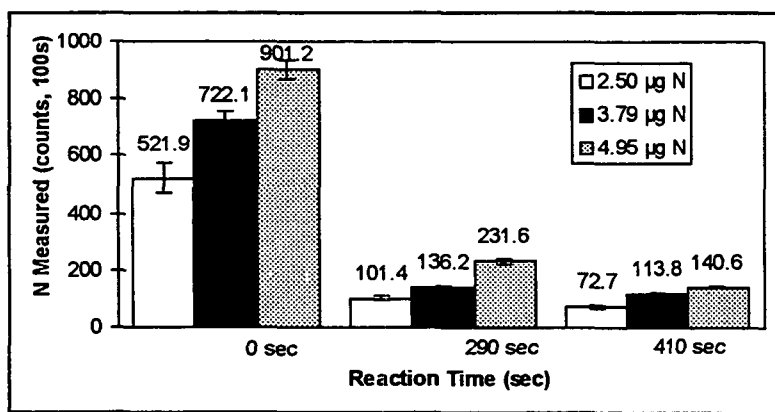


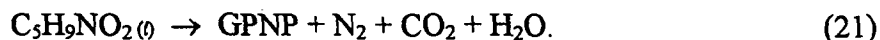
Figure 53. Effect of gas phase residence time on NO_x precursor depletion under static pyrolysis conditions where proline was the source of fuel nitrogen at the concentrations indicated.

Kinetic Analysis of Gas Phase NO_x Precursor Depletion

A kinetic evaluation was done using proline as the model fuel nitrogen source. An evaluation of the rate of depletion of the gas phase NO_x precursor nitrogen was conducted for pyrolysis conditions at various residence times. Proline at concentrations of 2.564, 3.789, and 4.954 $\mu\text{g N}/5 \mu\text{l}$ (0.0366, 0.0541, and 0.0707 mol/L) served as the source of fuel nitrogen species for the evaluation. Reaction of a fuel nitrogen species, such as proline ($\text{C}_5\text{H}_9\text{NO}_2$), during pyrolysis can be characterized as:



Measurements were taken of the GPNP species which are the sum of NO, HCN, NH_i, and any other fuel NO_x intermediate species, NX_x. As such, the initial pyrolysis reaction can be more simply written as:



As time progresses, some of the gas phase NO_x precursors will react irreversibly forming inert N₂. Therefore, the reaction in Eq. 21 can be written strictly in terms of the nitrogen species for complete reaction as:



This reaction describes the conversion of proline fuel nitrogen into a gas phase NO_x precursor-type (GPNP) species during pyrolysis with subsequent reaction of the GPNP species to inert N₂(g). For the experimental system used here, the pyrolysis reaction occurs as a batch process with the proline sample being rapidly pyrolyzed to GPNP species and N₂(g). This mixture is held in a static helium-based gas environment for a specified time at a specified temperature. At the end of the reaction time, a helium carrier gas is introduced into the system to move the “plug” product gases into the analytical-combustion chamber where the measurement of the residual gas phase NO_x precursory species occurs.

The system is assumed to be a homogeneous gas phase batch or plug flow process, and therefore, any dispersion of the pyrolytic gases due to the introduction of the carrier gas would invalidate the plug flow assumption. Calculations indicated that the nitrogen

pyrolysis gases would be well mixed in the reactor tube validating the homogeneous gas phase assumption (see Appendix IX). The effect of dispersion was also evaluated and found to be negligible for the reactor conditions. (See Appendix IX.) Thus, the reaction process is assumed to be a batch process with homogeneous gas-phase reactions occurring.

Determination of the Rate Equation. The basic kinetic theory is provided below for a first-order irreversible rate equation. This type of equation is chosen because reactions which form $N_2(g)$ are irreversible at these temperatures and because simple homogeneous gas-phase reactions tend to follow first-order kinetics. The kinetic theory is then applied for determination of the rate equation which is evaluated in two steps. Using the integral method, the concentration dependency is found followed by a determination of the temperature dependency. Determination of each of these steps is presented and discussed.

The first-order rate equation given by Levenspiel⁹⁰ in terms of reactant consumption or product formation is

$$-r_A = r_B = -\frac{dC_A}{dt} = kC_A \quad (23)$$

where separation and integration yields

$$-\int_{C_{Ao}}^{C_A} \frac{dC_A}{C_A} = k \int_0^t dt \quad (24)$$

and

$$-\ln \frac{C_A}{C_{Ao}} = kt \quad (25)$$

where A = the component of interest; here, nitrogen,
 C_A = the gas phase concentration of GPNP (mol/l) at a given time, t ,
 C_{Ao} = the gas phase concentration of GPNP (mol/l), at time $t = 0$,
 k = the rate constant (sec^{-1}), and
 t = the time of reaction (sec).

Concentration Dependency. Applying the rate equation for reaction of gas phase NO_x precursors from the fuel nitrogen pyrolysis experimental system, the concentration dependency is determined. A plot of $\ln (C_A/C_{Ao})$ versus time, t , as indicated in Fig. 54, gives a straight line supporting the assumption of a first-order expression. Note that it is assumed that any depletion in NO_x directly relates to a corresponding increase in N_2 . Concentration and reaction time data are provided in Table 13.

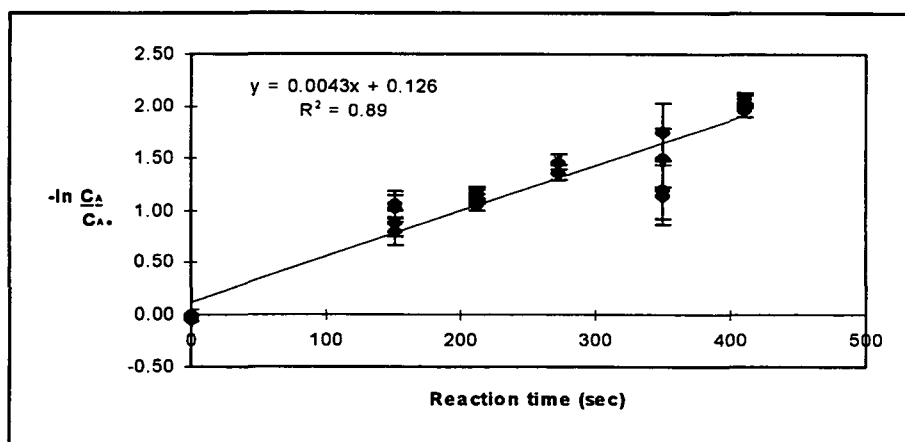


Figure 54. Test for the first-order reaction of gas phase NO_x precursors, Eq. 22, at 673 K.

Table 13. Concentrations of gas phase NO_x precursors at various reaction times where $C_{Ao} = 0.0393$ mol/l for $T = 673$ K.

Reaction Time (sec)	C_A (mol/l)	$-\ln(C_A/C_{Ao})$
152	0.014	1.016
152	0.018	0.791
152	0.014	1.056
152	0.016	0.871
212	0.012	1.162
212	0.013	1.105
212	0.012	1.139
212	0.014	1.045
272	0.0101	1.354
272	0.0091	1.459
350	0.0118	1.196
350	0.0124	1.143
350	0.0087	1.500
350	0.0068	1.746
410	0.0051	2.042
410	0.0055	1.957
410	0.0049	2.074

Verification that the gas phase NO_x precursor reaction was first-order with respect to the NO_x precursor gas phase concentration was accomplished by measuring the conversion was for initial gas phase NO_x precursor concentrations of 0.03663, 0.05405, and 0.07074 mol/L at a temperature of 673 K. If the reaction is first order, the conversion is a function of temperature but is independent of the initial concentrations. The results are given in Table 14 and are plotted in Fig. 55 as conversion vs. concentration. The percent conversion was defined as

$$X = 100 \left[1 - \left(\frac{C_A}{C_{Ao}} \right) \right] \quad (26)$$

Table 14. Percent conversions (Eq. 26) of gas phase NO_x precursor. Concentrations of initial reactant and the product gases are given at reaction times of 290 and 410 sec for 673 K.

C_{A0} (mole/l)	$C_{A\ 290}$ (mole/l)	$C_{A\ 410}$ (mole/l)	Percent Conversion	
			290 sec	410 sec
0.03663	0.00714	0.00506	80.50	86.18
0.03663	0.00781	0.00548	78.69	85.04
0.03663	0.00867	0.00713	76.32	80.53
0.03663	0.00000	0.00490	—	86.62
0.05405	0.01014	0.00932	81.24	82.75
0.05405	0.00971	0.00853	82.03	84.21
0.05405	0.01109	0.00800	79.48	85.20
0.07074	0.01793	0.01021	74.66	85.56
0.07074	0.01737	0.01096	75.45	84.51
0.07074	0.01731	0.01078	75.54	84.77

In Fig. 55, the average conversions are 78.2% and 84.5% with standard deviations of 1.77% and 3.78%, respectively, for 290 sec and 410 sec reaction times. The conversion in Fig. 55, as previously indicated in Fig. 51, is constant for the concentration ranges presented, which provides additional support for a first-order reaction.

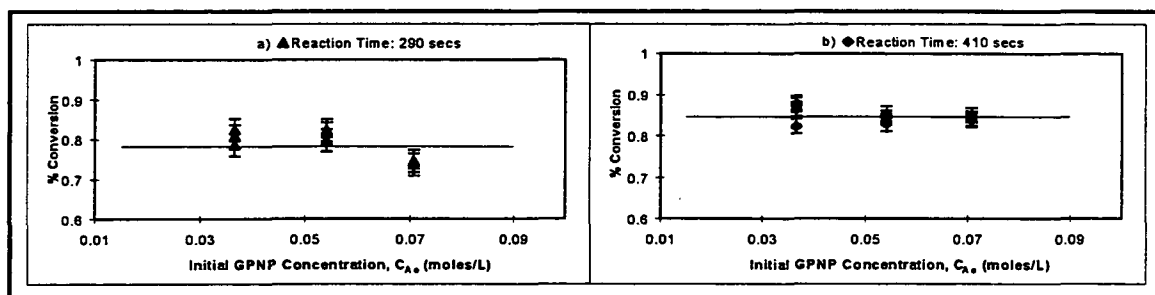


Figure 55. Conversion of gas phase NO_x precursors to N_2 during static pyrolysis is independent of initial concentration. a) 290 sec reaction time. b) 410 sec reaction time.

Temperature Dependency. Temperature dependency of the first-order reaction is determined by evaluating the rate constant for the gas phase NO_x precursor conversion at

temperatures of 573–973 K for a given reaction time of $t = 450$ sec. The data, given in Table 15, are plotted as $-\ln(C_A/C_{A0})$ versus time, t , in Fig. 56.

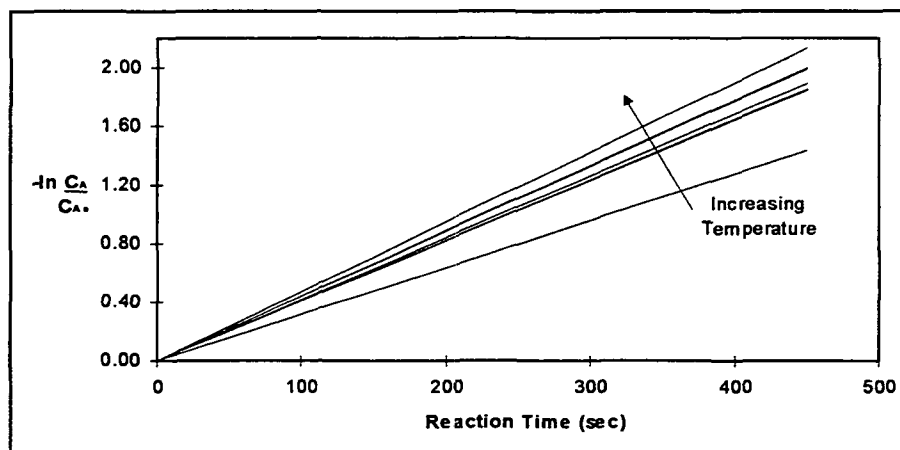


Figure 56. Temperature dependency of first-order rate equation.

Table 15. Concentration data for temperature dependency determination, $C_{A0} = 0.0366$ mol/l.

Sample ID	C_A (mol/l)	Reaction Time (sec)	$-\ln(C_A/C_{A0})$	T(K)	k
N4147071	0.00833	450	1.559	573	0.0032
N4147072	0.00955	450	1.421	573	0.0032
N4147073	0.01052	450	1.325	573	0.0032
N4147061	0.00639	450	1.824	673	0.0044
N4147063	0.00621	450	1.852	673	0.0044
N4147064	0.00632	450	1.835	673	0.0044
N4147051	0.00566	450	1.944	773	0.0044
N4147052	0.00522	450	2.025	773	0.0044
N4147053	0.00520	450	2.029	773	0.0044
N4147041	0.00627	450	1.842	873	0.0041
N4147042	0.00627	450	1.843	873	0.0041
N4147044	0.00615	450	1.861	873	0.0041
N4147031	0.00571	450	1.937	973	0.0044
N4147032	0.00583	450	1.916	973	0.0044
N4147033	0.00489	450	2.092	973	0.0044
N4146211	0.00471	450	2.128	873	0.0047
N4146212	0.00448	450	2.178	873	0.0047
N4146214	0.00493	450	2.082	873	0.0047
N4146205	0.00587	450	1.908	773	0.0042
N4146204	0.00731	450	1.689	773	0.0042
N4146203	0.00580	450	1.920	773	0.0042
N4146202	0.00511	450	2.047	773	0.0042

The Arrhenius equation, Eq. 27, is used to determine the energy of activation for the rate expression.

$$k = k_o e^{-E_a/RT} \quad (27)$$

The plot of $\ln k$ vs. $1/T$ (K^{-1}) in Fig. 57 indicates the slope, $-E_a/R$, to be -427.49 ± 35.10 K. As such, the energy of activation, E_a , equals 850 cal/mol for gas phase NO_x precursor depletion at 573–973 K. The activation energy indicates a weak temperature sensitivity. This follows closely to the weak temperature dependence found for the formation of fuel NO_x .² This further indicates that, for this reaction, the gas residence time is more important in the depletion reaction than the temperature at which the reaction occurs.

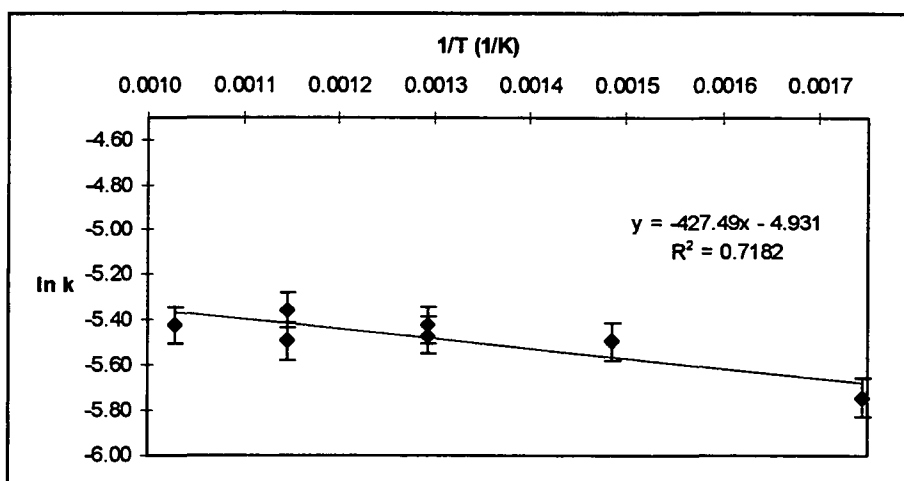


Figure 57. Arrhenius plot for determination of activation energy for the conversion of gas phase NO_x precursors.

Interpretation of Kinetic Data

The residence time of the GPNP species was important in understanding the fractional conversion of the fuel nitrogen to GPNP. At gas phase residence times up to 450 seconds, depletion of the GPNP species was determined to be as great as 85%. The depletion was noted to follow first-order reaction kinetics with a low energy of activation and in turn, a low temperature dependency.

A more complicated reaction mechanism for the depletion likely occurs. The low activation energy along with the correspondingly low temperature sensitivity suggests that either radical reactions are important in the depletion mechanism or that the depletion is assisted by some form of catalytic process to reduce the experimental activation energy.

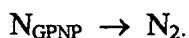
Radical reactions are known to decrease the activation energy for a reaction pathway.⁹² Likewise, catalytic reactions provide a lower activation energy such as observed for the depletion reaction of NO_x precursor species. For instance, the presence of CO has been noted to enhance the depletion of NO gas over black liquor char⁵⁸ as well as coal chars.⁴⁴ Carbon monoxide is present in this system as a pyrolysis product and may contribute to the depletion reactions which occur. It appears that a more complicated chemical and physical process is required to identify the complete mechanism for the depletion of the gas phase NO_x precursor species.

CONCLUSIONS

1. Conversion of nitrogen to NO for various nitrogen compounds ranged from 35–91% for the total nitrogen PCL measurement at 1100° C and > 75% O₂. The conversion was found to depend on the nitrogen species chemical structure. Nitrate and ammonium compounds, for example, converted at equivalent rates, ~ 90 and ~ 38%, respectively. The conversion was the same regardless if the nitrate was present as AgNO₃ or as NH₄NO₃ or if the ammonium was present as NH₄Cl, NH₄NO₃, or (NH₄)₂SO₄. Amine and heterocyclic nitrogen species conversion was variable depending on the chemical structure of the individual nitrogen compound. For instance, tryptophan, which has nitrogen bound in a five-member ring and also as an amino group, showed a nitrogen conversion to NO of ~ 62%, whereas glutamic acid, an amine, indicated only a 45% conversion to NO and proline, a five-member nitrogen species, indicated a conversion to NO of only 35%. The conversion of the fuel nitrogen to NO was found to be more dependent on the chemistry involved rather than the thermodynamics or kinetics of the experimental system.
2. Black liquor nitrogen content varied from 0.06–0.12%. The black liquor nitrogen was found primarily in the acid-precipitated liquor fraction which is composed of predominantly lignin-type compounds. Up to 97% of the total black liquor nitrogen can be accounted for in this fraction. This was confirmed by independent measurements of the nitrogen content in the remaining black liquor fraction which was

shown to contain only 3–6% of the total black liquor nitrogen. Closure of the nitrogen balance was achieved at levels of $\pm 10\%$.

3. Both straight-chain and five- and six-member heterocyclic nitrogen structures were found in black liquor. Various species of black liquor nitrogen present indicate that multiple fuel nitrogen pathways which form fuel NO_x may be possible. Several potential pathways for the formation of CN and NH_i as precursor species for fuel NO_x , from the pyrolysis of proline and glutamic acid, have been suggested. It was found that both species go through pyrrole-type intermediates which then may yield the CN or NH_i intermediates. The results indicate that these species may follow similar decomposition pathways such that both the CN and NH_i fuel NO_x intermediates may be formed.
4. A reduction in the conversion to NO_x was measured for increased residence times during static inert pyrolysis. Pyrolysis gases were held in the PCL reactor to allow for the gas phase NO_x precursor species to react. Reduction of the NO_x measured, by as much as 50%, was achieved for reaction times of ~ 150 sec. Greater reductions were measured at longer residence times.
5. The kinetics for the depletion of gas phase NO_x precursors, GPNP, in the PCL pyrolysis reactor followed a first-order irreversible gas phase reaction:



The first-order reaction provided an experimental activation energy of 850 cal/mol which indicates a weak temperature sensitivity. The low activation energy is suggestive that radical or catalytic reactions are involved in the depletion.

6. During pyrolysis of model fuel nitrogen compounds, all of the nitrogen was released by 400° C regardless of the heating rate. All black liquor nitrogen was released by about 500° C under inert pyrolysis conditions.
7. No effect on the total gas phase NO_x precursor concentration was observed for heating rates up to 150° C/min. At heating rates from 10 to 1000° C/sec, no effect was observed on the pyrolytic gas-phase composition.
8. The addition of alkali to model fuel nitrogen species reduced the fuel nitrogen conversion to NO_x precursors. The decrease in conversion was enhanced by increasing the concentration of alkali in the sample. The fuel nitrogen conversion was decreased about 10% when model compounds were added to black liquor and then pyrolyzed.
9. No significant effect of oxygen was observed under pyrolysis conditions in PCL pyrolysis furnace.

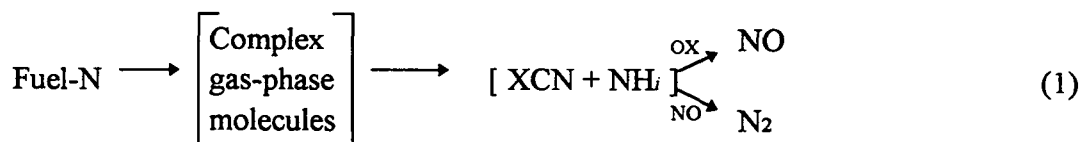
CONTRIBUTIONS

The results of this work have specific applications in providing understanding 1) of the total nitrogen analyses employed by industry and 2) of fuel NO_x formation in regard to general stationary combustion processes and specifically for black liquor combustion. The results of the total nitrogen measurement with the PCL method indicate the dependency of the accuracy of the PCL method on being able to match the chemical form of the nitrogen in the standard employed, as well as the matrix within which the nitrogen is bound, to the form of the nitrogen in the sample. Having this knowledge, accurate results could be obtained using the new PCL method as compared with the traditional Kjeldahl or the LECO methods. However, the overall comparison of the total nitrogen techniques indicates that a critical evaluation of any reported total nitrogen value is required.

In terms of the insight gained to enhance the understanding of fuel NO_x formation, the results provide increased knowledge of formation processes as well as specific applications to the combustion of black liquor. Both of these applications are discussed to emphasize the knowledge gained and to apply the results in a practical environment.

INSIGHT INTO FUEL NO_x FORMATION

The formation of fuel NO_x has been characterized in this thesis simply by Eq. 1, presented previously and shown below, despite its complicated pathway.



Many of the numerous reactions involved for the conversion of HCN and NH_i intermediates to NO have been characterized and reported in the literature from fossil fuel combustion.¹² These data can be applied to black liquor combustion. However, little knowledge was available for the types of fuel-N species in black liquor or for the conversion of the fuel nitrogen to NO_x intermediates HCN and NH_i . Results have been reported here identifying the types of fuel nitrogen species in black liquor. In addition, possible pathways that model fuel nitrogen species undergo during formation of the HCN and NH_i intermediates also have been reported. These findings, while specific to black liquor pyrolysis, can also be applied to the general knowledge of fuel NO_x formation from stationary combustion sources.

RECOVERY FURNACE APPLICATION

The empirical data collected in this thesis may be useful as input data for IPST's recovery furnace model. Implementation of the results into the computer model may provide a more complete understanding of the recovery furnace gas phase processes. Also, the data could be valuable if used to suggest alternative ways to control NO_x .

Application of the results for modification of recovery boiler operating conditions is limited, but the results may provide a better understanding of NO_x emissions from recovery boilers. It may be possible for a mill to evaluate its potential to emit NO_x based on the black liquor composition and to some extent on recovery boiler operating conditions. For instance, the relationships presented could be used as a basis for improving the understanding of gaseous nitrogen chemistry in the furnace. The

information obtained may also be instructive in selecting the best NO_x control techniques. Further, the information may be valuable in understanding how changes in operating conditions will affect NO_x emission levels. Some alternative NO_x control strategies are presented below.

Alternative NO_x Control Strategies

Current NO_x control strategies include the use of biased firing, air staging and low excess air firing, and fuel nitrogen doping.⁴⁹ However, these methods were developed for the reduction and elimination of thermal NO_x. These methods may have limited success in a recovery boiler where NO_x emissions are generated from the nitrogen in black liquor. Based on the reported conversions of the fuel nitrogen species and the results of their pyrolysis and combustion, some alternative NO_x control strategies may be available for recovery furnace operations.

The nitrogen species are important with respect to the degree of fuel nitrogen conversion attainable within a combustion environment. The amine type species tend to exhibit lower conversions and therefore, would be the preferable form of nitrogen in the pulp wood. This result is supported by the fact that ammonia and urea nitrogen species (both with R-NH₃ structures) are functional in reducing NO_x when injected into the gas stream.^{39, 91} Nitrate species should be avoided as their conversion during combustion remains high regardless of its structural bonding.

Evaluation of the sodium species in the matrices indicates that the inorganic composition of black liquor is likewise important. Modification of the sodium species

ratios may be a place to lower the conversion of fuel nitrogen to NO_x and NO_x precursors. The addition of both NaOH and Na_2CO_3 lowered the amounts of gas phase NO_x measured. Therefore, higher concentrations of both of these in the liquor, e.g. increasing the dead load in the furnace, should not adversely affect the anticipated NO_x emission levels.

In terms of operating conditions, pyrolysis in a static environment would be most preferable to enhance the depletion of NO_x intermediate species. Rapid mixing with O_2 is likely to increase fuel NO_x formation as well as any mixing environment which would dilute the nitrogen volatile gas concentrations locally thus inhibiting the likelihood of the in situ depletion reactions from occurring. Therefore, char bed combustion or liquor burning on the wall may be preferable to in-flight combustion.

SUGGESTIONS FOR FUTURE WORK

Based on the experimental work and the data analysis completed, the following suggestions are presented for continued work to gain further understanding of the fundamental nitrogen chemistry involved during NO_x formation from recovery boiler operations and to improve the analytical techniques used for nitrogen analyses.

Further investigation of the gas phase depletion which occurs among the pyrolysis products of the fuel nitrogen species is warranted. The results indicated the depletion to follow simple first-order kinetics. The system appeared to be more complex than what could be described by diffusion theory and requires further investigation to provide a more accurate explanation of the gas phase nitrogen chemistry involved. Catalytic processes were suggested to play a role and further investigation of these processes, specifically the reaction which occur in the presence of CO, would provide further insight.

The pyrolysis GC/MS is a valuable tool for identifying gas phase species during fuel NO_x formation. It is thought that a great deal of further information could be obtained to understand the nitrogen gas phase composition and subsequent NO_x formation and depletion mechanisms by continuing work in this area. It is recommended that a GC column be used to look more closely at the lower molecular weight nitrogen gases, such as NH_3 , HCN , and N_2 , and quantitative studies be completed to support the qualitative results reported here. The addition of CO or SO_2 to the gas phase during pyrolysis would also allow for quantification of the catalytic effects of these species in the reduction of NO to N_2 . In addition, the kinetics for the formation of the various fuel nitrogen model compounds is also recommended.

A thorough investigation of the nitrogen release with respect to the sulfur and carbon species could be achieved with the use of the high-temperature pyrochemiluminescence analyzer. The analyzer currently has a UV detector for sulfur species and a NDIR CO₂ analyzer could readily be situated on the exhaust line for detection of total carbon. In particular, the relationships with sulfur are important to black liquor combustion processes in light of the NO_x/SO_x tradeoff which has been noted to exist.

The comparison of total nitrogen measurements which was presented stresses the importance of being critical in evaluating absolute nitrogen values reported. It also presents a need to have a standardized method to use for the total nitrogen analysis of black liquor and char samples as well as other industry samples. Work to establish a standard for the PCL high temperature total nitrogen method would be valuable

EXPERIMENTAL EQUIPMENT AND METHODS

The experimental methods used to collect data throughout this work are given in the following section. An instrument description and the operating conditions are provided along with other pertinent experimental parameters for the four major pieces of equipment used. Finally, chemical analysis information is given.

Basic principles of the analytical and spectrometric techniques are briefly presented to provide an understanding of the instrumental analyses employed. Development and verification of methods used is given in the Appendices as indicated. Lists of equipment and materials are given in Appendix I, while sample preparation information is given in Appendix IV.

PYROCHEMILUMINESCENCE (PCL) NITROGEN ANALYZER

Instrument Description

Nitrogen analyses were conducted using a pyrochemiluminescence (PCL) nitrogen analyzer.⁷⁰ The relative conversions of the fuel nitrogen to gas phase NO_x and NO_x precursor species (GPNP which equals the sum of NO plus any oxidizable intermediates such as HCN and NH_i) for several nitrogen species were determined. The effects of various sodium salts at equivalent concentrations and at increasing concentrations on the nitrogen response of several model fuel nitrogen compounds were also evaluated.

Samples are placed in a quartz boat and are inserted into a horizontal tube reactor inside of a tube furnace where they are combusted. A sample drive was used to introduce

liquid and solid samples into the analyzer for combustion while the gas sampling inlet system was used for controlled introduction of gaseous samples.

Samples were combusted such that all of the fuel nitrogen was assumed to be converted to the oxidized form of nitrogen, NO. The NO and other combustion gases are sent through a membrane dryer before entering the ozone generator. Here, NO reacts with ozone, O_3 , to form excited nitrogen dioxide, NO_2^* . As the excited molecule decays, light is emitted and then detected with a photomultiplier tube within the nitrogen detector assembly.⁷⁰ The total nitrogen result is determined by the light response emitted by the unknown sample compared with that of a known standard material. The secondary ozone is sent back into the furnace to reduce it to inert O_2 before it is exhausted with the other combustion gases. Detail of the reactor is shown in Fig. 59.

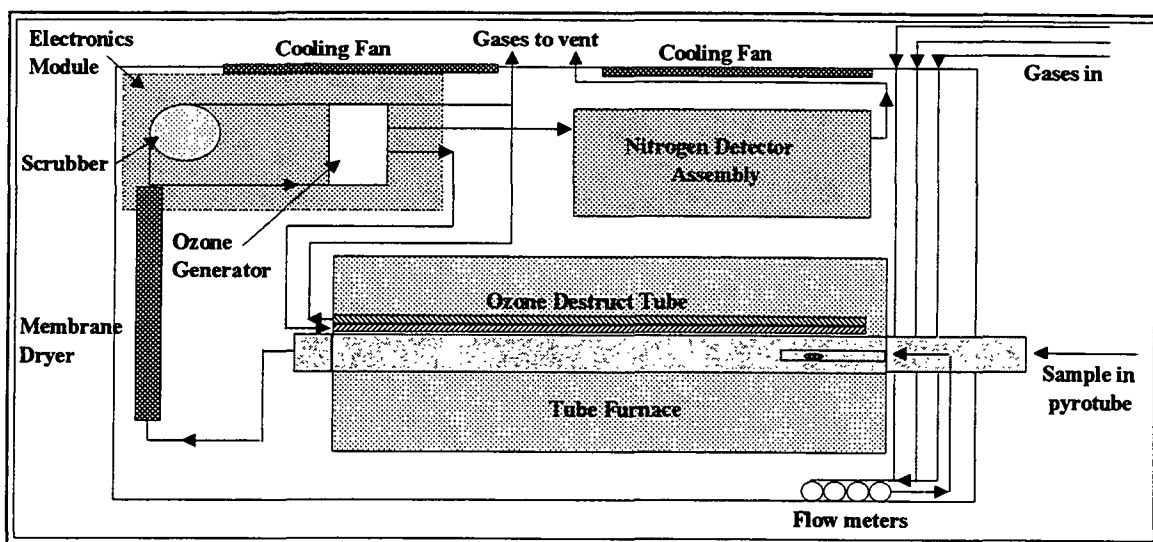


Figure 59. Overhead diagram of the PCL nitrogen analyzer system components.

Operating Conditions

High-temperature combustion followed by chemiluminescence detection is a relatively new method used to determine total nitrogen. For many sample types, very good results can be achieved in the range of 0.001–1% N or greater. The method employs combusting a small amount of sample in a high-temperature, oxygen-rich (>75% O₂) environment oxidizing all gas phase NO_x precursor (GPNP) species present to NO. Helium was used as a carrier gas. Note that the conditions employed do not generate thermal NO_x from N₂ in the atmosphere as the temperature is too low. Method development and verification data are provided in Appendix II.

PYROLYSIS USING THE PCL NITROGEN ANALYZER

Instrument Description

Pyrolysis experiments were carried out in a tube reactor with a temperature-programmable furnace which can be directly attached to the PCL nitrogen analyzer. Heating rates from 1–150° C/min were capable but most experiments were run at a rate of 150° C/min to a final temperature. Final pyrolysis temperatures from 300–700°C were used.

Operating Conditions

Conversion of fuel nitrogen to GPNP species was measured under various pyrolytic conditions. Pyrolysis of several model fuel nitrogen compounds was conducted in inert (pure helium gas) and oxidative (~15% O₂ in helium) environments. The pyrolysis

experiments were carried out at heating rates of 50–150° C/min at temperatures from ambient to 700° C. The effect of gas flow rate was evaluated by pyrolyzing the samples both in static and dynamic (0.170 liters/min) environments. The fuel nitrogen conversion to GPNP species was measured using the nitrogen analyzer described previously.

PYROLYSIS USING GAS CHROMATOGRAPHY/MASS SPECTROMETRY

Instrument Description

The effect of high heating rates on the composition of the gas phase nitrogen species was evaluated for model fuel nitrogen compounds during pyrolysis using a CDS Analytical Pyroprobe 2000 interfaced to a Hewlett Packard 5890 Series II gas chromatograph. Gas species identification was made with a Hewlett Packard 5971A mass selective detector with an electron impact source. A block diagram of the experimental setup is provided in Fig. 60.

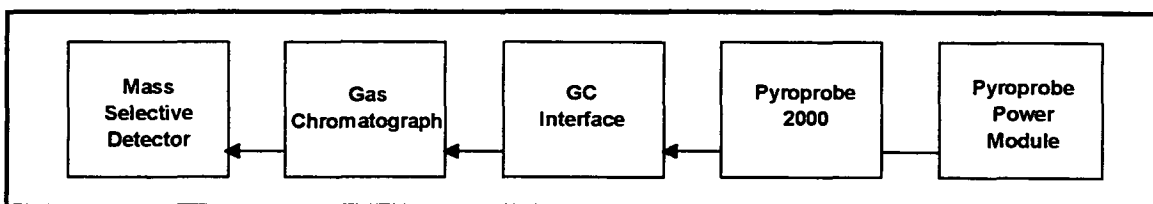


Figure 60. Block diagram for pyrolysis GC/MS.

The principle for pyrolysis GC/MS allows for extended use of the GC/MS analysis technique. The sample is pyrolyzed inside the pyroprobe. The pyrolysis gases enter the GC and are separated on the column using helium as the carrier gas. The sample gases remain inert in the system and do not interact with molecules of the carrier gas species.

Separation is mainly based on molecular size with the smaller molecules being eluted more rapidly than the larger molecules.

The separated gas species then enter a mass selective detector which converts the gas sample species to rapidly moving ions and resolves them based on their mass to charge ratios. A block diagram of the system components is given in Fig. 61. The electron impact source converts the gas molecules to charged particles by bombarding the gaseous sample with a beam of energetic electrons.⁷⁷ When the gas molecule is impacted, it enters an excited state. The subsequent relaxation, which is inherently accompanied by fragmentation of the main ion, leads to a large number of positive ions of various masses smaller than that the original molecule. Positive ions are separated from negative ions with the former being drawn into the mass analyzer. Within the analyzer, the ions are dispersed and focused onto a detector. From the analyzer, the ions collect on an electrode where the resulting ion current is amplified and recorded as a function of the scan time to provide the mass spectrum.

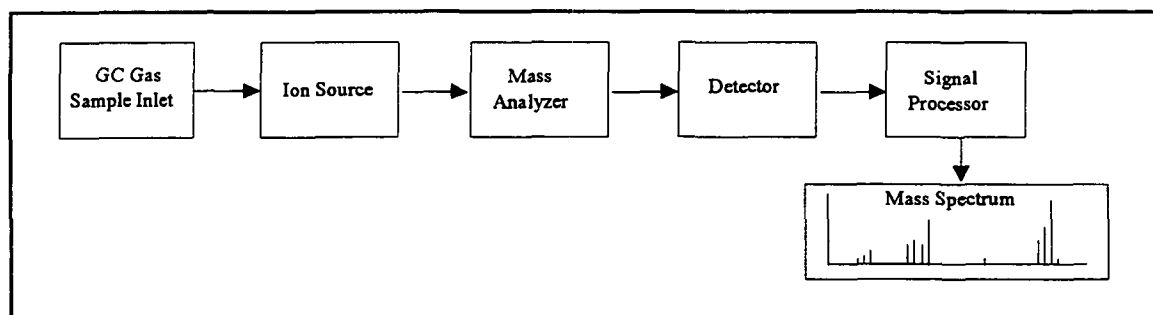


Figure 61. Block diagram for the components of the mass selective detector.

Operating Conditions

The heating rates used for the pyrolysis GC/MS were 10, 150, 400, and 1000° C/sec. Solid samples of approximately 0.02–0.1 mg were pyrolyzed in an inert, helium gas, atmosphere. Each sample was placed inside a 2 mm-I.D. quartz tube with a quartz wool plug on either end to retain the sample. The sample tube was then placed inside the probe heating coil which in turn was placed inside the interface to be pyrolyzed at the desired heating rate.

Pyrolysis gases are rapidly quenched and cooled by a helium carrier gas which also transports the gases about three inches to the head of the GC column. The column used was a HP-5 (crosslinked 5% Ph Me Silicone) column with the following dimensions: 25 m x 0.2 mm x 0.33 μ m film thickness. Within the column, the gases are separated by their molecular weights—higher molecular weight species being retained for a longer period of time. The separated gases then entered the mass selective detector which provided data for gas phase pyrolytic species identification.

The parameters for the GC/MS operation are provided in Table 16. The method for GC/MS data acquisition is “PYRO2.M.” Comparison of the results were made with the computer data base library “NBS54K” available from the National Bureau of Standards.⁹³

Table 16. Operational parameters for the pyrolysis GC/MS experiments.

<u>MS PARAMETERS</u>		<u>GC ZONE TEMPERATURES</u>	<u>° C</u>
Solvent Delay:	0 min	Injector A:	250
EM Absolute:	False	Injector B:	150
EMV Offset:	0	Detector A:	50, off
Resulting Voltage:	1729.4	Detector B:	325
		Auxiliary	50, off
<u>SCAN PARAMETERS</u>			
Low Mass:	1.2		
High Mass:	150		
Threshold:	150		
Sampling #:	2		
A/D Samples:	4		
<u>GC OVEN PARAMETERS</u>		<u>OVEN PROGRAM</u>	
Oven Equilibrium Time:	0.5 min	Ambient to 175° C	
Oven Max.:	325° C	at 10° C/min	
Oven:	On	hold temperature 2 min	
Ambient:	25° C	Total run time: 15 min	
<u>PYROPROBE PARAMETERS</u>		<u>INTERFACE PARAMETERS</u>	
Ambient for 10 sec		hold at ambient	
Ramp at selected rate to 500° C		no heating rate	
hold temperature 20 sec			

BLACK LIQUOR SINGLE DROP REACTOR

Description of Apparatus and Instrumentation

The single drop experiments were conducted to obtain preliminary measurements of the nitrogen evolution during black liquor pyrolysis and to try to characterize the total nitrogen evolved as NO_x species. These experiments were conducted in Åbo Akademi University's Combustion Chemistry Research Group's (CCRG) laboratory in Turku, Finland.

The general experimental setup includes a vertical quartz reactor inside a tube furnace and a NO_x analyzer connected for computer data acquisition. A block diagram of

the experimental arrangement is provided in Fig. 62. Calibration of the analyzer was completed with certified gases by directing the flow from the cylinders through the reactor in the tube furnace. Gases were then directed out of the furnace by the N_2 carrier gas where the flow was divided such that the appropriate flow rates were delivered to the analyzer for concentration measurements.

Verification of methods is provided in Appendix III. The data from the experimental work, as well as from calibration, was acquired using computer data acquisition. A CO_2 analyzer was set up in parallel with the NO analyzer to monitor the pyrolysis process and to check for air leaks in the system.

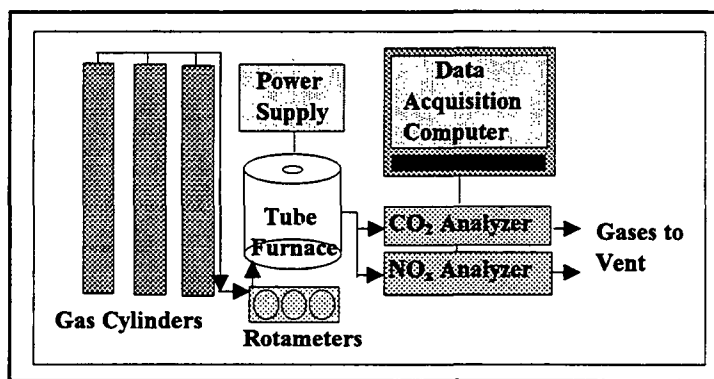


Figure 62. Experimental block diagram for the measurement of NO_x evolved during black liquor pyrolysis.

The CO_2 analyzer was an NDIR-industrial photometer. The NO analyzer was based on chemiluminescence principles for NO detection and included an ozone generator and vacuum pump. A filter was placed at the sample entrance for fume capture to prevent contamination of the internal reactor.

The quartz reactor is illustrated in Fig. 63. During calibration, all gases were sent through the reactor so that the measurements would have a similar response time as during experimental data collection. The reactor was airtight during calibration work. The quartz components of the reactor had ground glass joints, and the droplet insertion rod was in the down position which closed the top of the reactor. The gas lines to and from the analyzer were Teflon with Swaglock® fittings. All gas flows were measured and controlled with calibrated rotameters. A moisture trap of silica gel was used in the gas lines to assure the gases were dry. The total gas flow into the reactor through the calibration work was 300 L/h and therefore, all gases were in a laminar regime.

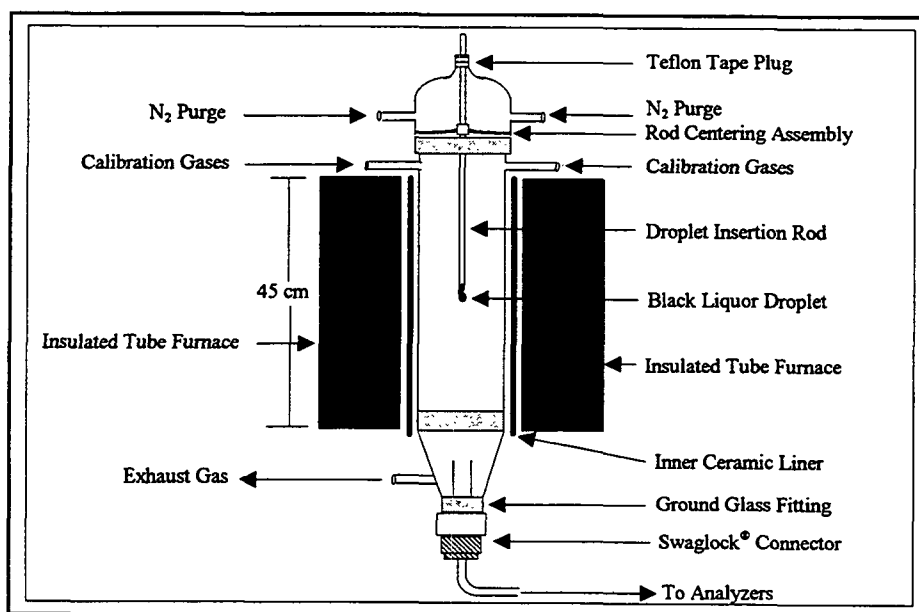


Figure 63. Quartz tube reactor for black liquor pyrolysis, CCRG, Åbo Akademi University.

Operating Conditions

Individual black liquor drops of $15\text{--}25 \pm 7$ mg were pyrolyzed in an inert (N₂) atmosphere. Black liquor was transferred from the storage container with a spatula to a

hook to make the drop. Each drop was weighed and the hook with the drop was placed in a holding container while the remaining drops of that set were prepared. Holding time ranged from 15–120 minutes before the test was started. Each drop was held in a nitrogen (N_2) purge for 3–5 minutes prior to being pyrolyzed. A weight loss of 5–10% (i.e. 1–2 mg) was observed during the “drying” period.

The hook with the drop was transferred to the insertion rod to be pyrolyzed. The purge drying occurred with the insertion rod in the up position allowing the nitrogen to flow over the drop and through the reactor. The data acquisition was started at the end of the purge drying. The drop was manually inserted to the pyrolysis position—approximately 30 cm into the furnace. A lag time of 7–12 seconds was noted between the start of data acquisition until the drop was in place. The gas flow through the analyzer had a residence time of about 10 seconds for the NO_x analyzer, which was measured at 300 L/h N_2 , ambient.

Data was collected for pyrolysis at temperatures of 300–1000° C. Two liquors each were pyrolyzed at 100° C and 200° C intervals. The remaining chars were lifted to the up position and allowed to cool in the nitrogen purge for a minimum of five minutes. Much longer times were required to cool the char from high temperature pyrolysis to an inert state. The cooled chars were then weighed and retained for nitrogen analysis.

Pyrolysis tests at a given temperature were done in random order to eliminate the possibility of instrument drift affecting the results. A minimum of seven replicates was pyrolyzed at each temperature as indicated. Calculations indicated seven replicates were

needed to provide a statistically sound sample size. (See Appendix III.) The chars for all replicates were combined for total nitrogen determination by the high-temperature pyrochemiluminescence method. The char samples were ground prior to analysis and the reported nitrogen values are the average of at least three replicates for each sample.

THERMOGRAVIMETRIC DIFFERENTIAL SCANNING CALORIMETER

Description of Apparatus and Instrumentation

An initial evaluation of the sodium salt effects was conducted as a screening experiment using a thermogravimetric-differential scanning calorimeter (Setaram TG-DSC 111) for combinations of sodium salts with organic nitrogen compounds. The total mass loss was measured upon pyrolysis of the sample. Note that the mass loss does not separate out the nitrogen loss. The purpose was to indicate if the addition of sodium salts to a model fuel nitrogen system would effect the mass loss of the entire compound and the temperature at which the initial composition occurred. The results of these screening experiments are reported in the results and discussion section and in Appendix XII. A block diagram for the experimental setup is indicated in Fig. 64 with greater detail of the calorimeter given in Fig. 65.

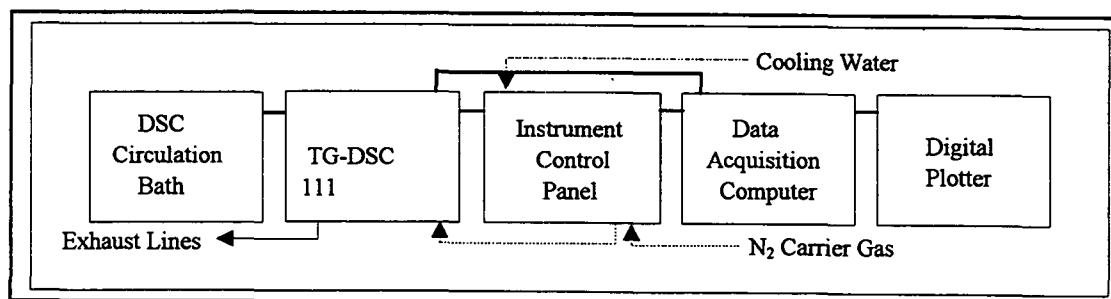


Figure 64. Block diagram for experimental equipment and data acquisition for the TG-DSC 111.

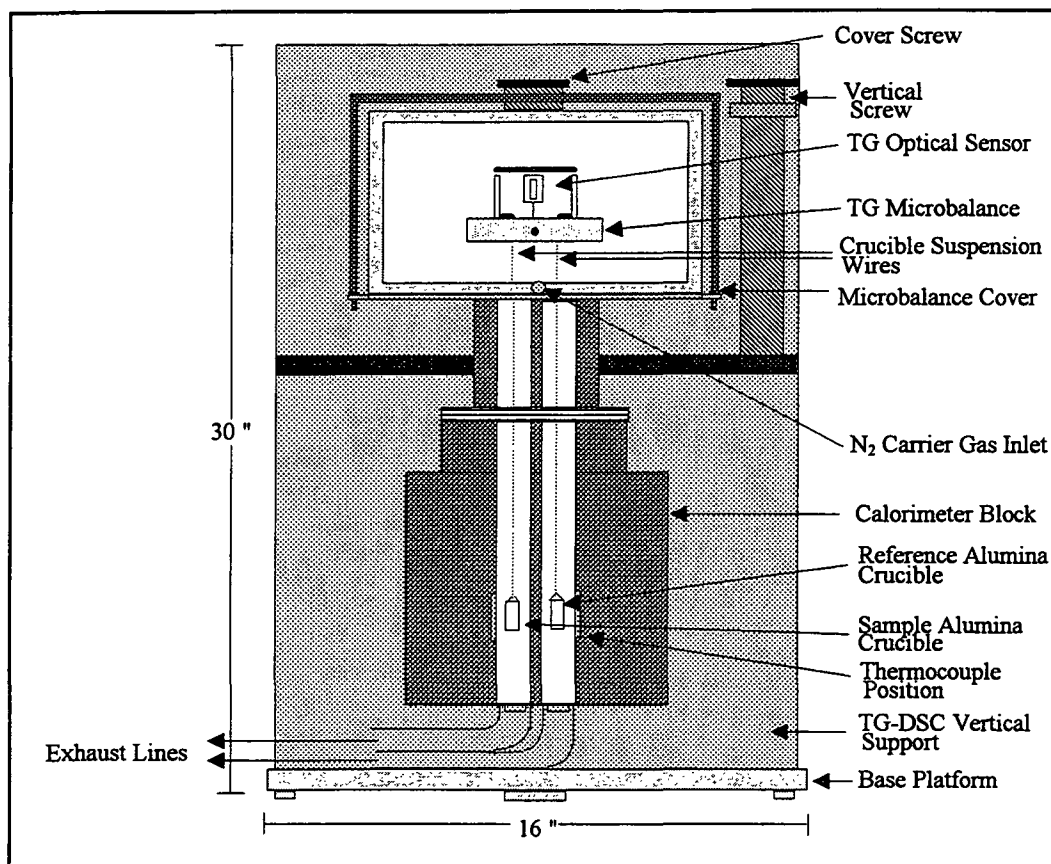


Figure 65. Schematic diagram of the TG-DSC 111 calorimeter and microbalance.

The principle of TG-DSC is based on the relationship between temperature and a property of the system of interest, such as mass, volume, or heat of reaction.⁷⁷

Thermogravimetric analysis continuously measures the mass of a sample as the temperature is increased linearly. The weight loss of the sample during heating is plotted as a thermogram, mass vs. temperature, and provides information on the decomposition of the sample. The derivative of the thermogram provides more visually accessible information on the decomposition which takes place. The derivative curve is characterized by peaks in which the peak area represents the total mass loss and the peak height represents the rate of mass loss.

In the screening experiments, samples were heated in parallel at a constant rate in alumina crucibles along with a reference material. Nitrogen gas, N_2 , was used as a carrier gas to prevent pyrolytic gases from entering the microbalance area and to vent the exhaust gases to a hood. Weight loss and power input data were collected and stored automatically using a computer data acquisition software package developed by Astra Scientific International, Inc. (ASI).

Operating Conditions

A factorial design experiment was conducted to test for significance of the inorganic content on the decomposition temperature, weight loss and enthalpy of decomposition of various nitrogen species during slow pyrolysis. The 2^3 factorial experimental design was presented in Table 5 on page 56. The inorganic components tested were Na_2SO_4 (factor a), Na_2S (factor b), and Na_2CO_3 (factor c). Each factor was tested individually and in combination with the other two factors. The base case or control for the experiment was designated "treatment combination 1" and consisted of two nitrogen compounds, glutamic acid and tryptophan, in a sodium hydroxide solution. Preparation of each treatment combination is given in Appendix IV. The nitrogen compounds were chosen based on the nitrogen structures observed in the black liquor from structural analysis where glutamic acid is a straight-chain amino compound while tryptophan contains both the amino group as well as heterocyclic bound nitrogen.

Eight different experiments (see Table 5, page 58) were done in triplicate for a total of 24 runs using the TG-DSC technique over a temperature range from ambient to

810° C with a heating rate of 5° C/min. Each run was completed in random order to eliminate effects of day-to-day variation by the operator and in the instrument. As the baseline for the screening experiments, the decomposition temperatures of each of the components to be added was initially established. By comparing the baseline black liquor nitrogen decomposition characteristics with those of each treatment, the effects of each factor and/or their interactions on these variables were established.

The operating conditions were the same for each sample and are identified in Table 17 below. A sample of each particular treatment (7.43 mg, \pm 0.39 mg on average) was placed in an alumina crucible and was measured against the reference material of similar weight (7.30 mg) in a second alumina crucible.

Table 17. Operating conditions for TG-DCS 111 screening experiments.

Parameter	Value
Type of Measurement	Linear Scan
Heating Rate	5° C/min
Initial Temperature	~ 20° C
Final Temperature	~ 810° C
Power Amplification	0.5 mW
TG Amplification	10 mg
Reference Material	Platinum Wire

Instrument performance was monitored by running periodic baseline tests to check stability of the measurements for noise or drift. The thermograms collected for each sample were corrected to provide measurements for the sample only. This was done by subtracting the baseline power or weight loss curve from those of the sample thermogram.

An enthalpy and weight region analysis was done. Data, including decomposition temperature, weight, and energy were abstracted from the thermogram for each replicate within the regions of interest. Three regions were chosen: region I for the overall decomposition; region II for glutamic acid decomposition; and region III for tryptophan decomposition. (See Fig. 66.) Data was analyzed for each region in each thermogram for all replicates according to the temperatures identified in Table 18. Data and methods verification are found in Appendix XI.

Table 18. Temperature designations for TG-DSC analysis regions.

Region	Initial Temperature (° C)	Final Temperature (° C)
I	159 ± 44	441 ± 17
II	184 ± 13	269 ± 14
III	271 ± 12	413 ± 18

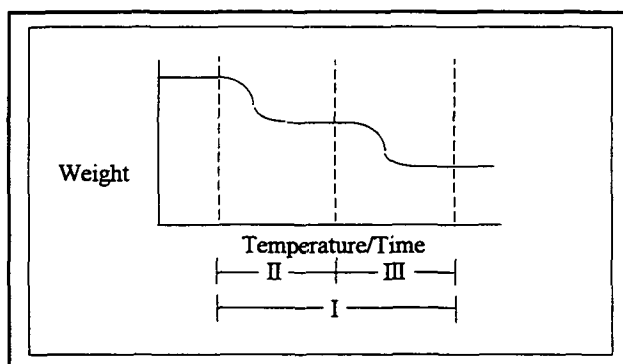


Figure 66. Thermogram regions for enthalpy and weight analysis. Region I = overall decomposition; Region II = glutamic acid decomposition; Region III = tryptophan decomposition.

CHEMICAL ANALYSES USED

For the compositional and structural analysis of the black liquor samples, numerous tests were run. In Table 19, a tabulated list of the analyses done, a brief description of the method, and laboratory where the analysis was completed is given. A listing of laboratory locations is provided in Appendix I.

Table 19. Summary of compositional and structural methods on which analyses of the black liquor samples was based.

Analysis	Test Method	Description	Laboratory	Ref.
Elemental	TAPPI T623, TAPPI T625	Digestion of samples followed by detection with ICP or AA	RSD, IPST; KCL; Galbraith Labs; Huffman Labs	94
Ionic	TAPPI T699 pm-83	Digestion of samples followed by IC	RSD, IPST; KCL; Huffman Labs	94
Organic structural	GC-MS	Fractionation of liquor samples followed by column separation	RSD, IPST	63
Amino acid; Protein	43.A08-43.A13, 43.259-43.264	Chemical assay	Hazelton Labs	68, 69
Kjeldahl total nitrogen	D 3590-89, D 3179-89	Acid digestion, detection of NH ₃	Galbraith Labs; KCL	72, 73
LECO total nitrogen	low temperature combustion	Thermoconductive measurement of N ₂	Galbraith Labs	--
High temperature combustion total nitrogen	D5176-91, D4629-91	High temperature combustion with pyrochemiluminescence detection of NO _x	EMPA, IPST	95, 96
Dry solids content	TAPPI T650 pm-84	Low temperature evaporation followed by weight determination	KCL, IPST	94

ACKNOWLEDGMENTS

A task which requires several years to complete cannot be done solely on the knowledge, efforts, and persistence of a single individual. It also requires the input and assistance of many others. Acknowledgment is given to the Institute of Paper Science and Technology and its member companies for the opportunity to continue my education and to pursue, in detail, a research topic of my choosing. The task of completing this dissertation could not have been completed without the technical expertise given by the faculty and staff and without the financial support provided.

In particular, my primary advisor, Dr. Earl Malcolm, has provided continual review and presented challenges into the how and why at the heart of the issue. He has helped me maintain a larger scope when details of the daily experimental work became mundane. Appreciation also goes out to my committee members, Dr. Jeff Empie, Dr. Tom Grace, and Dr. Junyong Zhu for helpful suggestions and guidance in this work.

The members of the Combustion Chemistry Research Group at Åbo Akademi University in Turku, Finland are greatly acknowledged for help and assistance in the completion of the single drop studies. Time spent doing these experiments was both technically and culturally expanding, which is important in a technologically and globally advancing industry. Specifically, I wish to thank Mikael (Peppe) Forssén for laboratory and practical assistance in making my transition into the CCRG and the Finnish community a smooth one. My appreciation is also extended to Professor Mikko Hupa for providing the opportunity to do joint research within the CCRG and for encouragement and

technical advice on many of the challenging problems which occurred while working under his direction. My time spent working in the CCRG will continue to be reflected through my broader perspective on pyrolysis research as well as on life in general.

Likewise, recognition must be given to members of the Institute community for their individual assistance: Kathleen Poll for assistance with GC/MS analytical techniques and data interpretation; Peter Froass for assistance with the acid precipitated lignin samples; Teri Ard for help in proofing this document; and fellow students, past and present, for providing a technical sounding board for ideas, concepts, and assistance with various challenging problems. To many others too numerous to name individually, I am sincerely thankful.

Finally, I wish to acknowledge the love received from my parents and family. They have continued to support me unconditionally, without understanding the how or why of what I do, as I have worked toward my goals. I would also like to express heartfelt thanks to Mick for bringing some balance into my life again.

LITERATURE CITED

1. 1994 Clean Air Act Compliance Tappi Short Course Notes, Tappi Press, Atlanta, GA, October 1994.
2. Nichols, K.M.; Thompson, L.M.; Empie, H.J. A Review of NO_x Formation Mechanisms in the Recovery Furnaces. *Tappi Journal*. 76(1):119–124 (1993).
3. Veverka, P.J.; Nichols, K.M. On the Form of Nitrogen in Wood and Its Fate During Kraft Pulping. *Tappi Environmental Conf.* TAPPI Press, Atlanta, GA, pp. 777–780 (1993).
4. Nichols, K.M.; Lien, S.J. Formation of Fuel-NO_x During Black Liquor Combustion. *Tappi Journal*. 76(3):185–191 (1993).
5. Aho, K., Hupa, M., Nikkanen, S., Release of Nitrogen Compounds During Black Liquor Pyrolysis, *Tappi Engineering Conference Proceedings*, TAPPI Press, Atlanta, GA, p. 377–384, 1993.
6. Pershing D.W.; Wendt, J.O.L. Pulverized Coal Combustion: The Influence of Flame Temperature and Coal Composition on Thermal and Fuel NO_x. *Sixteenth Symposium (International) on Combustion*. The Combustion Institute. Pittsburgh, PA. pp. 389–399 (1977).
7. Hupa, M.; Solin, P.; Hyöty, P. Combustion Behaviour of Black Liquor Droplets. *Tappi International Recovery Conf. Proc.*, TAPPI Press, Atlanta, GA, pp. 335–344 (1985).
8. Adams, T.N.; Frederick, W.J. *Kraft Recovery Boiler Physical and Chemical Processes*, American Paper Institute. New York, 1988.
9. Zeldovich, J. The Oxidation of Nitrogen in Combustion and Explosions. *Acta Physiochimica U.R.S.S.* 21(4):577–628 (1946).
10. Fenimore, C.P. Formation of Nitric Oxide in Premixed Hydrocarbon Flames. *Thirteenth Symposium (International) on Combustion*. The Combustion Institute. Pittsburgh, PA. pp. 372–380 (1971).
11. Hayhurst, A.N.; Vince, I. M. Nitric Oxide Formation From N₂ in Flames: The Importance of 'Prompt' NO. *Progress in Energy and Combustion Science*. 6:35–51 (1980).
12. Bowman, C.T. *Chemistry of Gaseous Pollutant Formation and Destruction*, Chapter 4 of *Fossil Fuel Combustion: A Source Book*. Bartok, W.; Sarofim, A.F., eds. John Wiley & Sons, Inc., New York (1991).

13. Nelson, P.F., Buckley, A.N., Kelly, M.D., Functional Forms of Nitrogen in Coals and the Release of Coal Nitrogen as NO_x Precursors (HCN and NH_3). Twenty-Fourth Symposium (International) on Combustion, Combustion Institute, Pittsburgh, PA, 24: 1259–1267 (1992).
14. Haynes, B.S. Reactions of Ammonia and Nitric Oxide in the Burnt Gases of Fuel-Rich Hydrocarbon-Air Flames. *Combustion and Flame*. 28:81–91 (1977).
15. Wendt, J.O.L.; Pershing, D.W.; Lee, J.W.; Glass, J.W. Pulverized Coal Combustion: NO_x Formation Mechanisms Under Fuel Rich and Staged Combustion Conditions. Seventeenth Symposium (International) on Combustion. The Combustion Institute. Pittsburgh, PA. pp. 77–87 (1979).
16. Merryman, E.L.; Levy, A. Nitrogen Oxide Formation in Flames: The Roles of NO_2 and Fuel Nitrogen. Fifteenth Symposium (International) on Combustion. The Combustion Institute. Pittsburgh, PA. pp. 1073–1083 (1975).
17. Takagi, T.; Ogasawara, M.; Daizo, M.; Tatsumi, T. NO_x Formation From Nitrogen in Fuel and Air During Turbulent Diffusion Combustion. Sixteenth Symposium (International) on Combustion. The Combustion Institute. Pittsburgh, PA. pp. 181–189 (1977).
18. Blair, D.W.; Wendt, J.O.L.; Bartok, W. Evolution of Nitrogen and Other Species During Controlled Pyrolysis Of Coal. Sixteenth Symposium (International) on Combustion. The Combustion Institute. Pittsburgh, PA. pp. 475–489 (1977).
19. Axworthy, A.E. Reactions of Fuel-Nitrogen Compounds Under Condition of Inert Pyrolysis, *Fuel*. 57: 29–35 (1978).
20. Levy, A. Unresolved Problems in SO_x , NO_x , Soot Control in Combustion. Nineteenth Symposium (International) on Combustion. The Combustion Institute. Pittsburgh, PA. pp. 1223–1242 (1982).
21. Fenimore, C.P. Effects of Diluents and Mixing on Nitric Oxide From Fuel-Nitrogen Species in Diffusion Flames. Sixteenth Symposium (International) on Combustion. The Combustion Institute. Pittsburgh, PA. pp. 1065–1071 (1977).
22. Chen, S.L.; Heap, M.P.; Pershing, D.W.; Martin, G.B. Influence of Coal Composition on the Fate of Volatile and Char Nitrogen During Combustion. Nineteenth Symposium (International) on Combustion. The Combustion Institute. Pittsburgh, PA. pp. 1271–1280 (1982).
23. Davidson, R.M. Perspectives: Nitrogen in Coal. IEA (International Energy Agency) Coal Research, London, UK 1994.

24. Snyder, L.R. Nitrogen and Oxygen Compound Types in Petroleum: Total Analysis of a 400–700 °F Distillate from a California Crude Oil. *Analytical Chemistry*. 41(2):314–323 (1969).
25. Cerný, J., Mitera, J., Vavrečka, P. Separation and Identification of Nitrogen Compounds in Coal-Tar Pitch. *Fuel*. 68(5):596–600. (1989).
26. Burchill, P.; Herod, A.A.; Pritchard, E. Investigation of Nitrogen Compounds in Coal Tar Products. 1. Unfractionated Materials. *Fuel*. 62:11–19 (1983).
27. Hayatsu, R.; Scott, R.G.; Moore, L.P.; Studier, M.H. Aromatic Units in Coal. *Nature*. 257: 378–380, (1975).
28. Solomon, P.R.; Colket, M.B. Evolution of Fuel Nitrogen in Coal Devolatilization. *Fuel*. 57:749–755 (1978).
29. Nelson, P.F.; Kelly, M.D.; Wornat, M.J. Conversion of Fuel Nitrogen in Coal Volatiles to NO_x Precursors Under Rapid Heating Conditions. *Fuel*. 70:403–407 (1991).
30. Nagai, M.; Masunaga, T. Hydrodenitrogenation of a Mixture of Basic and Non-basic Polynuclear Aromatic Nitrogen Compounds. *Fuel*. 67: (1988).
31. Masterson, W.L., Slowinski, E.J., Stanitski, C.L., *Chemical Principles*, 6th Ed. Saunders College Publishing, New York, NY, 1985.
32. Houser, T.J., Hull, H., Alway, R.M., Biftu, T., Kinetics of Formation of HCN during Pyridine Pyrolysis. *International Journal of Chemical Kinetics*. 12:569–574 (1980).
33. Pereira, F.J.; Beer, J.M.; Gibbs, B.; Hedley, A.B. NO_x Emissions From Fluidized-Bed Combustors. Fifteenth Symposium (International) on Combustion. The Combustion Institute. Pittsburgh, PA. pp. 1149–1155 (1975).
34. Pohl, J.H.; Sarofim, A.F. Devolatilization and Oxidation of Coal Nitrogen. Sixteenth Symposium (International) on Combustion. The Combustion Institute. Pittsburgh, PA. pp. 491–501 (1977).
35. Mackie, J.C.; Colket, M.B.; Nelson, P.F. Shock Tube Pyrolysis of Pyridine. *J. Phys. Chem.* 94:4099–4106 (1990).
36. Haussman, G.J.; Kruger, C.H. Evolution and Reaction of Coal Fuel Nitrogen During Rapid Oxidative Pyrolysis and Combustion. Twenty-Third Symposium (International) on Combustion. The Combustion Institute. Pittsburgh, PA. pp. 1265–1271 (1990).
37. Pershing D.W.; Wendt, J.O.L. Relative Contributions of Volatile Nitrogen and Char Nitrogen to NO_x Emissions from Pulverized Coal Flames. *Ind. Eng. Chem. Process Des. Dev.* 18(1):60–67 (1979).

38. Okazaki, K.; Shishido, H.; Nishikawa, T.; Ohtake, K. Separation of the Basic Factors Affecting NO Formation in Pulverized Coal Combustion. Twentieth Symposium (International) on Combustion. The Combustion Institute. Pittsburgh, PA. pp. 1381–1389 (1984).
39. Chen, S.L.; Cole, J.A.; Heap, M.P.; Kramlich, J.C.; McCarthy, J.M.; Pershing, D.W. Advanced NO_x Reduction Processes Using -NH and -CN Compounds in Conjunction with Staged Air Addition. Twenty-Second Symposium (International) on Combustion. The Combustion Institute. Pittsburgh, PA. pp. 1135–1145 (1988).
40. Song, Y.H.; Blair, D.W.; Siminski, V.J.; Bartok, W. Conversion of Fixed Nitrogen to N₂ in Rich Combustion. Eighteenth Symposium (International) on Combustion. The Combustion Institute. Pittsburgh, PA. pp. 53–63 (1981).
41. De Soete, G.G. Heterogeneous N₂O and NO Formation From Bound Nitrogen Atoms During Coal Char Combustion. Twenty-Third Symposium (International) on Combustion, The Combustion Institute, Pittsburgh, PA. pp. 1257–1264 (1990).
42. Mereb, J.B.; Wendt, J.O.L. Reburning Mechanisms in a Pulverized Coal Combustor. Twenty-Third Symposium (International) on Combustion. The Combustion Institute. Pittsburgh, PA. pp. 1273–1279 (1990).
43. Bose, A.C.; Wendt, J.O.L. Pulverized Coal Combustion: Fuel Nitrogen Mechanisms in the Rich Post-Flame. Twenty-Second Symposium (International) on Combustion. The Combustion Institute. Pittsburgh, PA. pp. 1127–1134 (1988).
44. Furusawa, T.; Tsunoda, M.; Tsujimura, M.; Adschiri, T. Nitric Oxide Reduction by Char and Carbon Monoxide. *Fuel*. 64:1306–1309 (1985).
45. Galeano, S.F.; Kahn, D.C.; Mack, R.A. Air Pollution: Controlled Operation of a NSSC Recovery Furnace. *Tappi Journal*. 54(5):741–744 (1971).
46. Galeano, S.F.; Leopold, K.M. A Survey of Emissions of Nitrogen Oxides in the Pulp Mill. *Tappi Journal*. 56(3):74–76 (1973).
47. Hood, K.T. A Study of Nitrogen Oxides Emissions from Kraft Recovery Furnaces. The National Council of the Paper Industry for Air and Stream Improvement. Atmospheric Quality Improvement Technical Bulletin No. 105. New York, NY, December 28, 1979.
48. Pinkerton, J.E. A Review of Preconstruction Air Quality Permits Issued for Pulp Mill Emission Sources. The National Council of the Paper Industry for Air and Stream Improvement. Special Report No. 90-03. New York, NY, May 31, 1990.
49. Anderson, P.H.; Jackson, J.C. An Analysis of Best Available Control Technology Options for Kraft Recovery Furnace NO_x Emissions. *Tappi Journal*. 74(1):115–118 (1991).

50. Oscarsson, B.; Bentley, K.M.; Hood, S.W. Characterizing Emissions From a Modern Kraft Recovery Furnace. Tappi Environmental Conf. TAPPI Press, Atlanta, GA, pp. 1053–1060 (1991).
51. Björklund, H.; Warnqvist, B.; Pettersson, B. Inside a Kraft Recovery Boiler - Combustion of (High-Sulphidity) Black Liquor at High Dry Solids. Proc. International Chemical Recovery Conf. Ottawa, Ontario. TAPPI Press, Atlanta, GA, pp. 177–181, 1989.
52. Barsin, J.A.; Johnson, R.L.; Rissler, C.E. The St. Francisville Recover Low Odor Conversion and Capacity Upgrade. Proc. International Chemical Recovery Conf. Ottawa, Ontario, TAPPI Press, Atlanta, GA, pp. 29–37, 1989.
53. Casale, F.S.; Fritz, P.A. Start Up and Operating Experience of a High-Solids Recovery Boiler at S.D. Warren Company Westbrook, Maine. Tappi Engineering Conf. TAPPI Press, Atlanta, GA, pp. 687–688 (1990).
54. Netherton, B.; Osborne, D.M. Arkansas Kraft's Modified Evaporator Produces 80% Solids. Tappi Journal. 74(11):71–74 (1991).
55. Someshewar, A.V. An Analysis of Kraft Recovery Furnace NO_x Emissions and Related Parameters, The National Council of the Paper Industry for Air and Stream Improvement. Technical Bulletin No. 636. New York, NY, July, 1992.
56. Brännland, R.; Nordén, S.; Lindström, L. Implementation in Full Scale—The Next Step for Prenox.[®] Tappi Journal. 73(5):231–237 (1990).
57. Thompson, L.M. The Depletion of Nitric Oxide by Reaction with Molten Sodium Carbonate and Sodium Carbonate/Sodium Sulfide Mixtures. Doctoral Dissertation. Atlanta, GA. Institute of Paper Science and Technology. 1995.
58. Iisa, K., Carangal, A., Scott, A., Pianpucktr, R., Tangpanyapinit, V., Nitrogen Oxide Formation and Destruction in Recovery Boilers. Proceedings of the International Chemical Recovery Conference. Toronto, Canada, TAPPI Press. Atlanta, GA, pp. B241–B250, 1995.
59. Forssén, M.; Hupa, M.; Pettersson, R.; Martin, D. NO Release During Black Liquor Char Combustion and Gasification, Proceedings of the 1995 International Chemical Recovery Conference, Toronto, Canada, TAPPI Press, Atlanta, GA, pp. B231–B239, April 24–27, 1995.
60. Forssén, M.; Hupa, M.; Hellström, P. Liquor-to-Liquor Differences in Combustion and Gasification Processes: Nitrogen Oxide Formation Tendency, Tappi Engineering Conference Proceedings, Dallas, TX, TAPPI Press, Atlanta, GA, pp. 825–832, September 11–14, 1995.

61. Thompson, L.M., Martin, D.M., Empie, J.H., Malcolm, E.W., Wood, M. The Fate of Nitrogen in a Kraft Recovery Furnace, Proceedings of the 1995 International Chemical Recovery Conference, Toronto, Canada, TAPPI Press, Atlanta, GA, pp. B225-B229, April 24-27, 1995.
62. Tarpey, T., Tran, H., Mao, X. Emissions of Gaseous Ammonia and Particulate Containing Ammonium Compounds from a Smelt Dissolving Tank, Proceedings of the 1995 International Chemical Recovery Conference, Toronto, Canada, TAPPI Press, Atlanta, GA, pp. B217-B224, April 24-27, 1995.
63. Niemelä, K. Low-Molecular Weight Organic Compounds in Birch Kraft Black Liquors. Doctoral Dissertation. University of Helsinki. (1990).
64. Dill, I.; Salnikow, J.; Kraepelin, G. Hydroxyproline-Rich Protein Material in Wood and Lignin of *Fagus sylvatica*. Applied and Environmental Microbiology. 48(6):1259-1261 (1984).
65. Fukuda, T.; Mott, F.L.; Harad, C. Studies on Tissue Culture of Tree-Cambium XI. Characterization of Lignin Suspension-Cultured Cells of Loblolly Pine. Mokuzaishi. 34(2):149-154 (1988).
66. Laidlaw, R.A.; Smith, G.A. The Proteins of the Timbers of Scots Pine (*Pinus sylvestris*). *Holzforschung*. 19(5):129-134 (1965).
67. Lin, S.Y., Commercial Spent Pulping Liquors in Methods in Lignin Chemistry. Lin, S.Y.; Dence, C.W., Eds., Springer Verlag. Berlin, Heidelberg. p. 75, 1992.
68. Official Methods of Analysis. First supplement. 14th Ed., Methods 43.A08-43.A13, Arlington, VA. (1985)
69. Official Methods of Analysis. 14th Ed., Methods 43.259-43.264, Arlington, VA, 1984.
70. ANTEK® Instruments, Inc., 7000B Operation Manual, Houston, TX, 1993.
71. Kostantinides, F.N.; Boehm, K.A.; Radmer, W.J. Storm, M.C.; Adderly, J.T.; Weisdorf, S.A.; Cerra, F.B. Pyrochemiluminescence™: Real-Time, Cost-Effective Method for Determination of Total Urinary Nitrogen in Clinical Nitrogen-Balance Studies. *Clinical Chemistry*. 34(12):2518-2520 (1988).
72. ASTM D3179-89. Standard Test Method for Nitrogen in the Analysis of Coal and Coke. Annual Book of ASTM Standards. American Society for Testing and Materials. Philadelphia, PA 1993.
73. ASTM D3590-90. Standard Test Method for Total Kjeldahl Nitrogen in Water. Annual Book of ASTM Standards. American Society for Testing and Materials. Philadelphia, PA. 1993.

74. Analytical Chemistry Group, Research Services Division, Kjeldahl Micro Analysis Method, Institute of Paper Science and Technology, Atlanta, GA. 1992.
75. Jäckel, H. Personal communication. EMPA, Dübendorf, Switzerland. 1993.
76. Jones, B.M.; Daughton, C.G. Chemiluminescence vs. Kjeldahl Determination of Nitrogen in Oil Shale Retort Waters and Organonitrogen Compounds. *Analytical Chemistry*. 57:2320–2325 (1985).
77. Skoog, D.A. *Principles of Instrumental Analysis*, 3rd Ed., Saunders College Publishing, Philadelphia, PA, 1989.
78. Thompson, L.M. Personal communication. Research Chemical Engineer, Westvaco Corp., Charleston, SC, September, 1995.
79. Jolly, W.J., *The Inorganic Chemistry of Nitrogen*, W.A. Benjamin, Inc., 1964.
80. *CRC Handbook of Chemistry and Physics*, 66th Ed., Weast, R.C. Ed., CRC Press Inc., Boca Raton, FL, 1985.
81. Prouty, A.L., Stuart, R.C., Caron, A.L. Nitrogen Oxide Emissions From a Kraft Recovery Furnace. *Tappi Journal*. 76(1):115–118 (1993).
82. Hurd, C.D., Macon, A.R., Simon, J.I., Levetan, R.V. Pyrolytic Formation of Arenes. I. Survey of General Principles and Findings. *Journal of the American Chemical Society*. 84:4509–4515 (1962).
83. Houser, T.J., McCarville, M.E., Biftu, T., Kinetics of the Thermal Decomposition of Pyridine in a Flow System. *International Journal of Chemical Kinetics*. 12:555–568 (1980).
84. Appleton, J.P., Heywood, J.B., The Effects of Imperfect Fuel-Air Mixing in a Burner on NO Formation From Nitrogen in the Air and the Fuel. Fourteenth Symposium (International) on Combustion, Combustion Institute, Pittsburgh, PA, 14:777–786 (1973).
85. Tsang, C.W.; Harrison, A.G., Chemical Ionization of Amino Acids. *Journal of the American Chemical Society*. 98(6): 1301–1308 (1976).
86. Hägg, G. *Allmän Och Oorganisk Kemi (General and Organic Chemistry)*, Allmqvist and Wiksell, Stockholm, Sweden, p. 518, 1963.
87. Clement, J.L., Barna, J.L. The Effect of Black Liquor Fuel-Bound Nitrogen on NO_x Emissions. TAPPI Environmental Conference Proceedings. Boston, MA, TAPPI Press. Atlanta, GA, pp. 653–660, March 28–31, 1993.

88. Jones, A.K., Stewart, R.I., The High Solids Breakpoint - A Trade-off Between SO_2 and NO_x . Proceedings of the International Chemical Recovery Conference. Seattle, WA, TAPPI Press. Atlanta, GA, pp. 365-370, 1992.
89. Chen, W. personal communication, ABB Combustion, NJ, August 1995.
90. Levenspiel, O., Chemical Reaction Engineering. 2nd Ed. John Wiley & Sons, Inc. New York, NY. 1972.
91. Lövblad, R., Moberg, G., Olausson, L., Boström, C., NO_x Reduction From a Recovery Boiler by Injection of an Enhanced Urea Solution (NOXOUT® Process). Tappi Environmental Conference Proceedings, Boston, MA, TAPPI Press, Atlanta, GA, p. 1071-1075, 1991.
92. Nonhebel, D.C.; Walton, J.C. Free-Radical Chemistry: Structure and Mechanism, Cambridge University Press, New York, NY 1974.
93. National Institute of Standards and Technology, Formerly the National Bureau of Standards, NIST/EPA/NIH Chemical Structures Database, G1036A Rev. A.00.00, U.S. Secretary of Commerce, 1992.
94. Tappi Test Methods, TAPPI Press, Atlanta, GA, 1992.
95. ASTM D4629-91. Test Method for Organically Bound Trace Nitrogen in Liquid Petroleum Hydrocarbons by Oxidative Combustion and Chemiluminescence Detection. Annual Book of ASTM Standards. Vol. 05.02 American Society for Testing and Materials. Philadelphia, PA 1993.
96. ASTM D5176-91. Test Method for Total Chemically Bound Nitrogen in Water by Pyrolysis and Chemiluminescence Detection. Annual Book of ASTM Standards. Vol. 11.02 American Society for Testing and Materials. Philadelphia, PA 1993.

APPENDIX I: LIST OF MATERIALS AND EXPERIMENTAL EQUIPMENT

Table I-1. List of experimental equipment.

<u>Item</u>	<u>Description</u>	<u>Vendor</u>
Thermogravimetric Differential Scanning Calorimeter (Setaram, TG-DSC 111)	Microbalance with calorimeter and data acquisition software.	Astra Scientific International, Inc., Pleasanton, CA
High Temperature Pyrochemiluminescence Nitrogen/Sulfur Analyzer (7000B)	Nitrogen analyzer with gas sampling inlet, multimatrix inlet with sample drive, and temperature programmable furnace	Antek Instruments, Inc., Houston, TX
Syringes	10 uL 701N Series with bevel point needle, for injection of aqueous sample into nitrogen analyzer	Hamilton via VWR Scientific, Marietta, GA
personal gas monitor for ammonia	GASMAN monitor for ammonia (NH ₃) with dual alarms: instantaneous and TWA	GASMAN via JR Environmental, Inc., Martinez, GA
borosilicate jars with septa	40 mL jars, open top closure with 0.125 septa, 200 series, for nitrogen compound calibration standards	VWR Scientific Inc., Marietta, GA
ceramic tube	protective liner for nitrogen analyzer pyrotube	Coors Ceramic, Golden, CO
quartz pyrotube	various models for sample inlet systems for nitrogen analyzer	Lillie Glass Blowers, Inc., Smyrna, GA
mass flow meters	NALL-10K, NALL-1K	Teledyne-Hasting-Raydist, Hampton, VA
computer data acquisition software	Labtech Acquire, Version 1.2.4	Laboratory Technologies Corporation
GC-MS	5890 Series II gas chromatograph with 5971A mass selective detector	Hewlett Packard Inc.
Pyroprobe 2000	for pyrolytic GC-MS	CDS Analytical Inc., Oxford, PA

Table I-2. List of compressed gases used.

<u>Item</u>	<u>Vendor</u>
Prepurified Nitrogen, N ₂	Holox Ltd., Atlanta, GA
Technical Grade Nitrogen, N ₂	Holox Ltd., Atlanta, GA
UPC Oxygen, O ₂	Air Products & Chemicals, Inc., Atlanta, GA
Certified Gas Mixture, ammonia (NH ₃) in He	Air Products & Chemicals, Inc., Atlanta, GA
UHP/Zero Grade He	Air Products & Chemicals, Inc., Atlanta, GA
Certified Gas Mixture, Nitric Oxide (NO) in He	Air Products & Chemicals, Inc., Atlanta, GA

Table I-3. List of chemicals used.

<u>Item</u>	<u>Vendor</u>
L-Glutamic Acid	Aldrich Chemical Co., Milwaukee, WI
Pyrazine (99% + purity)	Aldrich Chemical Co., Milwaukee, WI
L-Tryptophan (99% purity)	Aldrich Chemical Co., Milwaukee, WI
Ammonium Nitrate (99.999% purity)	Aldrich Chemical Co., Milwaukee, WI
Ammonium Sulfate (99.999% purity)	Aldrich Chemical Co., Milwaukee, WI
Ammonium Chloride (99.998% purity)	Aldrich Chemical Co., Milwaukee, WI
Benzoic Acid, Na Salt (99%) (sodium benzoate)	Aldrich Chemical Co., Milwaukee, WI
L-Proline (99% + purity)	Aldrich Chemical Co., Milwaukee, WI
Sodium Hydroxide	Fisher Chemical Co., Fair Lawn, NJ
Sodium Sulfide	Fisher Chemical Co., Fair Lawn, NJ
Sodium Sulfate	JT Baker Chemical Co., Phillipsburg, NJ
Sodium Carbonate	JT Baker Chemical Co., Phillipsburg, NJ
36.5–38.0% Hydrochloric Acid, Reagent Grade	VWR Scientific Inc., Marietta, GA

Table I-4. List of laboratories used.

<u>Laboratory</u>	<u>Location</u>
Analytical Chemistry Group, Research Services Div.	IPST, Atlanta, GA
Huffman Laboratories, Inc.	Golden, CO
Galbraith Laboratories, Inc.	Knoxville, TN
Hazleton Wisconsin Laboratories	Madison, WI
KCL (Finnish Central Laboratories)	Espoo, Finland
EMPA (Swiss Federal Lab. for Materials Testing)	Dübendorf, Switzerland

APPENDIX II: PYROCHEMILUMINESCENCE NITROGEN ANALYZER METHODS VERIFICATION

This appendices presents the results obtained to verify the methods used to obtain fixed nitrogen measurements as valid for both combustion and pyrolysis conditions. The data includes general optimization information for the experimental conditions and nitrogen measurements and then specific information for combustion and pyrolysis conditions.

METHODS OPTIMIZATION

Combustion Temperature

The effect of temperature on the nitrogen release was evaluated to understand the differences in the results observed between the total nitrogen measurements samples. Samples of ~3.75 µg N as AgNO₃ in H₂O, ~3.75 µg N and ~5.0 µg N as proline in H₂O, ~3.75 µg N as NH₄Cl in H₂O, and ~2.5 µg N as pyrazine in H₂O were combusted using Method 5. Temperatures were evaluated from 950-1100° C at 50° C intervals. All sample data are provided at the end of this section and the results are presented in the following table and figure.

Table II-1. Total nitrogen response determined by high temperature combustion Method 5 at several temperatures. Data are averages of all replicates at the temperature indicated.

Sample Identification	Combustion Temperature (° C)			
	950	1000	1050	1100
3.7698 µg N as AgNO ₃ in H ₂ O	67539	101271	106014	106418
4.954 µg N as Proline in H ₂ O	59782	51850	53471	42688
3.789 µg N as Proline in H ₂ O	51180	54398	55753	41613
3.782 µg N as NH ₄ Cl in H ₂ O	48260	48300	50620	47985
2.4857 µg N as Pyrazine in H ₂ O	42145	47396	48238	48793

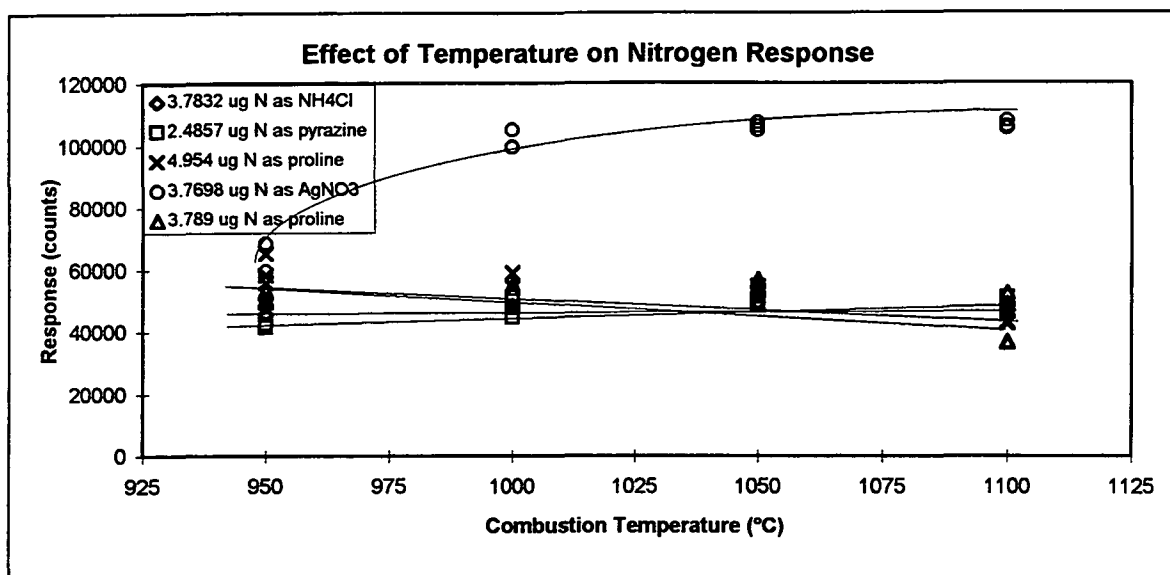


Figure II-1. Effect of combustion temperature on nitrogen response.

The data show that the greatest response can be achieved at the 1100° C combustion temperature for most of the nitrogen species. These samples indicate either an increasing response or a plateau value for the temperatures tested. For the proline samples at both concentrations examined, a slight loss of response was noted with increasing temperature.

Data Tables for Temperature Effect

Fixed nitrogen data collected under combustion conditions for the effect of temperature is provided below. The data is presented along with the statistical summaries. Error estimates can be taken from the correlation coefficients in the plots as well as the statistical standard deviation and coefficient of variation.

The sample numbers in the data tables, such as N4097022, are the same as the computer data acquisition (CDA) file names. The N identifies the sample as a nitrogen

release profile type of data file. The 4 represents the lab notebook #4264. The next three digits are the page number within the notebook where the data can be found and the last three digits are the sample number on that page. The last digit represents the number of the replicate. For the example, the values listed for the N4097022 sample would be found in notebook 4264 on page 97 as sample 2, replicate 2.

Table II-2. Summarized data for the effect of temperature on the nitrogen response.
Data collected using Method 5 and temperatures as indicated.

Temperature	3.7832 $\mu\text{g N/5 } \mu\text{l}$ sample of NH_4Cl in H_2O				
<u>(°C)</u>	<u>Replicate 1</u>	<u>Replicate 2</u>	<u>Replicate 3</u>		
1100	48187	46845	48921		
1050	51523	51177	49158		
1000	48550	48550	47799		
950	48310	50860	45608		
Temperature	2.4857 $\mu\text{g N/5 } \mu\text{l}$ sample of pyrazine in H_2O				
<u>(°C)</u>	<u>Replicate 1</u>	<u>Replicate 2</u>	<u>Replicate 3</u>		
1100	51009	47433	47937		
1050	48481	48100	48131		
1000	49956	47688	44542		
950	42618	41501	42316		
Temperature	3.789 $\mu\text{g N/5 } \mu\text{l}$ sample of proline in H_2O				
<u>(°C)</u>	<u>Replicate 1</u>	<u>Replicate 2</u>	<u>Replicate 3</u>	<u>Replicate 4</u>	<u>Replicate 5</u>
1100	36609	36329	52429	46015	36679
1050	56925	55843	54490	--	--
1000	54011	55265	53917	--	--
950	49551	50593	53393	--	--
Temperature	3.7698 $\mu\text{g N/5 } \mu\text{l}$ sample of AgNO_3 in H_2O				
<u>(°C)</u>	<u>Replicate 1</u>	<u>Replicate 2</u>	<u>Replicate 3</u>		
1100	105937	107918	105415		
1050	107196	104783	106063		
1000	99382	104948	99483		
950	59543	68462	74612		
Temperature	4.954 $\mu\text{g N/5 } \mu\text{l}$ sample of proline in H_2O				
<u>(°C)</u>	<u>Replicate 1</u>	<u>Replicate 2</u>	<u>Replicate 3</u>	<u>Replicate 4</u>	
1100	43129	42461	42473	--	
1050	53043	54573	52794	--	
1000	48102	48591	58856	54512	
950	65207	55920	58217	--	

Table II-3. Data for the effect of temperature on the nitrogen response of various nitrogen species during combustion.

Method Used:	5	PMT Voltage:	825
O ₂ to O ₃ :	30 ml/min	Furnace Temperature:	1100° C
O ₂ to pyro:	365 ml/min	Gain Setting:	HI
O ₂ to inlet:	20 ml/min	Gain Factor:	X1
He to inlet:	145 ml/min	Residence Time:	3 min
Nitrogen Species:	As Indicated	Matrix:	d,d-H ₂ O

<u>Sample #*</u>	<u>Sample ID</u>	<u>Sample Vol</u> <u>(μl)</u>	<u>Known N</u> <u>Mass (μg)</u>	<u>Response</u> <u>Counts</u>	<u>CDA Sum</u> <u>Response</u>
N4100011	~750 ppm N AgNO ₃	5	3.7698	105937	188.403
N4100012	~750 ppm N AgNO ₃	5	3.7698	107918	191.7728
N4100013	~750 ppm N AgNO ₃	5	3.7698	--**	191.2112
N4100014	~750 ppm N AgNO ₃	5	3.7698	105415	186.9385
N4100021	~1000 ppm N proline	5	4.954	43129	76.3182
N4100022	~1000 ppm N proline	5	4.954	42461	75.1705
N4100023	~1000 ppm N proline	5	4.954	42473	71.4846
N4102181	~750 ppm N NH ₄ Cl	5	3.7832	48187	85.2783
N4102182	~750 ppm N NH ₄ Cl	5	3.7832	46845	82.9103
N4102183	~750 ppm N NH ₄ Cl	5	3.7832	48921	86.7187
N4102201	~750 ppm N proline	5	3.789	36609	64.7701
N4102202	~750 ppm N proline	5	3.789	36329	64.2823
N4102203	~750 ppm N proline	5	3.789	--	--
N4102204	~750 ppm N proline	5	3.789	52429	92.8222
N4102205	~750 ppm N proline	5	3.789	46015	81.4453
N4102206	~750 ppm N proline	5	3.789	36679	64.7703
N4102191	~500 ppm N pyrazine	5	2.4857	51009	90.1854
N4102192	~500 ppm N pyrazine	5	2.4857	47433	83.8868
N4102193	~500 ppm N pyrazine	5	2.4857	47937	84.8143
N4101151	~500 ppm N pyrazine	5	2.4857	48481	85.86
N4101152	~500 ppm N pyrazine	5	2.4857	48100	85.1078
N4101153	~500 ppm N pyrazine	5	2.4857	48131	85.1808

*The sample # is the same as the Computer Data Acquisition filename. The N identifies it as a nitrogen data file.

The 4 represents the lab book #4264. The next three digits are the page number for the data and the last three digits are the sample number on that page.

**Data was thrown out experimentally or statistically thrown out according to the Q-test.

<u>Summarized Data</u>	<u>Ave. Counts</u>	<u>n</u>	<u>SD</u>	<u>RSD (%)</u>
~750 ppm N AgNO ₃	106418	3	1311	1.23
~1000 ppm N proline	42688	3	382	0.89
~750 ppm N NH ₄ Cl	47985	3	1053	2.19
~750 ppm N proline	41613	5	7309	17.56
~500 ppm N pyrazine	48793	3	1935	3.97
~500 ppm N pyrazine	48238	3	211	0.44

Table II-3. (cont.) Data for the effect of temperature on the nitrogen response of various nitrogen species during combustion.

Method Used:	5	PMT Voltage:	825
O ₂ to O ₃ :	30 ml/min	Furnace Temperature:	1050° C
O ₂ to pyro:	365 ml/min	Gain Setting:	HI
O ₂ to inlet:	20 ml/min	Gain Factor:	X1
He to inlet:	145 ml/min	Residence Time:	3 min
Nitrogen Species:	As Indicated	Matrix:	d,d-H ₂ O

<u>Sample #*</u>	<u>Sample ID</u>	<u>Sample Vol</u> <u>(μl)</u>	<u>Known N</u> <u>Mass (μg)</u>	<u>Response</u> <u>Counts</u>	<u>CDA Sum</u> <u>Response</u>
N4100041	~750 ppm N AgNO ₃	5	3.7698	107196	190.0145
N4100042	~750 ppm N AgNO ₃	5	3.7698	104783	185.474
N4100043	~750 ppm N AgNO ₃	5	3.7698	106063	187.7929
N4100031	~1000 ppm N proline	5	4.954	53043	93.9205
N4100032	~1000 ppm N proline	5	4.954	54575	96.6305
N4100033	~1000 ppm N proline	5	4.954	--	97.583
N4100034	~1000 ppm N proline	5	4.954	52794	93.5054
N4101171	~750 ppm N NH ₄ Cl	5	3.7832	51523	91.1377
N4101172	~750 ppm N NH ₄ Cl	5	3.7832	51177	90.5273
N4101173	~750 ppm N NH ₄ Cl	5	3.7832	49158	87.2557
N4101161	~750 ppm N proline	5	3.789	56925	100.8544
N4101162	~750 ppm N proline	5	3.789	27905*	49.17
N4101163	~750 ppm N proline	5	3.789	27011*	49.5583
N4101164	~750 ppm N proline	5	3.789	55843	98.8035
N4101165	~750 ppm N proline	5	3.789	54490	96.5334
N4101091	~500 ppm N pyrazine	5	2.4857	49956	88.379
N4101092	~500 ppm N pyrazine	5	2.4857	47688	84.2529
N4101093	~500 ppm N pyrazine	5	2.4857	44542	78.6135
N4101141	~500 ppm N pyrazine	5	2.4857	42618	75.1716
N4101142	~500 ppm N pyrazine	5	2.4857	41501	73.4134
N4101143	~500 ppm N pyrazine	5	2.4857	42316	74.7556

*The sample # is the same as the Computer Data Acquisition filename. The N identifies it as a nitrogen data file.

The 4 represents the lab book #4264. The next three digits are the page number for the data and the last three digits are the sample number on that page.

<u>Summarized Data</u>	<u>Ave. Counts</u>	<u>n</u>	<u>SD</u>	<u>RSD (%)</u>
~750 ppm N AgNO ₃	106014	3	1207	1.14
~1000 ppm N proline	53471	3	965	1.8
~750 ppm N NH ₄ Cl	50620	3	1277	2.52
~750 ppm N proline	55753	3	1220	2.19
~500 ppm N pyrazine	47396	3	2719	5.74
~500 ppm N pyrazine	42145	3	578	1.37

Table II-3. (cont.) Data for the effect of temperature on the nitrogen response of various nitrogen species during combustion.

Method Used:	5	PMT Voltage:	825
O ₂ to O ₃ :	30 ml/min	Furnace Temperature:	1000° C
O ₂ to pyro:	365 ml/min	Gain Setting:	HI
O ₂ to inlet:	20 ml/min	Gain Factor:	X1
He to inlet:	145 ml/min	Residence Time:	3 min
Nitrogen Species:	As Indicated	Matrix:	d,d-H ₂ O

<u>Sample #</u>	<u>Sample ID</u>	<u>Sample Vol</u> <u>(μl)</u>	<u>Known N</u> <u>Mass (μg)</u>	<u>Response</u> <u>Counts</u>	<u>CDA Sum</u> <u>Response</u>
N4100051	~750 ppm N AgNO ₃	5	3.7698	99382	175.6588
N4100052	~750 ppm N AgNO ₃	5	3.7698	104948	185.8638
N4100053	~750 ppm N AgNO ₃	5	3.7698	99483	175.9031
N4100061	~1000 ppm N proline	5	4.954	48102	85.1318
N4100062	~1000 ppm N proline	5	4.954	48591	85.8641
N4100063	~1000 ppm N proline	5	4.954	58856	104.1987
N4100064	~1000 ppm N proline	5	4.954	54512	96.5087
N4100071	~750 ppm N NH ₄ Cl	5	3.7832	48550	85.9619
N4100072	~750 ppm N NH ₄ Cl	5	3.7832	48550	85.8157
N4100073	~750 ppm N NH ₄ Cl	5	3.7832	47799	84.619
N4100181	~750 ppm N proline	5	3.789	54011	95.5807
N4100182	~750 ppm N proline	5	3.789	55265	97.6808
N4100183	~750 ppm N proline	5	3.789	53917	95.3856

*The sample # is the same as the Computer Data Acquisition filename. The N identifies it as a nitrogen data file.

The 4 represents the lab book #4264. The next three digits are the page number for the data and the last three digits are the sample number on that page.

<u>Summarized Data</u>	<u>Ave. Counts</u>	<u>n</u>	<u>SD</u>	<u>RSD (%)</u>
~750 ppm N AgNO ₃	101271	3	3185	3.14
~1000 ppm N proline	52516	4	5134	9.78
~750 ppm N NH ₄ Cl	48300	3	434	0.9
~750 ppm N proline	54398	3	753	1.38

Table II-3. (cont.) Data for the effect of temperature on the nitrogen response of various nitrogen species during combustion.

Method Used:	5	PMT Voltage:	825
O ₂ to O ₃ :	30 ml/min	Furnace Temperature:	950° C
O ₂ to pyro:	365 ml/min	Gain Setting:	HI
O ₂ to inlet:	20 ml/min	Gain Factor:	X1
He to inlet:	145 ml/min	Residence Time:	3 min
Nitrogen Species:	As Indicated	Matrix:	d,d-H ₂ O

<u>Sample #</u>	<u>Sample ID</u>	<u>Sample Vol</u> <u>(ul)</u>	<u>Known N</u> <u>Mass (ug)</u>	<u>Response</u> <u>Counts</u>	<u>CDA Sum</u> <u>Response</u>
N4101101	~750 ppm N AgNO ₃	5	3.7698	59543	99.5396
N4101102	~750 ppm N AgNO ₃	5	3.7698	68462	--
N4101103	~750 ppm N AgNO ₃	5	3.7698	74612	125.2698
N4101111	~1000 ppm N proline	5	4.954	65207	115.454
N4101112	~1000 ppm N proline	5	4.954	55920	98.9991
N4101113	~1000 ppm N proline	5	4.954	58217	103.0763
N4101131	~750 ppm N NH ₄ Cl	5	3.7832	48310	85.4001
N4101132	~750 ppm N NH ₄ Cl	5	3.7832	50860	90.0876
N4101133	~750 ppm N NH ₄ Cl	5	3.7832	45608	80.6885
N4101121	~750 ppm N proline	5	3.789	49551	87.6951
N4101122	~750 ppm N proline	5	3.789	50593	89.697
N4101123	~750 ppm N proline	5	3.789	53393	94.6292

*The sample # is the same as the Computer Data Acquisition filename. The N identifies it as a nitrogen data file.

The 4 represents the lab book #4264. The next three digits are the page number for the data and the last three digits are the sample number on that page.

<u>Summarized Data</u>	<u>Ave. Counts</u>	<u>n</u>	<u>SD</u>	<u>RSD (%)</u>
~750 ppm N AgNO ₃	67539	3	7577	11.22
~1000 ppm N proline	59782	3	4837	8.09
~750 ppm N NH ₄ Cl	48260	3	2627	5.44
~750 ppm N proline	51180	3	1987	3.88

Sample Boat Preparation

Because the use history of the quartz sample boats appeared to effect the reproducibility and accuracy of a nitrogen measurement, several methods for preparing the boats for analysis were evaluated. Because of cost, cleaning and reuse was required. For liquid samples, a small amount of quartz wool was placed in the boats to provide a greater surface area for the sample material. The quartz and wool was placed in the sample chamber. The chamber was under a vacuum and any air which entered the chamber was swept from the chamber into the pyrotube prior to the boats introduction into the pyrotube for data collection. The boat and wool were inserted into the pyrotube to clean it from contamination. At this point, the boat remained in the closed sample chamber and was no longer exposed to the laboratory environment preventing possible further contamination. The liquid sample was withdrawn through a septum from the sample bottle with a microliter syringe and was injected into the wool in the boat through a septum on the sample chamber. The total nitrogen measurement was when the boat with the sample was introduced into the pyrotube.

The manufacturers suggested that an individual boat with wool could be reused for multiple samples. When the wool visibly degraded, the boat and wool was and the boat washed in water to be reused. This was the first method tested. Using this boat preparation allows for gradual degradation of the wool surface and could affect the combustion process. This likely results in gradual loss of reproducibility and accuracy of measurement. The second method tested was to use one boat and wool for each sample

analyzed washing each boat with distilled water prior to its use. This eliminated the potential for effects from gradual degradation. The third preparation was similar to the second. However, the boat was soaked in a 0.5M HCl bath for a minimum 15 minutes prior to the distilled water wash. This was done to neutralize the sodium species which may have reacted on the quartz during the high temperature combustion. The results of the individual samples and the summarized data are presented in the following two tables.

Table II-4 . Results of total nitrogen analysis of 53.1 ppm N as tryptophan in 1N NaOH using analyzer Method Zero for three boat preparation methods.

<u>Method</u>	<u>Sample Number</u>	<u>Average Measured N Concentration (ppm)</u>	<u>Number of Replicates</u>	<u>Standard Deviation</u>	<u>% RSD</u>	<u>% Error</u>
1	1	54.5	3	4.2	7.7	2.6
1	2	52.0	3	2.5	4.9	-2.0
1	3	62.9	4	5.0	7.9	18.4
2	4	63.0	3	1.4	2.2	18.7
2	5	60.7	3	8.5	13.9	14.4
2	6	54.9	3	4.1	7.4	3.4
3	7	49.0	3	1.9	4.0	-7.7
3	8	56.5	3	1.2	2.2	6.5
3	9	46.9	3	2.1	4.5	-11.7
3	10	50.1	3	4.1	8.2	-5.6
3	11	54.4	3	5.2	9.6	2.5
3	12	56.2	3	6.1	10.9	5.9
3	13	50.4	3	1.7	3.3	-5.0
3	14	58.0	5	3.2	5.6	9.2

Table II-5. Summarized data for the three boat preparation methods.

<u>Method</u>	<u>Number of Replicates</u>	<u>Average % RSD</u>	<u>Average % Error</u>
1	3	6.8	7.7
2	3	6.9	12.2
3	8	5.5	-0.7

The summarized data in Table II-5 indicates that method 3, soaking the boats in HCl and then washing in water for use with individual samples, provided the least error on average in the total nitrogen measurement. Because the overall average percent error is very close to zero, little to no bias is indicated in the measurement. Both methods 1 and 2

indicated the error to be positive and therefore, likely a bias was present when these preparations were used that yielded concentrations higher than the known concentration. The average RSD (%) was also lower for method 3.

An analysis of variance (ANOVA) was done on the data to statistically support these findings and is outlined below. It was determined that the methods are statistically significantly different. Significant differences were also observed for the samples in Methods 1 and 3 and for all of the samples regardless of the method. Likewise, the least significant difference for each analysis was calculated to determine if there were significant differences between means within each analysis. It is likely that the significant differences between means for an individual method was due to the sodium species contamination in the boats due to previous use. The boats exhibited various degrees of contamination based on its individual history for sample analysis. Some of the boats remained heavily soiled with the inorganic ash material which had adhered to the internal walls of the boats.

Based on this analysis, method three provided the best reproducibility and accuracy for the analysis. This boat preparation technique was used for all liquid analyses. The same boat preparation was also used for solid samples. However, with solid samples, replicates were always run in separate cleaned boats for each sample and no wool was used.

Analysis of Variance for Sample Boat Preparation

An analysis of variance (ANOVA) was performed on the percent error of the measured concentrations for the three sample boat preparations evaluated. The ANOVA was done using NCSS using the GLM ANOVA method.⁹⁷ Five analyses were done providing "significance" at a 95% confidence level on methods, on individual samples within a method, and on all samples. Each analysis is significant if the "Prob>F" term is

less than $(1 - \text{confidence level})$ or $(1 - 0.95 = 0.05)$. The ANOVA reports are presented in the tables below.

All analyses were determined to be significant except that shown in Table II-8. In method 2, cleaning the boats with water only, the % error between samples was not significantly different.

Table II-6. ANOVA Table for Response Variable: % ERROR. Test for significance between methods.

<u>Source</u>	<u>DF</u>	<u>Sum-Squares</u>	<u>Mean Square</u>	<u>F-Ratio</u>	<u>Prob>F</u>	<u>Significant</u>
Method	2	1115	557.49	5.16	0.0099	yes
Error	42	4537	108.02			
Total	44	5652				

Table II-7. ANOVA Table for Response Variable: % ERROR. Test for significance between samples for method 1.

<u>Source</u>	<u>DF</u>	<u>Sum-Squares</u>	<u>Mean Square</u>	<u>F-Ratio</u>	<u>Prob>F</u>	<u>Significant</u>
Method 1	2	821	410.67	6.67	0.0239	yes
Error	7	431	61.61			
Total	9	1252				

Table II-8. ANOVA Table for Response Variable: % ERROR. Test for significance between samples for method 2.

<u>Source</u>	<u>DF</u>	<u>Sum-Squares</u>	<u>Mean Square</u>	<u>F-Ratio</u>	<u>Prob>F</u>	<u>Significant</u>
Method 2	2	371	185.52	1.74	0.2527	no
Error	6	638	106.32			
Total	8	1009				

Table II-9. ANOVA Table for Response Variable: % ERROR. Test for significance between samples for method 3.

<u>Source</u>	<u>DF</u>	<u>Sum-Squares</u>	<u>Mean Square</u>	<u>F-Ratio</u>	<u>Prob>F</u>	<u>Significant</u>
Method 3	7	1469	209.86	4.69	0.0038	yes
Error	18	806	44.79			
Total	25	2275				

Table II-10. ANOVA Table for Response Variable: % ERROR. Test for significance between samples for all methods.

<u>Source</u>	<u>DF</u>	<u>Sum-Squares</u>	<u>Mean Square</u>	<u>F-Ratio</u>	<u>Prob>F</u>	<u>Significant</u>
Method	13	3776	290.49	4.80	0.0002	yes
Error	31	1875	60.49			
Total	44	5652				

The least significant difference (LSD) between means was also determined because in a large collection of means, some of the observed differences may exceed the LSD even if no real differences among the means exist. For the data above and the means given in Table II-7, the LSD_T was used to determine the studentized range least significant difference.

$$LSD_T = Q S_x \quad (II-1)$$

where $Q = Q_{p, v_1, v_2}$ is the studentized range statistic taken from a table⁹⁷ with p = the confidence interval, v_1 is the number of means, v_2 is the number of error degrees of freedom; S_x is the standard error, (Mean Square Error/number of observations in the group)^{1/2}. The number of observations must be calculated as the harmonic mean because the number of observations in each group were not equal. The harmonic mean (n_h) is determined by the following equation.

$$n_h = a / \sum (1/n_i) \quad (II-2)$$

where a = number of means and n_i = number of observations within each group. The LSD are given in the following tables along with the determined significant differences between means for each analysis.

Table II-11. Determination of significance by the LSD_T for the ANOVAs as indicated.

<u>Analyses</u>	<u>#</u>	<u>Q</u>	<u>n_h</u>	<u>S_x</u>	<u>LSD_T</u>	<u># of Sig. Dif. Between Means</u>
% Error Between Methods	1	3.44	12.02	3.0	10.32	1
% Error Between Samples in Method 1	2	4.16	3.27	4.34	18.05	1
% Error Between Samples in Method 2	3	4.34	3.00	5.95	25.82	0
% Error Between Samples in Method 3	4	4.00	3.16	3.77	15.06	6
% Error Between Samples in All Methods	5	5.15	3.15	4.38	22.56	9

In analysis #1, the methods 2 and 3 were shown to be significantly different from each other by the LSD_T . This difference becomes apparent by the large positive overall average percent error for method 2 and the very small overall percent error in method 3. Method 3 appears to provide more accurate measurements with less bias for the error to fall in either a positive or negative direction. The significant differences between means are identified in Table II-12 and the remaining differences can be evaluated by inspection of the respective means. In many cases, the differences are significant because the boat used in the test was very heavily soiled by comparison to the others.

Table II-12. Significant difference between means evaluated by the LSD_T for the analyses indicated in Table II-11.

<u>Analyses #</u>	<u>Means with Significant Differences</u>
1	2 & 3
2	2 & 3
3	—
4	1 & 2, 1 & 8, 2 & 3, 3 & 6, 3 & 8, 4 & 8
5	3 & 7, 3 & 9, 3 & 10, 3 & 13, 4 & 7, 4 & 9, 4 & 10, 4 & 13, 5 & 9

Effect of Sample Size

The use of various sample sizes was evaluated to see if an effect on the measured nitrogen concentration existed. Three samples were used from the preparations for the TG-DSC experiments. These samples were prepared in aqueous solutions (distilled, deionized water (d, d-H₂O)) and the source of nitrogen in these samples was glutamic acid and tryptophan. The three samples used were A, BC, and ABC. As a reminder, A represented the addition of Na₂SO₄, B represented the addition of Na₂S, and C represented the addition of Na₂CO₃ for each specified treatment. Refer Appendix IV for more detail on the sample compositions.

The samples were injected into the boats for nitrogen analysis using Method Five for the analyzer. Five μ l samples were used to generate data in the range from 10-1000

ppm N as AgNO_3 in $\text{d,d-H}_2\text{O}$. The analyzer was operated under typical combustion conditions; however, the O_2 flow to the O_3 generator was at 1.5 units instead of 3.0 units. The concentrations of each sample and the resulting percent error for the measurement are provided for the sample size tested in the table below.

Table II-13. Effect of sample size on total nitrogen measurement accuracy.

<u>Sample Size (μl)</u>	% Error	% Error	% Error
	<u>Treatment A (96 ppm N)</u>	<u>Treatment BC (96 ppm N)</u>	<u>Treatment A (383 ppm N)</u>
2	-36.50	--	32.2
3	-35.41	35.68	42.55
4	-36.42	--	57.48
5	-37.04	35.94	58.89
5	-36.55	--	56.56

Note that the majority of the error is likely due to differences in conversions of the nitrogen species in the sample (nitrogen source as amine and heterocyclic from glutamic acid and tryptophan) and in the standard (nitrogen as nitrate). Even acknowledging this error, a trend in the results for Treatment ABC is apparent. Neither Treatment A nor BC shows a significant difference in the degree of error observed. The sample size was accounted for in the analysis method. Therefore, the effect observed for Treatment ABC was not fully understood but likely was associated with the sample composition.

Verification of Gas Loop Sample Size

Verification of the gas sample loop size for the gas sampling inlet of the nitrogen analyzer was required due to the unusually high response values obtained when comparing the initial response data for NO gas samples with liquid samples. The operating manual for the gas sampling inlet system identified the sample loop volume as 2.0 ml. All initial calculations were based on the 2.0 ml volume. The manufacturer was not able to verify the sample loop size as it was not standardized for every instrument. Therefore, the sample loop volume had to be measured. Measurements were made using several methods and are

discussed here. The first was by estimation based on physical dimensions. The equation for the volume of a cylinder (Eq. II-3) was used.

$$V_{\text{cyl}} = \pi r^2 h \quad (\text{II-3})$$

The sample loop was removed from the gas sample box and physically measured by tracing the external length of the coiled loop with fishing line. The loop was made of 0.125" stainless steel tubing with a 2 mm ID. The length of the loop was found to be 161.7 cm and therefore, the volume was found to be 5.08 cm³.

To verify the physical measurement, The gas sample loop was submersed in methanol and then the weight of the solvent inside the loop was determined. The sample loop volume was then calculated by dividing the solvent weight by its density. A second solvent, methylene chloride (CH₂Cl₂), was used and each test was repeated. The data and results are given in Table II-14. The sample loop was identified as 5.0 ml and the appropriate corrections for the previous sets of data were made.

Table II-14. Parameters for determination of gas sample loop volume by submersion in solvent. The sample loop weight was 64.19 g.

<u>Solvent ID/Sample #</u>	<u>Sample Loop + Solvent Wt. (g)</u>	<u>Solvent Wt. (g)</u>	<u>Solvent Density (g/cm³)</u>	<u>Calculated Loop Volume (cm³)</u>
Methanol/1	68.22	4.03	0.7917	5.09
Methanol/2	68.18	3.99	0.7917	5.04
CH ₂ Cl ₂ /1	70.80	6.61	1.325	4.99
CH ₂ Cl ₂ /2	70.81	6.62	1.325	5.00

TOTAL NITROGEN MEASUREMENT

Measurement of Multiple Fuel Nitrogen Species

The work to quantify the effects of additions of various nitrogen species injected into the NO and NH₃ gas stream on the fixed nitrogen results was completed. Several species of nitrogen compounds were injected into the NO gas stream at concentrations of 250, 500, and 750 ppm N as NO or NH₃. The nitrogen species included proline, NH₄Cl, pyrazine, glutamic acid, and AgNO₃. All data was collected in the concentration range from about 300-850 ppm N. A complete set of data is provided at the end of this section for these experiments.

Model Fuel-N Species with NO (g)

Early results indicated a slight reduction in the overall measurement of NO at NO gas concentrations of 500 and 750 ppm when combined with other nitrogen species, while NO at concentrations of 250 ppm injected with various nitrogen species seemed to enhance the total nitrogen response. This is shown in the figure below.

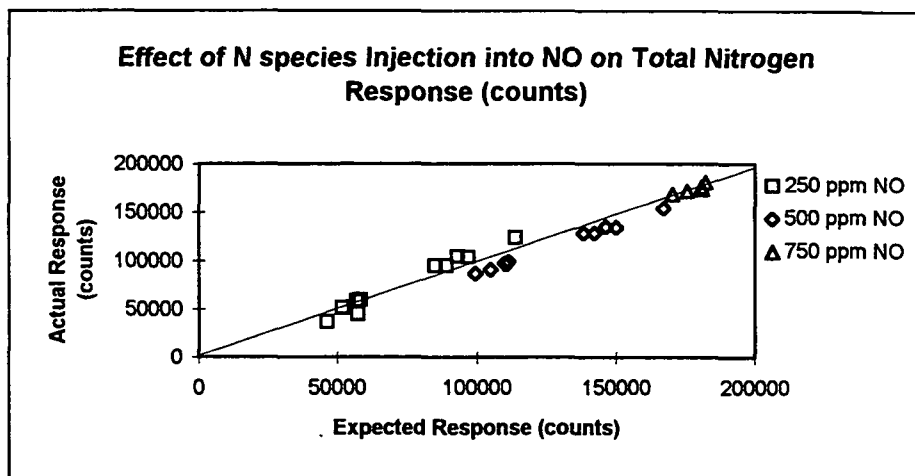


Figure II-2. Comparison of expected and actual response for the nitrogen measured during injection of aqueous nitrogen species into an NO gas stream.

Further analysis of the data suggests that the differences observed are likely the result of daily fluctuations in the analyzer performance. Further testing indicated this to be the case. Also, the carrier gas cylinder was switched out during the data collection and may be responsible for the differences observed in the response due to changes in pressure.

The differences for the various nitrogen species injected into 250 ppm NO ranged from -22.6% to 11.5% of the expected response with the injection of 0.4989 $\mu\text{g N}$ as AgNO_3 yielding the lowest response and 2.564 $\mu\text{g N}$ as proline yielding the greatest response. For 500 ppm NO, the response was -7.2 to -13.3 % lower than expected and for 750 ppm NO, the response was only -0.4 to -3.9% less than the expected values for the various nitrogen species injected.

Further results to quantify the effects of additions of various nitrogen species on the total nitrogen response when they were injected into the NO gas stream are provided in the table below. These results show no enhancement or reduction in the total nitrogen response indicating no competing reactions (i.e. formation of N_2) to be occurring with in the combustion environment of the analyzer. The relative differences in the experimental averages and the expected values are very small and can be explained by the variation within the measurements. All data was collected in the concentration range from about 300–850 ppm N total.

Table II-15. Comparative nitrogen response for aqueous nitrogen sample injection into NO gas stream.

[NO] (~ ppm N)	Injected Sample ID	Experimental Ave. N Response (counts)	Std. Dev. (counts)	Rel. Std. Dev. (%)	Expected Ave. N Response (counts)	Expected Std. Dev. (counts)	Absolute % Difference
250	50 ppm N as Glut. Acid	45437	100	0.22	44001	773	3.26
250	100 ppm N as Glut. Acid	50091	122	0.24	49439	820	1.32
250	100 ppm N as pyrazine	51775	171	0.33	50342	683	2.85
250	100 ppm N as NH ₄ Cl	50194	1027	2.05	49494	950	1.41
250	100 ppm N as AgNO ₃	47575	2458	5.17	47640	2099	0.14
500	50 ppm N as Glut. Acid	94716	657	0.69	93326	954	1.49
500	100 ppm N as Glut. Acid	100028	444	0.44	98764	1001	1.28
500	100 ppm N as pyrazine	96954	1261	1.30	99667	864	2.72
500	100 ppm N as NH ₄ Cl	99798	822	0.82	98819	1131	0.99
500	100 ppm N as AgNO ₃	87789	945	1.08	96965	2280	9.46
750	50 ppm N as Glut. Acid	150348	2484	1.65	149241	1499	0.74
750	100 ppm N as Glut. Acid	154439	3573	2.31	154679	1546	0.16
750	100 ppm N as pyrazine	155013	869	0.56	155582	1409	0.37
750	100 ppm N as NH ₄ Cl	153023	1118	0.73	154734	1676	1.11
750	100 ppm N as AgNO ₃	152810	1922	1.25	152880	2825	0.61

The data shows that there is little to no difference in the experimental and the expected total nitrogen response. The differences observed in nearly all of the sets of data can be accounted for within the standard deviation of the measurements. In only two sets of data is the % difference greater than 3%. At 250 ppm N as NO with an injection of 50 ppm N as glutamic acid, the % difference was 3.26%. Through out all of the testing, the variation in the nitrogen response from the glutamic acid samples was relatively high. A percent difference of 9.46% was observed for 500 ppm N as NO with an injection of 100 ppm N as AgNO₃. It was noted that the silver nitrate samples seemed to be absorbing in the injection port of the combustion chamber. While acid purges were used to flush nitrogen from the system, the absorption may account for the low value. Overall, no reactions were occurring between the NO gas and the nitrogen species within the combustion chamber when these species were measured together. The result can simply be taken as the sum of the individual nitrogen species measurements.

Model Fuel-N Species with NH₃ (g)

Similar experiments were conducted for gas phase reactions of NH₃ with the injected aqueous nitrogen species. All data required to evaluate the effects of additions of various nitrogen species on the fixed nitrogen response when injected into a NH₃ gas stream was collected. The results shown in Table II-16 below indicate no enhancement or reduction in the total nitrogen response indicating no reaction to be occurring within the combustion environment of the analyzer. The relative differences in the experimental averages and the expected values are very small and as with the NO results, can be explained by the variation within the measurements. All data was collected in the concentration range from about 300–850 ppm N total.

Table II-16. Comparative nitrogen response for aqueous nitrogen sample injection into NH₃ gas stream.

[NH ₃] (~ ppm N)	Injected Sample ID	Experimental Ave. N Response (counts)	Std. Dev. (counts)	Rel. Std. Dev. (%)	Expected Ave. N Response (counts)	Expected Std. Dev. (counts)	Absolute % Difference
250	50 ppm N as Glut. Acid	63324	1994	3.15	68422	2045	7.45
250	100 ppm N as Glut. Acid	71908	3938	5.48	74312	4091	3.24
250	100 ppm N as pyrazine	68799	5563	8.09	74679	5715	7.87
250	100 ppm N as NH ₄ Cl	71615	2452	3.42	74301	2470	3.62
250	100 ppm N as AgNO ₃	59935	796	1.33	73317	2278	18.25
500	50 ppm N as Glut. Acid	110583	6893	6.23	117103	6961	5.57
500	100 ppm N as Glut. Acid	119446	4504	3.77	122523	5005	2.51
500	100 ppm N as pyrazine	120643	4074	3.38	123511	4092	2.32
500	100 ppm N as NH ₄ Cl	118227	2951	2.50	123061	3088	3.93
500	100 ppm N as AgNO ₃	126673	7972	6.29	121353	9746	4.38
750	50 ppm N as Glut. Acid	158486	3345	2.11	164526	3365	3.67
750	100 ppm N as Glut. Acid	170416	1401	0.82	169908	1672	0.30
750	100 ppm N as pyrazine	158072	4896	3.10	170272	4988	7.16
750	100 ppm N as NH ₄ Cl	164313	7086	4.31	170050	7222	3.37
750	100 ppm N as AgNO ₃	168943	5427	3.21	170236	6851	0.76

Again, the data show that there is little to no difference in the experimental and expected total nitrogen response. The differences observed in nearly all sets of data can be accounted for within the standard deviation of the measurement. In general, however, the variation in the nitrogen measurements for NH₃ was greater than that for NO.

In only three sets of data is the absolute percent difference greater than 6% and all of these occurred with measurements of ~250 ppm N as NH_3 . With an injection of 50 ppm N as glutamic acid, the percent difference was 7.45%. When ~100 ppm N as pyrazine was injected, a percent difference of 7.87% was observed. With an injection of 100 ppm N as AgNO_3 , the percent difference was 18.25%. It was noted that the silver nitrate samples seemed to be absorbing in the injection port of the combustion chamber. While acid purges were used to flush nitrogen from the system, the absorption may account for the lower average value. It should also be noted that the dilution gas (He) cylinder pressure was approaching low levels for some of the samples which seemed to increase the variation observed. Overall, no reactions appeared to be occurring between the NH_3 gas and the nitrogen species within the combustion chamber when these species were measured together. As with the injections made into the NO gas stream, the results can simply be taken as the sum of the individual nitrogen species measurements.

Data Tables for Multiple Fuel Nitrogen Species Measurements

Fixed nitrogen data collected under combustion conditions for multiple fuel-nitrogen species is provided in this appendix. The data included are the following: 1) data for aqueous nitrogen sample injected into the gas stream used as a control for further measurements, 2) calibration data for NO and NH_3 , and 3) data for the injection of nitrogen samples into the NO and NH_3 gas streams for total nitrogen measurement and interactions between gas phase species. The correction data for NO and NH_3 gas concentrations for the conversion of ppm-mole for gas concentrations to ppm-gram for the aqueous nitrogen samples are provided in Appendix V.

Each set of data is presented along with the statistical summaries. Error estimates can be taken from the correlation coefficients in the plots as well as the statistical standard deviation and coefficient of variation.

The sample numbers in the data tables, such as N4097022, are the same as the computer data acquisition (CDA) file names. The N identifies the sample as a nitrogen release profile type of data file. The 4 represents the lab notebook #4264. The next three digits are the page number within the notebook where the data can be found and the last three digits are the sample number on that page. The last digit represents the number of the replicate. For the example, the values listed for the N4097022 sample would be found in notebook 4264 on page 97 as sample 2, replicate 2.

Table II-17. Data for measurement of nitrogen species during combustion; sample injected into the gas phase.

Method Used:	5	PMT Voltage:	825
O2 to O3:	30 ml/min	Furnace Temperature:	1100° C
O2 to pyro:	365 ml/min	Gain Setting:	HI
O2 to inlet:	20 ml/min	Gain Factor:	X1
He to inlet:	145 ml/min	Residence Time:	3 min
Nitrogen Species: Pyrazine		Matrix:	H ₂ O*

*Note: All samples were injected manually into the pyrotube as the gas sample box was in line.

Carrier gas (He) flow rate setting at 1.0 (25 ml/min).

Sample #	Sample ID	Sample Vol (μ l)	Known N Mass (μ g)	Response Counts	CDA Sum Response
N4113011	~500 ppm N	5	2.4857	51751*	89.8928
N4113012	~500 ppm N	5	2.4857	51638*	90.576
N4113013	~500 ppm N	5	2.4857	53405	94.3117
N4113014	~500 ppm N	5	2.4857	50989	89.9658
N4113015	~500 ppm N	5	2.4857	49910*	87.6955
N4113016	~500 ppm N	5	2.4857	56879	100.6346
N4113021	~100 ppm N	5	0.5076	12168	21.1425
N4113022	~100 ppm N	5	0.5076	12050	20.8985
N4113023	~100 ppm N	5	0.5076	12019	20.9961

*Note: These points have not been used in the analysis, because they are known to be in error experimentally.

Summarized Data	Ave. Counts	n	SD	RSD (%)
~100 ppm N	12079	3	78	0.65
~500 ppm N	53758	3	2961	5.51

Nitrogen Species: AgNO₃ Matrix: H₂O*

*Note: All samples were injected manually into the pyrotube as the gas sample box was in line.

Carrier gas (He) flow rate setting at 1.0 (25 ml/min).

Sample #	Sample ID	Sample Vol (μ l)	Known N Mass (μ g)	Response Counts	CDA Sum Response
N4113031	~100 ppm N	5	0.4989	11229	19.2628
N4113032	~100 ppm N	5	0.4989	8218	14.38
N4113033	~100 ppm N	5	0.4989	9948	17.2362
N4113034	~100 ppm N	5	0.4989	8112	13.8181

Summarized Data	Ave. Counts	n	SD	RSD (%)
~100 ppm N	9377	4	1494	15.9

Table II-17. (cont.) Data for measurement of nitrogen species during combustion; sample injected into the gas phase.

Method Used: 5 PMT Voltage: 825
 O2 to O3: 30 ml/min Furnace Temperature: 1100° C
 O2 to pyro: 365 ml/min Gain Setting: HI
 O2 to inlet: 20 ml/min Gain Factor: X1
 He to inlet: 145 ml/min Residence Time: 3 min
 Nitrogen Species: proline Matrix: H2O*

*Note: All samples were injected manually into the pyrotube as the gas sample box was in line.

Carrier gas (He) flow rate setting at 1.0 (25 ml/min).

Sample #	Sample ID	Sample Vol (μ l)	Known N Mass (μ g)	Response Counts	CDA Sum Response
N4113041	~500 ppm N	5	2.564	56855	100.0736
N4113042	~500 ppm N	5	2.564	57156	--
N4113043	~500 ppm N	5	2.564	52173	91.968

Summarized Data	Ave. Counts	n	SD	RSD (%)
~500 ppm N	55395	3	2794	5.04

Method Used: 5 PMT Voltage: 825 3/19/95
 O2 to O3: 30 ml/min Furnace Temperature: 1100C
 O2 to pyro: 365 ml/min Gain Setting: HI
 O2 to inlet: 20 ml/min Gain Factor: X1
 He to inlet: 145 ml/min Residence Time: 3 min
 Nitrogen Species: Glutamic Acid Matrix: H2O*

*Note: All samples were injected manually into the pyrotube as the gas sample box was in line.

Carrier gas (He) flow rate setting at 1.0 (25 ml/min).

Sample #	Sample ID	Sample Vol (μ l)	Known N Mass (μ g)	Response Counts	CDA Sum Response
N4113051	~500 ppm N	5	2.4791	49492	87.3046
N4113052	~500 ppm N	5	2.4791	48190	84.9601
N4113053	~500 ppm N	5	2.4791	42816	75.5613
N4113061	~50 ppm N	5	0.2564	5907	10.1563
N4113062	~50 ppm N	5	0.2564	5736	9.9365
N4113063	~50 ppm N	5	0.2564	5571	9.5948
N4113071	~100 ppm N	5	0.4953	11386	19.8244
N4113072	~100 ppm N	5	0.4953	11187	19.4093
N4113073	~100 ppm N	5	0.4953	10955	19.165

Summarized Data	Ave. Counts	n	SD	RSD (%)
~50 ppm N	5738	3	168	2.92
~100 ppm N	11176	3	215	1.93
~500 ppm N	46832	3	3539	7.56

Table II-17. (cont.) Data for measurement of nitrogen species by combustion;
sample injected into the gas phase.

Method Used:	5	PMT Voltage:	825
O2 to O3:	30 ml/min	Furnace Temperature:	1100° C
O2 to pyro:	365 ml/min	Gain Setting:	HI
O2 to inlet:	20 ml/min	Gain Factor:	X1
He to inlet:	145 ml/min	Residence Time:	3 min
Nitrogen Species:	NH ₄ Cl	Matrix:	H ₂ O*

*Note: All samples were injected manually into the pyrotube as the gas sample box was in line.

Carrier gas (He) flow rate setting at 1.0 (25 ml/min).

<u>Sample #</u>	<u>Sample ID</u>	<u>Sample Vol</u> <u>(μl)</u>	<u>Known N</u> <u>Mass (μg)</u>	<u>Response</u> <u>Counts</u>	<u>CDA Sum</u> <u>Response</u>
N4113081	~100 ppm N	5	0.5098	11494	20.0195
N4113082	~100 ppm N	5	0.5098	11358	19.8732
N4113083	~100 ppm N	5	0.5098	10840	18.872
N4113091	~500 ppm N	5	2.549	40371	71.4113
N4113092	~500 ppm N	5	2.549	45826	80.8834
N4113093	~500 ppm N	5	2.549	44306	78.1005
<u>Summarized Data</u>	<u>Ave. Counts</u>	<u>n</u>	<u>SD</u>	<u>RSD (%)</u>	
~100 ppm N	11231	3	345	3.07	
~500 ppm N	43501	3	2815	6.47	

Table II-18. Data for total measurement of nitrogen species with NO (g) during combustion; sample injected into the NO.

Method Used:	5	PMT Voltage:	825
O2 to O3:	30 ml/min	Furnace Temperature:	1100° C
O2 to pyro:	365 ml/min	Gain Setting:	HI
O2 to inlet:	20 ml/min	Gain Factor:	X1
He to inlet:	145 ml/min	Residence Time:	3 min
N Species:	~750 ppm N as NO	Matrix:	He
Carrier gas:	He(g)	Gas box carrier flow:	0.025 lpm

<u>Sample #</u>	<u>Injected* Sample ID</u>	<u>Inj. Sample Mass (ul)</u>	<u>Flow (lpm) NO in He</u>	<u>Flow (lpm) He</u>	<u>Known N Mass (ug)</u>	<u>Response Counts</u>	<u>CDA Sum Response</u>
N4114131	0.5098 ug N NH4Cl	5	0.686	3.60	4.8552	153274	270.1402
N4114132	0.5098 ug N NH4Cl	5	0.688	3.60	4.8628	153995	271.1165
N4114133	0.5098 ug N NH4Cl	5	0.688	3.59	4.8774	151801	267.6496
N4114141	0.5076 ug N pyrazine	5	0.688	3.59	4.8752	154652	272.6062
N4114142	0.5076 ug N pyrazine	5	0.686	3.59	4.8675	156005	274.8035
N4114143	0.5076 ug N pyrazine	5	0.686	3.60	4.852	154383	272.3365
N4114151	0.4989 ug N AgNO3	5	0.686	3.60	4.8443	155724	274.7793
N4114152	0.4989 ug N AgNO3	5	0.689	3.60	4.8595	153825	271.384
N4114153	0.4989 ug N AgNO3	5	0.685	3.60	4.8367	151881	267.8213
N4114171	0.4953 ug N glut.acid	5	0.689	3.60	4.8559	150986	--
N4114172	0.4953 ug N glut.acid	5	0.685	3.60	4.8331	154211	272.2161
N4114173	0.4953 ug N glut.acid	5	0.689	3.60	4.8559	158120	278.9779
N4114181	0.2564 ug N glut.acid	5	0.688	3.60	4.6094	147599	260.5941
N4114182	0.2564 ug N glut.acid	5	0.686	3.60	4.6018	151018	266.5037
N4114183	0.2564 ug N glut.acid	5	0.686	3.60	4.6018	152429	268.7728

<u>Summarized Data</u>	<u>Ave. Counts</u>	<u>n</u>	<u>SD</u>	<u>RSD (%)</u>
0.5098 ug N NH4Cl	153023	3	1118	0.73
0.5076 ug N pyrazine	155013	3	869	0.56
0.4989 ug N AgNO3	153810	3	1922	1.25
0.4953 ug N glut.acid	154439	3	3573	2.31
0.2564 ug N glut.acid	150348	3	2484	1.65

Table II-18. (cont.) Data for total measurement of nitrogen species with NO (g) during combustion; sample injected into the NO.

Method Used:	5	PMT Voltage:	825
O2 to O3:	30 ml/min	Furnace Temperature:	1100° C
O2 to pyro:	365 ml/min	Gain Setting:	HI
O2 to inlet:	20 ml/min	Gain Factor:	X1
He to inlet:	145 ml/min	Residence Time:	3 min
N Species: ~500 ppm N as NO		Matrix:	He
Carrier gas:	He(g)	Gas box carrier flow:	0.025 lpm

Sample #	Injected* Sample ID	Inj. Sample Mass (ul)	Flow (lpm) NO in He	Flow (lpm) He	Known N Mass (ug)	Response Counts	CDA Sum Response
N4115221	0.5098 ug N NH4Cl	5	0.436	3.86	3.2664	100713	176.1235
N4115222	0.5098 ug N NH4Cl	5	0.429	3.86	3.2257	99559	175.0488
N4115223	0.5098 ug N NH4Cl	5	0.433	3.85	3.2593	99121	174.2917
N4115241	0.5076 ug N pyrazine	5	0.432	3.88	3.2307	101256	177.8567
N4115242	0.5076 ug N pyrazine	5	0.432	3.89	3.2217	98570	173.5847
N4115243	0.5076 ug N pyrazine	5	0.432	3.88	3.2307	100398	176.4405
N4115251	0.4989 ug N AgNO3	5	0.432	3.88	3.222	97493	171.2651
N4115252	0.4989 ug N AgNO3	5	0.430	3.89	3.2049	95513	167.8232
N4115253	0.4989 ug N AgNO3	5	0.432	3.85	3.2402	97856	171.9473
N4115231	0.4953 ug N glut.acid	5	0.438	3.86	3.2636	100527	176.6597
N4115232	0.4953 ug N glut.acid	5	0.435	3.86	3.2473	99880	175.4629
N4115233	0.4953 ug N glut.acid	5	0.433	3.86	3.2392	99678	174.9025
N4114211	0.2564 ug N glut.acid	5	0.429	3.86	2.9723	94977	166.7976
N4114212	0.2564 ug N glut.acid	5	0.433	3.86	2.9967	93969	165.2338
N4114213	0.2564 ug N glut.acid	5	0.433	3.86	2.9967	95204	167.2607

Summarized Data	Ave. Counts	n	SD	RSD (%)
0.5098 ug N NH4Cl	99798	3	822	0.82
0.5076 ug N pyrazine	96954	3	1261	1.3
0.4989 ug N AgNO3	87789	3	945	1.08
0.4953 ug N glut.acid	100028	3	444	0.44
0.2564 ug N glut.acid	94716	3	657	0.69

Table II-18. (cont.) Data for total measurement of nitrogen species with NO (g) during combustion; sample injected into the NO.

Method Used:	5	PMT Voltage:	825
O2 to O3:	30 ml/min	Furnace Temperature:	1100C
O2 to pyro:	365 ml/min	Gain Setting:	HI
O2 to inlet:	20 ml/min	Gain Factor:	X1
He to inlet:	145 ml/min	Residence Time:	3 min
N Species:	~250 ppm N as NO	Matrix:	He
Carrier gas:	He(g)	Gas box carrier flow:	0.025 lpm

<u>Sample #</u>	<u>Injected*</u> <u>Sample ID</u>	<u>Inj. Sample</u> <u>Mass (ul)</u>	<u>Flow (lpm)</u> <u>NO in He</u>	<u>Flow (lpm)</u> <u>He</u>	<u>Known N</u> <u>Mass (ug)</u>	<u>Response</u> <u>Counts</u>	<u>CDA Sum</u> <u>Response</u>
N4115311	0.5098 ug N NH4Cl	5	0.204	4.08	1.8074	49042	85.7416
N4115312	0.5098 ug N NH4Cl	5	0.204	4.06	1.8117	50526	88.3775
N4115313	0.5098 ug N NH4Cl	5	0.204	4.06	1.8117	51015	88.842
N4115321	0.5076 ug N pyrazine	5	0.206	4.06	1.8182	51855	90.4775
N4115322	0.5076 ug N pyrazine	5	0.206	4.06	1.8182	51578	90.0384
N4115323	0.5076 ug N pyrazine	5	0.204	4.08	1.8052	51891	90.6491
N4115281	0.4989 ug N AgNO3	5	0.204	4.10	1.7879	49219	85.8878
N4115282	0.4989 ug N AgNO3	5	0.204	4.08	1.7965	48756	84.9593
N4115283	0.4989 ug N AgNO3	5	0.204	4.06	1.8008	44749	78.0018
N4115301	0.4953 ug N glut.acid	5	0.204	4.08	1.7929	49974	86.9607
N4115302	0.4953 ug N glut.acid	5	0.204	4.08	1.7929	50218	87.5966
N4115303	0.4953 ug N glut.acid	5	0.204	4.08	1.7929	50082	87.1333
N4116331	0.2564 ug N glut.acid	5	0.206	4.08	1.5626	45360	78.8568
N4116332	0.2564 ug N glut.acid	5	0.206	4.06	1.567	45402	79.344
N4116333	0.2564 ug N glut.acid	5	0.206	4.08	1.5626	45550	79.4166

<u>Summarized Data</u>	<u>Ave. Counts</u>	<u>n</u>	<u>SD</u>	<u>RSD (%)</u>
0.5098 ug N NH4Cl	50194	3	1027	2.05
0.5076 ug N pyrazine	51775	3	171	0.33
0.4989 ug N AgNO3	47575	3	2458	5.17
0.4953 ug N glut.acid	50091	3	122	0.24
0.2564 ug N glut.acid	45437	3	100	0.22

Table II-18. (cont.) Data for total measurement of nitrogen species with NO (g) during combustion; sample injected into the NO.

Method Used:	5	PMT Voltage:	825
O2 to O3:	30 ml/min	Furnace Temperature:	1100° C
O2 to pyro:	365 ml/min	Gain Setting:	HI
O2 to inlet:	20 ml/min	Gain Factor:	X1
He to inlet:	145 ml/min	Residence Time:	3 min
N Species: ~500 ppm N as NO		Matrix:	He
Carrier gas:	He(g)	Gas box carrier flow:	0.025 lpm

Sample #	Injected* Sample ID	Inj. Sample Mass (μl)	Flow (lpm) NO in He	Flow (lpm) He	Known N Mass (μg)	Response Counts	CDA Sum Response
N4109161	2.564 ug N proline	5	0.439	3.86	5.337	135770	239.355
N4109162	2.564 ug N proline	5	0.435	3.88	5.303	136624	240.7714
N4109163	2.564 ug N proline	5	0.432	3.88	5.287	134094	236.5481
N4109164	2.564 ug N proline	5	0.432	3.88	5.287	134872	238.0616
N4109171	3.789 ug N proline	5	0.430	3.88	6.504	152246	268.8235
N4109172	3.789 ug N proline	5	0.429	3.86	6.505	157622	278.2956
N4109173	3.789 ug N proline	5	0.429	3.86	6.505	152148	268.8483
N4109174	3.789 ug N proline	5	0.433	3.85	6.539	154224	272.168

N Species: ~250 ppm N as NO	Matrix:	He
Carrier gas:	He(g)	Gas box carrier flow: 0.025 lpm

Sample #	Injected* Sample ID	Inj. Sample Mass (μl)	Flow (lpm) NO in He	Flow (lpm) He	Known N Mass (μg)	Response Counts	CDA Sum Response
N4111351	2.564 ug N proline	5	0.207	4.08	3.879	104372	183.3251
N4111352	2.564 ug N proline	5	0.207	4.08	3.879	93346*	164.0389
N4111353	2.564 ug N proline	5	0.207	4.08	3.879	104292	183.4722
N4111354	2.564 ug N proline	5	0.209	4.08	3.888	103202	182.0552
N4111361	3.789 ug N proline	5	0.209	4.08	5.113	126874	223.5838
N4111362	3.789 ug N proline	5	0.210	4.08	5.121	122982	216.7971
N4111363	3.789 ug N proline	5	0.207	4.08	5.104	121654	214.2338
N4111331	0.5098 ug N NH4Cl	5	0.207	4.08	1.825	58452	102.3929
N4111332	0.5098 ug N NH4Cl	5	0.207	4.08	1.825	57900	101.3198
N4111333	0.5098 ug N NH4Cl	5	0.206	4.06	1.820	57780	100.8578
N4111341	2.5490 ug N NH4Cl	5	0.210	4.09	3.877	95934	168.7267
N4111342	2.5490 ug N NH4Cl	5	0.209	4.08	3.873	95594	167.8706
N4111343	2.5490 ug N NH4Cl	5	0.209	4.08	3.873	92624	162.9158

[NO]	Summarized Data	Ave. Counts	n	SD	RSD (%)
250 ppm	0.5098 ug N NH4Cl	58044	3	358	62
250 ppm	2.5490 ug N NH4Cl	94717	3	1821	1.92
250 ppm	2.564 ug N proline	103955	3	654	0.63
250 ppm	3.789 ug N proline	123837	3	2713	2.19
500 ppm	2.564 ug N proline	135340	4	1096	0.81
500 ppm	3.789 ug N proline	154060	4	2560	1.66

Table II-18. (cont.) Data for total measurement of nitrogen species with NO (g) during combustion; sample injected into the NO.

Method Used:	5	PMT Voltage:	825
O2 to O3:	30 ml/min	Furnace Temperature:	1100° C
O2 to pyro:	365 ml/min	Gain Setting:	HI
O2 to inlet:	20 ml/min	Gain Factor:	X1
He to inlet:	145 ml/min	Residence Time:	3 min
N Species: ~250 ppm N as NO		Matrix:	He
Carrier gas:	He(g)	Gas box carrier flow:	0.025 lpm

<u>Sample #</u>	<u>Injected*</u> <u>Sample ID</u>	<u>Inj. Sample</u> <u>Mass (µl)</u>	<u>Flow (lpm)</u> <u>NO in He</u>	<u>Flow (lpm)</u> <u>He</u>	<u>Known N</u> <u>Mass (µg)</u>	<u>Response</u> <u>Counts</u>	<u>CDA Sum</u> <u>Response</u>
N4111311	0.5076 ug N pyrazine	5	0.206	4.09	1.810	58468	101.8807
N4111312	0.5076 ug N pyrazine	5	0.210	4.09	1.835	60042	104.9077
N4111313	0.5076 ug N pyrazine	5	0.209	4.08	1.831	59170	103.5413
N4111321	2.4857 ug N pyrazine	5	0.207	4.08	3.801	102100	179.9073
N4111322	2.4857 ug N pyrazine	5	0.207	4.08	3.801	104558	183.6673
N4111323	2.4857 ug N pyrazine	5	0.207	4.08	3.801	104926	184.6676
N4111371	0.2564 ug N glut.acid	5	0.210	4.08	1.589	52158	91.0901
N4111372	0.2564 ug N glut.acid	5	0.209	4.08	1.580	52606	91.8958
N4111373	0.2564 ug N glut.acid	5	0.209	4.08	1.580	53872	93.7266
N4111381	2.4791 ug N glut.acid	5	0.209	4.09	3.798	92484	162.5982
N4111382	2.4791 ug N glut.acid	5	0.209	4.09	3.798	91688	161.4752
N4111383	2.4791 ug N glut.acid	5	0.209	4.09	3.798	99760	175.5862
N4111391	0.4953 ug N glut.acid	5	0.209	4.09	1.814	58090	101.5882
N4111392	0.4953 ug N glut.acid	5	0.209	4.09	1.814	57334	100.2701
N4111393	0.4953 ug N glut.acid	5	0.209	4.08	1.819	57214	100.1233
N4111291	0.4953 ug N glut.acid	5	0.206	4.09	1.801	46938	82.0789
N4111292	0.4953 ug N glut.acid	5	0.206	4.09	1.801	40874	70.604
N4111293	0.4953 ug N glut.acid	5	0.204	4.09	1.792	45428	78.9058

<u>[NO]</u>	<u>Summarized Data</u>	<u>Ave. Counts</u>	<u>n</u>	<u>SD</u>	<u>RSD (%)</u>
250 ppm	0.5076 ug N pyrazine	59227	3	788	1.33
250 ppm	2.4857 ug N pyrazine	103861	3	1536	1.48
250 ppm	0.2564 ug N glut.acid	51220	3	3397	6.63
250 ppm	2.4791 ug N glut.acid	94644	3	4448	4.70
250 ppm	0.4953 ug N glut.acid	57579	3	442	0.77
250 ppm	0.4989 ug N AgNO3	44413	3	3157	7.11

Table II-18. (cont.) Data for total measurement of nitrogen species with NO (g) during combustion; sample injected into the NO.

Method Used: 5 PMT Voltage: 825
 O2 to O3: 30 ml/min Furnace Temperature: 1100° C
 O2 to pyro: 365 ml/min Gain Setting: HI
 O2 to inlet: 20 ml/min Gain Factor: X1
 He to inlet: 145 ml/min Residence Time: 3 min
 N Species: ~500 ppm N as NO Matrix: He
 Carrier gas: He(g) Gas box carrier flow: 0.025 lpm

Sample #	Injected* Sample ID	Inj. Sample Mass (µl)	Flow (lpm) NO in He	Flow (lpm) He	Known N Mass (µg)	Response Counts	CDA Sum Response
N4110181	0.5098 ug N NH4Cl	5	0.433	3.86	3.250	97508	171.2163
N4110182	0.5098 ug N NH4Cl	5	0.430	3.86	3.234	95722	167.8966
N4110183	0.5098 ug N NH4Cl	5	0.448	3.86	3.331	95576	167.7245
N4110191	2.5490 ug N NH4Cl	5	0.432	3.86	5.281	127812	225.1959
N4110192	2.5490 ug N NH4Cl	5	0.430	3.85	5.282	127862	225.6109
N4110193	2.5490 ug N NH4Cl	5	0.430	3.86	5.273	129010	227.8078
N4110201	0.2564 ug N glut.acid	5	0.429	3.85	2.981	89940	158.0819
N4110202	0.2564 ug N glut.acid	5	0.438	3.86	3.021	92922	163.5502
N4110203	0.2564 ug N glut.acid	5	0.438	3.86	3.021	87650	153.9065
N4110211	0.4953 ug N glut.acid	5	0.438	3.86	3.260	98654	170.2881
N4110212	0.4953 ug N glut.acid	5	0.438	3.86	3.260	96212	169.0915
N4110213	0.4953 ug N glut.acid	5	0.438	3.86	3.260	98604	173.6331
N4110221	2.4791 ug N glut.acid	5	0.436	3.86	5.236	130738	230.5173
N4110222	2.4791 ug N glut.acid	5	0.436	3.86	5.236	129496	228.223
N4110223	2.4791 ug N glut.acid	5	0.436	3.86	5.236	124948	220.1903
N4110231	0.5076 ug N pyrazine	5	0.430	3.86	3.232	101122	177.7101
N4110232	0.5076 ug N pyrazine	5	0.433	3.86	3.248	98316	172.8517
N4110233	0.5076 ug N pyrazine	5	0.429	3.86	3.224	97110	170.7277
N4110241	2.4857 ug N pyrazine	5	0.433	3.86	5.226	133326	235.6452
N4110242	2.4857 ug N pyrazine	5	0.428	3.86	5.193	127552	224.6589
N4110243	2.4857 ug N pyrazine	5	0.439	3.86	5.259	142262	250.7572
N4110251	0.4989 ug N AgNO3	5	0.436	3.86	3.256	99374	174.8046
N4110252	0.4989 ug N AgNO3	5	0.433	3.86	3.239	93984	165.1859
N4110253	0.4989 ug N AgNO3	5	0.432	3.86	3.231	94248	167.5769
N4110261	H2O	5	0.429	3.86	2.716	85808	150.4163
N4110262	H2O	5	0.433	3.88	2.731	86783	151.8813
N4110263	H2O	5	0.438	3.88	2.756	86332	151.3924

[NO]	Summarized Data	Ave. Counts	n	SD	RSD (%)
500 ppm	0.5098 ug N NH4Cl	96268	3	1076	1.12
500 ppm	2.5490 ug N NH4Cl	128228	3	678	0.53
501 ppm	0.2564 ug N glut.acid	90171	3	2644	2.93
500 ppm	0.4953 ug N glut.acid	97223	3	1238	1.27
500 ppm	2.4791 ug N glut.acid	128394	3	3048	2.37
500 ppm	0.5076 ug N pyrazine	98849	3	2058	2.08
500 ppm	2.4857 ug N pyrazine	134380	3	7411	5.52
500 ppm	0.4989 ug N AgNO3	95869	3	3039	3.17
500 ppm	H2O	86308	3	488	0.57

Table II-19. Data for total measurement of nitrogen species with NO (g) during combustion; sample injected into the NO.

Method Used:	5	PMT Voltage:	825
O2 to O3:	30 ml/min	Furnace Temperature:	1100° C
O2 to pyro:	365 ml/min	Gain Setting:	HI
O2 to inlet:	20 ml/min	Gain Factor:	X1
He to inlet:	145 ml/min	Residence Time:	3 min
N Species: ~250 ppm N as NO		Matrix:	He
Carrier gas:	He(g)	Gas box carrier flow:	0.025 lpm

<u>Sample #</u>	<u>Injected*</u> <u>Sample ID</u>	<u>Inj. Sample</u> <u>Mass (μl)</u>	<u>Flow (lpm)</u> <u>NO in He</u>	<u>Flow (lpm)</u> <u>He</u>	<u>Known N</u> <u>Mass (μg)</u>	<u>Response</u> <u>Counts</u>	<u>CDA Sum</u> <u>Response</u>
N4110281	H2O	5	0.20592	4.104	1.2976	36813	63.6703
N4110282	H2O	5	0.20449	4.090	1.2933	36479	63.1091
N4110283	H2O	5	0.20735	4.090	1.3105	37423	64.8663

<u>[NO]</u>	<u>Summarized Data</u>	<u>Ave. Counts</u>	<u>n</u>	<u>SD</u>	<u>RSD (%)</u>
250 ppm	H2O	36905	3	479	1.30

N Species: ~750 ppm N as NO	Matrix:	He
Carrier gas:	He(g)	Gas box carrier flow: 0.025 lpm

<u>Sample #</u>	<u>Injected*</u> <u>Sample ID</u>	<u>Inj. Sample</u> <u>Mass (μl)</u>	<u>Flow (lpm)</u> <u>NO in He</u>	<u>Flow (lpm)</u> <u>He</u>	<u>Known N</u> <u>Mass (μg)</u>	<u>Response</u> <u>Counts</u>	<u>CDA Sum</u> <u>Response</u>
N4112421	H2O	5	0.6864	3.6036	4.3454	166782	294.2127
N4112422	H2O	5	0.6850	3.6036	4.3378	171017	301.8557
N4112423	H2O	5	0.6850	3.6036	4.3378	168608	297.5332
N4112411	0.4953 ug N glut.acid	5	0.6878	3.6036	4.8483	175138	309.2288
N4112412	0.4953 ug N glut.acid	5	0.6878	3.6036	4.8483	179354	316.4307
N4112413	0.4953 ug N glut.acid	5	0.6864	3.6036	4.8407	175638	309.9376
N4112431	0.2564 ug N glut.acid	5	0.6878	3.6036	4.6094	173962	306.8599
N4112432	0.2564 ug N glut.acid	5	0.6864	3.6036	4.6018	170428	300.8794
N4112433	0.2564 ug N glut.acid	5	0.6864	3.6036	4.6018	170640	301.0494
N4112441	0.5076 ug N pyrazine	5	0.6878	3.6036	4.8606	182494	321.8273
N4112442	0.5076 ug N pyrazine	5	0.6850	3.6036	4.8454	180344	318.2611
N4112443	0.5076 ug N pyrazine	5	0.6878	3.6036	4.8606	181000	319.971
N4112451	0.5098 ug N NH4Cl	5	0.6893	3.5893	4.885	172070	303.4931
N4112452	0.5098 ug N NH4Cl	5	0.6878	3.6036	4.8628	175704	309.766
N4112453	0.5098 ug N NH4Cl	5	0.6850	3.6036	4.8476	173790	306.8858

<u>[NO]</u>	<u>Summarized Data</u>	<u>Ave. Counts</u>	<u>n</u>	<u>SD</u>	<u>RSD (%)</u>
750	H2O	168802	3	2124	1.26
750	0.4953 ug N glut.acid	176710	3	2303	1.30
750	0.2564 ug N glut.acid	171677	3	1982	1.15
750	0.5076 ug N pyrazine	181279	3	1102	0.61
750	0.5098 ug N NH4Cl	173855	3	1818	1.05

Table II-20. Data for total measurement of nitrogen species with NH₃ (g) by combustion; sample injected into the gas phase.

Method Used:	5	PMT Voltage:	825
O ₂ to O ₃ :	30 ml/min	Furnace Temperature:	1100° C
O ₂ to pyro:	365 ml/min	Gain Setting:	HI
O ₂ to inlet:	20 ml/min	Gain Factor:	X1
He to inlet:	145 ml/min	Residence Time:	3 min
N Species:	~250 ppm N as NH ₃	Matrix:	He
Carrier gas:	He(g)	Gas box carrier flow:	0.025 lpm

Sample #	Injected* Sample ID	Inj. Sample Mass (μl)	Flow (lpm) NH ₃ in He	Flow (lpm) He	Known N Mass (μg)	Response Counts	CDA Sum Response
N4118121	0.5098 μg N NH ₄ Cl	5	0.19877	4.09	1.2588	74445	129.2419
N4118122	0.5098 μg N NH ₄ Cl	5	0.19877	4.09	1.2588	70119	121.8698
N4118123	0.5098 μg N NH ₄ Cl	5	0.2002	4.09	1.2674	70281	122.0407
N4118131	0.2564 μg N glut. acid	5	0.2002	4.09	1.2674	65598	114.0081
N4118132	0.2564 μg N glut. acid	5	0.19877	4.09	1.2588	61868	107.0017
N4118133	0.2564 μg N glut. acid	5	0.19877	4.09	1.2588	62507	108.0277
N4118141	0.4953 μg N glut. acid	5	0.19877	4.09	1.2588	86150*	145.1091
N4118142	0.4953 μg N glut. acid	5	0.19877	4.09	1.2588	72030	124.3842
N4118143	0.4953 μg N glut. acid	5	0.19734	4.09	1.2501	75785	130.1429
N4118144	0.4953 μg N glut. acid	5	0.19734	4.09	1.2501	67911	117.2065
N4118145	0.4953 μg N glut. acid	5	0.2002	4.09	1.2674	56978*	114.5156
N4119151	0.5076 μg N pyrazine	5	0.19734	4.09	1.2501	73633	127.2403
N4119152	0.5076 μg N pyrazine	5	0.19734	4.09	1.2501	54805*	95.0424
N4119153	0.5076 μg N pyrazine	5	0.19877	4.09	1.2588	57694*	99.7049
N4119154	0.5076 μg N pyrazine	5	0.19877	4.09	1.2588	73264	126.6296
N4119155	0.5076 μg N pyrazine	5	0.19877	4.09	1.2588	65922	114.0826
N4119156	0.5076 μg N pyrazine	5	0.19877	4.09	1.2588	62376	106.7308
N4119161	0.4989 μg N AgNO ₃	5	0.19877	4.08	1.2630	69264	119.5278
N4119162	0.4989 μg N AgNO ₃	5	0.19877	4.08	1.2630	64291	111.3982
N4119163	0.4989 μg N AgNO ₃	5	0.19877	4.08	1.2630	69739	120.2601

*Note: These points have not been used in the analysis, because they are known to be in error experimentally.

Summarized Data	Ave. Counts	n	SD	RSD (%)
0.5098 μg N NH ₄ Cl	71615	3	2452	3.42
0.5076 μg N pyrazine	68799	4	5563	8.09
0.4989 μg N AgNO ₃	67765	3	3018	4.45
0.4953 μg N glut. acid	71908	3	3938	5.48
0.2564 μg N glut. acid	63324	3	1994	3.15

Table II-20. (cont.) Data for total measurement of nitrogen species with NH_3 (g) by combustion; sample injected into the gas phase.

Method Used:	5	PMT Voltage:	825
O ₂ to O ₃ :	30 ml/min	Furnace Temperature:	1100° C
O ₂ to pyro:	365 ml/min	Gain Setting:	HI
O ₂ to inlet:	20 ml/min	Gain Factor:	X1
He to inlet:	145 ml/min	Residence Time:	3 min
N Species:	~500 ppm N as NH_3	Matrix:	He
Carrier gas:	He(g)	Gas box carrier flow:	0.025 lpm

Sample #	Injected* Sample ID	Inj. Sample Mass (μl)	Flow (lpm) NH ₃ in He	Flow (lpm) He	Known N Mass (μg)	Response Counts	CDA Sum Response
N4119191	0.4989 μg N AgNO ₃	5	0.41899	3.88	2.6499	129787	225.1625
N4119192	0.4989 μg N AgNO ₃	5	0.41756	3.88	2.6417	136485	232.317
N4119193	0.4989 μg N AgNO ₃	5	0.41613	3.88	2.6335	127035	220.5261
N4119194	0.4989 μg N AgNO ₃	5	0.41613	3.88	2.6335	125501	217.6483
N4119195	0.4989 μg N AgNO ₃	5	0.41613	3.88	2.6335	114559	198.9708
N4119201	0.5098 μg N NH ₄ Cl	5	0.41613	3.86	2.6423	118459	206.1988
N4119202	0.5098 μg N NH ₄ Cl	5	0.41756	3.88	2.6417	115167	200.5589
N4119203	0.5098 μg N NH ₄ Cl	5	0.41756	3.88	2.6417	121055	210.5919
N4119221	0.5076 μg N pyrazine	5	0.41756	3.88	2.6417	124127	216.0603
N4119222	0.5076 μg N pyrazine	5	0.41756	3.88	2.6417	116164	202.5118
N4119223	0.5076 μg N pyrazine	5	0.41899	3.88	2.6499	121639	208.5396
N4122231	0.4953 μg N glut. acid	5	0.41613	3.88	2.6335	124619	215.3995
N4122232	0.4953 μg N glut. acid	5	0.41899	3.86	2.6587	116399	202.6585
N4122233	0.4953 μg N glut. acid	5	0.41756	3.88	2.6417	117320	203.8525
N4122241	0.2564 μg N glut. acid	5	0.41756	3.88	2.6417	112018	195.0153
N4122242	0.2564 μg N glut. acid	5	0.41899	3.88	2.6499	103086	179.8806
N4122243	0.2564 μg N glut. acid	5	0.41756	3.89	2.6329	116645	202.7292

Summarized Data	Ave. Counts	n	SD	RSD (%)
0.5098 μg N NH ₄ Cl	118227	3	2951	2.50
0.5076 μg N pyrazine	120643	3	4074	3.38
0.4989 μg N AgNO ₃	126673	5	7972	6.29
0.4953 μg N glut. acid	119446	3	4504	3.77
0.2564 μg N glut. acid	110583	3	6893	6.23

Table II-20. (cont.) Data for total measurement of nitrogen species with NH_3 (g) by combustion; sample injected into the gas phase.

Method Used:	5	PMT Voltage:	825
O_2 to O_3 :	30 ml/min	Furnace Temperature:	1100° C
O_2 to pyro:	365 ml/min	Gain Setting:	HI
O_2 to inlet:	20 ml/min	Gain Factor:	X1
He to inlet:	145 ml/min	Residence Time:	3 min
N Species:	~750 ppm N as NH_3	Matrix:	He
Carrier gas:	He(g)	Gas box carrier flow:	0.025 lpm

Sample #	Injected* Sample ID	Inj. Sample Mass (μl)	Flow (lpm) NH ₃ in He	Flow (lpm) He	Known N Mass (μg)	Response Counts	CDA Sum Response
N4123371	0.4953 μg N glut. acid	5	0.65923	3.62	4.1860	169203	294.2826
N4123372	0.4953 μg N glut. acid	5	0.65923	3.62	4.1860	170096	294.7203
N4123373	0.4953 μg N glut. acid	5	0.65923	3.62	4.1860	171949	297.8447
N4123381	0.2564 μg N glut. acid	5	0.6578	3.62	4.1783	155139	270.4302
N4123382	0.2564 μg N glut. acid	5	0.6578	3.62	4.1783	158489	275.7766
N4123383	0.2564 μg N glut. acid	5	0.6578	3.62	4.1783	161830	281.4652
N4123391	0.5076 μg N pyrazine	5	0.65923	3.62	4.1860	159137	277.974
N4123392	0.5076 μg N pyrazine	5	0.65923	3.62	4.1860	162348	283.7118
N4123393	0.5076 μg N pyrazine	5	0.65923	3.62	4.1860	152731	266.77
N4123401	0.4989 μg N AgNO_3	5	0.65923	3.62	4.1860	170590	293.6235
N4123402	0.4989 μg N AgNO_3	5	0.6578	3.63	4.1643	165720	288.4957
N4123403	0.4989 μg N AgNO_3	5	0.65923	3.63	4.1720	156630	273.0441
N4123411	0.5098 μg N NH_4Cl	5	0.65923	3.63	4.1720	163632	284.9561
N4123412	0.5098 μg N NH_4Cl	5	0.66066	3.62	4.1936	168718	293.8427
N4123413	0.5098 μg N NH_4Cl	5	0.65923	3.63	4.1720	174479	303.4862

Summarized Data	Ave. Counts	n	SD	RSD (%)
0.5098 μg N NH_4Cl	164313	3	7086	4.31
0.5076 μg N pyrazine	158072	3	4896	3.10
0.4989 μg N AgNO_3	168943	3	5427	3.21
0.4953 μg N glut. acid	170416	3	1401	0.82
0.2564 μg N glut. acid	158486	3	3345	2.11

PYROLYSIS

Temperature Profile Accuracy

The temperature heating profile for the programmable furnace was checked for accuracy. The maximum heating rate of 150° C/min was used and the data is shown below. Very good results were achieved. Less than 2% error was calculated in this case.

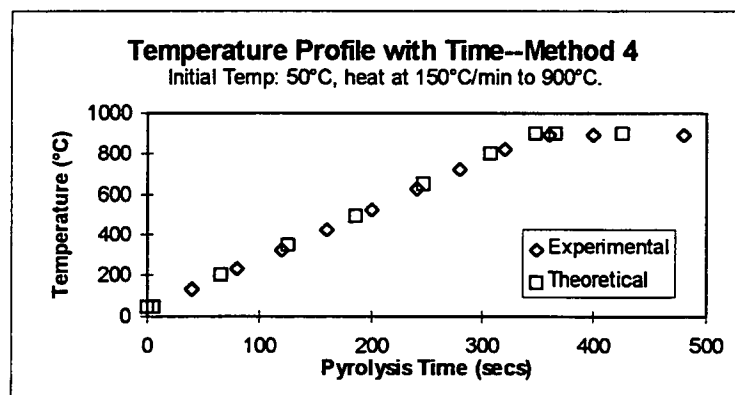


Figure II-3. Verification of heating rate accuracy for programmable inlet furnace on the nitrogen analyzer.

Carrier Gas Flow Rate

The effect of flow rate was also determined using 2.564 µg N as proline for the sample during pyrolysis. The results indicated the effect to be minimal at flow rates ≥ 62 cc/min. The data is shown in Table II-21 and Fig. II-4 below.

Table II-21. Effect of carrier gas flow rate on nitrogen response for 2.564 µg N as proline during pyrolysis.

Flow rate (cc/min)	0	0.1	4	13.6	62	102	165	250	307	369	444
Response (counts)	0	5282	42212	47695	55544	54558	57707	57407	54873	53012	52462

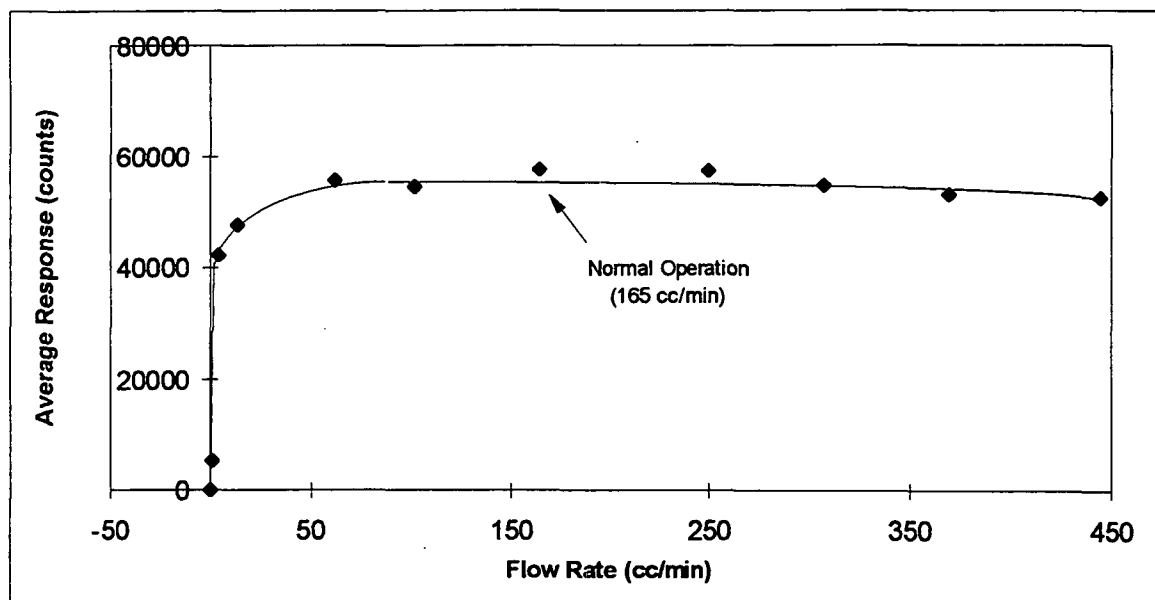


Figure II-4. Effect of flow rate on the pyrolysis nitrogen response for 2.564 μg N/ 5 μl proline sample.

Effect of Sample Placement

Some variation in the measurement is partially due to the way that the sample is placed into the quartz wool in the sample boats. See Figure II-5 below. In a), where the samples was injected into loosely packed quartz wool, the main peak is separated into two distinct peaks at a pyrolysis time of about 85 seconds. A second smaller release is noted at about 250 seconds. In b), where the sample was injected into densely packed quartz wool, a quicker initial release is noted by the increased upward slope of the main peak. Also, the second peak has reverted into a shoulder of the main peak with a slightly larger amount of nitrogen being measured in the second peak at about 300 seconds pyrolysis time.

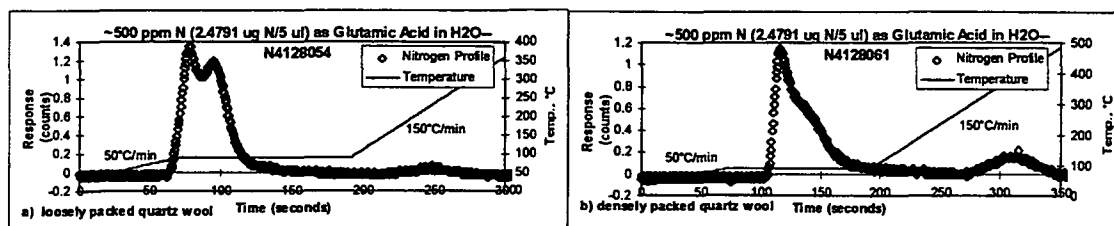


Figure II-5. Nitrogen profiles of glutamic acid during oxidative pyrolysis indicating variation that can occur due to sample introduction methods. a) loosely packed quartz wool. b) densely packed quartz wool.

A shift in the initial release from about 60 seconds to 100 seconds exists after the beginning of pyrolysis. The more densely packed wool would be expected to allow slower mass and heat transfer to the sample. The difference in these parameters in the two cases are likely responsible for the changes observed in the nitrogen release profiles and in the overall amount of nitrogen measured. A decrease of nearly 10% was observed in the later case. The summarized data are presented in the table below.

Table II-22. Data for oxidative pyrolysis of glutamic acid ($2.4791 \mu\text{g N} / 5 \mu\text{l}$ sample) when samples were injected into loosely or densely packed quartz wool.

Sample ID	n	Average (counts)	SD	RSD (%)
loosely packed	5	54260	1535	2.83
densely packed—replicate 1	4	49522	3198	6.46
densely packed—replicate 2	4	49316	2935	5.95

A test was done to see if there were any effects due to injecting a sample into the same location in the wool as the previous sample without changing the wool or acid washing the sample boat. Statistically, no difference was observed in the average counts for either sample; however, the relative standard deviation (RSD) was higher without acid washing the boat and using new wool.

Reproducibility

Good reproducibility was observed for the proline and glutamic acid samples; however, the reproducibility for the pyrazine samples remains poor. The poor reproducibility may be a result of the low temperature at which the nitrogen in proline is released. Glutamic acid nitrogen is released at about 90° C, proline at about 120° C, and pyrazine nitrogen is released at about 43° C. Based on the some of the early nitrogen measurements made, data is presented in Table II-23. This data was collected at the slowest heating rates in order to maximize peak separation for each of the individual nitrogen species. Better reproducibility was achieved for all species at higher heating rates

Table II-23. GPNP nitrogen measurement (as response counts) of model black liquor nitrogen compounds during slow oxidative pyrolysis.

Species	GPNP N Av. counts	n	SD	RSD (%)	Antek total N Av. counts	Conversion (%)*
2.4791 µg N as glutamic acid	56833	6	3764	6.62	34096	+66.69
2.564 µg N as proline	54840	5	2396	4.52	31079	+76.45
3.789 µg N as proline	78972	3	2327	2.95	46731	+69.00
4.954 µg N as proline	102570	4	5416	5.28	42688 [†]	+140.28
2.4857 µg N as pyrazine	27155	4	745	2.74	48603	-44.13

*Conversion is calculated as [(GPNP nitrogen - ANTEK Total nitrogen)/ANTEK Total nitrogen] * 100.

[†]Because the average counts presented is obviously incorrect (smaller than expected compared to the results at 3.789 µg N), the predicted value can be used to determine the conversion. Based on the predicted values for the concentration range of 50–750 ppm N as proline, the Antek total N Av. counts would be 58836 which would change the conversion to +74.33%.

Measurements were also made for the samples at 150° C/min and only a slight difference was observed in the GPNP nitrogen measured and the nitrogen release profiles. For proline, no difference (beyond that accounted for within experimental error) was observed for either the 2.564 µg N or the 3.789 µg N samples. The 4.954 µg N sample

did show a decrease (-8.6%) in the average counts observed going from the optimized (for nitrogen release and peak separation) to the 150° C/min heating rate.

Data for Pyrolysis Fixed Nitrogen Measurements

The data provided here have been discussed above and have been used to validate the pyrolysis conditions for accurate measurement of fixed nitrogen. Each set of data is presented along with the statistical summaries. Error estimates can be taken from the correlation coefficients in the plots as well as the statistical standard deviation and coefficient of variation.

The sample numbers in Tables II-25 and II-26, such as N4097022, are the same as the computer data acquisition (CDA) file names. The N identifies the sample as a nitrogen release profile type of data file. The 4 represents the lab notebook #4264. The next three digits are the page number within the notebook where the data can be found and the last three digits are the sample number on that page. The last digit represents the number of the replicate. For the example, the values listed for the N4097022 sample would be found in notebook 4264 on page 97 as sample 2, replicate 2.

The data presented in Table II-24 provide the heating methods employed during the various pyrolysis experiments and method development. The method number correlates to the heating program number presented at the top of Tables II-25 and II-26.

Table II-24. Heating program methods used during the pyrolysis experiments.

The following Methods have been used for the Antek Inlet Furnace Temperature Programming. Each method is identified with a number and has been used to describe operating parameters for the samples that have been pyrolyzed. The heating methods are outlined below.

Method #1

Level:	<u>1</u>	<u>2</u>	<u>3</u>
Temperature:	100° C	250° C	700° C
Delay Time:	0.10 min	2.00 min	1.00 min
Ramp Rate:	50° C/min	100° C/min	

Method #2

Level:	<u>1</u>	<u>2</u>	<u>3</u>
Temperature:	35° C	400° C	700° C
Delay Time:	0.10 min	3.00 min	0.1 min
Ramp Rate:	150° C/min	150° C/min	

Method #3

Level:	<u>1</u>	<u>2</u>	<u>3</u>
Temperature:	35° C	600° C	700° C
Delay Time:	0.10 min	3.00 min	0.1 min
Ramp Rate:	150° C/min	150° C/min	

Method #4

Level:	<u>1</u>	<u>2</u>
Temperature:	35° C	700° C
Delay Time:	0.10 min	3.00 min
Ramp Rate:	150° C/min	

Method #5

Level:	<u>1</u>	<u>2</u>	<u>3</u>
Temperature:	35° C	90° C	700° C
Delay Time:	0.10 min	2.00 min	1.0 min
Ramp Rate:	50° C/min	150° C/min	

Method #6

Level:	<u>1</u>	<u>2</u>	<u>3</u>
Temperature:	35° C	120° C	700° C
Delay Time:	0.10 min	3.00 min	1.0 min
Ramp Rate:	50° C/min	150° C/min	

Table II-25. Proline pyrolysis data for total nitrogen measurement; effect of [O₂] content.

Method Used: 5 PMT Voltage: 825
 O₂ to O₃: 30 ml/min Furnace Temperature: 1100° C
 O₂ to pyro: 365 ml/min Gain Setting: HI
 O₂ to inlet: 6.6 ml/min Gain Factor: X1
 He to inlet: 158 ml/min Heating Program #: 2

Nitrogen Species: proline Matrix: H₂O

***Pyrolysis at 4% oxygen.**

Sample #	Sample ID	Sample Vol (μl)	Known N Mass (μg)	Response Counts	CDA Sum Response
N4140171	~500 ppm N	5	2.564	55900	99.0964
N4140172	~500 ppm N	5	2.564	55849	98.8279
N4140173	~500 ppm N	5	2.564	56595	100.0973
Sample #	Ave. Counts	n	SD	RSD (%)	
N414017_	56115	3	416	0.74	

O₂ to inlet: 13.2 ml/min He to inlet: 152 ml/min

***Pyrolysis at 8% oxygen.**

Sample #	Sample ID	Sample Vol (μl)	Known N Mass (μg)	Response Counts	CDA Sum Response
N4140161	~500 ppm N	5	2.564	54175	95.8494
N4140162	~500 ppm N	5	2.564	52538	92.9929
N4140163	~500 ppm N	5	2.564	48764	86.5963
Sample #	Ave. Counts	n	SD	RSD (%)	
N414016_	51826	3	2775	5.35	

O₂ to inlet: 20 ml/min He to inlet: 145 ml/min

***Pyrolysis at 12% oxygen.**

Sample #	Sample ID	Sample Vol (μl)	Known N Mass (μg)	Response Counts	CDA Sum Response
N4140141	~500 ppm N	5	2.564	57008	101.2447
N4140142	~500 ppm N	5	2.564	52805	93.7494
N4140143	~500 ppm N	5	2.564	53327	94.5069
Sample #	Ave. Counts	n	SD	RSD (%)	
N414014_	54380	3	2291	4.21	

O₂ to inlet: 36.3 ml/min He to inlet: 129 ml/min

***Pyrolysis at 22% oxygen.**

Sample #	Sample ID	Sample Vol (μl)	Known N Mass (μg)	Response Counts	CDA Sum Response
N4140151	~500 ppm N	5	2.564	53821	95.4588
N4140152	~500 ppm N	5	2.564	54644	97.0452
N4140153	~500 ppm N	5	2.564	55826	98.901
Sample #	Ave. Counts	n	SD	RSD (%)	
N414015_	54764	3	1007	1.84	

O₂ to inlet: 0 ml/min He to inlet: 165 ml/min

***Pyrolysis at 0% oxygen.**

Sample #	Sample ID	Sample Vol (μl)	Known N Mass (μg)	Response Counts	CDA Sum Response
N4140121	~500 ppm N	5	2.564	55979	99.2917
N4140122	~500 ppm N	5	2.564	53606	95.1905
N4140123	~500 ppm N	5	2.564	53247	94.311
N4140124	~500 ppm N	5	2.564	53830	95.3613
N4140181	~500 ppm N	5	2.564	51154	90.6489
N4140182	~500 ppm N	5	2.564	54784	97.1187
N4140183	~500 ppm N	5	2.564	54354	96.3625
Sample #	Ave. Counts	n	SD	RSD (%)	
N414012_	54165	4	1233	2.28	
N414018_	53431	3	1983	3.71	

Table II-26. Data for the effect of flow rate during oxidative proline pyrolysis.

Method Used:	5	PMT Voltage:	825
O ₂ to O ₃ :	30 ml/min	Furnace Temperature:	1100° C
O ₂ to pyro:	365 ml/min	Gain Setting:	HI
O ₂ to inlet:	6.6 ml/min	Gain Factor:	X1
He to inlet:	55 ml/min	Heating Program #:	2
Nitrogen Species:	proline	Matrix:	H ₂ O

**Oxidative Pyrolysis at 12% oxygen, 62 ml/min total flow .*

Sample #	Sample ID	Sample Vol (μ l)	Known N Mass (μ g)	Response Counts	CDA Sum Response
N4141241	~500 ppm N	5	2.564	55820	98.7306
N4141242	~500 ppm N	5	2.564	54909	96.948
N4141243	~500 ppm N	5	2.564	55902	98.657

Sample #	Ave. Counts	n	SD	RSD (%)
N414124_	55544	3	551	0.99

**Oxidative Pyrolysis at 12% oxygen, 369 ml/min total flow .*

Sample #	Sample ID	Sample Vol (μ l)	Known N Mass (μ g)	Response Counts	CDA Sum Response
N4142251	~500 ppm N	5	2.564	52266	92.5291
N4142252	~500 ppm N	5	2.564	52926	93.4322
N4142253	~500 ppm N	5	2.564	53845	95.1168

Sample #	Ave. Counts	n	SD	RSD (%)
N414225_	53012	3	793	1.5

**Oxidative Pyrolysis at 12% oxygen, 13.6 ml/min total flow .*

Sample #	Sample ID	Sample Vol (μ l)	Known N Mass (μ g)	Response Counts	CDA Sum Response
N4142261	~500 ppm N	5	2.564	47835	84.008
N4142262	~500 ppm N	5	2.564	47436	83.3002
N4142263	~500 ppm N	5	2.564	48412	85.0582

Sample #	Ave. Counts	n	SD	RSD (%)
N414226_	47895	3	491	1.03

**Oxidative Pyrolysis at 12% oxygen, 4 ml/min total flow .*

Sample #	Sample ID	Sample Vol (μ l)	Known N Mass (μ g)	Response Counts	CDA Sum Response
N4142271	~500 ppm N	5	2.564	42752	75.1218
N4142272	~500 ppm N	5	2.564	44026	77.1235
N4142273	~500 ppm N	5	2.564	39856	69.4827

Sample #	Ave. Counts	n	SD	RSD (%)
N414227_	42212	3	2137	5.06

Table II-26. (cont.) Data for the effect of flow rate during oxidative proline pyrolysis.

*Oxidative Pyrolysis at 12% oxygen, 444 ml/min total flow .

<u>Sample #</u>	<u>Sample ID</u>	<u>Sample Vol</u> <u>(μl)</u>	<u>Known N</u> <u>Mass (μg)</u>	<u>Response</u> <u>Counts</u>	<u>CDA Sum</u> <u>Response</u>
N4143302	~500 ppm N	5	2.564	52577	--
N4143303	~500 ppm N	5	2.564	52702	92.7976
N4143304	~500 ppm N	5	2.564	52108	91.8943
<u>Sample #</u>	<u>Ave. Counts</u>	<u>n</u>	<u>SD</u>	<u>RSD (%)</u>	
N414330_	52462	3	313	0.60	

*Oxidative Pyrolysis at 12% oxygen, 102 ml/min total flow .

<u>Sample #</u>	<u>Sample ID</u>	<u>Sample Vol</u> <u>(μl)</u>	<u>Known N</u> <u>Mass (μg)</u>	<u>Response</u> <u>Counts</u>	<u>CDA Sum</u> <u>Response</u>
N4143321	~500 ppm N	5	2.564	53962	95.0924
N4143322	~500 ppm N	5	2.564	53947	95.1655
N4143324	~500 ppm N	5	2.564	55764	98.3395
<u>Sample #</u>	<u>Ave. Counts</u>	<u>n</u>	<u>SD</u>	<u>RSD (%)</u>	
N414332_	54558	3	1045	1.91	

*Oxidative Pyrolysis at 12% oxygen, 250 ml/min total flow .

<u>Sample #</u>	<u>Sample ID</u>	<u>Sample Vol</u> <u>(μl)</u>	<u>Known N</u> <u>Mass (μg)</u>	<u>Response</u> <u>Counts</u>	<u>CDA Sum</u> <u>Response</u>
N4143331	~500 ppm N	5	2.564	59018	104.1992
N4143332	~500 ppm N	5	2.564	55790	98.4372
N4143333	~500 ppm N	5	2.564	57411	101.2201
<u>Sample #</u>	<u>Ave. Counts</u>	<u>n</u>	<u>SD</u>	<u>RSD (%)</u>	
N414333_	57407	3	1614	2.81	

*Oxidative Pyrolysis at 12% oxygen, 307 ml/min total flow .

<u>Sample #</u>	<u>Sample ID</u>	<u>Sample Vol</u> <u>(μl)</u>	<u>Known N</u> <u>Mass (μg)</u>	<u>Response</u> <u>Counts</u>	<u>CDA Sum</u> <u>Response</u>
N4143341	~500 ppm N	5	2.564	55832	98.4127
N4143342	~500 ppm N	5	2.564	54282	95.6539
N4143343	~500 ppm N	5	2.564	54505	96.191
<u>Sample #</u>	<u>Ave. Counts</u>	<u>n</u>	<u>SD</u>	<u>RSD (%)</u>	
N414334_	54873	3	838	1.53	

*Oxidative Pyrolysis at 12% oxygen, 165 ml/min total flow .

<u>Sample #</u>	<u>Sample ID</u>	<u>Sample Vol</u> <u>(μl)</u>	<u>Known N</u> <u>Mass (μg)</u>	<u>Response</u> <u>Counts</u>	<u>CDA Sum</u> <u>Response</u>
N4143311	~500 ppm N	5	2.564	57501	101.3644
N4143312	~500 ppm N	5	2.564	56344	99.5356
N4143313	~500 ppm N	5	2.564	51000	100.5122
N4143314	~500 ppm N	5	2.564	59701	105.3954
<u>Sample #</u>	<u>Ave. Counts</u>	<u>n</u>	<u>SD</u>	<u>RSD (%)</u>	
N414331_	56137	4	3696	6.58	

Table II-26. (cont.) Data for the effect of flow rate during oxidative proline pyrolysis.

*Oxidative Pyrolysis at 12% oxygen, 165 ml/min total flow.

<u>Sample #</u>	<u>Sample ID</u>	<u>Sample Vol</u> <u>(μl)</u>	<u>Known N</u> <u>Mass (μg)</u>	<u>Response</u> <u>Counts</u>	<u>CDA Sum</u> <u>Response</u>
N4143351	~500 ppm N	5	2.564	55964	98.5589
N4143352	~500 ppm N	5	2.564	56187	98.9987
N4143353	~500 ppm N	5	2.564	55948	98.5103
<u>Sample #</u>	<u>Ave. Counts</u>	<u>n</u>	<u>SD</u>	<u>RSD (%)</u>	
N414335_	56033	3	134	0.24	

Table II-27. Inert pyrolysis data for nitrogen species; effect of multiple nitrogen types on the nitrogen response.

Method Used:	5	PMT Voltage:	825
O ₂ to O ₃ :	30 ml/min	Furnace Temperature:	1100° C
O ₂ to pyro:	365 ml/min	Gain Setting:	HI
O ₂ to inlet:	0 ml/min	Gain Factor:	X1
He to inlet:	165 ml/min	Heating Program #:	2
Nitrogen Species: as indicated		Matrix:	H ₂ O

<u>Sample #</u>	<u>Sample ID</u>	<u>Sample Vol</u> <u>(μl)</u>	<u>Known N</u> <u>Mass (μg)</u>	<u>Sample Vol</u> <u>(μl)</u>	<u>Known N</u> <u>Mass (μg)</u>	<u>Total</u> <u>Counts</u>	<u>CDA Sum</u> <u>Response</u>
N4134091	pyrazine	5	2.4857	proline	5	2.564	95162
N4134092	pyrazine	5	2.4857	proline	5	2.564	97118
N4134093	pyrazine	5	2.4857	proline	5	2.564	86247
N4134101	glutamic acid	5	2.4791	proline	5	2.564	102630
N4134102	glutamic acid	5	2.4791	proline	5	2.564	101589
N4134103	glutamic acid	5	2.4791	proline	5	2.564	99260
N4134111	glutamic acid	5	2.4791	pyrazine	5	2.4857	98271
N4134112	glutamic acid	5	2.4791	pyrazine	5	2.4857	98954
N4134113	glutamic acid	5	2.4791	pyrazine	5	2.4857	93804
<u>Sample #</u>	<u>Ave. Counts</u>	<u>n</u>	<u>SD</u>	<u>RSD (%)</u>			
N413409_	92843	3	5795	6.24			
N413410_	101160	3	1726	1.71			
N413411_	97010	3	2797	2.88			

APPENDIX III: SINGLE DROPLET METHODS VERIFICATION

Information for the calibration and to verify that NO measurements could be made with the single droplet reactor at Åbo Akademi, Turku, Finland. Included here are the data for the calibration and a discussion of the experimental work completed in this regard. Calculation of the Reynolds number is included along with the statistical determination of the appropriate sample size to be used in the single droplet experiments.

NO ANALYZER CALIBRATION

Prior to calibration of the analyzers, the zero and span point for the analyzers had to be set. For the zero point, a zero gas of nitrogen was fed to the reactor at 300 l/h and the sample stream to the analyzers was diluted in the same manner as that which would occur during calibration and experimentation. The system was allowed to stabilize and then the analyzer was adjusted such that the measured response was zero. For the span point adjustment, a calibration gas at 80% of R3 for each of the analyzers was fed to the system. When a stable measurement was observed, the analyzer was adjusted such that the measured response was likewise 80% of the full scale. The full scale response for all ranges was 5.0 volts and as such the sensitivity of the measurements remained high at all ranges for each of the analyzers.

During calibration, NO gas was fed into a T-joint which split the flow so that it entered the reactor on opposing sides. The N₂ carrier gas flow was split by a T-joint and entered the reactor, again on opposing sides, about 17 cm above the calibration gas

entrance. The gases traveled the length of the reactor (approximately 52 cm) where they exited. Approximately 52 L/h went to the CO₂ analyzer and 33 L/h went to the NO analyzer with the remainder being exhausted. The NO analyzer stream was brought to a total of ~53 L/h with air to provide for an 8% O₂ concentration.

The NO analyzers were calibrated individually by feeding known concentrations of certified calibration gas (195 ppm NO in N₂) to the reactor and thus to the analyzers for measurement. Five concentrations of NO were delivered to the reactor at 80, 60, 40, 20, and 10% of the full scale range of measurement for each analyzer. The concentration set points were determined based on the analyzer reaction cell concentrations. Thus, the air dilution was also taken into account in this way. For example, for the 072 analyzer at R3, concentrations of 160, 120, 80, 40 and 20 ppm NO were fed to the reactor in a total volumetric flow of 300 l/h. The NO flow rates were calculated and delivered to the reactor via the calibrated rotameters. The balance of the flow was calculated for the N₂ carrier gas. All calibration measurements were made at room temperature.

At each concentration within each range, the system was allowed to stabilize and then the analyzer voltage response was recorded. The linear relationship was calculated between the values of slope (m) and the intercept (b) for the true concentrations (x) and the measured response (y). The regression analysis was done on Microsoft EXCEL software. The calibration curves included the (0,0) point in the regression analysis. This allowed for more accurate determination of the concentrations in the lower portion of each range. The equation for the calibration curve and the corresponding correlation coefficient was obtained directly from the regression analysis.

The analyzers were monitored daily for stability and accuracy of the NO measurement by feeding known concentrations of the gas through the reactor to the analyzer. Because of the possibility for NO-NO reactions at higher gas concentrations, the concentrations of NO was always 10 ppm or less. The NO was fed to the system at concentrations of approximately 1.5, 2, and 4 ppm. For each test, the system was allowed to stabilize and the voltage response was taken. The appropriate calibration equation was then used to determine the measured concentration.

The relative error in the response was determined by subtracting the true values from the measured values. The averages for each set of tests, where $n = 3$, were determined and used as a basis to monitor the instruments' performance. Based on the analyzer response over a period of time and the known accuracy of rotameter controlled flows, a 10% margin of error in the average measurements was determined to be the limit for recalibration. The stability of the instruments came to a level where only weekly calibration was required. During the pyrolysis experiments, the system was calibrated three times: once initially and twice during the actual experimentation time period.

Discussion

The calibration curves throughout the set up and the experimental work indicated very good linearity. A typical calibration curve for the 072 analyzer provides an example of the linearity and is illustrated in Figure III-1. Since the system was set up to operate in the lower concentration ranges, the 072 R2 and R3 ranges were not used in these experiments. The use of only the lower concentration ranges was verified initially by burning several black liquor droplets to observe the level of nitrogen release. All

concentrations were observed to be 3 ppm NO or less even at conditions for maximum nitrogen release. The correlation coefficients were on average $0.999 (\pm 0.0005)$ for the 072 R1 NO calibration equation.

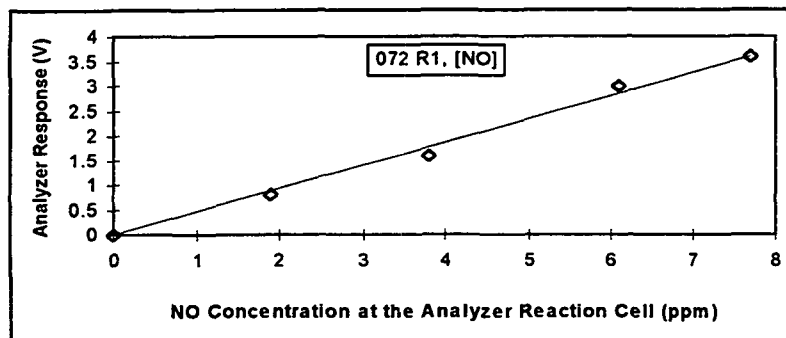


Figure III-1. Calibration curves for NO concentration measurements made with the 072 analyzer at R1.

Small differences were noted in the slope of the calibration equations for a given range when recalibration was required. The outcome of daily monitoring of the analyzer prior to experimental work confirmed its stability as well as its ability to make accurate measurements for the unknown NO gas concentrations during experimentation. The values for the monitoring tests, described in the previous section, are indicated in Table III-1. The first column provides the number of days of testing chronologically; however, they are not consecutive. The average was determined from three data points when the NO calibration gas was fed to the system.

Table III-1. Daily monitoring results for the NO analyzer's calibration stability.

<u>Day</u>	<u>072 Ave. % Dif. NO (Calculated - True) only NO used</u>
1*	0.41
2	-1.99
3	2.67
4	-6.40
5	2.31
6	9.34
7*	7.89
8	4.49
9	9.35
10*	3.08
11	8.60
12	7.00

*Indicates day of recalibration.

The values were found to be both higher and lower than the true values indicating no systematic error or bias in the measurements. All observed values were less than the set limit of 10% error. The error for any single measurement extended from about -6.4% to 9.35% for the NO measured analyzer. When an error of about 9% or greater was observed, the calibration was redone.

A high total flow rate for the pyrolysis experiments was used to maintain the concentrations of the nitrogen species in the gases at very low levels. In this way, the accuracy of the measurements was assured to be within the 10% margin that had been established. The results of the calibration work indicated that the analyzer could maintain the stability and accuracy for measurements of unknown NO gas concentrations during the black liquor pyrolysis experiments.

CALCULATION OF N_{Re}

To determine if the system is in the laminar or turbulent regime, the Reynolds number calculation was used. Here, the Reynolds number (Re) is equal to the inertial force over the viscous force.⁹⁸

$$Re = d u \rho / \mu = d G / \mu, \quad (\text{III-1})$$

where d is the diameter (in meters) of the flow chamber, ρ is the density of the gas (kg/m^3), μ is the viscosity ($\text{kg/m}\cdot\text{s}$), and u is the velocity of the gas (m/s). A Reynolds number less than 2100 represents laminar flow and one greater than 4000 represents turbulent flow. The density of air was taken to be $1.205 \text{ (kg/m}^3\text{)}$ at 20°C and 1 atm. The equation for a cylinder volume was $\pi r^2 h$. The area of a cylinder was $2\pi r h$. The reactor was 3.5 cm in diameter and 52 cm in length. Therefore, the reactor area was 0.5718 m^2 . The flow rate at 300 l/h is equivalent to $8.3 \times 10^{-5} \text{ m}^3/\text{s}$. Therefore, the velocity was $1.457 \times 10^{-5} \text{ m/s}$. The Reynolds number in the reactor was:

$$Re = \frac{(0.035 \text{ m}) (1.457 \times 10^{-5} \text{ m/s}) (1.205 \text{ kg/m}^3)}{(2.05 \times 10^{-5} \text{ kg/m}\cdot\text{s})} = 0.02969. \quad (\text{III-2})$$

Therefore, the gas flow through the reactor was in a laminar regime. At the location of the air addition to the gas sample stream, the flow rate was 53 l/h in a gas line 88 cm in length and 1.25 mm in diameter. The area of the gas line was determined to be 0.0069 m^2 . The velocity was 0.00213 m/s and the resulting Reynolds number was:

$$Re = \frac{(0.00125 \text{ m}) (0.00213 \text{ m/s}) (1.205 \text{ kg/m}^3)}{(2.05 \times 10^{-5} \text{ kg/m}\cdot\text{s})} = 0.1565. \quad (\text{III-3})$$

Again, the Reynolds number indicated the gas flow to be laminar. The experimental setup should allow for the gases to move through the reactor and gas lines evenly. Therefore, any variation in the analyzer response should not be due to turbulent flow.

DETERMINATION OF STATISTICALLY SOUND SAMPLE SIZE.

The sample size required to get statistically sound data during the pyrolysis experiments was determined. The data from Aho's experiments was used in the calculation as the same techniques were employed under similar operating conditions.⁹⁹

The sample size determination calculation was:¹⁰⁰

$$n = [Z_{\alpha/2} \sigma / E]^2 \quad (\text{III-4})$$

where

$$E = Z_{\alpha/2} (\sigma / \sqrt{n}) \quad (\text{where } \sigma \text{ is known or } n > 30) \quad (\text{III-5})$$

or

$$E = t_{\alpha/2} (s / \sqrt{n}) \quad (\text{where } n \leq 30). \quad (\text{III-6})$$

Because the sample size is known to be less than 30, the second equation is used to determine E by using the experimental data from Aho's work. During pyrolysis of a birch liquor, the nitrogen released was observed to be 24.1 mg N / 100 g BLS \pm 2.2 mg N/100 g BLS, where nine liquor droplets were pyrolyzed. Therefore, at a 95 % confidence interval, $\sigma = 0.05$ and $\alpha/2 = 0.025$. Thus, $t_{\alpha/2} = 2.306$ where the degrees of freedom are $(n-1) = 8$. From statistical tables, $Z = 1.96$. Substitution of these values to solve for E gives

$$E = (2.306) (2.2/\sqrt{9}) = 1.69107. \quad (\text{III-7})$$

Substitution of E into the first equation, results in

$$n = [(1.96)(2.2)/(1.69107)]^2 = 6.5. \quad (\text{III-8})$$

Therefore, seven replicates was sufficient to provide statistically sound data during the pyrolysis experiments.

APPENDIX IV: SAMPLE PREPARATION

This appendix contains sample preparation information for the model fuel nitrogen species, black liquor samples and for the screening experiment samples. The nitrogen samples used to examine the conversion of fuel nitrogen species etc. were prepared in the laboratory. The sample preparation data for each of the standard samples in a water or inorganic matrix is provided in this appendix. The information provided for black liquor sample preparation is in regards to liquor fractionation of the lignin organic material from the inorganics. This information is provided below.

MODEL FUEL NITROGEN SPECIES

Data for the nitrogen sample preparation, for the samples used in the combustion and pyrolysis experiments, are given in the following tables. All samples were prepared using distilled, deionized water ($\sim 18 \text{ M}\Omega$) and class A volumetric glassware. The glutamic acid and tryptophan samples were warmed in a hot tap water bath to bring the solid into solution. The 1000 ppm N as glutamic acid and the 750 ppm N tryptophan samples did not go into solution after a couple of hours of warming and therefore, these were not used in any of the nitrogen standard measurements.

Table IV-1. Sample preparation data for NH_4Cl , FW = 53.49 g/mole, 26.17% N.

Target Conc. (ppm)	Target NH_4Cl Wt. (g)	Actual Wt. Added (g)	Volume (ml)	Actual Conc. (μg)*
1000-a	0.3821	0.3896	100	5.09814
1000-b	0.3821	0.3855	100	5.09799

* Concentration as $\mu\text{g N/5 } \mu\text{l sample}$.

Table IV-2. Sample preparation data for NH_4Cl by dilution of 1000 ppm N solution.

Target Conc. (ppm)	1000 ppm N solution used	Volume Added (ml)	Total Vol. (ml)	Actual Conc. (μg)*
750	a	75	100	3.7832
500	b	25	50	2.5490
100	b	10	100	0.5098
50	b	5	100	0.2549

* Concentration as $\mu\text{g N} / 5 \mu\text{l sample}$.

Table IV-3. Sample preparation data for NH_4NO_3 . FW = 80.04 g/mole. 34.98% N.

Target Conc. (ppm)	Actual Wt. Added (g)	Volume (ml)	Actual Conc. (μg)*
1000	0.3191	100	5.58145
750	0.2077	100	3.6329
500	0.1425	100	2.4925
100	0.0317	100	0.55447
50	0.0136	100	0.23788

* Concentration as $\mu\text{g N} / 5 \mu\text{l sample}$.

Table IV-4. Sample preparation data for $(\text{NH}_4)_2\text{SO}_4$. FW = 132.14 g/mole. 21.19% N.

Target Conc. (ppm)	Actual Wt. Added (g)	Volume (ml)	Actual Conc. (μg)*
1000	0.4713	100	4.9934
750	0.3560	100	3.7618
500	0.2327	100	2.4655
100	0.0456	100	0.4831
50	0.0214	100	0.2267

* Concentration as $\mu\text{g N} / 5 \mu\text{l sample}$.

Table IV-5. Sample preparation data for Glutamic Acid. FW = 147.13 g/mole. 9.515% N.

Target Conc. (ppm)	Actual Wt. Added (g)	Volume (ml)	Actual Conc. (μg)*
1000	1.0595	100	5.0405
750	0.7856	100	3.7375
500	0.5211	100	2.4791
100	0.1041	100	0.4953
50	0.0539	100	0.2564

* Concentration as $\mu\text{g N} / 5 \mu\text{l sample}$.

Table IV-6. Sample preparation data for Tryptophan. FW = 204.23 g/mole.
13.71% N.

Target Conc. (ppm)	Actual Wt. Added (g)	Volume (ml)	Actual Conc. (μ g)*
750	0.5499	100	3.7696
500	0.3618	100	2.48014
100	0.0739	100	0.5066
50	0.0345	100	0.2365

* Concentration as μ g N/ 5 μ l sample.

Table IV-7. Sample preparation data for Pyrazine. FW = 80.09 g/mole.
34.96% N.

Target Conc. (ppm)	Actual Wt. Added (g)	Volume (ml)	Actual Conc. (μ g)*
1000	0.2904	100	5.0762
750	0.2258	100	3.9470
500	0.1422	100	2.4857

* Concentration as μ g N/ 5 μ l sample.

For the 100 ppm N solution as pyrazine, 5 ml of the 1000 ppm N solution was diluted to 50 ml providing 0.5076 μ g N/ 5 μ l sample. For the 50 ppm N solution as pyrazine, 2.5 ml of the 1000 ppm solution was diluted to 50 ml volume providing 0.2538 μ g N/ 5 μ l sample.

Table IV-8. Sample preparation data for AgNO₃. FW = 169.87 g/mole.
8.24% N.

Target Conc. (ppm)	Actual Wt. Added (g)	Volume (ml)	Actual Conc. (μ g)*
1000	1.2109	100	4.9889
750	0.9150	100	3.7698
500	0.6101	100	2.5136

* Concentration as μ g N/ 5 μ l sample.

For the 100 ppm N solution as AgNO₃, 5 ml of the 1000 ppm N solution was diluted to 50 ml providing 0.49889 μ g N/ 5 μ l sample. For the 50 ppm N solution as AgNO₃, 5 ml of the 500 ppm solution was diluted to 50 ml volume providing 0.25136 μ g N/ 5 μ l sample.

To obtain a calibration curve in the range of 5–100 ppm N, standards in this range were prepared by dilution of the AgNO_3 standards. One ml of the 1000 ppm N standard was diluted to 50 ml to obtain a 19.96 ppm N ($0.09978 \mu\text{g N}/5 \mu\text{l sample}$) standard. One ml of the 500 ppm N standard was diluted to 50 ml to obtain a 10.05 ppm N standard ($0.05272 \mu\text{g N}/5 \mu\text{l sample}$). Two ml of the 100 ppm N standard was diluted to 50 ml to obtain a 3.99 ppm N standard ($0.01995 \mu\text{g N}/5 \mu\text{l sample}$).

To verify the previously observed effects of NaOH , Na_2CO_3 , and Na_2SO_4 on the glutamic acid response, glutamic acid solutions at 50, 100, and 500 ppm N in 0.2 N solutions of the salts were prepared. Eight grams of NaOH was dissolved in 1000 ml of d, d- H_2O , 10.6 g of Na_2CO_3 was dissolved in 1000 ml of d, d- H_2O , and 14.2 g of Na_2SO_4 was dissolved in 1000 ml of d, d- H_2O . These solutions were used as the basis for preparing the glutamic acid solutions as identified in Table IV-9.

Table IV-9. Sample preparation data for Glutamic Acid in 0.2 N sodium salt matrix. FW = 147.13 g/mole. 9.515% N. All samples prepared to a 100 ml volume.

Target Conc. (ppm)	†Actual Wt. Added (g)	†Actual Conc. (μg)*	‡Actual Wt. Added (g)	‡Actual Conc. (μg)*	§Actual Wt. Added (g)	§Actual Conc. (μg)*
50	0.0567	0.2698	0.0625	0.29735	0.0514	0.2446
100	0.1103	0.5248	0.1055	0.5019	0.1069	0.5086
500	0.5246	2.4958	0.5346	2.5434	0.5280	2.5120

* Concentration as $\mu\text{g N}/5 \mu\text{l sample}$.

†For NaOH solutions.

‡For Na_2CO_3 solutions.

§For Na_2SO_4 solutions.

Two samples were prepared as mixed standards. The first was a 50/50 solution of nitrogen as glutamic acid and tryptophan where 20 ml of each 100 ppm N solution was mixed to provide $0.50095 \mu\text{g N}/5 \mu\text{l sample}$. The second was a 25/75 solution of nitrogen as glutamic acid and tryptophan where 10 ml of glutamic acid solution and 30 ml

of tryptophan solution each at 500 ppm N were mixed to provide 2.47988 $\mu\text{g N}/5\ \mu\text{l}$ sample.

Table IV-10. Preparation data for proline. FW = 115.13 g/mole. 12.17% N.

<u>Target Concentration*</u>	<u>Target Proline Weight (g)</u>	<u>Actual Weight Added (g)</u>	<u>Volume (ml)</u>	<u>Actual Concentration*</u>
5.0	0.4109	0.4071	50	4.954
3.75	0.6164	0.6228	100	3.789
2.50	0.4109	0.4214	100	2.564
1.25	0.2055	0.2080	100	1.265
0.50	0.0822	0.0865	100	0.526

* Concentration as $\mu\text{g N}/5\ \mu\text{l}$ sample.

Samples were also prepared for NH_4Cl in various concentrations of Na_2CO_3 to test the effect of the alkali matrix concentration on the nitrogen response. First, the Na_2CO_3 solutions were prepared. The sample preparation is given in Table IV-11. The Na_2CO_3 solutions were then used to prepare the NH_4Cl solutions. The preparation for these samples is given in Tables IV-12–IV-14. Chemical additions of NH_4Cl were made and diluted to volume with the corresponding Na_2CO_3 solution.

Table IV-11. Preparation data for Na_2CO_3 . FW = 106 g/mole.

<u>Target Concentration*</u>	<u>Target NH_4Cl Weight (g)</u>	<u>Actual Weight Added (g)</u>	<u>Volume (ml)</u>
0.1	2.65	2.6	500
0.1	1.325	1.4	250
0.2	5.3	5.3	500
0.2	5.3	5.3	500
0.5	13.25	13.25	500
0.5	6.625	6.6	250

* Concentration as N (normality).

Table IV-12. Preparation data for NH_4Cl in 0.1 N Na_2CO_3 . FW = 53.49 g/mole. 26.2% N.

<u>Target Concentration*</u>	<u>Target NH_4Cl Weight (g)</u>	<u>Actual Weight Added (g)</u>	<u>Volume (ml)</u>	<u>Actual Concentration*</u>
5.0	0.1911	0.1934	50	5.060
3.75	0.1433	0.1456	50	3.810
2.50	0.1911	0.1975	100	2.584
1.25	0.0956	0.0954	100	1.247
0.50	0.0382	0.0407	100	0.533

* Concentration as $\mu\text{g N/ 5 } \mu\text{l}$ sample.

Table IV-13. Preparation data for NH_4Cl in 0.2 N Na_2CO_3 . FW = 53.49 g/mole. 26.2% N.

<u>Target Concentration*</u>	<u>Target NH_4Cl Weight (g)</u>	<u>Actual Weight Added (g)</u>	<u>Volume (ml)</u>	<u>Actual Concentration*</u>
5.0	0.1911	0.1924	50	5.034
3.75	0.1433	0.1480	50	3.873
2.50	0.1911	0.1960	100	2.564
1.25	0.0956	0.0956	100	1.250
0.50	0.0382	0.0380	100	0.497

* Concentration as $\mu\text{g N/ 5 } \mu\text{l}$ sample.

Table IV-14. Preparation data for NH_4Cl in 0.5 N Na_2CO_3 . FW = 53.49 g/mole. 26.2% N.

<u>Target Concentration*</u>	<u>Target NH_4Cl Weight (g)</u>	<u>Actual Weight Added (g)</u>	<u>Volume (ml)</u>	<u>Actual Concentration*</u>
5.0	0.1911	0.2041	50	5.340
3.75	0.1433	0.1415	50	3.703
2.50	0.1911	0.1938	100	2.535
1.25	0.0956	0.0959	100	1.254
0.50	0.0382	0.0392	100	0.513

* Concentration as $\mu\text{g N/ 5 } \mu\text{l}$ sample.

BLACK LIQUORS

The commercial black liquors used for pyrolysis experiments were analyzed as whole liquors and as freeze dried liquors. Also, inorganic and lignin samples obtained from the liquors via acid precipitation⁶⁷ were also analyzed. To obtain the freeze dried material, the black liquor sample weight was determined and the sample was then attached to the freeze drier to dry. Samples were stored at 4° C in air tight containers until tested.

The acid precipitated lignin was obtained through an isolation technique adapted from Lin.⁶⁷ Basically, the high solids liquors were diluted to about 40% solids (the low solids liquor was used as received) and heated to 90–95° C, then acidified to pH 2 with sulfuric acid. The liquor is was cooled to 40° C, filtered, and freeze dried. The lignin obtained is heterogeneous with regard to the chemical components, however, all of the water is removed from the system. The inorganic fraction was obtained by freeze drying the filtrate from the precipitated lignin. Again, the samples were stored at 4° C in air tight containers until tested.

SCREENING EXPERIMENTS

For each treatment, the chemical addition was as indicated in Table IV-15 below. Each component was weighed out in a weighing tray and quantitatively transferred to a 100 ml beaker containing 30 ml of 0.1 M NaOH. The solution was stirred using a stir bar and was concentrated (at about 70° C) in a water bath (at about 95° C) on a hot plate. The pH of the solution was maintained at 11 and was adjusted with concentrated H₂SO₄. (Only the treatments containing Na₂S needed adjustment due to the addition of the buffer solution.) The beaker with the concentrated solution was then brought to dryness in a vacuum oven at 105–110° C and 25–30 psig. Each was then cooled and stored in a desiccator until used as samples in the TG-DSC.

Table IV-15. Chemical addition for each treatment combination.

Treatment Combinations	Amount Added (grams)				
	Tryptophan	Glutamic Acid	Na ₂ SO ₄ (factor A)	Na ₂ S (factor B)	Na ₂ CO ₃ (factor C)
I	0.5010	0.5015	--	--	--
A	0.5009	0.5006	0.5011	--	--
B	0.5009	0.5013	--	0.5012	--
AB	0.5003	0.5007	0.5010	0.5012	--
C	0.5007	0.5003	--	--	0.5011
AC	0.5003	4.995	0.5013	--	0.5017
BC	0.5010	0.5003	--	0.5012	0.5006
ABC	0.5002	0.5012	0.5006	0.5007	0.5011

The NaOH solution was made with deaerated H₂O to prevent the potential oxidation of species, particularly Na₂S, when brought into solution. To further prevent sulfide oxidation, a sulfide anti-oxidant buffer (SAOB II) was used to stabilize the sulfide in solution. Two ml of the SAOB II solution was added to each treatment containing Na₂S (treatments B, AB, BC, and ABC). The SAOB II solution was prepared by dissolving 80 g NaOH in a 1000 ml volumetric flask containing about 400 ml of distilled, deaerated water. To this, 67 g disodium EDTA and 35 g ascorbic acid was added and dissolved. The SAOB II solution was pale yellow in color and darkened as the solution oxidized. Because the solution volume for each treatment was small, the sulfide concentration could not be measured. However, the change in color of the SAOB II in the treatment solution served as a qualitative indicator of the degree of sulfide oxidation. All solutions in which the SAOB II was added were concentrated under a nitrogen purge to help reduce oxidation of the sulfide. If the treatment solution darkened to an orange-brown color during concentration, the solution was discarded and a new solution prepared.

APPENDIX V: GPNP NITROGEN DATA COLLECTED UNDER COMBUSTION CONDITIONS

GPNP nitrogen data collected under combustion conditions is provided in this appendix. The data included are the following: 1) data for aqueous nitrogen sample injected into the gas stream used as a control for further measurements, 2) calibration data for NO and NH₃, 3) data for the injection of nitrogen samples into the NO and NH₃ gas streams for total nitrogen measurement and interactions between gas phase species, and 4) correction data for NO and NH₃ gas concentrations for the conversion of ppm-mole for gas concentrations to ppm-gram for the aqueous nitrogen samples.

Each set of data is presented along with the statistical summaries. Error estimates can be taken from the correlation coefficients in the plots as well as the statistical standard deviation and coefficient of variation.

The sample numbers in the data tables, such as N4097022, are the same as the computer data acquisition (CDA) file names. The N identifies the sample as a nitrogen release profile type of data file. The 4 represents the lab notebook #4264. A 3 would represent the lab notebook #3917. The next three digits are the page number within the notebook where the data can be found and the last three digits are the sample number on that page. The last digit represents the number of the replicate. For the example, the values listed for the N4097022 sample would be found in notebook 4264 on page 97 as sample 2, replicate 2.

Table V-1. Calibration data for nitrogen as silver nitrate during combustion.

Method Used:	5	PMT Voltage:	825
O2 to O3:	30 ml/min	Furnace Temperature:	1100° C
O2 to pyro:	365 ml/min	Gain Setting:	HI
O2 to inlet:	20 ml/min	Gain Factor:	X1
He to inlet:	145 ml/min	Residence Time:	3 min
Nitrogen Species:	AgNO ₃	Matrix:	d,d-H ₂ O

<u>Sample #</u>	<u>Sample ID</u>	<u>Sample Vol</u> <u>(μl)</u>	<u>Known N</u> <u>Mass (μg)</u>	<u>Response</u> <u>Counts</u>	<u>CDA Sum</u> <u>Response</u>
N4083C03	50.27 ppm N	5	0.25136	4773	8.496
N4083C04	50.27 ppm N	5	0.25136	4494	7.9094
N4_83C02	50.27 ppm N	5	0.25136	4682	8.1536
N4_83C01	50.27 ppm N	5	0.25136	4298	7.2749
N4083C05	99.78 ppm N	5	0.4989	11931	21.0449
N4083C06	99.78 ppm N	5	0.4989	11862	21.0445
N4083C07	99.78 ppm N	5	0.4989	11803	20.6544
N4083C08	502.72 ppm N	5	2.5136	67938	120.2632
N4083C09	502.72 ppm N	5	2.5136	67564	119.7023
N4083C10	502.72 ppm N	5	2.5136	68060	120.4832
N4083C11	753.96 ppm N	5	3.7698	104290	184.717
N4083C12	753.96 ppm N	5	3.7698	104523	185.1069
N4083C13	753.96 ppm N	5	3.7698	104564	185.449
N4083C14	997.78 ppm N	5	4.9889	139284	247.0215
N4083C15	997.78 ppm N	5	4.9889	140200	248.6564
N4083C16	997.78 ppm N	5	4.9889	139831	247.9739

<u>Summarized Data</u>	<u>Ave. Counts</u>	<u>n</u>	<u>SD</u>	<u>RSD (%)</u>
50.27 ppm N	4560.5	4	212.8	4.67
99.78 ppm N	11865	3	64	0.54
502.72 ppm N	67854	3	258	0.38
753.96 ppm N	104459	3	148	0.14
997.78 ppm N	139772	3	461	0.33

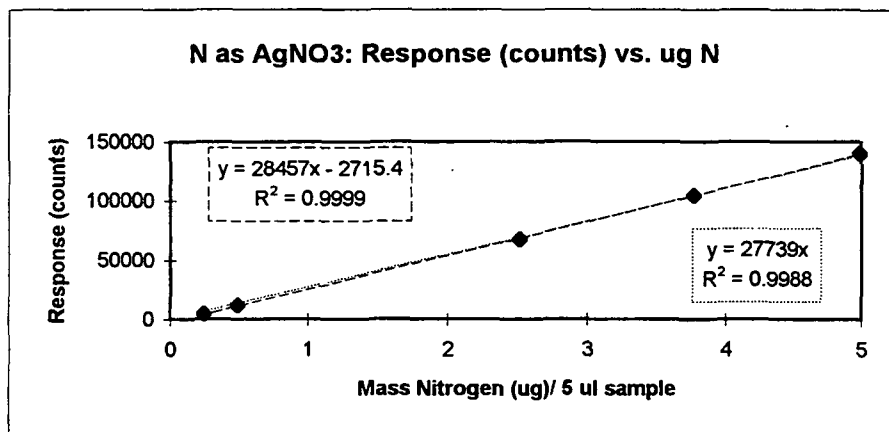


Table V-2. Calibration data for measurement of nitric oxide gas.

Method Used:	5	PMT Voltage:	825
O ₂ to O ₃ :	30 ml/min	Furnace Temperature:	1100° C
O ₂ to pyro:	365 ml/min	Gain Setting:	HI
O ₂ to inlet:	20 ml/min	Gain Factor:	X1
He to inlet:	145 ml/min	Residence Time:	3 min
Nitrogen Species:	NO(g)	Matrix:	He
Carrier gas:	He(g)	Gas box carrier flow:	0.025 lpm

<u>Sample #</u>	<u>Sample ID</u>	<u>Sample Vol</u> <u>(μl)</u>	<u>Flow (lpm)</u> <u>NO in He</u>	<u>Flow (lpm)</u> <u>He</u>	<u>Known N</u> <u>Mass (μg)</u>	<u>Response</u> <u>Counts</u>	<u>CDA Sum</u> <u>Response</u>
N4109131	~100 ppm N	5	0.0801	4.1899	0.5098	10822	17.8011
N4109132	~100 ppm N	5	0.0772	4.1899	0.4915	10749	17.8744
N4109133	~100 ppm N	5	0.0772	4.2042	0.4898	10987	18.0694
N4109141	~250 ppm N	5	0.2031	4.0898	1.2847	36590	63.4998
N4109142	~250 ppm N	5	0.2059	4.0755	1.3062	37184	64.6471
N4109143	~250 ppm N	5	0.2059	4.0755	1.3062	36234	62.6696
N4110271	~250 ppm N	5	0.20449	4.1041	1.289	38677	67.0152
N4110272	~250 ppm N	5	0.20878	4.0898	1.3191	38256	66.2333
N4110273	~250 ppm N	5	0.20735	4.0898	1.3105	38861	67.284
N4111301	~250 ppm N	5	0.20592	4.0898	1.3019	46073	80.2273
N4111302	~250 ppm N	5	0.21021	4.0898	1.3277	46629	81.1794
N4111303	~250 ppm N	5	0.20735	4.0755	1.3149	46120	80.0563
N4109151	~500 ppm N	5	0.4304	3.8324	2.7423	80810	141.9701
N4109152	~500 ppm N	5	0.4333	3.8610	2.7403	84273	147.8781
N4109153	~500 ppm N	5	0.4304	3.8753	2.7150	85325	149.4166
N4112401	~750 ppm N	5	0.6878	3.6036	4.353	168362	297.3641
N4112402	~750 ppm N	5	0.6878	3.6036	4.353	170945	301.416
N4112403	~750 ppm N	5	0.6893	3.5893	4.3752	168445	297.2418
N4112461	~750 ppm N	5	0.6850	3.5893	4.3523	170230	300.2201
N4112462	~750 ppm N	5	0.6864	3.6036	4.3454	173191	304.9574
N4112463	~750 ppm N	5	0.6864	3.6036	4.3454	169272	298.3874

<u>Summarized Data</u>	<u>Ave. Counts</u>	<u>n</u>	<u>SD</u>	<u>RSD (%)</u>
~100 ppm N	10853	3	122	1.12
~250 ppm N	40514	9	4412	10.89
~500 ppm N	83469	3	2362	2.83
~750 ppm N	170074	6	1829	1.075

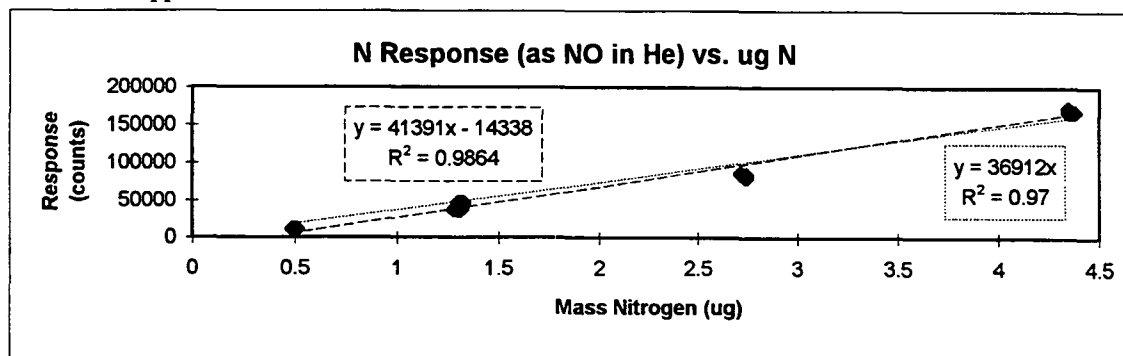


Table V-3. Data for measurement of nitrogen as NH₃ (g) by combustion.

Method Used:	5	PMT Voltage:	825
O ₂ to O ₃ :	30 ml/min	Furnace Temperature:	1100C
O ₂ to pyro:	365 ml/min	Gain Setting:	HI
O ₂ to inlet:	20 ml/min	Gain Factor:	X1
He to inlet:	145 ml/min	Residence Time:	3 min
Nitrogen Species:	NH ₃ (g)	Matrix:	He
Carrier gas:	He(g)	Gas box carrier flow:	0.025 lpm

Sample #	Sample ID	Sample Mass (ul)	Flow (lpm) NH ₃ in He	Flow (lpm) He	Known N Mass (ug)	Response Counts	CDA Sum Response
N4117051	~250 ppm N	5	0.1988	4.09	1.259	32433	55.1757
N4117052	~250 ppm N	5	0.1973	4.08	1.254	35077	59.2279
N4117053	~250 ppm N	5	0.1988	4.09	1.259	36887	62.3527
N4117054	~250 ppm N	5	0.1973	4.09	1.250	38441	63.8417
N4117055	~250 ppm N	5	0.1988	4.08	1.263	39594	66.9419
N4117056	~250 ppm N	5	0.1988	4.09	1.259	37910	64.0372
N4117061	~500 ppm N	5	0.4190	3.88	2.650	93785*	155.3491
N4117062	~500 ppm N	5	0.4190	3.88	2.650	94796*	158.6686
N4117063	~500 ppm N	5	0.4176	3.88	2.642	133716	219.0911
N4117064	~500 ppm N	5	0.4190	3.88	2.650	123793	210.6662
N4117065	~500 ppm N	5	0.4176	3.88	2.642	108188	--
N4117066	~500 ppm N	5	0.4176	3.88	2.642	126661	216.7689
N4117067	~500 ppm N	5	0.4161	3.89	2.625	117931	204.7063
N4117068	~500 ppm N	5	0.4176	3.88	2.642	126586	218.1612
N4118071	~250 ppm N	5	0.1988	4.09	1.259	67635	114.3974
N4118072	~250 ppm N	5	0.1973	4.08	1.254	38548*	70.111
N4118073	~250 ppm N	5	0.1988	4.09	1.259	62140	105.6083
N4118074	~250 ppm N	5	0.1988	4.09	1.259	61926	105.1688
N4118081	~500 ppm N	5	0.4176	3.88	2.642	127608	217.8895
N4118082	~500 ppm N	5	0.4190	3.88	2.650	121809	210.7877
N4118083	~500 ppm N	5	0.4190	3.86	2.659	127581	218.9661
N4118091	~750 ppm N	5	0.6592	3.63	4.172	173971	277.4914
N4118092	~750 ppm N	5	0.6607	3.63	4.180	176990	300.8217
N4118093	~750 ppm N	5	0.6592	3.63	4.172	149945	262.3008
N4118094	~750 ppm N	5	0.6592	3.63	4.172	153258	267.9635
N4118095	~750 ppm N	5	0.6592	3.63	4.172	186940	315.5935
N4118101	~500 ppm N	5	0.4176	3.88	2.642	126362*	215.9615
N4118102	~500 ppm N	5	0.4161	3.88	2.634	113978	197.3345
N4118103	~500 ppm N	5	0.4176	3.88	2.642	114591	198.8738
N4118104	~500 ppm N	5	0.4176	3.88	2.642	113213	196.3844
N4118111	~250 ppm N	5	0.1988	4.09	1.259	62898	106.7561
N4118112	~250 ppm N	5	0.2002	4.09	1.267	62835	104.7543
N4118113	~250 ppm N	5	0.1988	4.09	1.259	80916*	126.0965
N4118114	~250 ppm N	5	0.1988	4.09	1.259	66334	112.642
N4118115	~250 ppm N	5	0.1973	4.09	1.250	55067	94.9678
N4118116	~250 ppm N	5	0.1959	4.08	1.246	61217	105.4128

*Note: These points have not been used in the analysis, because they are known to be in error experimentally.

Table V-3. (cont.) Data for measurement of nitrogen as NH_3 (g) by combustion.

<u>Sample #</u>	<u>Sample ID</u>	<u>Sample Mass</u> <u>(ul)</u>	<u>Flow (lpm)</u> <u>NH_3 in He</u>	<u>Flow (lpm)</u> <u>He</u>	<u>Known N</u> <u>Mass (ug)</u>	<u>Response</u> <u>Counts</u>	<u>CDA Sum</u> <u>Response</u>
N4119171	~250 ppm N	5	0.1988	4.08	1.263	59056	101.557
N4119172	~250 ppm N	5	0.1988	4.08	1.263	52001*	89.3257
N4119173	~250 ppm N	5	0.1973	4.08	1.254	60605	103.7531
N4119174	~250 ppm N	5	0.1973	4.08	1.254	60145	103.1194
N4119181	~500 ppm N	5	0.4161	3.88	2.634	117838	204.0696
N4119182	~500 ppm N	5	0.4190	3.86	2.659	106730	185.6883
N4119183	~500 ppm N	5	0.4176	3.88	2.642	126037	212.2481
N4119184	~500 ppm N	5	0.4176	3.88	2.642	123128	210.5873
N4119185	~500 ppm N	5	0.4161	3.88	2.634	111783	194.2806
N4119211	~500 ppm N	5	0.4176	3.88	2.642	108762	188.5719
N4119212	~500 ppm N	5	0.4190	3.88	2.650	122401*	210.3701
N4119213	~500 ppm N	5	0.4190	3.88	2.650	111505	193.0146
N4119214	~500 ppm N	5	0.4190	3.88	2.650	105084	184.1283
N4122251	~500 ppm N	5	0.4176	3.89	2.633	112996	195.0643
N4122252	~500 ppm N	5	0.4190	3.88	2.650	108662	188.3507
N4122253	~500 ppm N	5	0.4190	3.89	2.641	105517	183.2236
N4123361	~750 ppm N	5	0.6578	3.63	4.164	175425	288.0069
N4123362	~750 ppm N	5	0.6592	3.63	4.172	154018	268.2568
N4123363	~750 ppm N	5	0.6592	3.63	4.172	159939	277.6796
N4123364	~750 ppm N	5	0.6592	3.63	4.172	147719	258.0301
N4123421	~750 ppm N	5	0.6592	3.63	4.172	160670	278.6818
N4123422	~750 ppm N	5	0.6607	3.63	4.180	157364	273.7015
N4123423	~750 ppm N	5	0.6621	3.63	4.187	157882	274.8006

*Note: These points have not been used in the analysis, because they are known to be in error experimentally.

<u>Sample #</u>	<u>Sample ID</u>	<u>Ave. Counts</u>	<u>n</u>	<u>SD</u>	<u>RSD (%)</u>
N411705_	~250 ppm N	36724	6	2598	7.07
N411706_	~500 ppm N	122813	6	8793	7.16
N411807_	~250 ppm N	63900	3	3236	5.06
N411808_	~500 ppm N	125666	3	3340	2.66
N411809_	~750 ppm N	198221	5	15955	9.48
N411810_	~500 ppm N	113927	3	690	0.61
N411811_	~250 ppm N	61470	5	4089	6.65
N411917_	~250 ppm N	59935	3	796	1.33
N411918_	~500 ppm N	117103	5	7946	6.79
N411921_	~500 ppm N	108450	3	3222	2.97
N412225_	~500 ppm N	109058	3	3755	3.44
N412336_	~750 ppm N	159275	4	11866	7.45
N412342_	~750 ppm N	158639	3	1778	1.12

Table V-3. (cont.) Calibration data for NH₃ (g) gas species during combustion.

Method Used:	5	PMT Voltage:	825
O ₂ to O ₃ :	30 ml/min	Furnace Temperature:	1100° C
O ₂ to pyro:	365 ml/min	Gain Setting:	HI
O ₂ to inlet:	20 ml/min	Gain Factor:	X1
He to inlet:	145 ml/min	Residence Time:	3 min
Nitrogen Species:	9770 ppm NH ₃	Matrix:	He
Carrier gas:	He(g)	Gas box carrier flow:	0.095 lpm

Sample #	Sample ID	Sample Vol/Mass (μ l)	Flow (lpm) NH ₃ in He	Flow (lpm) He	Known N Mass (μ g)	Response Counts	CDA Sum Response
N4097065	100 ppm N	5000	0.044	4.22	0.2899	10169	16.9184
N4097067	100 ppm N	5000	0.042	4.22	0.2799	10282	17.1623
N4097068	100 ppm N	5000	0.042	4.22	0.2799	11000	18.4806
N4097069	100 ppm N	5000	0.042	4.22	0.2799	10785	18.0898
N4098071	250 ppm N	5000	0.107	4.09	0.7181	31412	54.3446
N4098072	250 ppm N	5000	0.108	4.09	0.7231	32645	56.2736
N4098073	250 ppm N	5000	0.107	4.09	0.7181	32776	56.6889
N4098081	500 ppm N	5000	0.225	3.88	1.5440	63709	111.595
N4098082	500 ppm N	5000	0.224	3.88	1.5390	65280	114.0855
N4098083	500 ppm N	5000	0.225	3.88	1.5440	61657	108.398
N4098091	750 ppm N	5000	0.355	3.63	2.5067	96926	169.9442
N4098092	750 ppm N	5000	0.354	3.63	2.5017	96819	170.042
N4098093	750 ppm N	5000	0.354	3.63	2.5017	95109	166.8685
N4098101	1000 ppm N	5000	0.499	3.36	3.6401	123900	217.1605
N4098102	1000 ppm N	5000	0.500	3.36	3.6450	125131	219.7006
N4098103	1000 ppm N	5000	0.500	3.36	3.6450	126707	223.0204

Summarized Data	Ave. Counts	n	SD	RSD (%)
100 ppm N	10559	4	398	3.77
250 ppm N	32278	3	753	2.33
500 ppm N	63549	3	1817	2.86
750 ppm N	96285	3	1020	1.06
1000 ppm N	125246	3	1407	1.12

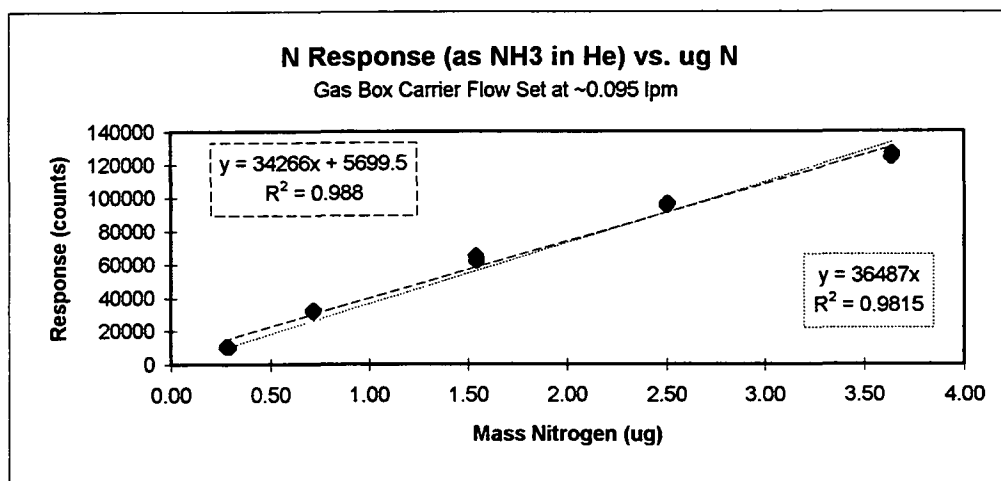


Table V-3. (cont.) Calibration data for NH₃ (g) gas species during combustion.

Method Used:	5	PMT Voltage:	825
O ₂ to O ₃ :	30 ml/min	Furnace Temperature:	1100C
O ₂ to pyro:	365 ml/min	Gain Setting:	HI
O ₂ to inlet:	20 ml/min	Gain Factor:	X1
He to inlet:	145 ml/min	Residence Time:	3 min
Nitrogen Species: 9770 ppm NH ₃		Matrix:	He
Carrier gas:	He(g)	Gas box carrier flow:	0.025 lpm

Sample #	Sample ID	Sample Vol/Mass (μ l or mg)	Flow (lpm) NH ₃ in He	Flow (lpm) He	Known N Mass (μ g)	Response Counts	CDA Sum Response
N4097061	100 ppm N	5000	0.042	4.22	0.2748	0	0
N4097062	100 ppm N	5000	0.044	4.22	0.2899	19	0.5124
N4098111	1000 ppm N	5000	0.498	3.36	3.6352	139786	241.381
N4098112	1000 ppm N	5000	0.498	3.36	3.6352	150043	260.6186
N4098113	1000 ppm N	5000	0.499	3.36	3.6401	153814	266.9673
N4098141	500 ppm N	5000	0.225	3.88	1.5440	68403	118.0896
N4098142	500 ppm N	5000	0.225	3.88	1.5440	67322	116.7475
N4098143	500 ppm N	5000	0.224	3.88	1.5390	66970	116.0393

Summarized Data	Ave. Counts	n	SD	RSD (%)
100 ppm N	10	2	13.4	141.4
500 ppm N	67565	3	747	1.11
1000 ppm N	147881	3	7260	4.91

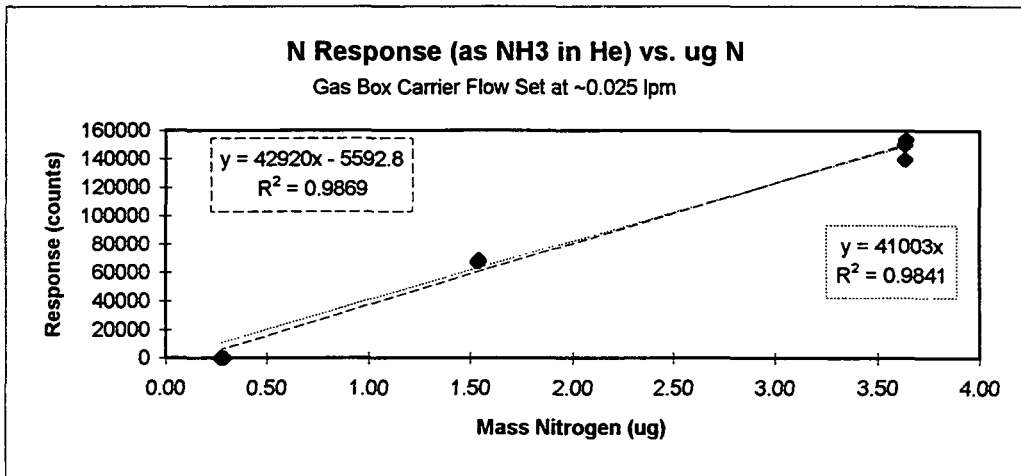


Table V-3. (cont.) Calibration data for NH₃ (g) gas species during combustion.

Method Used:	5	PMT Voltage:	825
O ₂ to O ₃ :	30 ml/min	Furnace Temperature:	1100° C
O ₂ to pyro:	365 ml/min	Gain Setting:	HI
O ₂ to inlet:	20 ml/min	Gain Factor:	X1
He to inlet:	145 ml/min	Residence Time:	3 min
Nitrogen Species:	9770 ppm NH ₃	Matrix:	He
Carrier gas:	He(g)	Gas box carrier flow:	0.220 lpm

<u>Sample #</u>	<u>Sample ID</u>	<u>Sample Vol/Mass</u> <u>(μl)</u>	<u>Flow (lpm)</u> <u>NO in He</u>	<u>Flow (lpm)</u> <u>He</u>	<u>Known N</u> <u>Mass (μg)</u>	<u>Response</u> <u>Counts</u>	<u>CDA Sum</u> <u>Response</u>
N4097063	100 ppm N	5000	0.042	4.22	0.2799	11475	19.5307
N4097066	100 ppm N	5000	0.044	4.22	0.2849	12369	21.0687
N4098121	1000 ppm N	5000	0.499	3.37	3.6266	98773	--
N4098122	1000 ppm N	5000	0.500	3.36	3.6450	98773	173.631
N4098123	1000 ppm N	5000	0.500	3.36	3.6450	99237	174.5833
N4098131	500 ppm N	5000	0.225	3.86	1.5494	58060	101.9376
N4098132	500 ppm N	5000	0.223	3.88	1.5340	57777	101.3418
N4098133	500 ppm N	5000	0.223	3.89	1.5287	53767	94.7264

<u>Summarized Data</u>	<u>Ave. Counts</u>	<u>n</u>	<u>SD</u>	<u>RSD (%)</u>
100 ppm N	11922	2	632	5.3
500 ppm N	56535	3	2401	4.25
1000 ppm N	98928	3	268	0.27

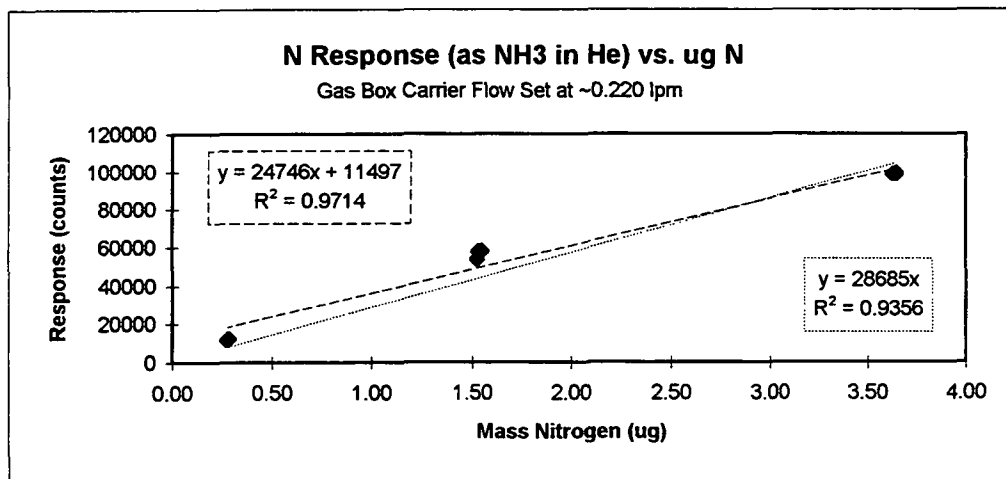


Table V-4. Data for total nitrogen measurement of NO (g) by combustion.

Method Used:	5	PMT Voltage:	825
O2 to O3:	30 ml/min	Furnace Temperature:	1100° C
O2 to pyro:	365 ml/min	Gain Setting:	HI
O2 to inlet:	20 ml/min	Gain Factor:	X1
He to inlet:	145 ml/min	Residence Time:	3 min
Nitrogen Species:	NO(g)	Matrix:	He
Carrier gas:	He(g)	Gas box carrier flow:	0.025 lpm

Sample #	Sample ID	Sample Vol (μ l)	Flow (lpm) NO in He	Flow (lpm) He	Known N Mass (μ g)	Response Counts	CDA Sum Response
N4113101	~250 ppm N	5	0.209	4.09	1.319	39401	67.8442
N4113102	~250 ppm N	5	0.207	4.09	1.310	37924	65.3784
N4113103	~250 ppm N	5	0.206	4.10	1.298	37804	65.3784
N4114111	~500 ppm N	5	0.436	3.88	2.747	87066	152.5147
N4114112	~500 ppm N	5	0.433	3.86	2.740	87520	153.3453
N4114113	~500 ppm N	5	0.435	3.86	2.748	88733	155.469
N4114121	~750 ppm N	5	0.688	3.60	4.353	144085	253.6111
N4114122	~750 ppm N	5	0.692	3.60	4.376	144429	254.5877
N4114123	~750 ppm N	5	0.686	3.60	4.345	145704	256.6624
N4114161	~750 ppm N	5	0.688	3.60	4.353	141862	250.2665
N4114162	~750 ppm N	5	0.685	3.60	4.338	142486	250.7556
N4114163	~750 ppm N	5	0.688	3.60	4.353	143313	252.6346
N4114191	~750 ppm N	5	0.686	3.60	4.345	144158	253.979
N4114192	~750 ppm N	5	0.685	3.60	4.338	141563	249.8041
N4114193	~750 ppm N	5	0.685	3.60	4.338	143935	253.8082
N4114201	~500 ppm N	5	0.433	3.86	2.740	87735	154.1027
N4114202	~500 ppm N	5	0.428	3.88	2.699	87465	153.3948
N4114203	~500 ppm N	5	0.432	3.86	2.732	86401	151.3929
N4115261	~500 ppm N	5	0.436	3.86	2.757	88860	156.1041
N4115262	~500 ppm N	5	0.436	3.88	2.747	87070	153.0038
N4115263	~500 ppm N	5	0.435	3.89	2.730	87438	153.2482
N4115271	~250 ppm N	5	0.204	4.09	1.293	37517	64.8661
N4115272	~250 ppm N	5	0.203	4.08	1.289	37854	65.8428
N4115273	~250 ppm N	5	0.203	4.09	1.285	37523	65.2327
N4115291	~250 ppm N	5	0.209	4.10	1.315	38656	67.5021
N4115292	~250 ppm N	5	0.206	4.10	1.298	38512	66.4044
N4115293	~250 ppm N	5	0.206	4.10	1.298	37762	65.526
N4116341	~250 ppm N	5	0.206	4.06	1.311	38667	67.2099
N4116342	~250 ppm N	5	0.206	4.06	1.311	38724	67.2339
N4116343	~250 ppm N	5	0.206	4.06	1.311	38808	67.5025
<u>Summarized Data</u>	<u>Ave. Counts</u>	<u>n</u>	<u>SD</u>	<u>RSD (%)</u>			
~250 ppm N	38263	12	605	1.58			
~500 ppm N	87588	9	786	0.90			
~750 ppm N	143503	9	1331	0.93			

Table V-5. Calibration data for nitrogen as silver nitrate during combustion.

Method Used:	6	PMT Voltage:	825
O2 to O3:	30 ml/min	Furnace Temperature:	1100° C
O2 to pyro:	365 ml/min	Gain Setting:	HI
O2 to inlet:	20 ml/min	Gain Factor:	X10
He to inlet:	145 ml/min	Residence Time:	3 min
Nitrogen Species:	AgNO3	Matrix:	d,d-H2O

<u>Sample #</u>	<u>Sample ID</u>	<u>Sample Vol</u> <u>(ul)</u>	<u>Known N</u> <u>Mass (ug)</u>	<u>Response</u> <u>Counts</u>	<u>CDA Sum</u> <u>Response</u>
N4085C01	3.99 ppm N	5	0.01995	2787	--
N4085C02	3.99 ppm N	5	0.01995	2623	--
N4085C03	3.99 ppm N	5	0.01995	2570	--
N4085C04	10.05 ppm N	5	0.05272	10268	--
N4085C05	10.05 ppm N	5	0.05272	10850	--
N4085C06	10.05 ppm N	5	0.05272	11254	--
N4085C07	19.96 ppm N	5	0.09978	24701	--
N4085C08	19.96 ppm N	5	0.09978	24110	--
N4085C09	19.96 ppm N	5	0.09978	24774	--
N4085C10	50.27 ppm N	5	0.25136	67982	--
N4085C11	50.27 ppm N	5	0.25136	66264	--
N4085C12	50.27 ppm N	5	0.25136	66254	--
N4085C13	99.78 ppm N	5	0.4989	136337	--
N4085C14	99.78 ppm N	5	0.4989	129883	--
N4085C15	99.78 ppm N	5	0.4989	127786	--

<u>Summarized Data</u>	<u>Ave. Counts</u>	<u>n</u>	<u>SD</u>	<u>RSD (%)</u>
3.99 ppm N	2660	3	113	4.25
10.05 ppm N	10791	3	495.7	4.59
19.96 ppm N	24528	3	364	1.48
50.27 ppm N	66833	3	995	1.49
99.78 ppm N	131335	3	4457	3.39

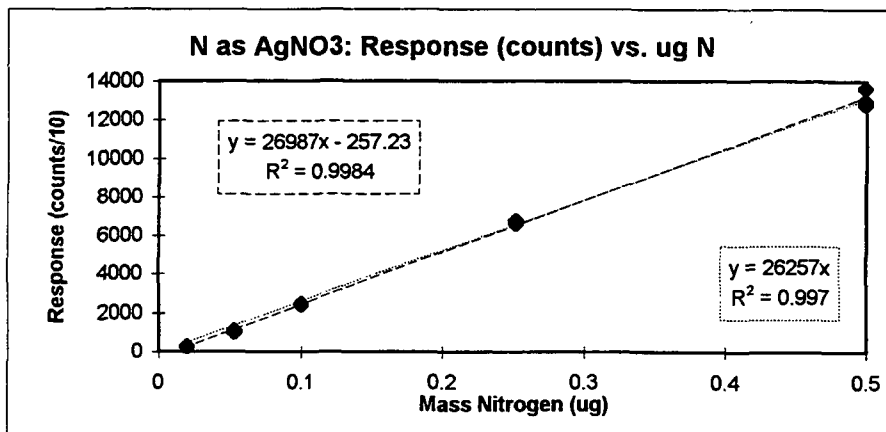


Table V-22. (cont.) Concentration corrections for NO gas samples. Initial [NO] = 9424 ppm NO in He. Flow rates in lpm as air conversion factors are 1.43 for He, 1.43 for NO in He.

Sample #	Flow Rate NO (l/min as air)	Flow Rate NO (l/min)	Flow Rate He (l/min as air)	Flow Rate He (l/min)	Conc. N ($\mu\text{g N/sample}$)
N4110271	0.143	0.20449	2.87	4.10	1.2890
N4110272	0.146	0.20878	2.86	4.09	1.3191
N4110273	0.145	0.20735	2.86	4.09	1.3105
N4110281	0.144	0.20592	2.87	4.10	1.2976
N4110282	0.143	0.20449	2.86	4.09	1.2933
N4110283	0.145	0.20735	2.86	4.09	1.3105
N4111291	0.144	0.20592	2.86	4.09	1.3019
N4111292	0.144	0.20592	2.86	4.09	1.3019
N4111293	0.143	0.20449	2.86	4.09	1.2933
N4111301	0.144	0.20592	2.86	4.09	1.3019
N4111302	0.147	0.21021	2.86	4.09	1.3277
N4111303	0.145	0.20735	2.85	4.08	1.3149
N4111311	0.144	0.20592	2.86	4.09	1.3019
N4111312	0.147	0.21021	2.86	4.09	1.3277
N4111313	0.146	0.20878	2.85	4.08	1.3235
N4111321	0.145	0.20735	2.85	4.08	1.3149
N4111322	0.145	0.20735	2.85	4.08	1.3149
N4111323	0.145	0.20735	2.85	4.08	1.3149
N4111331	0.145	0.20735	2.85	4.08	1.3149
N4111332	0.145	0.20735	2.85	4.08	1.3149
N4111333	0.144	0.20592	2.84	4.06	1.3106
N4111341	0.147	0.21021	2.86	4.09	1.3277
N4111342	0.146	0.20878	2.85	4.08	1.3235
N4111343	0.146	0.20878	2.85	4.08	1.3235
N4111351	0.145	0.20735	2.85	4.08	1.3149
N4111352	0.145	0.20735	2.85	4.08	1.3149
N4111353	0.145	0.20735	2.85	4.08	1.3149
N4111354	0.146	0.20878	2.85	4.08	1.3235
N4111361	0.146	0.20878	2.85	4.08	1.3235
N4111362	0.147	0.21021	2.85	4.08	1.3321
N4111363	0.145	0.20735	2.85	4.08	1.3149
N4111371	0.147	0.21021	2.85	4.08	1.3321
N4111372	0.146	0.20878	2.85	4.08	1.3235
N4111373	0.146	0.20878	2.85	4.08	1.3235
N4111381	0.146	0.20878	2.86	4.09	1.3191
N4111382	0.146	0.20878	2.86	4.09	1.3191
N4111383	0.146	0.20878	2.86	4.09	1.3191
N4111391	0.146	0.20878	2.86	4.09	1.3191
N4111392	0.146	0.20878	2.86	4.09	1.3191
N4111393	0.146	0.20878	2.85	4.08	1.3235
N4112401	0.481	0.68783	2.52	3.60	4.3530
N4112402	0.481	0.68783	2.52	3.60	4.3530
N4112403	0.482	0.68926	2.51	3.59	4.3752

Table V-5. (cont.) Calibration data for NO (g) gas species during combustion.

Method Used:	5	PMT Voltage:	825
O2 to O3:	30 ml/min	Furnace Temperature:	1100° C
O2 to pyro:	365 ml/min	Gain Setting:	HI
O2 to inlet:	20 ml/min	Gain Factor:	X1
He to inlet:	145 ml/min	Residence Time:	3 min
Nitrogen Species:	9424 ppm NO	Matrix:	He
Carrier gas:	He(g)	Gas box carrier flow:	0.220 lpm

Sample #	Sample ID	Sample Vol/Mass (μ l)	Flow (lpm) NO in He	Flow (lpm) He	Known N Mass (μ g)	Response Counts	CDA Sum Response
N4099171	100 ppm N	5000	0.056	4.204	0.3570	15718	27.368
N4099172	100 ppm N	5000	0.056	4.204	0.3570	14915	26.1962
N4099173	100 ppm N	5000	0.056	4.204	0.3570	15511	27.1728
N4099181	500 ppm N	5000	0.304	3.861	1.9823	89205	157.9104
N4099182	500 ppm N	5000	0.303	3.861	1.9763	89796	158.9844
N4099183	500 ppm N	5000	0.304	3.861	1.9823	90618	160.6198
N4099211	1000 ppm N	5000	0.677	3.318	4.6028	161690	338.1597
N4099212	1000 ppm N	5000	0.676	3.318	4.5972	162808	340.8448
N4099213	1000 ppm N	5000	0.678	3.318	4.6085	162673	340.6984

Summarized Data	Ave. Counts	n	SD	RSD (%)
100 ppm N	15382	3	417	2.71
500 ppm N	89873	3	710	0.79
1000 ppm N	162390	3	610	0.38

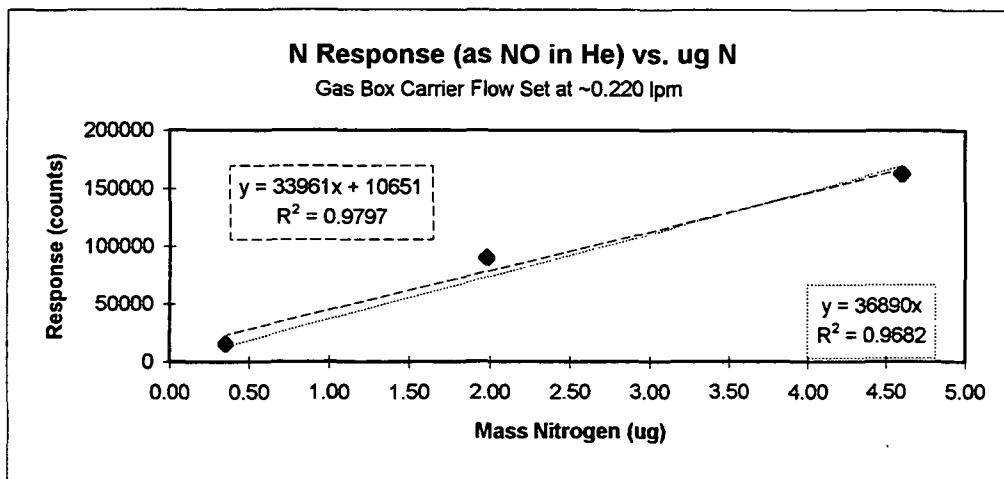


Table V-5. (cont.) Calibration data for NO (g) gas species during combustion.

Method Used:	5	PMT Voltage:	825
O2 to O3:	30 ml/min	Furnace Temperature:	1100° C
O2 to pyro:	365 ml/min	Gain Setting:	HI
O2 to inlet:	20 ml/min	Gain Factor:	X1
He to inlet:	145 ml/min	Residence Time:	3 min
Nitrogen Species:	9424 ppm NO	Matrix:	He(g)
Carrier gas:	He(g)	Gas box carrier flow:	0.025 lpm

Sample #	Sample ID	Sample Vol. (μ l)	Flow (lpm) NO in He	Flow (lpm) He	Known N Mass (μ g)	Response Counts	CDA Sum Response
N4097011	100 ppm N	5000	0.057	4.204	0.3633	10044	16.2629
N4097012	100 ppm N	5000	0.056	4.204	0.3570	9414	15.3343
N4097013	100 ppm N	5000	0.056	4.204	0.3570	9551	15.4071
N4097021	250 ppm N	5000	0.145	4.090	0.9299	32353	55.787
N4097022	250 ppm N	5000	0.146	4.090	0.9361	33657	57.6422
N4097023	250 ppm N	5000	0.146	4.090	0.9361	33665	57.8136
N4097031	500 ppm N	5000	0.304	3.861	1.9823	77224	134.5446
N4097032	500 ppm N	5000	0.304	3.861	1.9823	77649	134.9841
N4097033	500 ppm N	5000	0.304	3.861	1.9823	77683	135.2291
N4097041	750 ppm N	5000	0.480	3.604	3.1923	129075	226.6333
N4097042	750 ppm N	5000	0.482	3.604	3.2041	128221	224.974
N4097043	750 ppm N	5000	0.480	3.604	3.1923	126192	221.2391
N4097044	750 ppm N	5000	0.481	3.604	3.1982	129416	226.7074
N4097051	1000 ppm N	5000	0.677	3.318	4.6028	182668	321.7507
N4097052	1000 ppm N	5000	0.677	3.318	4.6028	--	331.7605
N4097053	1000 ppm N	5000	0.675	3.318	4.5915	187743	330.4666
N4097054	1000 ppm N	5000	0.677	3.318	4.6028	185690	326.9513

Summarized Data	Ave. Counts	n	SD	RSD (%)
100 ppm N	9670	3	331	3.43
250 ppm N	33225	3	755	2.27
500 ppm N	77519	3	256	0.33
750 ppm N	128226	3	1446	1.13
1000 ppm N	185367	3	2553	1.38

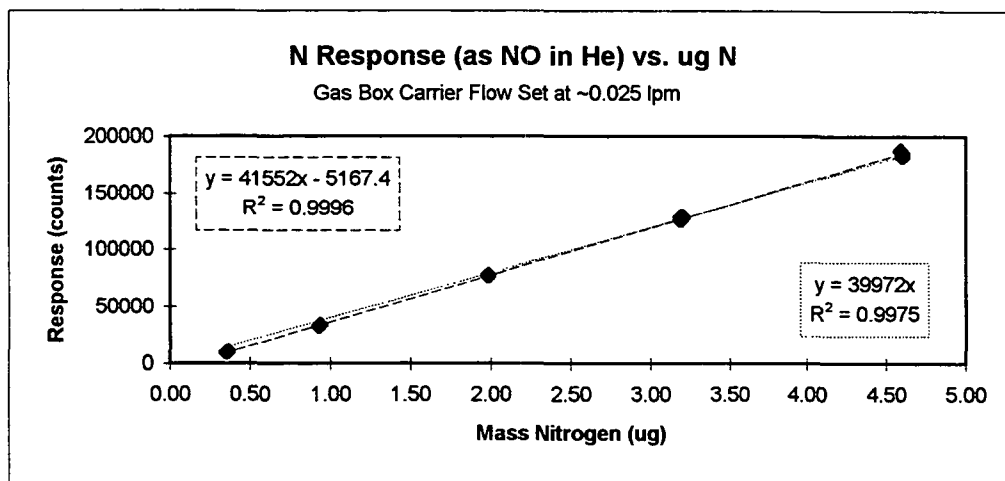


Table V-5. (cont.) Calibration data for NO (g) gas species during combustion.

Method Used:	5	PMT Voltage:	825
O2 to O3:	30 ml/min	Furnace Temperature:	1100° C
O2 to pyro:	365 ml/min	Gain Setting:	HI
O2 to inlet:	20 ml/min	Gain Factor:	X1
He to inlet:	145 ml/min	Residence Time:	3 min
Nitrogen Species:	9424 ppm NO	Matrix:	He
Carrier gas:	He(g)	Gas box carrier flow:	0.095 lpm

Sample #	Sample ID	Sample Vol/Ma: (ul)	Flow (lpm) NO in He	Flow (lpm) He	Known N Mass (ug)	Response Counts	CDA Sum Response
N4098161	100 ppm N	5000	0.056	4.2042	0.3570	14465	25.1709
N4098162	100 ppm N	5000	0.056	4.2042	0.3570	14503	25.2685
N4098163	100 ppm N	5000	0.056	4.2042	0.3570	14813	25.7811
N4099191	500 ppm N	5000	0.304	3.861	1.9823	89220	157.9105
N4099192	500 ppm N	5000	0.304	3.861	1.9823	89337	158.1786
N4099193	500 ppm N	5000	0.305	3.861	1.9883	88688	157.1044
N4099201	1000 ppm N	5000	0.677	3.3176	4.6028	199788	357.9831
N4099202	1000 ppm N	5000	0.678	3.3176	4.6085	199408	357.7594
N4099203	1000 ppm N	5000	0.676	3.3176	4.5972	200936	360.1317

Summarized Data	Ave. Counts	n	SD	RSD (%)
100 ppm N	14594	3	191	1.31
500 ppm N	89083	3	346	0.39
1000 ppm N	200044	3	795	0.40

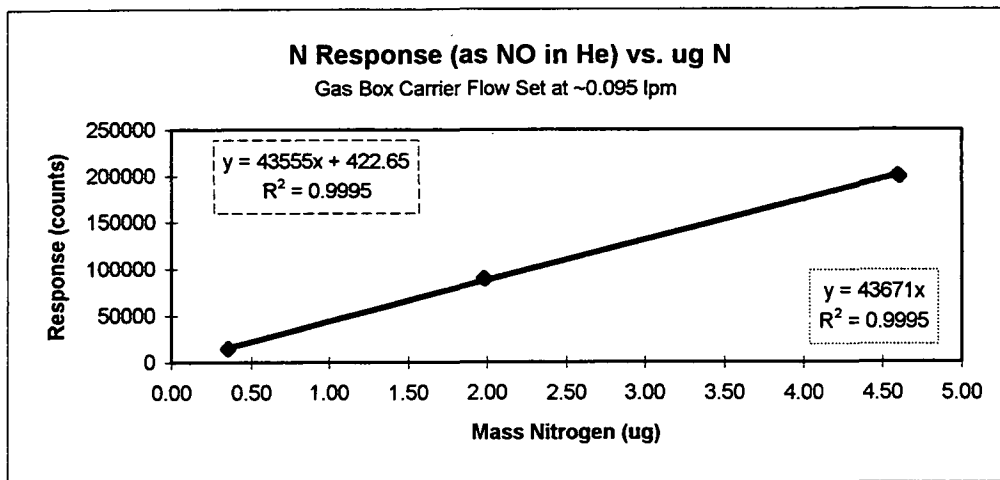


Table V-5. (cont.) Calibration data for NO (g) gas species during combustion.

Method Used:	5	PMT Voltage:	825
O2 to O3:	30 ml/min	Furnace Temperature:	1100° C
O2 to pyro:	365 ml/min	Gain Setting:	HI
O2 to inlet:	20 ml/min	Gain Factor:	X1
He to inlet:	145 ml/min	Residence Time:	3 min
Nitrogen Species:	9600 ppm NO	Matrix:	He
Carrier gas:	He(g)	Gas box carrier flow:	0.025 lpm

<u>Sample #</u>	<u>Sample ID</u>	<u>Sample Vol/Mass</u> <u>(μl)</u>	<u>Flow (lpm)</u> <u>NO in He</u>	<u>Flow (lpm)</u> <u>He</u>	<u>Known N</u> <u>Mass (μg)</u>	<u>Response</u> <u>Counts</u>	<u>CDA Sum</u> <u>Response</u>
4264-2211	10 ppm N	5000	0.014	2.99	0.1080	1	--
4264-2212	10 ppm N	5000	0.014	2.99	0.1080	1	--
4264-2213	10 ppm N	5000	0.014	2.98	0.1080	1	--
4264-2221	50 ppm N	5000	0.068	2.93	0.5256	9209	--
4264-2222	50 ppm N	5000	0.068	2.93	0.5256	9738	--
4264-2223	50 ppm N	5000	0.068	2.93	0.5256	9391	--
4264-2231	100 ppm N	5000	0.131	2.88	1.0083	27895	--
4264-2232	100 ppm N	5000	0.131	2.87	1.0116	28238	--
4264-2233	100 ppm N	5000	0.131	2.87	1.0116	26805	--
4264-2241	500 ppm N	5000	0.555	2.44	4.2944	160873	--
4264-2242	500 ppm N	5000	0.557	2.44	4.3070	162676	--
4264-2243	500 ppm N	5000	0.555	2.44	4.2944	161640	--
4264-2251	1000 ppm N	5000	0.94	2.06	7.2613	287752	--
4264-2252	1000 ppm N	5000	0.939	2.06	7.2560	285466	--
4264-2253	1000 ppm N	5000	0.939	2.06	7.2560	284023	--
<u>Summarized Data</u>		<u>Ave. Counts</u>	<u>n</u>	<u>SD</u>	<u>RSD (%)</u>		
10 ppm N		1	3	59	59.5		
50 ppm N		9446	3	269	2.85		
100 ppm N		27646	3	478	2.71		
500 ppm N		161396	3	1114	0.69		
1000 ppm N		285747	3	1880	0.66		

Table V-6. Calibration data for nitrogen as proline during combustion.

Method Used:	5	PMT Voltage:	825
O2 to O3:	30 ml/min	Furnace Temperature:	1100C
O2 to pyro:	365 ml/min	Gain Setting:	HI
O2 to inlet:	20 ml/min	Gain Factor:	X1
He to inlet:	145 ml/min	Residence Time:	3 min
Nitrogen Species:	Proline	Matrix:	d,d-H2O

Sample #	Sample ID	Sample Vol (μ l)	Known N Mass (μ g)	Response Counts	CDA Sum Response
N4091051	~100 ppm N	5	0.526	9606	16.7482
N4091052	~100 ppm N	5	0.526	9036	15.8201
N4091053	~100 ppm N	5	0.526	8068	13.8429
N4091054	~100 ppm N	5	0.526	11564	20.1658
N4091055	~100 ppm N	5	0.526	8328	14.3557
N4091061	~250 ppm N	5	1.265	22656	39.9169
N4091062	~250 ppm N	5	1.265	11183**	19.4581
N4091063	~250 ppm N	5	1.265	23110	40.5514
N4091064	~250 ppm N	5	1.265	23943	41.9679
N4091071	~750 ppm N	5	3.789	46154	81.3231
N4091072	~750 ppm N	5	3.789	30409**	53.6375
N4091073	~750 ppm N	5	3.789	48030	84.7651
N4091074	~750 ppm N	5	3.789	46010	81.1281
N4091081	~1000 ppm N	5	4.954	34268	60.3025
N4091082	~1000 ppm N	5	4.954	27015	47.4367
N4091083	~1000 ppm N	5	4.954	35758	63.0125
N4091084	~1000 ppm N	5	4.954	42038	74.1454
N4091085	~1000 ppm N	5	4.954	46774	82.4652
N4092091	~500 ppm N	5	2.564	29297	51.538
N4092092	~500 ppm N	5	2.564	33279	58.4962
N4092093	~500 ppm N	5	2.564	31189	54.8827
N4092094	~500 ppm N	5	2.564	30552	53.8574

*The sample # is the same as the Computer Data Acquisition filename. The N identifies it as a nitrogen data file. The 4 represents the lab book #4264. The next three digits are the page number for the data and the last three digits are the sample number on that page.

**Data was thrown out experimentally or statistically thrown out according to the Q-test.

Summarized Data	Ave. Counts	n	SD	RSD (%)
~100 ppm N	9320	5	1392	14.9
~250 ppm N	23236	3	653	2.81
~500 ppm N	31079	4	1664	5.4
~750 ppm N	46731	3	1127	2.41
~1000 ppm N	37171	5	4457	20.4

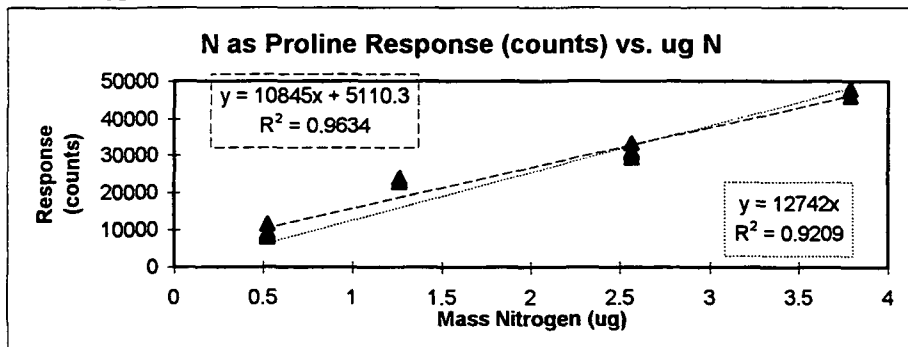


Table V-7. Calibration data for nitrogen as pyrazine during combustion.

Method Used:	5	PMT Voltage:	825
O2 to O3:	30 ml/min	Furnace Temperature:	1100° C
O2 to pyro:	365 ml/min	Gain Setting:	HI
O2 to inlet:	20 ml/min	Gain Factor:	X1
He to inlet:	145 ml/min	Residence Time:	3 min
Nitrogen Species:	pyrazine	Matrix:	d,d-H2O

Sample #	Sample ID	Sample Vol (µl)	Known N Mass (µg)	Response Counts	CDA Sum Response
N4075041	~500 ppm N	5	2.4857	52373	92.7487
N4075042	~500 ppm N	5	2.4857	52778	93.701
N4075043	~500 ppm N	5	2.4857	52322	92.7244
N4075012	~50 ppm N	5	0.2538	5088	9.1794
N4075013	~50 ppm N	5	0.2538	5104	9.2283
N4075014	~50 ppm N	5	0.2538	5002	8.8866
N4075021	~750 ppm N	5	3.947	75833	134.8632
N4075022	~750 ppm N	5	3.947	76392	135.6443
N4075023	~750 ppm N	5	3.947	72406	128.5159
N4075091	~1000 ppm N	5	5.0762	85443	151.6845
N4075092	~1000 ppm N	5	5.0762	90565	160.9617
N4075093	~1000 ppm N	5	5.0762	86991	154.077
N4075031	~100 ppm N	5	0.5076	11356	20.0441
N4075032	~100 ppm N	5	0.5076	11348	19.9953
N4075033	~100 ppm N	5	0.5076	11363	20.1902

Summarized Data	Ave. Counts	n	SD	RSD (%)
~50 ppm N	5065	3	55	1.08
~100 ppm N	11356	3	7.8	0.07
~500 ppm N	52491	3	250	0.48
~750 ppm N	74877	3	2158	2.88
~1000 ppm N	87667	3	2627	3.0

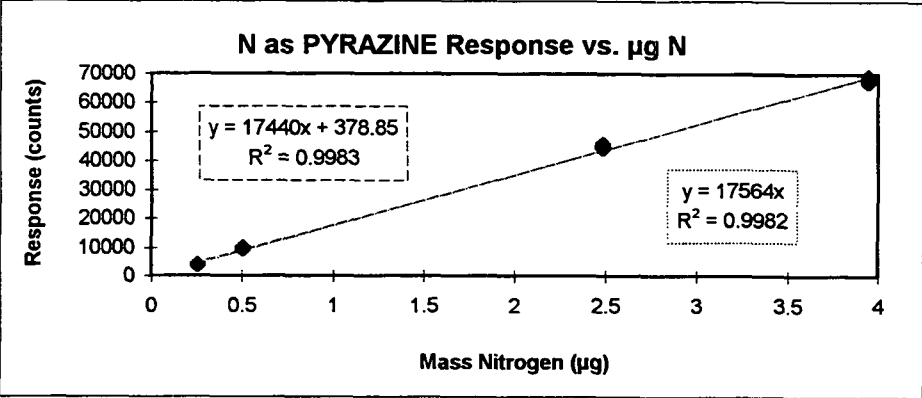


Table V-8. Calibration data for nitrogen as glutamic acid during combustion.

Method Used:	5	PMT Voltage:	825
O2 to O3:	30 ml/min	Furnace Temperature:	1100° C
O2 to pyro:	365 ml/min	Gain Setting:	HI
O2 to inlet:	20 ml/min	Gain Factor:	X1
He to inlet:	145 ml/min	Residence Time:	3 min
Nitrogen Species:	glutamic acid	Matrix:	d,d-H2O

Sample #	Sample ID	Sample Vol (ul)	Known N Mass (ug)	Response Counts	CDA Sum Response
N4075061	~500 ppm N	5	2.4791	36938	65.5763
N4075062	~500 ppm N	5	2.4791	35907	63.6962
N4075063	~500 ppm N	5	2.4791	36257	64.0135
N4075081	~100 ppm N	5	0.4953	9159	16.0643
N4075082	~100 ppm N	5	0.4953	9562	16.943
N4075083	~100 ppm N	5	0.4953	9407	16.5282
N4075051	~50 ppm N	5	0.2564	4509	8.0809
N4075052	~50 ppm N	5	0.2564	4274	7.7149
N4075053	~50 ppm N	5	0.2564	4211	7.422

Summarized Data	Ave. Counts	n	SD	RSD (%)
~50 ppm N	3950	3	542	13.7
~100 ppm N	9118	3	83	0.9
~500 ppm N	31679	4	3881	12.3
~750 ppm N	42433	4	2324	5.5

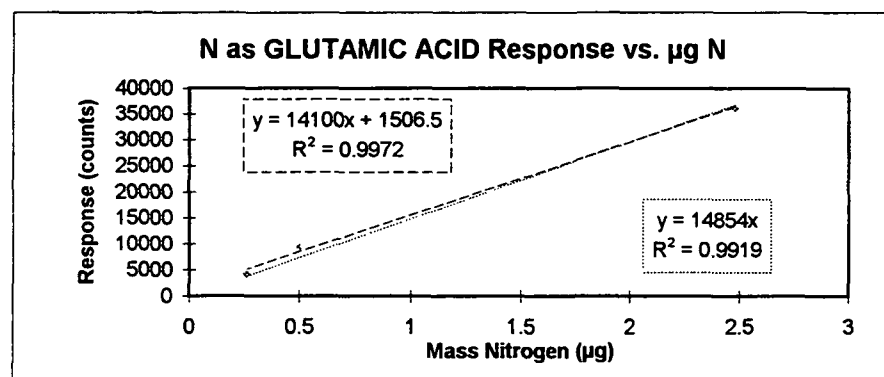


Table V-8. (cont.) Calibration data for combustion of glutamic acid.

Method Used:	5	PMT Voltage:	825
O2 to O3:	30 ml/min	Furnace Temperature:	1100° C
O2 to pyro:	365 ml/min	Gain Setting:	HI
O2 to inlet:	20 ml/min	Gain Factor:	X1
He to inlet:	145 ml/min	Residence Time:	3 min
Nitrogen Species:	Glutamic Acid	Matrix:	H2O

Sample #*	Sample ID	Sample Vol (μ l)	Known N Mass (μ g)	Response Counts	CDA Sum Response
N4106011	~50 ppm N	5	0.2564	4871	8.4961
N4106012	~50 ppm N	5	0.2564	4928	8.6669
N4106013	~50 ppm N	5	0.2564	4805	8.4471
N4106021	~500 ppm N	5	2.4791	32662**	57.7877
N4106022	~500 ppm N	5	2.4791	40663	72.2166
N4106023	~500 ppm N	5	2.4791	39811	70.5808
N4106024	~500 ppm N	5	2.4791	38541	68.3594
N4106031	~100 ppm N	5	0.4953	9782	17.2119
N4106032	~100 ppm N	5	0.4953	10218	18.0665
N4106033	~100 ppm N	5	0.4953	10183	18.0176
N4106041	~750 ppm N	5	3.7375	37744	66.9434
N4106042	~750 ppm N	5	3.7375	38067	67.4069
N4106043	~750 ppm N	5	3.7375	37721	66.9922
N4106071	~100 ppm N	5	0.4953	9884	17.2851
N4106072	~100 ppm N	5	0.4953	10047	17.9198
N4106073	~100 ppm N	5	0.4953	9604	16.9922

*The sample # is the same as the Computer Data Acquisition filename. The N identifies it as a nitrogen data file.

The 4 represents the lab book #4264. The next three digits are the page number for the data and the last three digits are the sample number on that page.

**These data are not used in the summary calculations as they are known to be in error experimentally or can be statistically thrown out.

Summarized Data	Ave. Counts	n	SD	RSD (%)
~50 ppm N	4867.5	3	60.3	1.24
~100 ppm N	9953	6	240	2.41
~500 ppm N	39672	3	1068	2.69
~750 ppm N	37844	3	194	0.51

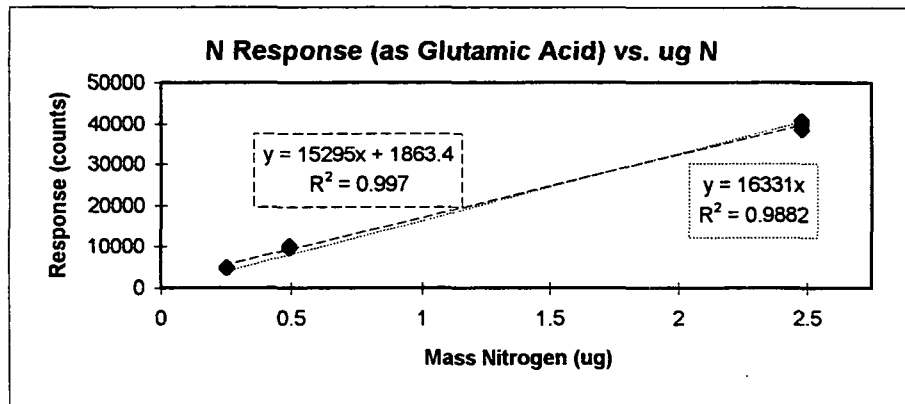


Table V-9. Calibration data for nitrogen as tryptophan during combustion.

Method Used:	5	PMT Voltage:	825
O2 to O3:	30 ml/min	Furnace Temperature:	1100° C
O2 to pyro:	365 ml/min	Gain Setting:	HI
O2 to inlet:	20 ml/min	Gain Factor:	X1
He to inlet:	145 ml/min	Residence Time:	3 min
Nitrogen Species:	TRYPTOPHAN	Matrix:	d,d-H2O

Sample #	Sample ID	Sample Vol (μl)	Known N Mass (μg)	Response Counts	CDA Sum Response
N4075071	~750 ppm N	5	3.7696	72557	128.5153
N4075072	~750 ppm N	5	3.7696	72298	128.0271
N4075073	~750 ppm N	5	3.7696	72552	128.4905
N4075101	100	5	0.5066	8778	15.747
N4075102	100	5	0.5066	8401	15.0384
N4075103	100	5	0.5066	9731	17.1142
N4075104	100	5	0.5066	7702	13.6228
N4076121	50	5	0.2365	2600	4.6874
N4076122	50	5	0.2365	2993	5.3223
N4076123	50	5	0.2365	2970	5.1758
N4076111	500	5	2.4801	42929	75.852
N4076112	500	5	2.4801	42957	75.9967
N4076113	500	5	2.4801	45388	80.1504

Summarized Data	Ave. Counts	n	SD	RSD (%)
~50 ppm N	2855	3	221	7.73
~100 ppm N	8653	5	846	9.77
~500 ppm N	43758	3	1412	3.23
~750 ppm N	72469.2	3	148	0.2

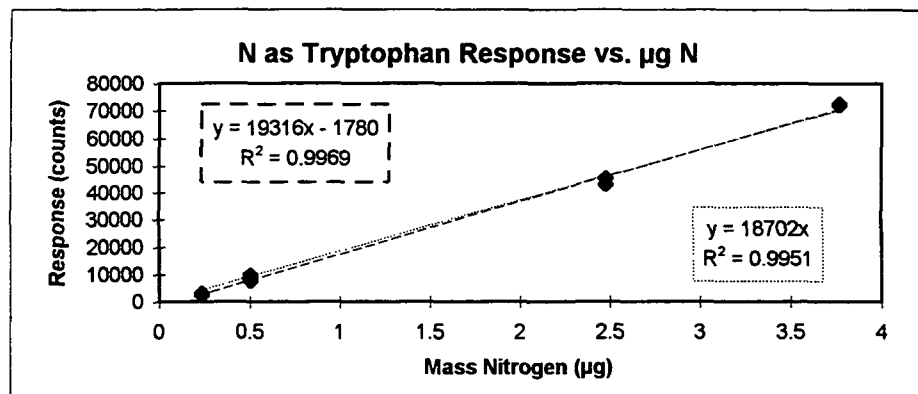


Table V-10. Calibration data for nitrogen (as ammonium nitrate) during combustion.

Method Used:	5	PMT Voltage:	825
O2 to O3:	30 ml/min	Furnace Temperature:	1100 ° C
O2 to pyro:	365 ml/min	Gain Setting:	HI
O2 to inlet:	20 ml/min	Gain Factor:	X1
He to inlet:	145 ml/min	Residence Time:	3 min
Nitrogen Species:	NH4NO3	Matrix:	d,d-H2O

<u>Sample #</u>	<u>Sample ID</u>	<u>Sample Vol</u> <u>(μl)</u>	<u>Known N</u> <u>Mass (μg)</u>	<u>Response</u> <u>Counts</u>	<u>CDA Sum</u> <u>Response</u>
N4076171	~750 ppm N	5	3.6329	66548	118.2368
N4076172	~750	5	3.6329	66526	118.1148
N4076173	~750	5	3.6329	66646	118.286
N4076161	~50	5	0.2379	3352	6.079
N4076162	~50	5	0.2379	2948	4.1502
N4076163	~50	5	0.2379	2882	5.1996
N4076164	~50	5	0.2379	2447	4.2968
N4076151	~100	5	0.5545	10350	18.3592
N4076152	~100	5	0.5545	10473	18.5544
N4076153	~100	5	0.5545	10302	18.2618
N4076141	~1000	5	5.5815	92114	163.279
N4076142	~1000	5	5.5815	93188	165.0862
N4076143	~1000	5	5.5815	94944	168.4548
N4076131	~500	5	2.4925	46852	—
N4076132	~500	5	2.4925	47325	84.3017
N4076133	~500	5	2.4925	47484	84.1309

<u>Summarized Data</u>	<u>Ave. Counts</u>	<u>n</u>	<u>SD</u>	<u>RSD (%)</u>
~50 ppm N	2907	4	371	12.7
~100 ppm N	10375	3	88	0.85
~500 ppm N	47220	3	329	0.7
~750 ppm N	66573	3	64	0.1
~1000 ppm N	93415	3	1429	1.53

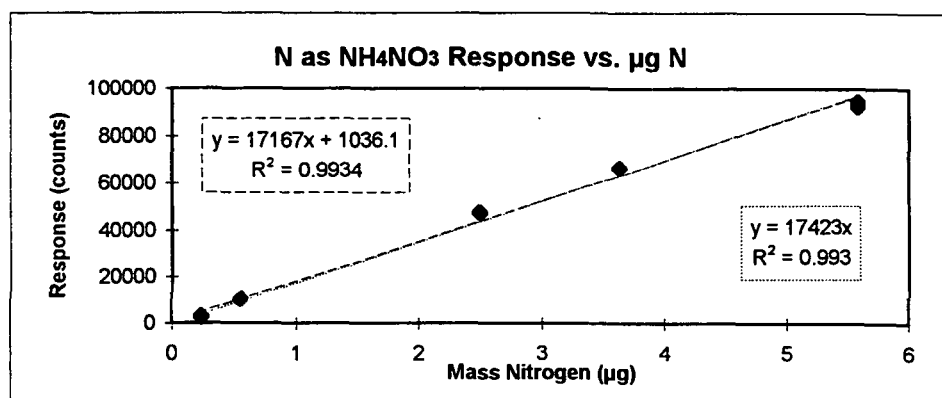


Table V-11. Calibration data for nitrogen as ammonium sulfate during combustion.

Method Used:	5	PMT Voltage:	825
O2 to O3:	30 ml/min	Furnace Temperature:	1100° C
O2 to pyro:	365 ml/min	Gain Setting:	HI
O2 to inlet:	20 ml/min	Gain Factor:	X1
He to inlet:	145 ml/min	Residence Time:	3 min
Nitrogen Species:	(NH ₄) ₂ SO ₄	Matrix:	d,d-H ₂ O

Sample #	Sample ID	Sample Vol (μ l)	Known N Mass (μ g)	Response Counts	CDA Sum Response
N4076191	~1000 ppm N	5	4.9934	49597	88.1591
N4076192	~1000 ppm N	5	4.9934	44651	79.1745
N4076193	~1000 ppm N	5	4.9934	60142	106.8604
N4076194	~1000 ppm N	5	4.9934	58148	103.1736
N4076195	~1000 ppm N	5	4.9934	57697	102.3924
N4077221	~100 ppm N	5	0.4831	8756	15.4297
N4077222	~100 ppm N	5	0.4831	8774	15.503
N4077223	~100 ppm N	5	0.4831	8607	15.21
N4076181	~50 ppm N	5	0.2267	4057	7.5927
N4076182	~50 ppm N	5	0.2267	3460	6.8361
N4076183	~50 ppm N	5	0.2267	3563	6.445
N4076184	~50 ppm N	5	0.2267	3593	6.4695
N4077211	~750 ppm N	5	3.7618	46509	82.251
N4077212	~750 ppm N	5	3.7618	48311	82.3483
N4077213	~750 ppm N	5	3.7618	46486	85.6204
N4076201	~500 ppm N	5	2.4655	34145	60.3758
N4076202	~500 ppm N	5	2.4655	35331	62.5487
N4076203	~500 ppm N	5	2.4655	35629	62.9641

Summarized Data	Ave. Counts	n	SD	RSD (%)
~50 ppm N	3743	4	226	6.05
~100 ppm N	8712	3	92	1.05
~500 ppm N	35035	3	785	2.24
~750 ppm N	47102	3	1047	2.22
~1000 ppm N	54047	5	6621	12.25

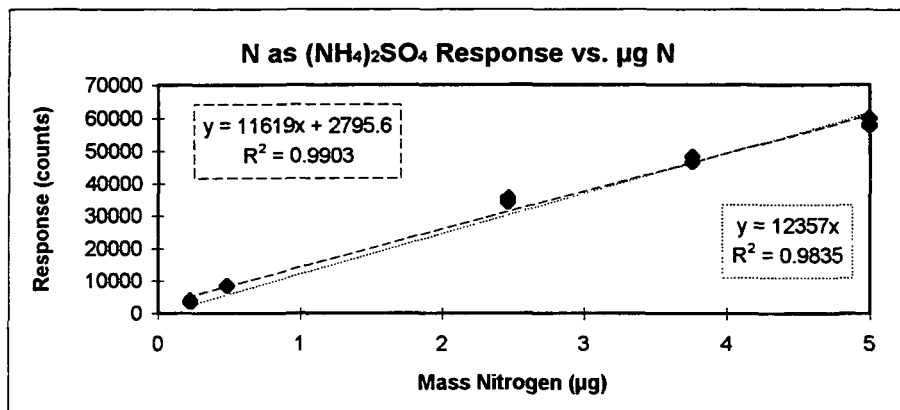


Table V-11. Calibration data for nitrogen (as ammonium sulfate) during combustion.

Method Used:	5	PMT Voltage:	825
O2 to O3:	30 ml/min	Furnace Temperature:	1100° C
O2 to pyro:	365 ml/min	Gain Setting:	HI
O2 to inlet:	20 ml/min	Gain Factor:	X1
He to inlet:	145 ml/min	Residence Time:	3 min
Nitrogen Species:	(NH ₄) ₂ SO ₄	Matrix:	d,d-H ₂ O

<u>Sample #</u>	<u>Sample ID</u>	<u>Sample Vol</u> <u>(μl)</u>	<u>Known N</u> <u>Mass (μg)</u>	<u>Response</u> <u>Counts</u>	<u>CDA Sum</u> <u>Response</u>
N4076191	~1000 ppm N	5	4.9934	49597	88.1591
N4076192	~1000 ppm N	5	4.9934	44651	79.1745
N4076193	~1000 ppm N	5	4.9934	60142	106.8604
N4076194	~1000 ppm N	5	4.9934	58148	103.1736
N4076195	~1000 ppm N	5	4.9934	57697	102.3924
N4077221	~100 ppm N	5	0.4831	8756	15.4297
N4077222	~100 ppm N	5	0.4831	8774	15.503
N4077223	~100 ppm N	5	0.4831	8607	15.21
N4076181	~50 ppm N	5	0.2267	4057	7.5927
N4076182	~50 ppm N	5	0.2267	3460	6.8361
N4076183	~50 ppm N	5	0.2267	3563	6.445
N4076184	~50 ppm N	5	0.2267	3593	6.4695
N4077211	~750 ppm N	5	3.7618	46509	82.251
N4077212	~750 ppm N	5	3.7618	48311	82.3483
N4077213	~750 ppm N	5	3.7618	46486	85.6204
N4076201	~500 ppm N	5	2.4655	34145	60.3758
N4076202	~500 ppm N	5	2.4655	35331	62.5487
N4076203	~500 ppm N	5	2.4655	35629	62.9641

<u>Summarized Data</u>	<u>Ave. Counts</u>	<u>n</u>	<u>SD</u>	<u>RSD (%)</u>
~50 ppm N	3743	4	226	6.05
~100 ppm N	8712	3	92	1.05
~500 ppm N	35035	3	785	2.24
~750 ppm N	47102	3	1047	2.22
~1000 ppm N	54047	5	6621	12.25

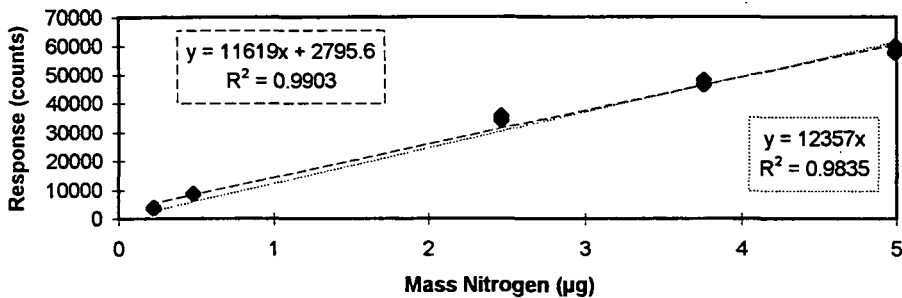
N as (NH₄)₂SO₄ Response vs. μg N

Table V-12. Calibration data for nitrogen as ammonium chloride during combustion.

Method Used:	5	PMT Voltage:	825
O2 to O3:	30 ml/min	Furnace Temperature:	1100° C
O2 to pyro:	365 ml/min	Gain Setting:	HI
O2 to inlet:	20 ml/min	Gain Factor:	X1
He to inlet:	145 ml/min	Residence Time:	3 min
Nitrogen Species:	NH4Cl	Matrix:	d,d-H2O

<u>Sample #</u>	<u>Sample ID</u>	<u>Sample Vol (μl)</u>	<u>Known N Mass (μg)</u>	<u>Response Counts</u>	<u>CDA Sum Response</u>
N4077271	~100 ppm N	5	0.5098	7698	13.5985
N4077272	~100	5	0.5098	9523	16.6991
N4077273	~100	5	0.5098	9074	15.9669
N4077274	~100	5	0.5098	9191	16.0645
N4077261	~1000	5	5.098	42831	75.8546
N4077262	~1000	5	5.098	50719	89.8683
N4077263	~1000	5	5.098	43724	77.5148
N4077264	~1000	5	5.098	43135	--
N4077251	~750 ppm N	5	3.7832	45208	79.9557
N4077252	~750	5	3.7832	47276	83.7402
N4077253	~750	5	3.7832	50150	88.8914
N4077254	~750	5	3.7832	51161	90.6737
N4077231	~50	5	0.2549	3941	6.958
N4077232	~50	5	0.2549	4231	7.4704
N4077233	~50	5	0.2549	4110	7.202
N4077241	~500	5	2.549	33938	59.9365
N4077242	~500	5	2.549	33161	58.789
N4077243	~500	5	2.549	26933	47.6323
N4077244	~500	5	2.549	27232	--

<u>Summarized Data</u>	<u>Ave. Counts</u>	<u>n</u>	<u>SD</u>	<u>RSD (%)</u>
~50 ppm N	4094	3	146	3.56
~100 ppm N	8872	4	805	9.08
~500 ppm N	30316	4	3749	12.37
~750 ppm N	48449	4	2716	5.61
~1000 ppm N	43230	3	454	1.05

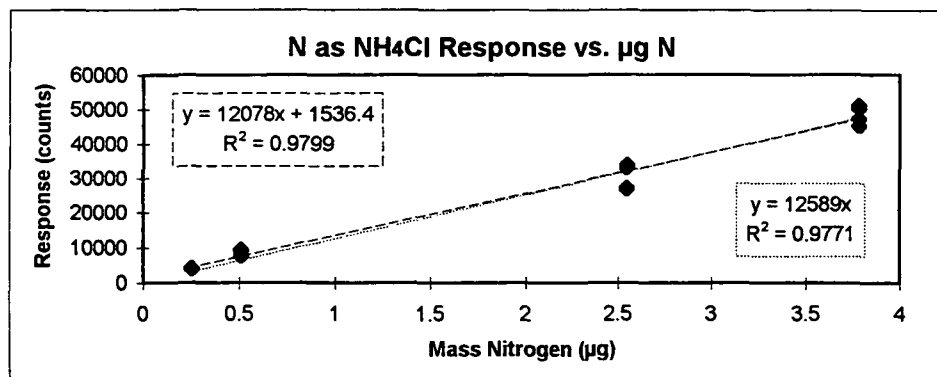


Table V-13. Calibration data for combustion of glutamic acid in 0.2N NaOH.

Method Used:	5	PMT Voltage:	825
O2 to O3:	30 ml/min	Furnace Temperature:	1100° C
O2 to pyro:	365 ml/min	Gain Setting:	HI
O2 to inlet:	20 ml/min	Gain Factor:	X1
He to inlet:	145 ml/min	Residence Time:	3 min
Nitrogen Species:	glutamic acid	Matrix:	0.2N NaOH

<u>Sample #</u>	<u>Sample ID</u>	<u>Sample Vol</u> <u>(μl)</u>	<u>Known N</u> <u>Mass (μg)</u>	<u>Response</u> <u>Counts</u>	<u>CDA Sum</u> <u>Response</u>
N4083081	499.16 ppm N	5	2.4958	31237	55.1747
N4083082	499.16 ppm N	5	2.4958	30130	52.9529
N4083083	499.16 ppm N	5	2.4958	29685	52.0009
N4084121	53.95 ppm N	5	0.26975	1415	2.4644
N4084122	53.95 ppm N	5	0.26975	1598	2.6841
N4084123	53.95 ppm N	5	0.26975	1953	3.2457
N4084124	53.95 ppm N	5	0.26975	1528	--
N4084131	104.95 ppm N	5	0.52475	7057	12.3047
N4084132	104.95 ppm N	5	0.52475	6127	10.7658
N4084133	104.95 ppm N	5	0.52475	5654	9.7407

<u>Summarized Data</u>	<u>Ave. Counts</u>	<u>n</u>	<u>SD</u>	<u>RSD (%)</u>
53.95 ppm N	1624	4	232	14.31
104.95 ppm N	6280	3	713.6	11.36
499.16 ppm N	30351	3	799	2.63

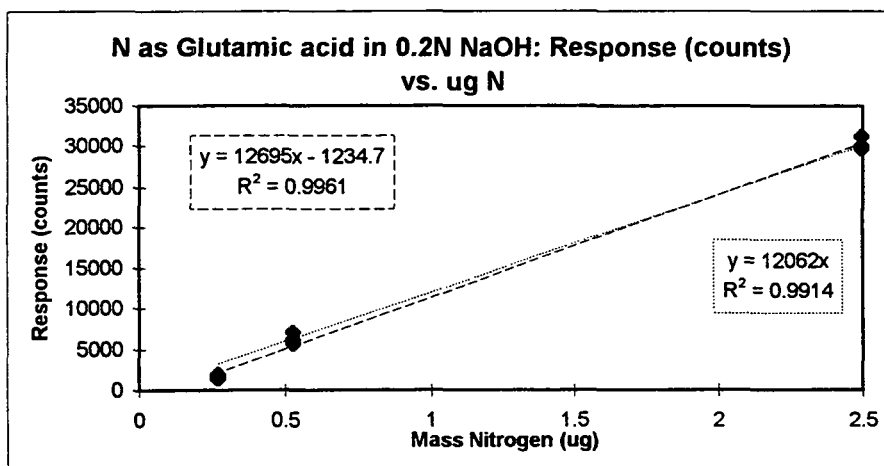


Table V-14. Calibration data for combustion of glutamic acid in 0.2N Na₂SO₄.

Method Used:	5	PMT Voltage:	825
O ₂ to O ₃ :	30 ml/min	Furnace Temperature:	1100° C
O ₂ to pyro:	365 ml/min	Gain Setting:	HI
O ₂ to inlet:	20 ml/min	Gain Factor:	X1
He to inlet:	145 ml/min	Residence Time:	3 min
Nitrogen Species:	glutamic acid	Matrix:	0.2N Na ₂ SO ₄

<u>Sample #</u>	<u>Sample ID</u>	<u>Sample Vol</u> <u>(μl)</u>	<u>Known N</u> <u>Mass (μg)</u>	<u>Response</u> <u>Counts</u>	<u>CDA Sum</u> <u>Response</u>
N4083071	48.91 ppm N	5	0.2445	3475	6.0053
N4083072	48.91 ppm N	5	0.2445	3504	6.0785
N4083073	48.91 ppm N	5	0.2445	3547	6.2006
N4083091	502.39 ppm N	5	2.51195	40206	71.3133
N4083092	502.39 ppm N	5	2.51195	42157	74.3161
N4083093	502.39 ppm N	5	2.51195	36421	64.4043
N4083094	502.39 ppm N	5	2.51195	44323	78.2466
N4083101	101.72 ppm N	5	0.5086	9864	17.5048
N4083102	101.72 ppm N	5	0.5086	9629	16.8945
N4083103	101.72 ppm N	5	0.5086	10278	18.1884

<u>Summarized Data</u>	<u>Ave. Counts</u>	<u>n</u>	<u>SD</u>	<u>RSD (%)</u>
53.95 ppm N	1624	4	232	14.31
104.95 ppm N	6280	3	713.6	11.36
499.16 ppm N	30351	3	799	2.63

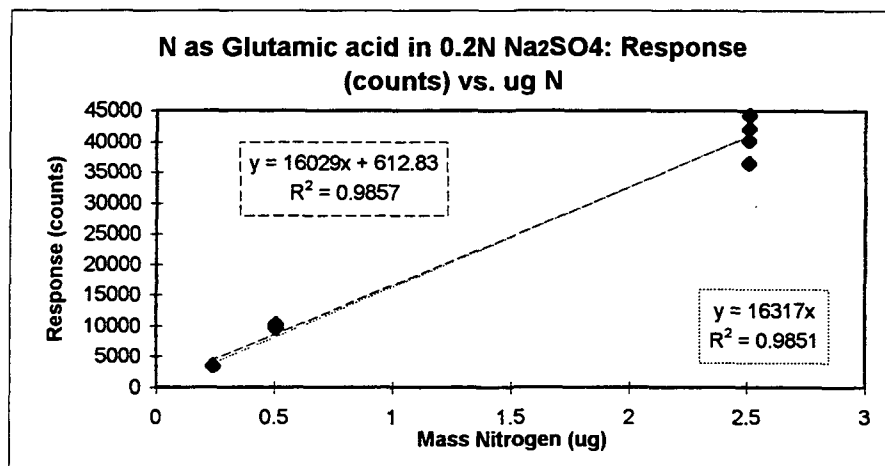


Table V-15. Calibration data for combustion of glutamic acid in 0.2N Na₂CO₃.

Method Used:	5	PMT Voltage:	825
O ₂ to O ₃ :	30 ml/min	Furnace Temperature:	1100° C
O ₂ to pyro:	365 ml/min	Gain Setting:	HI
O ₂ to inlet:	20 ml/min	Gain Factor:	X1
He to inlet:	145 ml/min	Residence Time:	3 min
Nitrogen Species:	glutamic acid	Matrix:	0.2N Na ₂ CO ₃

<u>Sample #</u>	<u>Sample ID</u>	<u>Sample Vol</u> (μ l)	<u>Known N</u> Mass (μ g)	<u>Response</u> Counts	<u>CDA Sum</u> Response
N4084111	508.67 ppm N	5	2.5434	31757	55.9813
N4084112	508.67 ppm N	5	2.5434	32268	57.2502
N4084113	508.67 ppm N	5	2.5434	31599	55.8346
N4084141	100.38 ppm N	5	0.5019	5705	--
N4084142	100.38 ppm N	5	0.5019	5831	10.1066
N4084143	100.38 ppm N	5	0.5019	5330	10.0336
N4084151	59.47 ppm N	5	0.2974	3275	5.8103
N4084152	59.47 ppm N	5	0.2974	3170	5.4441
N4084153	59.47 ppm N	5	0.2974	2901	4.9072

<u>Summarized Data</u>	<u>Ave. Counts</u>	<u>n</u>	<u>SD</u>	<u>RSD (%)</u>
59.47 ppm N	3115.5	3	193	6.18
100.38 ppm N	5789	3	73	1.25
508.67 ppm N	31875	3	349.7	1.1

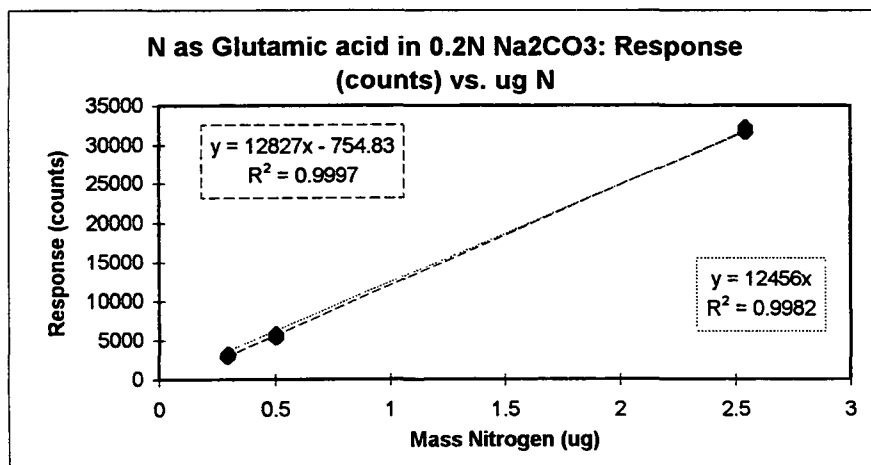


Table V-16. Calibration data for combustion of ammonium chloride in 0.1N Na₂CO₃.

Method Used:	5	PMT Voltage:	825
O ₂ to O ₃ :	30 ml/min	Furnace Temperature:	1100° C
O ₂ to pyro:	365 ml/min	Gain Setting:	HI
O ₂ to inlet:	20 ml/min	Gain Factor:	X1
He to inlet:	145 ml/min	Residence Time:	3 min
Nitrogen Species:	NH ₄ Cl	Matrix:	0.1N Na ₂ CO ₃

Sample #	Sample ID	Sample Vol (μ l)	Known N Mass (μ g)	Response Counts	CDA Sum Response
N4093241	~750 ppm N	5	3.810	55927	13.989
N4093242	~750 ppm N	5	3.810	57202	---
N4093243	~750 ppm N	5	3.810	58187	14.0871
N4094251	~100 ppm N	5	0.533	8057	33.4713
N4094252	~100 ppm N	5	0.533	8143	36.865
N4094253	~100 ppm N	5	0.533	8177	36.3278
N4094261	~250 ppm N	5	1.247	19120	37.7684
N4094262	~250 ppm N	5	1.247	21049	122.5099
N4094263	~250 ppm N	5	1.247	20751	123.462
N4094264	~250 ppm N	5	1.247	21508	129.6872
N4094271	~1000 ppm N	5	5.060	69253	130.4927
N4094272	~1000 ppm N	5	5.060	69826	60.4284
N4094273	~1000 ppm N	5	5.060	73357	73.1688
N4094274	~1000 ppm N	5	5.060	73875	73.2176
N4094281	~500 ppm N	5	2.584	34434**	75.2685
N4094282	~500 ppm N	5	2.584	41539	188.2569
N4094283	~500 ppm N	5	2.584	41577	187.7437
N4094284	~500 ppm N	5	2.584	42830	185.1805

*The sample # is the same as the Computer Data Acquisition filename. The N identifies it as a nitrogen data file.

The 4 represents the lab book #4264. The next three digits are the page number for the data and the last three digits are the sample number on that page.

**Data was thrown out experimentally or statistically thrown out according to the Q-test.

Summarized Data	Ave. Counts	n	SD	RSD (%)
~100 ppm N	8126	3	62	0.76
~250 ppm N	20607	4	1039	5.04
~500 ppm N	41982	3	735	1.75
~750 ppm N	57105	3	1133	1.98
~1000 ppm N	71578	4	2375	3.32

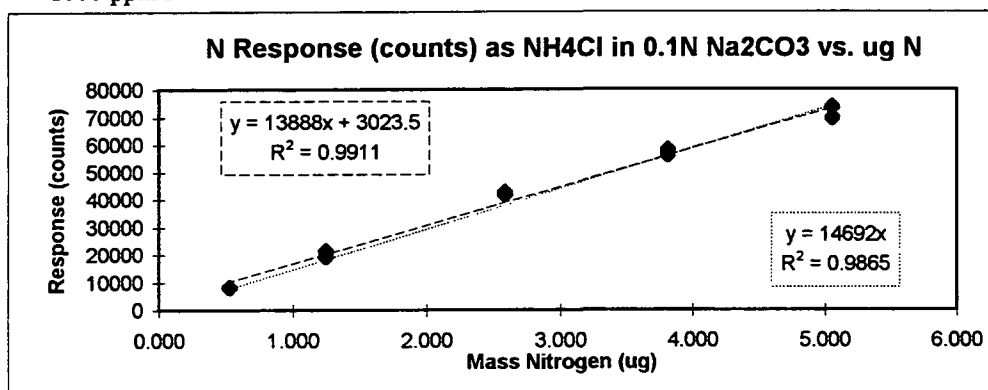


Table V-17. Calibration data for combustion of ammonium chloride in 0.2N Na₂CO₃.

Method Used:	5	PMT Voltage:	825
O2 to O3:	30 ml/min	Furnace Temperature:	1100° C
O2 to pyro:	365 ml/min	Gain Setting:	HI
O2 to inlet:	20 ml/min	Gain Factor:	X1
He to inlet:	145 ml/min	Residence Time:	3 min
Nitrogen Species:	NH ₄ Cl	Matrix:	0.2N Na ₂ CO ₃

Sample #	Sample ID	Sample Vol (μ l)	Known N Mass (μ g)	Response Counts	CDA Sum Response
N4093191	~250 ppm N	5	1.250	13435**	23.4128
N4093192	~250 ppm N	5	1.250	21621	37.9894
N4093193	~250 ppm N	5	1.250	20343	35.5954
N4093194	~250 ppm N	5	1.250	22208	38.916
N4093195	~250 ppm N	5	1.250	21353	37.2803
N4093201	~100 ppm N	5	0.497	6899	11.9632
N4093202	~100 ppm N	5	0.497	4629**	7.9833
N4093203	~100 ppm N	5	0.497	6406	11.0596
N4093204	~100 ppm N	5	0.497	7434	12.8175
N4093211	~750 ppm N	5	3.873	53408**	94.4821
N4093212	~750 ppm N	5	3.873	57843	102.0015
N4093213	~750 ppm N	5	3.873	61318	108.1295
N4093214	~750 ppm N	5	3.873	60284	106.2252
N4093221	~1000 ppm N	5	5.034	69874	123.5106
N4093222	~1000 ppm N	5	5.034	71785	126.8796
N4093223	~1000 ppm N	5	5.034	72981	128.9306
N4093224	~1000 ppm N	5	5.034	73392	129.6137
N4093231	~500 ppm N	5	2.564	40227	70.9717
N4093232	~500 ppm N	5	2.564	42582	75.024
N4093233	~500 ppm N	5	2.564	42978	75.7079

*The sample # is the same as the Computer Data Acquisition filename. The N identifies it as a nitrogen data file.
The 4 represents the lab book #4264. The next three digits are the page number for the data and the last three digits are the sample number on that page.

**Data was thrown out experimentally or statistically thrown out according to the Q-test.

Summarized Data	Ave. Counts	n	SD	RSD (%)
~100 ppm N	6913	3	514	7.44
~250 ppm N	21381	4	779	3.64
~500 ppm N	41929	3	1487	3.55
~750 ppm N	59815	3	1784	2.98
~1000 ppm N	72008	4	1578	2.19

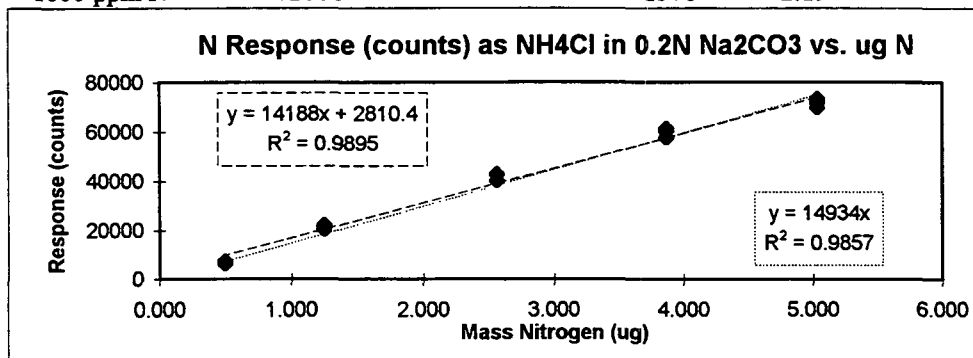


Table V-18. Calibration data for combustion of ammonium chloride in 0.5N Na₂CO₃.

Method Used:	5	PMT Voltage:	825
O ₂ to O ₃ :	30 ml/min	Furnace Temperature:	1100° C
O ₂ to pyro:	365 ml/min	Gain Setting:	HI
O ₂ to inlet:	20 ml/min	Gain Factor:	X1
He to inlet:	145 ml/min	Residence Time:	3 min
Nitrogen Species: NH ₄ Cl		Matrix:	0.5N Na ₂ CO ₃

<u>Sample #</u>	<u>Sample ID</u>	<u>Sample Vol</u> <u>(μl)</u>	<u>Known N</u> <u>Mass (μg)</u>	<u>Response</u> <u>Counts</u>	<u>CDA Sum</u> <u>Response</u>
N4092101	~750 ppm N	5	3.703	52537	92.627
N4092102	~750 ppm N	5	3.703	53381	93.9944
N4092103	~750 ppm N	5	3.703	57302	100.9273
N4092104	~750 ppm N	5	3.703	57922	98.1448
N4092105	~750 ppm N	5	3.703	59820	104.9801
N4092111	~500 ppm N	5	2.535	41965	73.7548
N4092112	~500 ppm N	5	2.535	42567	74.658
N4092113	~500 ppm N	5	2.535	38996**	67.0652
N4092114	~500 ppm N	5	2.535	42830	75.0727
N4092121	~100 ppm N	5	0.513	8946	15.3567
N4092122	~100 ppm N	5	0.513	7742	13.1349
N4092123	~100 ppm N	5	0.513	8305	14.3064
N4092124	~100 ppm N	5	0.513	8148	14.0623
N4092131	~1000 ppm N	5	5.340	74530**	131.8358
N4092132	~1000 ppm N	5	5.340	80670	142.2844
N4092133	~1000 ppm N	5	5.340	82110	144.5305
N4092134	~1000 ppm N	5	5.340	81684	143.8716
N4092141	~250 ppm N	5	1.254	22865	40.0389
N4092142	~250 ppm N	5	1.254	21552	18.3349
N4092143	~250 ppm N	5	1.254	22105	38.5009
N4092144	~250 ppm N	5	1.254	21426	37.2801

*The sample # is the same as the Computer Data Acquisition filename. The N identifies it as a nitrogen data file. The 4 represents the lab book #4264. The next three digits are the page number for the data and the last three digits are the sample number on that page.

**Data was thrown out experimentally or statistically thrown out according to the Q-test.

<u>Summarized Data</u>	<u>Ave. Counts</u>	<u>n</u>	<u>SD</u>	<u>RSD (%)</u>
~100 ppm N	8285	4	500	6.04
~250 ppm N	21987	4	655	2.98
~500 ppm N	42454	3	443	1.04
~750 ppm N	56192	5	3108	5.53
~1000 ppm N	81488	3	740	0.91

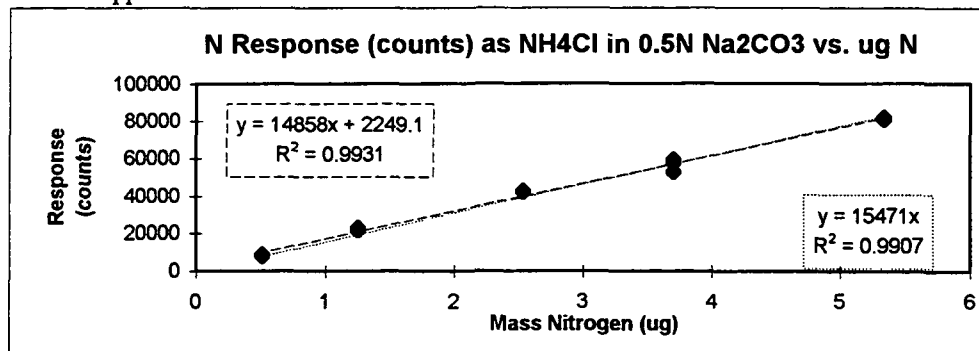


Table V-19. Calibration data for tryptophan in 0.1N NaOH during combustion.

Method Used:	5	PMT Voltage:	825
O ₂ to O ₃ :	30 ml/min	Furnace Temperature:	1100° C
O ₂ to pyro:	365 ml/min	Gain Setting:	HI
O ₂ to inlet:	20 ml/min	Gain Factor:	X1
He to inlet:	145 ml/min	Residence Time:	3 min
Nitrogen Species:	tryptophan	Matrix:	0.1N NaOH

Sample #	Sample ID	Sample Vol (μ l)	Response Counts
N3179031	53.1 ppm N	5	2556
N3179032	53.1 ppm N	5	2776
N3179033	53.1 ppm N	5	2734
N3179041	100.5 ppm N	5	5968
N3179042	100.5 ppm N	5	5909
N3179043	100.5 ppm N	5	6307
N3179051	502.1 ppm N	5	31867
N3179052	502.1 ppm N	5	31118
N3179053	502.1 ppm N	5	34516

Summarized Data	Ave. Counts	\bar{n}	SD	RSD (%)
53.1 ppm N	2689	3	117	4.34
100.5 ppm N	6061	3	215	3.54
502.1 ppm N	32500	3	1785	5.49

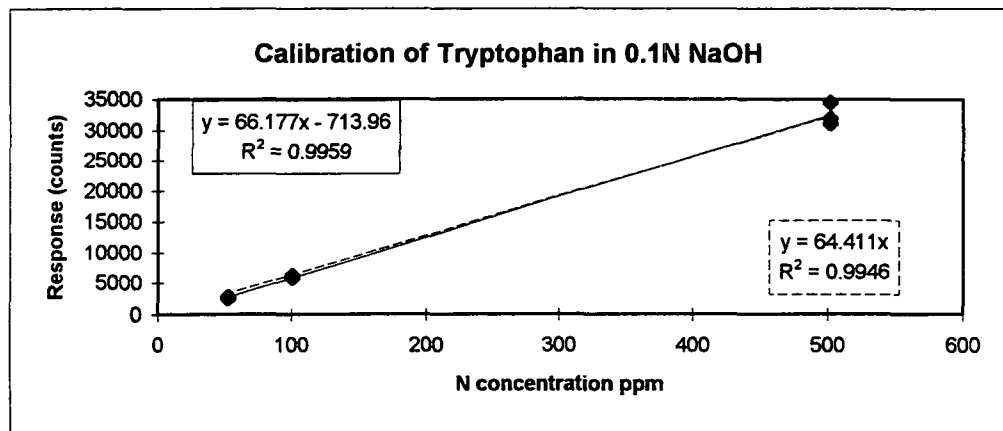


Table V-20. Calibration data for tryptophan in 0.01N NaOH during combustion.

Method Used:	5	PMT Voltage:	825
O ₂ to O ₃ :	30 ml/min	Furnace Temperature:	1100° C
O ₂ to pyro:	365 ml/min	Gain Setting:	HI
O ₂ to inlet:	20 ml/min	Gain Factor:	X1
He to inlet:	145 ml/min	Residence Time:	3 min
Nitrogen Species:	tryptophan	Matrix:	0.01N NaOH

Sample #	Sample ID	Sample Vol (μ l)	Response Counts
N3179061	49.4 ppm N	5	2491
N3179062	49.4 ppm N	5	2766
N3179063	49.4 ppm N	5	3067
N3179071	107.2 ppm N	5	7439
N3179072	107.2 ppm N	5	7504
N3179073	107.2 ppm N	5	7571
N3179081	525.5 ppm N	5	40340
N3179082	525.5 ppm N	5	40060
N3179083	525.5 ppm N	5	38158

Summarized Data	Ave. Counts	n	SD	RSD (%)
49.4 ppm N	2775	3	288	10.38
107.2 ppm N	7505	3	66	0.88
525.5 ppm N	39519	3	1187	3.00

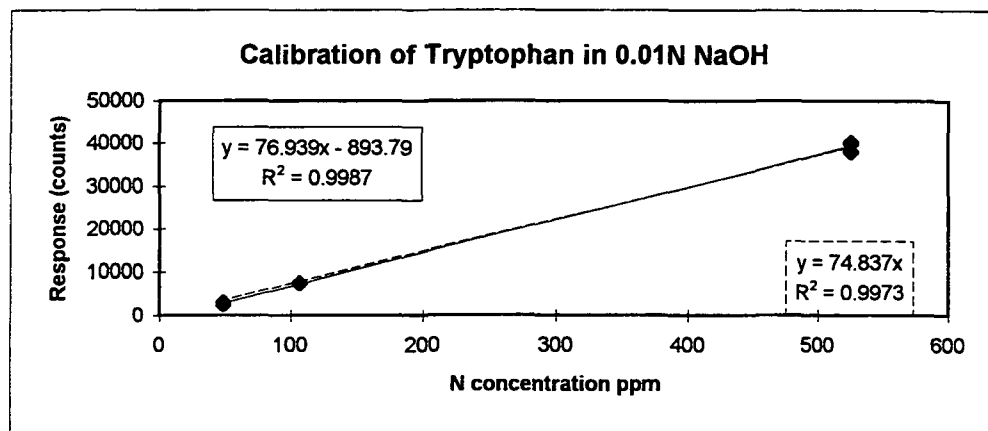


Table V-21. Calibration data for tryptophan in 1.0N NaOH during combustion.

Method Used:	5	PMT Voltage:	825
O ₂ to O ₃ :	30 ml/min	Furnace Temperature:	1100° C
O ₂ to pyro:	365 ml/min	Gain Setting:	HI
O ₂ to inlet:	20 ml/min	Gain Factor:	X1
He to inlet:	145 ml/min	Residence Time:	3 min
Nitrogen Species:	tryptophan	Matrix:	1.0N NaOH

<u>Sample #</u>	<u>Sample ID</u>	<u>Sample Vol (μl)</u>	<u>Response Counts</u>
N3179021	50.2 ppm N	5	2149
N3179022	50.2 ppm N	5	2066
N3179023	50.2 ppm N	5	2509
N3179011	101.7 ppm N	5	4935
N3179012	101.7 ppm N	5	5032
N3179013	101.7 ppm N	5	4702
N3179001	503.2 ppm N	5	31918
N3179002	503.2 ppm N	5	30847
N3179003	503.2 ppm N	5	35678

<u>Summarized Data</u>	<u>Ave. Counts</u>	<u>n</u>	<u>SD</u>	<u>RSD (%)</u>
50.2 ppm N	2241	3	235	10.51
101.7 ppm N	4890	3	170	3.47
503.2 ppm N	32814	3	2537	7.73

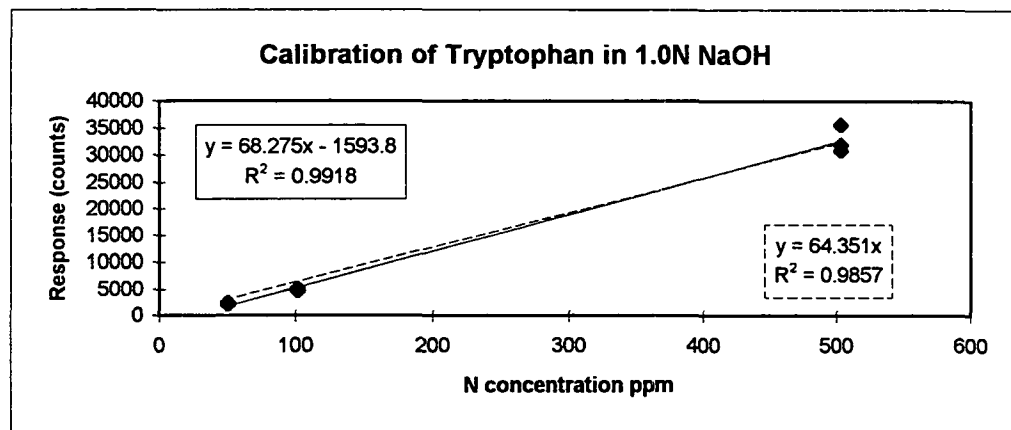


Table V-22. Concentration corrections for NO gas samples. Initial [NO] = 9424 ppm
 NO in He. Flow rates in lpm as air conversion factors are 1.43 for He, 1.43 for NO in He.

<u>Sample #</u>	<u>Flow Rate NO</u> <u>(l/min as air)</u>	<u>Flow Rate</u> <u>NO (l/min)</u>	<u>Flow Rate He</u> <u>(l/min as air)</u>	<u>Flow Rate</u> <u>He (l/min)</u>	<u>Conc. N</u> <u>(µg N/sample)</u>
N4109131	0.056	0.08008	2.93	4.19	0.5093
N4109132	0.054	0.07722	2.93	4.19	0.4915
N4109133	0.054	0.07722	2.94	4.20	0.4898
N4109141	0.142	0.20306	2.86	4.09	1.2847
N4109142	0.144	0.20592	2.85	4.08	1.3062
N4109143	0.144	0.20592	2.85	4.08	1.3062
N4109151	0.301	0.43043	2.68	3.83	2.7423
N4109152	0.303	0.43329	2.7	3.86	2.7403
N4109153	0.301	0.43043	2.71	3.88	2.7150
N4109161	0.307	0.43901	2.7	3.86	2.7728
N4109162	0.304	0.43472	2.71	3.88	2.7393
N4109163	0.302	0.43186	2.71	3.88	2.7231
N4109164	0.302	0.43186	2.71	3.88	2.7231
N4109171	0.301	0.43043	2.71	3.88	2.7150
N4109172	0.300	0.429	2.7	3.86	2.7159
N4109173	0.300	0.429	2.7	3.86	2.7159
N4109174	0.303	0.43329	2.69	3.85	2.7495
N4110181	0.303	0.43329	2.7	3.86	2.7403
N4110182	0.301	0.43043	2.7	3.86	2.7240
N4110183	0.313	0.44759	2.7	3.86	2.8213
N4110191	0.302	0.43186	2.7	3.86	2.7322
N4110192	0.301	0.43043	2.69	3.85	2.7331
N4110193	0.301	0.43043	2.7	3.86	2.7240
N4110201	0.300	0.429	2.69	3.85	2.7250
N4110202	0.306	0.43758	2.7	3.86	2.7647
N4110203	0.306	0.43758	2.7	3.86	2.7647
N4110211	0.306	0.43758	2.7	3.86	2.7647
N4110212	0.306	0.43758	2.7	3.86	2.7647
N4110213	0.306	0.43758	2.7	3.86	2.7647
N4110221	0.305	0.43615	2.7	3.86	2.7566
N4110222	0.305	0.43615	2.7	3.86	2.7566
N4110223	0.305	0.43615	2.7	3.86	2.7566
N4110231	0.301	0.43043	2.7	3.86	2.7240
N4110232	0.303	0.43329	2.7	3.86	2.7403
N4110233	0.3	0.429	2.7	3.86	2.7159
N4110241	0.303	0.43329	2.7	3.86	2.7403
N4110242	0.299	0.42757	2.7	3.86	2.7077
N4110243	0.307	0.43901	2.7	3.86	2.7728
N4110251	0.305	0.43615	2.7	3.86	2.7566
N4110252	0.303	0.43329	2.7	3.86	2.7403
N4110253	0.302	0.43186	2.7	3.86	2.7322
N4110261	0.300	0.429	2.7	3.86	2.7159
N4110262	0.303	0.43329	2.71	3.88	2.7312
N4110263	0.306	0.43758	2.71	3.88	2.7555

Table V-22. (cont.) Concentration corrections for NO gas samples. Initial [NO] = 9424 ppm NO in He. Flow rates in lpm as air conversion factors are 1.43 for He, 1.43 for NO in He.

Sample #	Flow Rate NO (l/min as air)	Flow Rate NO (l/min)	Flow Rate He (l/min as air)	Flow Rate He (l/min)	Conc. N ($\mu\text{g N/sample}$)
N4110271	0.143	0.20449	2.87	4.10	1.2890
N4110272	0.146	0.20878	2.86	4.09	1.3191
N4110273	0.145	0.20735	2.86	4.09	1.3105
N4110281	0.144	0.20592	2.87	4.10	1.2976
N4110282	0.143	0.20449	2.86	4.09	1.2933
N4110283	0.145	0.20735	2.86	4.09	1.3105
N4111291	0.144	0.20592	2.86	4.09	1.3019
N4111292	0.144	0.20592	2.86	4.09	1.3019
N4111293	0.143	0.20449	2.86	4.09	1.2933
N4111301	0.144	0.20592	2.86	4.09	1.3019
N4111302	0.147	0.21021	2.86	4.09	1.3277
N4111303	0.145	0.20735	2.85	4.08	1.3149
N4111311	0.144	0.20592	2.86	4.09	1.3019
N4111312	0.147	0.21021	2.86	4.09	1.3277
N4111313	0.146	0.20878	2.85	4.08	1.3235
N4111321	0.145	0.20735	2.85	4.08	1.3149
N4111322	0.145	0.20735	2.85	4.08	1.3149
N4111323	0.145	0.20735	2.85	4.08	1.3149
N4111331	0.145	0.20735	2.85	4.08	1.3149
N4111332	0.145	0.20735	2.85	4.08	1.3149
N4111333	0.144	0.20592	2.84	4.06	1.3106
N4111341	0.147	0.21021	2.86	4.09	1.3277
N4111342	0.146	0.20878	2.85	4.08	1.3235
N4111343	0.146	0.20878	2.85	4.08	1.3235
N4111351	0.145	0.20735	2.85	4.08	1.3149
N4111352	0.145	0.20735	2.85	4.08	1.3149
N4111353	0.145	0.20735	2.85	4.08	1.3149
N4111354	0.146	0.20878	2.85	4.08	1.3235
N4111361	0.146	0.20878	2.85	4.08	1.3235
N4111362	0.147	0.21021	2.85	4.08	1.3321
N4111363	0.145	0.20735	2.85	4.08	1.3149
N4111371	0.147	0.21021	2.85	4.08	1.3321
N4111372	0.146	0.20878	2.85	4.08	1.3235
N4111373	0.146	0.20878	2.85	4.08	1.3235
N4111381	0.146	0.20878	2.86	4.09	1.3191
N4111382	0.146	0.20878	2.86	4.09	1.3191
N4111383	0.146	0.20878	2.86	4.09	1.3191
N4111391	0.146	0.20878	2.86	4.09	1.3191
N4111392	0.146	0.20878	2.86	4.09	1.3191
N4111393	0.146	0.20878	2.85	4.08	1.3235
N4112401	0.481	0.68783	2.52	3.60	4.3530
N4112402	0.481	0.68783	2.52	3.60	4.3530
N4112403	0.482	0.68926	2.51	3.59	4.3752

Table V-22. (cont.) Concentration corrections for NO gas samples. Initial [NO] = 9424 ppm NO in He. Flow rates in lpm as air conversion factors are 1.43 for He, 1.43 for NO in He.

<u>Sample #</u>	<u>Flow Rate NO</u> <u>(l/min as air)</u>	<u>Flow Rate</u> <u>NO (l/min)</u>	<u>Flow Rate He</u> <u>(l/min as air)</u>	<u>Flow Rate</u> <u>He (l/min)</u>	<u>Conc. N</u> <u>(µg N/sample)</u>
N4112411	0.481	0.68783	2.52	3.60	4.3530
N4112412	0.481	0.68783	2.52	3.60	4.3530
N4112413	0.480	0.6864	2.52	3.60	4.3454
N4112421	0.480	0.6864	2.52	3.60	4.3454
N4112422	0.479	0.68497	2.52	3.60	4.3378
N4112423	0.479	0.68497	2.52	3.60	4.3378
N4112431	0.481	0.68783	2.52	3.60	4.3530
N4112432	0.480	0.6864	2.52	3.60	4.3454
N4112433	0.480	0.6864	2.52	3.60	4.3454
N4112441	0.481	0.68783	2.52	3.60	4.3530
N4112442	0.479	0.68497	2.52	3.60	4.3378
N4112443	0.481	0.68783	2.52	3.60	4.3530
N4112451	0.482	0.68926	2.51	3.59	4.3752
N4112452	0.481	0.68783	2.52	3.60	4.3530
N4112453	0.479	0.68497	2.52	3.60	4.3378
N4112461	0.479	0.68497	2.51	3.59	4.3523
N4112462	0.480	0.6864	2.52	3.60	4.3454
N4112463	0.480	0.6864	2.52	3.60	4.3454

Table V-22. (cont.) Concentration corrections for NO gas samples. Initial [NO] = 9424 ppm NO in He. Flow rates in lpm as air conversion factors are 1.43 for He, 1.43 for NO in He.

<u>Sample #</u>	<u>Flow Rate NO (l/min as air)</u>	<u>Flow Rate NO (l/min)</u>	<u>Flow Rate He (l/min as air)</u>	<u>Flow Rate He (l/min)</u>	<u>Conc. N ($\mu\text{g N/sample}$)</u>
N4113101	0.146	0.20878	2.86	4.09	1.3191
N4113102	0.145	0.20735	2.86	4.09	1.3105
N4113103	0.144	0.20592	2.87	4.10	1.2976
N4114111	0.305	0.43615	2.71	3.88	2.7474
N4114112	0.303	0.43329	2.7	3.86	2.7403
N4114113	0.304	0.43472	2.7	3.86	2.7484
N4114121	0.481	0.68783	2.52	3.60	4.3530
N4114122	0.484	0.69212	2.52	3.60	4.3758
N4114123	0.48	0.6864	2.52	3.60	4.3454
N4114131	0.48	0.6864	2.52	3.60	4.3454
N4114132	0.481	0.68783	2.52	3.60	4.3530
N4114133	0.481	0.68783	2.51	3.59	4.3676
N4114141	0.481	0.68783	2.51	3.59	4.3676
N4114142	0.48	0.6864	2.51	3.59	4.3599
N4114143	0.48	0.6864	2.52	3.60	4.3454
N4114151	0.48	0.6864	2.52	3.60	4.3454
N4114152	0.482	0.68926	2.52	3.60	4.3606
N4114153	0.479	0.68497	2.52	3.60	4.3378
N4114161	0.481	0.68783	2.52	3.60	4.3530
N4114162	0.479	0.68497	2.52	3.60	4.3378
N4114163	0.481	0.68783	2.52	3.60	4.3530
N4114171	0.482	0.68926	2.52	3.60	4.3606
N4114172	0.479	0.68497	2.52	3.60	4.3378
N4114173	0.482	0.68926	2.52	3.60	4.3606
N4114181	0.481	0.68783	2.52	3.60	4.3530
N4114182	0.48	0.6864	2.52	3.60	4.3454
N4114183	0.48	0.6864	2.52	3.60	4.3454
N4114191	0.48	0.6864	2.52	3.60	4.3454
N4114192	0.479	0.68497	2.52	3.60	4.3378
N4114193	0.479	0.68497	2.52	3.60	4.3378
N4114201	0.303	0.43329	2.7	3.86	2.7403
N4114202	0.299	0.42757	2.71	3.88	2.6987
N4114203	0.302	0.43186	2.7	3.86	2.7322
N4114211	0.3	0.429	2.7	3.86	2.7159
N4114212	0.303	0.43329	2.7	3.86	2.7403
N4114213	0.303	0.43329	2.7	3.86	2.7403
N4115221	0.305	0.43615	2.7	3.86	2.7566
N4115222	0.3	0.429	2.7	3.86	2.7159
N4115223	0.303	0.43329	2.69	3.85	2.7495
N4115231	0.306	0.43758	2.7	3.86	2.7647
N4115232	0.304	0.43472	2.7	3.86	2.7484

Table V-22. (cont.) Concentration corrections for NO gas samples. Initial [NO] = 9424 ppm NO in He. Flow rates in lpm as air conversion factors are 1.43 for He, 1.43 for NO in He.

<u>Sample #</u>	<u>Flow Rate NO (l/min as air)</u>	<u>Flow Rate NO (l/min)</u>	<u>Flow Rate He (l/min as air)</u>	<u>Flow Rate He (l/min)</u>	<u>Conc. N ($\mu\text{g N/sample}$)</u>
N4115233	0.303	0.43329	2.7	3.86	2.7403
N4115241	0.302	0.43186	2.71	3.88	2.7231
N4115242	0.302	0.43186	2.72	3.89	2.7141
N4115243	0.302	0.43186	2.71	3.88	2.7231
N4115251	0.302	0.43186	2.71	3.88	2.7231
N4115252	0.301	0.43043	2.72	3.89	2.7060
N4115253	0.302	0.43186	2.69	3.85	2.7413
N4115261	0.305	0.43615	2.7	3.86	2.7566
N4115262	0.305	0.43615	2.71	3.88	2.7474
N4115263	0.304	0.43472	2.72	3.89	2.7302
N4115271	0.143	0.20449	2.86	4.09	1.2933
N4115272	0.142	0.20306	2.85	4.08	1.2890
N4115273	0.142	0.20306	2.86	4.09	1.2847
N4115281	0.143	0.20449	2.87	4.10	1.2890
N4115282	0.143	0.20449	2.85	4.08	1.2976
N4115283	0.143	0.20449	2.84	4.06	1.3019
N4115291	0.146	0.20878	2.87	4.10	1.3147
N4115292	0.144	0.20592	2.87	4.10	1.2976
N4115293	0.144	0.20592	2.87	4.10	1.2976
N4115301	0.143	0.20449	2.85	4.08	1.2976
N4115302	0.143	0.20449	2.85	4.08	1.2976
N4115303	0.143	0.20449	2.85	4.08	1.2976
N4115311	0.143	0.20449	2.85	4.08	1.2976
N4115312	0.143	0.20449	2.84	4.06	1.3019
N4115313	0.143	0.20449	2.84	4.06	1.3019
N4115321	0.144	0.20592	2.84	4.06	1.3106
N4115322	0.144	0.20592	2.84	4.06	1.3106
N4115323	0.143	0.20449	2.85	4.08	1.2976
N4116331	0.144	0.20592	2.85	4.08	1.3062
N4116332	0.144	0.20592	2.84	4.06	1.3106
N4116333	0.144	0.20592	2.85	4.08	1.3062
N4116341	0.144	0.20592	2.84	4.06	1.3106
N4116342	0.144	0.20592	2.84	4.06	1.3106
N4116343	0.144	0.20592	2.84	4.06	1.3106

Table V-23. Concentration corrections for NH₃ gas samples. Initial [NH₃] = 9970 ppm
 NH₃ in He. Flow rates in lpm as air conversion factors are 1.43 for He, 1.43 for NH₃ in He.

Sample #	Flow Rate NH ₃ (l/min as air)	Flow Rate NH ₃ (l/min)	Flow Rate He (l/min as air)	Flow Rate He (l/min)	Conc. N (µg N/sample)
N4117051	0.139	0.19877	2.86	4.09	1.2588
N4117052	0.138	0.19734	2.85	4.08	1.2543
N4117053	0.139	0.19877	2.86	4.09	1.2588
N4117054	0.138	0.19734	2.86	4.09	1.2501
N4117055	0.139	0.19877	2.85	4.08	1.2630
N4117056	0.139	0.19877	2.86	4.09	1.2588
N4117061	0.293	0.41899	2.71	3.88	2.6499
N4117062	0.293	0.41899	2.71	3.88	2.6499
N4117063	0.292	0.41756	2.71	3.88	2.6417
N4117064	0.293	0.41899	2.71	3.88	2.6499
N4117065	0.292	0.41756	2.71	3.88	2.6417
N4117066	0.292	0.41756	2.71	3.88	2.6417
N4117067	0.291	0.41613	2.72	3.89	2.6248
N4117068	0.292	0.41756	2.71	3.88	2.6417
N4118071	0.139	0.19877	2.86	4.09	1.2588
N4118072	0.138	0.19734	2.85	4.08	1.2543
N4118073	0.139	0.19877	2.86	4.09	1.2588
N4118074	0.139	0.19877	2.86	4.09	1.2588
N4118081	0.292	0.41756	2.71	3.88	2.6417
N4118082	0.293	0.41899	2.71	3.88	2.6499
N4118083	0.293	0.41899	2.7	3.86	2.6587
N4118091	0.461	0.65923	2.54	3.63	4.1720
N4118092	0.462	0.66066	2.54	3.63	4.1797
N4118093	0.461	0.65923	2.54	3.63	4.1720
N4118094	0.461	0.65923	2.54	3.63	4.1720
N4118095	0.461	0.65923	2.54	3.63	4.1720
N4118101	0.292	0.41756	2.71	3.88	2.6417
N4118102	0.291	0.41613	2.71	3.88	2.6335
N4118103	0.292	0.41756	2.71	3.88	2.6417
N4118104	0.292	0.41756	2.71	3.88	2.6417
N4118111	0.139	0.19877	2.86	4.09	1.2588
N4118112	0.14	0.2002	2.86	4.09	1.2674
N4118113	0.139	0.19877	2.86	4.09	1.2588
N4118114	0.139	0.19877	2.86	4.09	1.2588
N4118115	0.138	0.19734	2.86	4.09	1.2501
N4118116	0.137	0.19591	2.85	4.08	1.2456
N4118121	0.139	0.19877	2.86	4.09	1.2588
N4118122	0.139	0.19877	2.86	4.09	1.2588
N4118123	0.14	0.2002	2.86	4.09	1.2674
N4118131	0.14	0.2002	2.86	4.09	1.2674
N4118132	0.139	0.19877	2.86	4.09	1.2588
N4118133	0.139	0.19877	2.86	4.09	1.2588
N4118141	0.139	0.19877	2.86	4.09	1.2588
N4118142	0.139	0.19877	2.86	4.09	1.2588

Table V-23.(cont.) Concentration corrections for NH₃ gas samples. Initial [NH₃] = 9970 ppm NH₃ in He. Flow rates in lpm as air conversion factors are 1.43 for He, 1.43 for NH₃ in He.

<u>Sample #</u>	<u>Flow Rate NH₃</u> <u>(l/min as air)</u>	<u>Flow Rate</u> <u>NH₃ (l/min)</u>	<u>Flow Rate He</u> <u>(l/min as air)</u>	<u>Flow Rate</u> <u>He (l/min)</u>	<u>Conc. N</u> <u>(µg N/sample)</u>
N4118143	0.138	0.19734	2.86	4.09	1.2501
N4118144	0.138	0.19734	2.86	4.09	1.2501
N4118145	0.14	0.2002	2.86	4.09	1.2674
N4119151	0.138	0.19734	2.86	4.09	1.2501
N4119152	0.138	0.19734	2.86	4.09	1.2501
N4119153	0.139	0.19877	2.86	4.09	1.2588
N4119154	0.139	0.19877	2.86	4.09	1.2588
N4119155	0.139	0.19877	2.86	4.09	1.2588
N4119156	0.139	0.19877	2.86	4.09	1.2588
N4119161	0.139	0.19877	2.85	4.08	1.2630
N4119162	0.139	0.19877	2.85	4.08	1.2630
N4119163	0.139	0.19877	2.85	4.08	1.2630
N4119171	0.139	0.19877	2.85	4.08	1.2630
N4119172	0.139	0.19877	2.85	4.08	1.2630
N4119173	0.138	0.19734	2.85	4.08	1.2543
N4119174	0.138	0.19734	2.85	4.08	1.2543
N4119181	0.291	0.41613	2.71	3.88	2.6335
N4119182	0.293	0.41899	2.7	3.86	2.6587
N4119183	0.292	0.41756	2.71	3.88	2.6417
N4119184	0.292	0.41756	2.71	3.88	2.6417
N4119185	0.291	0.41613	2.71	3.88	2.6335
N4119191	0.293	0.41899	2.71	3.88	2.6499
N4119192	0.292	0.41756	2.71	3.88	2.6417
N4119193	0.291	0.41613	2.71	3.88	2.6335
N4119194	0.293	0.41899	2.71	3.88	2.6499
N411919_	0.292	0.41756	2.71	3.88	2.6417
N411919-	0.291	0.41613	2.71	3.88	2.6335
N4119195	0.291	0.41613	2.71	3.88	2.6335
N4119201	0.291	0.41613	2.7	3.86	2.6423
N4119202	0.292	0.41756	2.71	3.88	2.6417
N4119203	0.292	0.41756	2.71	3.88	2.6417
N4119211	0.292	0.41756	2.71	3.88	2.6417
N4119212	0.293	0.41899	2.71	3.88	2.6499
N4119213	0.293	0.41899	2.71	3.88	2.6499
N4119214	0.293	0.41899	2.71	3.88	2.6499
N4119221	0.292	0.41756	2.71	3.88	2.6417
N4119222	0.292	0.41756	2.71	3.88	2.6417
N4119223	0.293	0.41899	2.71	3.88	2.6499
N4122231	0.291	0.41613	2.71	3.88	2.6335
N4122232	0.293	0.41899	2.7	3.86	2.6587
N4122233	0.292	0.41756	2.71	3.88	2.6417
N4122241	0.292	0.41756	2.71	3.88	2.6417
N4122242	0.293	0.41899	2.71	3.88	2.6499
N4122243	0.292	0.41756	2.72	3.89	2.6329

Table V-23.(cont.) Concentration corrections for NH₃ gas samples. Initial [NH₃] = 9970 ppm NH₃ in He. Flow rates in lpm as air conversion factors are 1.43 for He, 1.43 for NH₃ in He.

Sample #	Flow Rate NH ₃ (l/min as air)	Flow Rate NH ₃ (l/min)	Flow Rate He (l/min as air)	Flow Rate He (l/min)	Conc. N (μ g N/sample)
N4122251	0.292	0.41756	2.72	3.89	2.6329
N4122252	0.293	0.41899	2.71	3.88	2.6499
N4122253	0.293	0.41899	2.72	3.89	2.6411
N4123361	0.46	0.6578	2.54	3.63	4.1643
N4123362	0.461	0.65923	2.54	3.63	4.1720
N4123363	0.461	0.65923	2.54	3.63	4.1720
N4123364	0.461	0.65923	2.54	3.63	4.1720
N4123371	0.461	0.65923	2.53	3.62	4.1860
N4123372	0.461	0.65923	2.53	3.62	4.1860
N4123373	0.461	0.65923	2.53	3.62	4.1860
N4123381	0.46	0.6578	2.53	3.62	4.1783
N4123382	0.46	0.6578	2.53	3.62	4.1783
N4123383	0.46	0.6578	2.53	3.62	4.1783
N4123391	0.461	0.65923	2.53	3.62	4.1860
N4123392	0.461	0.65923	2.53	3.62	4.1860
N4123393	0.461	0.65923	2.53	3.62	4.1860
N4123401	0.461	0.65923	2.53	3.62	4.1860
N4123402	0.46	0.6578	2.54	3.63	4.1643
N4123403	0.461	0.65923	2.54	3.63	4.1720
N4123411	0.461	0.65923	2.54	3.63	4.1720
N4123412	0.462	0.66066	2.53	3.62	4.1936
N4123413	0.461	0.65923	2.54	3.63	4.1720
N4123421	0.461	0.65923	2.54	3.63	4.1720
N4123422	0.462	0.66066	2.54	3.63	4.1797
N4123423	0.463	0.66209	2.54	3.63	4.1873

APPENDIX VI: THERMODYNAMIC EVALUATION OF NITROGEN SPECIES CONVERSION

The results of the combustion studies conducted at slow heating rates indicated that the conversion of fuel nitrogen was dependent on the fuel nitrogen chemical structure. Thermodynamic equilibrium concentration calculations were made to theoretically evaluate the results for the various conversions observed for the different model fuel nitrogen compounds. This appendix provides examples of the data and reviews the calculation procedures. The original calculations were done using the HSC Chemistry software program.¹⁰¹

OVERVIEW OF THERMODYNAMIC EQUILIBRIUM CALCULATIONS

Calculations were made using the HSC Chemistry software package. This package calculates multiphase equilibrium compositions. By inputting the amounts of raw materials, the program calculates the products at a theoretical equilibrium state. The program uses a thermodynamic/thermochemical database of enthalpies (H), entropies (S), and heat capacities (C) for about 5600 compounds. The package uses the Gibbs Free Energy Minimization Method to calculate the equilibrium composition. It should be noted, however, that the minimization routines do not always find the correct equilibrium state. Therefore, the results can be in error. Accuracy of the calculations was improved by maximizing the number of iterations.

The Gibbs minimization method computes the composition of the phases where the total Gibbs energy of the system attains its minimum value at a fixed mass balance. The standard Gibbs energy of formation, ΔG°_f , is used to determine the extent of the chemical reaction. It is calculated from the standard enthalpies and entropies of formation,

$$\Delta G^\circ_f = \Delta H^\circ_f - T\Delta S^\circ_f, \text{ where}$$

$$\Delta H^\circ_f - = \Delta H^\circ_{298} + \int_{298}^T C_p(T)dT + H_{tr}$$

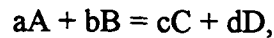
$$\Delta S^\circ_f - = \Delta S^\circ_{298} + \int_{298}^T (C_p/T)dT + H_{tr}/T_{tr}$$

and C_p is the specific heat and is represented by the power series,

$$C_p = \alpha + \beta T + \gamma T^2.$$

Here, H_{tr} and T_{tr} represent the enthalpy of phase transitions (such as vaporization) and the transformation temperature, respectively.

These equations are used for a chemical reaction, such as



where the equilibrium constant, K , is represented as

$$K = \{([C]^c)([D]^d)\}/\{([A]^a)([B]^b)\},$$

where $[A]$ is the activity (concentration) or partial pressure of A and a is the coefficient of A in the reaction equation. Finally,

$$\ln K = \Delta G_{rxn}/(-RT),$$

where R is the gas constant, $R = 1.987 \text{ cal}/(\text{K mol}) = 8.314 \text{ J}/(\text{K mol})$. The temperature is expressed in Kelvin (K).

In the software program, the user specifies the temperature range and the temperature step along with the pressure, input amounts of the reactants, and the number of iterations to be done at each temperature for the calculation. The program calculate the volume, reaction enthalpy and entropy to arrive at the equilibrium compositions.

Example Equilibrium Compositions

On the following pages are examples of the equilibrium compositions presented in graphical form. The input composition for the first set of data is presented below, while that for the second set of data is presented later. Discussion of each set of results is also given here.

Table VI-1. Input data for nitrogen species equilibrium composition calculations for temperatures from 100–1300° C.

AgNO ₃		NH ₄ NO ₃		NH ₄ Cl		(NH ₄) ₂ SO ₄	
Species	Input Amount (mol)	Species	Input Amount (mol)	Species	Input Amount (mol)	Species	Input Amount (mol)
H ₂ O(g)	1.0	H ₂ O(g)	1.0	H ₂ O(g)	1.0	H ₂ O(g)	1.0
O ₂ (g)	1.0	O ₂ (g)	1.0	O ₂ (g)	1.0	O ₂ (g)	2.0
e-	1.0	e-	1.0	e-	1.0	e-	1.0
He(g)	1.0	He(g)	1.0	He(g)	1.0	He(g)	1.0
AgNO ₃	1.0	NH ₄ NO ₃	2.0	NH ₄ Cl	2.0	(NH ₄) ₂ SO ₄	2.0
Ag(+a)	1.0	--	--	--	--	--	--

In each figure, the species of interest in terms of understanding the nitrogen chemistry and conversion to NO_x are presented. The combustion reactions in the nitrogen

analyzer occurred at 1100° C. In chart a), AgNO_3 equilibrium concentration indicates the only nitrogen species at 1100° C to be N_2 . This does not follow the experimental data in which 91% of the fuel nitrogen was converted to GPNP (the sum of NO , HCN , NH_3 , and other oxidizable intermediates).

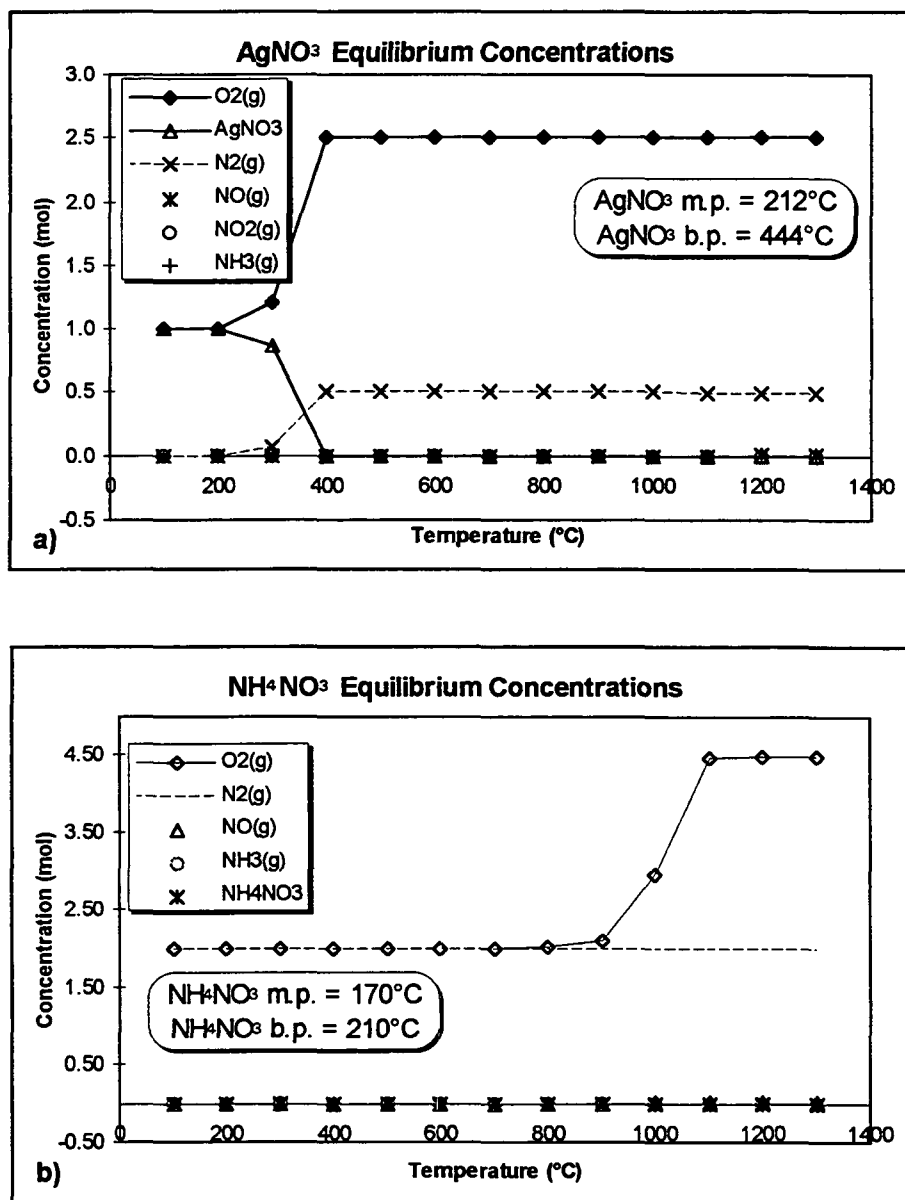


Figure VI-1. Examples of thermodynamic equilibrium concentration calculations for model inorganic fuel nitrogen species. a) AgNO_3 and b) NH_4NO_3 .

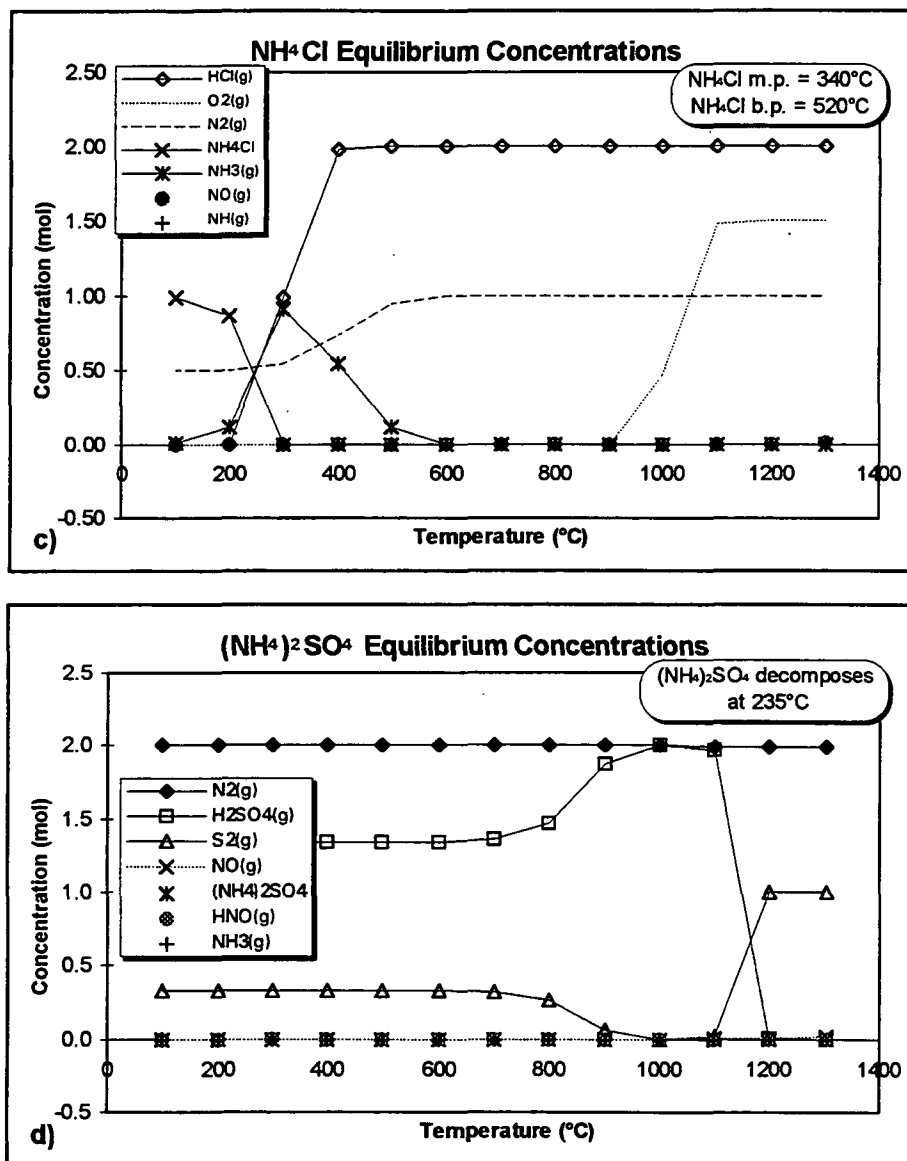


Figure Y-1. (cont.) Examples of thermodynamic equilibrium concentration calculations for model inorganic fuel nitrogen species. c) NH_4Cl , and d) $(\text{NH}_4)_2\text{SO}_4$.

Again in figure b), the only nitrogen species present at 1100°C is N_2 . Under combustion conditions, NH_4NO_3 yielded a 55% conversion of fuel nitrogen. In figure c), as the NH_4Cl decomposes starting at about 200°C , NH_3 is observed to increase until 300°

C at which time its decomposition triggers the increase of N_2 . Ultimately at 1100°C , the only nitrogen species present is N_2 . During combustion, NH_4Cl had a rather low conversion of only 39%. The $(NH_4)_2SO_4$ had similar results during combustion yielding a 37% conversion of fuel nitrogen to fixed nitrogen.

Similar results were also obtained from the equilibrium calculations as noted in d). The concentration of N_2 remains high and unchanged throughout the calculated temperature range. Only a slight amount of NO is detected starting at 1100°C . No other fixed nitrogen species were observed.

The output of the thermodynamic equilibrium calculations shown in Figure VI-2 were completed for C_4N_2 instead of pyrazine, $C_4H_4N_2$, as the later formulas was not accepted into the software program. The C_4N_2 species was used as the fuel nitrogen source to represent pyrazine. The species of interest are plotted in Figure VI-2.

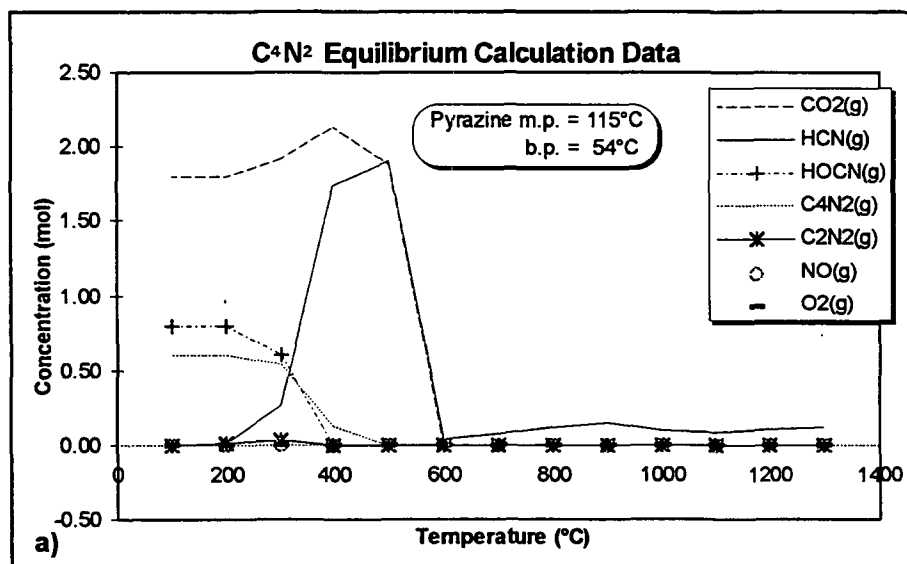


Figure VI-2. Examples of thermodynamic equilibrium concentration calculations for model organic fuel nitrogen species.

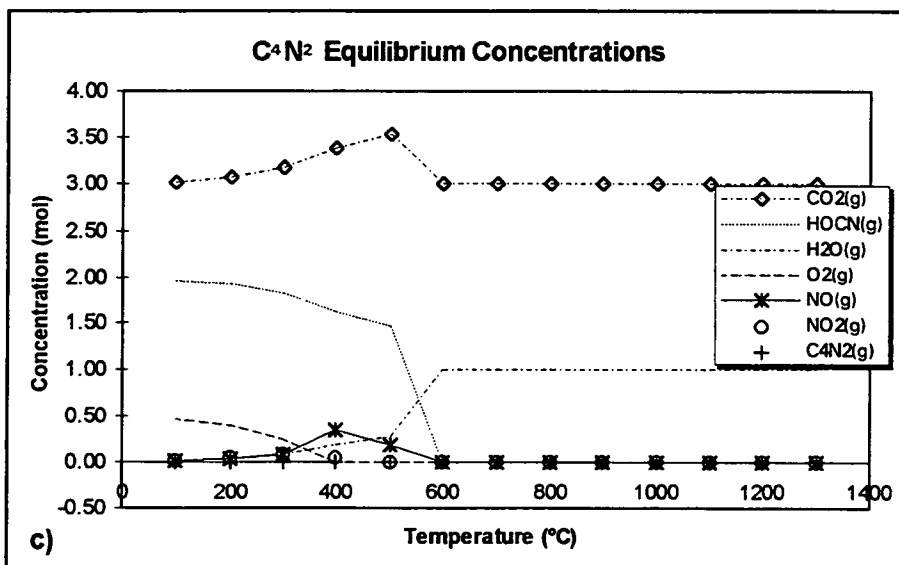
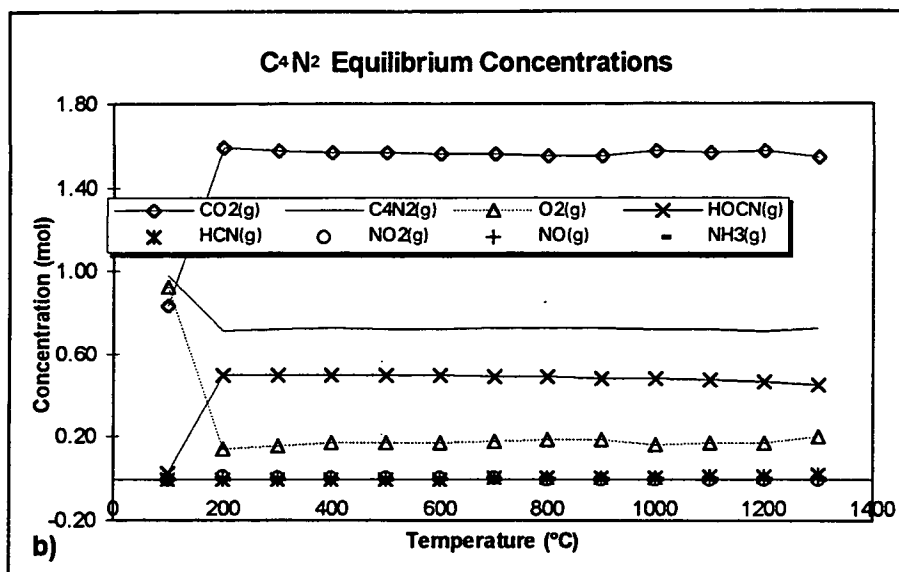


Figure VI-2. (cont.) Examples of thermodynamic equilibrium concentration calculations for model organic fuel nitrogen species.

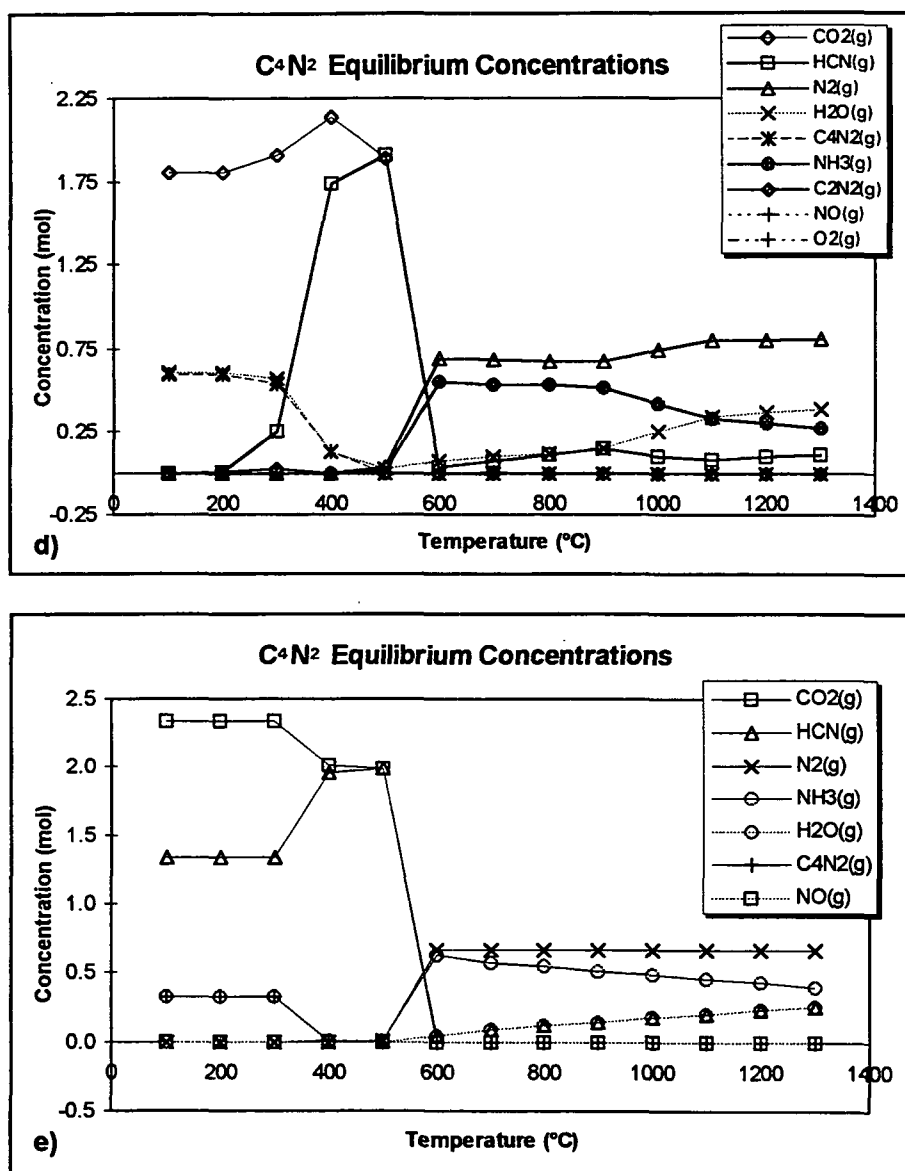


Figure VI-2. (cont.) Examples of thermodynamic equilibrium concentration calculations for model organic fuel nitrogen species.

The data in Figures VI-2 a), d), and e) indicates the formation of intermediate species HCN as H₂O and C₄N₂ degrade starting at a temperature of 200° C. The formation of NO is not observed at the temperatures and conditions provided for the calculations. From 500 to 600° C, HCN rapidly degrades and only a small amount is

present in the range of 1000° C and above. At about 500° C, NH_3 is formed but its degradation begins at about 900° C. Likewise, as the NH_3 increases, so does N_2 . The N_2 increase after 900° C occurs at the same time that NH_3 decreases.

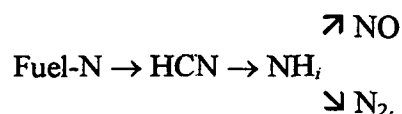
Figure VI-2 b) represents the outcome of calculations when no water is present in the gas phase as part of the system and was excluded during the calculations. Figure VI-2 c) represents the only case in which NO and NO_2 were formed. The input data for each set of initial compositions are provided in Table VI-2. For Figure VI-2 d), the thermodynamic equilibrium predicts that approximately 60% of the nitrogen in the gas phase at 1100° C is N_2 , HCN represents approximately 10%, and NH_3 represents about 30%.

Table VI-2. Input data for determination of equilibrium composition calculations for C_4N_2 over the temperature range from 100–1300° C. Input amount in moles.

Figure #	He(g)	H ₂ O(g)	C ₄ N ₂ (g)	O ₂ (g)	C(g)	H(g)
a)	1.0	1.0	1.0	2.0	1.0	0
b)	1.0	1.0	1.0	4.0	1.0	0
c)	1.0	0	1.0	2.0	1.0	0.5
d)	1.0	1.0	1.0	2.0	1.0	0
e)	1.0	1.0	1.0	1.0	1.0	0

APPENDIX VII: KINETICS OF NITROGEN OXIDATION IN THE PYROTUBE

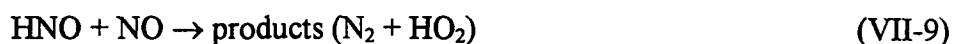
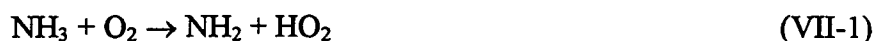
The kinetic evaluation of the gas phase nitrogen chemistry within the pyrotube in the analyzer was done to verify that the conditions were appropriate to allow all of the release nitrogen to be oxidized to NO. The intermediate gas phase reactions were included in the evaluation. The equations to be evaluated were based on the fuel nitrogen pathway,



The question of whether the rate of the reaction in the pyrotube for the NH_i species to be oxidized to NO or react with NO to form N_2 is of interest. Estimates for the kinetic parameters for the reactions of interest were obtained using the CHEM-KIN database.¹⁰² The estimated rates for the reactions were determined and compared with each other to verify that all of the nitrogen released during combustion in the pyrotube would be converted to NO and not reacted with other nitrogen gas phase species to form N_2 which cannot be measured.

The concentrations of the gas species were estimated based on the reported average 0.1% nitrogen concentration in the black liquor samples and the amount of oxygen present (about 73% O_2) in the pyrotube with the method used. It was assumed that all of the fuel-bound nitrogen was converted to gas phase species either as NO or NH_3 . When the rate of reaction of NH_i with NO was considered, it was assumed that half

of the nitrogen was available as NO and half was available as NH_i . Also, none of the oxygen in the sample was considered available for the reactions. The CHEM-KIN database was used to obtain the rate constants, and then, the rates of the reactions were compared. The following reactions were considered.



The rate constants obtained from the database along with calculated rates of the reactions are presented in Table VII-1. The calculations were based on the general equation $-r = kC_A C_B$ where the reaction is represented by $A + B \rightarrow \text{products}$. The temperature of the reaction is 1100° C.

Table VII-1. Kinetic rate data for the ammonia oxidation and nitric oxide reduction for the pyrotube.

Reaction Number	k (cm ³ /mol.s)	-r
VII-1	1E+12exp(-30,949K/T)	4.05E-08
VII-2	5E+14exp(-25,161K/T)	7.01E-07
VII-3	1E+14exp(-503K/T)	24872
VII-4	8.687E+12exp(-341.3K/T)	0.8635
VII-5	5.13E+13exp(-7598K/T)	50.6
VII-6	1E+14exp(-25,161K/T)	2.7E-04
VII-7	7E+13exp(-14,000K/T)	3.3E-04
VII-8	3.16E+12exp(-1510K/T)	260.2
VII-9	1.346E+04exp(-926.3K/T)	8.74E-10

It is desirable to have the oxidation of the NH_i species to be more rapid than the reduction of these species to N_2 . Comparing the rates of VII-1 and VII-2, VII-2 was found to be faster only by one order of magnitude. The intermediate species which results may further react via reactions VII-5, VII-6, R VII-7, and VII-8 and VII-9. The $\text{NH}_2 + \text{O}_2$ reaction (VII-5) to form $\text{HNO} +$ the hydroxyl radical would dominate over the formation of $\text{NH} + \text{HO}_2$. The reaction leading to the hydroxyl radical was estimated to be five orders of magnitude faster than the competing VII-7. For the HNO intermediate species, the oxidation reaction preferentially would occur before the reduction reaction. The NH intermediate species also shows that the oxidation reaction was five orders of magnitude greater than the reduction reaction and all NH intermediates would react to form NO or NO_2 and be measured by the analyzer.

The evaluation assumes no mass transfer limitations. The reaction tube construction allows for heavy mixing in an excess oxygen environment. The nitrogen concentrations were estimated for a typical sample to be analyzed. The oxygen

concentration was also estimated based on the analyzer method employed. Because of the extreme excess of oxygen in the system, it is thought that all of the nitrogen bound in the samples will be released and converted to NO or NO₂ to be detected with the chemiluminescence analyzer. This was shown kinetically to hold. No problems were expected with the analysis and the experiments that were planned.

APPENDIX VIII: GPNP NITROGEN DATA COLLECTED UNDER PYROLYSIS CONDITIONS

The data provided in this appendix represents the data collected under pyrolysis conditions. This data includes the following: oxidative pyrolysis data, nonoxidative pyrolysis data, data for matrices effects, and static inert pyrolysis data for various model fuel nitrogen species.

Each set of data is presented along with the statistical summaries. Error estimates can be taken from the correlation coefficients in the plots as well as the statistical standard deviation and coefficient of variation.

The sample numbers in the data tables, such as N4097022, are the same as the computer data acquisition (CDA) file names. The N identifies the sample as a nitrogen release profile type of data file. The 4 represents the lab notebook #4264. The next three digits are the page number within the notebook where the data can be found and the last three digits are the sample number on that page. The last digit represents the number of the replicate. For the example, the values listed for the N4097022 sample would be found in notebook 4264 on page 97 as sample 2, replicate 2.

Table VIII-1. Oxidative pyrolysis data for nitrogen species.

Method Used:	5	PMT Voltage:	825
O ₂ to O ₃ :	30 ml/min	Furnace Temperature:	1100° C
O ₂ to pyro:	365 ml/min	Gain Setting:	HI
O ₂ to inlet:	20 ml/min	Gain Factor:	X1
He to inlet:	145 ml/min	Heating Program #:	6
Nitrogen Species:	proline	Matrix:	H ₂ O

<u>Sample #</u>	<u>Sample ID</u>	<u>Sample Vol</u> <u>(μl)</u>	<u>Known N</u> <u>Mass (μg)</u>	<u>Response</u> <u>Counts</u>	<u>CDA Sum</u> <u>Response</u>
N4130081	~1000 ppm N	5	4.954	97475	172.2901
N4130082	~1000 ppm N	5	4.954	100143	177.41667
N4130083	~1000 ppm N	5	4.954	102596	181.4205
N4130084	~1000 ppm N	5	4.954	110064	194.3844
N4130091	~750 ppm N	5	3.789	76342	134.7656
N4130092	~750 ppm N	5	3.789	79810	140.8687
N4130093	~750 ppm N	5	3.789	80764	142.5533
N4130101	~750 ppm N	5	3.789	78770	139.331
N4130102	~750 ppm N	5	3.789	77183	136.1569
N4130103	~750 ppm N	5	3.789	83593	147.7289

<u>Sample #</u>	<u>Ave. Counts</u>	<u>n</u>	<u>SD</u>	<u>RSD (%)</u>
N413008_	102570	4	5416	5.28
N413009_	78972	3	2327	2.95
N413010_	79849	3	3339	4.18

Nitrogen Species: pyrazine Matrix: H₂O

<u>Sample #</u>	<u>Sample ID</u>	<u>Sample Vol</u> <u>(μl)</u>	<u>Known N</u> <u>Mass (μg)</u>	<u>Response</u> <u>Counts</u>	<u>CDA Sum</u> <u>Response</u>
N4130151	~500 ppm N	5	2.4857	17480	30.2004*
N4130152	~500 ppm N	5	2.4857	27443	47.9004
N4130153	~500 ppm N	5	2.4857	38787	67.9198
N4130154	~500 ppm N	5	2.4857	24291	42.2368
N4130155	~500 ppm N	5	2.4857	4837	8.2522*
N4130156	~500 ppm N	5	2.4857	36032	63.0126

*Note: These points have not been used in the analysis, because they are in error experimentally or can be rejected statistically .

<u>Sample #</u>	<u>Ave. Counts</u>	<u>n</u>	<u>SD</u>	<u>RSD (%)</u>
N413015_	31638	4	3880	21.75

Table VIII-1. (cont.) Oxidative pyrolysis data for nitrogen species.

Method Used:	5	PMT Voltage:	825
O ₂ to O ₃ :	30 ml/min	Furnace Temperature:	1100° C
O ₂ to pyro:	365 ml/min	Gain Setting:	HI
O ₂ to inlet:	20 ml/min	Gain Factor:	X1
He to inlet:	145 ml/min	Heating Program #:	6
Nitrogen Species: proline		Matrix:	H ₂ O

Sample #	Sample ID	Sample Vol (μ l)	Known N Mass (μ g)	Response Counts	CDA Sum Response
N4130111	~750 ppm N	5	3.789	81365	143.8475
N4130112	~750 ppm N	5	3.789	77859	137.6214
N4130113	~750 ppm N	5	3.789	73960	130.7373
N4130121	~1000 ppm N	5	4.954	93719	165.6981
N4130122	~1000 ppm N	5	4.954	95316	168.2124
N4130123	~1000 ppm N	5	4.954	92136	162.8906
N4130131	~500 ppm N	5	2.564	53227	93.8227
N4130132	~500 ppm N	5	2.564	55898	98.4371
N4130133	~500 ppm N	5	2.564	58180	102.4896
N4133021	~500 ppm N	5	2.564	58470	102.5875
N4133022	~500 ppm N	5	2.564	56466	98.9988
N4133023	~500 ppm N	5	2.564	56806	99.7312
N4135181	~500 ppm N	5	2.564	50700	89.3066
N4135182	~500 ppm N	5	2.564	53785	94.6527
N4135183	~500 ppm N	5	2.564	52855	93.066

Sample #	Ave. Counts	n	SD	RSD (%)
N413011_	77728	3	3704	4.77
N413012_	93724	3	1590	1.70
N413013_	55768	3	2479	4.45
N413302_	57247	3	1072	1.87
N413518_	52447	3	1582	3.02

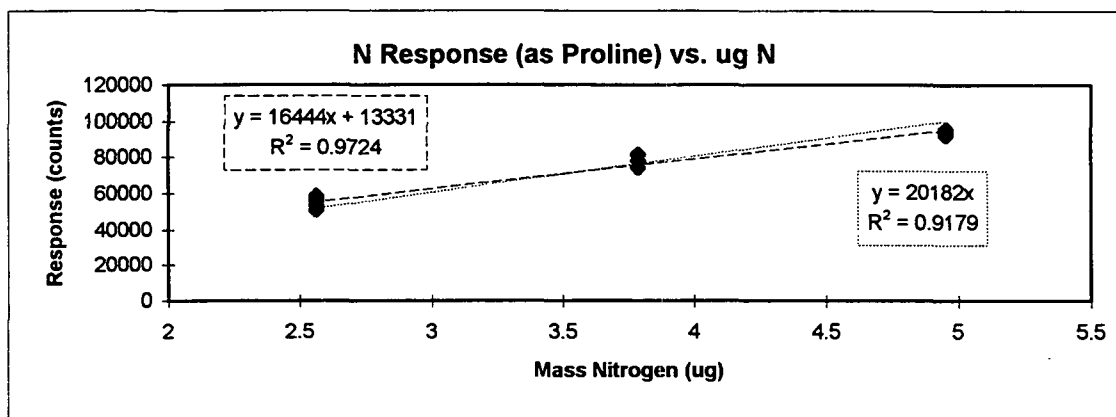


Table VIII-1. (cont.) Oxidative pyrolysis data for nitrogen species.

Method Used:	5	PMT Voltage:	825
O ₂ to O ₃ :	30 ml/min	Furnace Temperature:	1100° C
O ₂ to pyro:	365 ml/min	Gain Setting:	HI
O ₂ to inlet:	20 ml/min	Gain Factor:	X1
He to inlet:	145 ml/min	Heating Program #:	2
Nitrogen Species:	glutamic acid	Matrix:	H ₂ O

<u>Sample #</u>	<u>Sample ID</u>	<u>Sample Vol</u> <u>(μl)</u>	<u>Known N</u> <u>Mass (μg)</u>	<u>Response</u> <u>Counts</u>	<u>CDA Sum</u> <u>Response</u>
N4130141	~500 ppm N	5	2.4791	55978	98.2666
N4130142	~500 ppm N	5	2.4791	52759	92.7977
N4130143	~500 ppm N	5	2.4791	55821	97.8268
N4133011	~500 ppm N	5	2.4791	57558	101.1232
N4133012	~500 ppm N	5	2.4791	55849	97.7784
N4133013	~500 ppm N	5	2.4791	56221	98.6324
N4135191	~500 ppm N	5	2.4791	55.153	96.9969
N4135192	~500 ppm N	5	2.4791	52898	92.968
N4135193	~500 ppm N	5	2.4791	51433	90.4053
N4136281	~500 ppm N	5	2.4791	50035	87.7687
N4136282	~500 ppm N	5	2.4791	53775	94.1403
N4136283	~500 ppm N	5	2.4791	53987	94.7754

<u>Sample #</u>	<u>Ave. Counts</u>	<u>n</u>	<u>SD</u>	<u>RSD (%)</u>
N413014_	54853	3	1815	3.31
N413301_	56543	3	899	1.59
N413519_	53161	3	1873	3.52
N413628_	52599	3	2223	4.23

Nitrogen Species: pyrazine Matrix: H₂O

<u>Sample #</u>	<u>Sample ID</u>	<u>Sample Vol</u> <u>(μl)</u>	<u>Known N</u> <u>Mass (μg)</u>	<u>Response</u> <u>Counts</u>	<u>CDA Sum</u> <u>Response</u>
N4134121	~500 ppm N	5	2.4857	44536	78.3444
N4134122	~500 ppm N	5	2.4857	45078	79.1744
N4134123	~500 ppm N	5	2.4857	44307	77.7343

<u>Sample #</u>	<u>Ave. Counts</u>	<u>n</u>	<u>SD</u>	<u>RSD (%)</u>
N413412_	44641	3	396	0.89

Table VIII-2. Inert (non-oxidative) pyrolysis data for nitrogen species.

Method Used:	5	PMT Voltage:	825
O ₂ to O ₃ :	30 ml/min	Furnace Temperature:	1100° C
O ₂ to pyro:	365 ml/min	Gain Setting:	HI
O ₂ to inlet:	0 ml/min	Gain Factor:	X1
He to inlet:	165 ml/min	Heating Program #:	2
Nitrogen Species:	proline	Matrix:	H ₂ O

Sample #	Sample ID	Sample Vol (μ l)	Known N Mass (μ g)	Response Counts	CDA Sum Response
N4133031	~500 ppm N	5	2.564	56820	99.7551
N4133032	~500 ppm N	5	2.564	55323	97.072
N4133033	~500 ppm N	5	2.564	56799	99.9751
N4133041	~750 ppm N	5	3.789	75146	132.5679
N4133042	~750 ppm N	5	3.789	78889	138.9402
N4133043	~750 ppm N	5	3.789	77140	136.1328
N4133051	~1000 ppm N	5	4.954	90779	160.0341
N4133052	~1000 ppm N	5	4.954	92930	164.16
N4133053	~1000 ppm N	5	4.954	90951	160.4728

Sample #	Ave. Counts	n	SD	RSD (%)
N413303_	56314	3	858	1.52
N413304_	77058	3	1873	2.43
N413305_	91554	3	1195	1.31

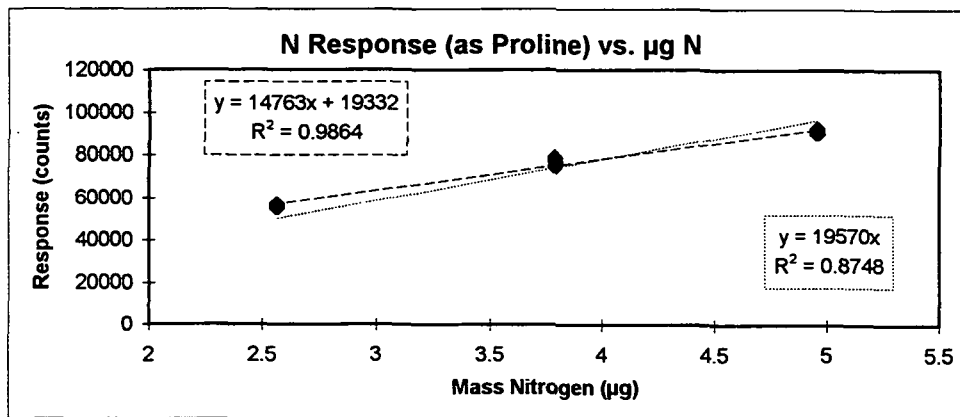


Table VIII-2. (cont.) Inert (nonoxidative) pyrolysis data for nitrogen species.

Method Used:	5	PMT Voltage:	825
O ₂ to O ₃ :	30 ml/min	Furnace Temperature:	1100° C
O ₂ to pyro:	365 ml/min	Gain Setting:	HI
O ₂ to inlet:	0 ml/min	Gain Factor:	X1
He to inlet:	165 ml/min	Heating Program #:	2
Nitrogen Species: pyrazine		Matrix:	H ₂ O

<u>Sample #</u>	<u>Sample ID</u>	<u>Sample Vol</u> <u>(μl)</u>	<u>Known N</u> <u>Mass (μg)</u>	<u>Response</u> <u>Counts</u>	<u>CDA Sum</u> <u>Response</u>
N4131161	~500 ppm N	5	2.4857	21894	38.2573
N4131162	~500 ppm N	5	2.4857	17016	29.785
N4131163	~500 ppm N	5	2.4857	26256	46.0935
N4131164	~500 ppm N	5	2.4857	36967	65.2343
N4133071	~500 ppm N	5	2.4857	32127*	55.9569
N4133072	~500 ppm N	5	2.4857	33460	58.3738
N4133073	~500 ppm N	5	2.4857	43758	76.9532
N4133074	~500 ppm N	5	2.4857	41845	73.34
N4133081	~500 ppm N	5	2.4857	36808	64.5263
N4133082	~500 ppm N	5	2.4857	31355	55.0783
N4133083	~500 ppm N	5	2.4857	28570	50.2199
N4134141	~500 ppm N	5	2.4857	30740*	53.6378
N4134142	~500 ppm N	5	2.4857	41393	72.5839
N4134143	~500 ppm N	5	2.4857	41545	73.0957
N4134144	~500 ppm N	5	2.4857	36205	63.1591
N4134145	~500 ppm N	5	2.4857	25860*	45.0444

*Note: These points have not been used in the analysis, because they are in error experimentally or can be rejected statistically .

<u>Sample #</u>	<u>Ave. Counts</u>	<u>n</u>	<u>SD</u>	<u>RSD (%)</u>
N413116_	25556	4	8476	33.2
N413307_	39688	3	5476	13.8
N413308_	32245	3	4190	13.0
N413414_	39714	3	3040	7.65

Nitrogen Species: glutamic acid Matrix: H₂O

<u>Sample #</u>	<u>Sample ID</u>	<u>Sample Vol</u> <u>(μl)</u>	<u>Known N</u> <u>Mass (μg)</u>	<u>Response</u> <u>Counts</u>	<u>CDA Sum</u> <u>Response</u>
N4133061	~500 ppm N	5	2.4791	54461	95.2625
N4133062	~500 ppm N	5	2.4791	53617	93.7491
N4133063	~500 ppm N	5	2.4791	54957	96.2398

<u>Sample #</u>	<u>Ave. Counts</u>	<u>n</u>	<u>SD</u>	<u>RSD (%)</u>
N413306_	54345	3	677	1.25

Table VIII-3. Inert pyrolysis data for nitrogen species; effect of matrices composition.

Method Used:	5	PMT Voltage:	825
O2 to O3:	30 ml/min	Furnace Temperature:	1100° C
O2 to pyro:	365 ml/min	Gain Setting:	HI
O2 to inlet:	0 ml/min	Gain Factor:	X1
He to inlet:	165 ml/min	Heating Program #:	2
Nitrogen Species:	glutamic acid	Matrix:	As indicated

<u>Sample #</u>	<u>Sample ID</u>	<u>Sample Vol</u> <u>(μl)</u>	<u>Known N</u> <u>Mass (μg)</u>	<u>Response</u> <u>Counts</u>	<u>CDA Sum</u> <u>Response</u>	<u>Matrix ID</u>
N4135201	~500 ppm N	5	2.4985	30967	53.7358	0.1N NaOH
N4135202	~500 ppm N	5	2.4985	33841	59.1309	0.1N NaOH
N4135203	~500 ppm N	5	2.4985	34034	59.1309	0.1N NaOH
N4135211	~500 ppm N	5	2.4958	31836	55.1508	0.2N NaOH
N4135212	~500 ppm N	5	2.4958	32808	57.1294	0.2N NaOH
N4135213	~500 ppm N	5	2.4958	34160	59.1553	0.2N NaOH
N4135221	~500 ppm N	5	2.5085	26725	46.0211	1.0N NaOH
N4135222	~500 ppm N	5	2.5085	24103	41.2117	1.0N NaOH
N4135223	~500 ppm N	5	2.5085	26095	44.971	1.0N NaOH
N4135231	~500 ppm N	5	2.5434	37283	64.9421	0.2N Na ₂ CO ₃
N4135232	~500 ppm N	5	2.5434	36980	64.4544	0.2N Na ₂ CO ₃
N4135233	~500 ppm N	5	2.5434	37192	64.7461	0.2N Na ₂ CO ₃
N4136241	~500 ppm N	5	2.5120	52201	91.2594	0.2N Na ₂ SO ₄
N4136242	~500 ppm N	5	2.5120	48104	83.9595	0.2N Na ₂ SO ₄
N4136243	~500 ppm N	5	2.5120	62405	109.375	0.2N Na ₂ SO ₄
N4136251	~500 ppm N	5	2.4965	35227	61.45	0.1N NaOH & 0.1N Na ₂ CO ₃
N4136252	~500 ppm N	5	2.4965	36019	62.5986	0.1N NaOH & 0.1N Na ₂ CO ₃
N4136253	~500 ppm N	5	2.4965	36939	64.0627	0.1N NaOH & 0.1N Na ₂ CO ₃
N4136261	~500 ppm N	5	2.478	35995	62.5251	0.1N NaOH & 0.1N Na ₂ SO ₄
N4136262	~500 ppm N	5	2.478	38956	67.9208	0.1N NaOH & 0.1N Na ₂ SO ₄
N4136263	~500 ppm N	5	2.478	38680	67.1871	0.1N NaOH & 0.1N Na ₂ SO ₄
N4136271	~500 ppm N	5	2.4925	10004*	63.3792	0.1N NaOH & 0.1N Na ₂ S
N4136272	~500 ppm N	5	2.4925	41041	71.4845	0.1N NaOH & 0.1N Na ₂ S
N4136273	~500 ppm N	5	2.4925	39207	68.2619	0.1N NaOH & 0.1N Na ₂ S
N4136274	~500 ppm N	5	2.4925	40357	70.3613	0.1N NaOH & 0.1N Na ₂ S

*Note: These points have not been used in the analysis, because they are in error experimentally or can be rejected statistically .

<u>Sample #</u>	<u>Ave. Counts</u>	<u>n</u>	<u>SD</u>	<u>RSD (%)</u>
N413520_	32947	3	1718	5.21
N413521_	32935	3	1590	3.54
N413522_	25641	3	2479	5.34
N413523_	37152	3	1072	0.42
N413624_	54237	3	7365	13.58
N413625_	36062	3	857	2.38
N413626_	37877	3	1636	4.32
N413627_	40202	3	927	2.31

Table VIII-4. Oxidative Proline Pyrolysis Data, NaCl Matrix

Method Used:	5	PMT Voltage:	825
O2 to O3:	30 ml/min	Furnace Temperature:	1100° C
O2 to pyro:	365 ml/min	Gain Setting:	HI
O2 to inlet:	20 ml/min	Gain Factor:	X1
He to inlet:	145 ml/min	Heating Program #:	2
Nitrogen Species:	proline	Matrix:	H2O w/ 5 µl 2597 ppm Cl as NaCl

<u>Sample #</u>	<u>Sample ID</u>	<u>Sample Vol</u> <u>(µl)</u>	<u>Known N</u> <u>Mass (µg)</u>	<u>Response</u> <u>Counts</u>	<u>CDA Sum</u> <u>Response</u>
N4149161	~500 ppm N	5	2.564	49497	87.1086
N4149162	~500 ppm N	5	2.564	43815	77.1238
N4149163	~500 ppm N	5	2.564	53562	93.7741
N4149164	~500 ppm N	5	2.564	53626	94.1892

<u>Sample #</u>	<u>Ave. Counts</u>	<u>n</u>	<u>SD</u>	<u>RSD (%)</u>
N414916_	50125	4	4629	9.23

Method Used:	5	PMT Voltage:	825
O2 to O3:	30 ml/min	Furnace Temperature:	1100° C
O2 to pyro:	365 ml/min	Gain Setting:	HI
O2 to inlet:	20 ml/min	Gain Factor:	X1
He to inlet:	145 ml/min	Heating Program #:	2
Nitrogen Species:	proline	Matrix:	H2O w/ 5 µl 2597 ppm Cl as NaCl

<u>Sample #</u>	<u>Sample ID</u>	<u>Sample Vol</u> <u>(µl)</u>	<u>Known N</u> <u>Mass (µg)</u>	<u>Response</u> <u>Counts</u>	<u>CDA Sum</u> <u>Response</u>
N4149171	~500 ppm N	5	2.564	50282	88.3543
N4149172	~500 ppm N	5	2.564	55263	97.2411
N4149173	~500 ppm N	5	2.564	52255	91.9187

<u>Sample #</u>	<u>Ave. Counts</u>	<u>n</u>	<u>SD</u>	<u>RSD (%)</u>
N414918_	52600	3	2508	4.77

Table VIII-5. Stagnant, Nonoxidative Glutamic Acid Pyrolysis Data, Effect of Delay Time

Method Used: 5 PMT Voltage: 825
 O2 to O3: 30 ml/min Furnace Temperature: 1100° C
 O2 to pyro: 365 ml/min Gain Setting: HI
 O2 to inlet: 0 ml/min Gain Factor: X1
 He to inlet: 165 ml/min Heating Program #: 2
 Nitrogen Species: Glut. Acid Matrix: H2O

*Stagnant Pyrolysis; He flow on at Ramp2, Delay2 = 2 minutes, quartz boat 2" from combustion entrance.

Sample #	Sample ID	Sample Vol (ul)	Known N Mass (ug)	Response Counts	CDA Sum Response	1st peak Counts	1st peak CDA Sum	2nd peak Counts	2nd peak CDA Sum
N4152131	~500 ppm N	5	2.4791	4839	10.8154	164	0.3172	4675	8.1543
N4152132	~500 ppm N	5	2.4791	6064	10.0829	381	0.61	5683	9.7653
N4152133	~500 ppm N	5	2.4791	6093	11.2058	350	0.6344	5743	9.6188
N4152134	~500 ppm N	5	2.4791	6874	11.0595	1388	2.1472	5486	9.3748
Sample #	Ave. Counts	n	SD	RSD (%)					
N415213_	5967	4	840	14.09					

Method Used: 5 PMT Voltage: 825
 O2 to O3: 30 ml/min Furnace Temperature: 1100° C
 O2 to pyro: 365 ml/min Gain Setting: HI
 O2 to inlet: 0 ml/min Gain Factor: X1
 He to inlet: 165 ml/min Heating Program #: 2
 Nitrogen Species: Glut. Acid Matrix: H2O

*Stagnant Pyrolysis; He flow on at Ramp2, Delay2 = 2 minutes, quartz boat 2" from combustion entrance.

Sample #	Sample ID	Sample Vol (ul)	Known N Mass (ug)	Response Counts	CDA Sum Response	1st peak Counts	1st peak CDA Sum	2nd peak Counts	2nd peak CDA Sum
N4153181	~500 ppm N	5	2.4791	7336	12.4743	1222	1.9764	6114	10.4979
N4153182	~500 ppm N	5	2.4791	8346	13.8402	2657	4.1724	5689	9.6678
N4153183	~500 ppm N	5	2.4791	6976	11.7173	1520	2.3668	5456	9.3505
Sample #	Ave. Counts	n	SD	RSD (%)					
N415318_	7552	3	710	9.39					

Method Used: 5 PMT Voltage: 825
 O2 to O3: 30 ml/min Furnace Temperature: 1100° C
 O2 to pyro: 365 ml/min Gain Setting: HI
 O2 to inlet: 0 ml/min Gain Factor: X1
 He to inlet: 165 ml/min Heating Program #: 2
 Nitrogen Species: Glut. Acid Matrix: H2O

*Stagnant Pyrolysis; He flow on at Ramp2, Delay2 = 4 minutes, quartz boat 2" from combustion entrance.

Sample #	Sample ID	Sample Vol (ul)	Known N Mass (ug)	Response Counts	CDA Sum Response	1st peak Counts	1st peak CDA Sum	2nd peak Counts	2nd peak CDA Sum
N4153191	~500 ppm N	5	2.4791	7254	11.9851	2464	3.7821	4790	8.203
N4153192	~500 ppm N	5	2.4791	5796	9.4467	1760	2.6352	4036	6.8115
N4153193	~500 ppm N	5	2.4791	6082	10.1304	1587	2.4156	4495	7.7148
N4153194	~500 ppm N	5	2.4791	4531	7.6417	1	0.0244	4530	7.6173
Sample #	Ave. Counts	n	SD	RSD (%)					
N415319_	5916	4	1118	18.90					

Table VIII-5. (cont.) Stagnant, Nonoxidative Glutamic Acid Pyrolysis Data, Effect of Delay Time

Method Used: 5 PMT Voltage: 825
 O2 to O3: 30 ml/min Furnace Temperature: 1100° C
 O2 to pyro: 365 ml/min Gain Setting: HI
 O2 to inlet: 0 ml/min Gain Factor: X1
 He to inlet: 165 ml/min Heating Program #: 2
 Nitrogen Species: Glut. Acid Matrix: H2O

**Stagnant Pyrolysis; He flow on at Ramp2, Delay2 = 2 minutes, quartz boat 2" from combustion entrance.*

Sample #	Sample ID	Sample Vol (ul)	Known N Mass (ug)	Response Counts	CDA Sum Response	1st peak Counts	1st peak CDA Sum	2nd peak Counts	2nd peak CDA Sum
N4152111	~500 ppm N	5	2.4791	8438	14.4271	1884	2.9524	6554	11.4747
N4152112	~500 ppm N	5	2.4791	6935	11.6928	1384	2.196	5551	9.4968
N4152113	~500 ppm N	5	2.4791	8432	14.5004	1741	2.806	6691	11.6944
N4152114	~500 ppm N	5	2.4791	6964	11.9122	1515	2.5376	5449	9.3746

Sample #	Ave. Counts	n	SD	RSD (%)
N415211_	7692	3	858	11.15

Method Used: 5 PMT Voltage: 825
 O2 to O3: 30 ml/min Furnace Temperature: 1100° C
 O2 to pyro: 365 ml/min Gain Setting: HI
 O2 to inlet: 0 ml/min Gain Factor: X1
 He to inlet: 165 ml/min Heating Program #: 2
 Nitrogen Species: Glut. Acid Matrix: H2O

**Stagnant Pyrolysis; He flow on at Ramp2, Delay2 = 4 minutes, quartz boat 2" from combustion entrance.*

Sample #	Sample ID	Sample Vol (ul)	Known N Mass (ug)	Response Counts	CDA Sum Response	1st peak Counts	1st peak CDA Sum	2nd peak Counts	2nd peak CDA Sum
N4152121	~500 ppm N	5	2.4791	8325	14.1607	4185	6.8852	4140	7.2755
N4152122	~500 ppm N	5	2.4791	6184	10.5209	1535	2.3912	4649	8.1297
N4152123	~500 ppm N	5	2.4791	7428	12.5724	3124	5.1993	4304	7.3731
N4152124	~500 ppm N	5	2.4791	6534	10.7646	2104	3.2452	4430	7.5194
N4152125	~500 ppm N	5	2.4791	7420	12.3293	3570	5.7132	3850	6.6161

Sample #	Ave. Counts	n	SD	RSD (%)
N415212_	7178	5	842	11.73

Table VIII-6. Stagnant inert pyrolysis data for nitrogen species; He carrier gas on at 400°C.

Method Used: 5 PMT Voltage: 825
 O₂ to O₃: 30 ml/min Furnace Temperature: 1100° C
 O₂ to pyro: 365 ml/min Gain Setting: HI
 O₂ to inlet: 0 ml/min Gain Factor: X1
 He to inlet: 165 ml/min Heating Program #: 2
 Nitrogen Species: glutamic acid Matrix: H₂O

<u>Sample #</u>	<u>Sample ID</u>	<u>Sample Vol</u> <u>(μl)</u>	<u>Known N</u> <u>Mass (μg)</u>	<u>Response</u> <u>Counts</u>	<u>CDA Sum</u> <u>Response</u>	<u>1st peak</u> <u>Counts</u>	<u>1st peak</u> <u>CDA Sum</u>	<u>2nd peak</u> <u>Counts</u>	<u>2nd peak</u> <u>CDA Sum</u>
N4135161	~500 ppm N	5	2.4791	24633	42.1388	10821	18.1398	13812	13.999
N4135162	~500 ppm N	5	2.4791	18531	31.9093	4535	7.5685	13996	24.3408
N4135163	~500 ppm N	5	2.4791	25114	43.1396	10333	17.3584	14781	25.7812
N4135164	~500 ppm N	5	2.4791	24452	42.2118	9907	16.2814	14545	25.3904

Nitrogen Species: proline Matrix: H₂O

<u>Sample #</u>	<u>Sample ID</u>	<u>Sample Vol</u> <u>(μl)</u>	<u>Known N</u> <u>Mass (μg)</u>	<u>Response</u> <u>Counts</u>	<u>CDA Sum</u> <u>Response</u>	<u>1st peak</u> <u>Counts</u>	<u>1st peak</u> <u>CDA Sum</u>	<u>2nd peak</u> <u>Counts</u>	<u>2nd peak</u> <u>CDA Sum</u>
N4135171	~500 ppm N	5	2.564	28538	49.678	12981	22.2896	15557	27.0506
N4135172	~500 ppm N	5	2.564	28878	49.9755	15231	26.2208	13647	23.7547
N4135173	~500 ppm N	5	2.564	30859	53.6132	15890	27.4413	14969	26.1719

Table VIII-7. Stagnant, Nonoxidative Pyrazine Pyrolysis Data, Effect of Delay Time

Method Used: 5 PMT Voltage: 825
 O2 to O3: 30 ml/min Furnace Temperature: 1100° C
 O2 to pyro: 365 ml/min Gain Setting: HI
 O2 to inlet: 0 ml/min Gain Factor: X1
 He to inlet: 165 ml/min Heating Program #: 2
 Nitrogen Species: pyrazine Matrix: H2O

**Stagnant Pyrolysis; He flow on at Ramp2, Delay2 = 2 minutes, quartz boat 2" from combustion entrance.*

Sample #	Sample ID	Sample Vol (ul)	Known N Mass (ug)	Response Counts	CDA Sum Response	1st peak Counts	1st peak CDA Sum	2nd peak Counts	2nd peak CDA Sum
N4153151	~500 ppm N	5	2.4857	12239	20.2618	8212	13.4746	4027	6.7872
N4153152	~500 ppm N	5	2.4857	11927	19.3596	7644	12.0597	4283	7.2999
N4153153	~500 ppm N	5	2.4857	12507	20.6771	8310	13.6214	4197	7.0557

Sample #	Ave. Counts	n	SD	RSD (%)
N415315_	12224	3	289	2.37

Method Used: 5 PMT Voltage: 825
 O2 to O3: 30 ml/min Furnace Temperature: 1100C
 O2 to pyro: 365 ml/min Gain Setting: HI
 O2 to inlet: 0 ml/min Gain Factor: X1
 He to inlet: 165 ml/min Heating Program #: 2
 Nitrogen Species: pyrazine Matrix: H2O

**Stagnant Pyrolysis; He flow on at Ramp2, Delay2 = 2 minutes, quartz boat 2" from combustion entrance.*

Sample #	Sample ID	Sample Vol (ul)	Known N Mass (ug)	Response Counts	CDA Sum Response	1st peak Counts	1st peak CDA Sum	2nd peak Counts	2nd peak CDA Sum
N4153162	~500 ppm N	5	2.4857	8809	14.3536	6280	10.0813	2529	4.2723
N4153163	~500 ppm N	5	2.4857	7720	12.5715	5331	8.6409	2389	3.9306
N4153164	~500 ppm N	5	2.4857	9227	15.2817	6581	10.741	2646	4.5407

Sample #	Ave. Counts	n	SD	RSD (%)
N415316_	8585	3	778	9.06

APPENDIX IX: KINETICS FOR GPNP CONVERSION

This appendix contains further calculations and data to support the kinetic evaluation completed for the static inert pyrolysis of proline nitrogen for the conversion of GPNP (gas phase NO_x and NO_x precursors) to N_2 . Included are the following: 1) calculations to verify the assumption of a homogeneous gas phase, 2) evaluation of the effect of dispersion including calculation of the Reynolds number, the vessel dispersion number and the kinetics for first-order irreversible reaction with dispersion; and 3) data for determination of the kinetic parameters including calibration data, and data for the effect of temperature and delay or residence time on the conversion of the GPNP used to determine the conversions.

VERIFICATION OF HOMOGENEOUS GAS PHASE

An assumption was made in the kinetic data that gas phase was homogeneous, i.e. both the reacting nitrogen gases and the helium carrier gas were well mixed. The assumption was verified by calculating the molar flux of the nitrogen gas into the helium within the pyrolysis reactor tube. The molar flux equation was used for steady-state diffusion of A (taken to be NH_3) through nondiffusing B (helium) and is given in the equation below.¹⁰³

$$N_A = \frac{D_{AB}P_t}{RTz\bar{p}_{B,M}}(\bar{p}_{A1} - \bar{p}_{A2}) \quad (\text{IX-1})$$

where N_A = molar flux relative to a fixed surface, $\text{mol/m}^2\cdot\text{sec}$,

D_{AB} = diffusivity of A in B, m^2/sec ,

R = gas constant, 1.9872 cal/mol·K

T = temperature, K

z = distance in z direction, m

p_t = total pressure, N/m²

$\bar{p}_{B,M}$ = partial pressure of B, N/m²

\bar{p}_{A1} = partial pressure of A at zero distance, N/m²

\bar{p}_{A2} = partial pressure of A at maximum distance, N/m²

Application of the ideal gas law,

$$\frac{p_t}{RT} = \frac{n}{V} = C \quad (\text{IX-2})$$

yields

$$N_A = \frac{D_{AB}C}{z\bar{p}_{B,M}}(\bar{p}_{A1} - \bar{p}_{A2}) \quad (\text{IX-3})$$

The diffusivity of A (NH₃) in B (helium) is estimated based on the kinetic theory of gases and is given in the following equation.¹⁰³

$$D_{AB} = \frac{10^{-4}(1.084 - 0.249\sqrt{1/M_A + 1/M_B})T^{3/2}\sqrt{1/M_A + 1/M_B}}{p_t(r_{AB})^2 f(\kappa T / \varepsilon_{AB})} \quad (\text{IX-4})$$

where M_A = molecular weight of A, g/mol,

M_B = molecular weight of B, g/mol,

r_{AB} = molecular separation at collision, nm = $(r_A + r_B)/2$

κ = Boltzmann's constant,

ε_{AB} = energy of molecular attraction = $\sqrt{\varepsilon_A \varepsilon_B}$,

The molecular separation and the energy of molecular attraction are determined from tabulated values for NH_3 and helium.¹⁰⁴ Thus, $r_{AB} = 0.2726 \text{ nm}$ and $\varepsilon_{AB}/\kappa = 75.537 \text{ K}$. At the reaction temperature of 300° C or 573 K , $\kappa T/\varepsilon_{AB} = 7.586$. The function of this value is obtained from the chart of the collision function for diffusion¹⁰⁵ such that $f(\kappa T/\varepsilon_{AB}) = f(7.586) = 0.39$. Finally, $\sqrt{1/M_A + 1/M_B} = 0.557$. Substitution of these values into Eq. IX-4 provides $D_{AB} = 2.444 \times 10^{-4} \text{ m}^2/\text{s}$.

Substitution of these values into Eq. IX-3 provides

$$\begin{aligned}
 N_A &= \frac{(2.444 \times 10^{-4} \text{ m}^2/\text{s})(0.0396 \text{ mol/L})(\bar{p}_{A1} - \bar{p}_{A2})}{(0.0508 \text{ m}) \bar{p}_{B,M}} \\
 &= 1.905 \times 10^{-4} \text{ mol/m}^2 \text{ s} \frac{(\bar{p}_{A1} - \bar{p}_{A2})}{\bar{p}_{B,M}}
 \end{aligned}
 \tag{IX-5}$$

The ratio of partial pressures is expected to be a very small number because the concentration of A, NH_3 , is much smaller than that of B, helium. Therefore, the molar flux, N_A , is said to be $< 1.905 \times 10^{-4} \text{ mol/m}^2 \text{ s}$. Then, dividing the flux by the concentration of A (0.0396 mol/L) and the distance z (0.07 m) it is calculated that diffusion will occur in less than 0.07 sec . Thus, the time for the nitrogen species to diffuse in the gas phase to a homogeneous mixture is negligible compared to the reactions which were $> 150 \text{ sec}$. Thus, the assumption made for the homogeneous gas phase for the kinetic calculations is valid.

EVALUATION OF THE EFFECT OF DISPERSION

An evaluation was made for the possibility of dispersion during GPNP nitrogen measurements to negate the assumption of a batch process with homogeneous gas-phase reactions. The outcome, which indicated the dispersion to be small and therefore, negligible, was derived by determination of the vessel dispersion number, D/uL , where D is the axial dispersion coefficient, u is the average volumetric flow rate in the reactor (cm^3/sec), and L is the reactor length (cm).⁹⁰ The experimental volumetric flow rate was $165 \text{ cm}^3/\text{sec}$ and the reactor length is 14 cm.

The axial dispersion coefficient, D , can be determined for low Reynolds numbers by

$$\sigma_{\theta}^2 = \frac{\sigma^2}{\bar{t}^2} = 2 \left(\frac{D}{uL} \right) \quad (\text{IX-6})$$

where σ_{θ}^2 = variance in dimensionless time,
 σ^2 = variance of the response curve, sec^2 , and
 \bar{t} = mean residence time in reactor, $= L/u = 22.91 \text{ sec}$.

The Reynolds number, N_{Re} , was calculated according to¹⁰⁶

$$N_{\text{Re}} = \frac{d\rho\bar{V}}{\mu} = \frac{d\bar{V}}{\nu} \quad (\text{IX-7})$$

where d = diameter of the reactor (2.1 cm),
 ρ = density of the liquid ($\rho_{\text{He}} = 0.17847 \text{ kg/m}^3$),

\bar{V} = average velocity, $\bar{V} = (\text{volumetric flow rate})/(\text{cross sectional surface area})$, 55.15 cm/sec,

μ = viscosity of the fluid (0.019 cP), and

ν = kinematic viscosity.

At reaction conditions (0.1223 MPa and 673 K), $N_{Re} = 1.813$. When $N_{Re} < 2000$, laminar flow is the governing regime. Therefore, the use of Eq. IX-6 to determine the vessel dispersion number is validated.

Because of the low Reynolds number and the likelihood that D/uL is small, the response curve, as seen in Fig. IX-1, can be used to determine the variance of the flow.

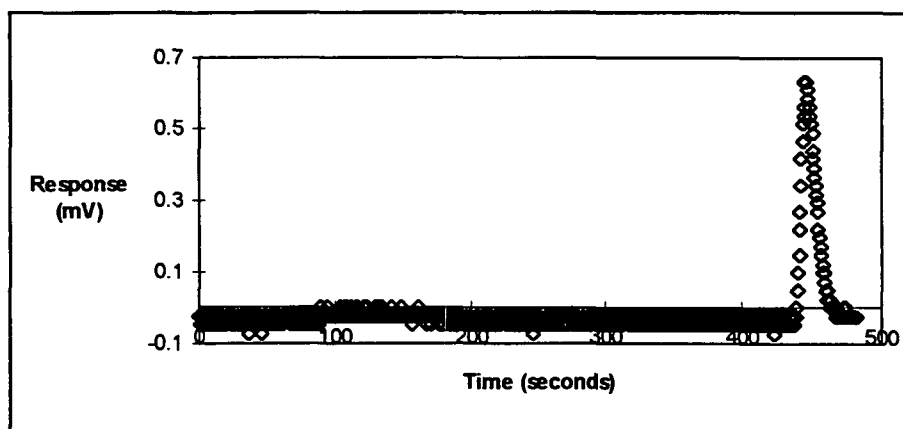


Figure IX-1. Total response curve for proline-nitrogen pyrolysis at $T = 673$ K.

Examining the response peak more closely in Fig. IX-2, it is observed that the curve follows quite closely the normal distribution. The variance and hence the vessel dispersion number can be obtained by following the properties of the normal curve.¹⁰⁰ By definition, one standard deviation, σ , on either side of the mean represents 68% of the

total curve area. By calculating the total curve area, and back calculating 34% of that total on either side of the mean, the distance of 2σ is achieved.

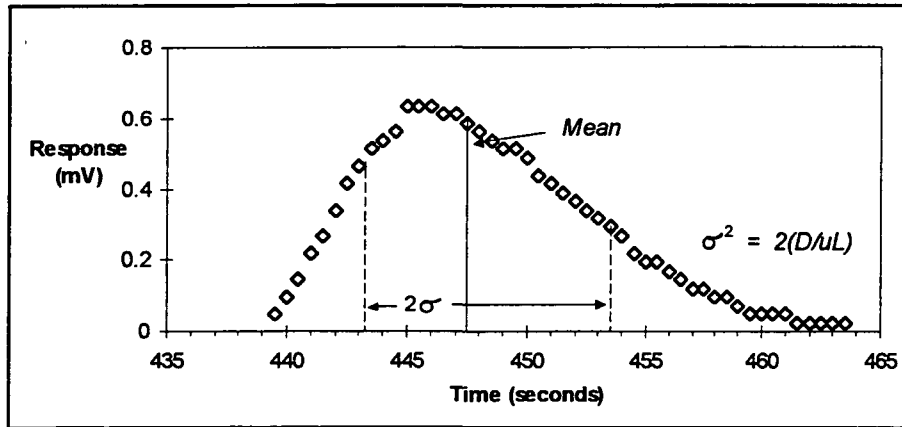


Figure IX-2. Response curve for proline-nitrogen pyrolysis at $T = 673$ for determination of the variance, σ^2 , and the vessel dispersion number, D/uL .

From Fig. IX-2, it is observed that the 2σ distance is 10.25 sec. Therefore, σ is 5.125 and $\sigma_\theta = 0.2237$. Employing Eq. IX-6, the vessel dispersion number then becomes

$$\frac{D}{uL} = \frac{\sigma_\theta^2}{2} = 0.0250 \quad (\text{IX-8})$$

A maximum error estimate of the vessel dispersion number is given by the relationship: error $< 5\%$ when $D/uL \leq 0.01$. For $D/uL = 0.025$, the maximum error $< 12.5\%$. Another evaluation of the vessel dispersion number indicates that as

$$\frac{D}{uL} \rightarrow 0 \quad (\text{IX-9})$$

negligible dispersion occurs; hence plug flow exists.

KINETICS FOR FIRST-ORDER REACTION WITH DISPERSION

To further validate the assumption of no dispersion, the kinetics for the first-order reaction with dispersion were calculated. The rate expression is given in Eq. IX-10 for the physical description presented in Fig. IX-3.

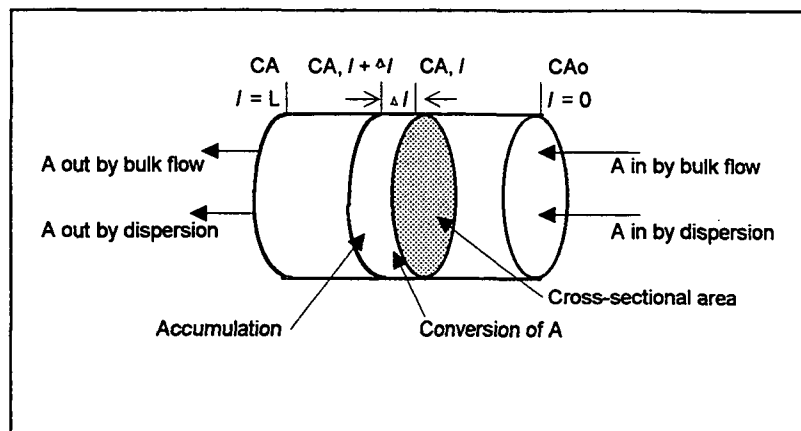


Fig. IX-3. Physical presentation of tube reactor for first-order reaction with dispersion.

The expression takes into account the reactant input and output due to bulk flow ($C_{A,l} uS$ and $C_{A,l+\Delta l} uS$), the input and output due to axial dispersion ($-(DS(dC_A/dl))_l$ and $-(DS(dC_A/dl))_{l+\Delta l}$), disappearance by reaction ($-r_A S \Delta l$), and accumulation (equals zero by the steady state approximation). Dividing each term by $S \Delta l$ yields

$$-r_A = u \frac{(C_{A,l+\Delta l} - C_{A,l})}{\Delta l} - D \frac{\left[\left(\frac{dC_A}{dl} \right)_{l+\Delta l} - \left(\frac{dC_A}{dl} \right)_l \right]}{\Delta l} \quad (\text{IX-10})$$

Application of the limits $\Delta l \rightarrow 0$ for the smooth continuous function of l gives

$$-kC_A = u \frac{dC_A}{dl} - D \frac{d^2C_A}{dl^2} \quad (\text{IX-11})$$

In dimensionless form, where $z = l/L$ and $\tau = \bar{t} = L/u = V/v$, Eq. IX-11 becomes

$$-k\tau C_A = \frac{D}{uL} \frac{d^2C_A}{dz^2} - \frac{dC_A}{dz} \quad (\text{IX-12})$$

This expression indicates the dependence of the disappearance of component A on the reaction rate group, $k\tau C_A$, and the dispersion group, D/uL , also known as the vessel dispersion number. The analytical solution to Eq. IX-12 is available in the literature for first order reactions.¹⁰⁷ The solution for reactors with entrance-exit boundary conditions is

$$\frac{C_A}{C_{Ao}} = \frac{4a \exp\left(\frac{1}{2} \frac{uL}{D}\right)}{(1+a)^2 \exp\left(\frac{a}{2} \frac{uL}{D}\right) - (1-a)^2 \exp\left(-\frac{a}{2} \frac{uL}{D}\right)} \quad (\text{IX-13})$$

where $a = \sqrt{1 + 4k\tau(D/uL)}$. Eq. IX-13 can be greatly simplified by dropping out the higher order terms if only small deviations from plug flow exists and the vessel dispersion number, D/uL , becomes small. Then, expansion of the exponential terms provides

$$\frac{C_A}{C_{Ao}} = \exp\left[-k\tau + (k\tau)^2 \frac{D}{uL}\right] \quad (\text{IX-14})$$

Plotting $\ln(C_A/C_{Ao})$ vs residence time, τ , yields Fig. IX-4. The good fit of the data to the straight line suggests the first-order rate expression with dispersion to be valid. As such, the temperature dependency was determined for the k value in the slope term of the

log of Eq. IX-14. The plot of these calculations are shown in Fig. IX-5 and the Arrhenius plot for the determination of the activation energy and the pre-exponential constant is provided in Fig. IX-6. The data used to generate these plots is given in Tables IX-1 and IX-2.

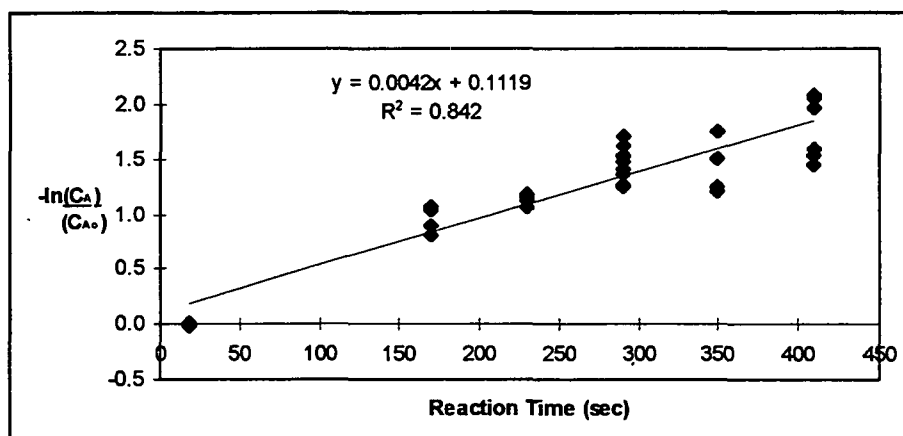


Figure IX-4. Test for first-order reaction with dispersion.

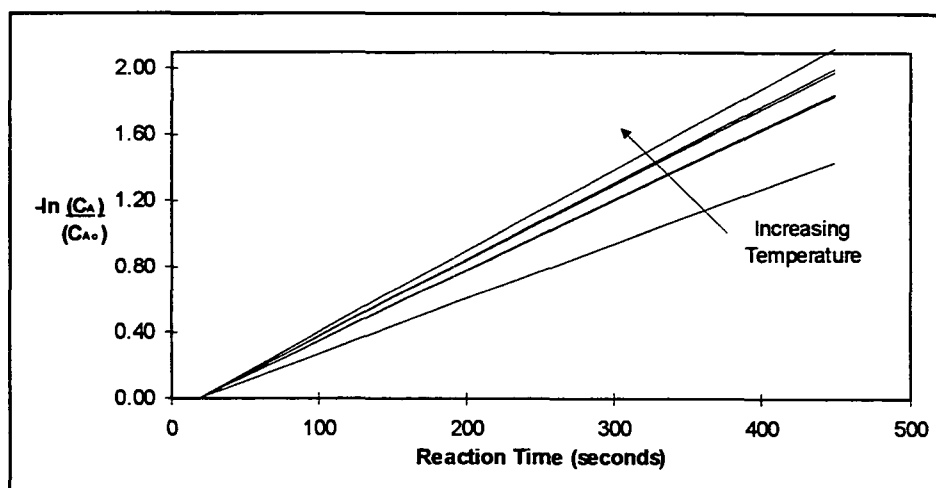


Figure IX-5. Temperature dependency of first-order rate equation accounting for dispersion.

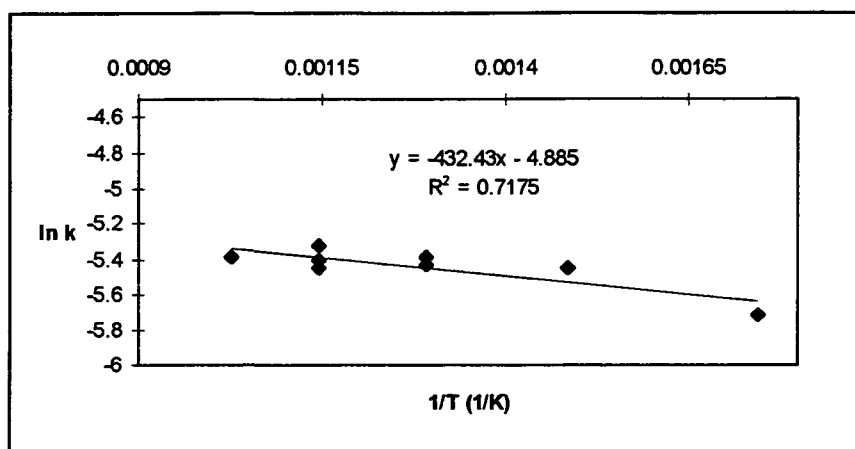


Figure IX-6. Arrhenius plot for determination of activation energy based on the dispersion "slope-k".

For the "slope-k" calculations, values obtained for E_a/R and for $\ln(k_0)$ indicate good agreement with those of the first-order rate expression without accounting for the dispersion. Only a one percent difference in the activation energy and a difference of about 4.7% in the pre-exponential constant. This follows a general rule of thumb which states that the real values agree well with those estimated as long as the vessel dispersion number is less than or equal to 0.05.¹⁰⁸ Thus, use of the simple first-order rate expression is valid.

Table IX-1. Sample data for determination of GPNP nitrogen concentration dependency at various reaction times.

Sample ID	C_{Ao} , Conc ($\mu\text{g N}/5 \mu\text{l}$)	C_A , Conc (mol/l)	$\frac{[C_A]}{[C_{Ao}]}$	$\ln\left(\frac{[C_A]}{[C_{Ao}]}\right)$	$-\ln(\)$	Rxn Time (sec)	T (K)
N4139061	2.7437	0.03917	20.3678	3.0140	-3.0140	0	673
N4139062	2.7531	0.03930	20.4376	3.0174	-3.0174	0	673
N4139063	2.8197	0.04025	20.9326	3.0413	-3.0413	0	673
N4139081	0.9888	0.01412	0.3568	-1.0307	1.0307	170	673
N4139082	1.2382	0.01768	0.4467	-0.8058	0.8058	170	673
N4139083	0.9504	0.01357	0.3429	-1.0704	1.0704	170	673
N4139084	1.1434	0.01632	0.4125	-0.8855	0.8855	170	673
N4139091	0.8550	0.01221	0.3085	-1.1761	1.1761	230	673
N4139093	0.9050	0.01292	0.3265	-1.1193	1.1193	230	673
N4139094	0.8748	0.01249	0.3156	-1.1532	1.1532	230	673
N4139095	0.9611	0.01372	0.3467	-1.0592	1.0592	230	673
N4139071	0.5926	0.00846	4.3993	1.4814	-1.4814	290	673
N4139072	0.7838	0.01119	5.8188	1.7611	-1.7611	290	673
N4139101	0.7974	0.01138	0.2877	-1.2459	1.2459	290	673
N4139102	0.7051	0.01007	0.2544	-1.3689	1.3689	290	673
N4139103	0.6348	0.00906	0.2290	-1.4739	1.4739	290	673
N4151021	0.5003	0.00714	5.9197	1.7783	-1.7783	290	673
N4151022	0.5468	0.00781	5.2341	1.6552	-1.6552	290	673
N4151023	0.6075	0.00867	4.7125	1.5502	-1.5502	290	673
N4140131	0.8261	0.01179	0.2981	-1.2105	1.2105	350	673
N4139111	0.7988	0.01140	4.0595	1.4011	-1.4011	350	673
N4139112	0.6097	0.00870	4.5096	1.5062	-1.5062	350	673
N4139114	0.4768	0.00681	3.5397	1.2640	-1.2640	350	673
N4151031	0.3545	0.00506	2.6316	0.9676	-0.9676	410	673
N4151032	0.3858	0.00551	2.8640	1.0522	-1.0522	410	673
N4151034	0.3433	0.00490	2.5486	0.9355	-0.9355	410	673
N4151051	0.7104	0.01014	5.2739	1.6628	-1.6628	290	673
N4151052	0.6805	0.00971	5.0514	1.6197	-1.6197	290	673
N4151053	0.7771	0.01109	5.7685	1.7524	-1.7524	290	673
N4151061	0.6530	0.00932	4.8478	1.5785	-1.5785	410	673
N4151062	0.5977	0.00853	4.4367	1.4899	-1.4899	410	673
N4151063	0.5603	0.00800	4.1595	1.4254	-1.4254	410	673

Table IX-2. Sample data for determination of GPNP temperature dependency.

Sample ID	Conc (ug N/5 ul)	Conc (mol/l)	$\frac{[C_A]}{[C_{Ao}]}$	$\ln\left(\frac{[C_A]}{[C_{Ao}]}\right)$	$-\ln()$	Rxn Time (sec)	T (K)
N4147071	0.5832	0.00833	0.2104	-1.5587	1.5587	450	573
N4147072	0.6692	0.00955	0.2414	-1.4212	1.4212	450	573
N4147073	0.7369	0.01052	0.2659	-1.3248	1.3248	450	573
N4147061	0.4474	0.00639	0.1614	-1.8238	1.8238	450	673
N4147063	0.4351	0.00621	0.1570	-1.8517	1.8517	450	673
N4147064	0.4424	0.00632	0.1596	-1.8350	1.8350	450	673
N4147051	0.3966	0.00566	0.1431	-1.9444	1.9444	450	773
N4147052	0.3657	0.00522	0.1319	-2.0254	2.0254	450	773
N4147053	0.3644	0.00520	0.1315	-2.0291	2.0291	450	773
N4147041	0.4394	0.00627	0.1585	-1.8419	1.8419	450	873
N4147042	0.4389	0.00627	0.1584	-1.8429	1.8429	450	873
N4147044	0.4311	0.00615	0.1556	-1.8608	1.8608	450	873
N4147031	0.3996	0.00571	0.1442	-1.9367	1.9367	450	973
N4147032	0.4081	0.00583	0.1472	-1.9158	1.9158	450	973
N4147033	0.3423	0.00489	0.1235	-2.0915	2.0915	450	973
N4146211	0.3302	0.00471	0.1191	-2.1275	2.1275	450	873
N4146212	0.3141	0.00448	0.1133	-2.1776	2.1776	450	873
N4146214	0.3454	0.00493	0.1246	-2.0824	2.0824	450	873
N4146205	0.4112	0.00587	0.1483	-1.9083	1.9083	450	773
N4146204	0.5121	0.00731	0.1848	-1.6886	1.6886	450	773
N4146203	0.4063	0.00580	0.1466	-1.9201	1.9201	450	773
N4146202	0.3579	0.00511	0.1291	-2.0468	2.0468	450	773

DATA FOR PROLINE-N CALIBRATION AND KINETIC CALCULATIONS

The data used to determine the molar concentrations is provided in the tables on the following pages. The original proline nitrogen concentrations were determined with the calibration curve provided in Fig. IX-8. Using the linear equation, the concentration of GPNP nitrogen is determined with units of ug N/5 μ L.

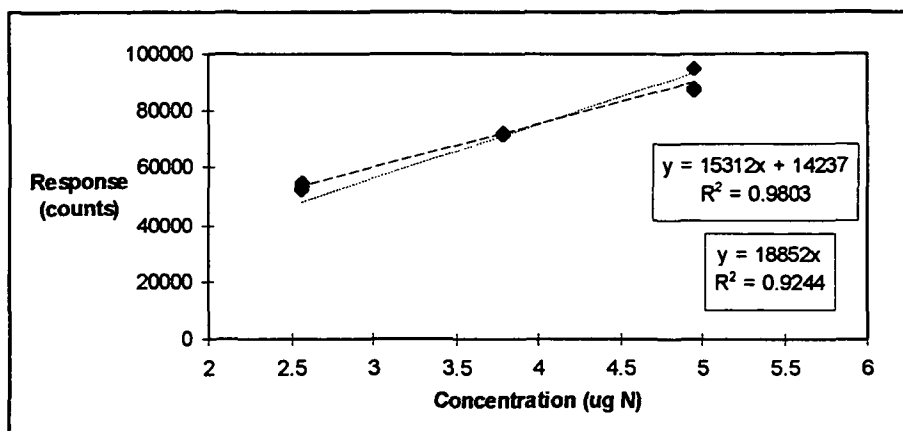


Figure IX-8. Calibration response for the proline GPNP nitrogen conversion kinetics data.

Conversion of these units to molar concentrations is made by dividing the $\mu\text{g N}/5$ μL concentration by the molecular weight of nitrogen. An example calculation is provided here.

$$\frac{2.564\mu\text{gN}}{5\mu\text{L}} \equiv \left(\frac{2.564\text{gN}}{5\text{L}} \right) \left(\frac{1\text{mole}}{14.01\text{g}} \right) = 0.0366 \text{ mole/l} \quad (\text{IX-10})$$

The data provided in tables on the following pages includes that used for the calibration and evaluation of the kinetic parameters. Each pyrolysis condition was replicated a minimum of three times. The summarized data is also provided giving an indication of the reproducibility of the measurements and the relative error. Each table identifies the properties being examined during the proline-nitrogen pyrolysis experiments and the GPNP measurements.

Each set of data is presented along with the statistical summaries. Error estimates can be taken from the correlation coefficients in the plots as well as the statistical standard deviation and coefficient of variation.

The sample numbers in the data tables, such as N4097022, are the same as the computer data acquisition (CDA) file names. The N identifies the sample as a nitrogen release profile type of data file. The 4 represents the lab notebook #4264. The next three digits are the page number within the notebook where the data can be found and the last three digits are the sample number on that page. The last digit represents the number of the replicate. For example, the values listed for the N4097022 sample would be found in notebook 4264 on page 97 as sample 2, replicate 2.

The CDA values in the tables represent the integrated area under the nitrogen release profile obtained with the computer data acquisition system. This value provides a check on the response values obtained directly from the nitrogen analyzer.

Table IX-3. Oxidative Proline Pyrolysis Data, Kinetic Calibration Data

Method Used: 5 PMT Voltage: 825
 O2 to O3: 30 ml/min Furnace Temperature: 1100° C
 O2 to pyro: 365 ml/min Gain Setting: HI
 O2 to inlet: 20 ml/min Gain Factor: X1
 He to inlet: 145 ml/min Heating Program #: 2*
 Nitrogen Species: proline Matrix: H2O

* Delay2 = 2 minutes

<u>Sample #</u>	<u>Sample ID</u>	<u>Sample Vol (μl)</u>	<u>Known N Mass (μg)</u>	<u>Response Counts</u>	<u>CDA Sum Response</u>
N4151011	~500 ppm N	5	2.564	53534	--
N4151012	~500 ppm N	5	2.564	54488	--
N4151013	~500 ppm N	5	2.564	52548	--
<u>Sample #</u>	<u>Ave. Counts</u>	<u>n</u>	<u>SD</u>	<u>RSD (%)</u>	
N415101_	53523	3	970	1.81	

Method Used: 5 PMT Voltage: 825
 O2 to O3: 30 ml/min Furnace Temperature: 1100° C
 O2 to pyro: 365 ml/min Gain Setting: HI
 O2 to inlet: 20 ml/min Gain Factor: X1
 He to inlet: 145 ml/min Heating Program #: 2
 Nitrogen Species: proline Matrix: H2O

<u>Sample #</u>	<u>Sample ID</u>	<u>Sample Vol (μl)</u>	<u>Known N Mass (μg)</u>	<u>Response Counts</u>	<u>CDA Sum Response</u>
N4151041	~750 ppm N	5	3.789	72554	127.8315
N4151042	~750 ppm N	5	3.789	72235	127.1485
N4151043	~750 ppm N	5	3.789	71838	126.489
<u>Sample #</u>	<u>Ave. Counts</u>	<u>n</u>	<u>SD</u>	<u>RSD (%)</u>	
N415104_	72209	3	358	0.49	

Method Used: 5 PMT Voltage: 825
 O2 to O3: 30 ml/min Furnace Temperature: 1100° C
 O2 to pyro: 365 ml/min Gain Setting: HI
 O2 to inlet: 20 ml/min Gain Factor: X1
 He to inlet: 145 ml/min Heating Program #: 2
 Nitrogen Species: proline Matrix: H2O

<u>Sample #</u>	<u>Sample ID</u>	<u>Sample Vol (μl)</u>	<u>Known N Mass (μg)</u>	<u>Response Counts</u>	<u>CDA Sum Response</u>
N4151071	1000 ppm N	5	4.954	95167	168.53
N4151072	1000 ppm N	5	4.954	87518	154.1261
N4151073	1000 ppm N	5	4.954	87670	154.7846
<u>Sample #</u>	<u>Ave. Counts</u>	<u>n</u>	<u>SD</u>	<u>RSD (%)</u>	
N415107_	90118	3	4372	4.85	

Table IX-4. Stagnant, Nonoxidative Proline Pyrolysis Data, Effect of Delay Time.

Method Used: 5 PMT Voltage: 825
 O2 to O3: 30 ml/min Furnace Temperature: 1100° C
 O2 to pyro: 365 ml/min Gain Setting: HI
 O2 to inlet: 0 ml/min Gain Factor: X1
 He to inlet: 165 ml/min Heating Program #: 2
 Nitrogen Species: proline Matrix: H2O

**Stagnant Pyrolysis; He flow on at Ramp2, Delay2 = 2 minutes, quartz boat 2" from combustion entrance.*

Sample #	Sample ID	Sample Vol (ul)	Known N Mass (ug)	Response Counts	CDA Sum Response	1st peak Counts	1st peak CDA Sum	2nd peak Counts	2nd peak CDA Sum
N4151021	~500 ppm N	5	2.564	9431	--	2280	--	7151	--
N4151022	~500 ppm N	5	2.564	10309	17.4318	4062	6.4941	6247	10.9377
N4151023	~500 ppm N	5	2.564	11452	19.0672	3909	5.9812	7543	13.086

Sample #	Ave. Counts	n	SD	RSD (%)
N415102_	10397	3	1013	9.75

Method Used: 5 PMT Voltage: 825
 O2 to O3: 30 ml/min Furnace Temperature: 1100° C
 O2 to pyro: 365 ml/min Gain Setting: HI
 O2 to inlet: 0 ml/min Gain Factor: X1
 He to inlet: 165 ml/min Heating Program #: 2
 Nitrogen Species: proline Matrix: H2O

**Stagnant Pyrolysis; He flow on at Ramp2, Delay2 = 4 minutes, quartz boat 2" from combustion entrance.*

Sample #	Sample ID	Sample Vol (ul)	Known N Mass (ug)	Response Counts	CDA Sum Response	1st peak Counts	1st peak CDA Sum	2nd peak Counts	2nd peak CDA Sum
N4151031	~500 ppm N	5	2.564	6683	10.8621	2396	3.6845	4287	7.1776
N4151032	~500 ppm N	5	2.564	7237	12.1819	3303	5.517	3934	6.6649
N4151034	~500 ppm N	5	2.564	6472	10.6915	1995	3.0012	4477	7.6903

Sample #	Ave. Counts	n	SD	RSD (%)
N415103_	6797	3	395	5.81

Method Used: 5 PMT Voltage: 825
 O2 to O3: 30 ml/min Furnace Temperature: 1100° C
 O2 to pyro: 365 ml/min Gain Setting: HI
 O2 to inlet: 0 ml/min Gain Factor: X1
 He to inlet: 165 ml/min Heating Program #: 2
 Nitrogen Species: proline Matrix: H2O

**Stagnant Pyrolysis; He flow on at Ramp2, Delay2 = 2 minutes, quartz boat 2" from combustion entrance.*

Sample #	Sample ID	Sample Vol (ul)	Known N Mass (ug)	Response Counts	CDA Sum Response	1st peak Counts	1st peak CDA Sum	2nd peak Counts	2nd peak CDA Sum
N4151051	~750 ppm N	5	3.789	13393	22.656	6612	10.9615	6781	11.6945
N4151052	~750 ppm N	5	3.789	12828	21.3864	5544	8.9599	7284	12.4265
N4151053	~750 ppm N	5	3.789	14649	24.609	6499	10.5711	8150	14.0379

Sample #	Ave. Counts	n	SD	RSD (%)
N415105_	13623	3	932	6.84

Table IX-4. (cont.) Stagnant, Nonoxidative Proline Pyrolysis Data, Effect of Delay Time.

Method Used: 5 PMT Voltage: 825
 O2 to O3: 30 ml/min Furnace Temperature: 1100° C
 O2 to pyro: 365 ml/min Gain Setting: HI
 O2 to inlet: 0 ml/min Gain Factor: X1
 He to inlet: 165 ml/min Heating Program #: 2
 Nitrogen Species: proline Matrix: H2O

*Stagnant Pyrolysis; He flow on at Ramp2, Delay2 = 4 minutes, quartz boat 2" from combustion entrance.

Sample #	Sample ID	Sample Vol (ul)	Known N Mass (ug)	Response Counts	CDA Sum Response	1st peak Counts	1st peak CDA Sum	2nd peak Counts	2nd peak CDA Sum
N4151061	~750 ppm N	5	3.789	12311	20.7034	6652	11.0108	5659	9.6926
N4151062	~750 ppm N	5	3.789	11267	18.6766	5943	9.5216	5324	9.155
N4151063	~750 ppm N	5	3.789	10563	17.6512	5603	9.1308	4960	8.5204

Sample #	Ave. Counts	n	SD	RSD (%)
N415106_	11381	3	879	7.72

Method Used: 5 PMT Voltage: 825
 O2 to O3: 30 ml/min Furnace Temperature: 1100° C
 O2 to pyro: 365 ml/min Gain Setting: HI
 O2 to inlet: 0 ml/min Gain Factor: X1
 He to inlet: 165 ml/min Heating Program #: 2
 Nitrogen Species: proline Matrix: H2O

*Stagnant Pyrolysis; He flow on at Ramp2, Delay2 = 2 minutes, quartz boat 2" from combustion entrance.

Sample #	Sample ID	Sample Vol (ul)	Known N Mass (ug)	Response Counts	CDA Sum Response	1st peak Counts	1st peak CDA Sum	2nd peak Counts	2nd peak CDA Sum
N4151081	~1000 ppm N	5	4.954	23697	40.5271	15194	25.8299	8503	14.6972
N4151083	~1000 ppm N	5	4.954	22937	39.2335	15192	25.9035	7745	13.33
N4151084	~1000 ppm N	5	4.954	22854	39.6238	15371	26.7332	7483	12.8906

Sample #	Ave. Counts	n	SD	RSD (%)
N415108_	23162	3	464	2.01

Method Used: 5 PMT Voltage: 825
 O2 to O3: 30 ml/min Furnace Temperature: 1100° C
 O2 to pyro: 365 ml/min Gain Setting: HI
 O2 to inlet: 0 ml/min Gain Factor: X1
 He to inlet: 165 ml/min Heating Program #: 2
 Nitrogen Species: proline Matrix: H2O

*Stagnant Pyrolysis; He flow on at Ramp2, Delay2 = 2 minutes, quartz boat 2" from combustion entrance.

Sample #	Sample ID	Sample Vol (ul)	Known N Mass (ug)	Response Counts	CDA Sum Response	1st peak Counts	1st peak CDA Sum	2nd peak Counts	2nd peak CDA Sum
N4152091	~1000 ppm N	5	4.954	13489	22.5587	6682	10.8889	6807	11.6698
N4152093	~1000 ppm N	5	4.954	14470	24.6327	8790	14.8673	5680	9.7654
N4152094	~1000 ppm N	5	4.954	14233	23.9259	7162	11.7189	7071	12.207

Sample #	Ave. Counts	n	SD	RSD (%)
N415209_	14064	3	512	3.64

Table IX-5. Stagnant, Nonoxidative Proline Pyrolysis Data, Effect of Temperature.

Method Used:	5	PMT Voltage:	825
O2 to O3:	30 ml/min	Furnace Temperature:	1100C
O2 to pyro:	365 ml/min	Gain Setting:	HI
O2 to inlet:	0 ml/min	Gain Factor:	X1
He to inlet:	165 ml/min	Heating Program #:	2
Nitrogen Species:	proline	Matrix:	H2O

**Stagnant Pyrolysis; T2 = 500°C, He flow on at Ramp2, quartz boat 2" from combustion entrance.*

<u>Sample #</u>	<u>Sample ID</u>	<u>Sample Vol</u> <u>(ul)</u>	<u>Known N</u> <u>Mass (ug)</u>	<u>Response</u> <u>Counts</u>	<u>CDA Sum</u> <u>Response</u>
N4146202	~500 ppm N	5	2.564	6748	11.792
N4146203	~500 ppm N	5	2.564	7660	13.3545
N4146204	~500 ppm N	5	2.564	9655	16.6749
N4146205	~500 ppm N	5	2.564	7751	13.3297

<u>Sample #</u>	<u>Ave. Counts</u>	<u>n</u>	<u>SD</u>	<u>RSD (%)</u>
N414620_	7953	4	1222	15.36

**Stagnant Pyrolysis; T2 = 600°C, He flow on at Ramp2, quartz boat 2" from combustion entrance.*

<u>Sample #</u>	<u>Sample ID</u>	<u>Sample Vol</u> <u>(ul)</u>	<u>Known N</u> <u>Mass (ug)</u>	<u>Response</u> <u>Counts</u>	<u>CDA Sum</u> <u>Response</u>
N4146211	~500 ppm N	5	2.564	6225	10.8154
N4146212	~500 ppm N	5	2.564	5921	10.0829
N4146213	~500 ppm N	5	2.564	--	11.2058
N4146214	~500 ppm N	5	2.564	6512	11.0595

<u>Sample #</u>	<u>Ave. Counts</u>	<u>n</u>	<u>SD</u>	<u>RSD (%)</u>
N414621_	6219	3	295	4.75

**Stagnant Pyrolysis; T2 = 800°C, He flow on at Ramp2, quartz boat 2" from combustion entrance.*

<u>Sample #</u>	<u>Sample ID</u>	<u>Sample Vol</u> <u>(ul)</u>	<u>Known N</u> <u>Mass (ug)</u>	<u>Response</u> <u>Counts</u>	<u>CDA Sum</u> <u>Response</u>
N4147011	~500 ppm N	5	2.564	7754	13.2811
N4147012	~500 ppm N	5	2.564	7376	12.7925
N4147013	~500 ppm N	5	2.564	8667	15.0877

<u>Sample #</u>	<u>Ave. Counts</u>	<u>n</u>	<u>SD</u>	<u>RSD (%)</u>
N414701_	7933	3	664	8.37

**Stagnant Pyrolysis; T2 = 700°C, He flow on at Ramp2, quartz boat 2" from combustion entrance.*

<u>Sample #</u>	<u>Sample ID</u>	<u>Sample Vol</u> <u>(ul)</u>	<u>Known N</u> <u>Mass (ug)</u>	<u>Response</u> <u>Counts</u>	<u>CDA Sum</u> <u>Response</u>
N4147031	~500 ppm N	5	2.564	7534	13.086
N4147032	~500 ppm N	5	2.564	7693	13.3545
N4147033	~500 ppm N	5	2.564	6453	11.3765

<u>Sample #</u>	<u>Ave. Counts</u>	<u>n</u>	<u>SD</u>	<u>RSD (%)</u>
N414703_	7226	3	675	9.34

Table IX-5.(cont.) Stagnant, Nonoxidative Pyrolysis Data, Effect of Temperature.

*Stagnant Pyrolysis; $T_2 = 600^\circ\text{C}$, He flow on at Ramp2, quartz boat 2" from combustion entrance.

<u>Sample #</u>	<u>Sample ID</u>	<u>Sample Vol</u> <u>(ul)</u>	<u>Known N</u> <u>Mass (ug)</u>	<u>Response</u> <u>Counts</u>	<u>CDA Sum</u> <u>Response</u>
N4147041	~500 ppm N	5	2.564	8283	10.8154
N4147042	~500 ppm N	5	2.564	8275	10.0829
N4147044	~500 ppm N	5	2.564	8128	11.0595
<u>Sample #</u>	<u>Ave. Counts</u>	<u>n</u>	<u>SD</u>	<u>RSD (%)</u>	
N414704_	8228	3	87	1.06	

*Stagnant Pyrolysis; $T_2 = 500^\circ\text{C}$, He flow on at Ramp2, quartz boat 2" from combustion entrance.

<u>Sample #</u>	<u>Sample ID</u>	<u>Sample Vol</u> <u>(ul)</u>	<u>Known N</u> <u>Mass (ug)</u>	<u>Response</u> <u>Counts</u>	<u>CDA Sum</u> <u>Response</u>
N4147051	~500 ppm N	5	2.564	7476	13.1346
N4147052	~500 ppm N	5	2.564	6894	12.1337
N4147053	~500 ppm N	5	2.564	6869	12.2069
<u>Sample #</u>	<u>Ave. Counts</u>	<u>n</u>	<u>SD</u>	<u>RSD (%)</u>	
N414705_	7079	3	343	4.85	

*Stagnant Pyrolysis; $T_2 = 400^\circ\text{C}$, He flow on at Ramp2, quartz boat 2" from combustion entrance.

<u>Sample #</u>	<u>Sample ID</u>	<u>Sample Vol</u> <u>(ul)</u>	<u>Known N</u> <u>Mass (ug)</u>	<u>Response</u> <u>Counts</u>	<u>CDA Sum</u> <u>Response</u>
N4147061	~500 ppm N	5	2.564	8434	14.6726
N4147063	~500 ppm N	5	2.564	8202	14.3308
N4147064	~500 ppm N	5	2.564	8340	14.5265
<u>Sample #</u>	<u>Ave. Counts</u>	<u>n</u>	<u>SD</u>	<u>RSD (%)</u>	
N414706_	8325	3	117	1.40	

*Stagnant Pyrolysis; $T_2 = 300^\circ\text{C}$, He flow on at Ramp2, quartz boat 2" from combustion entrance.

<u>Sample #</u>	<u>Sample ID</u>	<u>Sample Vol</u> <u>(ul)</u>	<u>Known N</u> <u>Mass (ug)</u>	<u>Response</u> <u>Counts</u>	<u>CDA Sum</u> <u>Response</u>
N4147071	~500 ppm N	5	2.564	10995	19.1406
N4147072	~500 ppm N	5	2.564	12615	21.9724
N4147073	~500 ppm N	5	2.564	13892	24.2922
N4147074	~500 ppm N	5	2.564	14493	25.2685
<u>Sample #</u>	<u>Ave. Counts</u>	<u>n</u>	<u>SD</u>	<u>RSD (%)</u>	
N414707_	12999	4	1549	11.91	

*Stagnant Pyrolysis; $T_2 = 500^\circ\text{C}$, He flow on at Ramp2, quartz boat 2" from combustion entrance.

<u>Sample #</u>	<u>Sample ID</u>	<u>Sample Vol</u> <u>(ul)</u>	<u>Known N</u> <u>Mass (ug)</u>	<u>Response</u> <u>Counts</u>	<u>CDA Sum</u> <u>Response</u>
N4148081	~500 ppm N	5	2.564	9126	15.9666
N4148082	~500 ppm N	5	2.564	6471	11.255
N4148083	~500 ppm N	5	2.564	7825	13.7694
N4148084	~500 ppm N	5	2.564	8089	13.9891
<u>Sample #</u>	<u>Ave. Counts</u>	<u>n</u>	<u>SD</u>	<u>RSD (%)</u>	
N414808_	7878	4	1093	13.87	

Table IX-5.(cont.) Stagnant, Nonoxidative Pyrolysis Data, Effect of Temperature.

**Stagnant Pyrolysis; T₂ = 600°C, He flow on at Ramp2, quartz boat 2" from combustion entrance.*

<u>Sample #</u>	<u>Sample ID</u>	<u>Sample Vol</u> <u>(ul)</u>	<u>Known N</u> <u>Mass (ug)</u>	<u>Response</u> <u>Counts</u>	<u>CDA Sum</u> <u>Response</u>
N4148091	~500 ppm N	5	2.564	7547	13.281
N4148092	~500 ppm N	5	2.564	7487	13.0616
N4148093	~500 ppm N	5	2.564	7431	--

<u>Sample #</u>	<u>Ave. Counts</u>	<u>n</u>	<u>SD</u>	<u>RSD (%)</u>
N414809_	7488	3	57	0.77

**Stagnant Pyrolysis; T₂ = 700°C, He flow on at Ramp2, quartz boat 2" from combustion entrance.*

<u>Sample #</u>	<u>Sample ID</u>	<u>Sample Vol</u> <u>(ul)</u>	<u>Known N</u> <u>Mass (ug)</u>	<u>Response</u> <u>Counts</u>	<u>CDA Sum</u> <u>Response</u>
N4148102	~500 ppm N	5	2.564	7996	13.794
N4148103	~500 ppm N	5	2.564	5851	9.9603
N4148104	~500 ppm N	5	2.564	7708	13.2078
N4148105	~500 ppm N	5	2.564	7114	12.2802

<u>Sample #</u>	<u>Ave. Counts</u>	<u>n</u>	<u>SD</u>	<u>RSD (%)</u>
N414810_	7167	4	951	13.27

**Stagnant Pyrolysis; T₂ = 500°C, He flow on at Ramp2, quartz boat 2" from combustion entrance.*

<u>Sample #</u>	<u>Sample ID</u>	<u>Sample Vol</u> <u>(ul)</u>	<u>Known N</u> <u>Mass (ug)</u>	<u>Response</u> <u>Counts</u>	<u>CDA Sum</u> <u>Response</u>
N4148113	~500 ppm N	5	2.564	7506	12.9395
N4148114	~500 ppm N	5	2.564	7981	13.452
N4148115	~500 ppm N	5	2.564	7755	13.1828

<u>Sample #</u>	<u>Ave. Counts</u>	<u>n</u>	<u>SD</u>	<u>RSD (%)</u>
N414811_	7747	3	237	3.07

APPENDIX X: EFFECT OF HEAT RATE ON GASEOUS NITROGEN SPECIES

This appendix contains pyrolysis gas chromatography/mass spectrometry (GC/MS) data used to evaluate the effects of heating rate on the pyrolysis gas composition. The data was also employed to look into potential pathways for the formation of HCN and NH_3 from the model fuel nitrogen compounds. This section contains the results of the spectral interpretations along with the original spectra and tabulated data. One series of spectra from each set of replicates is given as an example for each heating rate and sample tested. Because the spectral data was collected only up to $m/z = 150$, identification of the gases at retention times greater than 6 min can not be made and therefore the spectra and data tables are only presented up to 6 min. The mass spectra for the peaks at these times only allow for identification of fragments, although it is thought that these species at higher retention times result from condensation reaction of the smaller molecular weight pyrolytic species.

Representative gas total ion chromatographs and mass spectra for each species tested at the different heating rates is provided in the collection of figures and tables. Note that little to no change in the peak shape occurs. A decrease in the retention times for the pyrolytic gases is observed at higher heating rates. The gas species volatilize more rapidly at higher temperatures; however, the composition of the gases does not change greatly. This suggests that the rate of heating has little effect on the gas-phase components during pyrolysis.

Some basic definitions, helpful in referring to spectra, are: the "base peak" has the most abundant mass in the spectra; the "molecular ion" or "parent ion" is the ion that has the same nominal mass as the neutral molecule; the mass/charge ratio (m/z) is often referred to simply as mass. Signals at masses less than the molecular ions represent fragments in the spectra of the parent peak and are used to arrive at a chemical structure for the compound represented by the spectrum.

It should be noted that, in general, the EI (electron impact) spectra of amino acids give very weak or nonexistent molecular ion peaks.¹⁰⁹ This is because amino acids quickly lose their carboxyl group upon electron impact. The loss of COOH or COOH₂ is nearly always present and clearly marked. Sometimes the species may be noted as the loss of H₂O and the subsequent loss of CO yielding R-CH=NH₂⁺. The presence of these fragments of the amino acid may or may not appear due to further decomposition of the ions. If, during pyrolysis, some of the amino acid volatilized without any decomposition, then these fragments would be expected.

Also to be noted is that there was no contamination in the spectra due to air or water. The retention time for air in the GC column is about 1.0 min. There are no peaks at this retention time. Likewise, water can be observed at about 2.6 min.

PYROLYSIS GC/MS FOR PROLINE

Spectral Identification of Proline Pyrolysis Products

Several of the species identifications are given here for proline pyrolysis at 10^5 C/sec as an example of the determination methods. Only the detailed identification of several of the initial peaks in this series is provided to eliminate redundancy for the reader yet provide information on the structural identification for the pyrolytic gases. As mentioned previously, because the spectral data was collected only up to $m/z = 150$, identification of the gases at retention times greater than 6 min can not be made and therefore the spectra and data tables are only presented up to 6 min. The mass spectra for the peaks at these times only allow for identification of fragments, although it is thought that these species at higher retention times result from condensation reaction of the smaller molecular weight pyrolytic species.

Several basic rules can be applied to make spectrometric identification of compounds. In general, the highest mass in the spectrum indicates the formula weight of the parent peak compound. The base peak indicates the fragment or molecular ion of the highest population. This information and some knowledge of the sample's behavior allows for an educated guess for the species identification. Exact identification by examining other spectral techniques, such as fourier transform infrared spectroscopy, were not attempted. Tables of mass and abundance data are available to assist in identification.¹⁰⁹⁻¹¹¹

Proline Pyrolysis Spectral Data Tables and Figures

Mass spectral data for proline pyrolysis at the four heating rates employed (10, 150, 400, and 1000° C/sec), as tables and spectra for peaks less than 6 min, are provided on the following pages of this section. Spectra and tables are provided for the results of the first heating rate, while the remaining data is provided strictly as tables. The tables include information for the heating rates employed, peak retention times, the mass/charge ratios and abundances for each peak at the given retention time. Each abundance has been normalized to the base peak for simplified identification of the mass/charge ratios from the noise of the spectrum.

The figures presented include the gas chromatogram and the individual mass spectra for the retention time of interest. Each figure contains the retention time value and the filename for the data. The filename can be used to identify the sample with its tabulated data.

Figure X-1. Comparison chromatograms for proline pyrolysis at heating rates of a) 10° C/sec, b) 150° C/sec, c) 400° C/sec, and d) 1000° C/sec.

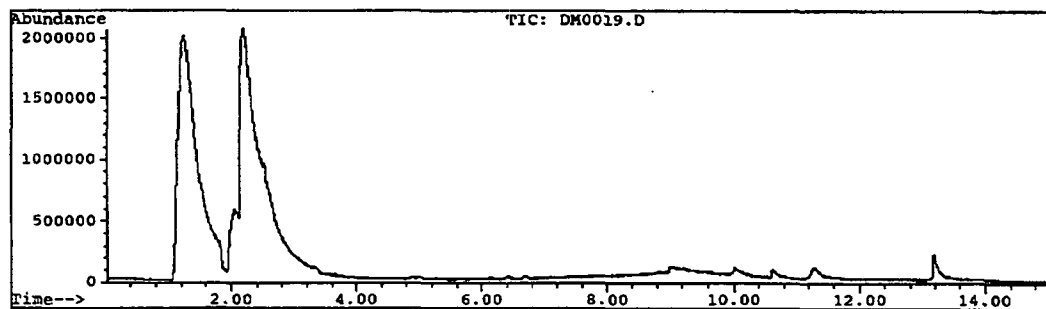
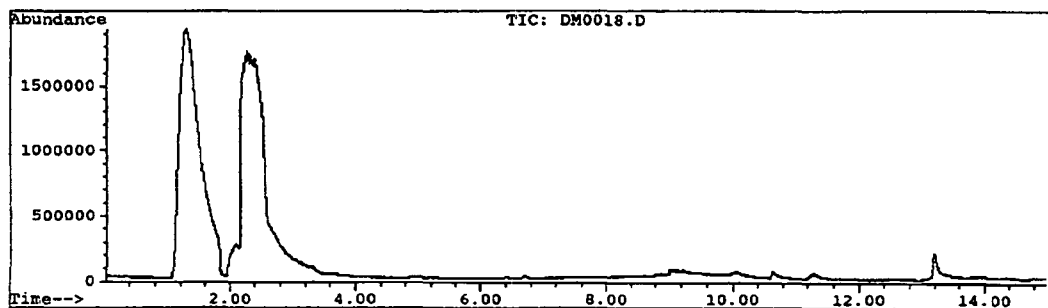
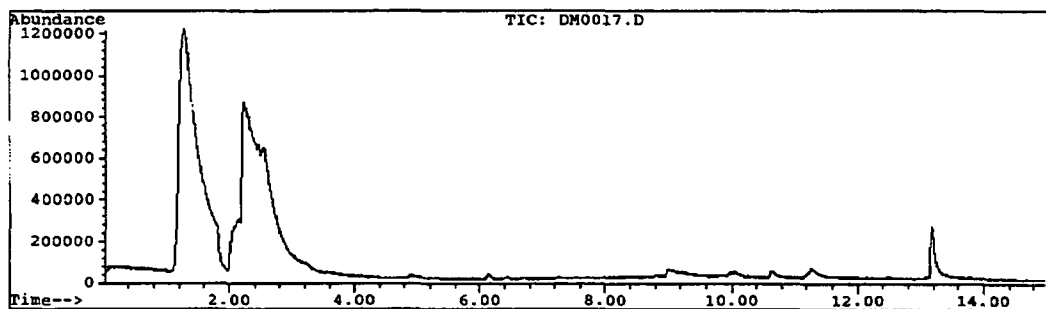
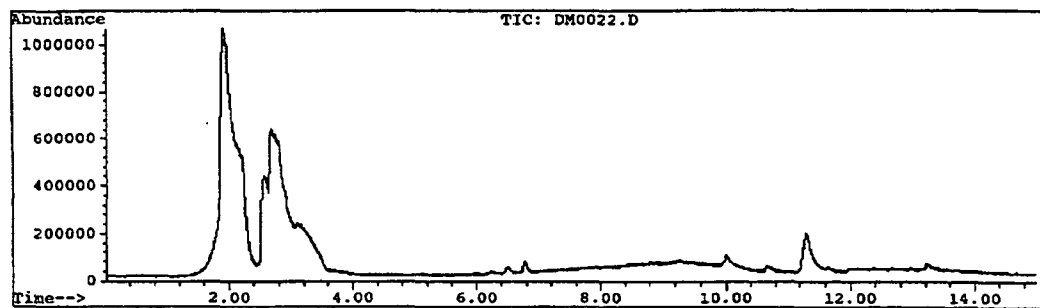


Table X-1. Mass spectral data for proline pyrolysis at 10° C/sec.

Proline pyrolysis at 600° C/min (0.01° C/msec) to 500° C (spectral name=DM0022.D).

Gas chromatography peaks at the following retention times:

1.9 min with shoulder at 2.1 min 2.6 min 6.2 min 6.8 min 10.6 min 13.2 min
 2.7 min 6.5 min 10.0 min 11.3 min

At each peak, the mass abundance is provided at the given mass/charge ratios (m/z).

At 1.9 min, the following abundances* were observed at the given mass/charge ratios (m/z).

<u>m/z</u>	<u>Abundance</u>	<u>m/z</u>	<u>Abundance</u>	<u>m/z</u>	<u>Abundance</u>	<u>m/z</u>	<u>Abundance</u>
4	2	17	11	26	3	44	100
12	1	18	25	27	3	45	1
13	0	19	0	28	10	46	0
14	0	20	0	29	0	51	0
15	0	24	0	32	0	77	0
16	4	25	1	42	0		

*Abundances are normalized against the base peak.

At 2.1 min, the following abundances* were observed at the given mass/charge ratios (m/z).

<u>m/z</u>	<u>Abundance</u>	<u>m/z</u>	<u>Abundance</u>	<u>m/z</u>	<u>Abundance</u>	<u>m/z</u>	<u>Abundance</u>
4	4	17	15	26	3	44	100
12	1	18	37	27	3	45	1
13	0	19	1	28	9	46	0
14	0	20	0	29	1	51	0
15	0	24	0	32	0	77	0
16	5	25	1	41	1		

*Abundances are normalized against the base peak.

At 2.6 min, the following abundances* were observed at the given mass/charge ratios (m/z).

<u>m/z</u>	<u>Abundance</u>	<u>m/z</u>	<u>Abundance</u>	<u>m/z</u>	<u>Abundance</u>	<u>m/z</u>	<u>Abundance</u>
4	10	30	0	49	0	66	0
14	1	32	1	50	0	67	1
15	1	36	0	51	1	68	46
16	1	37	4	52	1	69	72
17	4	38	6	54	4	70	4
18	12	39	21	55	0	77	0
25	1	40	13	57	0	82	0
26	4	41	100	62	0	84	1
27	7	42	36	63	1	85	0
28	8	43	3	64	1		
29	1	44	2	65	0		

*Abundances are normalized against the base peak.

Table X-1. (cont.) Mass spectral data for proline pyrolysis at 10° C/sec.

At 2.7 min, the following abundances* were observed at the given mass/charge ratios (m/z).

<u>m/z</u>	<u>Abundance</u>	<u>m/z</u>	<u>Abundance</u>	<u>m/z</u>	<u>Abundance</u>	<u>m/z</u>	<u>Abundance</u>
4	11	32	1	50	0	66	0
14	1	34	1	51	1	67	2
15	2	36	0	52	1	68	44
16	1	37	4	53	1	69	58
17	3	38	7	54	4	70	63
18	9	39	25	55	0	71	43
25	1	40	14	56	1	72	2
26	5	41	95	57	0	77	0
27	11	42	45	62	0	84	1
28	24	43	100	63	0	85	0
29	2	44	4	64	1		
30	4	49	0	65	0		

*Abundances are normalized against the base peak.

Figure X-2. Mass spectral data for proline pyrolysis at 10° C/sec (DM0022.D).

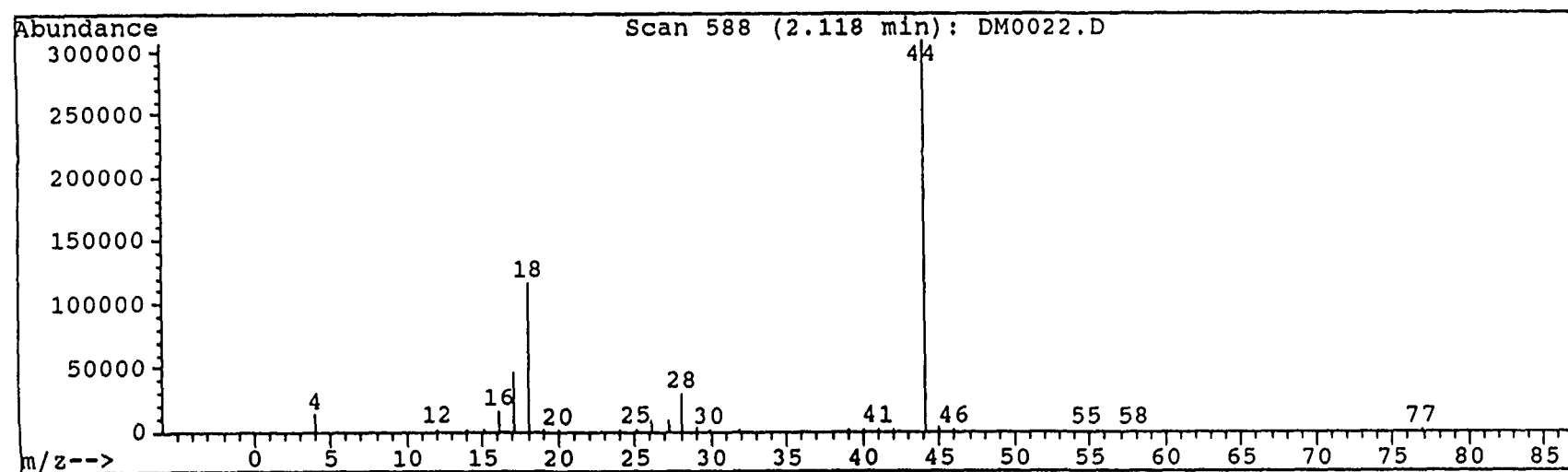
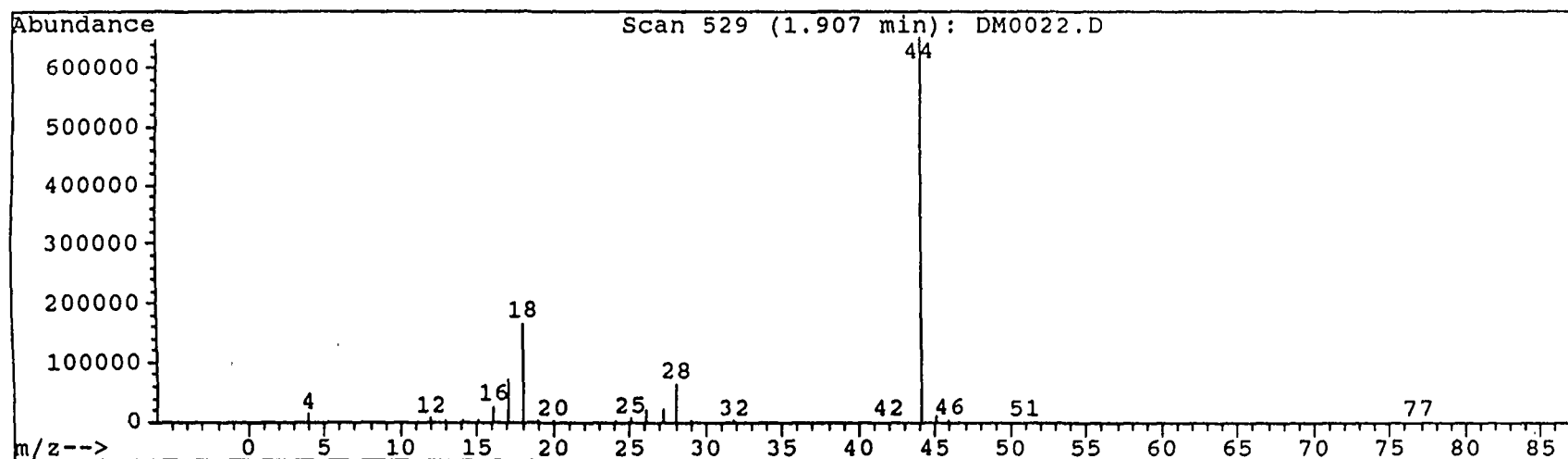


Figure X-2. (cont.) Mass spectral data for proline pyrolysis at 10° C/sec (DM0022.D).

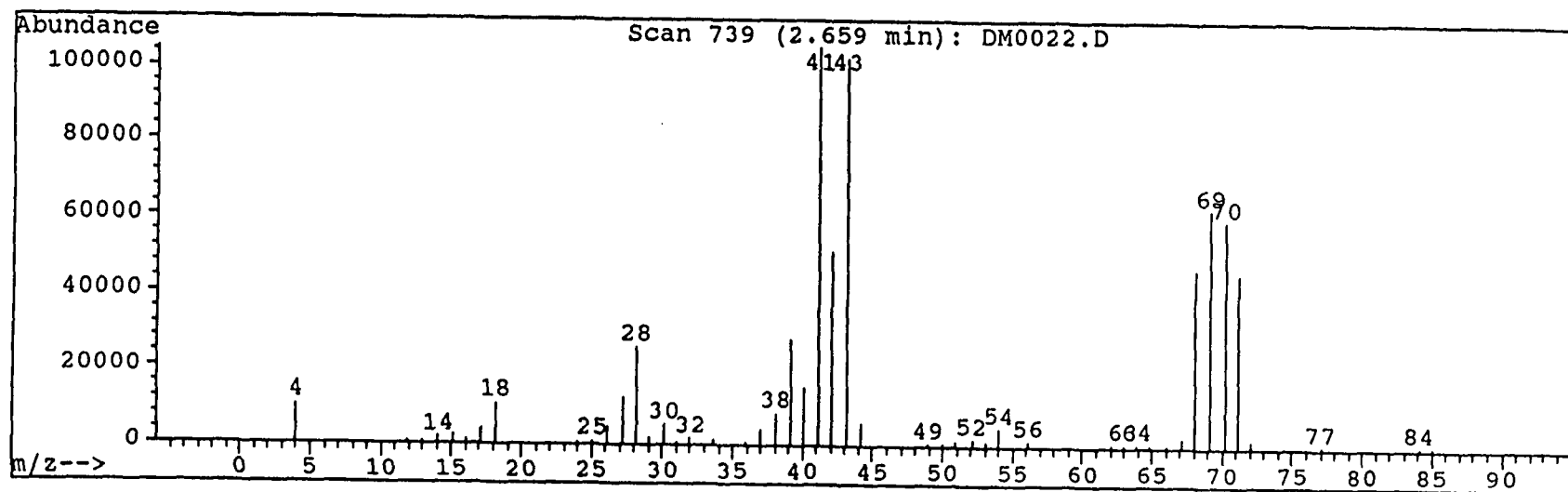
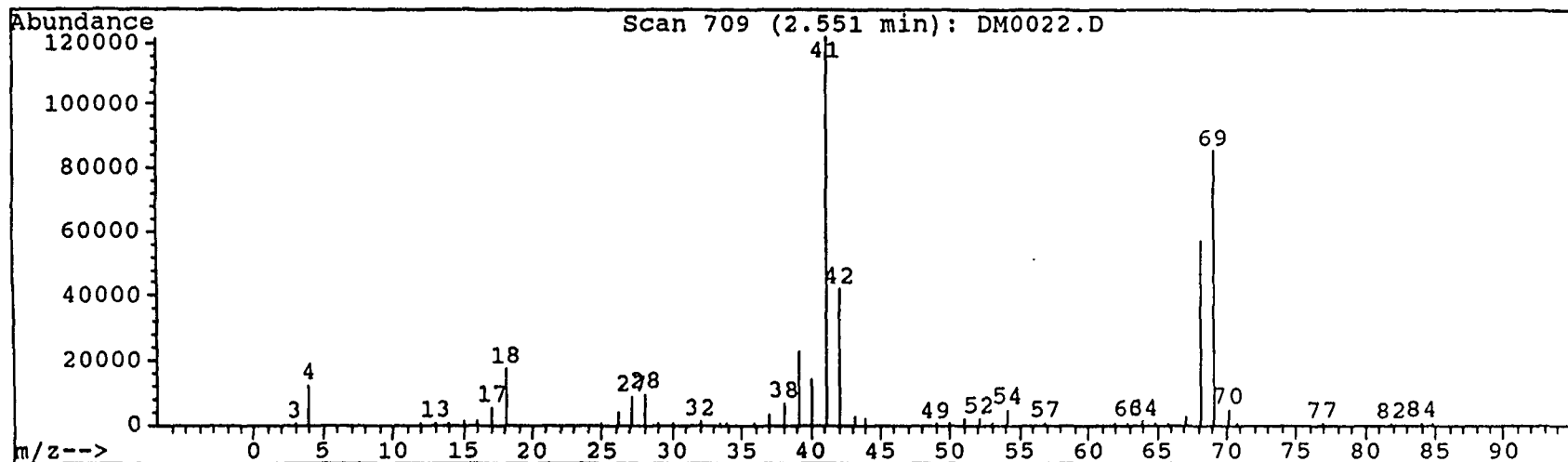


Table X-2. Mass spectral data for proline pyrolysis at 150° C/sec.

Proline pyrolysis at 150° C/sec (0.15° C/msec) to 500° C (spectral name=DM0017.D).

Gas chromatography peaks at the following retention times:

1.3 min	2.1 min	2.6 min	6.4 min	10.0 min	11.3 min
	2.3 min	6.2 min	6.7 min	10.6 min	13.2 min

At each peak, the mass abundance is provided at the given mass/charge ratios (m/z).

At 1.3 min, the following abundances* were observed at the given mass/charge ratios (m/z)

<u>m/z</u>	<u>Abundance</u>	<u>m/z</u>	<u>Abundance</u>	<u>m/z</u>	<u>Abundance</u>	<u>m/z</u>	<u>Abundance</u>
16	2	26	1	42	0	59	0
17	2	27	1	43	1	60	0
18	4	28	8	44	100	68	0
22	0	29	0	45	1	70	0
25	0	32	1	46	0	71	0

*Abundances are normalized against the base peak.

At 2.1 min, the following abundances* were observed at the given mass/charge ratios (m/z)

<u>m/z</u>	<u>Abundance</u>	<u>m/z</u>	<u>Abundance</u>	<u>m/z</u>	<u>Abundance</u>	<u>m/z</u>	<u>Abundance</u>
16	2	36	0	50	1	65	0
17	6	37	3	51	1	66	0
18	18	38	6	52	1	67	2
25	0	39	19	53	0	68	47
26	4	40	13	54	3	69	72
27	7	41	100	55	0	70	8
28	9	42	36	56	0	71	4
29	0	43	10	57	1	84	0
30	1	44	9	62	0		
32	1	45	0	63	0		
34	0	49	0	64	1		

*Abundances are normalized against the base peak.

At 2.3 min, the following abundances* were observed at the given mass/charge ratios (m/z)

<u>m/z</u>	<u>Abundance</u>	<u>m/z</u>	<u>Abundance</u>	<u>m/z</u>	<u>Abundance</u>	<u>m/z</u>	<u>Abundance</u>
17	2	36	0	52	1	68	21
18	5	37	2	54	1	69	22
25	0	38	4	55	2	70	62
26	2	39	14	56	0	71	46
27	8	40	7	57	1	72	2
28	22	41	45	62	0	73	0
29	2	42	31	63	0	82	0
30	5	43	100	64	0	84	0
31	0	44	6	65	0	85	0
32	1	50	0	66	0		
35	0	51	1	67	1		

*Abundances are normalized against the base peak.

Table X-2. (cont.) Mass spectral data for proline pyrolysis at 150° C/sec.

At 2.6 min, the following abundances* were observed at the given mass/charge ratios (m/z)

<u>m/z</u>	<u>Abundance</u>	<u>m/z</u>	<u>Abundance</u>	<u>m/z</u>	<u>Abundance</u>	<u>m/z</u>	<u>Abundance</u>
16	0	34	1	50	0	68	8
17	1	36	0	51	0	69	2
18	3	37	1	52	1	70	61
25	0	38	2	53	1	71	45
26	2	39	10	54	1	72	2
27	5	40	3	55	0	77	0
28	17	41	17	56	1	82	0
29	2	42	19	63	0	83	0
30	5	43	100	65	0		
31	0	44	5	66	0		
32	1	45	0	67	1		

*Abundances are normalized against the base peak.

Table X-3. Mass spectral data for proline pyrolysis at 400° C/sec.

Proline pyrolysis at 400° C/sec (0.4° C/msec) to 500° C (spectral name=DM0018.D).

Gas chromatography peaks at the following retention times:

1.3 min	2.1 min	6.4 min	10.1 min	11.3 min
	2.3 min	6.7 min	10.6 min	13.2 min

At each peak, the mass abundance is provided at the given mass/charge ratios (m/z).

At 1.3 min, the following abundances* were observed at the given mass/charge ratios (m/z).

<u>m/z</u>	<u>Abundance</u>	<u>m/z</u>	<u>Abundance</u>	<u>m/z</u>	<u>Abundance</u>	<u>m/z</u>	<u>Abundance</u>
16	2	26	1	38	0	46	0
17	2	27	1	41	0	68	0
18	5	28	7	42	0	70	0
22	0	29	0	44	100	71	0
25	0	32	0	45	1	82	0

*Abundances are normalized against the base peak.

At 2.1 min, the following abundances* were observed at the given mass/charge ratios (m/z).

<u>m/z</u>	<u>Abundance</u>	<u>m/z</u>	<u>Abundance</u>	<u>m/z</u>	<u>Abundance</u>	<u>m/z</u>	<u>Abundance</u>
16	1	36	0	52	1	68	46
17	3	37	3	53	0	69	72
18	11	38	6	54	4	70	7
25	1	39	18	55	0	71	3
26	3	40	12	56	1	73	0
27	8	41	100	57	1	77	0
28	9	42	36	63	0	82	0
29	1	43	8	64	1	84	2
30	3	44	9	65	0	85	1
32	1	50	0	67	2		

*Abundances are normalized against the base peak.

At 2.3 min, the following abundances* were observed at the given mass/charge ratios (m/z).

<u>m/z</u>	<u>Abundance</u>	<u>m/z</u>	<u>Abundance</u>	<u>m/z</u>	<u>Abundance</u>	<u>m/z</u>	<u>Abundance</u>
16	0	32	0	45	0	66	0
17	0	34	1	50	0	67	1
18	1	37	1	51	1	68	9
25	0	38	2	52	0	69	3
26	2	39	11	53	1	70	60
27	6	40	4	54	1	71	45
28	21	41	20	55	0	72	2
29	2	42	21	57	1	73	0
30	5	43	100	64	0	77	0
31	0	44	5	65	0	84	0

*Abundances are normalized against the base peak.

Table X-4. Mass spectral data for proline pyrolysis at 1000°C/sec.

Proline pyrolysis at 1000° C/sec (1.0° C/msec) to 500° C (spectral name=DM0019.D).

Gas chromatography peaks at the following retention times:

1.2 min	2.0 min	6.1 min	6.7 min	10.6 min	13.2 min
	2.2 min	6.4 min	10.0 min	11.3 min	

At each peak, the mass abundance is provided at the given mass/charge ratios (m/z).

At 1.2 min, the following abundances* were observed at the given mass/charge ratios (m/z).

<u>m/z</u>	<u>Abundance</u>	<u>m/z</u>	<u>Abundance</u>	<u>m/z</u>	<u>Abundance</u>	<u>m/z</u>	<u>Abundance</u>
16	2	25	0	39	0	46	0
17	2	26	2	41	0	68	0
18	4	27	2	42	0	70	0
19	0	28	7	43	1	71	0
20	0	29	0	44	100		
22	0	32	0	45	1		

*Abundances are normalized against the base peak.

At 2.0 min, the following abundances* were observed at the given mass/charge ratios (m/z).

<u>m/z</u>	<u>Abundance</u>	<u>m/z</u>	<u>Abundance</u>	<u>m/z</u>	<u>Abundance</u>	<u>m/z</u>	<u>Abundance</u>
16	1	36	0	44	7	64	1
17	4	37	3	48	0	67	2
18	10	38	5	50	0	68	43
26	4	39	20	51	1	69	66
27	7	40	13	52	1	70	5
28	10	41	100	54	4	71	2
30	2	42	33	57	0	78	0
32	0	43	6	63	1	85	0

*Abundances are normalized against the base peak.

At 2.2 min, the following abundances* were observed at the given mass/charge ratios (m/z).

<u>m/z</u>	<u>Abundance</u>	<u>m/z</u>	<u>Abundance</u>	<u>m/z</u>	<u>Abundance</u>	<u>m/z</u>	<u>Abundance</u>
17	1	38	3	56	1	85	1
18	2	39	13	57	0		
25	0	40	6	67	0		
26	2	41	31	68	0		
27	7	42	25	69	1		
28	22	43	100	70	1		
29	2	44	4	71	4		
30	5	50	0	72	0		
33	0	52	1	73	0		
34	0	53	1	77	0		
37	2	54	1	84	1		

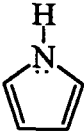
*Abundances are normalized against the base peak.

PYROLYSIS GC/MS FOR GLUTAMIC ACID

Spectral Identification of Glutamic Acid Pyrolysis Products

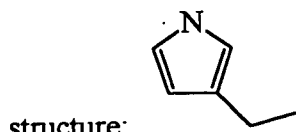
Glutamic acid pyrolysis indicated one primary peak at a retention time of 1.8 min. At least three other peaks were observed but relative to the peak at 1.8 min. were small. The species represented by these much smaller peaks were observed at later retention times. The peak at 1.8 min. was determined to be CO_2 represented by the base peak at mass 44. Likely fragments for this molecule would be CO, C, and O. All three of these species are represented in the mass spectrum with mass charge ratios of 28, 12, and 16, respectively.

At retention time 2.3 min. representing the shoulder of the main peak, a combination of species is observed. The base peak at mass 18 is primarily water, but NH_4^+ may also be contributing; there is a weak abundance at 14 indicating nitrogen to be present. A small amount of CO_2 ($m/z = 44$) is also thought to be present along with pyrrole which is seen at mass 67.

Pyrrole ($m/z = 67$), , is the dominant species at a 2.9 min. retention time.

A spectral library search matched the experimental spectrum at 86% confidence.⁹² The quantity of the pyrrole is shown to be small as indicated by the relatively large abundance of He, the carrier gas for the system, at mass 4 in the spectrum.

In the mass spectrum collected at 4.8 min., the parent ion molecule is observed at mass 95; a possible structure, is 3-ethyl-1H-pyrrole, which is represented by the chemical



83% confidence.⁹² Mass 94 is represented by the loss of a hydrogen while mass 80 is represented by the loss of a methyl group. These species appear to be the predominant pyrolytic gases at this retention time.

Glutamic Acid Pyrolysis Spectral Data Tables and Figures

Mass spectral data tables and spectra (up to a 6 min retention time) for glutamic acid pyrolysis are provided on the following pages of this section. Spectra and tables are provided for the results of the first heating rate, while the remaining data is provided strictly as tables. The tables include information for the heating rates employed, peak retention times, the mass/charge ratios and abundances for each peak at the given retention time. Each abundance has been normalized to the base peak for simplified identification of the informational mass/charge ratios from the noise of the spectrum.

The figures presented include the gas chromatogram and the individual mass spectra for the retention time of interest. Each figure contains the retention time value and the filename for the data. The filename can be used to identify the sample with its tabulated data.

Table X-5. Mass spectral data for glutamic acid pyrolysis at 10° C/sec.

Glutamic acid pyrolysis at 600° C/min (0.01° C/msec) to 500° C (spectral name=DM0023.D).

Gas chromatography peaks at the following retention times:

1.8 min 2.3 min 2.9 min 4.8 min 9.8 min

At each of these peaks, the mass abundance data are presented below.

At 1.8 min, the following abundances* were observed at the given mass/charge ratios (m/z).

<u>m/z</u>	<u>Abundance</u>	<u>m/z</u>	<u>Abundance</u>	<u>m/z</u>	<u>Abundance</u>	<u>m/z</u>	<u>Abundance</u>
12	1	17	2	26	0	44	100
14	0	18	3	27	0	45	1
15	0	19	0	28	7	60	0
16	2	25	0	29	0	64	0

*Abundances are normalized against the base peak.

At 2.3 min, the following abundances* were observed at the given mass/charge ratios (m/z).

<u>m/z</u>	<u>Abundance</u>	<u>m/z</u>	<u>Abundance</u>	<u>m/z</u>	<u>Abundance</u>	<u>m/z</u>	<u>Abundance</u>
4	29	26	2	44	10	68	1
14	1	27	4	51	2	69	1
15	1	28	6	52	3	70	1
16	9	38	3	53	5	71	1
17	39	39	3	54	4	72	1
18	100	40	4	55	2		
19	1	41	8	56	2		
20	1	42	2	66	1		
25	1	43	4	67	2		

*Abundances are normalized against the base peak.

At 2.9 min, the following abundances* were observed at the given mass/charge ratios (m/z).

<u>m/z</u>	<u>Abundance</u>	<u>m/z</u>	<u>Abundance</u>	<u>m/z</u>	<u>Abundance</u>	<u>m/z</u>	<u>Abundance</u>
4	24	32	1	45	4	66	7
14	1	33	1	50	1	67	100
15	1	36	1	52	2	68	5
16	1	37	6	53	1	69	2
17	4	38	9	54	1	73	2
18	10	39	31	55	1	74	1
26	2	40	22	60	2	77	2
27	2	41	36	62	1	78	1
28	14	43	6	63	1	79	3
29	1	44	5	65	1	81	1

*Abundances are normalized against the base peak.

Table X-5. (cont.) Mass spectral data for glutamic acid pyrolysis at 10° C/sec.

At 4.7 min, the following abundances* were observed at the given mass/charge ratios (m/z).

<u>m/z</u>	<u>Abundance</u>	<u>m/z</u>	<u>Abundance</u>	<u>m/z</u>	<u>Abundance</u>	<u>m/z</u>	<u>Abundance</u>
4	61	40	4	57	3	79	4
14	1	41	13	59	3	80	100
15	2	42	18	60	6	81	7
16	2	43	7	61	2	84	4
17	5	44	25	62	2	85	3
18	15	45	5	63	3	85	5
26	2	46	2	65	5	91	2
27	7	50	4	66	5	92	3
28	18	51	5	67	14	93	11
29	6	52	5	72	2	94	55
31	2	53	16	73	6	95	75
32	5	54	6	74	2	96	7
38	3	55	6	77	3	106	2
39	13	56	3	78	4	140	1

*Abundances are normalized against the base peak.

Table X-6. Mass spectral data for glutamic acid pyrolysis at 400° C/sec.

Glutamic acid pyrolysis at 400° C/sec (0.4° C/msec) to 500° C (spectral name=DM0026.D).

Gas chromatography peaks at the following retention times:

1.2 min 2.6 min 6.1 min 9.8 min

At each of these peaks, the mass abundance data are presented below.

At **1.2 min**, the following abundances* were observed at the given mass/charge ratios (m/z).

<u>m/z</u>	<u>Abundance</u>	<u>m/z</u>	<u>Abundance</u>	<u>m/z</u>	<u>Abundance</u>	<u>m/z</u>	<u>Abundance</u>
4	0	17	1	26	0	44	100
12	1	18	2	27	1	45	1
15	0	19	1	28	13	60	0
16	2	25	0	29	0	64	0

*Abundances are normalized against the base peak.

At **2.6 min**, the following abundances* were observed at the given mass/charge ratios (m/z).

<u>m/z</u>	<u>Abundance</u>	<u>m/z</u>	<u>Abundance</u>	<u>m/z</u>	<u>Abundance</u>	<u>m/z</u>	<u>Abundance</u>
4	6	36	1	50	1	68	6
17	1	37	5	51	1	73	1
18	3	38	9	52	3	74	1
25	1	39	29	55	1	77	1
26	1	40	24	60	1	79	1
27	1	41	34	63	1		
28	10	42	1	64	1		
29	1	43	2	65	1		
32	1	44	2	66	7		
34	1	45	1	67	100		

*Abundances are normalized against the base peak.

Figure X-3. Mass spectral data for glutamic acid pyrolysis at 10° C/sec (DM0023.D) and 400° C/sec (DM0026.D).

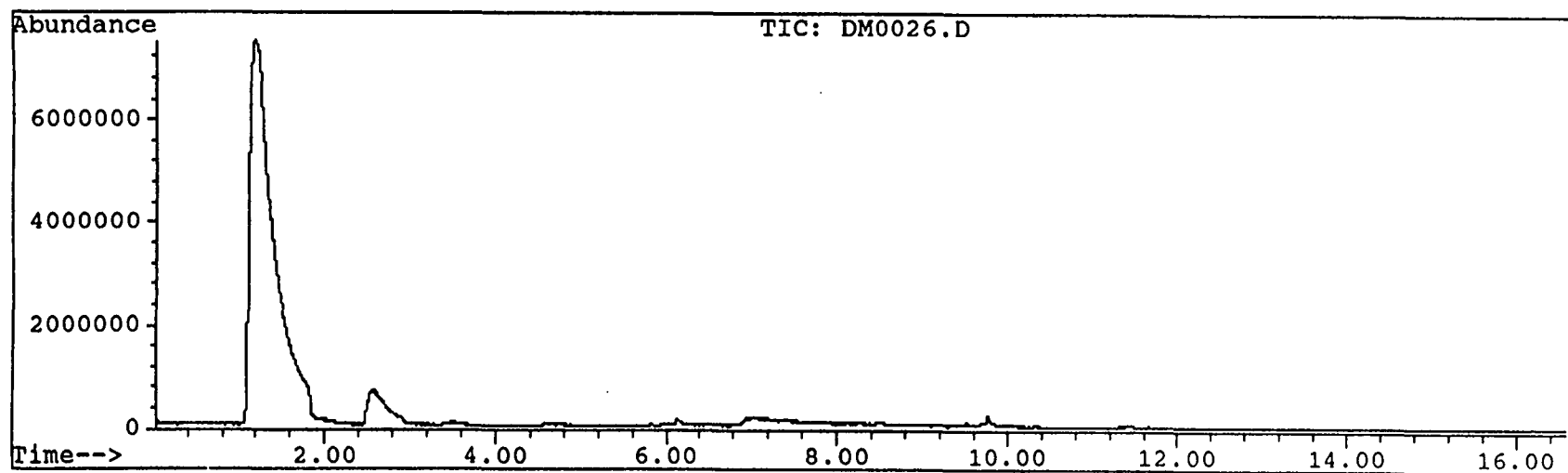
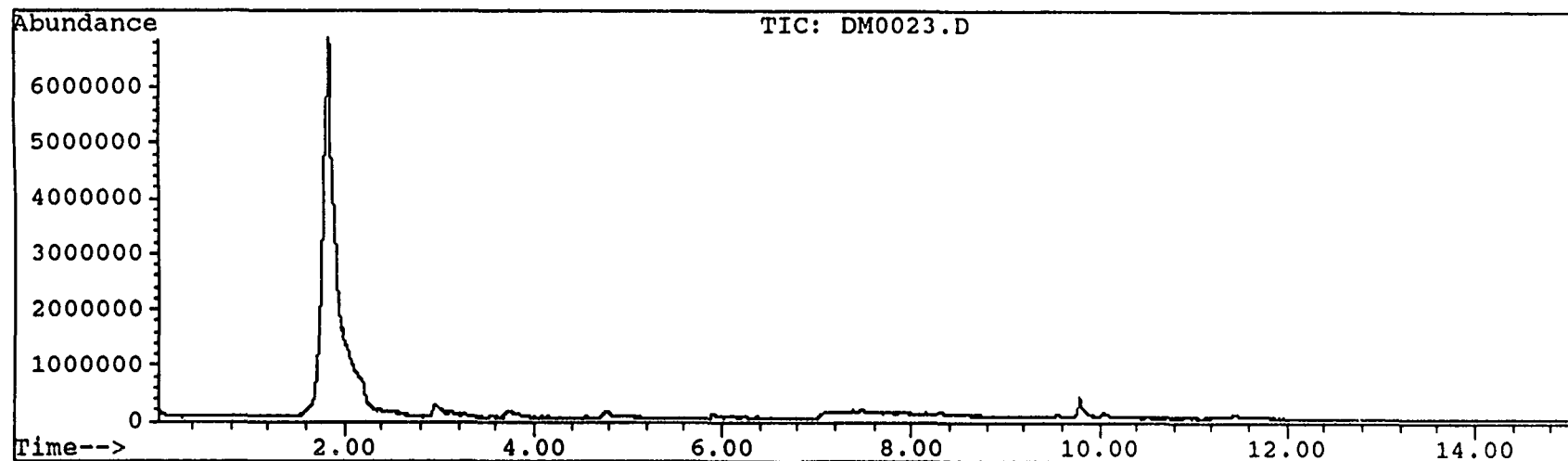


Figure X-4. Mass spectral data for glutamic acid pyrolysis at 10° C/sec (DM0023.D).

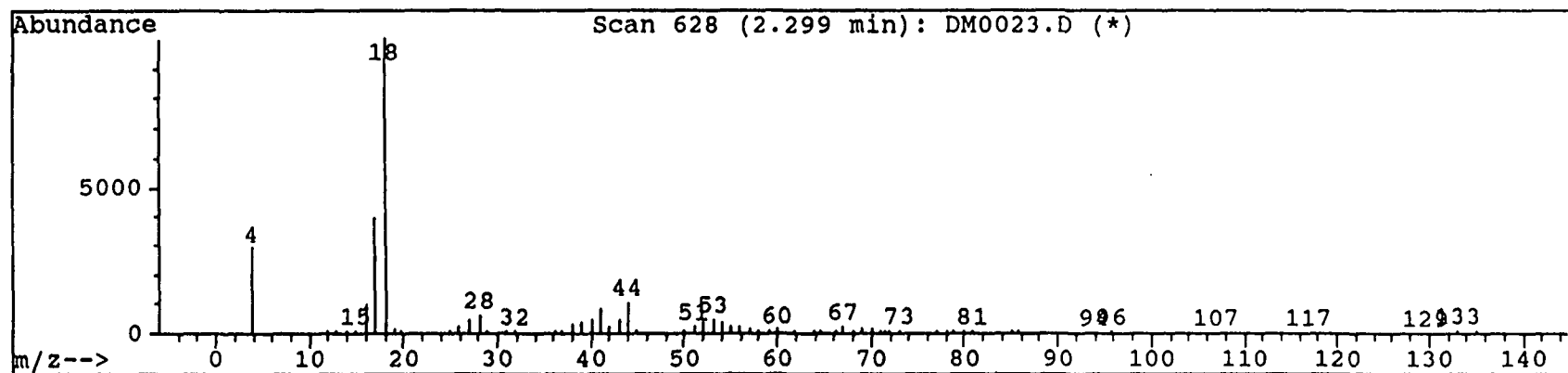
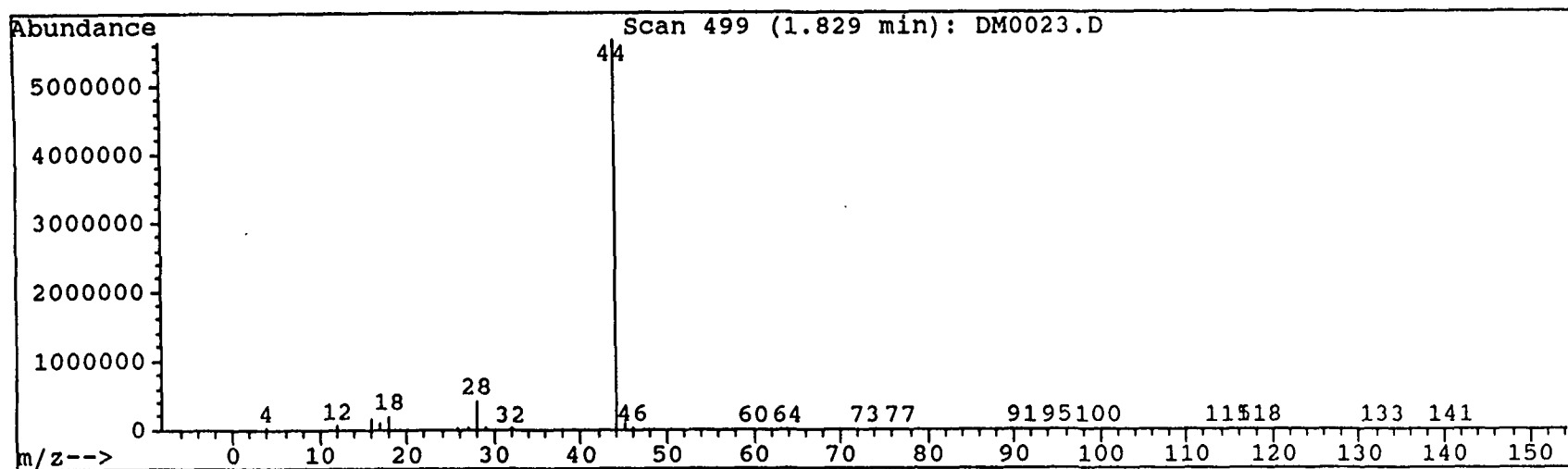


Figure X-4. (cont.) Mass spectral data for glutamic acid pyrolysis at 10° C/sec (DM0023.D).

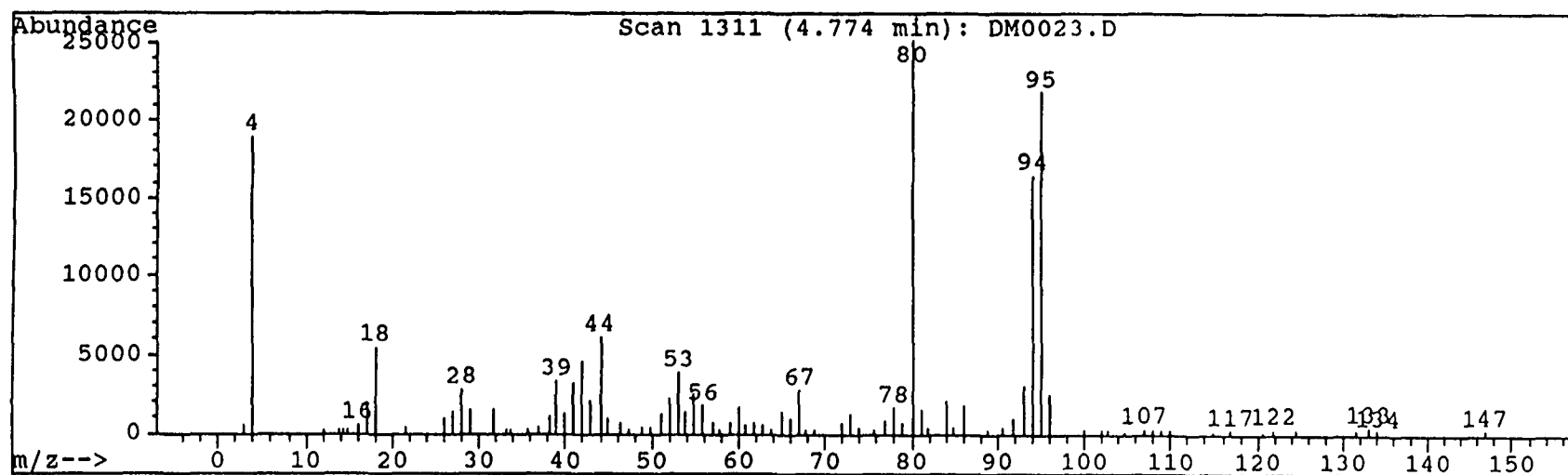
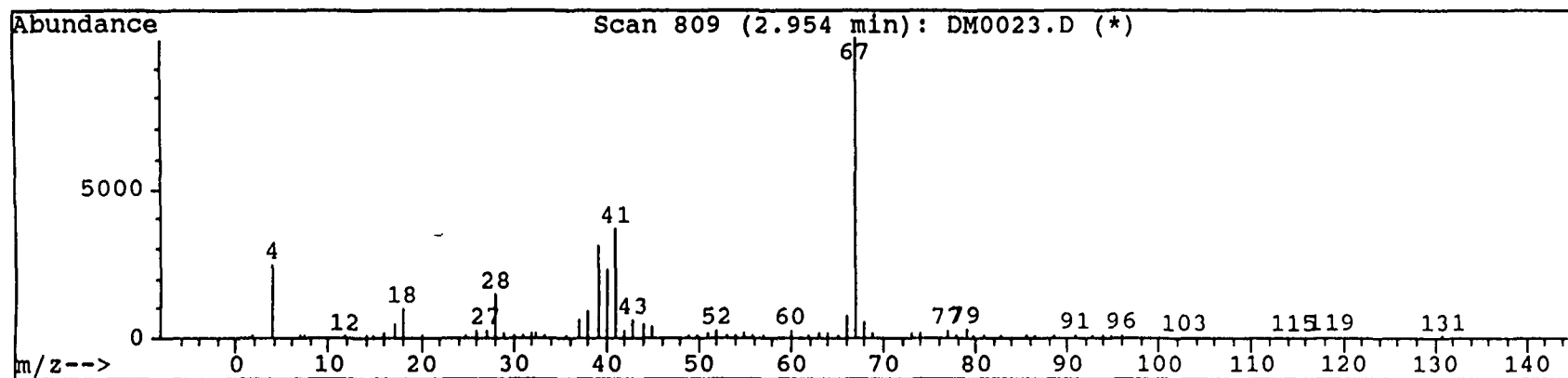
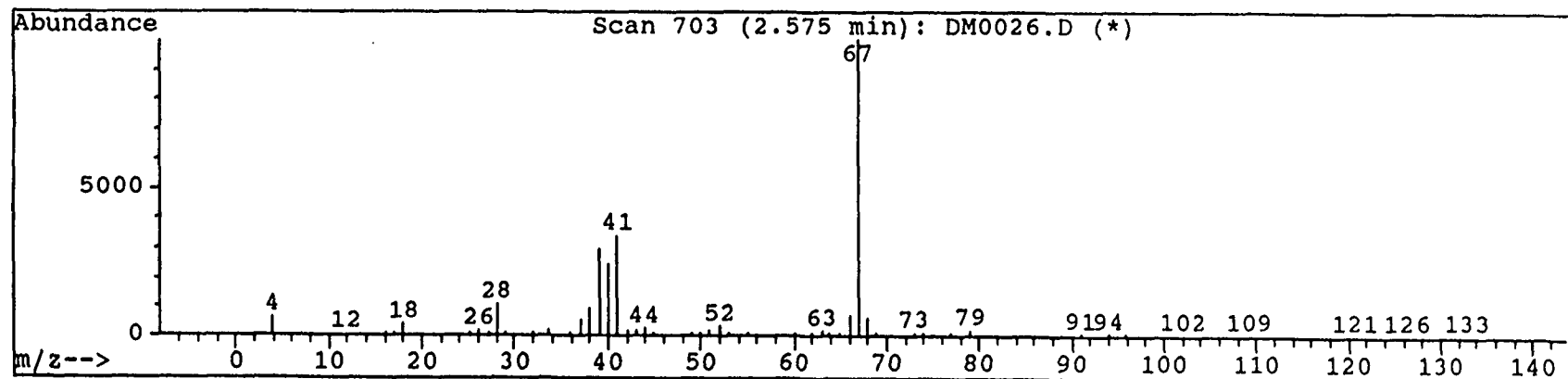
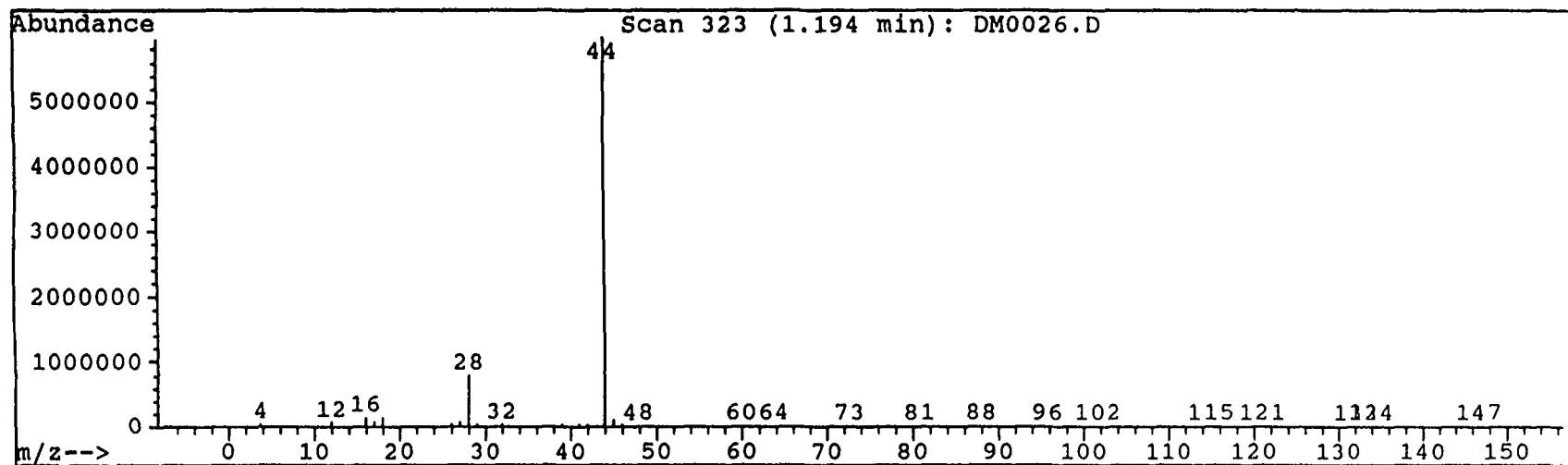


Figure X-8. Mass spectral data for glutamic acid pyrolysis at 400° C/sec (DM0026.D).



PYROLYSIS GC/MS FOR AMMONIUM SALTS

Spectral Identification of Ammonium Salt Pyrolysis Products

The mass spectrum for the chromatographic peaks observed from ammonium sulfate pyrolysis indicated the expected reaction products, ammonia and sulfur dioxide, SO₂. At a retention time of 1.9 min., the dominant species indicated as the group around mass 16 is ammonia (m/z = 17) and likely ammonium ion, NH₄⁺, (m/z = 18). Because both species are susceptible to losing hydrogen atoms, the base peak is represented by mass 16.

A very similar spectrum is observed at a retention time of 2.2 min. with a combination of the ammonia/ammonium ion being dominant. At a retention time of 2.3 min., sulfur dioxide is present at mass 64 with the main fragment at mass 48 being SO due to the loss of oxygen. Mass 32 is represented by O₂ while mass 18 is likely represented by the ammonium ion.

For ammonium chloride, little to nothing is observed in the chromatograms and the mass spectra due to the reversible reaction of the gas phase species NH₃ and HCl to form NH₄Cl. The reaction, given in Eq. X-1, forms the ammonium chloride precipitate when the gases are quenched after pyrolysis. This reaction proceeds at ambient temperatures. White deposits were observed after ammonium chloride pyrolysis suggesting that the following reaction occurred



The mass spectra for ammonium chloride indicate the presence of ammonium ion at mass 18. HCl, which would have been observed as a pyrolysis product, is not present. The dominant species is He at mass 4 indicating only the background to be present in the spectra. Other species such as N, N₂, O₂, and CO₂ observed in the spectra at masses 14, 28, 32, and 44, respectively, are in very low abundance.

Ammonium Salt Pyrolysis Spectral Data Tables and Figures

Mass spectral data tables and spectra for the ammonium salts are provided on the following pages of this section. Spectra and tables are provided for the results of the first heating rate, while the remaining data is provided strictly as tables. The tables include information for the heating rates employed, peak retention times, the mass/charge ratios and abundances for each peak at the given retention time. Each abundance has been normalized to the base peak for simplified identification of the informational mass/charge ratios from the noise of the spectrum.

The figures presented include the gas chromatogram and the individual mass spectra for the retention time of interest. Each figure contains the retention time value and the filename for the data. The filename can be used to identify the sample with its tabulated data.

Table X-7. Mass spectral data for ammonium sulfate pyrolysis at 10° C/sec.

Ammonium sulfate pyrolysis at 10° C/sec (0.01° C/msec) to 500° C (spectral name=DM0032.D).

Gas chromatography peaks at the following retention times:

1.9 min 2.2 min 2.3 min

At each of these peaks, the mass abundance data are presented below.

At 1.9 min, the following abundances* were observed at the given mass/charge ratios (m/z).

<u>m/z</u>	<u>Abundance</u>	<u>m/z</u>	<u>Abundance</u>	<u>m/z</u>	<u>Abundance</u>	<u>m/z</u>	<u>Abundance</u>
4	9	17	89	26	0	44	5
14	7	18	34	27	0	45	0
15	29	19	1	28	2	60	1
16	100	25	0	29	0	64	1

*Abundances are normalized against the base peak.

At 2.2 min, the following abundances* were observed at the given mass/charge ratios (m/z).

<u>m/z</u>	<u>Abundance</u>	<u>m/z</u>	<u>Abundance</u>	<u>m/z</u>	<u>Abundance</u>	<u>m/z</u>	<u>Abundance</u>
4	9	17	89	26	0	44	5
14	7	18	34	27	0	45	0
15	29	19	1	28	2	60	1
16	100	25	0	29	0	64	1

*Abundances are normalized against the base peak.

At 2.3 min, the following abundances* were observed at the given mass/charge ratios (m/z).

<u>m/z</u>	<u>Abundance</u>	<u>m/z</u>	<u>Abundance</u>	<u>m/z</u>	<u>Abundance</u>	<u>m/z</u>	<u>Abundance</u>
4	9	17	9	32	5	50	2
14	0	18	13	33	0	64	100
15	2	19	0	44	2	65	1
16	7	28	1	48	42	66	5

*Abundances are normalized against the base peak.

Table X-8. Mass spectral data for ammonium sulfate pyrolysis at 400° C/sec.

Ammonium sulfate pyrolysis at 400° C/sec (0.4° C/msec) to 500° C (spectral name=DM0034.D).

Gas chromatography peaks at the following retention times:

1.2 min 2.1 min

At each of these peaks, the mass abundance data are presented below.

At 1.2 min, the following abundances* were observed at the given mass/charge ratios (m/z).

<u>m/z</u>	<u>Abundance</u>	<u>m/z</u>	<u>Abundance</u>	<u>m/z</u>	<u>Abundance</u>	<u>m/z</u>	<u>Abundance</u>
4	5	17	83	26	0	32	2
14	8	18	17	27	0	44	2
15	31	19	1	28	5	45	0
16	100	25	0	29	0		

*Abundances are normalized against the base peak.

At 2.1 min, the following abundances* were observed at the given mass/charge ratios (m/z).

<u>m/z</u>	<u>Abundance</u>	<u>m/z</u>	<u>Abundance</u>	<u>m/z</u>	<u>Abundance</u>	<u>m/z</u>	<u>Abundance</u>
4	66	28	5	49	1	84	1
5	1	32	9	50	3	94	1
6	1	41	1	55	1	96	2
14	1	42	1	60	2	119	1
16	19	43	1	64	100	133	1
17	27	44	10	65	2	138	1
18	70	45	2	66	5		
20	1	46	1	73	3		
26	1	46	1	77	2		
27	1	48	49	78	1		

*Abundances are normalized against the base peak.

Figure X-6. Chromatogram for ammonium sulfate pyrolysis at 10° C/sec (DM0032.D) and 400° C/sec (DM0034.D).

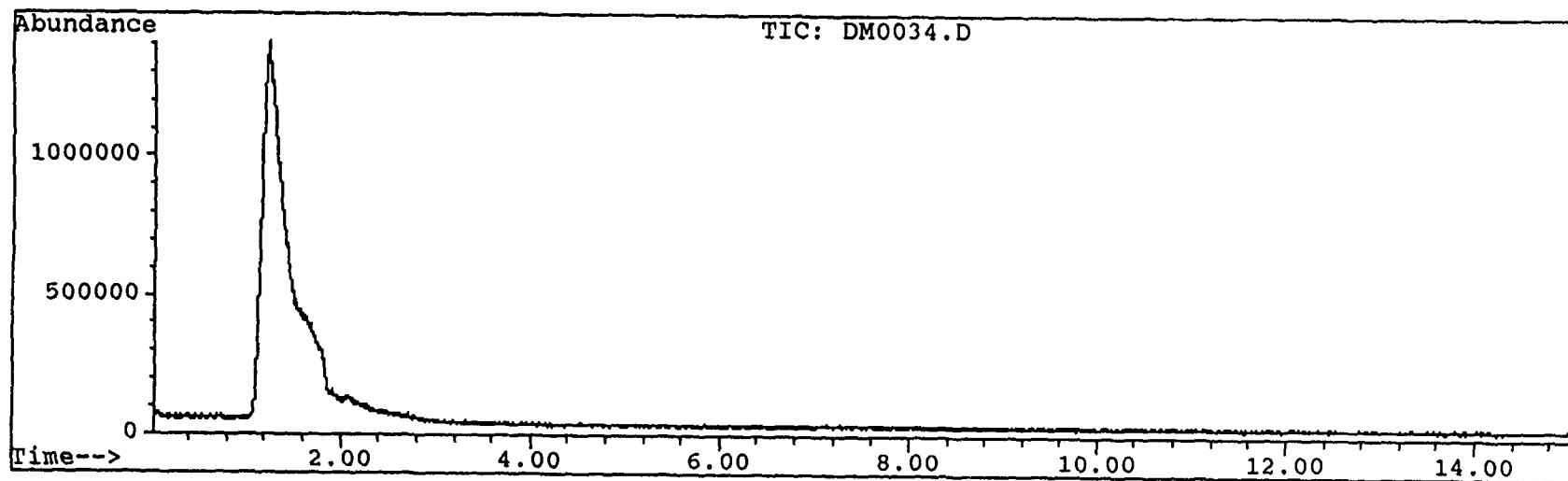
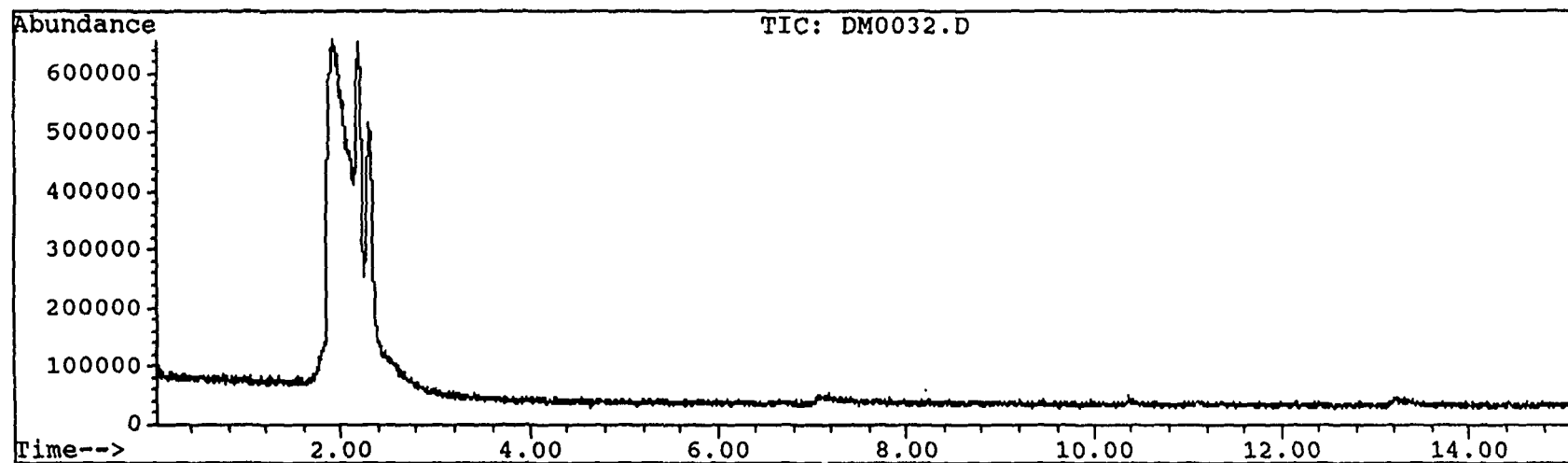


Figure X-7. Mass spectral data for ammonium sulfate pyrolysis at 10° C/sec (DM0032.D).

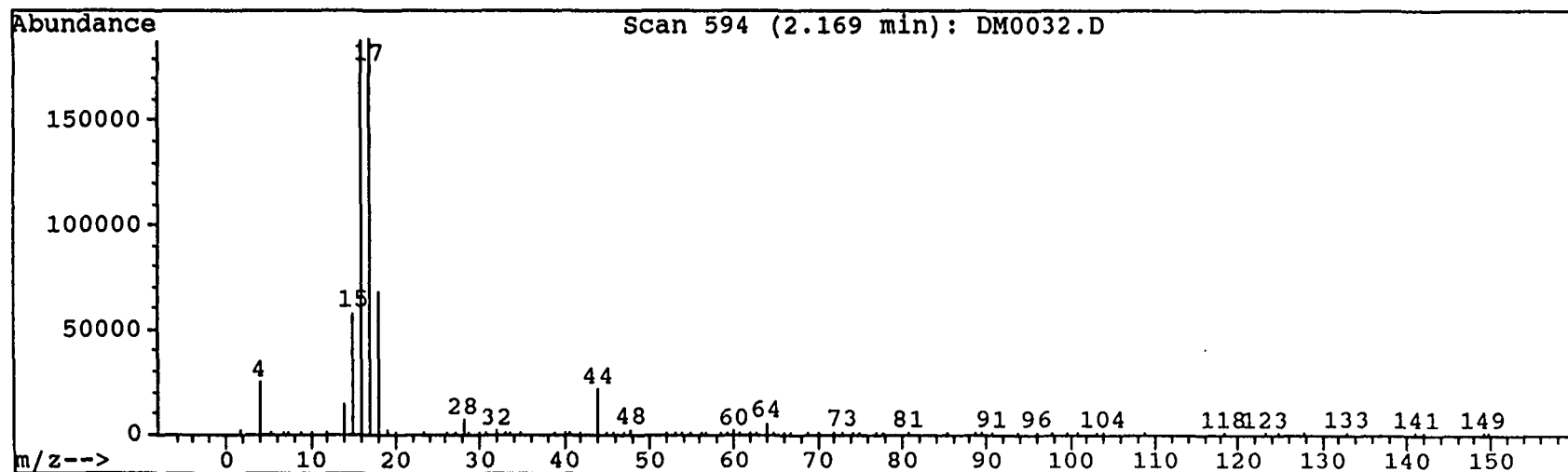
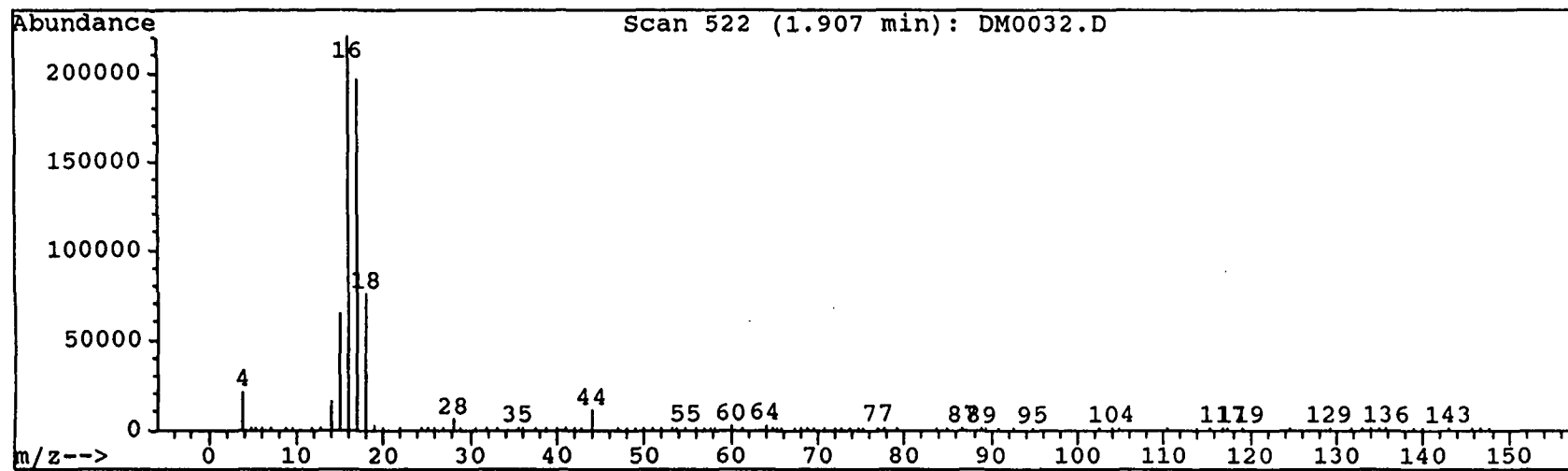


Figure X-7. (cont.) Mass spectral data for ammonium sulfate pyrolysis at 10° C/sec (DM0032.D).

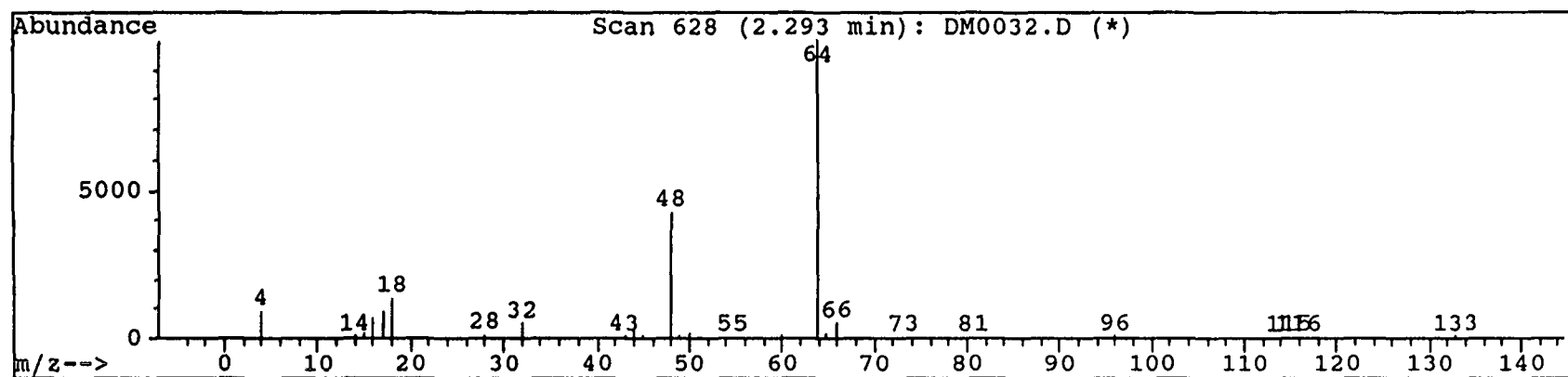


Figure X-8. Mass spectral data for ammonium sulfate pyrolysis at 4000° C/sec (DM0034.D).

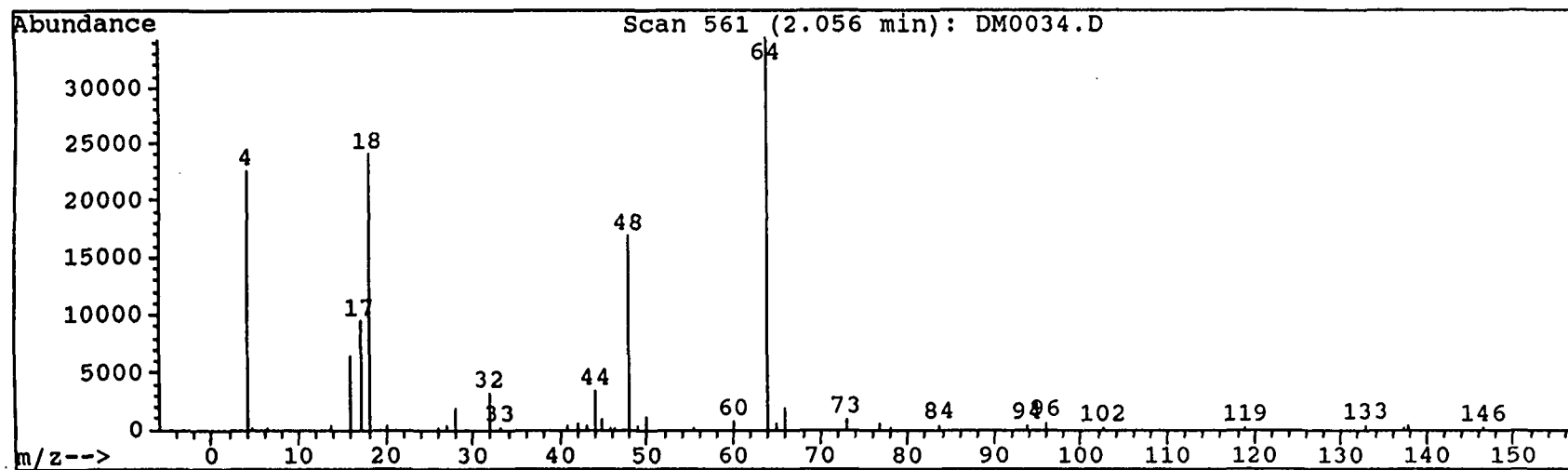
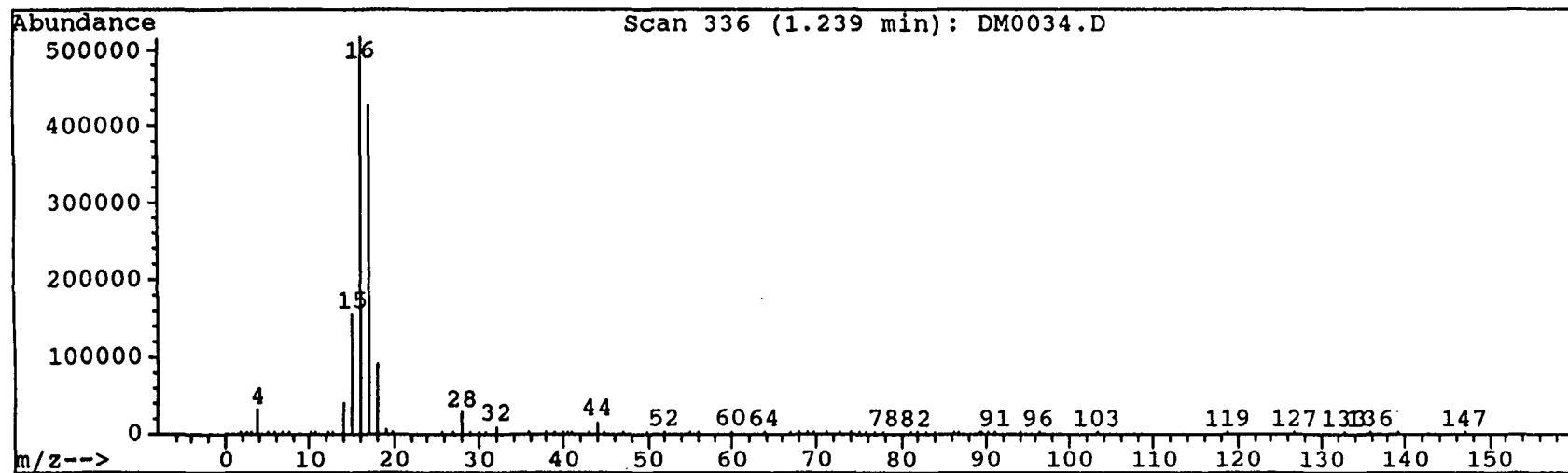


Table X-9. Mass spectral data for ammonium chloride pyrolysis at 10° C/sec.

Ammonium chloride pyrolysis at 600° C/min (0.01° C/msec) to 500° C (spectral name=DM0036.

Gas chromatography peak at the following retention times: 2.3 min

At each of these peaks, the mass abundance data are presented below.

At 2.3 min, the following abundances* were observed at the given mass/charge ratios (m/z).

<u>m/z</u>	<u>Abundance</u>	<u>m/z</u>	<u>Abundance</u>	<u>m/z</u>	<u>Abundance</u>	<u>m/z</u>	<u>Abundance</u>
4	73	18	17	43	2	64	100
14	2	27	1	44	16	66	7
15	5	28	6	48	45	79	2
16	14	32	6	50	3	149	2
17	22	34	2	58	2		

*Abundances are normalized against the base peak.

Table X-10. Mass spectral data for ammonium chloride pyrolysis at 400° C/sec.

Ammonium chloride pyrolysis at 400° C/sec (0.4° C/msec) to 500° C (spectral name=DM0035.D

Gas chromatography peak at the following retention times: 1.3 min

At each of these peaks, the mass abundance data are presented below.

At 1.3 min, the following abundances* were observed at the given mass/charge ratios (m/z).

<u>m/z</u>	<u>Abundance</u>	<u>m/z</u>	<u>Abundance</u>	<u>m/z</u>	<u>Abundance</u>	<u>m/z</u>	<u>Abundance</u>
2	2	18	23	40	2	60	4
4	100	27	2	42	2	64	9
14	9	28	49	44	37	69	2
15	1	29	2	48	6	73	3
16	10	32	19	51	2	96	2
17	12	34	2	55	2	117	2

*Abundances are normalized against the base peak.

Figure X-9. Chromatogram for ammonium chloride pyrolysis at 10° C/sec (DM0051.D) and 400° C/sec (DM0050.D).

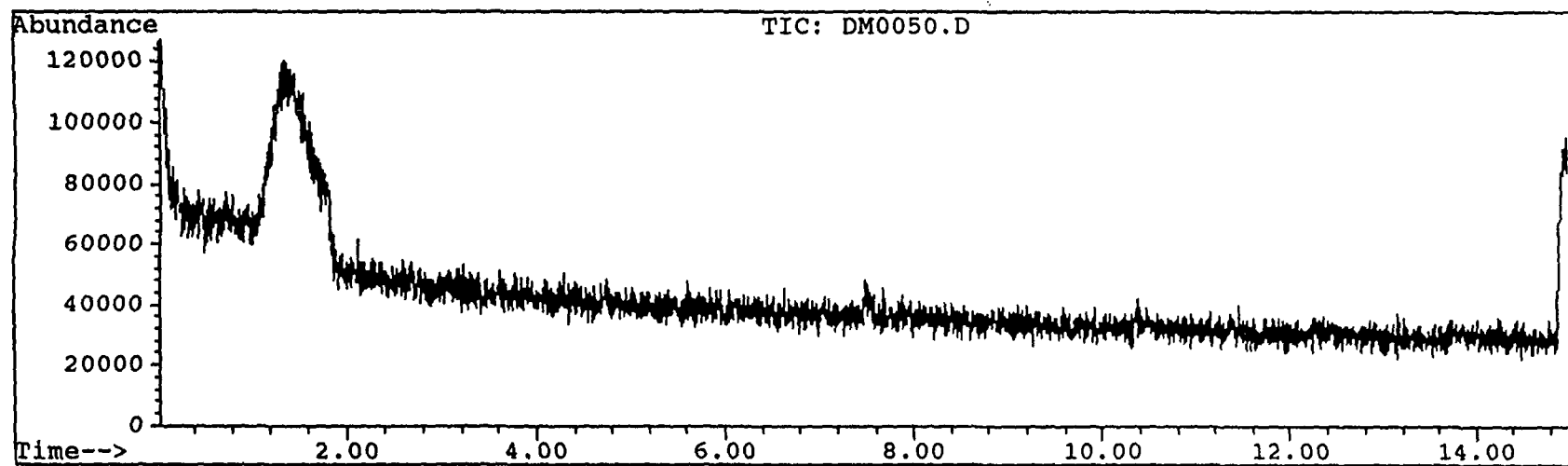
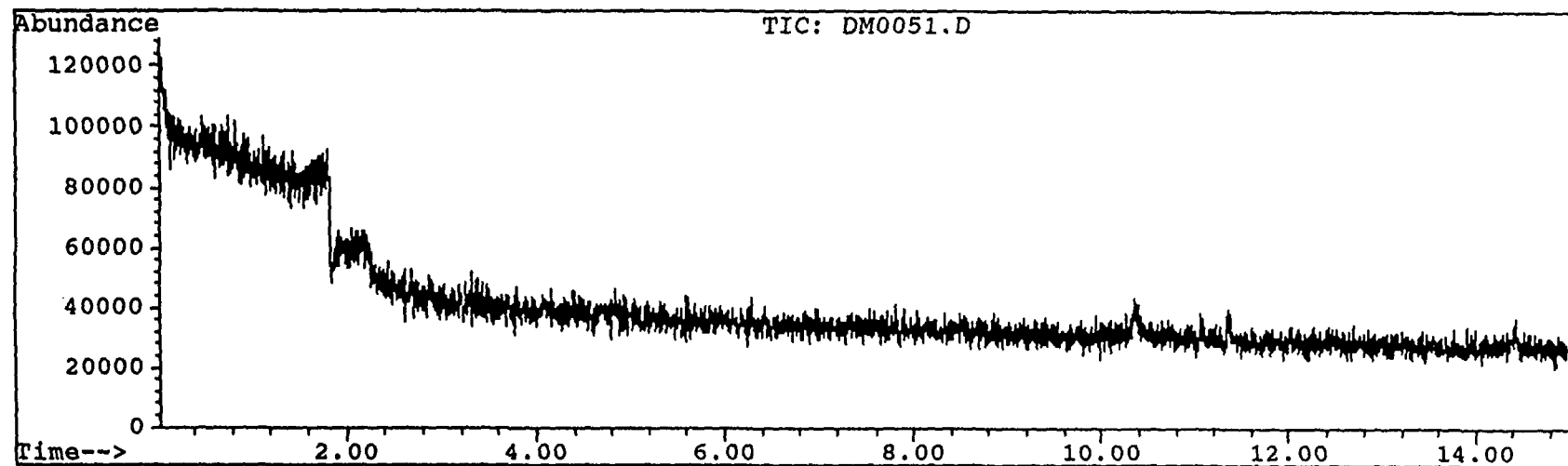


Figure X-10. Mass spectral data for ammonium chloride pyrolysis at 10° C/sec (DM0051.D) and 400° C/sec (DM0050.D).

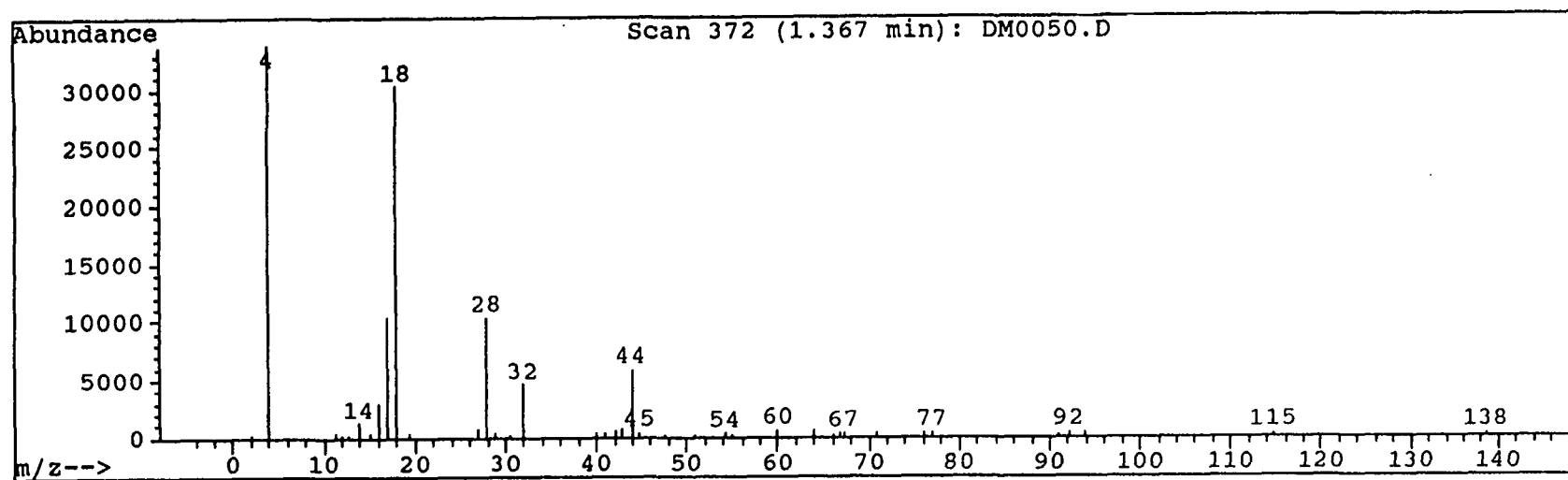
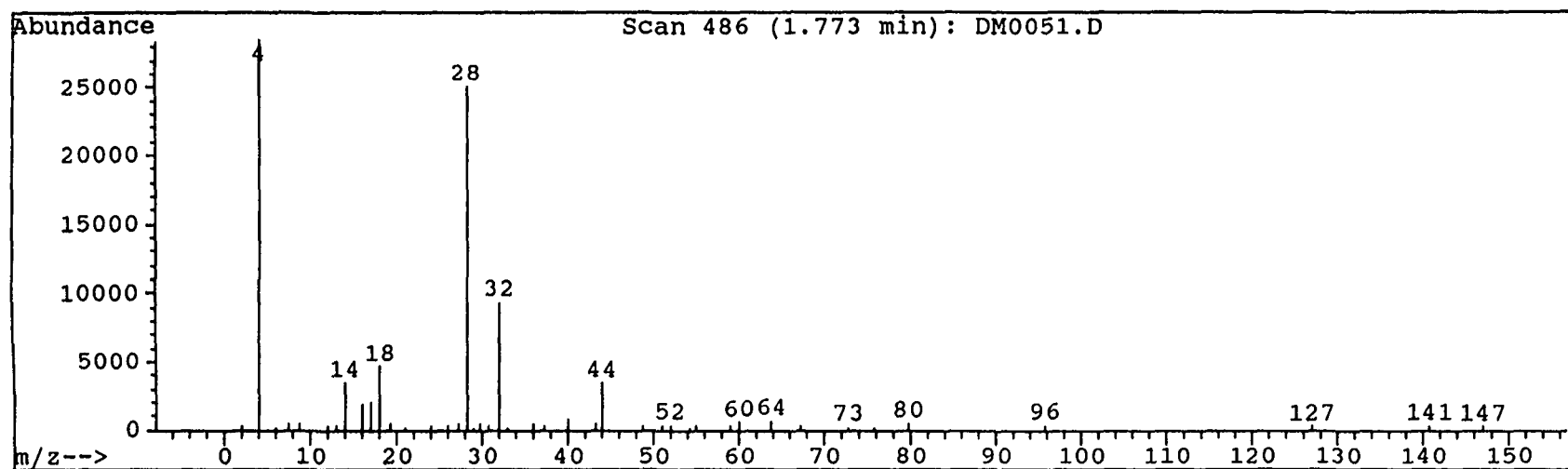


Table X-11. Mass spectral data for ammonia gas, direct injection into the GC as reference material. (DM0049.D)

Gas chromatography peaks at the following retention times: 1.01 min, initiated at 0.90 min

At each of these peaks, the mass abundance data are presented below.

At **1.01 min**, the following abundances* were observed at the given mass/charge ratios (m/z).

<u>m/z</u>	<u>Abundance</u>	<u>m/z</u>	<u>Abundance</u>	<u>m/z</u>	<u>Abundance</u>	<u>m/z</u>	<u>Abundance</u>
4	100	17	27	29	2	60	2
14	10	18	11	32	43	69	2
15	7	20	2	40	6		
16	20	28	88	44	10		

*Abundances are normalized against the base peak.

Table X-12. Mass spectral data for air, direct injection into the GC as reference material. (DM0047.D)

Gas chromatography peaks at the following retention times: 1.01 min, initiated at 0.91 min

At each of these peaks, the mass abundance data are presented below.

At **1.01 min**, the following abundances* were observed at the given mass/charge ratios (m/z).

<u>m/z</u>	<u>Abundance</u>	<u>m/z</u>	<u>Abundance</u>	<u>m/z</u>	<u>Abundance</u>
4	0	17	0	29	2
14	10	18	0	32	72
15	0	20	0	40	7
16	5	28	100	44	1

*Abundances are normalized against the base peak.

Figure X-11. Chromatogram and mass spectral data for injection of air (DM0047.D).

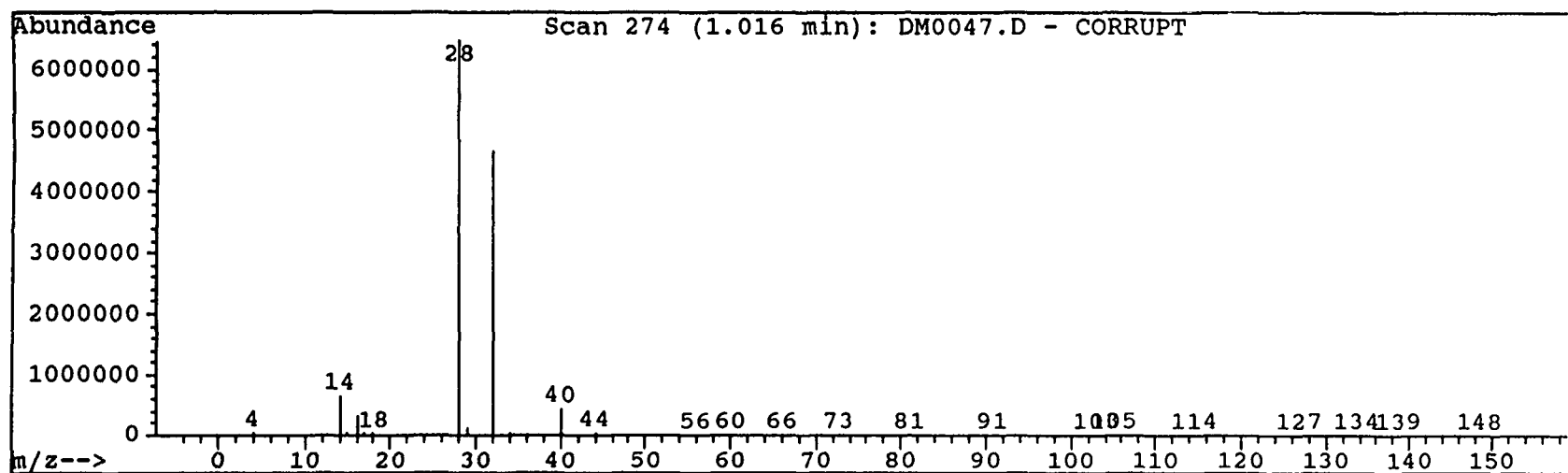
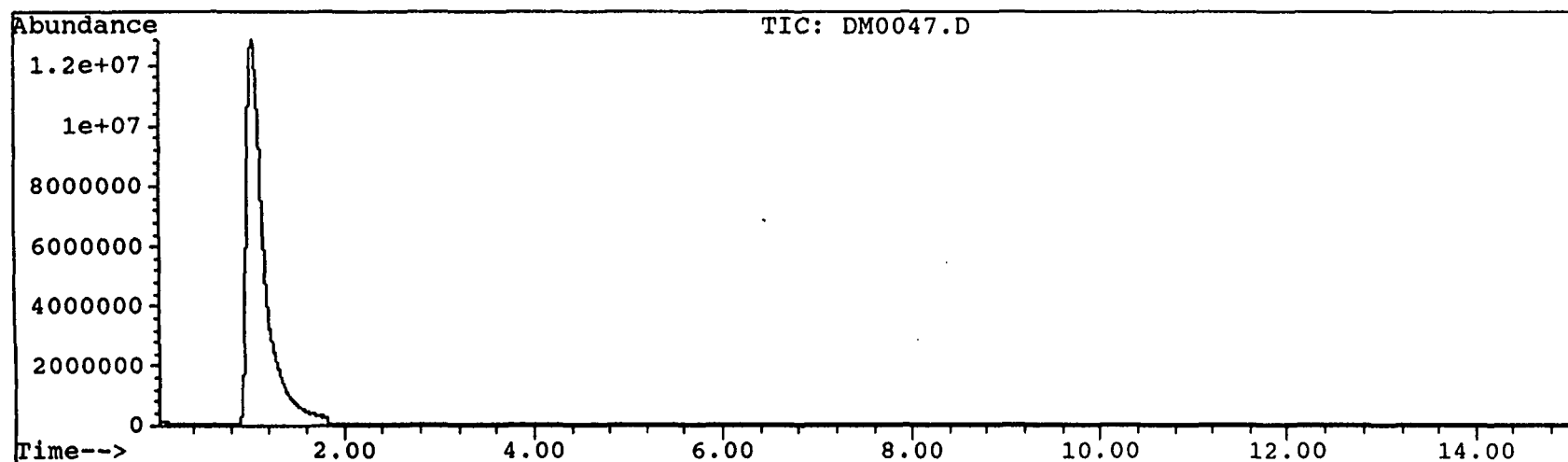
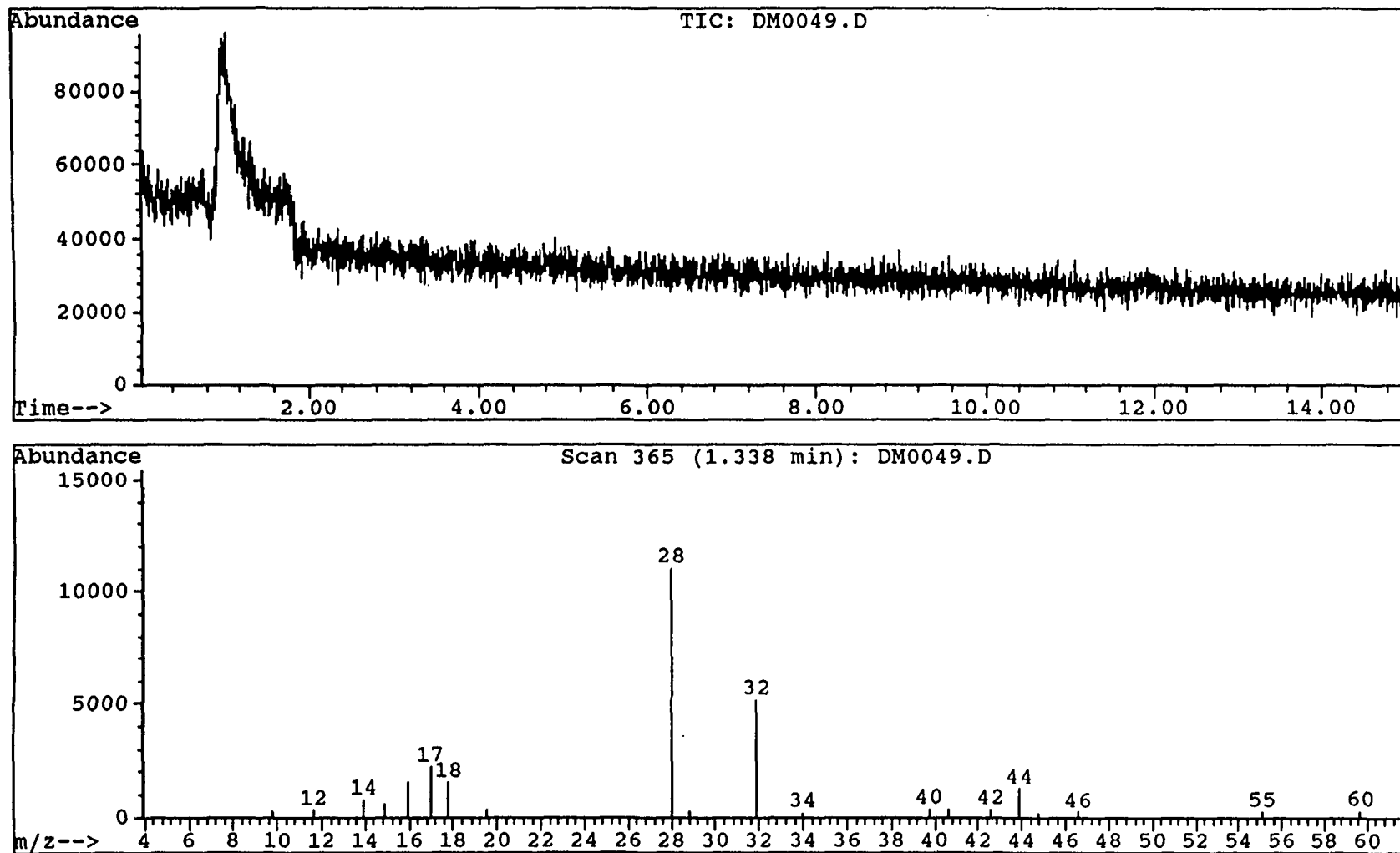


Figure X-12. Chromatogram and mass spectral data for injection of ammonia gas (DM0049.D).



APPENDIX XI: NITROGEN MEASUREMENTS FOR BLACK LIQUOR PYROLYSIS AND COMBUSTION

This appendices contains the nitrogen measurements data for pyrolysis and combustion of black liquor samples. The data is provided in two parts. First, data for total nitrogen measurements under combustion conditions for the black liquors and the liquor fractions is presented. This is followed by the GPNP nitrogen data for the black liquor samples and fractions for pyrolysis conditions. The calibration curve used to calculate the nitrogen concentrations is also presented. Second, the data that was obtained from single drop pyrolysis, %N as NO and %N in the char is presented.

Each set of data is presented along with the statistical summaries. Error estimates can be taken from the correlation coefficients in the plots as well as the statistical standard deviation and coefficient of variation.

For the GPNP nitrogen data, the sample numbers in the data tables, such as N4097022, are the same as the computer data acquisition (CDA) file names. The N identifies the sample as a nitrogen release profile type of data file. The 4 represents the lab notebook #4264. The next three digits are the page number within the notebook where the data can be found and the last three digits are the sample number on that page. The last digit represents the number of the replicate. For the example, the values listed for the N4097022 sample would be found in notebook 4264 on page 97 as sample 2, replicate 2.

Table XI-1. Black liquor acid precipitated fraction pyrolysis data for total nitrogen measurement.

Method Used:	5	PMT Voltage:	825	
O ₂ to O ₃ :	30 ml/min	Furnace Temperature:	1100 ° C	Acid ppt #1 So. Pine III
O ₂ to pyro:	365 ml/min	Gain Setting:	HI	Acid ppt #2 So. Pine IV
O ₂ to inlet:	20 ml/min	Gain Factor:	X1	Acid ppt #3 So. Pine I
He to inlet:	145 ml/min	Heating Program #:	2	Acid ppt #4 So. Pine II
Sample ID:	Acid precipitated fraction	Matrix:	none	

<u>Sample #</u>	<u>Sample ID</u>	<u>Sample Mass (µg)</u>	<u>Response Counts</u>	<u>CDA Sum Response</u>	<u>Calculated** %N (dry basis)</u>
N4145131	Acid ppt #1	4.05	155805	222.4365	0.1927
N4145132	Acid ppt #1	8.69	153107	470.557	0.1890
N4145133	Acid ppt #1	4.27	175309	265.5995	0.2193

<u>Sample #</u>	<u>Ave. Counts</u>	<u>n</u>	<u>SD</u>	<u>RSD (%)</u>
N414513_	161407	3	12114	7.51

<u>Sample #</u>	<u>Sample ID</u>	<u>Sample Mass (µg)</u>	<u>Response Counts</u>	<u>CDA Sum Response</u>	<u>Calculated** %N (dry basis)</u>
N4146151	Acid ppt #2	5.53	177768	347.338	0.2189
N4146152	Acid ppt #2	6.03	179578	382.6661	0.2213
N4146153	Acid ppt #2	5.72	187579	379.2488	0.2320

<u>Sample #</u>	<u>Ave. Counts</u>	<u>n</u>	<u>SD</u>	<u>RSD (%)</u>
N414615_	181642	3	5221	2.87

<u>Sample #</u>	<u>Sample ID</u>	<u>Sample Mass (µg)</u>	<u>Response Counts</u>	<u>CDA Sum Response</u>	<u>Calculated** %N (dry basis)</u>
N4146171	Acid ppt #3	6.47	1505279	205.0293	0.1224
N4146172	Acid ppt #3	5.58	104451	178.6619	0.1213
N4146173	Acid ppt #3	4.73	107319	186.474	0.1251

<u>Sample #</u>	<u>Ave. Counts</u>	<u>n</u>	<u>SD</u>	<u>RSD (%)</u>
N414617_	105683	3	1476	1.39

<u>Sample #</u>	<u>Sample ID</u>	<u>Sample Mass (µg)</u>	<u>Response Counts</u>	<u>CDA Sum Response</u>	<u>Calculated** %N (dry basis)</u>
N4146181	Acid ppt #4	3.93	134835	186.474	0.1639
N4146182	Acid ppt #4	3.40	127243	152.2458	0.1535
N4146183	Acid ppt #4	4.99	126659	222.7546	0.1528

<u>Sample #</u>	<u>Ave. Counts</u>	<u>n</u>	<u>SD</u>	<u>RSD (%)</u>
N414618_	129579	3	4561	3.52

**Nitrogen content determined by proline calibration curve.

Table XI-2. Black liquor non-precipitated fraction pyrolysis data for total nitrogen measurement.

Method Used:	5	PMT Voltage:	825	
O ₂ to O ₃ :	30 ml/min	Furnace Temperature:	1100 °C	Non- ppt #1 So. Pine III
O ₂ to pyro:	365 ml/min	Gain Setting:	HI	Non- ppt #2 So. Pine IV
O ₂ to inlet:	20 ml/min	Gain Factor:	X1	Non- ppt #3 So. Pine I
He to inlet:	145 ml/min	Heating Program #:	2	Non- ppt #4 So. Pine II
Sample ID:	Non-precipitated fraction	Matrix:	none	

<u>Sample #</u>	<u>Sample ID</u>	<u>Sample Mass (µg)</u>	<u>Response Counts</u>	<u>CDA Sum Response</u>	<u>Calculated** %N (dry basis)</u>
N4155291	Non- ppt #1	5.99	52317	109.0801	0.0551
N4155292	Non- ppt #1	6.31	56186	123.7549	0.0607
N4155293	Non- ppt #1	6.55	58992	135.1804	0.0648

<u>Sample #</u>	<u>Ave. Counts</u>	<u>n</u>	<u>SD</u>	<u>RSD (%)</u>
N415529_	55832	3	3351	6.00

<u>Sample #</u>	<u>Sample ID</u>	<u>Sample Mass (µg)</u>	<u>Response Counts</u>	<u>CDA Sum Response</u>	<u>Calculated** %N (dry basis)</u>
N4155301	Non- ppt #2	4.41	64703	99.3179	0.0733
N4155302	Non- ppt #2	4.28	66572	99.1226	0.0760
N4155303	Non- ppt #2	4.15	60429	87.0351	0.0671

<u>Sample #</u>	<u>Ave. Counts</u>	<u>n</u>	<u>SD</u>	<u>RSD (%)</u>
N415530_	63902	3	3149	4.93

<u>Sample #</u>	<u>Sample ID</u>	<u>Sample Mass (µg)</u>	<u>Response Counts</u>	<u>CDA Sum Response</u>	<u>Calculated** %N (dry basis)</u>
N4155311	Non- ppt #3	2.33	19948	15.5271	0.0085
N4155312	Non- ppt #3	4.13	23036	31.7117	0.0130
N4155313	Non- ppt #3	4.34	21893	31.395	0.0113

<u>Sample #</u>	<u>Ave. Counts</u>	<u>n</u>	<u>SD</u>	<u>RSD (%)</u>
N415532_	21626	3	1561	7.22

<u>Sample #</u>	<u>Sample ID</u>	<u>Sample Mass (µg)</u>	<u>Response Counts</u>	<u>CDA Sum Response</u>	<u>Calculated** %N (dry basis)</u>
N4155321	Non- ppt #4	4.43	22161	33.2282	0.0112
N4155322	Non- ppt #4	3.02	18738	--	0.0064
N4155323	Non- ppt #4	5.91	23521	47.6083	0.0132

<u>Sample #</u>	<u>Ave. Counts</u>	<u>n</u>	<u>SD</u>	<u>RSD (%)</u>
N415532_	21473	3	2464	11.48

**Nitrogen content determined by proline calibration curve.

Table XI-3. Black liquor pyrolysis data for total nitrogen measurement.

Method Used:	5	PMT Voltage:	825	
O ₂ to O ₃ :	30 ml/min	Furnace Temperature:	1100C	blk liq. #1 So. Pine III
O ₂ to pyro:	365 ml/min	Gain Setting:	HI	blk liq. #2 So. Pine IV
O ₂ to inlet:	20 ml/min	Gain Factor:	X1	blk liq. #3 So. Pine I
He to inlet:	145 ml/min	Heating Program #:	2	blk liq. #4 So. Pine II
Sample ID:	whole black liquor	Matrix:	none	

Sample #	Sample ID	Sample Mass (μ g)	Response Counts	CDA Sum Response	Calculated** %N (dry basis)
N4155331	black liquor #1	23.65	62819	525.0733	0.0982
N4155332	black liquor #1	14.45	62413	318.0186	0.0974
N4155333	black liquor #1	12.02	63204	267.8712	0.0990

Sample #	Ave. Counts	n	SD	RSD (%)
N415533_	62812	3	396	0.63

Sample #	Sample ID	Sample Mass (μ g)	Response Counts	CDA Sum Response	Calculated** %N (dry basis)
N4155341	black liquor #2	35.39	62500	793.6532	0.0982
N4155342	black liquor #2	16.00	65871	371.6302	0.1051
N4155343	black liquor #2	14.46	66302	338.5259	0.1059

Sample #	Ave. Counts	n	SD	RSD (%)
N415534_	64891	3	2082	3.21

Sample #	Sample ID	Sample Mass (μ g)	Response Counts	CDA Sum Response	Calculated** %N (dry basis)
N4155351	black liquor #3	11.94	35515	148.0226	0.0382
N4155352	black liquor #3	19.17	36909	249.1208	0.0407
N4155353	black liquor #3	8.89	34549	106.9587	0.0365

Sample #	Ave. Counts	n	SD	RSD (%)
N415535_	35658	3	1186	3.33

Sample #	Sample ID	Sample Mass (μ g)	Response Counts	CDA Sum Response	Calculated** %N (dry basis)
N4155361	black liquor #4	27.05	21789	—	0.0302
N4155362	black liquor #4	33.86	21131	252.2207	0.0275
N4155363	black liquor #4	39.26	20765	287.427	0.0261

Sample #	Ave. Counts	n	SD	RSD (%)
N415536_	21229	3	519	2.44

**Nitrogen content determined by proline calibration curve.

Table XI-4. Black liquor acid precipitated fraction combustion data for total nitrogen measurement.

Method Used:	5	PMT Voltage:	825	
O ₂ to O ₃ :	30 ml/min	Furnace Temperature:	1100° C	Acid ppt #1 So. Pine III
O ₂ to pyro:	365 ml/min	Gain Setting:	HI	Acid ppt #2 So. Pine IV
O ₂ to inlet:	20 ml/min	Gain Factor:	X1	Acid ppt #3 So. Pine I
He to inlet:	145 ml/min	Matrix:	none	Acid ppt #4 So. Pine II
Sample ID:	Acid precipitated fraction			

<u>Sample #</u>	<u>Sample ID</u>	<u>Sample Mass (µg)</u>	<u>Response Counts</u>	<u>CDA Sum Response</u>	<u>Calculated** %N (dry basis)</u>
N4159041	Acid ppt #1	3.42	177670	214.0623	0.3044
N4159042	Acid ppt #1	5.89	168425	351.1719	0.2884
N4159043	Acid ppt #1	4.23	179567	268.1643	0.3077

<u>Sample #</u>	<u>Ave. Counts</u>	<u>n</u>	<u>SD</u>	<u>RSD (%)</u>
N415904_	175221	3	5961	3.40

<u>Sample #</u>	<u>Sample ID</u>	<u>Sample Mass (µg)</u>	<u>Response Counts</u>	<u>CDA Sum Response</u>	<u>Calculated** %N (dry basis)</u>
N4159051	Acid ppt #2	9.47	172680	578.9308	0.2908
N4159052	Acid ppt #2	5.36	174477	330.396	0.2939
N4159053	Acid ppt #2	7.42	176893	464.2338	0.2980

<u>Sample #</u>	<u>Ave. Counts</u>	<u>n</u>	<u>SD</u>	<u>RSD (%)</u>
N415905_	181642	3	5221	2.87

<u>Sample #</u>	<u>Sample ID</u>	<u>Sample Mass (µg)</u>	<u>Response Counts</u>	<u>CDA Sum Response</u>	<u>Calculated** %N (dry basis)</u>
N4159061	Acid ppt #3	5.42	105825	202.3686	0.1777
N4159062	Acid ppt #3	4.51	105018	166.9916	0.1763
N4159063	Acid ppt #3	3.47	106891	130.3948	0.1795

<u>Sample #</u>	<u>Ave. Counts</u>	<u>n</u>	<u>SD</u>	<u>RSD (%)</u>
N415906_	105911	3	939	0.89

<u>Sample #</u>	<u>Sample ID</u>	<u>Sample Mass (µg)</u>	<u>Response Counts</u>	<u>CDA Sum Response</u>	<u>Calculated** %N (dry basis)</u>
N4159071	Acid ppt #4	6.27	123166	273.0957	0.2096
N4159072	Acid ppt #4	4.75	124905	209.6927	0.2126
N4159073	Acid ppt #4	3.40	129174	154.6633	0.2200

<u>Sample #</u>	<u>Ave. Counts</u>	<u>n</u>	<u>SD</u>	<u>RSD (%)</u>
N415907_	125748	3	3092	2.46

**Nitrogen content determined by glutamic acid calibration curve.

Table XI-5. Black liquor non-precipitated fraction combustion data for total nitrogen measurement.

Method Used:	5	PMT Voltage:	825	
O ₂ to O ₃ :	30 ml/min	Furnace Temperature:	1100° C	Non- ppt #1 So. Pine III
O ₂ to pyro:	365 ml/min	Gain Setting:	HI	Non- ppt #2 So. Pine IV
O ₂ to inlet:	20 ml/min	Gain Factor:	X1	Non- ppt #3 So. Pine I
He to inlet:	145 ml/min	Matrix:	none	Non- ppt #4 So. Pine II
Sample ID:	Non-precipitated fraction			

<u>Sample #</u>	<u>Sample ID</u>	<u>Sample Mass (µg)</u>	<u>Response Counts</u>	<u>CDA Sum Response</u>	<u>Calculated** %N (dry basis)</u>
N4160082	Non- ppt #1	3.84	37081	48.9248	0.0647
N4160083	Non- ppt #1	3.53	37104	--	0.0647
N4160084	Non- ppt #1	6.92	39731	94.9452	0.0696

<u>Sample #</u>	<u>Ave. Counts</u>	<u>n</u>	<u>SD</u>	<u>RSD (%)</u>
N416008_	37972	3	1523	4.01

<u>Sample #</u>	<u>Sample ID</u>	<u>Sample Mass (µg)</u>	<u>Response Counts</u>	<u>CDA Sum Response</u>	<u>Calculated** %N (dry basis)</u>
N4160091	Non- ppt #2	7.04	44829	109.4957	0.0792
N4160092	Non- ppt #2	9.92	44986	138.0842	0.0795
N4160093	Non- ppt #2	5.25	37298	67.2357	0.0653
N4160094	Non- ppt #2	3.18	38783	42.5766	0.0681

<u>Sample #</u>	<u>Ave. Counts</u>	<u>n</u>	<u>SD</u>	<u>RSD (%)</u>
N416009_	41474	4	4011	9.67

<u>Sample #</u>	<u>Sample ID</u>	<u>Sample Mass (µg)</u>	<u>Response Counts</u>	<u>CDA Sum Response</u>	<u>Calculated** %N (dry basis)</u>
N4160101	Non- ppt #3	4.28	17336	24.6543	0.0290
N4160102	Non- ppt #3	3.52	14011	16.037	0.0227
N4160103	Non- ppt #3	5.06	13660	22.9932	0.0221
N4160104	Non- ppt #3	4.42	11908	17.3559	0.0188

<u>Sample #</u>	<u>Ave. Counts</u>	<u>n</u>	<u>SD</u>	<u>RSD (%)</u>
N416010_	14229	4	2267	15.93

<u>Sample #</u>	<u>Sample ID</u>	<u>Sample Mass (µg)</u>	<u>Response Counts</u>	<u>CDA Sum Response</u>	<u>Calculated** %N (dry basis)</u>
N4160111	Non- ppt #4	3.20	12831	13.9644	0.0197
N4160112	Non- ppt #4	4.41	12037	18.1879	0.0182
N4160113	Non- ppt #4	3.37	12029	13.8421	0.0182

<u>Sample #</u>	<u>Ave. Counts</u>	<u>n</u>	<u>SD</u>	<u>RSD (%)</u>
N416011_	12299	3	461	3.75

**Nitrogen content determined by glutamic acid calibration curve.

Table X1-6. Black liquor combustion data for total nitrogen measurement.

Method Used: 5 PMT Voltage: 825
 O₂ to O₃: 30 ml/min Furnace Temperature: 1100° C
 O₂ to pyro: 365 ml/min Gain Setting: HI
 O₂ to inlet: 20 ml/min Gain Factor: X1
 He to inlet: 145 ml/min Matrix: none
 Sample ID: whole black liquor

blk liq. #1 So. Pine III
 blk liq. #2 So. Pine IV
 blk liq. #3 So. Pine I
 blk liq. #4 So. Pine II

Sample #	Sample ID	Sample Mass (µg)	Response Counts	CDA Sum Response	Calculated** %N (dry basis)
N4156071	black liquor #1	10.49	48723	--	0.1204
N4156072	black liquor #1	9.76	45354	154.0505	0.1117
N4157074	black liquor #1	9.03	43590	136.1298	0.1071

Sample #	Ave. Counts	n	SD	RSD (%)
N415607_	46215	3	3111	6.73

Sample #	Sample ID	Sample Mass (µg)	Response Counts	CDA Sum Response	Calculated** %N (dry basis)
N4156081	black liquor #2	6.38	51312	--	0.1278
N4156082	black liquor #2	12.18	44131	187.6426	0.1092
N4156083	black liquor #2	7.86	44180	120.3577	0.1093

Sample #	Ave. Counts	n	SD	RSD (%)
N415608_	46541	3	4132	8.88

Sample #	Sample ID	Sample Mass (µg)	Response Counts	CDA Sum Response	Calculated** %N (dry basis)
N4157091	black liquor #3	6.58	33205	75.4626	0.0715
N4157092	black liquor #3	9.26	32377	103.5888	0.0696
N4157093	black liquor #3	8.03	34929	97.2175	0.0754

Sample #	Ave. Counts	n	SD	RSD (%)
N415709_	33504	3	1302	3.89

Sample #	Sample ID	Sample Mass (µg)	Response Counts	CDA Sum Response	Calculated** %N (dry basis)
N4157101	black liquor #4	15.97	17735	98.3169	0.0803
N4157102	black liquor #4	21.19	19008	140.6253	0.0867
N4157103	black liquor #4	10.11	15573	54.1016	0.0693

Sample #	Ave. Counts	n	SD	RSD (%)
N415710_	17438	3	1737	9.96

**Nitrogen content determined by glutamic acid calibration curve.

Table XI-8. Calibration data for glutamic acid during combustion.

Method Used:	5	PMT Voltage:	825
O2 to O3:	30 ml/min	Furnace Temperature:	1100C
O2 to pyro:	365 ml/min	Gain Setting:	HI
O2 to inlet:	20 ml/min	Gain Factor:	X1
He to inlet:	145 ml/min	Residence Time:	3 min
Nitrogen Species:	glutamic acid	Matrix:	d,d-H2O

Sample #	Sample ID	Sample Vol (μ l)	Known N Mass (μ g)	Known N ppm	Response Counts
N4072161	~500 ppm N	5	2.4791	495.82	31999
N4072162	~500 ppm N	5	2.4791	495.82	31967
N4072163	~500 ppm N	5	2.4791	495.82	36108
N4072164	~500 ppm N	5	2.4791	495.82	26641
N4072171	~100 ppm N	5	0.4953	99.06	9196
N4072172	~100 ppm N	5	0.4953	99.06	9127
N4072174	~100 ppm N	5	0.4953	99.06	9030
N4072181	~750 ppm N	5	3.7375	747.5	39931
N4072182	~750 ppm N	5	3.7375	747.5	45273
N4072183	~750 ppm N	5	3.7375	747.5	41308
N4072184	~750 ppm N	5	3.7375	747.5	43218
N4072191	~50 ppm N	5	0.2564	51.28	3337
N4072192	~50 ppm N	5	0.2564	51.28	4151
N4072193	~50 ppm N	5	0.2564	51.28	4363

Summarized Data	Ave. Counts	n	SD	RSD (%)
~50 ppm N	3950	3	542	13.7
~100 ppm N	9118	3	83	0.9
~500 ppm N	31679	4	3881	12.3
~750 ppm N	42433	4	2324	5.5

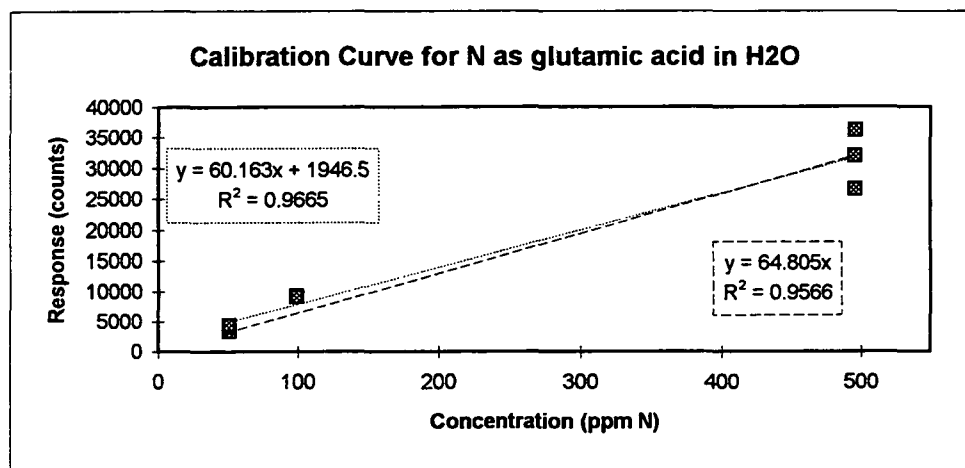


Table XI-9. Summarized data for black liquor droplet pyrolysis.

NOTE: Average % values reported on a dry basis.

Char nitrogen results included and done by Antek method. (EMPA)

LIQUOR: Pine

<i>Furnace temp.</i>	<i>Average % Weight Loss</i>	<i>Std. Dev. (Sample)</i>	<i>Average % N as NO</i>	<i>Std. Dev. (Sample)</i>	<i>% N in Char</i>	<i>Total N Released</i>
300	12.23	1.57	2.08	0.39	91.76	8.24
400	23.49	0.83	2.9	0.52	84.91	15.09
500	29.47	0.25	5.47	0.28	50.67	49.33
600	31.84	2.36	9.2	2.1	44.51	55.49
700	33.07	1.62	8.2	1.26	48.85	51.15
800	36.61	2.2	8.11	1.07	52.5	47.5
900	73.18	2.08	7.02	0.5	147.22	-47.22
1000	78.48	2.05	7.63	3.96	46.79	53.21

LIQUOR: Pine/Birch

<i>Furnace temp.</i>	<i>Average % Weight Loss</i>	<i>Std. Dev. (Sample)</i>	<i>Average % N as NO</i>	<i>Std. Dev. (Sample)</i>	<i>% N in Char</i>	<i>Total N Released</i>
400	22.87	1.25	2.5	0.28	93.29	6.71
600	31.27	1.42	8.61	1.05	53.57	46.43
800	40.18	3.82	7.72	1.38	63.5	36.5
1000	77.69	2.83	10	1.35	15.1	84.9

LIQUOR: Eucalyptus

<i>Furnace temp.</i>	<i>Average % Weight Loss</i>	<i>Std. Dev. (Sample)</i>	<i>Average % N as NO</i>	<i>Std. Dev. (Sample)</i>	<i>% N in Char</i>	<i>Total N Released</i>
300	8.73	1.19	1.28	0.26	97.95	2.05
400	23.2	2.85	5.41	1.23	77.36	22.64
500	30.32	0.9	2.73	0.22	58.54	41.46
600	29.74	1.82	3.47	0.38	66.48	33.52
700	33.36	1.13	6.08	0.68	58.24	41.76
800	47.31	0.88	6.36	0.83	62.95	37.05
900	76.92	1.92	4.36	0.46	154.43	-54.43
1000	78.49	1.28	7.18	1.5	61.63	38.37

LIQUOR: Southern Pine I

<i>Furnace temp.</i>	<i>Average % Weight Loss</i>	<i>Std. Dev. (Sample)</i>	<i>Average % N as NO</i>	<i>Std. Dev. (Sample)</i>	<i>% N in Char</i>	<i>Total N Released</i>
400	21.46	0.78	2.97	0.11	98.02	1.98
600	28.53	2.88	8.05	0.64	66.69	33.31
800	42.83	3.42	6.85	0.55	62.4	37.6
1000	79.03	2.07	9.43	1.51	30.53	69.47

Table XI-7. Proline combustion data for calibration of total nitrogen measurement.

Method Used:	5	PMT Voltage:	825
O2 to O3:	30 ml/min	Furnace Temperature:	1100° C
O2 to pyro:	365 ml/min	Gain Setting:	HI
O2 to inlet:	20 ml/min	Gain Factor:	X1
He to inlet:	145 ml/min	Matrix:	none
Sample ID:	proline		

Sample #	Sample ID	Sample Vol (ul)	Known N Mass (ug)	Response Counts	CDA Sum Response
N4156031	~100 ppm N	5	0.526	9971	17.3584
N4156032	~100 ppm N	5	0.526	10025	17.3584
N4156033	~100 ppm N	5	0.526	10255	17.6757
N4156041	~250 ppm N	5	1.265	20797	36.5232
N4156042	~250 ppm N	5	1.265	22876	40.2587
N4156043	~250 ppm N	5	1.265	22272	39.0869
N4157121	~750 ppm N	5	3.789	52171	92.3093
N4157122	~750 ppm N	5	3.789	49295	86.8407
N4157123	~750 ppm N	5	3.789	50991	90.0877
N4159032	~250 ppm N	5	1.265	21693	37.0125
N4159033	~250 ppm N	5	1.265	20451	35.7176
N4159034	~250 ppm N	5	1.265	21446	37.5979

Sample #	Ave. Counts	n	SD	RSD (%)
N415602_	27488	3	1059	3.85
N415603_	10083	3	151	1.50
N415604_	21972	3	1085	4.94
N415605_	38983	3	519	1.33
N415606_	43448	3	530	1.22
N415712_	50819	3	1445	2.84
N415902_	35872	3	787	2.22
N415903_	21197	3	657	3.10
N416012_	19540	2	2075	10.65

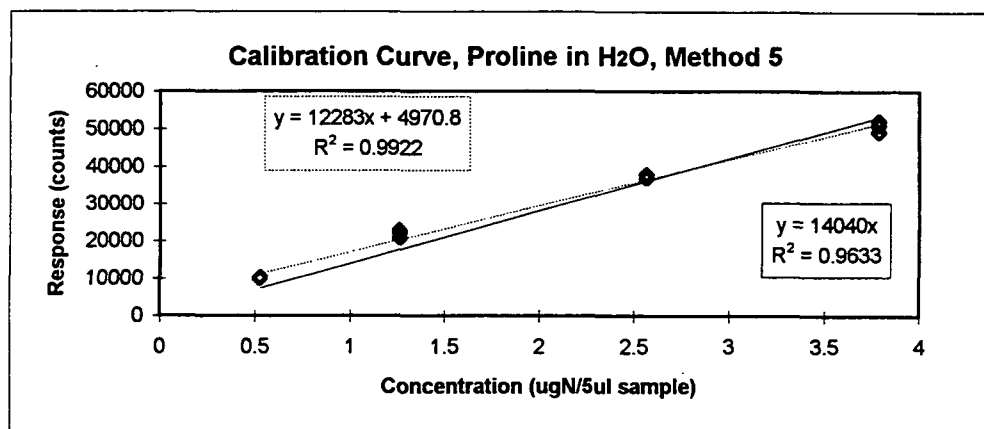


Table XI-10. Summary Data Single droplet Burns at the Temperatures indicated.

Liquor: Pine Furnace Temperature (C): 300
 Jar #: 3 % N (Dry solids Basis): 0.06
 Integration Time: 300 Sec. Dry solids (%): 71.2

Droplet #	Droplet Wt. (mg)	Droplet Dry Wt. (mg)	Char Wt. (mg)	Based on Dry Solids		Droplet N (mg)	Droplet N (mg/kg)	Droplet N mg/100 g BLS	072 NO at 8% O2 (ppm)	072 total N-Release asNO(ppm)
				Released Wt. (mg)	% Wt. Loss					
30	19.1	13.6	12.0	1.6	11.8	8.16E-03	427.2	8.15952E-05	0.95	5.47
31	22.4	15.9	14.0	1.9	12.2	9.57E-03	427.2	9.56928E-05	11.74	67.68
32	17.0	12.1	10.7	1.4	11.6	7.26E-03	427.2	0.000072624	0	0
33	19.7	14.0	12.0	2.0	14.4	8.42E-03	427.2	8.41584E-05	0.79	4.54
34	13.4	9.5	8.5	1.0	10.9	5.72E-03	427.2	5.72448E-05	0	0
35	25.4	18.1	15.5	2.6	14.3	1.09E-02	427.2	0.000108509	5.87	33.59
36	17.4	12.4	11.1	1.3	10.4	7.43E-03	427.2	7.43328E-05	0.79	4.52
SUMS:	134.4	95.7	83.8	11.9	85.6	5.74E-02	2990.4	5.74E-04	20.1	115.8
AVES:	19.20	13.67	11.97	1.70	12.23	8.20E-03	427.20	8.20E-05	2.88	16.54
Std.Dev.P:	3.60	2.56	2.10	0.49	1.46	0.00	0.00	0.00	4.08	23.50
Std.Dev.S:	3.89	2.77	2.27	0.52	1.57	0.00	0.00	0.00	4.41	25.38

Kjeldahl Droplet N (mg)	Droplet N mg/100 g BLS	Kjeldahl Droplet N mg/kg	ANTEK Droplet N mg/kg as recv'd	ANTEK Droplet N mg/kg as BLS	ANTEK Char-N mg/kg as recv'd	ANTEK Char-N mg/kg as BLS	Total N Remaining Char %	Total N Released %
0.008202	0.00008	427.20	318.30	447.05	402	410	91.76	8.24

Difference between Kjeldahl N & Antek N

-4.65

Table XI-10. (cont.) Summary Data Single droplet Burns at the Temperatures indicated.

Liquor: Pine Furnace Temperature (C): 400
 Jar #: 3 % N (Dry solids Basis): 0.06
 Integration Time: 300 Sec. Dry solids (%): 71.2

Droplet #	Droplet Wt. (mg)	Droplet Dry Wt. (mg)	Char Wt. (mg)	Released Wt. (mg)	% Wt. Loss	Droplet N (mg)	Droplet N (mg/kg)	Droplet N mg/100 g BLS	072 NO at 8% O2 (ppm)	072 total N-Release asNO(ppm)
12	17.6	12.5	9.6	2.9	23.4	7.52E-03	427.2	7.51872E-05	53.35	308.01
13.0	28.3	20.1	15.5	4.6	23.1	1.21E-02	427.2	0.000120898	62.73	359.48
14.0	20.6	14.7	11.2	3.5	23.6	8.80E-03	427.2	8.80032E-05	57.35	328.82
15.0	21.7	15.5	12.0	3.5	22.3	9.27E-03	427.2	9.27024E-05	58.98	340.88
16.0	23.2	16.5	12.5	4.0	24.3	9.91E-03	427.2	9.91104E-05	61.34	355.99
17.0	19.5	13.9	10.7	3.2	22.9	8.33E-03	427.2	0.000083304	56.66	330.65
18.0	20.9	14.9	11.2	3.7	24.7	8.93E-03	427.2	8.92848E-05	54.65	324.2
SUMS:	151.8	108.1	82.7	25.4	164.4	0.1	2990.4	0.0	405.1	2348.0
AVES:	21.69	15.44	11.81	3.63	23.49	9.26E-03	427.20	9.26E-05	57.87	335.43
Std.Dev.P:	3.15	2.24	1.73	0.53	0.77	0.00	0.00	0.00	3.15	16.80
Std.Dev.S:	3.40	2.42	1.87	0.57	0.83	0.00	0.00	0.00	3.40	18.14

Kjeldahl Droplet N (mg)	Droplet N mg/100 g BLS	Kjeldahl Droplet N mg/kg	ANTEK Droplet N mg/kg as recv'd	ANTEK Droplet N mg/kg as BLS	ANTEK Char-N mg/kg as recv'd	ANTEK Char-N mg/kg as BLS	Total N Remaining Char %	Total N Released %
0.009264	0.00009	427.20	318.30	447.05	372	380	84.91	15.09

Difference between Kjeldahl N & Antek N

-4.65

355

Droplet #	Droplet Wt. (mg)	Droplet Dry Wt. (mg)	Char Wt. (mg)	Based on Dry Solids		Droplet N (mg)	Droplet N (mg/kg)	Droplet N	072 NO at	072 total
				Released	% Wt.			mg/100 g	8% O2	N-Release
				Wt. (mg)	Loss			BLS	(ppm)	asNO(ppm)
11	26.2	18.7	13.1	5.6	29.8	1.12E-02	427.2	0.00011193	134.1	761.11
12	20.8	14.8	10.4	4.4	29.8	8.89E-03	427.2	8.8858E-05	115.48	660.61
13	21.5	15.3	10.8	4.5	29.4	9.18E-03	427.2	9.1848E-05	111.6	643.5
14	17.1	12.2	8.6	3.6	29.4	7.31E-03	427.2	7.3051E-05	97.42	558.22
15	19.6	14.0	9.9	4.1	29.1	8.37E-03	427.2	8.3731E-05	108.17	619.43
16	19.1	13.6	9.6	4.0	29.4	8.16E-03	427.2	8.1595E-05	103.66	593.99
17	24.1	17.2	12.1	5.1	29.5	1.03E-02	427.2	0.00010296	112.41	648.58
SUMS:	148.4	105.7	74.5	31.2	206.3	6.34E-02	2990.4	6.34E-04	782.8	4485.4
AVES:	21.20	15.09	10.64	4.45	29.47	9.06E-03	427.20	9.06E-05	111.83	640.78
Std.Dev.P:	2.86	2.04	1.42	0.62	0.23	0.00	0.00	0.00	10.67	59.04
Std.Dev.S:	3.09	2.20	1.53	0.67	0.25	0.00	0.00	0.00	11.53	63.77
					ANTEK	ANTEK	ANTEK	ANTEK	Total N	
		Kjeldahl	Droplet N	Kjeldahl	Droplet N	Droplet N	Char-N	Char-N	Remaining	Total N
		Droplet	mg/100 g	Droplet N	mg/kg	mg/kg	mg/kg	mg/kg	Char	Released
		N (mg)	BLS	mg/kg	as recv'd	as BLS	as recv'd	as BLS	%	%
		0.009057	0.00009	427.20	318.30	447.05	222	227	50.67	49.33

-4.65

Table XI-10. (cont.) Summary Data Single droplet Burns at the Temperatures indicated.

Liquor: 1-K-ME Furnace Temperature (C): 600
 Jar #: 3 % N (Dry solids Basis): 0.06
 Integration Time: 300 Sec. Dry solids (%): 71.2

Droplet #	Droplet Wt. (mg)	Droplet Dry Wt. (mg)	Char Wt. (mg)	Based on Dry Solids		Droplet N (mg)	Droplet N (mg/kg)	Droplet N mg/100 g BLS	072 NO at 8% O2 (ppm)	072 total N-Release asNO(ppm)
				Released Wt. (mg)	% Wt. Loss					
1	14.2	10.1	6.7	3.4	33.7	6.07E-03	427.2	6.0662E-05	71.93	415.56
2.0	23.4	16.7	12.2	4.5	26.8	1.00E-02	427.2	9.9965E-05	100.67	584.84
3.0	20.2	14.4	9.7	4.7	32.6	8.63E-03	427.2	8.6294E-05	95.24	555.27
4.0	19.0	13.5	9.3	4.2	31.3	8.12E-03	427.2	8.1168E-05	82.26	469.65
5.0	12.0	8.5	5.7	2.8	33.3	5.13E-03	427.2	5.1264E-05	66.13	378.95
6.0	20.6	14.7	9.9	4.8	32.5	8.80E-03	427.2	8.8003E-05	93.67	540.58
7.0	14.2	10.1	6.8	3.3	32.7	6.07E-03	427.2	6.0662E-05	78.48	452.81
SUMS:	123.6	88.0	60.3	27.7	222.8	0.1	2990.4	0.0	588.4	3397.7
AVES:	17.66	12.57	8.61	3.96	31.84	7.54E-03	427.20	7.54E-05	84.05	485.38
Std.Dev.P:	3.89	2.77	2.12	0.70	2.19	0.00	0.00	0.00	11.93	71.05
Std.Dev.S:	4.20	2.99	2.30	0.76	2.36	0.00	0.00	0.00	12.89	76.74

Kjeldahl Droplet N (mg)	Droplet N mg/100 g BLS	Kjeldahl Droplet N mg/kg	ANTEK Droplet N mg/kg as recv'd	ANTEK Droplet N mg/kg as BLS	ANTEK Char-N mg/kg as recv'd	ANTEK Char-N mg/kg as BLS	Total N Remaining Char %	Total N Released %
0.007543	0.00008	427.20	318.30	447.05	195	199	44.51	55.49

Difference between Kjeldahl N & Antek N

-4.65

Table XI-10. (cont.) Summary Data Single droplet Burns at the Temperatures indicated.

Liquor: 1-K-ME Furnace Temperature (C): 700
 Jar #: 3 % N (Dry solids Basis): 0.06
 Integration Time: 300 Sec. Dry solids (%): 71.2

Droplet #	Droplet Wt. (mg)	Droplet Dry Wt. (mg)	Based on Dry Solids			Droplet N (mg)	Droplet N (mg/kg)	Droplet N mg/100g BLS	072 NO at 8% O2 (ppm)	072 total N-Release asNO(ppm)
			Char Wt. (mg)	Released Wt. (mg)	% Wt. Loss					
13	19.4	13.8	9.0	4.8	34.8	8.29E-03	427.2	8.2877E-05	106.79	614.14
15	21.3	15.2	10.0	5.2	34.1	9.10E-03	427.2	9.0994E-05	93.97	536.18
17	22.5	16.0	10.6	5.4	33.8	9.61E-03	427.2	0.00009612	117.84	671.91
18	17.4	12.4	8.5	3.9	31.4	7.43E-03	427.2	7.4333E-05	67.62	385.8
19	25.9	18.4	12.3	6.1	33.3	1.11E-02	427.2	0.00011064	113.92	653.22
20	27.2	19.4	13.5	5.9	30.3	1.16E-02	427.2	0.0001162	122.21	702.85
21	17.6	12.5	8.3	4.2	33.8	7.52E-03	427.2	7.5187E-05	78.2	451.78
SUMS:	151.3	107.7	72.2	35.5	231.5	6.46E-02	2990.4	6.46E-04	700.6	4015.9
AVES:	21.61	15.39	10.31	5.08	33.07	9.23E-03	427.20	9.23E-05	100.08	573.70
Std.Dev.P:	3.57	2.54	1.83	0.76	1.50	0.00	0.00	0.00	19.31	110.75
Std.Dev.S:	3.86	2.75	1.97	0.82	1.62	0.00	0.00	0.00	20.86	119.63
	Kjeldahl Droplet N (mg)	Droplet N mg/100 g BLS	Kjeldahl Droplet N mg/kg	ANTEK Droplet N mg/kg as recv'd	ANTEK Droplet N mg/kg as BLS	ANTEK Char-N mg/kg as recv'd	ANTEK Char-N mg/kg as BLS	Total N Remaining Char %	Total N Released %	
	0.009234	0.00009	427.20	318.30	447.05	214	218	48.85	51.15	

Difference between Kjeldahl N & Antek N

-4.65

Table XI-10. (cont.) Summary Data Single droplet Burns at the Temperatures indicated.

Liquor: Pine Furnace Temperature (C): 800
 Jar #: 3 % N (Dry solids Basis): 0.06
 Integration Time: 300 Sec. Dry solids (%): 71.2

Droplet #	Droplet Wt. (mg)	Droplet Dry Wt. (mg)	Char Wt. (mg)	Released Wt. (mg)	% Wt. Loss	Droplet N (mg)	Droplet N (mg/kg)	072 NO at mg/100 g BLS	072 total 8% O2 (ppm)	N-Release asNO(ppm)
1	22.2	15.8	10.1	12.1	54.5	9.48E-03	427.2	0.948384	84.74	489.76
2	15.4	11.0	7.0	8.4	54.5	6.58E-03	427.2	0.657888	83.6	476.99
5	34.0	24.2	15.6	18.4	54.1	1.45E-02	427.2	1.45248	186.62	1078.19
6	30.6	21.8	14.3	16.3	53.3	1.31E-02	427.2	1.307232	182.42	1079.02
8	32.2	22.9	14.8	17.4	54.0	1.38E-02	427.2	1.375584	154.46	877.2
9	20.0	14.2	8.9	11.1	55.5	8.54E-03	427.2	0.8544	139.68	813.05
10	26.0	18.5	10.9	15.1	58.1	1.11E-02	427.2	1.11072	138.87	811.74
SUMS:	180.4	128.4	81.6	98.8	384.0	7.71E-02	2990.4	7.71	970.4	5626.0
AVES:	25.77	18.35	11.66	14.11	54.86	1.10E-02	427.2	1.10	138.63	803.71
Std.Dev.P:	6.39	4.55	3.04	3.40	1.45	0.00	0.00	0.27	38.55	227.41
Std.Dev.S:	6.90	4.92	3.28	3.67	1.57	0.00	0.00	0.29	41.64	245.63

Kjeldahl Droplet N (mg)	Droplet N mg/100 g BLS	Kjeldahl Droplet N mg/kg	ANTEK Droplet N mg/kg as recv'd	ANTEK Droplet N mg/kg as BLS	ANTEK Char-N mg/kg as recv'd	ANTEK Char-N mg/kg as BLS	Total N Remaining Char %	Total N Released %
0.011010	1.10096	427.20	318.30	447.05	230	235	52.50	47.50

Difference between Kjeldahl N & Antek N

-4.65

Table XI-10. (cont.) Summary Data Single droplet Burns at the Temperatures indicated.

Liquor: Pine Furnace Temperature (C): 900
 Jar #: 3 % N (Dry solids Basis): 0.06
 Integration Time: 300 Sec. Dry solids (%): 71.2

Droplet #	Droplet Wt. (mg)	Droplet Dry Wt. (mg)	Char Wt. (mg)	Based on Dry Solids		Droplet N (mg)	Droplet N (mg/kg)	Droplet N mg/100g BLS	072 NO at 8% O2 (ppm)	072 total N-Release asNO(ppm)
				Released Wt. (mg)	% Wt. Loss					
6	22.3	15.9	4.1	11.8	74.2	9.53E-03	427.2	9.5266E-05	132.06	780.92
7	19.2	13.7	3.3	10.4	75.9	8.20E-03	427.2	8.2022E-05	137.87	779.87
8	15.4	11.0	2.9	8.1	73.6	6.58E-03	427.2	6.5789E-05	122.35	691.63
9	15.4	11.0	3.4	7.6	69.0	6.58E-03	427.2	6.5789E-05	172.85	966.63
10	14.7	10.5	2.8	7.7	73.2	6.28E-03	427.2	6.2798E-05	160.58	921.08
11	17.5	12.5	3.3	9.2	73.5	7.48E-03	427.2	0.00007476	142.99	821.23
12	17.1	12.2	3.3	8.9	72.9	7.31E-03	427.2	7.3051E-05	142.23	823.3
SUMS:	121.6	86.6	23.1	63.5	512.2	5.19E-02	2990.4	5.19E-04	1010.9	5784.7
AVES:	17.37	12.37	3.30	9.07	73.18	7.42E-03	427.20	7.42E-05	144.42	826.38
Std.Dev.P:	2.47	1.76	0.39	1.43	1.93	0.00	0.00	0.00	15.85	85.41
Std.Dev.S:	2.67	1.90	0.42	1.54	2.08	0.00	0.00	0.00	17.12	92.25

Kjeldahl Droplet N (mg)	Droplet N mg/100 g BLS	Kjeldahl Droplet N mg/kg	ANTEK Droplet N mg/kg as recv'd	ANTEK Droplet N mg/kg as BLS	ANTEK Char-N mg/kg as recv'd	ANTEK Char-N mg/kg as BLS	Total N Remaining Char %	Total N Released %
0.007421	0.00007	427.20	318.30	447.05	645	658	147.22	47.22

Difference between Kjeldahl N & Antek N

-4.65

Table XI-10. (cont.) Summary Data Single droplet Burns at the Temperatures indicated.

Liquor: Pine Furnace Temperature (C): 1000
 Jar #: 3 % N (Dry solids Basis): 0.06
 Integration Time: 300 Sec. Dry solids (%): 71.2

Droplet #	Droplet Wt. (mg)	Droplet Dry Wt. (mg)	Char Wt. (mg)	Based on Dry Solids		Droplet N (mg)	Droplet N (mg/kg)	Droplet N mg/100g BLS	072 NO at 8% O2 (ppm)	072 total N-Release asNO(ppm)
				Released Wt. (mg)	% Wt. Loss					
1	24.5	17.4	3.9	13.5	77.6	1.05E-02	427.2	0.000104664	208.29	1194.74
2	22.7	16.2	3.4	12.8	79.0	9.70E-03	427.2	9.69744E-05	152.44	880.98
3	25.4	18.1	4.5	13.6	75.1	1.09E-02	427.2	0.000108509	163.07	935.36
4	24.4	17.4	3.6	13.8	79.3	1.04E-02	427.2	0.000104237	142.61	812.06
5	23.0	16.4	3.7	12.7	77.4	9.83E-03	427.2	0.000098256	123.72	708.93
6	19.6	14.0	2.9	11.1	79.2	8.37E-03	427.2	8.37312E-05	109.42	630.08
7	14.6	10.4	1.9	8.5	81.7	6.24E-03	427.2	6.23712E-05	112.23	643.13
SUMS:	154.2	109.8	23.9	85.9	549.3	6.59E-02	2990.4	6.59E-04	1011.8	5805.3
AVES:	22.03	15.68	3.41	12.27	78.48	9.41E-03	427.20	9.41E-05	144.54	829.33
Std.Dev.P:	3.50	2.49	0.76	1.76	1.89	0.00	0.00	0.00	32.04	183.85
Std.Dev.S:	3.78	2.69	0.83	1.90	2.05	0.00	0.00	0.00	34.60	198.58

Kjeldahl Droplet N (mg)	Droplet N mg/100 g BLS	Kjeldahl Droplet N mg/kg	ANTEK Droplet N mg/kg as recv'd	ANTEK Droplet N mg/kg as BLS	ANTEK Char-N mg/kg as recv'd	ANTEK Char-N mg/kg as BLS	Total N Remaining Char %	Total N Released %
0.009411	0.00009	427.20	318.30	447.05	205	209	46.79	53.21

Difference between Kjeldahl N & Antek N

-4.65

Table XI-11. Summary Data Single droplet Burns at the Temperatures indicated.

Liquor: Pine/Birch Furnace Temperature (C): 400
 Jar #: 2 % N (Dry solids Basis): 0.07
 Integration Time: 300 Sec. Dry solids (%): 74.8

Droplet #	Based on Dry Solids					Droplet N (mg)	Droplet N (mg/kg)	Droplet N mg/100 g BLS	072 NO at 8% O2 (ppm)	072 total N-Release asNO(ppm)
	Droplet Wt. (mg)	Droplet Dry Wt. (mg)	Char Wt. (mg)	Released Wt. (mg)	% Wt. Loss					
19	11.3	8.5	6.5	2.0	23.1	5.92E-03	523.6	5.9167E-05	15.4	89
20	25.1	18.8	14.7	4.1	21.7	1.31E-02	523.6	0.00013142	40.58	230.6
21	13.2	9.9	7.4	2.5	25.1	6.91E-03	523.6	6.9115E-05	25.68	148.37
23	15.7	11.7	9.1	2.6	22.5	8.22E-03	523.6	8.2205E-05	29.11	166.96
24	15.7	11.7	9.2	2.5	21.7	8.22E-03	523.6	8.2205E-05	26.08	148.23
25	19.5	14.6	11.1	3.5	23.9	1.02E-02	523.6	0.0001021	37.98	214.71
26	14.6	10.9	8.5	2.4	22.2	7.64E-03	523.6	7.6446E-05	32.64	184.04
SUMS:	115.1	86.1	66.5	19.6	160.1	6.03E-02	3665.2	6.03E-04	207.5	1181.9
AVES:	16.44	12.30	9.50	2.80	22.87	8.61E-03	523.60	8.61E-05	29.64	168.84
Std.Dev.P:	4.24	3.17	2.51	0.67	1.15	2.22E-03	0.00	2.22E-05	7.83	43.71
Std.Dev.S:	4.58	3.42	2.72	0.73	1.25	2.40E-03	0.00	2.40E-05	8.46	47.21

Kjeldahl Droplet N (mg)	Droplet N mg/100 g BLS	Kjeldahl Droplet N mg/kg	ANTEK Droplet N mg/kg as recv'd	ANTEK Droplet N mg/kg as BLS	ANTEK Char-N mg/kg as recv'd	ANTEK Char-N mg/kg as BLS	Total N Remaining Char %	Total N Released %
0.008609	0.00009	523.60	369.00	493.32	451	460	93.29	6.71

Difference between Kjeldahl N & Antek N

5.78 (Kjeldahl - Antek)/ Antek

Table XI-11. (cont.) Summary Data Single droplet Burns at the Temperatures indicated.

Liquor: Pine/Birch Furnace Temperature (C): 600
 Jar #: 2 % N (Dry solids Basis): 0.07
 Integration Time: 300 Sec. Dry solids (%): 74.8

Droplet #	Droplet Wt. (mg)	Droplet Dry Wt. (mg)	Based on Dry Solids			Droplet N (mg)	Droplet N (mg/kg)	Droplet N mg/100 g BLS	072 NO at 8% O2 (ppm)	072 total N-Release asNO(ppm)
			Char Wt. (mg)	Released Wt. (mg)	% Wt. Loss					
20	11.1	8.3	5.6	2.7	32.6	5.81E-03	523.6	5.81196E-05	71.98	412.87
21	15.8	11.8	8.1	3.7	31.5	8.27E-03	523.6	8.27288E-05	92.74	534.01
22	23.7	17.7	12.0	5.7	32.3	1.24E-02	523.6	0.000124093	116.71	672.1
23	21.0	15.7	11.2	4.5	28.7	1.10E-02	523.6	0.000109956	114.95	670.42
24	12.8	9.6	6.5	3.1	32.1	6.70E-03	523.6	6.70208E-05	76.76	451.99
25	24.5	18.3	12.5	5.8	31.8	1.28E-02	523.6	0.000128282	110.98	661.27
26	22.9	17.1	12.0	5.1	29.9	1.20E-02	523.6	0.000119904	127.22	762.82
SUMS:	131.8	98.6	67.9	30.7	218.9	6.90E-02	3665.2	6.90E-04	711.3	4165.5
AVES:	18.83	14.08	9.70	4.38	31.27	9.86E-03	523.60	9.86E-05	101.62	595.07
Std.Dev.P:	5.11	3.82	2.68	1.16	1.32	0.00	0.00	0.00	19.73	120.43
Std.Dev.S:	5.51	4.12	2.89	1.25	1.42	0.00	0.00	0.00	21.31	130.08

Kjeldahl Droplet N (mg)	Droplet N mg/100 g BLS	Kjeldahl Droplet N mg/kg	ANTEK Droplet N mg/kg as recv'd	ANTEK Droplet N mg/kg as BLS	ANTEK Char-N mg/kg as recv'd	ANTEK Char-N mg/kg as BLS	Total N Remaining Char %	Total N Released %
0.009859	0.00010	523.60	369.00	493.32	259	264	53.57	46.43

Difference between Kjeldahl N & Antek N

5.78 (Kjeldahl - Antek)/ Antek

Table XI-11. (cont.) Summary Data Single droplet Burns at the Temperatures indicated.

Liquor: Pine/Birch Furnace Temperature (C): 800
 Jar #: 2 % N (Dry solids Basis): 0.07
 Integration Time: 300 Sec. Dry solids (%): 74.8

Droplet #	Droplet Wt. (mg)	Droplet Dry Wt. (mg)	Char Wt. (mg)	Based on Dry Solids		Droplet N (mg)	Droplet N (mg/kg)	Droplet N mg/100 g BLS	072 NO at 8% O2 (ppm)	072 total N-Release asNO(ppm)
				Released Wt. (mg)	% Wt. Loss					
1	22.8	17.1	10.8	6.3	36.7	1.19E-02	523.6	0.000119381	119.03	687.89
2	17.7	13.2	8.2	5.0	38.1	9.27E-03	523.6	9.26772E-05	115.8	664.22
3	21.6	16.2	8.6	7.6	46.8	1.13E-02	523.6	0.000113098	125.76	725.62
4	22.2	16.6	10.3	6.3	38.0	1.16E-02	523.6	0.000116239	142.17	811.19
5	22.2	16.6	10.5	6.1	36.8	1.16E-02	523.6	0.000116239	131.9	755.31
6	26.5	19.8	11.4	8.4	42.5	1.39E-02	523.6	0.000138754	124.18	712.28
7	17.9	13.4	7.7	5.7	42.5	9.37E-03	523.6	9.37244E-05	124.28	717.09
SUMS:	150.9	112.9	67.5	45.4	281.2	7.90E-02	3665.2	7.90E-04	883.1	5073.6
AVES:	21.56	16.12	9.64	6.48	40.18	1.13E-02	523.60	1.13E-04	126.16	724.80
Std.Dev.P:	2.80	2.10	1.34	1.06	3.53	1.47E-03	0.00	1.47E-05	8.06	44.15
Std.Dev.S:	3.03	2.27	1.45	1.14	3.82	1.59E-03	0.00	1.59E-05	8.71	47.69

Kjeldahl Droplet N (mg)	Droplet N mg/100 g BLS	Kjeldahl Droplet N mg/kg	ANTEK Droplet N mg/kg as recv'd	ANTEK Droplet N mg/kg as BLS	ANTEK Char-N mg/kg as recv'd	ANTEK Char-N mg/kg as BLS	Total N Remaining Char %	Total N Released %
0.011287	0.00011	523.60	369.00	493.32	307	313	63.50	36.50

Difference between Kjeldahl N & Antek N

5.78 (Kjeldahl - Antek)/ Antek

Table XI-11. (cont.) Summary Data Single droplet Burns at the Temperatures indicated.

Liquor: Pine/Birch Furnace Temperature (C): 1000
 Jar #: 2 % N (Dry solids Basis): 0.07
 Integration Time: 300 Sec. Dry solids (%): 74.8

Droplet #	Droplet Wt. (mg)	Droplet Dry Wt. (mg)	Char Wt. (mg)	Based on Dry Solids		Droplet N (mg)	Droplet N (mg/kg)	Droplet N mg/100 g BLS	072 NO at 8% O2 (ppm)	072 total N-Release asNO(ppm)
				Released Wt. (mg)	% Wt. Loss					
10	19.8	14.8	4.1	10.7	72.3	1.04E-02	523.6	0.000103673	124.41	713.62
11	14.5	10.8	2.2	8.6	79.7	7.59E-03	523.6	0.000075922	116.63	659.73
12	11.5	8.6	1.8	6.8	79.1	6.02E-03	523.6	0.000060214	104.04	600.29
14	13.3	9.9	2.4	7.5	75.9	6.96E-03	523.6	6.96388E-05	104.63	627.36
15	13.7	10.2	2.2	8.0	78.5	7.17E-03	523.6	7.17332E-05	104.99	602.19
18	14.9	11.1	2.5	8.6	77.6	7.80E-03	523.6	7.80164E-05	122.82	749.92
19	11.8	8.8	1.7	7.1	80.7	6.18E-03	523.6	6.17848E-05	97.77	616.48
SUMS:	99.5	74.4	16.9	57.5	543.8	5.21E-02	3665.2	5.21E-04	775.3	4569.6
AVES:	14.21	10.63	2.41	8.22	77.69	7.44E-03	523.60	7.44E-05	110.76	652.80
Std.Dev.P:	2.56	1.92	0.74	1.21	2.62	0.00	0.00	0.00	9.64	54.07
Std.Dev.S:	2.77	2.07	0.80	1.31	2.83	0.00	0.00	0.00	10.42	58.40

Kjeldahl Droplet N (mg)	Droplet N mg/100 g BLS	Kjeldahl Droplet N mg/kg	ANTEK	ANTEK	ANTEK	ANTEK	Total N	Total N Released %
			Droplet N mg/kg as recv'd	Droplet N mg/kg as BLS	Char-N mg/kg as recv'd	Char-N mg/kg as BLS	Remaining Char %	
0.007443	0.00007	523.60	369.00	493.32	73	74	15.10	84.90

Difference between Kjeldahl N & Antek N

5.78 (Kjeldahl - Antek)/ Antek

Table XI-12. Summary Data Single droplet Burns at the Temperatures indicated.

Liquor: Eucalyptus Furnace Temperature (C): 300
 Jar #: 3 % N (Dry solids Basis): 0.09
 Integration Time: 300 Sec. Dry solids (%): 67.6

Droplet #	Droplet Wt. (mg)	Droplet Dry Wt. (mg)	Char Wt. (mg)	Based on Dry Solids		Droplet N (mg)	Droplet N (mg/kg)	Droplet N mg/100 g BLS	072 NO at 8% O2 (ppm)	072 total N-Release asNO(ppm)
				Released Wt. (mg)	% Wt. Loss					
20	19.4	13.1	12.0	1.1	8.5	1.18E-02	608.4	0.00011803	1.39	8.02
21	17.8	12.0	11.1	0.9	7.8	1.08E-02	608.4	0.0001083	9.74	55.96
22	23.0	15.5	14.1	1.4	9.3	1.40E-02	608.4	0.00013993	7.28	41.9
23	25.2	17.0	15.3	1.7	10.2	1.53E-02	608.4	0.00015332	17.93	102.83
24	24.3	16.4	14.8	1.6	9.9	1.48E-02	608.4	0.00014784	15.71	90.44
25	15.4	10.4	9.7	0.7	6.8	9.37E-03	608.4	9.3694E-05	9.36	53.67
26	21.7	14.7	13.4	1.3	8.7	1.32E-02	608.4	0.00013202	13.99	80.55
SUMS:	146.8	99.2	90.4	8.8	61.1	8.93E-02	4258.8	8.93E-04	75.4	433.4
AVES:	20.97	14.18	12.91	1.26	8.73	1.28E-02	608.40	1.28E-04	10.77	61.91
Std.Dev.P:	3.32	2.24	1.90	0.34	1.10	0.00	0.00	0.00	5.20	29.87
Std.Dev.S:	3.59	2.42	2.06	0.37	1.19	0.00	0.00	0.00	5.62	32.26

Kjeldahl Droplet N (mg)	Droplet N mg/100 g BLS	Kjeldahl Droplet N mg/kg	ANTEK Droplet N mg/kg as recv'd	ANTEK Droplet N mg/kg as BLS	ANTEK Char-N mg/kg as recv'd	ANTEK Char-N mg/kg as BLS	Total N Remaining Char %	Total N Released %
0.012759	0.00013	608.40	469.00	693.79	666	680	97.95	2.05

Difference between Kjeldahl N & Antek N

-14.03 (Kjeldahl - Antek)/ Antek

Table XI-12. (cont.) Summary Data Single droplet Burns at the Temperatures indicated.

Liquor: Eucalyptus Furnace Temperature (C): 400
 Jar #: 3 % N (Dry solids Basis): 0.09
 Integration Time: 300 Sec. Dry solids (%): 67.6

Droplet #	Droplet Wt. (mg)	Droplet Dry Wt. (mg)	Char Wt. (mg)	Based on Dry Solids		Droplet N (mg)	Droplet N (ppm)	Droplet N mg/100 g BLS	072 NO at 8% O2 (ppm)	072 total N-Release asNO(ppm)
				Released Wt. (mg)	% Wt. Loss					
1	17.2	11.6	9.0	2.6	22.6	1.05E-02	608.4	0.00010464	78.51	452.1
2	25.5	17.2	13.3	3.9	22.8	1.55E-02	608.4	0.00015514	87.93	506.36
3	29.6	20.0	15.3	4.7	23.5	1.80E-02	608.4	0.00018009	95.76	553.21
4	15.3	10.3	8.2	2.1	20.7	9.31E-03	608.4	9.3085E-05	71.52	416.99
5	20.8	14.1	11.1	3.0	21.1	1.27E-02	608.4	0.00012655	72.2	423.91
6	24.2	16.4	12.7	3.7	22.4	1.47E-02	608.4	0.00014723	84.56	482.44
7	25.3	17.1	12.1	5.0	29.3	1.54E-02	608.4	0.00015393	84.48	482.32
8	16.1	10.9	8.3	2.6	23.7	9.80E-03	9795.24	9.7952E-05	70.13	401.85
SUMS:	174.0	117.6	90.0	27.6	186.1	1.06E-01	14054.0	1.06E-03	645.1	3719.2
AVES:	24.86	16.80	12.86	3.95	26.59	1.51E-02	2007.72	1.51E-04	92.16	531.31
Std.Dev.P:	4.87	3.29	2.41	0.98	2.47	0.00	3038.26	0.00	8.52	47.75
Std.Dev.S:	5.20	3.52	2.58	1.05	2.64	0.00	3248.04	0.00	9.11	51.05

Kjeldahl Droplet N (mg)	Droplet N mg/100 g BLS	Kjeldahl Droplet N mg/kg	ANTEK Droplet N mg/kg as recv'd	ANTEK Droplet N mg/kg as BLS	ANTEK Char-N mg/kg as recv'd	ANTEK Char-N mg/kg as BLS	Total N Remaining Char %	Total N Released %
0.015123	0.00015	2007.72	469.00	693.79	526	537	77.36	22.64

Difference between Kjeldahl N & Antek N

65.44

Table XI-12. (cont.) Summary Data Single droplet Burns at the Temperatures indicated.

Liquor: Eucalyptus Furnace Temperature (C): 500
 Jar #: 3 % N (Dry solids Basis): 0.09
 Integration Time: 300 Sec. Dry solids (%): 67.6

Droplet #	Droplet Wt. (mg)	Droplet Dry Wt. (mg)	Char Wt. (mg)	Based on Dry Solids		Droplet N (mg)	Droplet N (mg/kg)	Droplet N mg/100 g BLS	072 NO at 8% O2 (ppm)	072 total N-Release asNO(ppm)
				Released Wt. (mg)	% Wt. Loss					
1	19.0	12.8	8.8	4.0	31.5	1.16E-02	608.4	0.000115596	108.87	629.01
2	24.4	16.5	11.5	5.0	30.3	1.48E-02	608.4	0.00014845	136.99	783.69
3	22.7	15.3	10.9	4.4	29.0	1.38E-02	608.4	0.000138107	125.45	715.32
4	18.9	12.8	8.9	3.9	30.3	1.15E-02	608.4	0.000114988	115	655.74
5	21.0	14.2	10.0	4.2	29.6	1.28E-02	608.4	0.000127764	124.48	709.75
6	23.7	16.0	11.0	5.0	31.3	1.44E-02	608.4	0.000144191	139.01	795.26
7	15.7	10.6	7.4	3.2	30.3	9.55E-03	608.4	9.55188E-05	103.28	595.52
SUMS:	145.4	98.3	68.5	29.8	212.2	8.85E-02	4258.8	8.85E-04	853.1	4884.3
AVES:	20.77	14.04	9.79	4.26	30.32	1.26E-02	608.40	1.26E-04	121.87	697.76
Std.Dev.P:	2.88	1.94	1.37	0.59	0.83	0.00	0.00	0.00	12.56	69.99
Std.Dev.S:	3.11	2.10	1.48	0.64	0.90	0.00	0.00	0.00	13.56	75.59

Kjeldahl Droplet N (mg)	Droplet N mg/100 g BLS	Kjeldahl Droplet N mg/kg	ANTEK Droplet N mg/kg as recv'd	ANTEK Droplet N mg/kg as BLS	ANTEK Char-N mg/kg as recv'd	ANTEK Char-N mg/kg as BLS	Total N Remaining Char %	Total N Released %
0.012637	0.00013	608.40	469.00	693.79	398	406	58.54	41.46

Difference between Kjeldahl N & Antek N

-14.03 (Kjeldahl - Antek)/ Antek

Table XI-12. (cont.) Summary Data Single droplet Burns at the Temperatures indicated.

Liquor: Eucalyptus Furnace Temperature (C): 600
 Jar #: 3 % N (Dry solids Basis): 0.09
 Integration Time: 300 Sec. Dry solids (%): 67.6

Droplet #	Droplet Wt. (mg)	Droplet Dry Wt. (mg)	Char Wt. (mg)	Based on Dry Solids		Droplet N (mg)	Droplet N (mg/kg)	Droplet N mg/100 g BLS	072 NO at 8% O2 (ppm)	072 total N-Release asNO(ppm)
				Released Wt. (mg)	% Wt. Loss					
1	24.6	16.6	11.5	5.1	30.8	1.50E-02	608.4	0.000149666	88.65	524.2
2	13.9	9.4	6.8	2.6	27.6	8.46E-03	608.4	8.45676E-05	65.38	392.05
4	19.9	13.5	9.6	3.9	28.6	1.21E-02	608.4	0.000121072	80.35	460.58
5	14.6	9.9	6.8	3.1	31.1	8.88E-03	608.4	8.88264E-05	59.27	341.77
6	14.3	9.7	6.7	3.0	30.7	8.70E-03	608.4	8.70012E-05	63.18	363.85
7	11	7.4	5.4	2.0	27.4	6.69E-03	608.4	0.000066924	49.85	287.07
8	13.9	9.4	6.4	3.0	31.9	8.46E-03	608.4	8.45676E-05	61.23	355.39
SUMS:	112.2	75.8	53.2	22.6	208.2	6.83E-02	4258.8	6.83E-04	467.9	2724.9
AVES:	16.03	10.84	7.60	3.24	29.74	9.75E-03	608.40	9.75E-05	66.84	389.27
Std.Dev.P:	4.27	2.89	1.98	0.92	1.68	2.60E-03	0.00	2.60E-05	12.25	73.48
Std.Dev.S:	4.62	3.12	2.14	1.00	1.82	2.81E-03	0.00	2.81E-05	13.24	79.37

Kjeldahl Droplet N (mg)	Droplet N mg/100 g BLS	Kjeldahl Droplet N mg/kg	ANTEK Droplet N mg/kg as recv'd	ANTEK Droplet N mg/kg as BLS	ANTEK Char-N mg/kg as recv'd	ANTEK Char-N mg/kg as BLS	Total N Remaining Char %	Total N Released %
0.009752	0.00010	608.40	469.00	693.79	452	461	66.48	33.52

Difference between Kjeldahl N & Antek N

-14.03 (Kjeldahl - Antek)/ Antek

Table XI-12. (cont.) Summary Data Single droplet Burns at the Temperatures indicated.

Liquor: Eucalyptus Furnace Temperature (C): 700
 Jar #: 3 % N (Dry solids Basis): 0.09
 Integration Time: 300 Sec. Dry solids (%): 67.6

Droplet #	Droplet Wt. (mg)	Droplet Dry Wt. (mg)	Char Wt. (mg)	Based on Dry Solids		Droplet N (mg)	Droplet N (mg/kg)	Droplet N mg/100 g BLS	072 NO at 8% O2 (ppm)	072 total N-Release asNO(ppm)
				Released Wt. (mg)	% Wt. Loss					
10	14.8	10.0	6.7	3.3	33.0	9.00E-03	608.4	9.0043E-05	88.61	510.25
11	17.4	11.8	8.0	3.8	32.0	1.06E-02	608.4	0.00010586	94.78	550.07
12	18.5	12.5	8.1	4.4	35.2	1.13E-02	608.4	0.00011255	94.66	55.83
13	14.7	9.9	6.5	3.4	34.6	8.94E-03	608.4	8.9435E-05	98.23	562.52
14	12.8	8.7	5.8	2.9	33.0	7.79E-03	608.4	7.7875E-05	79.61	456.64
15	18.1	12.2	8.2	4.0	33.0	1.10E-02	608.4	0.00011012	97.54	563.68
16	25.5	17.2	11.6	5.6	32.7	1.55E-02	608.4	0.00015514	124.51	710.9
SUMS:	121.8	82.3	54.9	27.4	233.5	7.41E-02	4258.8	7.41E-04	677.9	3409.9
AVES:	17.40	11.76	7.84	3.92	33.36	1.06E-02	608.40	1.06E-04	96.85	487.13
Std.Dev.P:	3.83	2.59	1.76	0.84	1.05	0.00	0.00	0.00	12.77	190.14
Std.Dev.S:	4.13	2.79	1.90	0.91	1.13	0.00	0.00	0.00	13.79	205.37

Kjeldahl Droplet N (mg)	Droplet N mg/100 g BLS	Kjeldahl Droplet N mg/kg	ANTEK Droplet N mg/kg as recv'd	ANTEK Droplet N mg/kg as BLS	ANTEK Char-N mg/kg as recv'd	ANTEK Char-N mg/kg as BLS	Total N Remaining Char %	Total N Released %
0.010586	0.00011	608.40	469.00	693.79	396	404	58.24	41.76

Difference between Kjeldahl N & Antek N

-14.03 (Kjeldahl - Antek)/ Antek

Table XI-12. (cont.) Summary Data Single droplet Burns at the Temperatures indicated.

Liquor: Eucalyptus Furnace Temperature (C): 800
 Jar #: 3 % N (Dry solids Basis): 0.09
 Integration Time: 300 Sec. Dry solids (%): 67.6

Droplet #	Droplet Wt. (mg)	Droplet Dry Wt. (mg)	Char Wt. (mg)	Based on Dry Solids		Droplet N (mg)	Droplet N (mg/kg)	Droplet N mg/100 g BLS	072 NO at 8% O2 (ppm)	072 total N-Release asNO(ppm)
				Released Wt. (mg)	% Wt. Loss					
20	25.5	17.2	8.9	8.3	48.4	1.55E-02	608.4	0.000155142	140.14	803.8
21	15.0	10.1	5.3	4.8	47.7	9.13E-03	608.4	0.00009126	127.1	731.92
22	18.4	12.4	6.5	5.9	47.7	1.12E-02	608.4	0.000111946	159.08	912.46
23	16.7	11.3	6.1	5.2	46.0	1.02E-02	608.4	0.000101603	152.97	875.13
24	18.1	12.2	6.5	5.7	46.9	1.10E-02	608.4	0.00011012	163.33	931.29
25	22.2	15.0	7.8	7.2	48.0	1.35E-02	608.4	0.000135065	167.99	950.26
26	19.9	13.5	7.2	6.3	46.5	1.21E-02	608.4	0.000121072	153.77	881.99
SUMS:	135.8	91.8	48.3	43.5	331.2	8.26E-02	4258.8	8.26E-04	1064.4	6086.9
AVES:	19.40	13.11	6.90	6.21	47.31	1.18E-02	608.40	1.18E-04	152.05	869.55
Std.Dev.P:	3.27	2.21	1.10	1.12	0.82	0.00	0.00	0.00	13.09	71.33
Std.Dev.S:	3.53	2.38	1.18	1.21	0.88	0.00	0.00	0.00	14.14	77.05

Kjeldahl Droplet N (mg)	Droplet N mg/100 g BLS	Kjeldahl Droplet N mg/kg	ANTEK Droplet N mg/kg as recv'd	ANTEK Droplet N mg/kg as BLS	ANTEK Char-N mg/kg as recv'd	ANTEK Char-N mg/kg as BLS	ANTEK Remaining Char %	Total N Released %
0.011803	0.00012	608.40	469.00	693.79	428	437	62.95	37.05

Difference between Kjeldahl N & Antek N

-14.03 (Kjeldahl - Antek)/ Antek

Table XI-12. (cont.) Summary Data Single droplet Burns at the Temperatures indicated.

Liquor: Eucalyptus Furnace Temperature (C): 900
 Jar #: 3 % N (Dry solids Basis): 0.09
 Integration Time: 300 Sec. Dry solids (%): 67.6

Droplet #	Droplet Wt. (mg)	Droplet Dry Wt. (mg)	Char Wt. (mg)	Based on Dry Solids		Droplet N (mg)	Droplet N (mg/kg)	Droplet N mg/100 g BLS	072 NO at 8% O2 (ppm)	072 total N-Release asNO(ppm)
				Released Wt. (mg)	% Wt. Loss					
20	21.0	14.2	3.3	10.9	76.8	1.28E-02	608.4	0.00012776	166.45	941.25
21	17.6	11.9	2.7	9.2	77.3	1.07E-02	608.4	0.00010708	168.25	959.36
22	18.6	12.6	2.7	9.9	78.5	1.13E-02	608.4	0.00011316	198.65	1136.46
23	17.3	11.7	3.0	8.7	74.3	1.05E-02	608.4	0.00010525	175.47	1013.09
24	23.7	16.0	3.3	12.7	79.4	1.44E-02	608.4	0.00014419	176.75	1031.49
25	25.5	17.2	4.4	12.8	74.5	1.55E-02	608.4	0.00015514	198.95	1164.05
26	22.5	15.2	3.4	11.8	77.6	1.37E-02	608.4	0.00013689	185.93	1098.71
SUMS:	146.2	98.8	22.8	76.0	538.5	8.89E-02	4258.8	8.89E-04	1270.5	7344.4
AVES:	20.89	14.12	3.26	10.86	76.92	1.27E-02	608.40	1.27E-04	181.49	1049.20
Std.Dev.P:	2.94	1.99	0.54	1.54	1.77	0.00	0.00	0.00	12.42	79.82
Std.Dev.S:	3.18	2.15	0.58	1.67	1.92	0.00	0.00	0.00	13.41	86.21

Kjeldahl Droplet N (mg)	Droplet N mg/100 g BLS	Kjeldahl Droplet N mg/kg	ANTEK Droplet N mg/kg as recv'd	ANTEK Droplet N mg/kg as BLS	ANTEK Char-N mg/kg as recv'd	ANTEK Char-N mg/kg as BLS	Total N Remaining Char %	Total N Released %
0.012707	0.00013	608.40	469.00	693.79	1050	1071	154.43	54.43

Difference between Kjeldahl N & Antek N

-14.03 (Kjeldahl - Antek)/ Antek

Table XI-12. (cont.) Summary Data Single droplet Burns at the Temperatures indicated.

Liquor: Eucalyptus Furnace Temperature (C): 1000
 Jar #: 3 % N (Dry solids Basis): 0.09
 Integration Time: 300 Sec. Dry solids (%): 67.6

Droplet #	Droplet Wt. (mg)	Droplet Dry Wt. (mg)	Char Wt. (mg)	Based on Dry Solids		Droplet N (mg)	Droplet N (mg/kg)	Droplet N mg/100 g BLS	072 NO at 8% O2 (ppm)	072 total N-Release asNO(ppm)
				Released Wt. (mg)	% Wt. Loss					
1	15.0	10.1	2.3	7.8	77.3	9.13E-03	608.4	0.00009126	104.14	596.33
2	9.5	6.4	1.5	4.9	76.6	5.78E-03	608.4	5.7798E-05	92.26	528.33
3	15.3	10.3	2.2	8.1	78.7	9.31E-03	608.4	9.3085E-05	113.03	644.46
4	9.0	6.1	1.3	4.8	78.6	5.48E-03	608.4	5.4756E-05	92.2	527.96
6	17.9	12.1	2.5	9.6	79.3	1.09E-02	608.4	0.0001089	112.53	665.83
7	15.2	10.3	2.0	8.3	80.5	9.25E-03	608.4	9.2477E-05	119.48	682.18
8	13.6	9.2	2.0	7.2	78.2	8.27E-03	608.4	8.2742E-05	111.79	645
SUMS:	95.5	64.6	13.8	50.8	549.4	5.81E-02	4258.8	5.81E-04	745.4	4290.1
AVES:	13.64	9.22	1.97	7.25	78.49	8.30E-03	608.40	8.30E-05	106.49	612.87
Std.Dev.P:	3.02	2.04	0.40	1.66	1.19	0.00	0.00	0.00	9.92	58.88
Std.Dev.S:	3.26	2.21	0.43	1.79	1.28	0.00	0.00	0.00	10.71	63.60

Kjeldahl Droplet N (mg)	Droplet N mg/100 g BLS	Kjeldahl Droplet N mg/kg	ANTEK Droplet N mg/kg as recv'd	ANTEK Droplet N mg/kg as BLS	ANTEK Char-N mg/kg as recv'd	ANTEK Char-N mg/kg as BLS	Total N Remaining Char %	Total N Released %
0.008300	0.00008	608.40	469.00	693.79	419	428	61.63	38.37

Difference between Kjeldahl N & Antek N

-14.03 (Kjeldahl - Antek)/ Antek

Table XI-13. Summary Data Single droplet Burns at the Temperatures indicated.

Liquor: Southern Pine I Furnace Temperature (C): 400
 Jar #: 5 % N (Dry solids Basis): 0.06
 Integration Time: 300 Sec. Dry solids (%): 72.7

Droplet #	Droplet Wt. (mg)	Droplet Dry Wt. (mg)	Char Wt. (mg)	Based on Dry Solids		Droplet N (mg)	Droplet N (mg/kg)	Droplet N mg/100 g BLS	072 NO at 8% O2 (ppm)	072 total N-Release asNO(ppm)
				Released Wt. (mg)	% Wt. Loss					
2	21.7	15.8	12.5	3.3	20.8	9.47E-03	436.2	9.4655E-05	64.2	369.67
3	23.6	17.2	13.6	3.6	20.7	1.03E-02	436.2	0.00010294	64.98	375.44
4	21.1	15.3	12.2	3.1	20.5	9.20E-03	436.2	9.2038E-05	62.21	361.39
5	21.4	15.6	12.1	3.5	22.2	9.33E-03	436.2	9.3347E-05	62.37	357.14
6	20.2	14.7	11.5	3.2	21.7	8.81E-03	436.2	8.8112E-05	59.48	341.19
7	18.2	13.2	10.3	2.9	22.2	7.94E-03	436.2	7.9388E-05	55.63	321.42
8	19.8	14.4	11.2	3.2	22.2	8.64E-03	436.2	8.6368E-05	57.37	326.03
SUMS:	146.0	106.1	83.4	22.7	150.2	6.37E-02	3053.4	6.37E-04	426.2	2452.3
AVES:	20.86	15.16	11.91	3.25	21.46	9.10E-03	436.20	9.10E-05	60.89	350.33
Std.Dev.P:	1.57	1.14	0.97	0.19	0.72	0.00	0.00	0.00	3.24	19.58
Std.Dev.S:	1.69	1.23	1.05	0.21	0.78	0.00	0.00	0.00	3.50	21.15

Kjeldahl Droplet N (mg)	Droplet N mg/100 g BLS	Kjeldahl Droplet N mg/kg	ANTEK Droplet N mg/kg as recv'd	ANTEK Droplet N mg/kg as BLS	ANTEK Char-N mg/kg as recv'd	ANTEK Char-N mg/kg as BLS	Total N Remaining Char %	Total N Released %
0.009098	0.00009	436.20	285.00	381.02	366	373	98.02	1.98

Difference between Kjeldahl N & Antek N

12.65 (Kjeldahl - Antek)/ Antek

Table XI-13. (cont.) Summary Data Single droplet Burns at the Temperatures indicated.

Liquor: Southern Pine I Furnace Temperature (C): 600
 Jar #: 5 % N (Dry solids Basis): 0.06
 Integration Time: 300 Sec. Dry solids (%): 72.7

Droplet #	Droplet Wt. (mg)	Droplet Dry Wt. (mg)	Char Wt. (mg)	Based on Dry Solids		Droplet N (mg)	Droplet N (mg/kg)	Droplet N mg/100 g BLS	072 NO at 8% O2 (ppm)	072 total N-Release asNO(ppm)
				Released Wt. (mg)	% Wt. Loss					
10	21.5	15.6	10.7	4.9	31.5	9.38E-03	436.2	0.000093783	80.82	471.22
12	28.2	20.5	14.9	5.6	27.3	1.23E-02	436.2	0.000123008	121.07	687.14
13	18.1	13.2	9.3	3.9	29.3	7.90E-03	436.2	7.89522E-05	90.05	513.43
14	19.8	14.4	9.9	4.5	31.2	8.64E-03	436.2	8.63676E-05	92.32	526.41
15	24.1	17.5	12.5	5.0	28.7	1.05E-02	436.2	0.000105124	99.56	570.12
16	19.3	14.0	10.0	4.0	28.7	8.42E-03	436.2	8.41866E-05	87.79	503.55
18	19.1	13.9	10.7	3.2	22.9	8.33E-03	436.2	8.33142E-05	84.46	487.62
SUMS:	150.1	109.1	78.0	31.1	199.7	6.55E-02	3053.4	6.55E-04	656.1	3759.5
AVES:	21.44	15.59	11.14	4.45	28.53	9.35E-03	436.20	9.35E-05	93.72	537.07
Std.Dev.P:	3.31	2.41	1.80	0.76	2.66	0.00	0.00	0.00	12.45	67.81
Std.Dev.S:	3.57	2.60	1.94	0.82	2.88	0.00	0.00	0.00	13.45	73.25

Kjeldahl Droplet N (mg)	Droplet N mg/100 g BLS	Kjeldahl Droplet N mg/kg	ANTEK Droplet N mg/kg as recv'd	ANTEK Droplet N mg/kg as BLS	ANTEK Char-N mg/kg as recv'd	ANTEK Char-N mg/kg as BLS	Total N Remaining Char %	Total N Released %
0.009353	0.00009	436.20	285.00	381.02	249	254	66.69	33.31

Difference between Kjeldahl N & Antek N

12.65 (Kjeldahl - Antek)/ Antek

Table XI-13. (cont.) Summary Data Single droplet Burns at the Temperatures indicated.

Liquor: Southern Pine I Furnace Temperature (C): 800
 Jar #: 5 % N (Dry solids Basis): 0.06
 Integration Time: 300 Sec. Dry solids (%): 72.7

Droplet #	Droplet Wt. (mg)	Droplet Dry Wt. (mg)	Char Wt. (mg)	Based on Dry Solids		Droplet N (mg)	Droplet N (mg/kg)	Droplet N mg/100 g BLS	072 NO at 8% O2 (ppm)	072 total N-Release asNO(ppm)
				Released Wt. (mg)	% Wt. Loss					
9	16.0	11.6	7.0	4.6	39.8	6.98E-03	436.2	6.9792E-05	70.29	403.71
10	23.1	16.8	10.2	6.6	39.3	1.01E-02	436.2	0.00010076	69.03	400.65
11	15.6	11.3	6.5	4.8	42.7	6.80E-03	436.2	6.8047E-05	71.98	412.58
14	18.5	13.4	8.1	5.3	39.8	8.07E-03	436.2	8.0697E-05	71.2	480.97
15	14.5	10.5	5.8	4.7	45.0	6.32E-03	436.2	6.3249E-05	72.16	402.99
16	13.0	9.5	5.2	4.3	45.0	5.67E-03	436.2	5.6706E-05	53.92	311.54
17	13.3	9.7	5.0	4.7	48.3	5.80E-03	436.2	5.8015E-05	64.8	371.46
SUMS:	114.0	82.9	47.8	35.1	299.8	4.97E-02	3053.4	4.97E-04	473.4	2783.9
AVES:	16.29	11.84	6.83	5.01	42.83	7.10E-03	436.20	7.10E-05	67.63	397.70
Std.Dev.P:	3.27	2.38	1.70	0.71	3.17	1.43E-03	0.00	1.43E-05	6.06	46.81
Std.Dev.S:	3.53	2.57	1.83	0.77	3.42	1.54E-03	0.00	1.54E-05	6.55	50.56

Kjeldahl Droplet N (mg)	Droplet N mg/100 g BLS	Kjeldahl Droplet N mg/kg	ANTEK Droplet N mg/kg as recv'd	ANTEK Droplet N mg/kg as BLS	ANTEK Char-N mg/kg as recv'd	ANTEK Char-N mg/kg as BLS	Total N Remaining Char %	Total N Released %
0.007104	0.00007	436.20	285.00	381.02	233	238	62.40	37.60

Difference between Kjeldahl N & Antek N

12.65 (Kjeldahl - Antek)/ Antek

Table XI-13. (cont.) Summary Data Single droplet Burns at the Temperatures indicated.

Liquor: Southern Pine I Furnace Temperature (C): 1000
 Jar #: 5 % N (Dry solids Basis): 0.06
 Integration Time: 300 Sec. Dry solids (%): 72.7

Droplet #	Droplet Wt. (mg)	Droplet Dry Wt. (mg)	Char Wt. (mg)	Based on Dry Solids		Droplet N (mg)	Droplet N (mg/kg)	Droplet N mg/100 g BLS	072 NO at 8% O2 (ppm)	072 total N-Release asNO(ppm)
				Released Wt. (mg)	% Wt. Loss					
2	11.9	8.7	2.1	6.6	75.7	5.19E-03	436.2	5.19078E-05	99.25	565.15
3	21.4	15.6	3.6	12.0	76.9	9.33E-03	436.2	9.33468E-05	104.26	602.36
4	20.3	14.8	2.9	11.9	80.3	8.85E-03	436.2	8.85486E-05	110.91	665.47
5	16.0	11.6	2.5	9.1	78.5	6.98E-03	436.2	0.000069792	106.37	592.47
6	11.6	8.4	1.7	6.7	79.8	5.06E-03	436.2	5.05992E-05	93.55	527.39
7	15.1	11.0	2.1	8.9	80.9	6.59E-03	436.2	6.58662E-05	101.52	586.68
8	16.7	12.1	2.3	9.8	81.1	7.28E-03	436.2	7.28454E-05	95.94	575.3
SUMS:	113.0	82.2	17.2	65.0	553.2	4.93E-02	3053.4	4.93E-04	711.8	4114.8
AVES:	16.14	11.74	2.46	9.28	79.03	7.04E-03	436.20	7.04E-05	101.69	587.83
Std.Dev.P:	3.48	2.53	0.58	2.01	1.92	0.00	0.00	0.00	5.59	38.89
Std.Dev.S:	3.76	2.74	0.63	2.17	2.07	0.00	0.00	0.00	6.04	42.00

Kjeldahl Droplet N (mg)	Droplet N mg/100 g BLS	Kjeldahl Droplet N mg/kg	ANTEK Droplet N mg/kg as recv'd	ANTEK Droplet N mg/kg as BLS	ANTEK Char-N mg/kg as recv'd	ANTEK Char-N mg/kg as BLS	Total N Remaining Char %	Total N Released %
0.007042	0.00007	436.20	285.00	381.02	114	116	30.53	69.47

Difference between Kjeldahl N & Antek N

12.65 (Kjeldahl - Antek)/ Antek

APPENDIX XII: THERMOGRAVIMETRIC DIFFERENTIAL SCANNING CALORIMETRY SCREENING EXPERIMENTS

The contents of this appendix include further details of the experimental procedures for the TG-DSC screening experiments, the experimental results and discussion, and the experimental data.

Differential thermal analysis (DTA) measures the temperature difference between the sample and an inert reference as both are heated at a constant temperature rate. The temperature difference indicates the heat absorbed or emitted by the sample due to chemical reaction. In differential scanning calorimetry (DSC), a sample and a reference are heated at a constant rate. However, measurement is made of the heat added to either the sample or the reference to maintain the two at the same temperature. The added heat offsets that consumed or given off by exothermic or endothermic reactions of the sample. Peaks of the DTG are positive for exothermic reactions resulting from physical or chemical changes in the sample such as adsorption. Endothermic peaks are negative in the thermogram representing physical processes including fusion, vaporization, sublimation, and desorption. When a DTG is obtained in an inert atmosphere, the reactions tend to be endothermic.

SCREENING EXPERIMENTS OVERVIEW

Screening experiments were employed to make an initial test for significance of inorganic content on the decomposition temperatures of various nitrogen species. A 2^3 factorial designed experiment was conducted using a thermogravimetric-differential scanning calorimeter and statistical analysis was done to provide an analysis of variance to

determine the significance of factors and interactions.¹⁰⁰ The use of this type of analysis assumed a linear response for the significant effects of the individual factors and of their interactions. The standard order of treatment combinations and the independent variables for the experimentation were previously identified in the experimental section and are given again in Table XII-1 below. Each treatment combination was tested in triplicate to provide for a direct estimate of the experimental error variance. Significance was determined using F-ratio comparisons with tabulated F-values at the 95% confidence level.

Table XII-1. Experimental design, 2^3 factorial, for screening experiments.

Treatment Combinations	Factor A, Na_2SO_4	Factor B, Na_2S	Factor C, Na_2CO_3	Experiment #
1	-	-	-	1
a	+	-	-	2
b	-	+	-	3
ab	+	+	-	4
c	-	-	+	5
ac	+	-	+	6
bc	-	+	+	7
abc	+	+	+	8

Statistical analysis (an unweighted means ANOVA) was performed using the computer program "Number Cruncher Statistical System" (NCSS)⁹⁷ on the data which included an analysis of variance and error estimation to determine the significance of individual factors and interactions. The three independent variables examined in each of the regions were the decomposition onset temperature, the percent weight loss for the nitrogen species, and the enthalpy at the onset of decomposition. Significance was determined at the 95% confidence level ($\alpha = 0.05$). The analysis of variance reports for each of the independent variables are provided at the end of this appendix. The results of the analysis are presented and discussed below.

RESULTS AND DISCUSSION

The three data regions for each thermogram were manually set taking into account the observed weight loss and the endothermic peak for the decomposition of glutamic acid and tryptophan both as their pure substance and as treatment 1. Data collected for each of the pure components, at the conditions previously indicated, is provided in Table XII-2.

The same "enthalpy and weight" analysis was performed on the thermograms. The weight loss data for each sample treatment was corrected (taking into account the decomposition of the SAOB in the sample) such that the weight loss observed could be directly correlated with the decomposition on the nitrogen compound of interest. An example of the correction calculation for the weight loss is provided at the end of this section. Therefore, the weight loss for each treatment combination is reported only on a percent basis for the nitrogen compounds within each of the region analyses. The overall weight loss for pure glutamic acid was 79.7 % and it was 71.5 % for tryptophan, while the weight loss observed in treatment one averaged 17.2 % and 101.6 % for each, respectively.

Table XII-2. Data for the thermal decomposition of glutamic acid and tryptophan obtained using the TG-DSC 111.

	Glutamic Acid		Tryptophan	
	Parameter	Value	Parameter	Value
1st Endothermic peak	Temperature Region	193-283° C	Temperature Region	276-313° C
	Decomposition Onset Temperature	203° C	Decomposition Onset Temperature	291.72° C
	% Weight Loss	37.6%	% Weight Loss	20.2%
2nd Endothermic peak	Temperature Region	227-284° C	Temperature Region	311-436° C
	Decomposition Onset Temperature	264° C	Decomposition Onset Temperature	357° C
	% Weight Loss	21.8%	% Weight Loss	51.5%

Decomposition Onset Temperature

The results for the overall decomposition of the nitrogen species indicated that all factors and two-way interactions were significant for the decomposition onset temperature. For the overall temperature range, the onset temperature was defined as the temperature at which the greatest weight loss was initiated. When the sample treatment was Na_2SO_4 , the sum mean onset temperature was 308°C . When the sample was not treated with the Na_2SO_4 , the sum mean onset temperature was 301°C . When the sample treatment was Na_2S , the sum mean onset temperature was 307°C , whereas when the sample was not treated with Na_2S , the sum mean onset temperature was 302°C .

Table XII-3. Sum mean decomposition onset temperatures for the total nitrogen species with significance of Na_2SO_4 , Na_2S , and Na_2CO_3 individual and two-way treatment combinations.

Significant Factor or Treatment Combination	Treatment	Sum Mean Onset Temperature ($^\circ\text{C}$)
Na_2SO_4	-1	301
	1	308
Na_2S	-1	302
	1	307
Na_2CO_3	-1	300
	1	309
$\text{Na}_2\text{SO}_4, \text{Na}_2\text{S}$	-1, -1	302
	-1, 1	300
	1, -1	301
	1, 1	315
$\text{Na}_2\text{SO}_4, \text{Na}_2\text{CO}_3$	-1, -1	295
	-1, 1	307
	1, -1	306
	1, 1	310
$\text{Na}_2\text{S}, \text{Na}_2\text{CO}_3$	-1, -1	292
	-1, 1	311
	1, -1	309
	1, 1	306

The sum mean onset temperature was 309°C when Na_2CO_3 was applied to the sample and the sum mean onset temperature was 300°C when the Na_2CO_3 treatment was

not applied. The two-way interactions between these variables were also significant. The sum mean onset temperatures are provided in Table XII-3 for each of significant individual treatment and combination.

For region II which is primarily the glutamic acid decomposition, the addition of Na_2S was determined significant with respect to the onset temperature. When the sample was treated with Na_2S , the sum mean onset temperature was 202°C . When the sample was not treated with Na_2S , the sum mean onset temperature was 218°C .

For region III, the addition of Na_2CO_3 and the interaction between Na_2S and Na_2CO_3 was determined significant to the tryptophan onset decomposition temperature. The effects for the significant factors and treatments for the onset temperature in region III are given in Table XII-4. When Na_2CO_3 was added to the sample, the sum mean onset temperature was 315°C , while the Na_2CO_3 untreated samples indicated a sum mean onset temperature of 305°C .

Table XII-4. Sum mean onset temperatures for the decomposition of nitrogen species in region III with significant treatment combinations.

Significant Factor or Treatment Combination	Treatment	Sum Mean Onset Temperature ($^\circ\text{C}$)
Na_2CO_3	-1	305
	1	315
$\text{Na}_2\text{S}, \text{Na}_2\text{CO}_3$	-1, -1	302
	-1, 1	318
	1, -1	307
	1, 1	311

For the interaction between the combination sulfide and carbonate treatment, when both sodium salts were added, the sum mean onset temperature was 311°C , while when neither salt was added, the sample sum mean onset temperature was 302°C . When

Na_2CO_3 was added and Na_2S was not added, the sum mean onset temperature was 318°

C. However, the reverse treatment, addition of Na_2S and not Na_2CO_3 , yielded a sum mean onset temperature of 307° C.

Percent Weight Loss

For the overall percent weight loss, only the addition of Na_2S and the addition of Na_2CO_3 was significant. When the sample was treated with Na_2S , the sum mean weight loss was 49.4 %. When the sample was not treated with Na_2S , the sum mean weight loss was 62.7 %. When the sample was treated with Na_2CO_3 , the sum mean weight loss was 54.0 %, while the Na_2CO_3 untreated sum mean weight loss was 58.1 %. These values are shown in the following table.

Table XII-5. Sum mean decomposition percent weight loss for the total nitrogen species with significance of Na_2S and Na_2CO_3 individual treatments.

Significant Factor	Treatment	Sum Mean % Weight Loss
Na_2S	-1	62.7
	1	49.4
Na_2CO_3	-1	58.1
	1	54.0

Within region II, the addition of each individual factor and two two-way interactions was determined significant to the percent weight loss observed. When the sample treatment consisted of the addition of Na_2SO_4 , the sum mean weight loss observed was 7.0% while when the sample was not treated with the Na_2SO_4 , the sum mean weight loss was 9.2%. When treated with Na_2S , the sum mean weight loss was 6.2%. When the sample was not treated with Na_2S , the sum mean weight loss was 9.9%. When the sample was treated with Na_2CO_3 , the sum mean was 2.9%, while the Na_2CO_3 untreated sample

sum mean weight loss was 13.2%. The application of both Na_2SO_4 and Na_2S yielded a weight loss of 3.5%. When Na_2SO_4 was added and Na_2S was not, the sum mean weight loss was 10.5%. The reverse treatment yielded a sum mean weight loss of 9.0%. When neither of the components was added, the sum mean weight loss was 9.3%. When the sample was treated with both Na_2S and Na_2CO_3 , the sum mean weight loss was 3.3% in region II. When the sample was treated with neither, the sum mean weight loss was 17.3%. When the treatment consisted of only the Na_2CO_3 addition and not the Na_2S , the sum mean weight loss was 9.2%, while the inverse of this yielded a sum mean weight loss of 2.6%. This data is tabulated in Table XII-6 for the percent weight loss observed in region II.

Table XII-6. Sum mean decomposition percent weight loss for the total nitrogen species with significant treatments in region II.

Significant Factor or Treatment Combination	Treatment	Sum Mean % Weight Loss
Na_2SO_4	-1	9.2
	1	7.0
Na_2S	-1	9.9
	1	6.2
Na_2CO_3	-1	13.2
	1	2.9
$\text{Na}_2\text{SO}_4, \text{Na}_2\text{S}$	-1, -1	9.3
	-1, 1	9.0
	1, -1	10.5
	1, 1	3.5
$\text{Na}_2\text{S}, \text{Na}_2\text{CO}_3$	-1, -1	17.3
	-1, 1	2.6
	1, -1	9.2
	1, 1	3.3

For the tryptophan decomposition percent weight loss, the addition of Na_2S and of Na_2CO_3 , each individually, was significant. When the Na_2S was added to the sample, the sum mean weight loss in the tryptophan region was 79.7%, while when the Na_2S was not

added, the sum mean weight loss was 105.5%. When the treatment consisted of carbonate addition, the sum mean weight loss was 95.9%, while the samples which were not treated with carbonate indicated a sum mean weight loss of 89.3%. This data is tabulated in Table XII-7.

Table XII-7. Sum mean decomposition percent weight loss for nitrogen species in region III with significance of Na_2S and Na_2CO_3 individual treatments.

Significant Factor	Treatment	Sum Mean % Weight Loss
Na_2S	-1	105.5
	1	79.7
Na_2CO_3	-1	89.3
	1	95.9

Enthalpy at the Onset of Decomposition

The third dependent variable examined was the enthalpy at the onset of decomposition within each of the three regions. In region I, the addition of individual factors Na_2S and Na_2CO_3 were significant along with the interaction between Na_2SO_4 and Na_2CO_3 and between Na_2S and Na_2CO_3 . These results are shown in the following table.

Table XII-8. Sum mean enthalpy at the onset of decomposition for region I.

Significant Factor or Treatment Combination	Treatment	Sum Mean Enthalpy (Joules)
Na_2S	-1	4.05
	1	2.05
Na_2CO_3	-1	3.84
	1	2.27
$\text{Na}_2\text{SO}_4, \text{Na}_2\text{S}$	-1, -1	4.69
	-1, 1	2.00
	1, -1	2.98
	1, 1	2.53
$\text{Na}_2\text{S}, \text{Na}_2\text{CO}_3$	-1, -1	5.26
	-1, 1	2.85
	1, -1	2.42
	1, 1	1.69

In region II, which is characterized by the glutamic acid decomposition, only two individual factors were significant to the enthalpy value at the onset of the decomposition. These were Na_2S and Na_2CO_3 . When Na_2S was the treatment of interest, its addition left the enthalpy at the onset decomposition at 0.25 Joules (J). When the Na_2S was not added, the enthalpy was 0.96 J. When the sample treatment was the addition of Na_2CO_3 , the enthalpy was 0.24 J while the non-treatment indicated a sum mean enthalpy of 0.96 J. These effects are presented in Table XII-9.

Table XII-9. Sum mean enthalpy at the onset of decomposition for region II.

Significant Factor or Treatment Combination	Treatment	Sum Mean Enthalpy (Joules)
Na_2S	-1	0.96
	1	0.25
Na_2CO_3	-1	0.97
	1	0.24

Two factors and two two-way interactions were determined significant for the enthalpy at the decomposition onset in region III. The addition of Na_2SO_4 yielded a mean sum enthalpy of 1.21 J, while the mean sum enthalpy was 1.76 J when Na_2SO_4 was not added. The addition of Na_2S was also significant and its addition yielded a sum mean enthalpy of 1.12 J. When Na_2S was not added, the reported sum mean enthalpy was 1.86 J. The interaction between Na_2SO_4 and Na_2S was significant. When the treatment consisted of the addition of both, the mean onset enthalpy was 1.02 J. When the Na_2SO_4 was added and the Na_2S was not, the sum mean onset enthalpy was 1.41 J. When the Na_2S was added and the Na_2SO_4 was not, the sum mean onset enthalpy was 1.22 J. When neither was added, the enthalpy at the onset of decomposition averaged 2.30 J.

The other interaction which was found significant was that between Na_2SO_4 and Na_2CO_3 . When both were added, the resulting sum mean enthalpy at the decomposition onset in region III was 1.21 J. When the Na_2SO_4 was added and the Na_2CO_3 was not, the sum mean onset enthalpy was 0.96 J. When the Na_2CO_3 was added and the Na_2SO_4 was not, the sum mean onset enthalpy was 1.60 J. When neither was added, the enthalpy at the onset of decomposition averaged 1.92 J. The effects for the significant treatments for the enthalpy in region III are listed in Table XII-10.

Table XII-10. Sum mean enthalpy at the decomposition onset of region III.

Significant Factor or Treatment Combination	Treatment	Sum Mean Enthalpy (Joules)
Na_2SO_4	-1	1.76
	1	1.21
Na_2S	-1	1.86
	1	1.12
$\text{Na}_2\text{SO}_4, \text{Na}_2\text{S}$	-1, -1	2.30
	-1, 1	1.22
	1, -1	1.41
	1, 1	1.02
$\text{Na}_2\text{SO}_4, \text{Na}_2\text{CO}_3$	-1, -1	1.92
	-1, 1	1.60
	1, -1	0.96
	1, 1	1.47

Summary

Several comments can be made, in general, about the results of the experiments. The straight chain nitrogen component, glutamic acid, was found to decompose at a lower temperature and with a greater percent weight loss than the heterocyclic ring structure, tryptophan. This is to be expected based on the literature for coal pyrolysis and combustion. The stability of nitrogen compounds is greatest for six-member rings,

followed by five-member ring structures, and then straight chain nitrogen compounds which are the least stable.

Solomon and Colket thought that the initial nitrogen release from ring structural species occurred without any changes initially to the heterocyclic ring.²⁸ A similar phenomena was observed during the TG-DSC slow pyrolysis of phenylalanine (a straight chain amino acid) where the phenylalanine entered the gas phase in its undisturbed structure. At higher temperatures, the rings are broken and the nitrogen species of HCN and NH₃ could then be observed.²⁸ The decomposition of straight chain structures occurs more readily than the decomposition of heterocyclic ring structures because the C-C bond is more easily broken than the C-H bond. However, the reverse tends to be true for the aromatic compounds.¹¹²

The addition of inorganic species has been found to affect the nature of the organic species decomposition. The general trends observed included a slight increase in the onset decomposition temperature, decreased weight loss, and a decrease in the enthalpy at the onset of decomposition. The degree to which the effect was observed was dependent on the inorganic species, or combination thereof, indicating that the sodium concentration may not be as important as the anion of the salt. In many of the significant treatments, either the sulfide or carbonate salts were involved. However, as in many situations, the general trends are not without exceptions.

The onset temperature for the nitrogen species decomposition shifts to higher temperature ranges for all treatments when compared to the decomposition of the individual pure components and to the results of the treatment combination 1. This is

likely explained by the amino acid compounds complexing with the inorganic sodium species and creating new sodium salts. In the overall region, all individual treatments and all two-way interactions were found significant. The addition of the individual inorganic components generally increased the decomposition temperature by 5–10° C. The combination of the sulfate and sulfide had the least effect on the onset temperature. When neither or only one was added, the temperature remained quite similar in all three cases but sulfate seemed to increase the temperature slightly more. When both were added, the onset temperature increased by nearly 14° C.

A similar trend was observed for the combination treatment of sulfate and carbonate. The onset temperature remained low and with each addition increased by 10–15° C with carbonate appearing to have a slightly greater effect. The treatment combination of sulfide and carbonate also increased the temperature but the greatest effect was observed when the carbonate was added and the sulfide was not. A temperature increase of 20° C was noted.

In region II, the only factor determined significant was the addition of sulfide. However, the addition of sulfide lowered the onset temperature by about 15° C. In region II, carbonate and sulfide were significant but the carbonate seemed to have a larger effect. Again, an increase of about 15° C was observed for the carbonate alone. The next greatest effect was for the sulfide-carbonate combination followed by the sulfide alone.

The possibility for sulfate conversion to sulfide exists due to the reducing environment during pyrolysis in the experimental system. This could enhance the effects observed where sulfide is involved. However, the conversion could not be verified as no

proximate or ultimate analyses were performed on the sample. Likewise, the nature of the decomposition products can not be determined as no gas phase analyses were done.

When the significant treatments for the effect on weight loss are examined, the sulfide and carbonate again play large roles and the effect is generally to reduce the weight loss observed. The sulfide seems to have the greatest effect in the overall region and in region III which corresponds to the tryptophan decomposition range. In the third region, the weight loss increased 25% with the sulfide addition. In region II, carbonate has the largest effect of any single factor while the combination of carbonate and sulfide has the greatest effect which appears to be synergistic in nature. In region III, the treatment of carbonate, while significant, has a reverse effect of sulfide and the observed effects of the other regions. The observed effect was an increase in the weight loss by about 6.5%.

The effects of the significant treatments for the variable of enthalpy at the onset of decomposition showed sulfide and carbonate to again be important with sulfide generally indicating a larger effect. Over the entire range (region I), the significant treatment combination of sulfide and carbonate again showed a synergistic effect. In region II, the carbonate treatment exhibited a larger decrease in the enthalpy. The sulfide has a greater effect in region III, however, sulfate also seems to have some relative importance. The differences observed for the enthalpy variable appeared to be less sensitive than the weight loss variable or the temperature variable effects.

The complete interpretation of these preliminary results is impossible. The data examined can account for activities which occur in the solid or liquid state. Therefore, explanations for the observed results need to be derived from solid-solid, solid-liquid, or

liquid-liquid reactions or possibly from solid-gas reactions at the sample surface. As mentioned above, the possibility exists for sulfate to be reduced to sulfide. The properties of the anions could be important in the effects observed. Consideration was therefore given to the possibilities for such reactions and their significance during pyrolysis.

Example of Weight Loss Correction Calculations

An example of the correction made to account for the SAOB in the organic model fuel nitrogen compound sample is given here. An example is provided for the treatment 1 for the total nitrogen compounds and for treatment B which contained only glutamic acid.

Treatment 1, Overall Region: Total Nitrogen Compounds

<u>Components:</u>	<u>% Based on Total Weight</u>
0.1200 g NaOH (from 0.1 M NaOH solution)	
0.5010 g Tryptophan	44.6% Tryptophan
<u>0.5015 g Glutamic Acid</u>	<u>44.7% Glutamic Acid</u>
1.1225 g TOTAL	89.3% Total Nitrogen Compounds
Initial Sample Weight: 8.05 mg	
Overall Weight Loss: 5.01 mg	

Calculation

$8.05 \text{ mg} \times 0.893 = 7.19 \text{ mg}$ Total Nitrogen Compounds

$5.01 \text{ mg} / 7.19 \text{ mg} = 69.7\%$ Weight Loss For The Total Nitrogen Compounds

Treatment B, Glutamic Acid Region: Weight Loss Glutamic Acid Only.

<u>Components:</u>	<u>% Based on Total Weight</u>
0.1200 g NaOH (from 0.1 M NaOH solution)	
0.5009 g Tryptophan	33.0% Tryptophan & Na ₂ EDTA
0.5013 g Glutamic Acid	26.7% Glutamic Acid & Ascorbic Acid
0.5012 g Na ₂ S	
0.4015 g NaOH (from SAOB II solution)	
0.3380 g Na ₂ EDTA (from SAOB II solution)	
<u>0.1765 g Ascorbic Acid (from SAOB II solution)</u>	
2.5394 g TOTAL	59.7% Total Nitrogen Compounds
Initial Sample Weight: 7.01 mg	
Glutamic Acid Weight Loss: 0.05 mg	

Calculation

$7.01 \text{ mg} \times 0.267 = 1.87 \text{ mg}$ Total Nitrogen Compounds

$0.05 \text{ mg} / 1.87 \text{ mg} = 2.67\%$ Weight Loss For The Total Nitrogen Compounds in the Glutamic Acid Decomposition Temperature Region.

DATA

The data extracted from the thermograms is provided below. These values were used to determine the ANOVA results. The ANOVA tables are also presented below.

Treatments

A	Na ₂ SO ₄
B	Na ₂ S
C	Na ₂ CO ₃

Temperature Regions

I	Overall = 150-450° C
II	Glutamic Acid = 150-280° C
III	Tryptophan = 280-450 °C

% Weight Loss 150-450° C		(-) S	(+) S
(-) SO ₄	(-) CO ₃	69.7	48.9
		70.9	50.5
		69.2	54.2
	(+) CO ₃	62.9	52.3
		60.1	51.4
		56.8	42.5
(+) SO ₄	(-) CO ₃	64.6	56.9
		56.3	47
		64.4	44.1
	(+) CO ₃	58.1	51.7
		56.6	44.6
		62.9	48.3

Decomp Onset Temp 150-450° C		(-) S	(+) S
(-) SO ₄	(-) CO ₃	296	298
		284	300
		291	299
	(+) CO ₃	313	300
		315	300
		313	301
(+) SO ₄	(-) CO ₃	291	320
		293	317
		295	319
	(+) CO ₃	309	313
		310	311
		308	308

% Weight Loss 150-280° C		(-) S	(+) S
(-) SO ₄	(-) CO ₃	17.2	15.5
		16.9	10.9
		17.5	13.4
	(+) CO ₃	2.1	5
		1.3	6.1
		1	3.2
(+) SO ₄	(-) CO ₃	19.5	6.9
		14.8	6.8
		17.6	1.7
	(+) CO ₃	2.3	3.2
		1.2	1.4
		7.4	0.7

Decomp Onset Temp 150-280° C		(-) S	(+) S
(-) SO ₄	(-) CO ₃	255	192
		210	199
		213	242
	(+) CO ₃	193	207
		202	206
		208	209
(+) SO ₄	(-) CO ₃	225	199
		222	249
		226	211
	(+) CO ₃	195	219
		172	239
		187	192

% Weight Loss 280-450° C		(-) S	(+) S
(-) SO ₄	(-) CO ₃	97.2	70
		105.7	73.7
		102	76.9
	(+) CO ₃	119.7	86
		109.7	81.7
		111	71.7
(+) SO ₄	(-) CO ₃	102.9	92.4
		88.1	83.5
		104.7	74.4
	(+) CO ₃	110.7	85.8
		96.7	79
		117.7	81.1

Decomp Onset Temp 280-450° C		(-) S	(+) S
(-) SO ₄	(-) CO ₃	305	311
		301	310
		304	328
	(+) CO ₃	312	305
		301	306
		302	306
(+) SO ₄	(-) CO ₃	295	310
		305	328
		304	323
	(+) CO ₃	308	317
		309	317
		308	316

Onset Enthalpy 150-450° C		(-) S	(+) S
(-) SO ₄	(-) CO ₃	6.76	5.07
		6.45	2.16
		6.23	1.49
	(+) CO ₃	3.03	1.62
		2.83	0.93
		2.45	1.13
(+) SO ₄	(-) CO ₃	4.36	2.03
		3.54	2.27
		4.22	1.49
	(+) CO ₃	2.08	2.19
		4.65	2.22
		2.04	2.03

Onset Enthalpy 150-280° C		(-) S	(+) S
(-) SO ₄	(-) CO ₃	1.58	1.43
		1.51	0.56
		1.27	0.07
	(+) CO ₃	0.51	-0.13
		0.13	-0.21
		0.19	-0.2
(+) SO ₄	(-) CO ₃	1.34	0.49
		1.38	0.41
		1.52	0.11
	(+) CO ₃	0.12	0.15
		1.82	0.18
		0.13	0.19

Onset Enthalpy 280-450° C		(-) S	(+) S
(-) SO ₄	(-) CO ₃	2.4	0.85
		3.27	1.74
		1.91	1.34
	(+) CO ₃	2.44	1.47
		1.79	0.96
		2	0.96
(+) SO ₄	(-) CO ₃	1.41	0.78
		0.84	0.52
		1.29	0.93
	(+) CO ₃	2.01	1.62
		1.24	1.06
		1.68	1.2

ANALYSIS OF VARIANCE REPORT: Unweighted Means ANOVA.

ANOVA Table for Response Variable: Temperature at decomposition onset, overall region.

<u>Source</u>	<u>DF</u>	<u>Sum-Squares</u>	<u>Mean-Squares</u>	<u>F-Ratio</u>	<u>Probability>F</u>	<u>Significant</u>
A (Na ₂ SO ₄)	1	294.0	294.0	43.42	0.0000	yes
B (Na ₂ S)	1	186.4	186.4	27.52	0.0001	yes
AB	1	368.0	368.0	54.35	0.0000	yes
C (Na ₂ CO ₃)	1	423.5	423.5	62.55	0.0000	yes
AC	1	96.6	96.6	14.27	0.0016	yes
BC	1	801.3	801.3	118.35	0.0000	yes
ABC	1	1.7	1.7	0.24	0.6277	no
ERROR	16	108.3	6.8			
TOTAL(Adj)	23					

Means & Effects for Response Variable: Temperature at decomposition onset, overall region.

<u>Term</u>	<u>Count</u>	<u>Mean</u>	<u>Std. Error</u>	<u>Effect</u>
ALL	24	304.3		304.3
A (Na ₂ SO ₄)				
-1	12	300.8	0.75	-3.5
1	12	307.8	0.75	3.5
B (Na ₂ S)				
-1	12	301.5	0.75	-2.8
1	12	307.0	0.75	2.8
C (Na ₂ CO ₃)				
-1	12	300.1	0.75	-4.2
1	12	308.5	0.75	4.2
AB (Na ₂ SO ₄ , Na ₂ S)				
-1, -1	6	301.9	1.06	3.9
-1, 1	6	299.6	1.06	-3.9
1, -1	6	301.0	1.06	-3.9
1, 1	6	314.5	1.06	3.9
AC				
-1, -1	6	294.5	1.06	-2.0
-1, 1	6	307.0	1.06	2.0
1, -1	6	305.6	1.06	2.0
1, 1	6	309.9	1.06	-2.0
BC				
-1, -1	6	291.5	1.06	-5.8
-1, 1	6	311.4	1.06	5.8
1, -1	6	308.6	1.06	5.8
1, 1	6	305.5	1.06	-5.8
ABC				
-1, -1, -1	3	290.2	1.50	0.26
-1, -1, 1	3	313.6	1.50	-0.26
-1, 1, -1	3	298.9	1.50	-0.26
-1, 1, 1	3	300.3	1.50	0.26
1, -1, -1	3	292.8	1.50	-0.26
1, -1, 1	3	309.3	1.50	0.26
1, 1, -1	3	318.3	1.50	0.26
1, 1, 1	3	310.6	1.50	-0.26

ANOVA Table for Response Variable: Glutamic acid onset decomposition temperature.

<u>Source</u>	<u>DF</u>	<u>Sum-Squares</u>	<u>Mean-Squares</u>	<u>F-Ratio</u>	<u>Probability>F</u>	<u>Significant</u>
A (Na ₂ SO ₄)	1	38.9	38.9	0.14	0.7133	no
B (Na ₂ S)	1	1448.5	1448.5	5.20	0.0366	yes
AB	1	212.7	212.7	0.76	0.3950	yes
C (Na ₂ CO ₃)	1	326.0	326.0	1.17	0.2953	yes
AC	1	272.6	272.6	0.98	0.3371	yes
BC	1	836.7	836.7	3.01	0.1022	yes
ABC	1	255.0	255.0	0.92	0.3526	yes
ERROR	16	4455.1	278.4			
TOTAL(Adj)	23	7845.8				

ANOVA Table for Response Variable: Tryptophan onset decomposition temperature.

<u>Source</u>	<u>DF</u>	<u>Sum-Squares</u>	<u>Mean-Squares</u>	<u>F-Ratio</u>	<u>Probability>F</u>	<u>Significant</u>
A (Na ₂ SO ₄)	1	110.4	110.4	3.32	0.0873	yes
B (Na ₂ S)	1	12.3	12.3	0.37	0.5525	no
AB	1	59.5	59.5	1.8	0.1990	yes
C (Na ₂ CO ₃)	1	616.6	616.6	18.53	0.0001	yes
AC	1	65.4	65.4	1.97	0.1800	yes
BC	1	196.0	196.0	8.89	0.0274	yes
ABC	1	0.9	0.9	0.03	0.8697	no
ERROR	16	532.6	33.3			
TOTAL(Adj)	23	1593.9				

ANOVA Table for Response Variable: Overall decomposition % weight loss.

<u>Source</u>	<u>DF</u>	<u>Sum-Squares</u>	<u>Mean-Squares</u>	<u>F-Ratio</u>	<u>Probability>F</u>	<u>Significant</u>
A (Na ₂ SO ₄)	1	47.9	47.9	2.78	0.1148	yes
B (Na ₂ S)	1	1068.0	1068.0	65.04	0.0000	yes
AB	1	15.8	15.8	0.92	0.3517	yes
C (Na ₂ CO ₃)	1	98.0	98.0	5.69	0.0297	yes
AC	1	28.8	28.8	1.67	0.2141	yes
BC	1	30.2	30.2	1.75	0.2043	yes
ABC	1	14.0	14.0	0.81	0.3813	yes
ERROR	16	275.5	17.2			
TOTAL(Adj)	23	1578.1				

ANOVA Table for Response Variable: Glutamic acid decomposition % weight loss.

<u>Source</u>	<u>DF</u>	<u>Sum-Squares</u>	<u>Mean-Squares</u>	<u>F-Ratio</u>	<u>Probability>F</u>	<u>Significant</u>
A (Na ₂ SO ₄)	1	29.6	29.6	6.77	0.0192	yes
B (Na ₂ S)	1	80.8	80.8	18.51	0.0005	no
AB	1	67.2	67.2	15.39	0.0012	yes
C (Na ₂ CO ₃)	1	638.2	638.2	146.18	0.0000	yes
AC	1	19.4	19.4	4.44	0.0513	yes
BC	1	115.1	115.1	26.37	0.0001	yes
ABC	1	3.6	3.6	0.81	0.3801	no
ERROR	16	69.9	69.9			
TOTAL(Adj)	23	1023.6				

ANOVA Table for Response Variable: Tryptophan decomposition % weight loss.

<u>Source</u>	<u>DF</u>	<u>Sum-Squares</u>	<u>Mean-Squares</u>	<u>F-Ratio</u>	<u>Probability>F</u>	<u>Significant</u>
A (Na ₂ SO ₄)	1	5.8	5.8	0.11	0.7399	yes
B (Na ₂ S)	1	4002.9	4002.9	79.4	0.0000	yes
AB	1	153.3	153.3	3.0	0.1004	yes
C (Na ₂ CO ₃)	1	262.4	262.4	5.2	0.0366	yes
AC	1	35.6	35.6	0.71	0.4128	yes
BC	1	106.5	106.5	2.11	0.1655	yes
ABC	1	12.3	12.3	0.24	0.6287	no
ERROR	16	806.7	806.7			
TOTAL(Adj)	23	5385.3				

ANOVA Table for Response Variable: Overall decomposition onset enthalpy.

<u>Source</u>	<u>DF</u>	<u>Sum-Squares</u>	<u>Mean-Squares</u>	<u>F-Ratio</u>	<u>Probability>F</u>	<u>Significant</u>
A (Na ₂ SO ₄)	1	2.1	2.1	2.55	0.1301	yes
B (Na ₂ S)	1	24.0	24.0	29.6	0.0001	yes
AB	1	1.9	1.9	2.3	0.1487	yes
C (Na ₂ CO ₃)	1	14.9	14.9	18.29	0.0006	yes
AC	1	7.6	7.6	9.31	0.0076	yes
BC	1	4.3	4.3	5.25	0.0359	yes
ABC	1	0.2	0.2	0.22	0.6437	no
ERROR	16	13.0	13.0			
TOTAL(Adj)	23	67.9				

ANOVA Table for Response Variable: glutamic acid decomposition onset enthalpy.

<u>Source</u>	<u>DF</u>	<u>Sum-Squares</u>	<u>Mean-Squares</u>	<u>F-Ratio</u>	<u>Probability>F</u>	<u>Significant</u>
A (Na ₂ SO ₄)	1	0.052	0.052	0.27	0.6102	no
B (Na ₂ S)	1	6.0	6.0	15.35	0.0012	yes
AB	1	0.052	0.052	0.27	0.6114	no
C (Na ₂ CO ₃)	1	3.2	3.2	16.57	0.0009	yes
AC	1	0.5	0.5	2.6	0.1261	yes
BC	1	0.3	0.3	1.44	0.2474	yes
ABC	1	0.023	0.023	0.12	0.7330	no
ERROR	16	3.1	3.1			
TOTAL(Adj)	23	10.17				

ANOVA Table for Response Variable: tryptophan decomposition onset enthalpy.

<u>Source</u>	<u>DF</u>	<u>Sum-Squares</u>	<u>Mean-Squares</u>	<u>F-Ratio</u>	<u>Probability>F</u>	<u>Significant</u>
A (Na ₂ SO ₄)	1	1.8	1.8	11.51	0.0037	yes
B (Na ₂ S)	1	3.3	3.3	21.2	0.0003	yes
AB	1	0.7	0.7	4.58	0.0482	yes
C (Na ₂ CO ₃)	1	0.055	0.055	0.35	0.5603	no
AC	1	1.0	1.0	6.54	0.0211	yes
BC	1	0.048	0.048	0.31	0.5871	no
ABC	1	0.012	0.012	0.07	0.7883	no
ERROR	16	2.5	2.5			
TOTAL(Adj)	23	9.4				

APPENDIX XIII: DISSERTATION PUBLICATIONS

The following list of presentations/publications have been made to report the findings of this work to the IPST and general scientific community. The first four papers have been published at the time of writing this document. The remaining articles are pending publication.

1. Martin, D.M.; Malcolm, E.W.; Hupa, M. The Effect of Fuel Composition on Nitrogen Release During Black Liquor Pyrolysis. Proceedings of the 1994 Technical Meeting of the Eastern States Section, Combustion Institute, Philadelphia, PA. pp. 294–297, 1994. Also in IPST's Technical Paper Series as #543.
2. Martin, D.M.; Malcolm, E.W. The Impact of Black Liquor Composition on the Release of Nitrogen in the Kraft Recovery Furnace. Proceedings of the 1995 Tappi Engineering Conference, TAPPI Press, Atlanta, GA, pp. 833–840, 1995. Submitted for publication in Tappi Journal August 1995. Also in IPST's Technical Paper Series as #584.
3. Forssén, M.; Hupa, M.; Pettersson, R.; Martin, D. NO Release During Black Liquor Char Combustion and Gasification, Proceedings of the 1995 International Chemical Recovery Conference, Toronto, Canada, TAPPI Press, Atlanta, GA, pp. B231–B239, 1995.
4. Thompson, L.M., Martin, D.M., Empie, H.J., Malcolm, E.W., Wood, M. The Fate of Nitrogen in a Kraft Recovery Furnace, Proceedings of the 1995 International Chemical Recovery Conference, Toronto, Canada, TAPPI Press, Atlanta, GA, pp. B225–B229, April 24–27, 1995. Also in IPST's Technical Paper Series as #557.
5. Martin, D.M.; Malcolm, E.W.; Empie, H.J. The Depletion of Proline Gaseous NO_x Intermediates at 573–973 K. To be submitted for publication in the Journal of Pulp and Paper Science.
6. Martin, D.M.; Malcolm, E.W. Evaluation of Heating Rate Effects on Fuel Nitrogen Pyrolysis Gas Phase Composition with Gas Chromatography-Mass Spectroscopy. To be submitted for publication in the Journal of Chromatographic Science.

ADDITIONAL CITATIONS

97. Hintze, J. L., programmer. Number Cruncher Statistical System (NCSS). Version 5.0 Kaysville, Utah 1987.
98. Levenspiel, O. Engineering Flow and Heat Exchange. Plenum Press, New York, NY, 1984.
99. Aho, K. Nitrogen Oxides Formation in Recovery Boilers. Licentiate Thesis, Åbo Akademi University, Turku, Finland, 1994.
100. Walpole, R.E.; Myers, R.H., Probability and Statistics for Engineers, 4th Ed., Macmillan Publishing Co. New York, NY, 1989
101. Roine, A., HSC Chemistry Software, Version 1.10, Outokumpu Research Oy, Pori, Finland, 1991.
102. Westley, F.; Frizzell, D.H.; Herron, J.T.; Hampson, R.F.; Mallard, W.G., Eds., National Institute of Standards and Technology Standard Reference Database 17, Chemical Kinetics Database, Version 5.0, U.S. Secretary of Commerce, 1993.
103. Treybal, R.E. Mass-Transfer Operations, 3rd Ed. McGraw-Hill Book Company, New York, NY 1980.
104. *ibid.*, p. 33.
105. *ibid.*, p.32
106. McCabe, W.L.; Smith, J.C.; Harriott, P., Unit Operations of Chemical Engineering, 4th Ed., McGraw-Hill, Inc., New York, NY, 1985.
107. Wehner, J.F.; Wilhelm, R.H., Boundary Conditions of Flow Reactor, Chemical Engineering Science, 6:89-93, (1956).
108. Tichacek, L.J., Selectivity in Experimental Reactors, AIChE Journal, 9(3):394-399 (1963).
109. Silverstein, R.M.; Bassler, G.C.; Morrill, T.C., Spectrometric Identification of Organic Compounds, 4th Ed., John Wiley and Sons, New York, NY, 1972.
110. Beynon, J.H.; Williams, A.E., Mass and Abundance Tables for Use in Mass Spectrometry, Elsevier Publishing Co., New York, NY, 1963.

111. Chapman, J.R., Practical Organic Mass Spectrometry, 2nd Ed., John Wiley & Sons, West Sussex, England, 1993.
112. Wendlandt, W.W., Thermal Analysis, 3rd Ed. John Wiley & Sons, New York, NY, 1986.